ISSN 0021-9673

VOL. 514 NO. 2 AUGUST 29, 1990
THIS ISSUE COMPLETES VOL. 514

JOURNAL OF CHROMATOGRAPHY

INTERNATIONAL JOURNAL ON CHROMATOGRAPHY, ELECTROPHORESIS AND RELATED METHODS

ELSEVIER

JOURNAL OF CHROMATOGRAPHY

Scope. The *Journal of Chromatography* publishes papers on all aspects of chromatography, electrophoresis and related methods. Contributions consist mainly of research papers dealing with chromatographic theory, instrumental development and their applications. The section *Biomedical Applications*, which is under separate editorship, deals with the following aspects: developments in and applications of chromatographic and electrophoretic techniques related to clinical diagnosis or alterations during medical treatment; screening and profiling of body fluids or tissues with special reference to metabolic disorders; results from basic medical research with direct consequences in clinical practice; drug level monitoring and pharmacokinetic studies; clinical toxicology; analytical studies in occupational medicine.

Submission of Papers. Manuscripts (in English; *four* copies are required) should be submitted to: The Editor of *Journal of Chromatography*, P.O. Box 681, 1000 AR Amsterdam, The Netherlands, or to: The Editor of *Journal of Chromatography, Biomedical Applications*, P.O. Box 681, 1000 AR Amsterdam, The Netherlands. Review articles are invited or proposed by letter to the Editors. An outline of the proposed review should first be forwarded to the Editors for preliminary discussion prior to preparation. Submission of an article is understood to imply that the article is original and unpublished and is not being considered for publication elsewhere. For copyright regulations, see below.

Subscription Orders. Subscription orders should be sent to: Elsevier Science Publishers B.V., P.O. Box 211, 1000 AE Amsterdam, The Netherlands, Tel. 5803 911, Telex 18582 ESPA NL. The *Journal of Chromatography* and the *Biomedical Applications* section can be subscribed to separately.

Publication. The *Journal of Chromatography* (incl. *Biomedical Applications*) has 37 volumes in 1990. The subscription prices for 1990 are:

J. Chromatogr. (incl. *Cum. Indexes, Vols. 451–500*) + *Biomed. Appl.* (Vols. 498–534):
Dfl. 6734.00 plus Dfl. 1036.00 (p.p.h.) (total *ca.* US$ 3885.00)

J. Chromatogr. (incl. *Cum. Indexes, Vols. 451–500*) only (Vols. 498–524):
Dfl. 5616.00 plus Dfl. 756.00 (p.p.h.) (total *ca.* US$ 3186.00)

Biomed. Appl. only (Vols. 525–534):
Dfl. 2080.00 plus Dfl. 280.00 (p.p.h.) (total *ca.* US$ 1180.00).

Our p.p.h. (postage, package and handling) charge includes surface delivery of all issues, except to subscribers in Argentina, Australia, Brasil, Canada, China, Hong Kong, India, Israel, Malaysia, Mexico, New Zealand, Pakistan, Singapore, South Africa, South Korea, Taiwan, Thailand and the U.S.A. who receive all issues by air delivery (S.A.L. — Surface Air Lifted) at no extra cost. For Japan, air delivery requires 50% additional charge; for all other countries airmail and S.A.L. charges are available upon request. Back volumes of the *Journal of Chromatography* (Vols. 1–497) are available at Dfl. 195.00 (plus postage). Claims for missing issues will be honoured, free of charge, within three months after publication of the issue. Customers in the U.S.A. and Canada wishing information on this and other Elsevier journals, please contact Journal Information Center, Elsevier Science Publishing Co. Inc., 655 Avenue of the Americas, New York, NY 10010. Tel. (212) 633-3750.

Abstracts/Contents Lists published in Analytical Abstracts, ASCA, Biochemical Abstracts, Biological Abstracts, Chemical Abstracts, Chemical Titles, Chromatography Abstracts, Clinical Chemistry Lookout, Current Contents/Life Sciences, Current Contents/Physical, Chemical & Earth Sciences, Deep-Sea Research/Part B: Oceanographic Literature Review, Excerpta Medica, Index Medicus, Mass Spectrometry Bulletin, PASCAL-CNRS, Pharmaceutical Abstracts, Referativnyi Zhurnal, Science Citation Index and Trends in Biotechnology.

See inside back cover for Publication Schedule, Information for Authors and information on Advertisements.

0021-9673/90/$03.50

Printed in The Netherlands

VOL. 514, NO. 2 JOURNAL OF CHROMATOGRAPHY AUGUST 29, 1990

CONTENTS

(Abstracts/Contents Lists published in Analytical Abstracts, ASCA, Biochemical Abstracts, Biological Abstracts, Chemical Abstracts, Chemical Titles, Current Contents/Life Sciences, Current Contents/Physical, Chemical & Earth Sciences, Deep-Sea Research/Part B: Oceanographic Literature Review, Excerpta Medica, Chromatography Abstracts, Index Medicus, Mass Spectrometry Bulletin, PASCAL-CNRS, Referativnyi Zhurnal and Science Citation Index)

(Continued overleaf)

In articles with more than one author, the name of the author to whom correspondence should be addressed is indicated in the article heading by a 6-pointed asterisk (*)

Chromatography and Modification of Nucleosides

Part C
Modified Nucleosides in Cancer and Normal Metabolism - Methods and Applications

Journal of Chromatography Library, 45C

edited by **C.W. Gehrke** *and* **K.C.T. Kuo,** *Department of Biochemistry, University of Missouri-Columbia, and Cancer Research Center, P.O. Box 1268, Columbia, MO, USA*

Chromatography and Modification of Nucleosides is a four-volume work which provides state-of-the-art chromatography and analytical methods for use in a wide spectrum of nucleic acid modification research.

The focus of Part A is the presentation of advanced methods for modification research on tRNAs, mRNAs, mtRNAs, tRNAs and DNAs. HPLC-UV, GC-MS, NMR, FT-IR and affinity chromatography approaches to nucleic acid modification studies are presented, as are nucleoside, oligonucleotide and nucleic acid isolation techniques. Part B has as its central theme the modified nucleosides of tRNA and the current analytical means for studying rRNA modifications. Modified nucleoside synthesis, function, structural conformation, biological regulation, and occurrence of modification in a wide range of tRNAs are presented, as is a chapter on DNA modification and a chapter on solid phase immunoassay for determining a particular modification.

The study of modified nucleosides in biological matrices (blood, urine) is the major thrust of Part C. As potential biological markers of disease, and for the insight that the modified nucleosides in fluids provide into the catabolism of the nucleic acids, a number of advanced methods for modified nucleoside isolation, separation, detection, characterization and measurement have been developed world-wide. Part C provides the reader with a comprehensive treatment of modified nucleosides as biochemical signals of neoplasia and normal metabolism. The final volume, Part D, will present structural characterization of unknown nucleosides as well as extensive biochemical, chemical and physical properties of RNA and DNA nucleosides, as a "database" for researchers in the field. Chromatographic methodology will be described for analysis of total modification of tRNAs and DNAs.

The chapters are written by leading scientists in their respective fields and present an up-to-date review on the roles of modified nucleosides in nucleic acids which will be extremely useful for workers in chromatography, molecular biology, genetics, biochemistry, biotechnology and the pharmaceutical industry.

Contents: Introduction. Early development of nucleoside markers for cancer *(T.P. Waalkes, C.W. Gehrke).* 1. Progress and future prospects of modified nucleosides as biological markers of cancer *(R.W. Zumwalt et al.).* 2. Ribonucleosides in biological fluids by a high-resolution quantitative RPLC-UV method *(K.C. Kuo et al.).* 3. Ribonucleosides in body fluids: On-line chromatographic cleanup and analysis by a column switching technique *(E. Schlimme, K. Siegfried-Boos).* 4. High-performance liquid chromatography of free nucleotides, nucleosides, and their bases in biological samples *(P.R. Brown, Y.-N. Kim).* 5. Isolation and characterization of modified nucleosides from human urines *(G.B. Chheda et al.).* 6. High performance liquid chromatography of modified nucleosides in human serum *(E.P. Mitchell et al.).* 7. Modified nucleosides in human blood serum as biochemical signals for neoplasia *(F. Salvatore et al.).* 8. Biochemical correlations between pseudouridine excretion and neoplasias *(F. Cimino et al.).* 9. High-performance liquid chromatography analysis of nucleosides and bases in mucosa tissues and urine of gastrointestinal cancer patients *(K. Nakano).* 10. Modified nucleosides as biochemical markers of asbestos exposure and AIDS *(O.K. Sharma, A. Fischbein).* 11. RNA catabolites in health and disease *(I. Clark et al.).* 12. Serum nucleoside chromatography for classification of lung cancer and controls *(J.E. McEntire et al.).* 13. Modified nucleosides and nucleobases in urine and serum as selective markers for the whole-body turnover of tRNA, rRNA, and mRNA-cap - Future prospects and impact *(G. Schöch et al.).* Combined Subject Index for Parts A, B and C.

1990 lvi + 452 pages ISBN 0-444-88598-6
Price: US$ 179.50 / Dfl. 350.00

ELSEVIER SCIENCE PUBLISHERS

P.O. Box 211, 1000 AE Amsterdam, The Netherlands.
P.O. Box 882, Madison Square Station, New York, NY 10159, USA.

Journal of Chromatography, 514 (1990) 97–109
Elsevier Science Publishers B.V., Amsterdam

CHROM. 22 540

Retention reproducibility of basic drugs in high-performance liquid chromatography on a silica column with a methanol–high-pH buffer eluent

Effect of operating conditions on separations using an organic buffer

ROGER M. SMITH* and JAMES P. WESTLAKE
Department of Chemistry, Loughborough University of Technology, Loughborough, Leics. LE11 3TU (U.K.)
and
RICHARD GILL and M. DAVID OSSELTON
Central Research and Support Establishment, Home Office Forensic Science Service, Aldermaston, Reading, Berks. RG7 4PN (U.K.)
(First received August 1st, 1989; revised manuscript received January 29th, 1990)

ABSTRACT

Basic drugs can be separated by high-performance liquid chromatography on silica using a methanol–aqueous pH-10 buffer eluent prepared from 3-(cyclohexylamino)-1-propanesulphonic acid and sodium 3-(cyclohexylamino)-2-hydroxy-1-propanesulphonate. The buffer could be reproducibly prepared. The effects of small changes in the buffer and eluent composition and in the operating temperature on the relative retentions of the different groups of drugs were determined.

INTRODUCTION

Basic drugs often cause problems in high-performance liquid chromatography (HPLC) because of interactions with the stationary phase. In reversed-phase HPLC poor peak shapes are often seen unless a deactivating agent, such as an aliphatic amine, is added to the eluent[1,2]. An alternative approach has been to use silica as an ion-exchange material with eluents containing high proportions of methanol and either perchloric acid[3,4] or high-pH buffers[5–9].

Jane[5] reported that retention was primarily controlled by analyte pK_a and stereochemistry. Subsequently, Bidlingmeyer *et al.*[10] suggested that the silica column also showed marked hydrophobicity and that the order of retention of related compounds often resembled that on reversed-phase HPLC. They attributed this effect

to the presence of siloxane groupings. To test these findings Law[11] examined 69 monobasic aryl alkylamines using an aqueous methanol eluent at pH 9.1. He showed that there was a linear relationship between the retention times of the amines and the reciprocal of the ionic strength and concluded that cation exchange was the predominant mechanism of retention and the separation was primarily controlled by eluent pH. Although there were deviations from the expected linearity these were small and the proposed hydrophobic mechanism was ruled out. Non-polar compounds were effectively unretained. There was only a fair correlation between pK_a and capacity factors. The sizes of the substituents were important but this was difficult to rationalise. Law and Chan[12] have also confirmed the long-term stability of silica columns towards mixed aqueous–organic eluents at high pH.

Lingeman *et al.*[13] have shown that the retention of amines is predominantly controlled by the pH of the eluent. They also found that as the proportion of modifier increased the retention of the amines initially decreased and then increased again at high proportions. This effect was attributed to the solvation of organic competing ions.

In recent studies Cox and Stout[14] have looked in detail at the retention of ionic compounds on silica using "pseudo-reversed-phase" conditions. They used a limited set of test compounds and concentrated on the pH ranges 2.1–7.0 and 15–75% methanol. They also observed a minimum capacity factor at approximately 50% organic modifier and found a linear relationship between reciprocal ionic strength and capacity factors. However, the curve showed a positive intercept suggesting that a second retention mechanism was effective in addition to the ion-exchange mode. This extra effect depended on the method of preparation of the silica.

Schmid and Wolf[15] examined a group of tricyclic antidepressants at pH 7.9 and also suggested that some hydrophobic interaction was present. They noted that at low buffer concentration the systems could be unstable. They found that as the pH increased from 4 to 10 the retentions of primary and secondary amines were affected more than tertiary amines. Above pH 10.0 the capacity factors of all three groups of amines decreased and this was attributed to a reduction in the degree of protonation of the bases. They claimed that there was little difference in selectivity between different brands of silica but the chromatograms in the paper showed significant changes.

Over the past few years, work in our laboratories on the development of robust and reliable methods for the analysis of basic drugs on silica columns by HPLC has examined the use of a methanol–aqueous ammonia–ammonium nitrate eluent[6–9]. The reproducibility of the experimental conditions[6] and the stationary phase[8] has been determined and the conclusions have been tested in national[7] and international collaborative studies[9]. Within a single laboratory good reproducibility could be obtained under controlled conditions[8], but in interlaboratory studies[7,9] the variations were much larger and it appeared that the method was very sensitive to changes in the operating conditions. Two areas of particular concern were the column temperature and the differences in concentrations of the ammonia stock solutions used to prepare the buffer. Although the pH appeared to remain unaltered, significant changes in the ionic strength would result from changes in the ammonia concentration[8,9]. It was concluded that this eluent lacked the required reproducibility for the analysis of basic drugs and it was therefore decided to examine alternative buffer systems, preferably those which could be made up by weight from single-component bases.

In an initial study, ethylenediamine was examined[16] and found to be better than ammonia. However, solid buffer components were still considered preferable. The present paper describes separations carried out using buffers prepared from non-volatile organic sulphonic acid amine buffer components. The effects of changes in the operating conditions on the selectivity and retentions were examined, and the robustness of the method with respect to the buffer composition was studied.

EXPERIMENTAL

Chemicals

Sodium 3-(cyclohexylamino)-2-hydroxy-1-propanesulphonate (CAPSO-Na), and 3-(cyclohexylamino)-1-propanesulphonic acid (CAPS) were obtained from Sigma (Poole, U.K.). Sodium nitrate was analytical-reagent grade and methanol was HPLC grade, both from FSA Laboratory Supplies (Loughborough, U.K.). Water was reagent grade, purified on site using a Millipore Liquipure water purification system. The drug samples were obtained from the reference collection of the Central Research and Support Establishment of the Home Office Forensic Science Service.

Buffer solution

The buffer solution was prepared by mixing CAPS (0.8852 g) and CAPSO-Na (1.0372 g) in water and making up to 50 ml.

HPLC separations

The HPLC separations were performed using a Pye Unicam 4010 pump and a Pye Unicam 4020 UV detector set at 254 nm. The eluent consisted of methanol–buffer (90:10, v/v) and was pumped at 2 ml min^{-1}. The samples (1 μl) were injected using a 7125 Rheodyne valve, fitted with a 20-μl loop, onto a Shandon column (25 cm $\times$ 5 mm I.D.) packed with Spherisorb S5W (5 μm, batches 5123 and 5493/1; Phase Separations, Queensferry, U.K.). The temperature of the analytical column was maintained at 30°C using a circulating water bath. The system was fitted with a pre-column (3 cm $\times$ 5 mm I.D.) filled with open-column-grade silica sieved to 60 mesh. The retention times were determined using a Hewlett-Packard 3390 integrator or a Shimadzu Chromatopac C-R3A integrator.

Test solutions of basic drugs

A set of nine solutions of basic drugs, which have been described previously[9], was used in the study. With the second column, solutions G, H and I were replaced by solutions K, L, M and N below.

Compositions in mg ml^{-1} in ethanol–water (90:10,v/v):

(K) Papaverine, 0.036– dipipanone hydrochloride, 0.82– methdilazine hydrochloride, 0.07– protriptyline hydrochloride, 0.24.

(L) Procaine hydrochloride, 0.044– promazine, 0.04– ethoheptazine citrate, 7.32– protriptyline hydrochloride, 0.40.

(M) Codeine phosphate, 3.20– L-phenylephrine hydrochloride, 1.05– protriptyline hydrochloride, 0.22.

(N) Nortriptyline hydrochloride (used as a secondary standard), 0.16– strychnine hydrochloride, 0.13.

CALCULATIONS

The retention times (t_R) were measured in duplicate and the capacity factors (k') were calculated as $k' = (t_R - t_0)/t_0$, where t_0 is the retention time of methanolic sodium nitrate (solution I). Relative capacity factors were calculated as k'/k'_p where k'_p is the capacity factor for protriptyline present as an internal standard. Solution N contained nortriptyline as a secondary standard whose k' value from solution C was used to determine the relative k' of strychnine.

RESULTS AND DISCUSSION

Because it was difficult to control the concentration of ammonia stock solutions used in the buffer, it was considered necessary to devise an alternative method for the analysis of basic drugs on silica. In developing the new method, the following desirable properties were identified based on experience gained from the use of the ammonia eluent. The buffer solution must be easy to prepare reproducibly and should not contain any volatile components. It should have a similar pH to that used in the ammonia system (pH 10.1)[7] but the eluting power of the eluent should be weaker than that of the ammonia eluent so that weakly retained compounds can be resolved from the solvent front. It should also extend the overall retention times and thus increase the discrimination capacity. However, the retention of the longest retained compounds should not be excessive and unduly extend the analysis time.

Trials using buffers based on the liquid base ethylenediamine[16] and on ethanolamine hydrochloride (unpublished) gave acceptable results but failed to meet all of the criteria. So the present study concentrated on potential solid organic buffer components of high pK_a including 2-(N-cyclohexylamino)ethanesulphonic acid (CHES, $pK_a = 9.3$), CAPSO-Na ($pK_a = 9.6$) and CAPS ($pK_a = 10.4$). A range of buffers of different composition and pH were prepared and examined. Buffers prepared from ethanolamine hydrochloride and CHES with a lower pH were found to be unsuitable because they gave poor peak shapes and long retention times.

Combinations of CAPS and CAPSO-Na gave buffer solutions of high pH, in the region of 9.6–10.4. In initial studies using a simplified test set of drug compounds (from ref. 8) a buffer containing the two compounds in a 1:1 molar ratio, 0.1 *M* for each component, gave reasonable retention times (protriptyline 10.6 min), longer than those on the ammonia system, but the efficiencies of some compounds were very low and their peak shapes where poor. On increasing the concentration of CAPSO-Na in the aqueous buffer to 0.2 *M*, giving a 2:1 molar ratio of CAPSO-Na/CAPS, much better results were obtained, although phenylephrine still exhibited low efficiency.

Since the results for these eluents seemed to be promising, a further set of experiments was performed in which an extended test set of drug solutions[9] was used. Six separations were carried out using buffers varying in composition from 1:2 to 4:1 CAPSO-Na/CAPS and with different overall ionic strengths. The eluents giving the best results were those prepared from a buffer with a calculated pH about 10.0 and ionic strength 0.075–0.080 *M*. If the pH was lower (1:2, pH 9.79) the later peaks were too highly retained (*e.g.* protriptyline, 15.6 min; strychnine, 16.70 min) whilst buffers of higher pH (4:1, pH 10.43) caused more rapid elution (protriptyline, 7.75 min) and thus reduced the resolution of the earlier eluting drugs.

TABLE I

CAPACITY FACTORS AND RELATIVE CAPACITY FACTORS USING THE CAPS/CAPSO-Na ELUENT AND THE AMMONIUM NITRATE ELUENT IN THE CHROMATOGRAPHY OF BASIC DRUGS ON A SILICA COLUMN

Conditions: column, Spherisorb S5W (batch 5123); eluent methanol–aqueous CAPS/CAPSO-Na buffer (each component 0.08 *M*) (90:10, v/v); temperature 30°C.

Compound	*Ionisation constant*[a]	*Capacity factor*		*Relative capacity factor (× 100)*[b]	
		CAPS/CAPSO-Na	*Ammonia*[c]	*CAPS/CAPSO-Na*	*Ammonia*[c]
Nitrazepam	3.2,10.8	0.22	0.02	2.7	1.3
Diazepam	3.3	0.25	0.02	3.1	1.3
Papaverine	6.4	0.31	0.06	3.9	2.6
Caffeine	14.0	0.41	0.10	5.1	5.0
Dextropropoxyphene	6.3	0.56	0.09	7.0	4.5
Cocaine	8.6	0.71	0.11	8.9	6.0
Procaine	9.0	0.81	0.17	10.2	8.8
Amitriptyline	9.4	1.44	0.39	18.0	19.9
Chlorpromazine	9.3	1.53	0.44	19.9	22.4
Propranolol	9.5	1.66	0.44	20.8	22.5
Imipramine	9.5	2.13	0.60	26.7	31.1
Dipipanone	8.5	2.32	0.45	29.0	22.9
Promazine	9.4	2.56	0.75	32.0	38.5
Phentermine	10.1	2.60	0.61	32.5	31.4
Codeine	8.2	2.64	0.91	33.0	46.6
Morphine	8.0,9.9	2.69	0.96	33.7	49.7
Amphetamine	9.9	2.72	0.69	34.1	35.6
Phenylephrine	8.9,10.1	3.51	1.24	43.9	63.8
Pholcodine	8.0,9.3	3.53	1.23	44.2	63.4
Prolintane	9.7[d]	3.89	0.93	48.6	47.7
Ethoheptazine	8.5	4.03	1.19	50.0	61.1
Nortriptyline	9.7	4.32	1.19	54.1	60.9
Methdilazine	7.5	4.36	1.32	54.6	67.9
Ephedrine	9.6	4.62	1.35	57.8	69.5
Pipazethate	n/a	4.64	1.07	58.1	54.9
Methylamphetamine	10.1	5.61	1.54	70.2	79.1
Protriptyline[e]	10.0	8.00	1.94	100.0	100.0
Strychnine	2.3,8.0	8.75	2.71	109.3	139.5

[a] From ref. 17 (n/a = not available).
[b] Relative capacity factors relative to protriptyline.
[c] Data taken from ref. 7.
[d] pK_a unpublished value from Boehringer Ingelheim.
[e] Based on test solution H. pK_a from ref. 15.

From these conclusions a buffer of pH 10.0 containing the two compounds in a 1:1 molar ratio at 0.08 *M* for each component was chosen for a more detailed study (Table I) as it gave better efficiencies than a more concentrated 1:1 molar buffer (0.1 *M* for each component) (*e.g* ephedrine, plate number $N = 3497$ compared to $N = 2573$ and prolintane, 3718 compared to 2957). The eluent had a good UV range, with an absorbance < 1 at 215 nm and the retentions of the drugs ranged from 1.60 to 13.06 min.

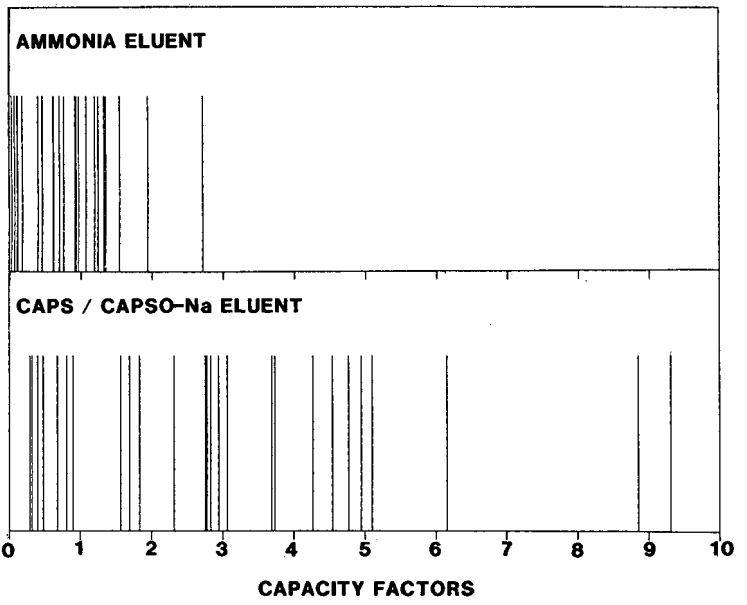

Fig. 1. Comparison of capacity factors using the ammonia–ammonium nitrate buffer (upper) and the CAPS/CAPSO-Na buffer (lower) showing the improvement in resolution and discriminating power with the latter eluent.

Comparison of the results for this eluent and the previous ammonia system showed that the present eluent gave an increase in retention time for all the drug compounds. This greater separation of the basic drugs (Fig. 1) would improve the resolution and thus enable better discrimination between similarly retained compounds, aiding more positive identification. The capacity factors and relative retentions with the two eluents differed significantly particularly for moderately retained compounds (relative capacity factors of 30–50) (Table I).

The changes in relative retentions caused some compounds to be eluted relatively more rapidly in the new system including imipramine, 26.7 (ammonia system, 31.1); promazine, 32.0 (38.5); codeine, 33.0 (46.6); morphine, 33.7 (49.7); phenylephrine 43.9 (63.8); pholcodine 44.2 (63.4); ethoheptazine, 50.0 (61.1); and strychnine, 109.3 (139.5). Other basic drugs were relatively more highly retained, including cocaine, 8.9 (6.0); dipipanone, 29.0 (22.9); prolintane, 48.6 (47.7); and pipazethate, 58.1 (54.9). These changes reflect those caused by decreasing the ionic strength of the buffer in the ammonia system[7], when the retentions of the last four compounds all increased whereas the earlier compounds decreased. There is no correlation with the pK_a of the analytes; dipipanone and ethoheptazine, both pK_a 8.5 behaving in a markedly different manner.

These results therefore contrast with the earlier studies[11,14,15], where, except at very low ionic strengths, there was generally no change in the relative order of retention with the strength of the buffer. However, a wider range of structural types is being examined in this study.

The development of the new eluent was carried out on Spherisorb S5W (batch

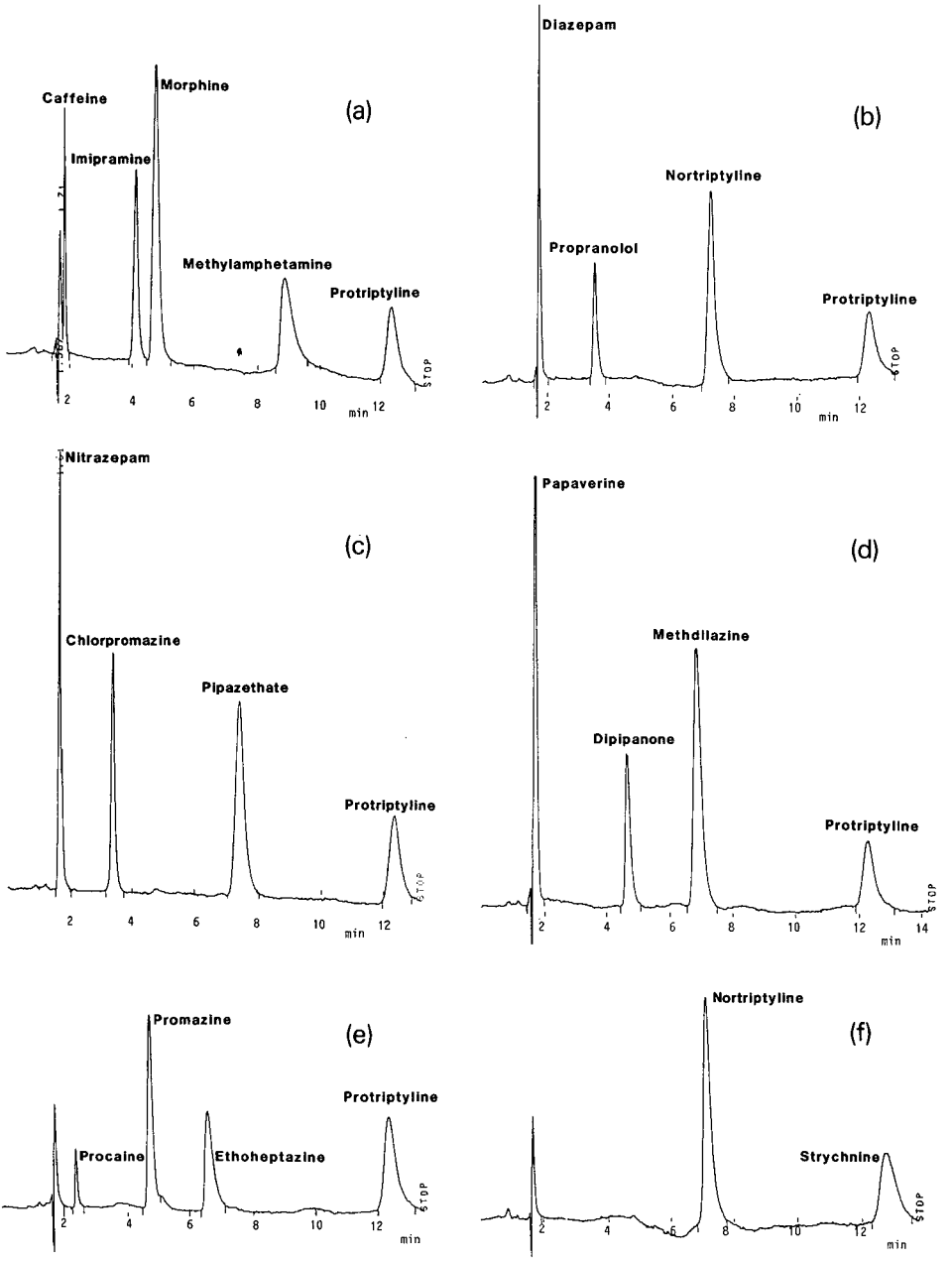

Fig. 2. Examples of separations of basic drugs on silica using the CAPS/CAPSO-Na eluent. Conditions: column: 25 cm × 5 mm I.D. packed with Spherisorb S5W (batch 5493/1); eluent: methanol–aqueous CAPS/CAPSO-Na buffer (90:10, v/v); buffer composition: each component 0.08 *M*; flow-rate = 2 ml/min; temperature: 30°C; detection wavelength = 254 nm. (a) Solution A; (b) solution C; (c) solution E; (d) solution K; (e) solution L; (f) solution N.

5123) but when the method was transferred to a new column containing a different batch of Spherisorb S5W (batch 5493/1) significantly different results were obtained and some of the components of the mixtures were unresolved. Strychnine was now unresolved from the internal standard protriptyline, whilst codeine and dipipanone in solution G co-eluted. Consequently the test mixtures G, H and I were replaced by mixtures K, L, M and N with nortriptyline as a secondary standard for strychnine in solution N (see Experimental). Good separations were now observed for all the test compounds, and examples are shown in Fig. 2.

TABLE II

REPRODUCIBILITY OF THE CAPACITY FACTORS AND RELATIVE CAPACITY FACTORS FOR THE SEPARATION OF BASIC DRUGS ON A SILICA COLUMN

Five repeated separations; column Spherisorb S5W (batch 5493/1); eluent, methanol–aqueous CAPS/CAPSO-Na buffer (each component 0.08 *M* (90:10, v/v); temperature 30°C.

Compound	*Capacity factor*			*Relative capacity factor (× 100)*[a]		
	Mean	*S.D.*	*C.V.*	*Mean*	*S.D.*	*C.V.*
Nitrazepam	0.29	0.00	–	3.3	0.1	3.0
Diazepam	0.32	0.01	3.1	3.7	0.1	2.7
Papaverine	0.40	0.01	2.5	4.5	0.1	2.7
Caffeine	0.48	0.01	2.1	5.5	0.2	3.6
Dextropropoxyphene	0.68	0.02	3.0	7.7	0.0	–
Cocaine	0.81	0.03	3.7	9.2	0.1	1.1
Procaine	0.90	0.03	3.3	10.1	0.1	1.0
Amitriptyline	1.57	0.05	3.2	17.8	0.2	1.1
Chlorpromazine	1.67	0.05	3.0	18.9	0.2	1.1
Propranolol	1.83	0.06	3.3	20.7	0.1	0.5
Imipramine	2.32	0.07	3.0	26.3	0.2	0.8
Codeine	2.75	0.10	3.6	31.1	0.2	0.6
Promazine	2.77	0.10	3.6	31.3	0.2	0.6
Dipipanone	2.78	0.14	5.0	31.4	0.5	1.6
Morphine	2.83	0.09	3.2	32.1	0.3	0.9
Phentermine	2.94	0.11	3.8	33.3	0.2	0.6
Amphetamine	3.06	0.12	3.9	34.6	0.1	0.3
Phenylephrine	3.69	0.14	3.8	41.7	0.2	0.5
Pholcodine	3.73	0.15	4.0	42.2	0.2	0.5
Ethoheptazine	4.27	0.17	4.0	48.2	0.2	0.4
Prolintane	4.27	0.18	4.2	48.4	0.3	0.6
Methdilazine	4.54	0.17	3.7	51.3	0.3	0.6
Nortriptyline	4.77	0.17	3.6	54.0	0.3	0.6
Pipazethate	4.94	0.22	4.5	55.8	0.4	0.7
Ephedrine	5.10	0.19	3.7	57.7	0.2	0.4
Methylamphetamine	6.15	0.24	3.9	69.6	0.2	0.3
Protriptyline[b]	8.85	0.38	4.3	100.0	–	–
Strychnine	9.31	0.35	3.8	105.2	0.7	0.7

[a] Relative capacity factors relative to protriptyline.
[b] Based on test solution L.

Effect of changes in the operating conditions

The robustness and reproducibility of the method was determined by varying the experimental parameters temperature, flow-rate, injection volume, and buffer composition. These included five runs using the selected standard conditions to monitor the reproducibility over a period of time (Table II). This included two eluents prepared from one batch of buffer solution, and three eluents prepared from a second batch of buffer.

The coefficient of variation (C.V.) in capacity factors was about 4% and, except for the rapidly eluting compounds, the variation in relative capacity factors was much lower (Table II) although dipipanone stood out as being poorer than other compounds with similar retentions. In previous studies with the ammonia eluent this compound was particularly sensitive to changes in experimental conditions[7]. The variations in retention were much smaller than the difference between the results on the two columns and suggested that batch-to-batch variations in the silica cause significant effects on retention in a similar manner to the differences observed with the ammonia[8,9] and diamine eluents[16].

In this series of separations the retention times and capacity factors showed a consistent downward drift with each subsequent analysis, although the relative capacity factors remained consistent. Inspection of the column at the end of the series of experiments revealed a 1-mm void at the top, indicating that the analytical column was slowly dissolving or being etched by the eluent. It is possible that the drift in retention was related to the dissolution of the silica during the study. A silica pre-column was being used between the pump and the injector to extend the column lifetime and its presence would appear to be essential, despite the study by Law and Chan[12] which found dissolution to be negligible.

To investigate the effect of small pH changes in the buffer on the separation of the drugs, buffers of pH 9.7 and 10.3, with ionic strengths equal to that of the standard buffer (0.080 *M*), were tested. For all of the analytes the retention times decreased on going from low to higher pH, which is probably caused by a reduction in the degree of protonation of the bases as observed earlier by Schmid and Wolf[15]. However, some of the bases were affected more than the others but for most of the drugs, the relative capacity factors also decreased as the pH was increased (Fig. 3). Particularly large decreases were observed for dipipanone (36.05 to 28.13), prolintane (52.41 to 45.25), pipazethate (61.64 to 51.43) and methylamphetamine (74.53 to 67.30). However, the pK_a values of these compounds are similar to those of many of the other drugs (Table I). The steric environment of the basic groups appears to be an important factor as the first three of these compounds all contain a cyclic tertiary amine with a substituted N-alkyl side chain. As noted earlier these three compounds also showed particular sensitivity to changes in separation conditions. In contrast, tertiary amines containing only N-methyl substituents, such as methdilazine and cocaine, showed much smaller effects relative to protriptyline which is also an N-methyl compound. In his study Law[11] had found that size of alkyl substituents had a marked effect. The introduction of N-methyl groups caused positive retention changes whereas larger alkyl substituents had a negative effect on retention. These effects may suggest that the larger substituents on a cyclic amine may limit the interaction of the basic group to a particular type of silanol site on the silica surface whose ionisation changes to a different extent than the other silanol groups with changes in eluent pH.

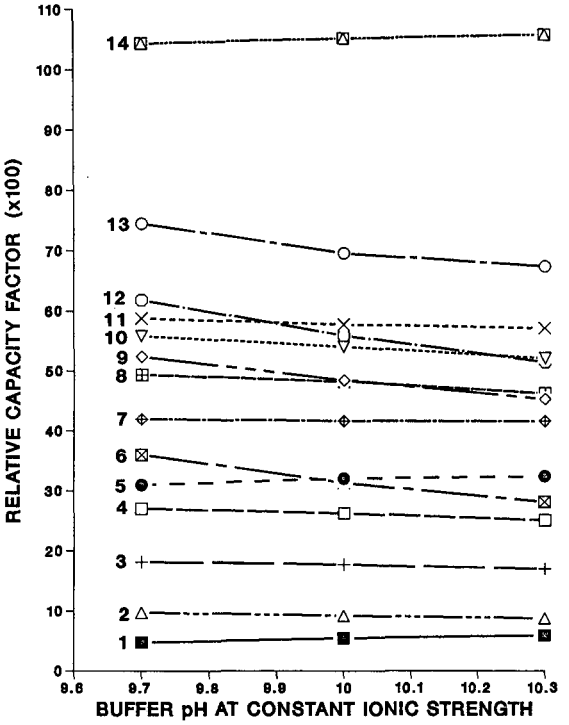

Fig. 3. Variation of relative capacity factors with pH. Conditions as in Fig. 2, but ratio of buffer components varied to give different buffer pH values at constant ionic strength. Compounds: 1 = caffeine; 2 = cocaine; 3 = amitriptyline; 4 = imipramine; 5 = morphine; 6 = dipipanone; 7 = phenylephrine; 8 = ethoheptazine; 9 = prolintane; 10 = nortriptyline; 11 = ephedrine; 12 = pipazethate; 13 = methylamphetamine; 14 = strychnine.

The relative retentions increased for a few compounds, including strychnine, codeine and morphine (31.03 to 32.40, pK_a 8.0 and 9.9). In the last case this might reflect the ionisation of the phenolic group to give a doubly charged species although phenylephrine which also contains a phenolic group changed very little. These relative changes were significant as a test of the robustness of the assay and emphasise the need for a constant buffer pH to obtain reproducible results. The lower pH also caused many of the compounds to elute with a lower efficiency but the higher pH reduced the efficiency of protriptyline. Clearly, although systematic changes with pH have been observed for small sample sets such as the tricyclic antidepressants[15] or aryl alkylamines[11], the resulting conclusions cannot be generalised to account for the relative changes observed in the present larger range of sample types.

The ionic strength of the present eluent was much lower than the previous ammonia eluent and this was a major factor leading to an increase in retention times. These changes agree with the predominant mode of retention being cation exchange. The effects of changes in the buffer concentration of $\pm$ 20% were examined by using buffers with ionic strengths of 0.096 and 0.064 *M* at a constant pH of 10.0. Most of the compounds showed a decrease in retention time on increasing the ionic strength, with

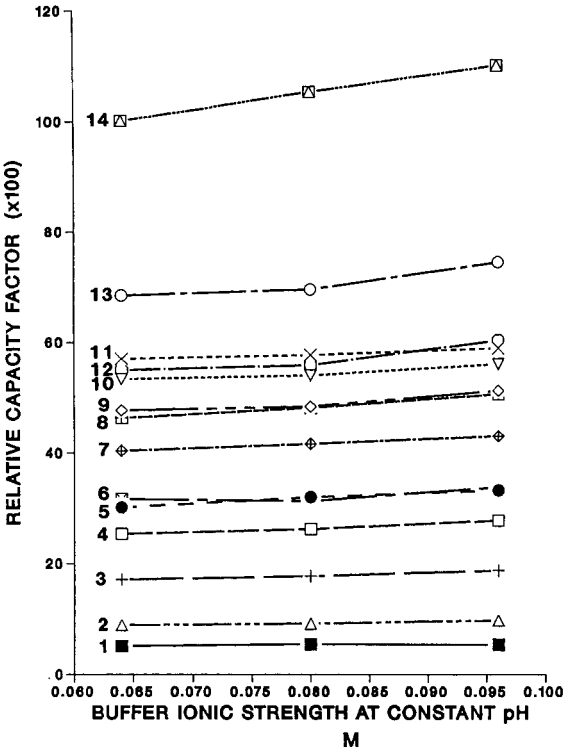

Fig. 4. Variation of relative capacity factors with ionic strength. Conditions as in Fig. 2, but ratio of buffer components varied to give different buffer ionic strengths at constant pH. Compounds as in Fig. 3.

protriptyline showing a quite significant change (13.4 min decreasing to 12.6 min) but strychnine (13.4 min to 13.7 min) and pipazethate (7.42 to 8.19 min) increased slightly. For most compounds the relative capacity factor increased slightly with some compounds showing a more marked effect (Fig. 4). The changes in the relative capacity factors were outside the experimental range for the repeated assays and suggest that small changes in the buffer could have a significant effect on an analysis. Again the compounds most affected were those which also markedly changed with pH.

The retention times of the drugs decreased as the temperature increased from 20 to 40°C, but for most of the compounds the relative capacity factors increased with increasing temperature. The increases were proportionally more significant for the weakly retained compounds (relative $k' < 10.1$, see Fig. 5). For the rest of the compounds the changes were $\pm$ 4%. Exceptions to this trend were methylamphetamine and strychnine which both showed decreases in relative capacity factor with increasing temperature, whilst pipazethate, methdilazine and ephedrine did not exhibit any obvious trend. The relative capacity factors recorded at 20 and 40°C were outside the range of experimental error determined for the five standard assays. Thus to obtain reproducible results it is necessary to thermostat the column and to specify the temperature in any description of the method.

When the proportion of methanol in the eluent was changed from 90 to 88 or

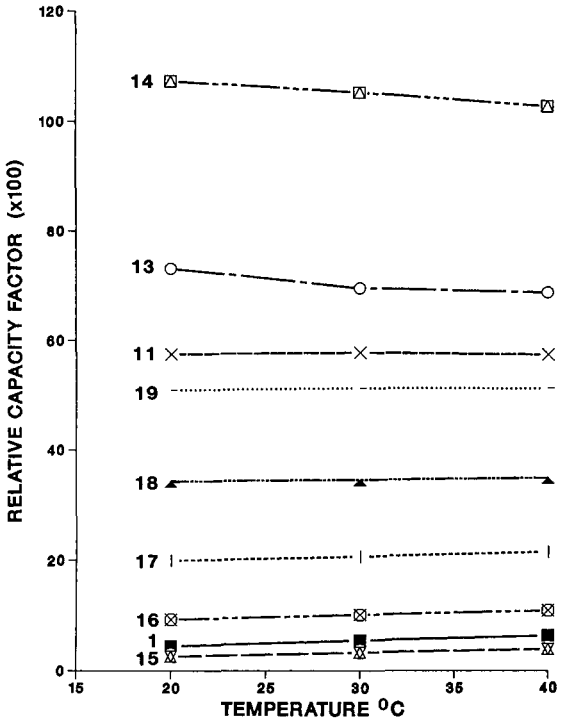

Fig. 5. Variation of relative capacity factors with temperature. Other conditions as in Fig. 2. Compounds as in Fig. 3, plus: 15 = nitrazepam; 16 = procaine; 17 = propranolol; 18 = amphetamine; 19 = methdilazine.

92%, variations in retention times and relative capacity factors were observed. Increasing methanol content caused an increase in the retention times but a very small change in the relative capacity factors for most compounds. Decreasing the methanol content had a more significant effect and the relative capacity factors were between 1.8 and 12% higher than the standard results. Thus care will be needed in the preparation of the eluent.

In a recent study Tanaka *et al.*[18] reported large changes in retention on changing the operating pressure in the column; these were ascribed to changes in the equilibria. An ion-exchange chromatographic separation might therefore be susceptible to similar effects, particularly if the drug is partially ionised. On changing the flow-rate from 2.0 ml min^{-1} to 1.0 ml min^{-1}, which changed the operating pressure from 145–148 bar to 76–78 bar, the capacity factors and relative capacity factors were unaffected.

In a case of a real-life sample submitted for analysis the concentration of the drug present in the solution will be unknown. Variations in relative capacity factors caused by changing the loading of the analyte on the column may therefore cause problems in identification. A sample of solution L was diluted to 20% of its original concentration and four replicate 1-μl injections were examined. The retention time of protriptyline was unaltered but the retentions and relative capacity factors of the test compounds were slightly increased. The changes were small and were less than two standard deviations (from Table II) for procaine and promazine and about three standard deviations for ethoheptazine.

CONCLUSIONS

This study has shown that the organic buffer salts CAPS and CAPSO-Na can be used to prepare reproducible buffer solutions for use in the analysis of basic drugs on silica. These eluents gave an increase in retention time and a better discrimination than the methanol–ammonium nitrate eluent.

The new method is susceptible to changes in the operating conditions and these parameters would need to be closely specified in the method protocol. Increases in the operating temperature or the ionic strength of the eluent, or a decrease in the proportion of the buffer caused the relative capacity factors to increase, whilst increasing the pH of the eluent or the proportion of methanol caused the relative capacity factors to decrease.

ACKNOWLEDGEMENTS

The authors thank the Home Office Forensic Science Service for a studentship to J.P.W. and Phase Separations for a gift of Spherisorb S5W.

REFERENCES

1 R. Gill, S. P. Alexander and A. C. Moffat, *J. Chromatogr.*, 247 (1982) 39.
2 R. W. Roos and C. A. Lau-Cam, *J. Chromatogr.*, 370 (1986) 403.
3 R. J. Flanagan, G. C. A. Storey, R. K. Bhrama and I. Jane, *J. Chromatogr.*, 247 (1982) 15.
4 R. J. Flanagan and I. Jane, *J. Chromatogr.*, 323 (1985) 173.
5 I. Jane, *J. Chromatogr.*, 111 (1975) 227.
6 R. Gill, M. D. Osselton, R. M. Smith and T. G. Hurdley, *J. Chromatogr.*, 386 (1987) 65.
7 R. M. Smith, T. G. Hurdley, R. Gill and M. D. Osselton, *J. Chromatogr.*, 398 (1987) 73.
8 R. M. Smith, T. G. Hurdley, J. P. Westlake, R. Gill and M. D. Osselton, *J. Chromatogr.*, 455 (1988) 77.
9 R. Gill, M. D. Osselton and R. M. Smith, *J. Pharm. Biomed. Anal.*, 7 (1989) 447.
10 B. A. Bidlingmeyer, J. K. Del Rios and J. Korpi, *Anal. Chem.*, 54 (1982) 442.
11 B. Law, *J. Chromatogr.*, 407 (1987) 1.
12 B. Law and P. F. Chan, *J. Chromatogr.*, 467 (1989) 267.
13 H. Lingeman, H. A. van Munster, J. H. Beynen, W. J. M. Underberg and A. Hulshoff, *J. Chromatogr.*, 352 (1986) 261.
14 G. B. Cox and R. W. Stout, *J. Chromatogr.*, 384 (1987) 315.
15 R. W. Schmid and Ch. Wolf, *Chromatographia*, 24 (1987) 713.
16 R. M. Smith and J. O. Rabuor, *J. Chromatogr.*, 464 (1989) 117.
17 J. E. F. Reynolds (Editor), *Martindale: The Extra Pharmacopoeia*, Pharmaceutical Press, London, 29th, ed., 1989.
18 N. Tanaka, T. Yoshimura and M. Araki, *J. Chromatogr.*, 406 (1987) 247.

Journal of Chromatography, 514 (1990) 111–122
Elsevier Science Publishers B.V., Amsterdam

CHROM. 22 565

Anomalous behavior of selected methyl-substituted polycyclic aromatic hydrocarbons in reversed-phase liquid chromatography

STEPHEN A. WISE* and LANE C. SANDER
Organic Analytical Research Division, National Institute of Standards and Technology, Gaithersburg, MD 20899 (U.S.A.)
and
RENE LAPOUYADE and PHILIPPE GARRIGUES
UA 348 CNRS, Université de Bordeaux I, F-33405 Talence Cedex (France)
(Received April 18th, 1990)

ABSTRACT

In the reversed-phase liquid chromatographic separation of polycyclic aromatic hydrocarbons (PAHs) on C_{18} phases, methyl-substituted PAHs are expected to elute after the unsubstituted parent PAH based on the increase in hydrocarbonaceous contact area of the methyl-substituted PAHs. However, we have observed that several methyl-substituted PAHs elute prior to the parent compound, *e.g.*, 1-methylperylene, 1-methylpicene and 13-methylpicene. To investigate this anomalous retention behavior, the retention characteristics of all methyl-substituted isomers of chrysene, picene and perylene were compared on a series of sixteen commercially prepared C_{18} phases. The anomalous retention behavior was observed only on polymeric C_{18} phases (*i.e.*, those prepared using trifunctional silanes) whereas the methyl-substituted PAHs elute after the parent PAH, as would be expected, on monomeric C_{18} phases (*i.e.*, those prepared using monofunctional silanes). The early elution of some of these methyl-substituted isomers is related to the non-planarity of these PAHs due to the presence of the methyl group in the so-called "bay-region" of the PAH structure. The non-planarity of these methyl-PAHs can be characterized by the dihedral angle of distortion between the aromatic rings.

INTRODUCTION

Reversed-phase liquid chromatography (LC) on C_{18} stationary phases provides excellent separations of polycyclic aromatic hydrocarbons (PAHs), particularly isomeric PAHs[1–4]. Polymeric C_{18} phases (*i.e.*, those prepared using trifunctional silanes with the addition of water) have been shown to provide greater selectivity for the separation of isomeric PAHs than the more commonly used monomeric C_{18}

0021-9673/90/$03.50

phases (*i.e.*, those prepared using monofunctional silanes with the exclusion of water)[2–4]. The factors responsible for the unique selectivity of polymeric C_{18} phases have been discussed in several previous publications[1,3]. The excellent selectivity of polymeric C_{18} phases for PAH separations has also been demonstrated for methyl-substituted PAH isomers. Comparisons of retention for methyl-substituted phenanthrene, pyrene, fluoranthene, chrysene, benz[*a*]anthracene, benzo[*c*]phenanthrene and benzo[*a*]pyrene isomers on monomeric and polymeric C_{18} phases have been reported[1,4]. In general, these methyl-PAH isomers were resolved on polymeric C_{18} phases and eluted in order of increasing rod-like shape, which was characterized by the length-to-breadth (*L/B*) ratio of the isomer[4].

In the reversed-phase LC separation of PAHs on C_{18} phases, methyl-substituted PAHs are generally expected to elute after the unsubstituted parent PAH because of the greater hydrocarbonaceous contact area (*i.e.*, hydrophobic character) of the methyl-PAH. However, we have observed that several methyl-PAHs elute prior to the parent compound, *e.g.*, 1-methylbenzo[*c*]phenanthrene[4], 13-methylpicene[1] and 1-methylperylene[5]. The anomalous behavior of these methyl-PAHs led to the investigation of the retention characteristics of all methyl-substituted isomers of chrysene, perylene and picene on a series of sixteen commercially prepared monomeric and polymeric C_{18} columns.

EXPERIMENTAL[a]

PAH standards

The methylchrysene isomers were obtained from the Community Bureau of Reference (Brussels, Belgium). The methylperylene isomers were synthesized as reported previously[6]. The methylpicene isomers (except 13-methylpicene) were obtained from oxidative photocyclization of the appropriate 1,2-diarylethylene[7]. 13-Methylpicene was obtained from the Rare Chemical Collection of Aldrich (Milwaukee, WI, U.S.A.). Standard Reference Material (SRM) 869, "Column Selectivity Test Mixture for Liquid Chromatography" was obtained from the Office of Standard Reference Materials at the National Institute of Standards and Technology (Gaithersburg, MD, U.S.A.).

LC columns

The following C_{18} columns were used in this study: Vydac 201TP reversed-phase C_{18} and Vydac 218TP protein and peptide C_{18} (Separations Group, Hesperia, CA, U.S.A.); Bakerbond C_{18} and Bakerbond C_{18} wide pore (J. T. Baker, Philipsburg, NJ, U.S.A.) (the Bakerbond C_{18} is on a narrow pore silica substrate, 120 Å pore diameter, whereas the Bakerbond C_{18} wide pore is on a silica with a 300 Å pore diameter); Erbasil C_{18}/H (Farmitalia Carlo Erba, Milan, Italy); Sepralyte C_{18} (Analytichem, Harbor City, CA, U.S.A.); Zorbax ODS (Mac Mod, Chadds Ford, PA, U.S.A.); and Hypersil ODS (Keystone, State College, PA, U.S.A.). Three different Vydac 201TP

[a] Certain commercial equipment, instruments or materials are identified in this report to specify adequately the experimental procedure. Such identification does not imply recommendation or endorsement by the National Institute of Standards and Technology, nor does it imply that the materials or equipment identified are the best available for the purpose.

columns were used. Vydac 201TP (normal) has the selectivity of C_{18} columns typically obtained from the manufacturer. Columns designated as Vydac 201TP (high) and (intermediate) are columns with percent carbon loadings higher than those typically obtained from the manufacturer. The Vydac 218TP phase has selectivity that is designated as "low" when compared to the "normal" Vydac 201TP columns. Five different Bakerbond C_{18} (wide pore) columns were used. These columns were experimental columns (A–E) which had been prepared by the manufacturer with varying percent carbon loadings on two different batches of silica (column A: 104 m^2/g and 10.4% C; column B: 78 m^2/g and 7.1% C; column C: 78 m^2/g and 6.8% C; column D: 78 m^2/g and 6.2% C; column E: 104 m^2/g and 5.6% C)[8]; columns B and C are typical of the carbon loading and selectivity for Bakerbond C_{18} (wide pore) columns.

LC conditions

Each of the LC columns was characterized using the Column Selectivity Test Mixture for Liquid Chromatography (SRM 869), as described previously[9,10], and selectivity ratios for tetrabenzonaphthalene (TBN) and benzo[*a*]pyrene (BaP) ($\alpha_{TBN/BaP}$) were calculated. The $\alpha_{TBN/BaP}$ values were determined with a mobile phase of acetonitrile–water (85:15) at a flow-rate of 1.5 ml/min and at a column temperature of 28°C. The selectivity ratios for the methyl-PAHs, relative to the unsubstituted parent PAH, were determined using a mobile phase of acetonitrile–water (80:20) for the methylchrysenes and methylperylenes and acetonitrile–water (95:5) for the methylpicenes. A multiwavelength ultraviolet absorption detector (Spectroflow 783, Kratos, Ramsey, NJ, U.S.A.) or a fluorescence spectrometer (LS-4, Perkin-Elmer, Norwalk, CT, U.S.A.) was used for detection of the solutes.

Calculation of solute shape and planarity parameters

The length-to-breadth (L/B) values for each of the methyl-PAH isomers were calculated using the approach described previously[4]. A new computer program was written to calculate L/B values using coordinates generated for space filling models of the PAH as shown in Fig. 1. The space filling models of the PAHs were determined using the X1CAMM Molecular Modeling program (XIRIS Corporation, New Monmouth, NJ, U.S.A.). The dihedral angles between aromatic rings were determined from calculations of the geometry of the molecule at the energy minimum using the MM2MP2 (version 1985) empirical force field method[11] on a VAX computer at the University of Bordeaux. Dihedral angles represent the angle formed by the bonds which link carbon atoms belonging to three aromatic rings, *i.e.*, it is the angle defined by the two aromatic rings connected to a common aromatic ring. For example in Fig. 1, α represents the dihedral angle of the two planes defined by ring A and ring C, whereas β represents the angle between the two planes defined by ring B and ring D. The sign (+ or −) represents dihedral distortion relative to an average molecular plane (− for down, + for up).

RESULTS AND DISCUSSION

In previous studies[1,2,4,12], the retention behavior of isomeric PAHs has been shown to be significantly different on monomeric C_{18} phases compared to polymeric C_{18} phases. Polymeric C_{18} phases are prepared using trifunctional silanes with the

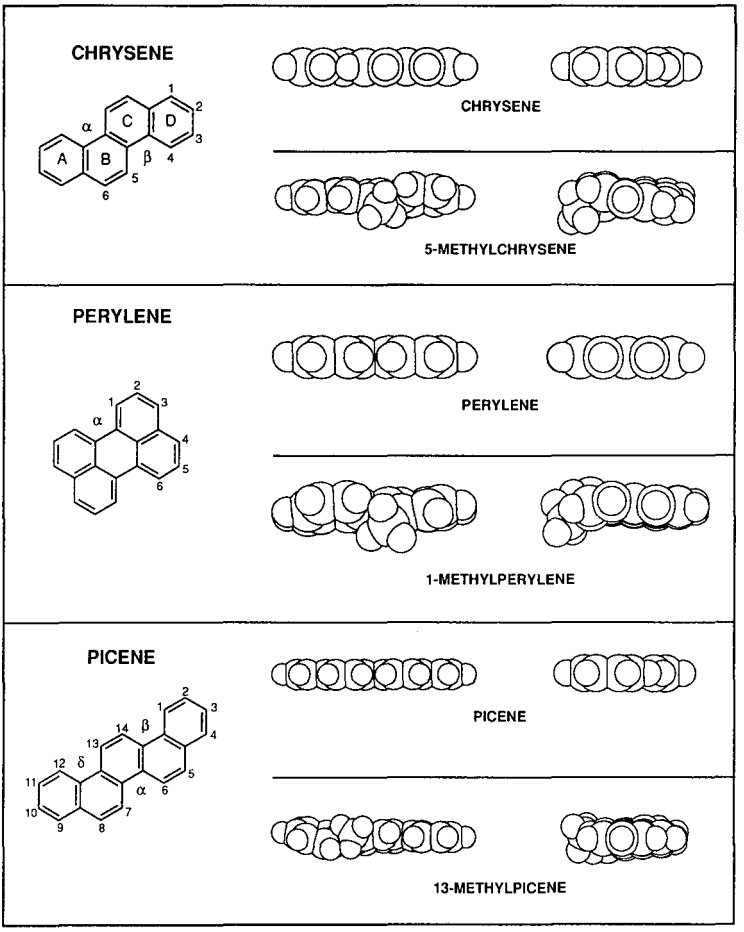

Fig. 1. Structures and space filling models of chrysene, picene and perylene and space filling models of selected non-planar methyl-substituted chrysene, picene and perylene isomers. The symbols α, β and δ designate the specific dihedral angles of distortion (see Table II).

addition of water, whereas monomeric C_{18} phases are prepared using monofunctional silanes, generally with the exclusion of water during the synthesis[2]. Methyl-substituted PAH isomers have different selectivity characteristics on monomeric and polymeric C_{18} phases[1,4]. In the present study, a series of sixteen commercially prepared C_{18} columns was selected and used to investigate the selectivity of several isomeric sets of methyl-substituted PAHs. These columns were characterized using the selectivity ratio (α) of tetrabenzonaphthalene and benzo[*a*]pyrene, which has been used previously to classify phase selectivity for the separation of PAHs[9,10]. Based on a previous study[10] in which the $\alpha_{TBN/BaP}$ values were determined for 25 different commercial C_{18} columns, this series of columns was selected to cover a broad range of selectivity characteristics. The $\alpha_{TBN/BaP}$ values for the sixteen columns used in this study are summarized in Table I. The majority of the phases used in this study were designated as polymeric C_{18}

TABLE I

LC COLUMNS INVESTIGATED FOR SELECTIVITY OF METHYL-SUBSTITUTED PAHs

Column	*Selectivity ratio* $\alpha_{TBN/BaP}$[a]	*Phase type*[b]
Bakerbond C_{18} (wide pore) (A)[c]	0.27	Polymeric
Vydac 201TP (high)[d]	0.39	Polymeric
Vydac 201TP (high)[d]	0.46	Polymeric
Vydac 201TP (intermediate)[d]	0.60	Polymeric
Bakerbond C_{18} (wide pore) (B)[c]	0.62	Polymeric
Vydac 201TP (intermediate)[d]	0.63	Polymeric
Vydac 201TP (normal)[e]	0.72	Polymeric
Bakerbond C_{18} (wide pore) (C)[c]	0.78	Polymeric
Bakerbond C_{18} (wide pore) (D)[c]	1.00	Polymeric
Erbasil C18/H	1.00	Polymeric
Vydac 218TP (protein and peptide)	1.12	Polymeric
Bakerbond C_{18}	1.32	Polymeric
Bakerbond C_{18} (wide pore) (E)[c]	1.43	Polymeric
Sepralyte C_{18}	1.72	Monomeric
Zorbax ODS	1.94	Monomeric
Hypersil ODS	1.98	Monomeric

[a] Selectivity factor (α) for tetrabenzonaphthalene and benzo[*a*]pyrene as described by Sander and Wise[10].

[b] Phase designation based on manufacturers' information regarding phase preparation.

[c] Columns designated as A–E were Bakerbond C_{18} (wide pore) that had been prepared with varying % carbon loadings; columns B and C are typical of the selectivity for Bakerbond C_{18} (wide pore) columns.

[d] Columns designated as Vydac 201TP (high) and Vydac 201TP (intermediate) are columns with % carbon loadings higher than those typically obtained from this manufacturer.

[e] Vydac 201TP (normal) has the selectivity of columns typically obtained from this manufacturer.

phases based on information from the manufacturers regarding the phase preparation. Based on the scheme proposed by Sander and Wise[10], which utilizes the $\alpha_{TBN/BaP}$ values to classify the characteristics of C_{18} phases for PAH selectivity, ten of the columns were classified as "polymeric" ($\alpha_{TBN/BaP} \leqslant 1$), three columns were classified as "intermediate" ($1 < \alpha_{TBN/BaP} < 1.7$), and only three were classified as "monomeric" ($\alpha_{TBN/BaP} \geqslant 1.7$). The $\alpha_{TBN/BaP}$ values for the sixteen columns in this study varied from 0.27, which indicates extremely high polymeric-like behavior, to 1.98 which indicates conventional monomeric-like selectivity. To provide a wide range of phases with polymeric-like selectivity, several columns, which had been prepared with varying percent carbon on the same wide-pore silica substrate, were obtained from two of the manufacturers. Even though the majority of commercially available C_{18} phases are designated as monomeric phases[10], only three monomeric C_{18} phases were included in this study since all monomeric C_{18} phases generally have very similar selectivity characteristics for the separation of isomeric PAHs.

The retention characteristics of three sets of methyl-substituted PAH isomers, *i.e.*, methylchrysenes, methylpicenes and methylperylenes (se Fig. 1), were investigated in this study. For each of these sets of methyl-PAHs, all possible isomers were available, *i.e.*, chrysene (six isomers), perylene (three isomers) and picene (seven isomers). These methyl-PAHs are of particular interest in the study of geochemical

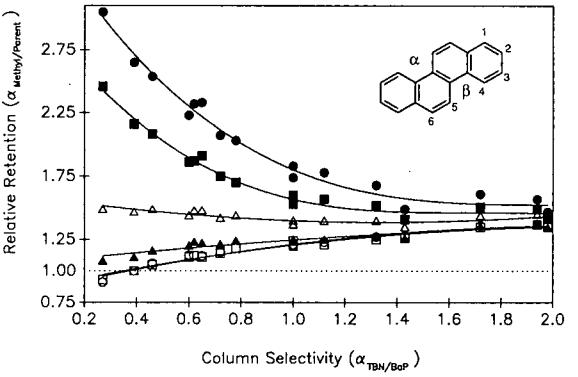

Fig. 2. Plot of retention of the methylchrysene isomers relative to chrysene *versus* column selectivity ($\alpha_{TBN/BaP}$) for sixteen different C_{18} columns. ● = 2-Methyl; ■ = 1-methyl; △ = 3-methyl; ▲ = 4-methyl; □ = 5-methyl; ○ = 6-methyl; ····· = chrysene.

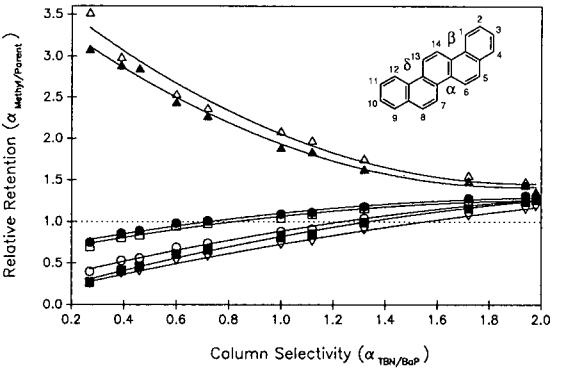

Fig. 3. Plot of retention of the methylpicene isomers relative to picene *versus* column selectivity ($\alpha_{TBN/BaP}$) for eleven different C_{18} columns. △ = 3-Methyl; ▲ = 4-methyl; ● = 2-methyl; □ = 5-methyl; ○ = 1-methyl; ■ = 6-methyl; ▽ = 13-methyl; ····· = picene.

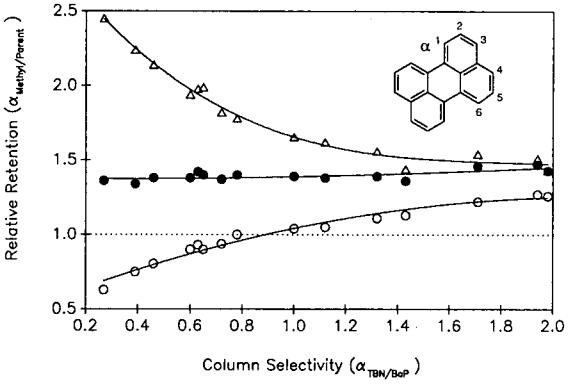

Fig. 4. Plot of retention of the methylperylene isomers relative to perylene *versus* column selectivity ($\alpha_{TBN/BaP}$) for fifteen different C_{18} columns. △ = 3-Methyl; ● = 2-methyl; ○ = 1-methyl; ····· = perylene.

processes. They have been identified in sediments, petroleum and several rare PAH minerals[13] as diagenetic maturity indicators[14], and in marine sediments as pollution origin markers[15].

The selectivity ratios (*i.e.*, relative retention) of the methyl-substituted isomers to the unsubstituted parent PAH were plotted *versus* the $\alpha_{TBN/BaP}$ values for the different LC columns (*i.e.*, the monomeric or polymeric nature of the stationary phase). These selectivity plots are shown in Figs. 2, 3 and 4 for the methylchrysene, methylpicene and methylperylene isomers, respectively. Several trends are apparent for all three groups of methyl-PAHs. For the three monomeric stationary phases, all of the methyl-substituted isomers elute after the parent PAHs, as would be expected based on the increased molecular weight and conctact area of the PAH solute, and the methyl-PAHs tend to elute as a group (*i.e.*, very little separation of the individual isomers). As the polymeric nature of the phase increases (*i.e.*, decreasing $\alpha_{TBN/BaP}$ values), the relative separation of the methyl isomers increases. This increased relative separation of the methyl-PAHs and the parent PAHs cannot be attributed to an increase in absolute retention. In fact, the absolute retention of chrysene, picene and perylene is generally greater on the monomeric phases than on the polymeric phases. These trends will be discussed in more detail below for each group of isomers.

The elution order of methyl-PAHs in reversed-phase LC correlates with the shape of the solute as described by the L/B ratio[4]. In addition to the shape, the planarity of the solute also affects the elution behavior of PAHs[3]. Recently, Garrigues *et al.*[16] calculated the dihedral angle of distortion for dimethylphenanthrene isomers and found that the isomers with large distortion angles eluted earlier than predicted by the L/B ratio. The distortion angle is defined as the dihedral angle between the aromatic rings opposite each other (*i.e.*, not adjacent rings) in the bay region. For example in Fig. 1, α represents the dihedral angle of the two planes defined by ring A and ring C, whereas β represents the angle between the two planes defined by ring B and ring D. The calculation of an angle of distortion by Garrigues *et al.*[16] represents the first attempt to quantify a parameter associated with non-planarity for correlation with chromatographic behavior. The L/B ratios and the angles of distortion for the methylchrysene, methylpicene and methylperylene isomers are summarized in Table II. For each of the PAHs, substitution of a methyl group in the "bay regions" (designated as α, β and δ in Fig. 1) results in varying degrees of distortion between the carbon atoms in the aromatic rings. For example, 4-methyl- and 5-methylchrysene have angles of 8.7 and 11.4 in the β bay region. For picene, which has three bay regions, distortion of varying amounts occurs in all three regions for 1-methyl-, 6-methyl- and 13-methylpicene.

Methylchrysene isomers

The selectivity ratios of the methylchrysenes relative to chrysene are plotted *versus* the stationary phase characteristics of sixteen C_{18} columns in Fig. 2. The chromatograms for the separation of the six methylchrysene isomers and chrysene on three different C_{18} phases, which have $\alpha_{TBN/BaP}$ of 0.27, 0.60 and 1.98, are illustrated in Fig. 5. The elution order of the methylchrysene isomers follows increasing L/B ratio. As shown in Fig. 2, the selectivity generally increases as the phase becomes more polymeric in nature (*i.e.*, decreasing $\alpha_{TBN/BaP}$ values). For the isomers with the largest L/B ratios (1-methyl and 2-methyl), the selectivity relative to chrysene increases as the

TABLE II

LENGTH-TO-BREADTH (L/B) RATIOS AND DIHEDRAL ANGLES OF DISTORTION FOR METHYLCHRYSENES, METHYLPICENES AND METHYLPERYLENES

See Experimental section for detailed definitions of the terms used. Methyl isomers listed in order of elution from Vydac 201TP (normal) column.

Isomers	L/B[a]	*Angle of distortion*		
		α	β	δ
Chrysene				
5-Methyl	1.48	4.3	−11.4	
6-Methyl	1.48	0.0	0.0	
4-Methyl	1.51	−3.6	−8.7	
3-Methyl	1.63	0.0	0.0	
1-Methyl	1.71	0.1	0.0	
2-Methyl	1.85	0.0	0.0	
Picene				
13.Methyl	1.75	−14.1	3.8	−25.4
6-Methyl	1.70	−26.9	−11.2	−12.0
1-Methyl	1.76	−14.0	−25.4	3.7
5-Methyl	1.76	−0.2	−0.7	0.4
2-Methyl	1.83	−1.5	−1.4	−0.4
4-Methyl	2.00	0.4	−1.0	0.0
3-Methyl	2.13	−1.1	−0.2	−0.2
Perylene				
1-Methyl	1.14	9.0		
2-Methyl	1.18	0.0		
3-Methyl	1.37	0.0		

[a] L/B is the length-to-breadth ratio of the solute as described previously[4].

phase becomes more polymeric in character; whereas for the isomers with the lowest L/B ratios and/or some non-planarity (as indicated by the angle of distortion), the selectivity ratio decreases and eventually becomes less than 1 (*i.e.*, elutes prior to chrysene) for the 5-methyl and 6-methyl isomers on the most highest loaded polymeric phase. For 3-methylchrysene, which has no distortion from planar (distortion angle of 0.0), the retention relative to chrysene changes very little on the different phases. The 5-methyl- and 6-methylchrysene have very similar behavior even though the 5-methyl isomer has angles of distortion of 4.3 and 11.4 degrees, whereas the 6-methyl isomer has no distortion. However, Sander and Wise[17] reported a separation of 5-methyl- and 6-methylchrysene at subambient temperatures with the 5-methyl isomer eluting first as would be expected based on non-planarity considerations.

Methylpicenes

The selectivity ratios of the methylpicenes relative to picene are plotted *versus* the stationary phase characteristics of eleven C_{18} columns in Fig. 3. As with the methylchrysenes, the α values for the isomers with the largest L/B ratios (3-methyl and 4-methyl) increase as the phases become more polymeric, and the retention relative to picene for the remaining isomers decreases. The chromatograms for the separation of

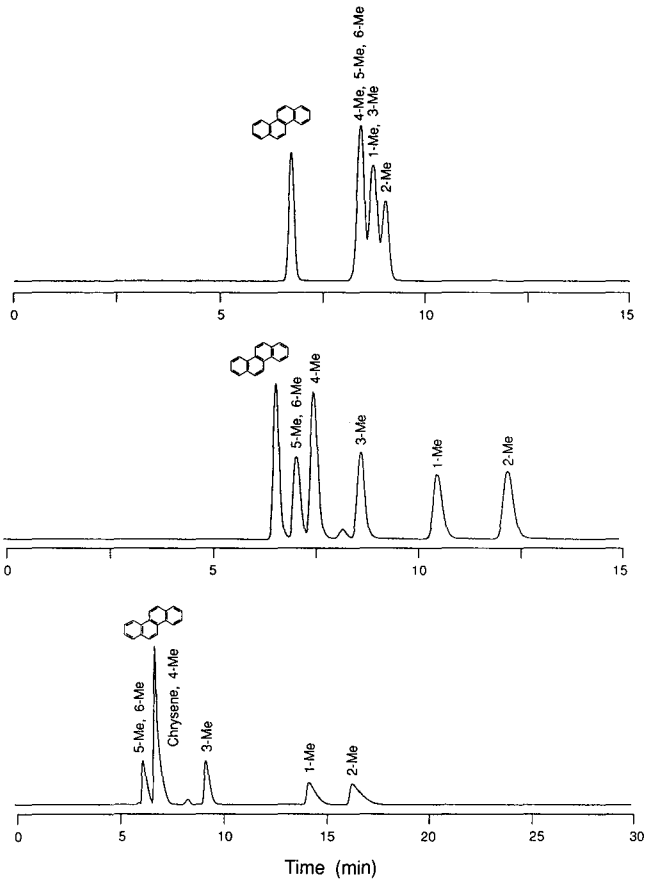

Fig. 5. Reversed-phase separation of chrysene and methylchrysene isomers on Hypersil ODS, $\alpha_{TBN/BaP}$ = 1.98 (upper chromatogram); Vydac 201TP, $\alpha_{TBN/BaP}$ = 0.60 (middle chromatogram); and Bakerbond C_{18} (wide pore) (A), $\alpha_{TBN/BaP}$ = 0.27 (lower chromatogram). Mobile phase: acetonitrile–water (80:20) at 1.5 ml/min. Fluorescence detection at 265 nm excitation and 365 nm emission. Me = Methyl.

the seven methylpicene isomers on three different C_{18} phases are shown in Fig. 6. The three methylpicene isomers that elute the earliest (13-methyl, 6-methyl and 1-methyl) have large angles of distortion (about 12 to 27 degrees) in the α, β and δ bay regions as well as the smallest L/B ratios for the isomer set (see Table II). As the polymeric nature of the phase increases (*i.e.*, decreasing $\alpha_{TBN/BaP}$ values), the relative separation of the methyl isomers increases and several methyl isomers eventually elute before picene, *i.e.*, 13-methyl-, 6-methyl-, 1-methyl-, 5-methyl- and 2-methylpicene.

Methylperylenes

The selectivity ratios of the methylperylenes relative to perylene are plotted *versus* the stationary phase characteristics of fifteen C_{18} columns in Fig. 4. The chromatograms for the separation of the three methylperylene isomers and perylene

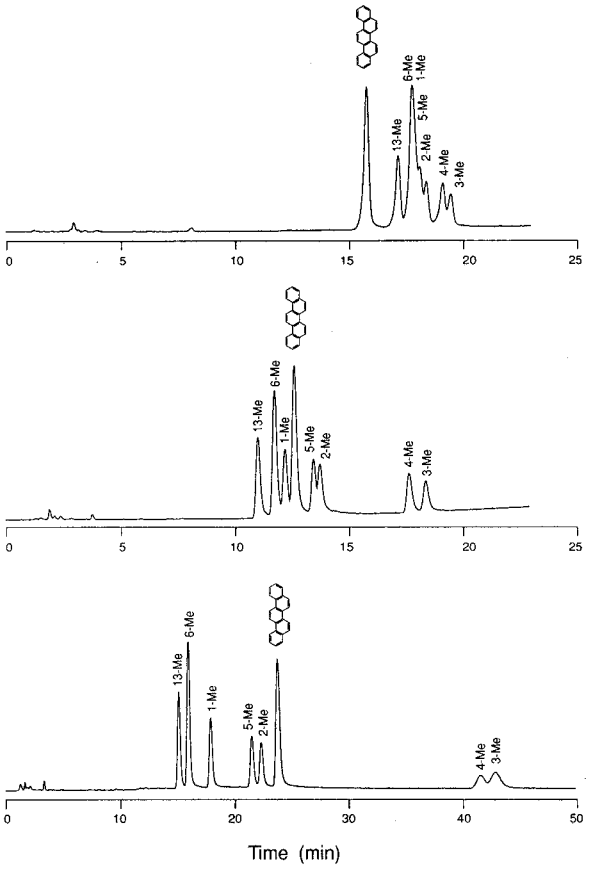

Fig. 6. Reversed-phase separation of picene and methylpicene isomers on Zorbax ODS, $\alpha_{TBN/BaP} = 1.94$ (upper chromatogram); Vydac 218TP, $\alpha_{TBN/BaP} = 1.12$ (middle chromatogram); and Vydac 201TP, $\alpha_{TBN/BaP} = 0.39$ (lower chromatogram). Mobile phase: gradient from acetonitrile–water (80:20) to 100% acetonitrile at 1%/min at 1.5 ml/min. Fluorescence detection at 284 nm excitation and 382 nm emission.

on two different C_{18} phases are shown in Fig. 7. Both of the C_{18} phases used in Fig. 7 were from the same manufacturer, and both columns had selectivity characteristics outside the normal range. Using a column with typical selectivity for this manufacturer ($\alpha_{TBN/BaP}$ value between approximately 0.70 and 0.90) would have resulted in 1-methylperylene coeluting with perylene (see Fig. 4). Garrigues *et al.*[5] first observed that 1-methylperylene eluted prior to perylene using a polymeric C_{18} column with a higher than normal carbon loading. The elution order of the three isomers follows increasing L/B ratios. The elution of the 1-methylperylene before perylene on the polymeric C_{18} phases can be attributed to the non-planarity of this isomer since the methyl group in the 1-position results in a distortion angle of 9 degrees.

The following trends can be summarized for all three groups of methyl-substituted isomers investigated: (1) The relative separation of the methyl-substituted PAH isomers increases as the C_{18} phase becomes more polymeric in nature ($\alpha_{TBN/BaP}$

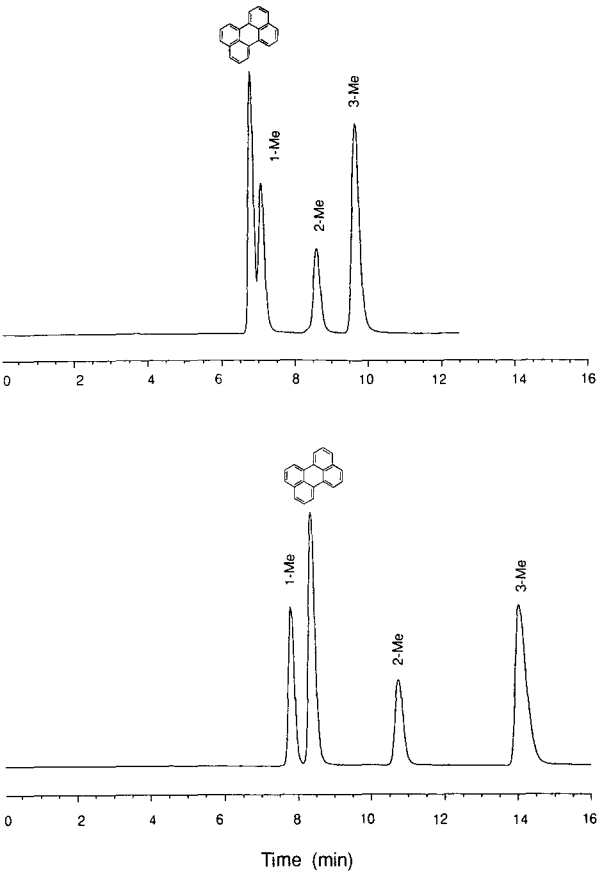

Fig. 7. Reversed-phase separation of perylene and methylperylene isomers on Vydac 201TP, $\alpha_{TBN/BaP} = 1.12$ (upper chromatogram); and Vydac 210TP, $\alpha_{TBN/BaP} = 0.60$ (lower chromatogram). Mobile phase: acetonitrile–water (80:20) at 1.5 ml/min. Fluorescence detection at 406 nm excitation and 440 nm emission.

decreases). (2) The order of elution of methyl-PAH isomers generally follows increasing L/B ratio, particularly on polymeric C_{18} phases. (3) On monomeric C_{18} phases, the methyl isomers elute after the parent PAH and tend to elute as a group, with little separation of individual isomers. (4) As the polymeric nature of the phase increases, isomers with some non-planarity and small L/B values eventually elute prior to the parent PAH. (5) As the polymeric nature of the phase increases, the retention of the isomers with large L/B values and planar structures increases relative to the parent PAH.

Retention model

The behavior of these non-planar methyl-substituted PAHs can be explained in terms of the "slot model", as proposed previously[3]. In this model the bonded alkyl phase is represented schematically as a surface with slots into which the PAH solute molecules can penetrate. Long, narrow solutes (large L/B values) can penetrate to

a greater extent than more compact, square solutes. Non-planar PAH solutes are partially excluded from the narrow slots resulting in reduced retention relative to planar PAHs.

CONCLUSIONS

For methyl-substituted PAH isomers, the characteristics of the C_{18} stationary phase and the planarity of the solute significantly influence the selectivity of the reversed-phase LC separation. By understanding the behavior of these isomers on various C_{18} phases, the appropriate phase can be selected for a particular application. For example, using a monomeric C_{18} phase provides a separation of the unsubstituted parent PAH from the methyl-substituted isomers with little differentiation among the methyl isomers. Garrigues *et al.*[18,19] have used this approach to isolate the methylphenanthrene isomers as a group prior to determination of the individual isomers using low temperature fluorescence spectroscopy. However, a C_{18} phase with extreme polymeric-like behavior may be required to provide an adequate separation of all methyl isomers of a particular PAH to determine the relative distributions of each isomer in various samples.

ACKNOWLEDGEMENT

The authors thank F. R. Guenther (NIST) for writing the computer program to calculate length-to-breadth values and M. Henry (J. T. Baker) for providing LC columns for this study.

REFERENCES

1 L. C. Sander and S. A. Wise. *Adv. Chromatogr.*, 25 (1986) 139.
2 L. C. Sander and S. A. Wise, *Anal. Chem.*, 56 (1984) 504.
3 S. A. Wise and L. C. Sander, *J. High Resolut. Chromatogr. Chromatogr. Commun.*, 8 (1985) 248.
4 S. A. Wise, W. J. Bonnett, F. R. Guenther and W. E. May, *J. Chromatogr. Sci.*, 19 (1981) 457.
5 P. Garrigues, E. Parlanti, R. Lapouyade and J. Bellocq, *Geochim. Cosmochim. Acta*, 52 (1988) 901.
6 R. Lapouyade, J. Pereyre and P. Garrigues, *C. R. Acad. Sci., Ser. 2*, 303 (1986) 903.
7 R. Lapouyade and J. H. Zhu, (1990) unpublished data.
8 D. Baschke, M. Jendziezyck, D. Youngs and M. Henry, *Book of Abstracts for Twelfth International Symposium of Polynuclear Aromatic Hydrocarbons, Gaithersburg, MD, Sept. 19–21, 1989.*
9 L. C. Sander and S. A. Wise, *LC · GC*, 8 (1990) 378.
10 L. C. Sander and S. A. Wise, *J. High Resolut. Chromatogr. Chromatogr. Commun.*, 11 (1988) 383.
11 J. Kao and N. Allinger, *J. Am. Chem. Soc.*, 99 (1977) 975.
12 S. A. Wise, B. A. Benner, H. Liu, G. D. Byrd and A. Colmsjö, *Anal. Chem.*, 60 (1988) 630.
13 S. A. Wise, R. M. Campbell, W. R. West, M. L. Lee and K. D. Bartle, *Chem. Geol.*, 54 (1986) 339.
14 P. Garrigues, R. De Sury, M. L. Angelin, J. Bellocq, J. L. Oudin and M. Ewald, *Geochim. Cosmochim. Acta*, 52 (1990) 375.
15 P. Garrigues, H. H. Soclo, M. P. Marniesse and M. Ewald, *Int. J. Environ. Anal. Chem.*, 28 (1987) 121.
16 P. Garrigues, M. Radke, O. Druez, H. Willsch and J. Bellocq, *J. Chromatogr.*, 473 (1989) 207.
17 L. C. Sander and S. A. Wise, *Anal. Chem.*, 61 (1989) 1749.
18 P. Garrigues and M. Ewald, *Anal. Chem.*, 55 (1983) 2155.
19 P. Garrigues, E. Parlanti, M. Radke, J. Bellocq, H. Willsch and M. Ewald, *J. Chromatogr.*, 395 (1987) 217.

Journal of Chromatography, 514 (1990) 123–136
Elsevier Science Publishers B.V., Amsterdam

CHROM. 22 507

Hydrophobicity parameters determined by reversed-phase liquid chromatography

I. Relationship between capacity factors and octanol–water partition coefficients for monosubstituted pyrazines and the related pyridines

CHISAKO YAMAGAMI*, TAMAKI OGURA and NARAO TAKAO
Kobe Women's College of Pharmacy, Motoyamakita-machi, Higashinada, Kobe, 658 (Japan)
(First received December 1st, 1989; revised manuscript received March 27th, 1990)

ABSTRACT

The capacity factors (k') of monosubstituted pyrazines and 2-substituted pyridines were measured on a Capcellpack C_{18} column using methanol–buffer (pH 9.2) mobile phases of different compositions, and the relationship between log P (n-octanol–water partition coefficient) and log k' was analysed. In all instances the amphiprotic substituents were eluted faster than expected on the assumption of log P–log k' linearity, reflecting that these groups act as hydrogen donors. For other substituents, a good linear relationship between log P and log k' was obtained with eluents containing 50–70% (v/v) of methanol. However, as the methanol content decreased, linearity no longer held and correction terms for the electronic effects and specific effects attributed to ester and amide groups were required. The relationship between log k'(pyrazine) and log k'(pyridine) was studied by applying a modified bidirectional Hammett-type correction for the component in π-value attributable to electronic effects of substituents and aza functions on the hydrogen-bonding solvation effect. The retention behaviour changed systematically with changes in mobile phase composition.

INTRODUCTION

The n-octanol–water partition coefficient (log P) is extensively used as a hydrophobicity parameter in quantitative structure–activity relationships (QSAR)[1,2]. Although the measurement of log P values by the shake-flask method is conventional and standard, it is sometimes time consuming and laborious. For some systems the log P values can be predicted by taking advantage of the additive property of substituent hydrophobic constants. However, this method has its limitations for compounds where electronic and steric effects are involved[3].

0021-9673/90/$03.50

Reversed-phase high-performance liquid chromatography (RP-HPLC) has increasingly been used as an alternative method for rapidly measuring the hydrophobicity of bioactive compounds in terms of the logarithm of the capacity factor, k', defined by the equation[4,5]

$$k' = (t_r - t_0)/t_0 \tag{1}$$

where t_r is the retention time of the compound and t_0 is that of an unretained compound. Most HPLC methods for predicting log P have used a combination of a commercially available alkyl-bonded stationary phase and methanol–water eluents[4–6]. Although the partition mechanism between the stationary phase and the mobile phase is complex, the extensive studies so far reported show that, with methanol–water as the eluent, the hydrogen-bonding behaviour of the HPLC system is similar to that of the octanol–water system[5] and log k' values are correlated with log P values by a Collander-type equation[7]:

$$\log k' = a \log P + b \tag{2}$$

It should be noted that an HPLC system using an alkyl-bonded stationary phase often discriminates among the analytes according to the hydrogen-bonding properties of the molecule; non-hydrogen bonders, hydrogen acceptors and hydrogen donors (amphiprotic groups)[4,8–10]. The correlation is then improved by introducing correction terms for differential hydrogen bonding, HB_A ($HB_A = 1$ for hydrogen acceptors and $HB_A = 0$ for others) and HB_D ($HB_D = 1$ for hydrogen donors and $HB_D = 0$ for others), as shown by the equation

$$\log k' = a \log P + bHB_A + cHB_D + d \tag{3}$$

Much effort to minimize this type of hydrogen-bond discrimination has been made[5,8].

Another problem in predicting log P values using eqns. 2 and 3 is the possibility of peak inversion The elution order of solutes is sometimes observed to be reversed, depending on the methanol concentration in the eluent[11–13]. For such a system, the accuracy of the predicted log P values depends on the mobile phase composition used to measure the capacity factors for the series of compounds. To eliminate this uncertainty, recent studies have proposed using a normalized parameter, log k_W, which can be obtained by extrapolation from the linear portion of the plot of log k' against the percentage by volume of methanol in the eluents to 100% water[14]. Many successful examples associated with this log k_w approach have been reported[5,8,10,15–17]. For this purpose, however, retention data at many mobile phase compositions should be measured over a wide range of retention times under the same stationary phase conditions. The linear relationship between log k' and methanol concentration does not always hold. In fact, the plot over a sufficiently wide range of methanol concentrations tends to show a curvature that may fit a quadratic equation better than a linear relationship[18,19]. In addition, the log k_W value estimated using these approximations has no distinct physical meaning, since the log k_W value thus obtained is not the same as the log k' value measured with pure water as the mobile phase[20]. It was claimed that the log k_W approach had the merit of reducing the effect of hydrogen

bonds[10]. Under such circumstances, it still seems doubtful whether the use of log k_W can be regarded as a standard method in every case. To gain more insight into this problem, systematic studies on the relationship between log k' and log P at different mobile phase compositions for a variety types of compounds are required

While interest in heterocyclic hydrophobicity has been increasing, little has been studied comprehensively except for the investigation of Lewis *et al.*[21]. We have previously measured and analysed log P values of monosubstituted diazines (pyrazines, pyrimidines and pyridazines) in terms of substituent effects[22]. It was shown that the π value (increment in log P attributable to a substitution) for diazine substituents ($\pi_{diazine}$) had considerably different features to the corresponding π value for substituents in monosubstituted benzenes (π_{PhX}), indicating that the electron-withdrawing property of the diazine ring caused a change in the hydrogen-bonding behaviour on the substituent as well as the ring nitrogen atoms. We were interested in analysing the HPLC retention parameters of these azines for several reasons: (1) to examine relationships between log P and log k' measured under various mobile and stationary phase conditions; (2) to compare the retention parameters for the heterocyclic system with those for other systems such as the benzenoid system to examine the influence of the hetero (ring-N) atom(s); (3) to ascertain whether the log k_W value is a reliable measure as a counter part of the *n*-octanol–water partition coefficient, as the retention time for these compounds could be measured experimentally even in mobile phases with high water concentrations; and (4) to find optimum HPLC conditions for the prediction of log P.

It has been difficult to obtain accurate retention times for basic compounds in their non-ionized form because the conventional chemically bonded silica gels cannot be used under alkaline conditions. Recently, silicone-coated silica gels modified with octadecyl or octyl groups have been developed as packing materials (Capcellpack) to ensure long-term stability under alkaline conditions[23]. In this study, as the first step of a systematic study of the HPLC retention behaviour of heterocyclic compounds, we have measured retention data for monosubstituted-pyrazines (2PR) on Capcellpack C_{18} with methanol–water eluents of different compositions. Corresponding data for 2-substituted pyridines (2PY) were also measured. The relationships between log k' and log P and between log k'(2PR) and log k'(2PY) were analysed in terms of substituent effects at each of the various eluent compositions. The changes in the retention behaviour as a function of the eluent composition are discussed.

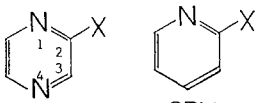

2PR

2PY

EXPERIMENTAL

Materials

The compounds tested are listed in Table I; their preparation has been described elsewhere[22].

Partition coefficients

n-Octanol–water log *P* values necessary for the discussion were taken from our previous work[22]. Measurements were done at pH values where the solute existed as the neutral form. All the log *P* values of pyrazines (2PR) were measured using an unbuffered aqueous phase. In fact, the log *P* values of even amino derivatives (16–18; pK_a = 3.1–3.5[24]), which are the most basic in the 2PR series, remained unchanged when measured using basic buffer (pH 9.2) solutions. For some pyridines (2PY) having strongly electron-donating substituents, such as alkyl ($pK_a \approx 6.0$[25]) and amino groups ($pK_a \approx 6.9$[25]), basic buffered solutions (pH 9.2) were used.

HPLC procedure

A Shimadzu LC5A liquid chromatograph equipped with a Model 7125 valve loop injector (Rheodyne) and SPD-2A UV (Shimadzu) and Shodex SE-31 refractive index (Shoden) detectors was used. Retention times were measured using a C-R4A Chromatopac (Shimadzu). A commercial Capcellpack C_{18} (15 cm × 4.6 mm I.D.) column (Shiseido)[23] was used without further treatment. This column was demonstrated to be more effective in suppressing the peak tailing caused by hydrogen bonding ion exchange and chelate formation than trimethylsilylation of ODS phases[26]. Commercial HPLC-grade methanol was used without further purification. As an aqueous buffer, 0.01 *M* sodium borate (pH 9.2) was used. Eluents containing 15–70% (v/v) of methanol were prepared. Appropriate amounts of samples were dissolved in methanol and 1–2 μl were injected at 25°C. The concentration of the eluents was adjusted to give an appropriate peak intensity. The flow-rate was 0.2–1.0 ml/min and the peak of methanol was used to estimate the t_0 value.

For 2PR, preliminary examinations showed that methanol–buffer (pH 7.4) and methanol–buffer (pH 9.2) eluents gave identical log k' values. However, to compare the results with those for 2PY, all the retention data in this work were taken with methanol–buffer (pH 9.2) eluents.

RESULTS

The capacity factors were measured for 2PR in the range 15–70% methanol and for 2PY in the range 15–50% methanol. The results are summarized in Table I. To check the possibility of the silanol effects, if any, the effects of amines added as masking agents and the effects of buffer concentration were examined for 2PR with the M15 eluent. Neither addition of triethylamine (0.1%) to the aqueous phase nor the use of increased buffer concentrations (0.02 instead of 0.01 *M*) had any significant influence on the retention behaviour, suggesting that the silanol effects are effectively suppressed on this stationary phase.

The parameters used for the correlations are given in Table II. The substituents in Table I can be classified into three groups: non-hydrogen bonders (1–6), hydrogen acceptors (7–16) and amphiprotic substituents (17–20)[9].

Relationship between log k' and log P

Plots of log k' against log *P* for 2PR at different methanol concentrations are shown in Fig. 1. For comparison, the corresponding retention data for mono-substituted benzenes were measured for 30% methanol (data not shown), and the plot

TABLE I

LOG k' VALUES FOR PYRAZINES (2PR) AND PYRIDINES (2PY)

No.	*Substituent*[a]	*2PR*				*2PY*		
		M15[b]	*M30*[b]	*M50*[b]	*M70*[b]	*M15*[b]	*M30*[b]	*M50*[b]
1	H	0.027	−0.301	−0.651	−0.957	0.801	0.442	−0.084
2	F	0.256	−0.016	−0.354	−0.688	0.667	0.349	−0.130
3	Cl	0.603	0.311	−0.106	−0.477	1.004	0.620	0.067
4	Br	–	–	–	–	1.115	0.711	0.147
5	Me	0.398	0.012	−0.482	−0.843	1.196	0.745	0.098
6	Et	0.816	0.367	−0.175	−0.609	1.565	1.066	0.349
7	OMe	0.767	0.392	−0.063	−0.475	1.195	0.796	0.241
8	OEt	1.247	0.847	0.272	−0.233	1.628	1.181	0.516
9	OPr	1.772	1.281	0.629	0.015	–	–	0.881
10	SMe	1.065	0.662	0.144	−0.313	1.396	0.967	0.334
11	CN	0.120	−0.192	−0.549	−0.932	0.471	0.086	−0.386
12	Ac	0.453	0.081	−0.366	−0.744	0.861	0.429	−0.095
13	CO_2Me	0.369	−0.120	−0.602	−1.035	0.781	0.301	−0.277
14	CO_2Et	0.845	0.306	−0.257	−0.749	1.256	0.709	0.031
15	$CONMe_2$	0.063	−0.439	−0.951	–	0.376	−0.175	−0.715
16	NMe_2	1.089	0.542	−0.078	−0.512	1.630	1.113	0.406
17	NH_2	−0.090	−0.463	−0.968	−1.277	0.633	0.294	−0.306
18	NHMe	0.457	−0.027	−0.536	−0.912	–	–	
19	NHAc	0.214	−0.234	−0.797	−1.279	0.628	0.162	−0.406
20	$CONH_2$	−0.195	−0.623	−1.153	–	0.324	−0.111	−0.638

[a] Me = methyl; Et = ethyl; Pr = propyl; Ac = acetyl.

[b] Methanol–buffer (pH 9.2, 0.01 *M* sodium borate); the figures represent the percentage by volume of methanol.

is shown in Fig. 2. It is clear that log k' for 2PR cannot be correlated with log P by a single relationship; in other words, the points for amphiprotic substituents (depicted by triangles) generally deviate downwards. This trend is in sharp contrast with that observed with benzene derivatives, which showed good linearity between log P and log k', reflecting how the electron-withdrawing property of the azine ring affects the hydrogen-bonding capability of these substituents. For simplicity, we first tried to analyse the relationship between log k' and log P, excluding those compounds having amphiprotic substituents. Good linear correlations were obtained when the methanol contents in eluents were 50% (M50) and 70% (M70), as shown by the equations

$$\log k' = 0.581 \log P - 0.511 \quad (4)$$
$$n = 15,\ r = 0.990,\ s = 0.059,\ F = 635.4$$

and

$$\log k' = 0.489 \log P - 0.884 \quad (5)$$
$$n = 14,\ r = 0.986,\ s = 0.052,\ F = 414.2$$

TABLE II

n-OCTANOL–WATER PARTITION COEFFICIENTS (LOG *P*) AND OTHER PARAMETERS USED FOR CORRELATION

No.	*Substituent*[a]	*Log P*		σ_I[c]	HB_{CO}	HB_{NH}	σ_m^{0}[b]	ρ[b]
		2PR[b]	*2PY*[b]					
1	H	−0.26	0.65	0.00	0.0	0.0	0.00	0.00
2	F	0.29	0.84	0.54	0.0	0.0	0.34	0.00
3	Cl	0.70	1.27	0.47	0.0	0.0	0.37	0.00
4	Br	0.93	1.38	0.47	0.0	0.0	0.37	0.00
5	Me	0.21	1.11	−0.01	0.0	0.0	−0.06	0.00
6	Et	0.69	1.60	−0.01	0.0	0.0	−0.08	0.00
7	OMe	0.73	1.34	0.30	0.0	0.0	0.10	0.27
8	OEt	1.28	1.81	0.28	0.0	0.0	0.10	0.27
9	OPr	1.84	2.38	0.28	0.0	0.0	0.10	0.27
10	SMe	1.17	1.71	0.30	0.0	0.0	0.14	0.20
11	CN	−0.01	0.40	0.57	0.0	0.0	0.62	0.00
12	Ac	0.20	0.83	0.30	0.0	0.0	0.36	0.16
13	CO_2Me	−0.23	0.36	0.32	1.0	0.0	0.35	0.13
14	CO_2Et	0.28	0.87	0.30	1.0	0.0	0.35	0.13
15	$CONMe_2$	−0.80[d]	−0.45[d]	0.28	1.0	0.0	–	–
16	NMe_2	0.93	1.65	0.17	0.0	0.0	−0.10	0.46
17	NH_2	−0.05	0.48	0.17	0.0	1.0	−0.09	0.74
18	NHMe	0.56[d]	1.12[d]	0.13	0.0	1.0	−0.10	–
19	NHAc	−0.03	0.54	0.28	1.0	1.0	0.14	0.91
20	$CONH_2$	−0.50	0.29	0.28	1.0	1.0	0.28	0.45

[a] See Table I.
[b] Taken from ref. 22.
[c] Taken from ref. 27.
[d] Newly measured.

respectively, where n is the number of compounds used for calculations, r is the correlation coefficient, s is the standard deviation and F is the value of the F-ratio between the variances of the observed and calculated values. When the methanol content decreases (M30 and M15), esters and amides containing functional groups such as $-CO_2R$ and $-CON=$ were observed to be retained longer than other hydrogen acceptors. To describe this differentiation effect, an indicator variable, HB_{CO}, was introduced, where $HB_{CO} = 1$ only for ester and amide groups and $HB_{CO} = 0$ for others. Addition of this parameter improved the correlations for M15 and M30 to give

$$\log k' = 0.824 \log P + 0.447 HB_{CO} + 0.184 \quad (6)$$
$$n = 15,\ r = 0.982,\ s = 0.100,\ F = 163.3$$

and

$$\log k' = 0.746 \log P + 0.253 HB_{CO} - 0.151 \quad (7)$$
$$n = 15,\ r = 0.994,\ s = 0.054,\ F = 507.5$$

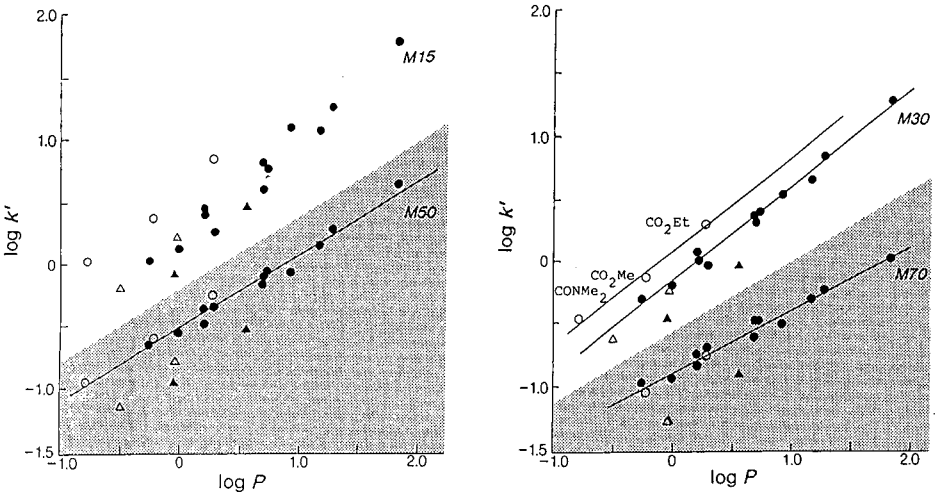

Fig. 1. Relationship between log P and log k' for monosubstituted pyrazines. Non-hydrogen bonders and hydrogen acceptors (substituents 1–16) are represented by the circles (●, HB_{CO} = 0; ○, HB_{CO} = 1) and amphiprotic substituents (17–20) are represented by the triangles (▲, HB_{CO} = 0; △, HB_{CO} = 1). The straight lines are the regression lines for non-hydrogen bonders and hydrogen acceptors coresponding to eqns. 12, 14 and 16.

respectively. Although eqn. 6 is statistically acceptable, examination of the residuals from the calculated values showed large deviations for electron-withdrawing substituents such as halogens and acetyl groups, suggesting that the electronic properties of the substituent participate in the retention mechanism. Among the electronic parameters examined, Charton's σ_I constant[27] was found most useful. Addition of σ_I helped significantly in minimizing the residuals and for M15 yielded

$$\log k' = 0.830 \log P + 0.465 HB_{CO} - 0.347\sigma_I + 0.273 \quad (8)$$
$$n = 15,\ r = 0.990,\ s = 0.078,\ F = 181.8$$

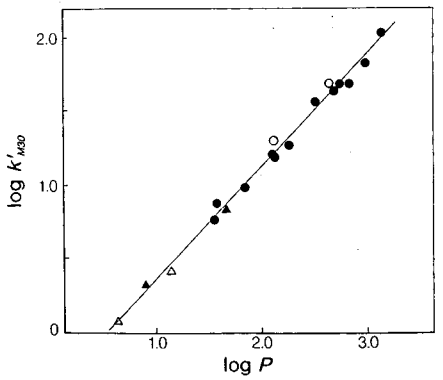

Fig. 2. Relationship between log P and log k' for monosubstituted benzenes [methanol–water (30:70); Capcellpack C_{18}; data taken from our unpublished results]. For symbols, see Fig. 1.

TABLE III

RELATIONSHIP BETWEEN LOG P AND LOG k'[a]

$\text{Log}k' = a\log P + h_1HB_{CO} + h_2HB_{AM} + \rho\sigma_I + c$

System	*Mobile phase*[b]	*Log P*	HB_{CO}	HB_{NH}	σ_I	*c*	*n*	*r*	*s*	*F*	*Eqn. no.*
2PR	M15	0.817	0.385	−0.292		0.200	19	0.984	0.099	152.7	10
		0.824	0.414	−0.319	−0.371	0.292	19	0.991	0.078	186.7	11
	M30	0.744	0.237	−0.305		−0.147	19	0.996	0.050	565.7	12
		0.747	0.248	−0.315	−0.137[c]	−0.113	19	0.997	0.045	513.6	13
	M50	0.582		−0.349		−0.511	19	0.992	0.060	503.2	14
		0.620	0.100	−0.361		−0.549	19	0.995	0.047	543.2	15
	M70	0.495		−0.348		−0.887	17	0.991	0.051	376.7	16
2PY[d]	M15	0.760	0.403	−0.446		0.203	17	0.964	0.126	56.7	17
		0.719	0.374	−0.451	−0.543	0.407	17	0.988	0.076	123.6	18
	M30	0.706	0.244	−0.362		−0.150	17	0.980	0.091	107.5	19
		0.674	0.222	−0.365	−0.414	0.006	17	0.995	0.048	299.5	20
	M50	0.540		−0.235	−0.219	−0.450	18	0.991	0.060	260.8	21
		0.591	0.117	−0.293		−0.591	18	0.991	0.061	251.6	22
		0.579	0.109[e]	−0.296	−0.205	−0.518	18	0.994	0.050	284.4	23

[a] Unless noted otherwise, all of the terms except for the intercept values are justified above the 99.5% level
[b] See the footnotes in Table I.
[c] Justified at the 94% level.
[d] Substituent NH_2 was not included for correlations 17–23.
[e] Justified at the 98% level.

Next, analyses including amphiprotic substituents were done by using an additional indicator variable, HB_{AM}, which takes the value 1 only for amphiprotic substituents (17–20) and 0 for others, as shown in Table II. Stepwise regression analyses were made in terms of the following general equation:

$$\log k' = a \log P + h_1HB_{CO} + h_2HB_{AM} + \rho\sigma_I + c \qquad (9)$$

The significance of each term was judged on the basis of statistical considerations. The most plausible correlations at each methanol concentration and statistically equivalent equations are summarized in Table III together with other equations necessary for the discussion.

For pyridines (2PY), plots of log k' against log P were generally similar to those for the pyrazine series, although the points became more scattered with decrease in the methanol content in the mobile phase than in the case of 2PR (Fig. 3). Excellent correlation equations were also obtained by application of eqn. 9 as the general formula, except for NH_2, which showed large deviations in all the mobile phases studied, for which rationalization is difficult at present[a]. The results are included in Table III.

[a] A possible explanation might be that aminopyridine is partially ionized under the experimental conditions. The log P values for octanol–water, octanol–buffer (pH 9.2) and octanol–0.1 M sodium hydroxide systems are 0.4–0.44, 0.48 and 0.51, respectively. It is difficult to judge whether the difference between the last two values should be regarded as significant to support this reasoning or not.

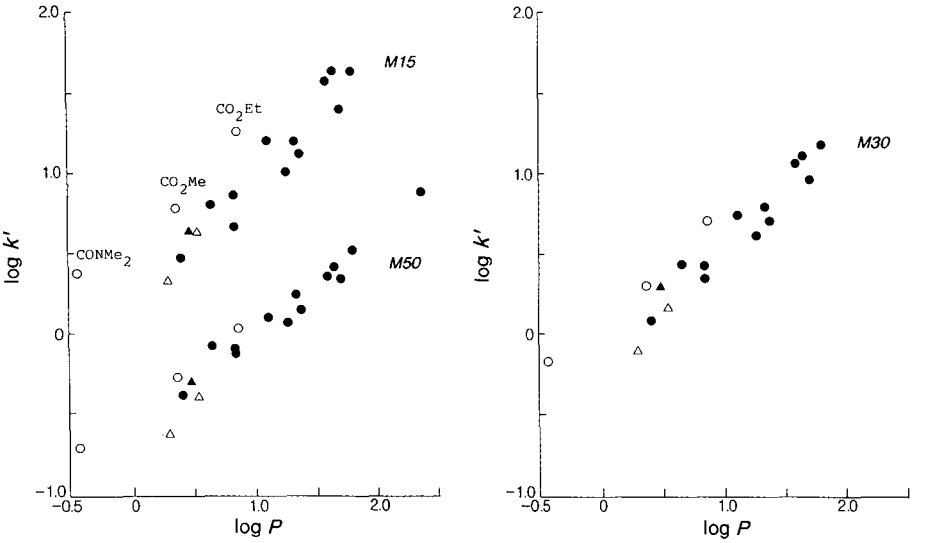

Fig. 3. Relationship between log P and log k' for 2-substituted pyridines. For symbols, see Fig. 1.

It should be noted that eqn. 9 shows that hydrogen-bonding acceptors other than ester and amide groups, such as alkoxy and cyano, behave similarly to non-hydrogen bonders. To examine the hydrogen-bond effect, if any, attributable to these ordinary hydrogen acceptors, we tried to introduce an additional indicator variable, HB_A, which takes the value 1 for the hydrogen-bond acceptors other than ester and amide groups (substituents 7–12 and 16). Regression analyses using log P, σ_I and three kinds of HB parameters (HB_{CO}, HB_{AM} and HB_A) indicated that the HB_A parameter was statistically significant (at the 93% level) only for M15 in 2PY. Even in this instance, the correlation was not much improved by the introduction of the parameter HB_A, indicating that eqn. 9 is sufficient as a general empirical equation to relate two kinds of hydrophobicity parameters from octanol–water and HPLC systems.

Relationship between log k'(2PR) and log k'(2PY)

In our previous work[22], we tried to analyse the π value of 2PR (π_{2PR}) in terms of physico-chemical parameters of substituent, such as π_{PhX}, and electronic and steric parameters. Contrary to our initial expectation in correlating π_{2PR} with π_{PhX}, no simple correlation could be derived because of strong electronic interactions between the substituent and ring nitrogen atoms. Therefore, as a preliminary step, we tried to correlate π_{2PR} with the π value of structurally related 2-substituted pyridines (π_{2PY}). Applying the bidirectional Hammett-type treatment proposed for the analysis of π values for disubstituted benzenes, YC_6H_4X (X and Y are variable and fixed substituents respectively)[3], to the pyrazine series where the ring N-4 atom is considered as the substituent Y, the π_{2PR} value was demonstrated to fit excellently the equation

$$\pi_{2PR} = a\pi_{2PY} + \rho_Y\sigma^0_X(m) + \sigma^0_Y(m)\rho_X + c \qquad (24)$$

TABLE IV

RELATIONSHIP BETWEEN LOG k'(2PR) AND LOG k'(2PY)

$k^*_{2PR} = ak^*_{2PY} + \rho_Y\sigma^0_X(m) + \sigma^0_Y(m)\rho_X + c$

Mobile phase[a]	*Correlation*[b]	n[c]	r	s	F	*Eqn.no*
M15	$k^*_{2PR} = 1.257k^*_{2PY} + 0.940\sigma^0_X(m) + 0.323\rho_X - 0.022$	16	0.990	0.068	205.1	26
M30	$k^*_{2PR} = 1.312k^*_{2PY} + 1.034\sigma^0_X(m) + 0.286\rho_X - 0.020$	16	0.991	0.064	209.4	27
M50	$k^*_{2PR} = 1.302k^*_{2PY} + 0.847\sigma^0_X(m) + 0.106\rho_X$[d] $- 0.002$	16	0.993	0.059	308.0	28

[a] See the footnotes in Table I.

[b] Unless noted otherwise, all of the terms except for the intercept values are justified above the 99.5% level

[c] The substituents NHMe and $CONMe_2$ were not included in calculations because their ρ_X values were unknown.

[d] Justified at the 90% level.

where $\sigma^0_X(m)$ is the electronic substituent constant σ^0_m of the substituent X and ρ_X is the susceptibility constant of X to the solubility-modifying effects of the Y (N-4) atom. While the interaction between X and N-1 is assumed to be cancelled by using π_{2PY} as the reference, the interaction between X and N-4 is expressed by the $\sigma^0_X(m)$ and ρ_X terms: the former expresses the effects of X (or strictly N-1 + X) on the change in the hydrogen-bonding ability of N-4, and the latter expresses the reversed effect of N-4 on X (or N-1 + X). The intercept, c, should theoretically be zero. By introducing the values of π_{2PY}, σ^0_m and ρ for X substituents the regression coefficients, a, ρ_Y and $\sigma^0_Y(m)$ are calculated by the least-squares method. If the analysis is limited to the series of 2PR, the use of σ_I instead of σ^0_m gave a statistically equivalent correlation to that formulated by eqn. 24. However, a comprehensive analysis of the π value of diazines, including not only pyrazines but also pyrimidines and pyridazines, showed that σ^0_m works better than σ_I in this type of analysis.

To compare the chromatographic retention behaviour with that observed from the octanol–water partitioning system, analogous analyses for log k' were tried at M15, M30 and M50, for which the retention data for 2PY are available. The correlation equation corresponding to eqn. 24 can be formulated by

$$k^*_{2PR} = ak^*_{2PY} + \rho_Y\sigma^0_X(m) + \sigma^0_Y(m)\rho_X + c \qquad (25)$$

where k^* is the increment in log k' attributable to the substitution. The analysis using eqn. 25 yielded excellent correlations at each mobile phase composition, as shown in Table IV.

DISCUSSION

Examination of Table III shows that the quality of correlation equations varies with the mobile phase composition, suggesting that the retention mechanism becomes more complicated with the decrease in methanol concentration. It is clearly demonstrated that the linearity of the log P–log k' relationship becomes perturbed more significantly by other factors as the methanol concentration decreases. For instance, the HB_{CO} term is statistically significant at M50, but neglecting this term from

ithe correlation would have little effect on the estimated log P value. However, for M15 and M30, the HB_{CO} term is essential.

In both series, 2PR and 2PY, the slope of log P and the intercept, c, increased with decreasing methanol concentration according to the general trend so far observed[4]. At a constant mobile phase composition, the slope of log P for 2PR is slightly but significantly higher than that for 2PY.

The coefficient of the HB_{AM} term was found to be negative in all the cases examined here, in accordance with the general behaviour that hydrogen donors have shorter retention times than expected from the log k' *vs.* log P calibration line[4]. Typical examples are the acceleration effects of phenol derivatives when eluted with methanol–water mixtures[6,8,28]. In this instance, the OH group is thought to undergo hydrogen bonding with the solvent as follows (type A):

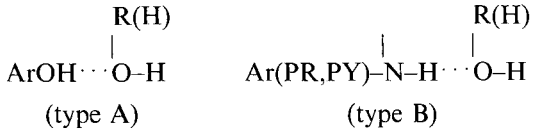

As octanol is more basic than methanol and water, this type of solvation participates to a greater extent in an octanol–water system than in a stationary phase–aqueous methanol mobile phase system, and hence the OH derivatives appear to be more hydrophobic in the former system. The present results could be understood in a similar way, as the electron-withdrawing property of the azine rings increases the hydrogen-donating ability of the amphiprotic groups and, hence, hydrogen bonding as in type B would occur.

The coefficient of the HB_{CO} term is positive and becomes larger with a decrease in methanol concentration. The reason why only functional groups such as ester and amide are retained more than the other ordinary hydrogen acceptors is difficult to explain. A similar effect was observed with other modifiers such as dioxane and also with other stationary phases such as phenyl- and cyano-bonded columns, although the slopes of the HB_{CO} term varied[29]. Interestingly, our current work has demonstrated that such an ester effect is also observed when the log P values of 2PR are compared between octanol–water and chloroform–water partitioning systems[29]. It seems from these results that the structural characteristics of solutes are responsible for the origin of the apparent retardation effect associated with ester and amide groups. Further studies of the retention behaviour exerted by such substituents involved in other reference systems would be required to explain this problem.

The fact that the σ_I term is significant, especially in water-rich mobile phases, demonstrates that the selective solute–solvent interactions are important in governing the log k' values. Probably this effect is associated with the pK_a of the solute. Ehrenson *et al.*[30] have shown that the pK_a values of 2-substituted pyridines can be described mainly by σ_I. The observed tendency that the contribution of the σ_I term becomes greater with an increase in the polarity of the mobile phase could be understood by the fact that the electronic effects are generally more important in a polar solution. At a fixed methanol concentration, the coefficient σ_I is larger for 2PY than for 2PR, probably because the electronic substituent effects affect the pK_a value for stronger bases (2PY) to a greater extent than for weaker bases (2PR). With increase in the

contribution from the electronic effects to the overall retention, the linear relationship between log P and log k' becomes poorer.

It should be noted that although the HPLC partitioning mechanism seems very complex, the relationship expressed by eqn. 25 holds very well in the range from M15 to M50. We had also found that the same type of correlation held in correlating the capacity factors of *m*- and *p*-substituted phenylacetanilides (PhA) with those of monosubstituted benzenes in the range from M50 to M70[6]. These results suggest that the partitioning in the HPLC system may be governed by similar factors to those operating in the octanol–water system. Table IV shows that the coefficient of k^*_{2PY} is fairly constant (*ca.* 1.3) and those of σ^0_m and ρ_X seem to reflect the properties of the mobile phase. The coefficient of σ^0_X(m), ρ_Y, increased by a factor of 1.2 on going from M50 to M30 [$\rho_{Y(M30)}/\rho_{Y(M50)} = 1.2$]. The same factor had been obtained with PhA when the equations for M50 and M70 were compared [$\rho_{Y(M50)}/\sigma_{Y(M70)} = 1.2$], indicating that the overall hydrogen-bonding behaviour of methanol–water mixtures varies linearly with the methanol concentration in the M30–M70 region. This linear change no longer seems assured when the methanol content is lower than 30%, as demonstrated by a decrease in the ρ_Y value at M15 relative to that at M30, indicative of a discontinuity in the retention mechanism at very high water contents in the mobile phase. In such a region of methanol concentrations it is possible that the properties of the stationary phase would also be changed non-linearly[31].

From the above discussion, the log k_W value obtained as an extrapolated value would have complex characteristics. To examine the validity of the log k_W approach, precise measurements of capacity factors over a wide range of methanol concentrations are required. Therefore, we shall discuss this problem only briefly here. In Table V, the log k_W values obtained by the linear extrapolation are presented. It is clearly seen that log k_W depends on the range over which the retention data were measured, as has often been observed[8]. The analysis of these log k_W values using eqn. 9 gave the following equations:

2PR, for the range 15–50% methanol:

$$\log k_{W(15-50)} = 0.949 \log P + 0.521HB_{CO} - 0.267HB_{AM} - 0.499\sigma_I + 0.606 \quad (29)$$
$$n = 16,\ r = 0.985,\ s = 0.105$$

2PR, for the range 30–70% methanol:

$$\log k_{W(50-70)} = 0.961 \log P + 0.403HB_{CO} - 0.153HB_{AM} - 0.264\sigma_I + 0.447 \quad (30)$$
$$n = 16,\ r = 0.991,\ s = 0.084$$

2PY, for the range 15–50% methanol:

$$\log k_{W(15-50)} = 0.844 \log P + 0.459HB_{CO} - 0.386HB_{AM} - 0.656\sigma_I + 0.722 \quad (31)$$
$$n = 16,\ r = 0.986,\ s = 0.089$$

It is worth noting that the correlation becomes more complex with the log k_W parameter, although the coefficient of log P becomes nearly unity. As an alternative extrapolation method, a quadratic model was also tried, but led to poorer correlations. Use of the $E_T(30)$ solvent polarity parameter[32] did not improve the correlation (data not shown). As studies on the log k_W approach have mostly treated benzenoid compounds, we also attempted to examine some monosubstituted benzenes on the

TABLE V

LOG k_W VALUES DERIVED BY LINEAR EXTRAPOLATION

No.	*Substituent*	*2PR*		*2PY:*	*PhX:*	
		$k_{W(30-70)}$[a]	$k_{W(15-50)}$[b]	$k_{W(15-50)}$[b]	k_W[c]	*(log P)*[d]
1	H	0.18(0.9993)[e]	0.30(0.9980)	1.19(0.9997)	2.04	(2.13)
2	F	0.49(1.0000)	0.51(0.9998)	1.02(0.9994)	2.22	(2.27)
3	Cl	0.89(0.9994)	0.89(0.9998)	1.41(0.9998)	2.77	(2.84)
4	Br	–	–	1.54(0.9999)	2.94	(2.99)
5	Me	0.63(0.9960)	0.77(0.9999)	1.68(0.9998)	2.65	(2.69)
6	Et	1.08(0.9980)	1.23(0.9996)	2.10(0.9998)	3.21	(3.15)
7	OMe	1.04(0.9996)	1.11(0.9997)	1.61(0.9999)	2.12	(2.11)
8	OEt	1.65(0.9993)	1.67(0.9998)	2.12(0.9995)	2.60	(2.51)
9	OPr	2.22(0.9999)	2.26(1.0000)	–	–	–
10	SMe	1.38(0.9994)	1.45(0.9999)	1.86(0.9999)	–	–
11	CN	0.37(0.9998)	0.40(0.9990)	0.83(0.9997)	1.65	(1.56)
12	Ac	0.69(0.9988)	0.80(0.9996)	1.26(0.9996)	1.77	(1.58)
13	CO_2Me	0.56(0.9995)	0.76(0.9963)	1.22(0.9996)	2.30	(2.12)
14	CO_2Et	1.09(0.9993)	1.29(0.9980)	1.77(0.9998)	2.85	(2.64)
15	$CONMe_2$	–[f]	–[f]	–	–	–
16	NMe_2	1.30(0.9949)	1.57(0.9990)	2.16(1.0000)	–	–
17	NH_2	–[f]	–[f]	–[f]	–	–
18	NHMe	0.86(0.9963)	0.86(0.9977)	–	–	–
19	NHAc	0.54(0.9990)	0.64(0.9999)	1.06(0.9997)	1.21	(1.16)
20	$CONH_2$	–[f]	–[f]	0.73(0.9997)	0.90	(0.64)

[a] Log k_W derived from the linear extrapolation using the data for 30–70% methanol.
[b] Log k_W derived from the linear extrapolation using the data for 15–50% methanol.
[c] Log k_W derived from the linear extrapolation using our unpublished data dor 30–70% methanol[29].
[d] Taken from ref. 22.
[e] Correlation coefficients.
[f] Not accurately determined.

same column. The log k_W values obtained are included in Table V for comparison. It is seen that the log k_W value agrees well with the log P value, indicative of the usefulness of log k_W as a possible candidate for the hydrophobicity of the benzenoid compounds. The different features observed in our system could therefore be produced by the ring nitrogen atom(s), which must increase the solute–solvent interactions by the hydrogen-bond effect. The difference in relative solvation effects through the hydrogen bonding between the stationary phase–mobile phase and octanol–water systems is expected to be increased with decrease in the methanol concentration in the eluent. In such instances, the eluent composition used to predict log P should be selected very carefully.

In conclusion, this work has shown that the log k' value of 2PR at different methanol concentrations can be expressed by eqn. 9 as a general equation. One of the most troublesome problems hampering the use of the RP-HPLC techniques for the determination of log P arises from the contribution of electronic effects (the $\rho\sigma$ term) which is responsible for perturbing the log P *vs.* log k' linearity. These electronic effects were more important in highly water-rich mobile phases. This finding leads us to conclude that the log k_W obtained as an extrapolated value would fail to describe the

hydrophobic properties of very polar solutes. To gain a closer insight into this subject, the analysis by eqn. 9 should be extended to a wider range of eluent compositions and to different kinds of stationary phases and also to other heterocyclic systems of solutes. Detailed discussion on this subject will be presented in a forthcoming paper. The physical meaning of the HB_{CO} parameter remains to be studied and work is in progress.

REFERENCES

1 T. Fujita, J. Iwasa and C. Hansch, *J. Am. Chem. Soc.*, 86 (1964) 5175.
2 A. Leo, C. Hansch and D. Elkins, *Chem. Rev.*, 71 (1971) 525.
3 T. Fujita, *Prog. Phys. Org. Chem.*, 14 (1983) 75.
4 H. Terada, *Quant. Struct.-Act. Relat.*, 5 (1986) 81.
5 Th. Braumann, *J. Chromatogr.*, 373 (1986) 191.
6 C. Yamagami, H. Takami, K. Yamamoto, K. Miyoshi and N. Takao, *Chem. Pharm. Bull.*, 32 (1984) 4994.
7 R. Collander, *Acta Chem. Scand.*, 5 (1951) 774.
8 D. J. Minick, J. H. Frenz, M. A. Patrick and D. A. Brent, *J. Med. Chem.*, 31 (1988) 1923.
9 T. Fujita, T. Nishioka and M. Nakajima, *J. Med. Chem.*, 20 (1977) 1071.
10 K. Miyake, N. Mizuno and H. Terada, *J. Chromatogr.*, 439 (1988) 227.
11 K. Valkó, T. Friedmann, J. Báti and A. Nagykáldi, *J. Liq. Chromatogr.*, 7 (1984) 2073.
12 G. E. Berendsen and L. de Galan, *J. Chromatogr.*, 196 (1980) 21.
13 L. R. Snyder, M. A. Quarry and J. L. Glajch, *Chromatographia*, 24 (1987) 33.
14 Th. Braumann, G. Weber and L. H. Grimme, *J. Chromatogr.*, 261 (1983) 329.
15 J. L. G. Thus and J. C. Kraak, *J. Chromatogr.*, 320 (1985) 271.
16 N. El Tayar, A. Tsantili-Kakoulidou, T. Roethlisberger, B. Testa and J. Gal, *J. Chromatogr.*, 439 (1988) 237.
17 W. E. Hammers, G. J. Meurs and C. L. de Ligny, *J. Chromatogr.*, 247 (1982) 1.
18 P. J. Schoenmakers, H. A. H. Billiet and L. de Galan, *J. Chromatogr.*, 282 (1983) 107.
19 N. E. Tayar, H. van de Waterbeemd and B. Testa, *J. Chromatogr.*, 320 (1985) 293.
20 P. J. Schoenmakers, H. A. H. Billiet and L. de Galan, *J. Chromatogr.*, 282 (1983) 107.
21 S. J. Lewis, M. S. Mirrlees and P. J. Taylor, *Quant. Struc.-Act. Relat.*, 2 (1983) 100.
22 C. Yamagami, N. Takao and T. Fujita, *Quant. Struct.-Act. Relat.*, in press.
23 Y. Ohtsu, H. Fukui, T. Kanda, K. Nakamura, M. Nakano, O. Nakata and Y. Fujiyama, *Chromatographia*, 24 (1987) 380.
24 G. B. Barlin, *The Pyrazines*, Wiley, New York, 1982.
25 D. D. Perrin, *Dissociation constants of Organic Bases in Aqueous Solution: Supplement*, Butterworth, London, 1972.
26 Y. Ohtsu, Y. Shiojima, T. Okumura, J. Koyama, K. Nakamura, O. Nakata, K. Kimata and N. Tanaka, *J. Chromatogr.*, 481 (1989) 147.
27 M. Charton, *Prog. Phys. Org. Chem.*, 13 (1981) 119.
28 N. Tanaka, H. Goodell and B. Karger, *J. Chromatogr.*, 158 (1978) 233.
29 C. Yamagami and N. Takao, in preparation.
30 S. Ehrenson, R. T. C. Brownlee and R. W. Taft, *Prog. Phys. Org. Chem.*, 10 (1973) 1.
31 R. P. W. Scott and C. F. Simpson, *J. Chromatogr.*, 197 (1980) 11.
32 B. P. Johnson, M. G. Khaledi and J. G. Dorsey, *Anal. Chem.*, 58 (1986) 2354.

Journal of Chromatography, 514 (1990) 137–146
Elsevier Science Publishers B.V., Amsterdam

CHROM. 22 504

Chemical properties of and solute–support interactions with the gel filtration medium Superdex 75 prep grade

INGRID DREVIN, LOTTA LARSSON, INGEGERD ERIKSSON and BO-LENNART JOHANSSON*

Pharmacia LKB Biotechnology AB, S-751 82 Uppsala (Sweden)

(First received December 11th, 1989; revised manuscript received April 10th, 1990)

ABSTRACT

The influence of the ionic strength and pH of the mobile phase on the distribution coefficient of proteins with different p*I* values was studied on Superdex 75 prep grade. Superdex contains small amounts of negatively charged groups which are responsible for electrostatic interactions between ionic solutes and the gel. Ion-exchange or ion-exclusion interactions were observed at low ionic strengths when the pH of the mobile phase was lower or higher than the p*I* values of the proteins. For some proteins, hydrophobic interactions were also observed at high ionic strengths.

The chemical stability of Superdex 75 prep grade was studied by comparing the chromatographic results from Superdex treated in acidic or basic solutions with those from untreated Superdex. The separation characteristics of Superdex 75 prep grade were unaffected after 25 washes with 1.0 *M* sodium hydroxide solution or 0.1 *M* hydrochloric acid with a contact time of 4 h for each wash. However, storage for 2 weeks in 0.01 *M* hydrochloric acid or 0.1 *M* sodium hydroxide solution partly hydrolysed the covalently bounded dextran in the agarose pores. This hydrolysation resulted in leakage of dextran and an increase in the K_{av} values of the test proteins.

INTRODUCTION

Dextran (*e.g.*, Sephadex) and agarose (*e.g.*, Sepharose) based gel filtration chromatography (GFC) media have played an essential part in the separation of biological samples for many years[1,2]. Dextran gels are known to give high selectivity in GFC as they have an evenly distributed polymer network[3]. However, agarose gels, which have a macroreticular structure[3], tend to have less steep selectivity curves and separate at considerably higher masses than Sephadex gels. On the other hand, agarose gels have a higher matrix rigidity, allowing higher flow-rates to be used.

The GFC medium investigated in this work, Superdex 75 prep grade, is composed of both dextran and agarose and the mean bead size is *ca.* 34 μm. It has been produced to combine high selectivity and high matrix rigidity. The selectivity of

0021-9673/90/$03.50

Superdex 75 prep grade is the same as that of Sephadex G-75, 3000-70 000 daltons. A comprehensive description of the selectivity, efficiency (N), bead structure and flow-rate properties of Superdex is presented elsewhere[4,5].

In addition to the exclusion properties and physical characteristics of a GFC medium, important considerations in GFC are also the non-size-related separation effects and the chemical stability of the medium[6,7]. The purpose of this study was to interpret the chromatographic results obtained with this packing under different elution conditions for a number of proteins. The separation characteristics of Superdex 75 prep grade were also studied after treatment under extreme acidic or basic conditions.

EXPERIMENTAL

Equipment

Chromatographic experiments were carried out with two Pharmacia FPLC systems, each consisting of an LCC-500 control unit, two P-500 high-precision pumps, a UV-1 UV monitor (280 nm, HR 10 cell), an MV-7 sample injector with a 500-μl loop, an MV 8 sample holder, a P-1 peristaltic pump and an REC-481 recorder. Superdex 75 prep grade was packed in Pharmacia HR 16/50 columns (50 cm × 1.6 cm I.D.) according to the packing instructions for the gel. A Shimadzu C-R3A integrator was used to store data.

Reagents

The mobile phase buffers were made from sodium acetate and acetic acid (pH 4.2), sodium dihydrogenphosphate and disodium hydrogenphosphate (pH 7.0) or sodium hydrogencarbonate and sodium carbonate (pH 10.0). The buffers were prepared from 0.020 M stock solutions of these acid and base components. Variations of the ionic strength were obtained by adding different amounts of sodium chloride to the stock solutions. The proteins used are listed in Tables I and II. These proteins were dissolved in the mobile phase at a concentration of *ca.* 2 mg/ml and kept frozen until used. All buffers and protein solutions were filtered through a 0.45-μm filter before use.

TABLE I

PROTEINS USED FOR STUDYING CHROMATOGRAPHIC BEHAVIOUR BEFORE AND AFTER BULK TREATMENT OF SUPERDEX 75 PREP GRADE

Protein	*Source*	*Concentration (mg/ml)*	*Molecular weight*	*Isoelectric point (pI)*
Lysozyme	Egg white	2.0	13 900	11.0
Myoglobin	Horse heart	3.0	17 500	7.0
α-Chymotrypsinogen A	Bovine pancrease	1.0	25 000	8.8
Pepsin	Bovine	8.0	33 000	2.9
Serum albumin	Bovine	2.0	69 000	4.7
Transferrin	Human	2.0	76 500	5.5

TABLE II

PROTEINS USED FOR STUDYING CHROMATOGRAPHIC BEHAVIOR ON SUPERDEX 75 PREP GRADE DURING CLEANING-IN-PLACE EXPERIMENTS

	Protein[a]	*Source*	*Concentration (mg/ml)*	*Molecular weight*	*Isoelectric point (pI)*
A	Cytidine		0.1	323	
B	Lysozyme	Egg white	1.2	13900	11.0
C	Cytochrome C	Horse heart	1.2	12400	10.2
D	Myoglobin	Horse heart	1.2	17500	7.0
E	α-Chymotrypsinogen A	Bovine pancrease	1.2	25000	8.8
F	β-Lactoglobulin	Bovine milk	1.2	35000	5.2
G	Ovalbumin	Egg white	2.5	45000	4.7
H	Serum albumin	Bovine	2.5	69000	4.7
I	IgG	Human	1.2	160000	7.7

[a] The letters A–I refer to the designation of the proteins in Figs. 5 and 6.

Treatment of Superdex 75 prep grade before packing

The chemical stability of Superdex 75 prep grade under static conditions was studied by incubating the gel (about 150 ml) for 14 days in 0.01 *M* hydrochloric acid or 0.1 *M* sodium hydroxide solution. Before the gel was incubated it was washed with 300 ml of the incubation solution. The incubation was done at ambient temperature (*ca.* 20°C). The two treated gel samples were packed in HR 16/50 columns and their chromatographic behaviour was compared with that of untreated Superdex 75 prep grade.

Chromatographic procedure for treated and untreated Superdex 75 prep grade

The columns were equilibrated by passage of at least three bed volumes of mobile phase before being used for experimental observations. The chromatographic runs were performed by individual injections of the proteins in Table I to avoid possible interactions between proteins. The flow-rate was 1.0 ml/min and the injection volume was 500 μl. The resulting retention volumes were used to calculate the distribution coefficient (K_{av}) from the equation

$$K_{av} = (V_e - V_0)/(V_t - V_0)$$

where V_e, V_0 and V_t represent solute elution volume, void volume and the total bed volume of fluid and gel combined, respectively. Blue Dextran 2000 (8.0 mg/ml) was employed as a marker of the void volume. V_0 was determined for all three buffers used: the relative standard deviation of V_0 was 0.75% ($n = 18$) when calculated from V_0 data acquired from all mobile phases investigated. V_t was calculated from the bed height and the inner diameter of the column. V_t was about 102 ml and the void fraction (V_0/V_t) was 0.34 for all packed columns.

Treatment of Superdex 75 prep grade after packing

The chemical stability of Superdex 75 prep grade was also studied by treating the gel after it had been packed in the column. One packed HR 16/50 column was

repeatedly treated with 0.1 *M* hydrochloric acid and another with 1.0 *M* sodium hydroxide solution. The solutions were pumped into the columns at a flow-rate of 1.0 ml/min for the acid and 0.67 ml/min for the sodium hydroxide solution. The flow was stopped when 100 ml had passed and after a specified time stated below and in Figs. 5 and 6 the gels were equilibrated with 0.02 *M* sodium phosphate buffer (pH 7.0) containing 0.3 *M* sodium chloride. A series of proteins, listed in Table II, were then injected onto the columns and the chromatographic behaviour was evaluated. The total time of exposure was 2 weeks, divided into 25 treatments of 4 h each, five treatments of 10 h, three of 24 h and finally two lasting 48 h. The chromatographic behaviour was tested after each treatment and the chromatographic procedure was the same as above except that 1.0 mg/ml of Blue Dextran 2000 was used as a V_0 marker. The number of plates (N) was determined by injection of 500 µl of 1% (v/v) acetone after each treatment. The retention volume (V_e) and the peak width at half-height ($w_{0.5}$) were used to calculate N [$N = 5.54 \cdot (V_e/w_{0.5})^2$].

RESULTS AND DISCUSSION

In gel filtration chromatography, the influence of mechanisms other than the size-separation mechanism is well documented. The most important non-size-related mechanisms are ion-exchange, ion-exclusion and hydrophobic interactions between the stationary phase and the sample molecules[7,8]. In addition, intramolecular electrostatic repulsive interactions[8] can also influence the separation behaviour of the sample molecule. Manipulation of these interactions by changing the mobile phase can increase selectivity in GFC. To test the extent of these separation mechanisms of Superdex 75 prep grade the influence of ionic strength on the K_{av} values of various proteins (Table I) was studied at different pH.

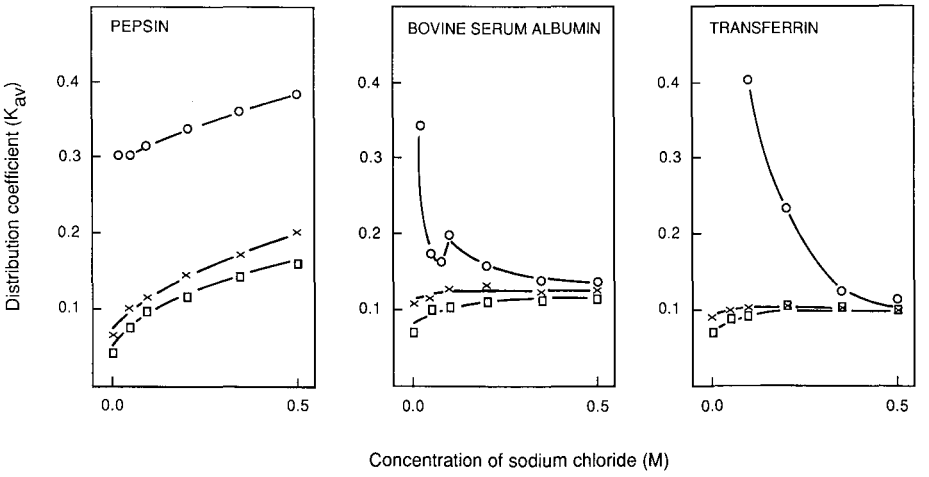

Fig. 1. Influence of sodium chloride on K_{av} of pepsin, bovine serum albumin and transferrin on untreated Superdex 75 prep grade with various mobile phase buffers. Mobile phases: ○ = 0.020 *M* acetate, pH 4.2; × = 0.020 *M* phosphate, pH 7.0; □ = 0.020 *M* carbonate, pH 10.0.

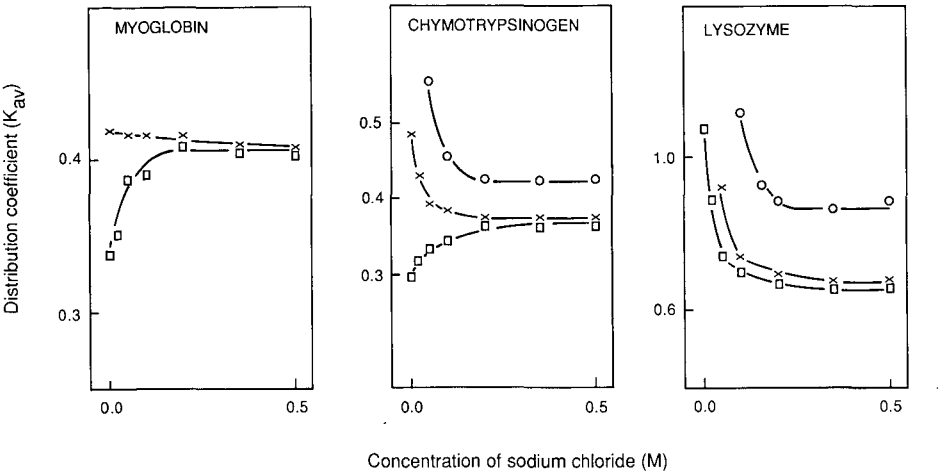

Fig. 2. Influence of sodium chloride on K_{av} of myoglobin, α-chymotrypsinogen and lysozyme on untreated Superdex 75 prep grade with various mobile phase buffers. Mobile phases: ○ = 0.020 *M* acetate, pH 4.2; × = 0.020 *M* phosphate, pH 7.0; □ = 0.020 *M* carbonate, pH 10.0.

Influence of ionic strength and pH on the performance of Superdex 75 prep grade

Figs. 1 and 2 show that the K_{av} values of the six investigated proteins were strongly influenced by the pH and the ionic strength of the mobile phase buffers used.

Pepsin. The increase in the K_{av} value of pepsin with increasing ionic strength at pH 10.0 and 7.0 (Fig. 1) is probably related to a decreasing ion-exclusion effect. This interpretation is supported by the fact that dextran and agarose gels contain small amounts of carboxyl groups[2,9] which are negatively charged at pH 7.0 and 10.0 [like pepsin (p*I* = 2.9)]. However, at pH 4.2 pepsin and Superdex 75 prep grade are charged to a lesser extent because the acid groups are ionized to a lower degree. The much higher K_{av} values observed at pH 4.2 than at pH 7.0 and 10.0 indicate that ion-exclusion effects did not influence the result to a great extent. Therefore, the increase in K_{av} with increasing ionic strength at pH 4.2 is probably related to hydrophobic interations. Such interactions between dextran-based gels and pepsin have been observed previously at acidic pH values[6].

Bovine serum albumin (BSA). Ion exclusion seems to influence significantly the K_{av} value of BSA only at low ionic strenght at pH 10.0 (Fig. 1). This may be attributed to the higher p*I* value of BSA compared with pepsin (Table I). Minimal interactions between Superdex 75 prep grade and BSA occurred at pH 7.0 and 10.0 at [NaCl] > 0.2 *M*, according to the K_{av} plateau (0.11). On the other hand, at pH 4.2, where BSA has a positive net charge, the results in Fig. 1 suggest that several non-size-related mechanisms are involved. Ion exchange between the positively charged BSA and anionic groups on Superdex 75 prep grade explains why K_{av} increases with decreasing ionic strength. In addition, it is known that BSA molecules expand in acidic solutions because of intramolecular repulsive interactions[10,11]. These interactions are most pronounced at low ionic strength and will be superimposed on the ion-exchange mechanism. The molecular expansion counteracts the ion-exchange effect and can therefore explain the decrease in K_{av} of BSA at about 0.05 *M* NaCl (Fig. 1).

Transferrin. In contrast to BSA, no effects from intramolecular interactions were observed for transferrin. However, like BSA, both ion exclusion and ion exchange influenced the retention time of transferrin (Fig. 1). Ion-exchange interactions affect the retention of transferrin more than for BSA because of the higher p*I* value of transferrin (Table I).

Myoglobin. The effect of ionic strength on the K_{av} of myoglobin at pH 10.0 is caused by ion-exclusion interaction, as discussed previously for pepsin, BSA and transferrin (Figs. 1 and 2). No significant trend of the retention of myoglobin was observed at pH 7.0 (Fig. 2), indicating that only an ideal size separation mechanism is involved. In the acidic mobile phase buffer myoglobin was denatured and precipitated in the column top filter.

Chymotrypsinogen. The high p*I* value of chymotrypsinogen means that it is positively charged at pH < 8.8. The increasing K_{av} value of chymotrypsinogen with decreasing ion strength at pH 4.2 and 7.0 (Fig. 2) is therefore attributed to an ion-exchange mechanism. The K_{av} plateau at pH 4.2 is higher compared with the K_{av} plateau at pH 7.0 (Fig. 2). This indicates an increasing hydrophobic interaction superimposed on a decreasing ion-exchange interaction when the sodium chloride concentration increases from 0.2 to 0.5 *M* at pH 4.2. The ideal K_{av} value of chymotrypsinogen is probably about 0.37, as the K_{av} plateaux at pH 7.0 and 10.0 merge at this value when [NaCl] > 0.2 *M*. However, at low ionic strength at pH 10 chymotrypsinogen is excluded from the pores because of electrostatic repulsion between the protein and the negatively charged Superdex 75 prep grade.

Lysozyme. Fig. 2 shows that the K_{av} of lysozyme increases with decreasing ionic strength for all the mobile phase buffers used. As lysozyme is positively charged at pH < 11 (Table I) and Superdex 75 prep grade is negatively charged at pH $>$ *ca.* 4, ion exchange can explain this behaviour. The levels of the K_{av} plateaux at [NaCl] > 0.4 *M* are much higher for all investigated buffers than could be expected from the molecular weight of lysozyme alone. It has been shown[12] that lysozyme exhibits a strong hydrophobic nature. Therefore we postulate that hydrophobic interactions also contribute to the retardation of lysozyme at high ionic strengths. Fig. 2 indicates that these interactions are highest at pH 4.2.

Chemical stability of Superdex 75 prep grade during long-term incubation at pH 2 and 13

The chromatographic behaviour of six proteins (Table I) on Superdex 75 prep grade treated with 0.01 *M* hydrochloric acid or 0.1 *M* sodium hydroxide solution for 14 days is shown in Figs. 3 and 4. Fig. 3 and 4 show that the K_{av} values of the proteins are influenced by the ionic strength in the same way on untreated and on acid- and base-treated Superdex 75 prep grade. This similiar behaviour indicates that no charged groups were formed on Superdex 75 prep grade during long-term incubation at pH 2 or 13. On the other hand the K_{av} values obtained after acid or base treatment of the gel are about 0.05 units higher than for the untreated Superdex 75 prep grade (Figs. 3 and 4). These results can be explained if the available pore volume has increased after the long-term incubation (see also the next section). Superdex 75 prep grade consists of spherical agarose beads to which dextran has been covalently bonded. Therefore, an increase in the available pore volume of Superdex 75 prep grade can be caused by a certain breakdown of dextran. The observed release of dextran at pH 2 and 13, verified with an immunochemical method[13], proves that dextran decomposes. This

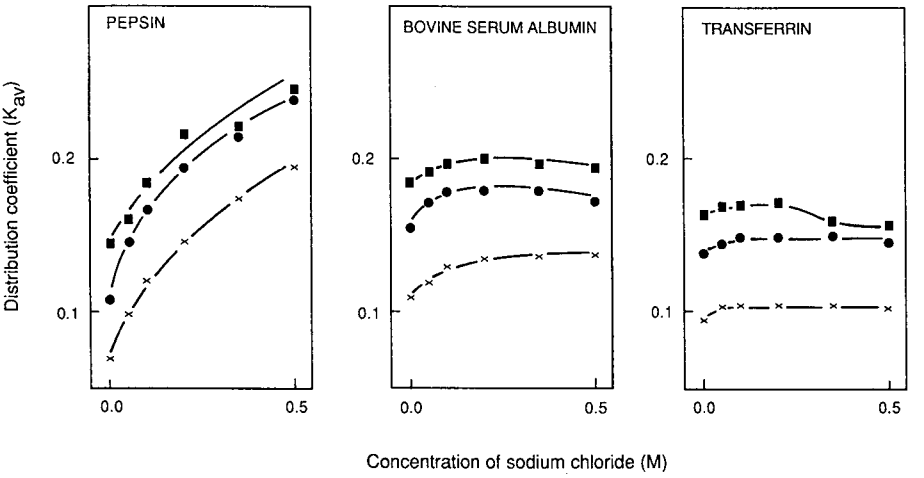

Fig. 3. Influence of sodium chloride on K_{av} of pepsin, bovine serum albumin and transferrin on (×) untreated, (●) acid-treated and (■) base-treated Superdex 75 prep grade. The mobile phase was 0.020 *M* phosphate (pH 7.0).

leakage will be investigated more carefully in a forthcoming study. Figs, 3 and 4 also show that the changes in available pore volume were higher after incubation at pH 13 than at pH 2.

Chemical stability of Superdex 75 prep grade with repeated column washes at pH 1 and 14

Cleaning procedures for prepacked gel filtration columns normally consist of rinsing with sodium hydroxide solution or hydrochloric acid. For example, cleaning-

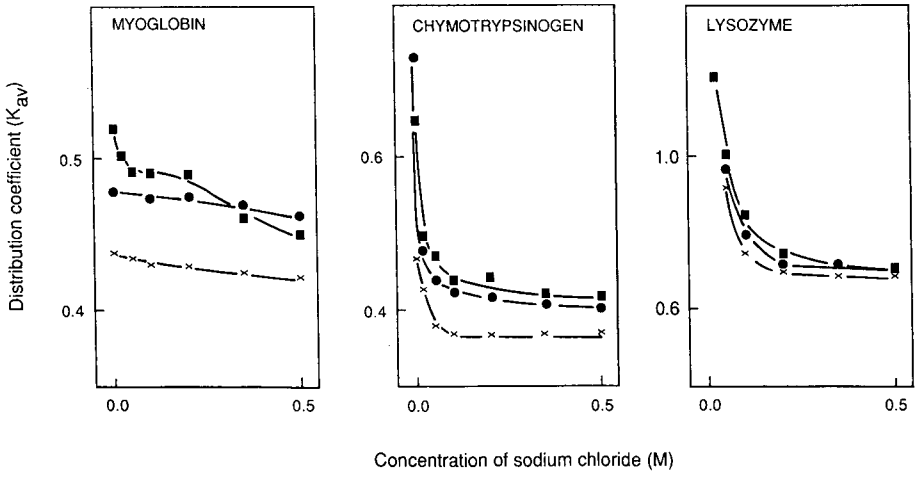

Fig. 4. Influence of sodium chloride on K_{av} of myoglobin, α-chymotrypsinogen and lysozyme on (×) untreated, (●) acid-treated and (■) base-treated Superdex 75 prep grade. The mobile phase was 0.020 *M* phosphate (pH 7.0).

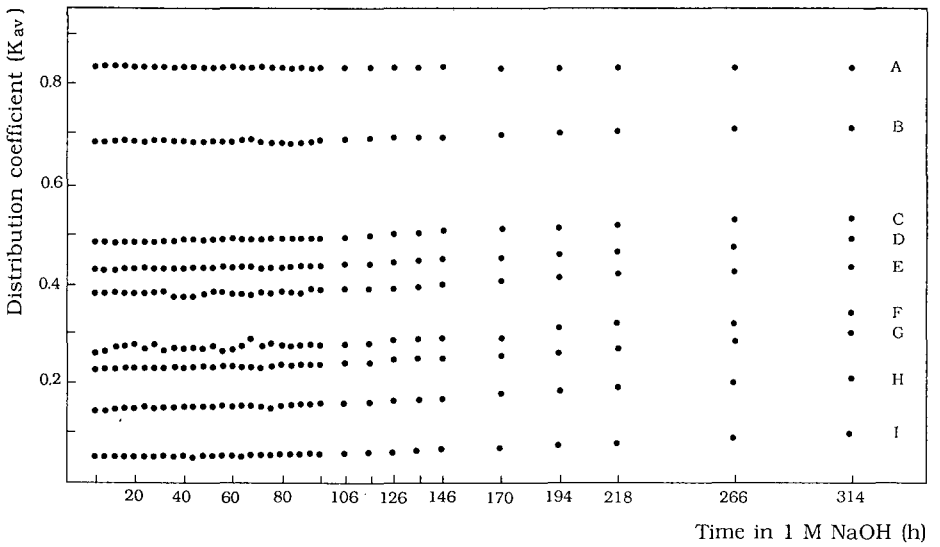

Fig. 5. Influence of repeated CIP treatments with 1.0 *M* NaOH on the distribution coefficients of a series of proteins (Table II) on Superdex 75 prep grade in an HR 16/50 column.

in-place (CIP) with 1.0 *M* sodium hydroxide for *ca.* 2 h is a very effective means of removing bacterial contamination from the purification system[14]. Therefore it is very important that a liquid chromatographic medium intended for purification of biomolecules can withstand many short-term treatments at extreme pH values.

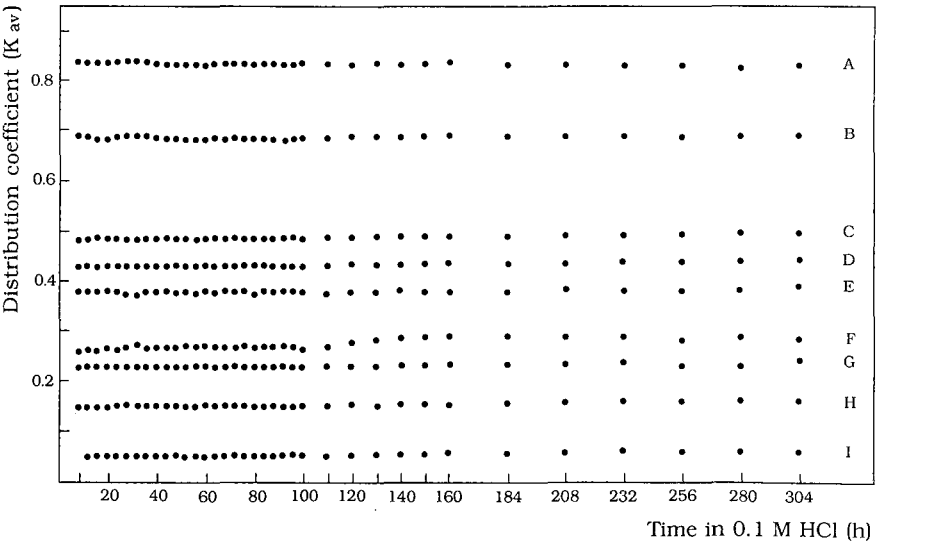

Fig. 6. Influence of repeated CIP treatments with 0.1 *M* HCl on the distribution coefficients of a series of proteins (Table II) on Superdex 75 prep grade in an HR 16/50 column.

The change in the K_{av} values of eight different proteins (Table II) after repeated short-term treatments of two Superdex 75 prep grade columns with 1.0 *M* sodium hydroxide solution and 0.1 *M* hydrochloric acid is shown in Figs. 5 and 6, respectively. A slight and gradual increase in retention volume was observed for all proteins in CIP with 1.0 *M* sodium hydroxide solution (Fig. 5). This trend increased when the washing time was prolonged. It can also be noted that the K_{av} of cytidine and V_0 (determined using Blue Dextran) were not influenced by the washing procedure. These results can be rationalized if the pore volume is constant and the available pore volume for protein molecules increases after the gel has been treated with 1.0 *M* sodium hydroxide solution. Partial breakdown of dextran (as suggested in the previous section) in the agarose pores at extreme pH values can cause such an effect on the separation behaviour. The total increase in the K_{av} values of the proteins after repeated washings with 1.0 *M* sodium hydroxide solution resulting in a total contact time of 14 days was in the range 0.04–0.09 (Fig. 5). This increase can be compared with the long-term treatment of the medium at pH 13 (experiments before packing reported in Figs. 3 and 4). Even though the pH value in the long-term treatment experiments was one unit lower, th K_{av} values of the proteins increased as much as for the total increase in the repeated washes experiments. The cause of these results has not been elucidated but may be attributed to the catalytic action of a hydrolysis product of dextran or the decomposition of dextran being independent of the sodium hydroxide concentration in the range investigated.

The results obtained after repeated column washes with 0.1 *M* hydrochloric acid (Fig. 6) show that the increase in the K_{av} values of the proteins was less than with 1.0 *M* sodium hydroxide solution (Fig. 5). However, long-term treatment with 0.01 *M* hydrochloric acid (pH 2) resulted in about the same effect on the K_{av} values (Figs. 3 and 4) as the total effect observed in the repeated CIP treatments with 0.1 *M* hydrochloric acid (Fig. 6). This effect can probably be explained similarly to for the results at high pH (see above).

The number of plates per metre for both columns were randomly varied between 13 500 and 16 500 during the tests. Further, the bed heights and the column back-pressure were constant throughout the experiments. The results indicate that the rigidity of Superdex 75 prep grade was unchanged after repeated CIP cycles with 0.1 *M* hydrochloric acid and 1.0 *M* sodium hydroxide solution.

CONCLUSION

The objectives of this work were to investigate the interactions of various proteins with the gel filtration medium Superdex 75 prep grade and to investigate the chemical stability of the gel.

It was shown that the presence of negatively charged groups on Superdex 75 prep grade can explain the electrostatic characteristics of the gel at low ionic strengths of the mobile phase. Ideal gel filtration chromatography was observed for proteins with intermediate p*I* values (5–9) using mobile phases of pH 7.0 and 10.0 at sodium chloride concentrations higher than about 0.2 *M*. In addition, the results obtained with lysozyme and chymotrypsinogen at acidic pH also show that Superdex 75 prep grade has hydrophobic properties at high ionic strengths.

The study of the chemical resistance of Superdex 75 prep grade shows that

dextran in the agarose pores was partly hydrolysed under extreme acidic and basic conditions. Nevertheless, a column packed with Superdex 75 prep grade can withstand at least 25 CIP cycles with 1.0 *M* sodium hydroxide solution or 0.1 *M* hydrochloric acid (contact time 4 h for each) without any significant change in separation performance.

REFERENCES

1 J.-C. Janson, *Chromatographia*, 23 (1987) 361.
2 L. Fischer, in T. S. Work and R. H. Burdon (Editors), *Laboratory Techniques in Biochemistry and Molecular Biology, Gel Filtration Chromatography*, Elsevier, Amsterdam, 1980, pp. 24–54.
3 L. Hagel, in P. L. Dubin (Editor), *Aqueous Size-Exclusion Chromatography*, Elsevier, Amsterdam, 1988, pp. 120–121.
4 *Data File 3020*, Pharmacia LKB Biotechnology, Uppsala, 1989.
5 L. Kågedal, H. Ellergren, B. Engtröm, A.-K. Lieber, H. Lundström, A. Persson and M. Schenning, *J. Chromatogr.*, submitted for publication.
6 B.-L. Johansson and J. Gustavsson, *J. Chromatogr.*, 457 (1988) 205.
7 P. L. Dubin, in P. L. Dubin (Editor), *Aqueous Size-Exclusion Chromatography*, Elsevier, Amsterdam, 1988, pp. 55–75.
8 H. G. Barth, *J. Chromatogr. Sci.*, 18 (1980) 409.
9 H. D. Crone, *J. Chromatogr.*, 92 (1974) 127.
10 K. Aoki and J. F. Forster, *J. Am. Chem. Soc.*, 79 (1957) 3385.
11 C. Tanford, J. G. Buzzel, D. G. Rands and S. A. Swanson, *J. Am. Chem. Soc.*, 77 (1955) 6421.
12 D. E. Schmidt, R. W. Giese, D. Conron and B. L. Karger, *Anal. Chem.*, 52 (1980) 177.
13 K. Hellsing and W. Richter, *J. Immunol. Methods*, 5 (1974) 147.
14 S. Yamamoto, K. Nakanihi and R. Matsuno, *Ion-Exchange Chromatography of Proteins*, Marcel Dekker, New York, Basle, 1988, p. 327.

Journal of Chromatography, 514 (1990) 147–159
Elsevier Science Publishers B.V., Amsterdam

CHROM. 22 514

Optical resolution of flavanones by high-performance liquid chromatography on various chiral stationary phases

MARTIN KRAUSE and RUDOLF GALENSA*
Institut für Lebensmittelchemie der Technischen Universität Braunschweig, Pockelsstr. 4, 3300 Braunschweig (F.R.G.)
(First received December 28th, 1989; revised manuscript received April 19th, 1990)

ABSTRACT

Six commercially available chiral stationary phases [Chiralcel OD, Chiralpak OP (+), ChiraSpher, Cyclobond I, acetylated Cyclobond I and Cyclobond II) were evaluated for the high-performance liquid chromatographic separation of flavanone, six monosubstituted flavanones and one disubstituted flavanone. At least some of the flavanones were resolved on each column, except on Cyclobond II. For the β-cyclodextrin stationary phases possible inclusion phenomena are discussed.

INTRODUCTION

The flavanones naringenin (5,7,4′-trihydroxyflavanone) and eriodictyol (5,7,3′,4′-tetrahydroxyflavanone) are central intermediates in the biosynthesis of flavonoids[1]. A large number of flavanones have been isolated as secondary plant metabolites, many of them in an optically active form[2]. However, there are many reports that do not comment on the stereochemistry of flavanones.

Of primary interest to us was the development of a high-performance liquid chromatographic (HPLC) method to determine flavanone enantiomers in plant extracts, *i.e.*, to gain information about the optical purity of flavanones without isolating them. It has been demonstrated for a flavanoneglycoside (naringin) by NMR that racemization of the aglycone occurred during maturation[3].

Chalcones, which also have been reported as natural products[4], are isomeric forms of the flavanones. Some chalcones cyclize spontaneously in aqueous medium in a pH-dependent reaction to racemic flavanones[5]. Stereochemical investigations therefore may be helpful in deciding whether chalcones or the corresponding flavanones were originally accumulated in plant cells.

During our search for a suitable HPLC column we tested many chiral stationary phases (CSP) with a series of different flavanones. We did not find a CSP for the resolution of all flavanones. Polyhydroxylated flavanones were separated on microcrystalline cellulose triacetate[6] or cellulose triacetate supported on silica gel diol[7]. In this paper we report the enantiomeric separation of flavanones with a low degree of

0021-9673/90/$03.50

substitution (hydroxyl or/and methoxyl groups) by HPLC on five CSPs. The parent compound flavanone also has been resolved on various cellulose- and amylose-carbamate CSPs by Okamoto and co-workers[8–11] and several 3-hydroxyflavanones[12] and a biflavanone[13] on Chiralpak OT (+).

EXPERIMENTAL

Materials

Flavanones (Fig. 1) were purchased from Roth (Karlsruhe, F.R.G.) and methanol, 2-propanol (HPLC grade), *n*-hexane, dioxane and *tert.*-butyl methyl ether (analytical-reagent grade) from Baker (Gross-Gerau, F.R.G.).

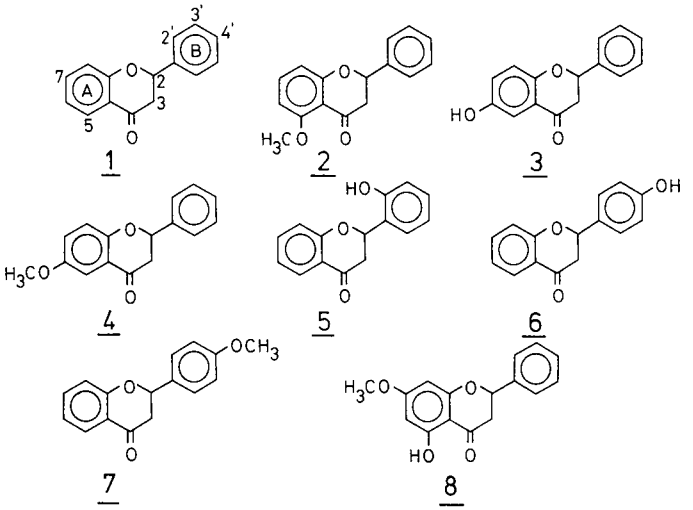

Fig. 1. Structures of flavanones tested. 1 = Flavanone; 2 = 5-methoxyflavanone; 3 = 6-hydroxyflavanone; 4 = 6-methoxyflavanone; 5 = 2′-hydroxyflavanone; 6 = 4′-hydroxyflavanone; 7 = 4′-methoxyflavanone; 8 = pinostrobin (5-hydroxy-7-methoxyflavanone).

HPLC

The HPLC apparatus used consisted of a gradient system from Beckman (Munich, F.R.G.) with two pumps (114 M) and a high-pressure mixing chamber, a sampling valve (Altex 210; Beckman) equipped with a 20-μl sample loop and a Pye Unicam variable-wavelength UV detector set at 254 nm (Philips, Kassel, F.R.G.). The results were recorded with an integrator (3390 A from Hewlett-Packard, Waldbronn, F.R.G. or C-R6A from Shimadzu, Duisburg, F.R.G.) or a video chromatographic control center (Pye Unicam 4850; Philips).

Chromatography was performed at ambient temperature unless specified otherwise. The column temperatures were adjusted, if necessary, with a column oven from Techlab (Erkerode, F.R.G.).

Some of the results were monitored with a polarimetric detector (Chiramonitor 750/25) from ACS (Macclesfield, U.K.), supplied by Zinsser (Frankfurt, F.R.G.).

Columns

The following columns were used:

Chiralcel OD (250 × 4.6 mm I.D.), 10 μm (Daicel, Baker);

Chiralpak OP (+) (250 × 4.6 mm I.D.), 10 μm (Daicel, Baker);

ChiraSpher (250 × 4.0 mm I.D.), 5 μm (Merck, Darmstadt, F.R.G.);

Cyclobond I (β-cyclodextrin) (250 × 4.6 mm I.D.), 5 μm (ASTEC; ICT, Frankfurt, F.R.G.);

Acetylated Cyclobond I (250 × 4.6 mm I.D.), 5 μm (ASTEC; ICT);

Cyclobond II (γ-cyclodextrin) (250 × 4.6 mm I.D.), 5 μm (ASTEC, ICT).

RESULTS AND DISCUSSION

Chiralcel OD

This chiral stationary phase consists of macroporous silica gel coated with cellulose tris(3,5-dimethylphenylcarbamate) (Fig. 2). Okamoto and co-workers[8–11] reported only the separation of flavanone on various cellulose- and amylose-derived CSPs. Table I shows that Chiralcel OD is capable of resolving many other substituted flavanones. Of the 8 flavanones studied (Fig. 1), only 4′-hydroxyflavanone is not separated, not even partially, as monitored with a polarimetric detector. The first-eluted enantiomer of the other seven flavanones is always leavorotatory.

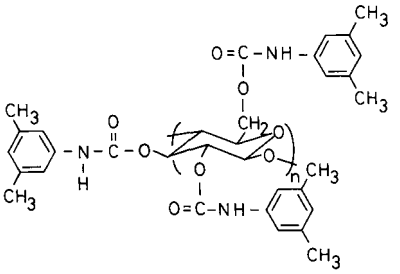

Fig. 2. Structure of Chiralcel OD [cellulose tris(3,5-dimethylphenylcarbamate)].

TABLE I

ENANTIOMERIC SEPARATION OF FLAVANONES ON CHIRALCEL OD

Mobile phase, *n*-hexane–2-propanol (90:10, v/v); flow-rate, 1 ml/min. k'_1 = Capacity factor of the first-eluted enantiomer as indicated; α = separation factor.

Compound	k'_1	α
Flavanone	1.34 (−)	1.49
5-Methoxy-	2.90 (−)	1.37
6-Hydroxy-	2.56 (−)	1.16
6-Methoxy-	1.62 (−)	1.29
2′-Hydroxy-	1.76 (−)	1.23
4′-Hydroxy-	4.99	1.00
4′-Methoxy-	1.85 (−)	1.25
Pinostrobin	1.96 (−)	1.60

Substituted flavanones have larger k' values than flavanone. The influence of a hydroxyl group on the retention behaviour is different depending on its position; 6- and 4'-hydroxyflavanones ($k' = 2.56$ and 4.99, respectively) are more retained than 2'-hydroxyflavanone ($k' = 1.76$) or pinostrobin (5-hydroxy-7-methoxy-) ($k' = 1.96$). The capacity factors of the hydroxy-substituted flavanones are larger in the pairs 6-hydroxy–6-methoxyflavanone and 4'-hydroxy–4'-methoxyflavanone, but the enantioselectivity decreases for 6-hydroxy- and is lost for 4'-hydroxyflavanone. It seems that hydrogen bonding between the hydroxyl groups of the flavanones and the carbamate function of the CSP hinders chiral recognition in these instances. Pinostrobin (with a hydroxyl group in the 5-position, $\alpha = 1.60$), on the other hand, is better resolved than flavanone ($\alpha = 1.49$). With pinostrobin intramolecular hydrogen bonding between the 5-hydroxy and the carbonyl groups is also possible. Other polyhydroxylated flavanones such as naringenin (5,7,4'-trihydroxyflavanone) were not resolved on this column without derivatization. However, the separation of naringenin tribenzoate was possible, indicating that hydroxyl groups of the solutes hinder chiral recognition.

In conclusion, Chiralcel OD is a CSP with relatively high separation factors for many flavanones. Fig. 3 demonstrates the resolution of pinostrobin with *n*-hexane–2-propanol (90:10) as the mobile phase.

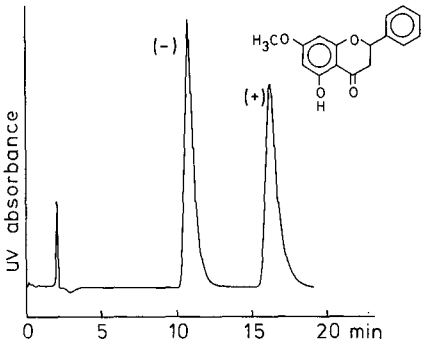

Fig. 3. Enantiomeric separation of pinostrobin on Chiralcel OD with *n*-hexane–2-propanol (90:10) at 1 ml/min as the mobile phase.

Chiralpak OP (+)

Chiralpak OP (+) is based on macroporous silica gel coated with poly(diphenyl 2-pyridylmethylmethacrylate). This type of CSP is chiral only due to its helicity[14], as shown in Fig. 4. As demonstrated in Table II, the chromatographic behaviour of four flavanones was studied. The polar modifier plays an important role in the separation process. *n*-Hexane–2-propanol (95:5) resulted in separation factors between 1.09 and 1.22. Small amounts of methanol in the mobile phase (eluent B) decrease the capacity factors and enantioselectivity is observed only for 5-methoxyflavanone. On the other hand, increasing the concentration of 2-propanol to 50% (eluent C) decreases the capacity factors even more but, except for 4'-methoxyflavanone, a separation is achieved. It seems that with apolar eluents polar interactions between the chiral

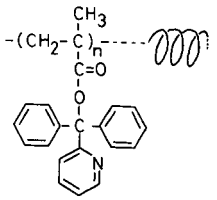

Fig. 4. Structure of Chiralpak OP (+) [poly(diphenyl 2-pyridylmethylmethacrylate)].

TABLE II

SEPARATION OF RACEMIC FLAVANONES ON CHIRALPAK OP (+)

Mobile phases: A = *n*-hexane–2-propanol (95:5, v/v); B = *n*-hexane–methanol–2-propanol (95:5:2.5, v/v/v); C = *n*-hexane–2-propanol (50:50, v/v); D = methanol. Flow-rate, 1 ml/min; temperature, 5°C.

Compound	*Mobile phase*							
	A		*B*		*C*		*D*	
	k'_1	α	k'_1	α	k'_1	α	k'_1	α
Flavanone	4.19	1.14	3.56	1.00	2.48	1.07	3.45	1.14
5-Methoxy-	8.46	1.22	4.99	1.07	2.23	1.20	1.28	1.00
6-Methoxy-	4.87	1.11	3.56	1.00	2.55	1.12	2.09	1.00
4'-Methoxy-	5.66	1.09	3.39	1.00	2.57	1.00	1.16	1.00

polymer and the solutes are important for the recognition process, although a general rule cannot be derived from the results obtained. With methanol as eluent flavanone is most retained (probably owing to a non-polar interaction) and a separation (α = 1.14) is also possible.

In general, the resolving power and efficiency of this CSP is not as good as those of Chiralcel OD. The elution order has only been determined for flavanone, as shown in Fig. 5.

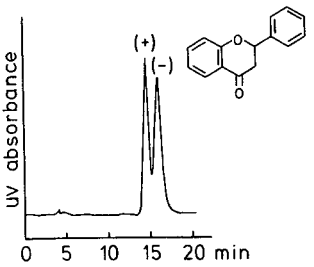

Fig. 5. Optical resolution of flavanone on Chiralpak OP (+) with *n*-hexane–2-propanol (95:5) at 1 ml/min as the mobile phase at 5°C.

ChiraSpher

In contrast to the above two CSPs, ChiraSpher is based on small-pore silica gel (pore size 10 nm). The chiral polymer [poly-N-acryloyl-(*S*)-phenylalanine ethyl ester] (Fig. 6) is fixed on the silica gel by an *in situ* polymerization procedure[15]. Table III illustrates that all flavanones were resolved (at least partially) on this CSP. The hydroxylated flavanones are much more retained than the methoxylated type (except pinostrobin) and therefore the eluents were not the same. Small amounts of dioxane in *n*-hexane (eluent A) as polar modifier resulted in a separation of flavanone and 6-methoxy- and 4'-methoxyflavanone (5-methoxyflavanone was not eluted within 30 min). The same separation factor as with eluent A was observed for flavanone and 6-methoxyflavanone with *n*-hexane–2-propanol (98:2) (eluent B), whereas α decreased slightly for 4'-methoxyflavanone. The capacity factor for 5-methoxyflavanone (k' = 5.33) was much higher than those for the other methoxyflavanones.

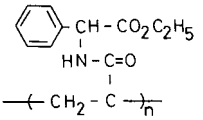

Fig. 6. Structure of ChiraSpher [poly-N-acryloyl-(*S*)-phenylalanine ethyl ester].

The hydroxylated flavanones were analysed with a mobile phase containing a larger amount of 2-propanol [*n*-hexane–2-propanol (90:10) (eluent C)]. Pinostrobin was eluted relatively fast (k' = 1.65) compard with 6-hydroxy- (k' = 5.37), 2'-hydroxy- (k' = 6.06) and 4'-hydroxyflavanone (k' = 13.09). Hydrogen bonding between the

TABLE III

OPTICAL RESOLUTION OF FLAVANONES ON CHIRASPHER

Mobile phases: A = *n*-hexane–dioxane (96:4, v/v); B = *n*-hexane–2-propanol (98:2, v/v); C = *n*-hexane–2-propanol (90;10, v/v). Flow-rate, 0.5 ml/min.

Compound	k'_1	α	*Mobile phase*
Flavanone	2.46 (+)	1.07	A
	1.48	1.07	B
5-Methoxy-	5.33	1.03	B
6-Hydroxy-	5.37 (+)	1.03	C
6-Methoxy-	4.12 (+)	1.07	A
	1.83	1.07	B
2'-Hydroxy-	6.06 (+)	1.04	C
4'-Hydroxy-	13.09 (+)	1.04	C[a]
4'-Methoxy-	3.13 (+)	1.07	A
	2.53	1.05	B
Pinostrobin	1.65 (+)	1.03	C

[a] Flow-rate 1 ml/min.

hydroxyl group of the flavanones and the amide and/or ester group of the stationary phase seems to be responsible for the strong retention of these compounds, with the exception of pinostrobin. The latter deviation may be due to intramolecular hydrogen bonding of the hydroxyl group to the keto group of pinostrobin.

The reason for the observed large differences in retention behaviour between the positional isomers 5-methoxy- and 6-methoxyflavanone and 2′-hydroxy- and 4′-hydroxyflavanone may be attributed to different tight fits in the cavities of the polymer of the CSP.

Although this type of CSP was regarded as most suitable for the resolution of polar racemates[15], no separation of polyhydroxylated flavanones such as naringenin (5,7,4′-trihydroxyflavanone) or naringenin tribenzoate was achieved.

A good resolution can be achieved for several flavanones in a single chromatographic run with *n*-hexane-dioxane (100:4) as the mobile phase owing to the high efficiency of the column, as shown in Fig. 7. Other polar modifiers such as *tert.*-butyl methyl ether were also tested with good results.

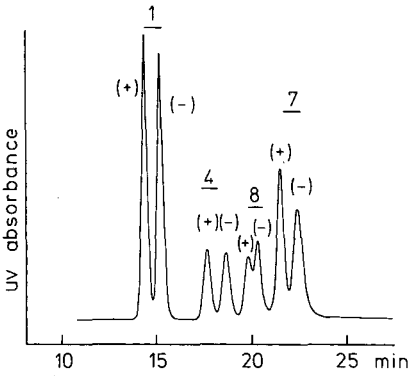

Fig. 7. Enantiomeric separation of flavanones on ChiraSpher with *n*-hexane–dioxane (100:4) at 1 ml/min as the mobile phase. For peak identification, see Fig. 1.

Cyclobond I

Cyclodextrins are cyclic glucoamyloses which have the form of a truncated cone. In the presence of water the cavity is relatively hydrophobic and lipophilic molecules or parts of a molecule can form inclusion complexes[16]. When enantiomers form inclusion complexes and there are interactions between the chiral centre or substituents near the chiral centre with the mouth of the cyclodextrin cavity, chiral recognition may occur[17]. Most optical resolutions reported in the literature were performed with β-cyclodextrins either as mobile phase additives or bonded to silicagel as stationary phase[17–19]. Only a few enantiomeric separations with α- or γ-cyclodextrins have been described[20,21].

A molecule of the size of benzene, naphthalene or biphenyl fits in the cavity of the β-cyclodextrin. Better enantioselectivity has been observed for molecules with naphthalene or biphenyl moieties than for smaller molecules, because of the requirement for a "tight fit" between the hydrophobic part of a compound and the

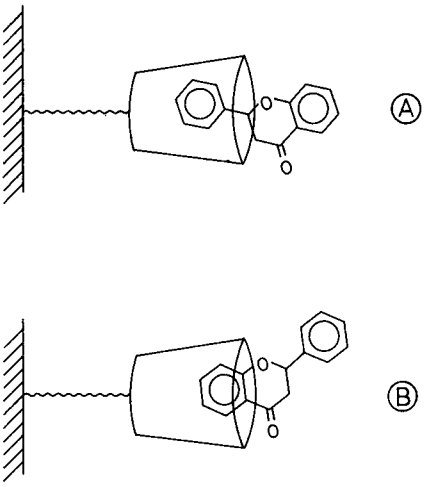

Fig. 8. Proposed inclusion orientations of flavanone in the β-cyclodextrin cavity: (A) inclusion of the phenyl group (ring A); (B) inclusion of ring B (see Fig. 1).

cyclodextrin cavity[17]. However, it was shown recently that single-ring compounds were resolved on β-cyclodextrin CSP when certain structural features are present[22].

Regarding the structure of the flavanones, an inclusion with the phenyl group (ring B) (Fig. 8A) or parts of the bicycle (ring A) (Fig. 8B) is possible. Recently the complexation of β-cyclodextrin with catechin and epicatechin, which have some structural similiarities with the flavanones, has been reported[23].

Table IV shows that inclusion with the β-cyclodextrin CSP also results in chiral discrimination for several flavanones. Compared with flavanone (k'_1 = 2.93) the introduction of a hydroxy group in 6- or 4'-position decreases the capacity factors (1.81; 1.93), which might be attributed to the higher polarity. 2'-Hydroxyflavanone (k'_1 = 2.54) is more strongly retained than 4'-hydroxyflavanone and the difference in

TABLE IV

ENANTIOMERIC SEPARATION OF FLAVANONES ON CYCLOBOND I (β-CYCLODEXTRIN)

Mobile phase, methanol–water (50:50, v/v); flow-rate, 1 ml/min.

Compound	k'_1	α	R_s
Flavanone	2.93 (−)	1.11	1.3
5-Methoxy-	1.78	1.00	–
6-Hydroxy-	1.81 (+)	1.11	1.2
6-Methoxy-	2.85 (−)	1.11	1.1
2'-Hydroxy-	2.54 (−)	1.33	3.5
4'-Hydroxy-	1.93	1.00	–
4'-Methoxy-	2.98 (−)	1.06	0.7
Pinostrobin	3.35[a]	[a]	[a]

[a] k' of the second peak; first peak eluted as a shoulder.

retention behaviour between 5-methoxyflavanone (k'_1 = 1.78) and 6-methoxyflavanone (k'_1 = 2.85) is also very large.

Regarding the chiral separations it is remarkable that 2'-hydroxyflavanone is best resolved (α = 1.33) and 4'-hydroxyflavanone not at all (not even with a larger amount of water in the mobile phase). 4'-Methoxyflavanone, on the other hand, is partially resolved. The reason for this behaviour is not clear. Maguire[24], in a study of hydantoin derivatives, observed that the introduction of a *p*-hydroxy group increased retention and separation factors. An inclusion of the *p*-hydroxyphenyl moiety of 4'-hydroxyflavanone with hydrogen bonding to the primary hydroxyl groups of the cyclodextrin molecule (as observed for the hydantoins) seems not to occur, because then the retention should also increase. Hydrogen bonding of the 4'-hydroxy group, however, may be one reason for the loss of enantioselectivity, because racemic 4'-methoxyflavanone is differentiated. Perhaps with 4'-hydroxyflavanone a different inclusion complex is formed.

It is further of interest that the elution order for 6-hydroxyflavanone [(+)- before (−)-enantiomer] is opposite to that for the other flavanones. 5-Methoxyflavanone is not separated, although a partial resolution was monitored with a polarimetric detector, also with the opposite elution order [(+)- before (−)-enantiomer].

The chiral recognition mechanism involving inclusion phenomena with Cyclobond I has been described in detail for several compounds[25]. One requirement is that inclusion occurs and that interaction with the rim of the cyclodextrin cavity can occur to result in chiral differentiation.

Both proposed inclusion orientations for the flavanones will probably contribute to the overall chromatographic behaviour. A definite recognition model cannot be derived from the results obtained. With the flavanones without B-ring oxygenation inclusion complex A (Fig. 8) seems more probable to be responsible for enantioselectivity because in complex B (Fig. 8) no polar groups are present at the phenyl group opposite the chiral centre to interact with the (polar) rim of the cyclodextrin cavity. Additionally, substituents in 5- and 6-positions may preclude full penetration of the A-ring of the flavanones into the cyclodextrin cavity. This may also limit the extent to wich complex B is involved in enantioselectivity. However, the difference in retention between 5-methoxyflavanone (k' = 1.78) and 6-methoxyflavanone (k' = 2.85) could also be explained by steric hindrance of 5-methoxyflavanone in complex B. The extent to which one of the complexes contributes to retention (achiral interaction) and enantioselectivity may be different for each flavanone.

Fig. 9 shows the influence of methanol concentration on the capacity factors for 2'-hydroxyflavanone. Up to a concentration of 80% methanol resolution is attained. The high separation factors may be due to rigid fixation of the B-ring with additional hydrogen bonding via the 2'hydroxy group in the β-cyclodextrin molecule (as in Fig. 8A), although the other orientation (as in Fig. 8B) may also explain the enantioselectivity. Neither interaction seems to be possible with the hydroxy group in the 4'-position.

Although the situation with the flavanones might be different, it should be noted that there is a carbonyl group opposite the chiral centre (on the other side of the phenyl group), a structural requirement which was thought to be important in resolving singel-ring compounds[22].

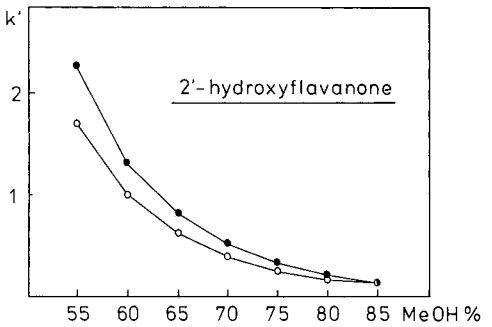

Fig. 9. Plot of methanol concentration in water against capacity factors (k') of 2'-hydroxyflavanone on Cyclobond I. Flow-rate, 1 ml/min. ○ = (−)-Enantiomer; ● = (+)-enantiomer.

Acetylated Cyclobond I

The mouth of the cyclodextrin molecule is extended by acetylating the 2-hydroxyl groups[19] and further binding sites are introduced. On bonded acetylated Cyclodextrin CSP (acetylated Cyclobond I) there have been only a few reports of enantiomeric separations[19,26,27]. Table V demonstrates that several flavanones were successfully resolved on this CSP, although the separation factors are smaller than with Cyclobond I. With the same eluent [methanol–water (50:50)] all capacity factors are higher than on Cyclobond I, which may be due to the increase in hydrophobicity. The most striking difference from Cyclobond I is that 5-methoxyflavanone is resolved, whereas 4'-methoxyflavanone is not. 5-Methoxy- and 6-hydroxyflavanone are eluted with the (+)-enantiomer first and flavanone and 6-hydroxy- and 2'-hydroxyflavanone are eluted with the opposite elution order [(−)- before (+)-enantiomer]. This behaviour is comparable to the situation on Cyclobond I (Table IV). Fig. 10 demonstrates that (except that the capacity factors are generally higher) the elution behaviour of 2'-hydroxyflavanone with respect to methanol concentration is similar to that with β-cyclodextrin (Fig. 9). Fig. 11 shows a chromatogram of 2'-hydroxy-

TABLE V

ENANTIOMERIC SEPARATION OF FLAVANONES ON ACETYLATED CYCLOBOND I (ACETYLATED β-CYCLODEXTRIN)

Mobile phase, methanol–water (50:50, v/v); flow-rate, 1 ml/min.

Compound	k'_1	α	R_s
Flavanone	4.40 (−)	1.07	0.7
5-Methoxy-	3.05 (+)	1.07	0.6
6-Hydroxy-	3.55 (+)	1.08	0.8
6-Methoxy-	5.00 (−)	1.06	0.7
2'-Hydroxy-	3.61 (−)	1.25	2.3
4'-Hydroxy-	3.22	1.00	–
4'-Methoxy-	5.11	1.00	–
Pinostrobin	7.06[a]	[a]	[a]

[a] k' of the second peak; first peak eluted as a shoulder.

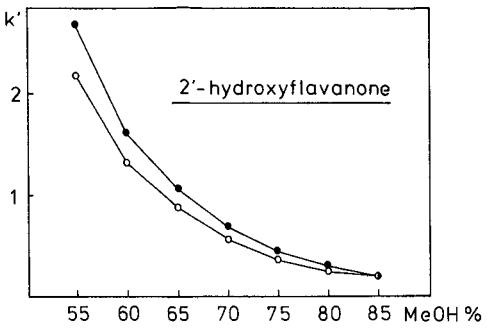

Fig. 10. Plot of methanol concentration in water against capacity factors (k') of 2'-hydroxyflavanone on acetylated Cyclobond I. Flow-rate, 1 ml/min. ○ = (−)-Enantiomer; ● = (+)-enatiomer.

flavanone separated on acetylated Cyclobond I with (a) UV and (b) polarimetric detection.

The inclusion phenomena are thought to be similar to those discussed for native β-cyclodextrin. Although the flavanones are more retained than on Cyclobond I, a decrease in the separation factors of the enantiomers (with the exception of 5-methoxyflavanone) is observed. The increase in retention may be due mainly to the increase in hydrophobicity of the CSP and not to a tighter fit of the solutes in the acetylated cyclodextrin cavity. The reduction of the hydrogen bonding sites of the cyclodextrin or steric reasons (acetoxy groups) may be responsible for the decrease in enantioselectivity. It has also been reported that acetylation of β-cyclodextrin enhanced (with one exception) the separation of dansylamino acid enantiomers[27].

Except for 5-methoxyflavanone, it can be concluded that the acetylated form of β-cyclodextrin results in a poorer resolution than β-cyclodextrin.

γ-Cyclodextrin has eight glucose units and the cavities are larger than those in β-cyclodextrin. With Γ-cyclodextrin bonded CSP (Cyclobond II) no enantiomeric separation was observed with UV detection, as demonstrated in Table VI. Although

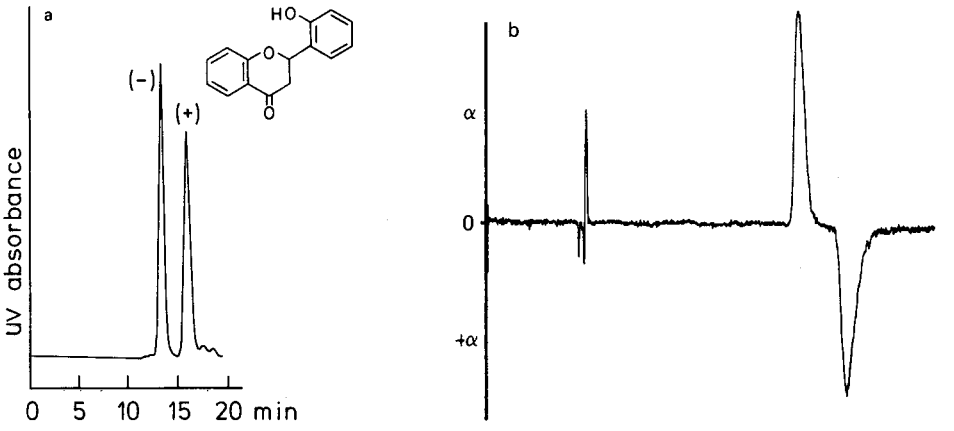

Fig. 11. Enantiomeric separation of 2'-hydroxyflavanone on acetylated Cyclobond I with methanol–water (50:50) at 1 ml/min as the mobile phase. (a) UV detection; (b) polarimetric detection.

TABLE VI

RETENTION BEHAVIOUR OF FLAVANONES ON CYCLOBOND II (γ-CYCLODEXTRIN)

Mobile phase, methanol–water (40:60, v/v); flow-rate, 1 ml/min.

Compound	*k'*	*Compound*	*k'*
Flavanone	1.70	2-Hydroxy-	1.56
5-Methoxy-	1.55	4'-Hydroxy-	1.05
6-Hydroxy-	1.19	4'-Methoxy-	1.68
6-Methoxy-	1.65	Pinostrobin	2.28

complexation is also possible with γ-cyclodextrin, the large cavity probably includes the whole molecule, not differentiating between the enantiomers. Capacity factors between Cyclobond I and II cannot be compared directly because the amounts of cyclodextrin bonded to the silica gel are different[28]. It is interesting, however, that the difference in the capacity factors of 5- and 6-methoxyflavanone is very small compared with the situation on β-cyclodextrin.

In conclusion, various chiral stationary phases can be used to resolve flavanones with a low degree of substitution. Except for ChiraSpher, not all of the tested flavanones were separated on each column. Minor structural changes can greatly affect enantioselectivity and resolution.

ACKNOWLEDGEMENTS

We thank Fa. Zinsser (Frankfurt, F.R.G.) for cooperation.

REFERENCES

1 W. Heller and G. Forkman, in J. B. Harborne (Editor), *The Flavonoids, Advances in Research*, Chapman & Hall, London and New York, 1988, pp. 399–422.
2 H. Arakawa and M. Nakazaki, *Justus Liebigs Ann. Chem.*, 636 (1960) 111.
3 W. Gaffield, R. E. Lundin, B. Gentili and R. M. Horowitz, *Bioorg. Chem.*, 4 (1975) 259.
4 B. A. Bohm, in J. B. Harborne (Editor), *The Flavonoids, Advances in Research*, Chapman & Hall, London and New York, 1988, pp. 329–340.
5 J. N. M. Mol, M. P. Robbins, R. A. Dixon and E. Veltkamp, *Phytochemistry*, 24 (1985) 2267.
6 M. Krause and R. Galensa, *J. Chromatogr.*, 441 (1988) 417.
7 M. Krause and R. Galensa, *J. Chromatogr.*, 502 (1990) 287.
8 Y. Okamoto, R. Aburatani, S.-I. Miura and K. Hatada, *J. Liq. Chromatogr.*, 10 (1987) 1613.
9 Y. Okamoto, M. Kawashima and K. Hatada, *J. Chromatogr.*, 363 (1986) 173.
10 Y. Okamoto, R. Aburatani, T. Fukumoto and K. Hatada, *Chem. Lett.*, (1987) 1857.
11 Y. Okamoto, H. Sakamoto, K. Hatada and M. Irie, *Chem. Lett.*, (1986) 983.
12 H. Takahashi, S. Li, Y. Harigaya and M. Onda, *Heterocycles*, 26 (1987) 3239.
13 M. Niwa, S. Otsuji, H. Tatematsu, G.-Q. Liu, X-F. Chen and Y. Hirata, *Chem. Pharm. Bull.*, 34 (1986) 3249.
14 Y. Okamoto and K. Hatada, *J. Liq. Chromatogr*, 9 (1986) 369.
15 G. Blaschke, *J. Chromatogr. Sci.*, 40 (1988) 179.
16 J. Szejtli, *Cyclodextrins and Their Inclusion Complexes*, Akadémiai Kiadó, Budapest, 1982.
17 T. J. Ward and D. W. Armstrong, *Chromatogr. Sci.*, 40 (1988) 131.
18 J. Szejtli, *Starch*, 39 (1987) 357.
19 T. J. Ward and D. W. Armstrong, *J. Liq. Chromatogr.*, 9 (1986) 407.

20 D. W. Armstrong, X. Yang, S. M. Han and R. A. Menges, *Anal. Chem.*, 59 (1987) 2594.
21 M. Gazdag, G. Szepesi and L. Huszar, *J. Chromatogr.*, 436 (1988) 31.
22 D. W. Armstrong, Y. I. Han and S. M. Han, *Anal. Chim. Acta*, 208 (1988) 275.
23 E. Haslam, T. H. Lilley, Y. Cai, R. Martin and D. Magnolato, *Planta Med.*, 55 (1989) 1.
24 J. H. Maguire, *J. Chromatogr.*, 387 (1987) 453.
25 D. W. Armstrong, T. J. Ward, R. D. Armstrong and T. E. Beesley, *Science (Washington, D.C.)*, 232 (1986) 1132.
26 P. Macaudiere, M. Claude, R. Rosset and A. Tambute, *J. Chromatogr.*, 450 (1988) 255.
27 M. Tanaka, T. Shono, D. Q. Zhu and Y. Kawaguchi, *J. Chromatogr.*, 469 (1989) 429.
28 D. W. Armstrong and W. Li, *Chromatography*, March (1987) 43.

Journal of Chromatography, 514 (1990) 161–170
Elsevier Science Publishers B.V., Amsterdam

CHROM. 22 521

Filled tubes as generation elements in electrokinetic detection in liquid chromatography

J. NEČA and R. VESPALEC*
Institute of Analytical Chemistry, Czechoslovak Academy of Sciences, Leninova 82, 611 42 Brno (Czechoslovakia)
(First received November 15th, 1989; revised manuscript received April 27th, 1990)

ABSTRACT

A chromatographic column with an electrically conductive wall can be used as an electrokinetic detector even for separations in reversed-phase systems. The high detection sensitivity is comparable to that of electrokinetic detectors placed behind the column. Solutes eluted from the column are detected without additional band broadening. Hence electrokinetic detection using the column as the detector is also promising for microcolumns. The filling increases the detection sensitivity only if the solute responses generated on the tube wall and tube filling are of identical polarities.

INTRODUCTION

Liquid chromatography and streaming current generation involve one common feature, *viz.*, movement of liquid along a solid surface. Hence any chromatographic experiment implicitly provides conditions for streaming current generation. Streaming current generation results from the fact that the streaming liquid carries part of the spatial charge of the electric double layer existing on the boundary between the solid surface (a generating element of the electrokinetic detector) and the flowing liquid[1]. The carried charge can be measured if it is collected by an electrode (sensing element) effected, for instance, by an electrically isolated conductive tube.

The magnitude and polarity of a streaming current depend on the composition of the flowing liquid[1–3]. It is therefore expedient to utilize a streaming current for detection[4]. Measurement of electrokinetic responses to different compounds[2,3] and analyses of bile[5] and carboxylic acids[6–9] and tributyl phosphate hydrolysis products[10] showed that electrokinetic detection of ionizable compounds is sensitive and selective. The properties of electrokinetic detectors behind the column, consisting of empty[6–9] and filled[2,11] capillaries or packs of capillaries[6,7,11], and the properties of the chromatographic columns acting as a detector[11–13] have been studied from different viewpoints[2,6–8,11–14]. However, the influence of the tube wall and its filling on the detection sensitivity and the current generated by the mobile phase stream (background current) were not explained.

0021-9673/90/$03.50

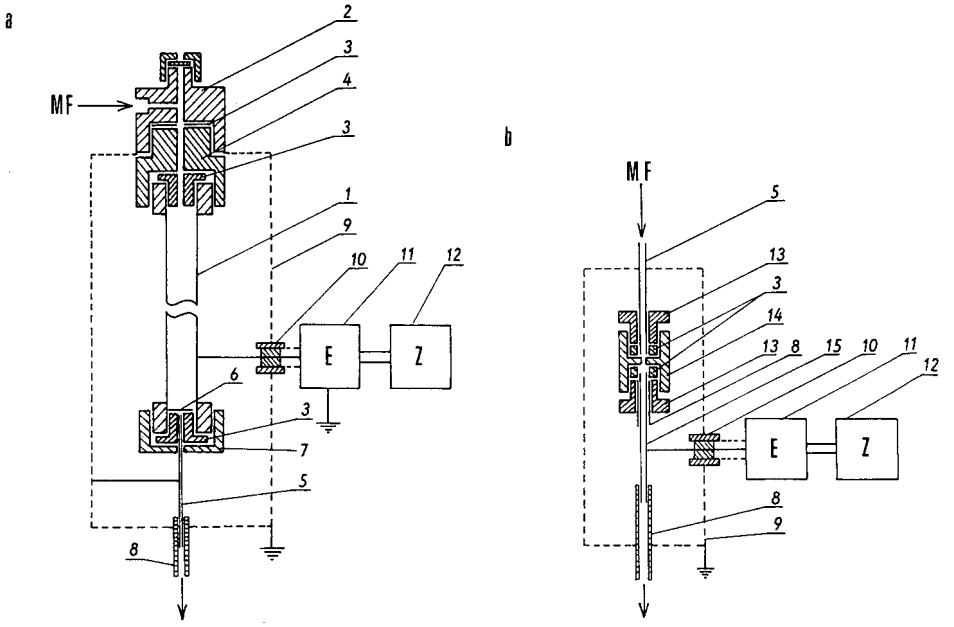

Fig. 1. Scheme of streaming current sensing. (a) From the chromatographic column; (b) from the capillary behind the chromatographic column. 1 = Column; 2 = injection block; 3 = PTFE seal; 4 = isolation element; 5 = stainless-steel capillary (45 × 0.8 mm I.D.); 6 = filter-paper; 7 = end screw joint; 8 = PTFE capillary; 9 = shielding; 10 = connector to electrometer; 11 = electrometer; 12 = recorder; 13 = screw; 14 = stainless-steel couple joint; 15 = stainless-steel capillary (40 × 0.5 mm I.D.).

The Helmholtz–Smoluchovsky equation describing the generation of a streaming current, I_s, has the general form

$$I_s = A\zeta P \tag{1}$$

for both empty[1] and filled[15–17] tubes. Constant A depends on the geometry of the generation element and the composition of the streaming liquid; ζ is the zeta potential and P is the pressure gradient on the generation element. The high additional pressure drop on an electrokinetic detector placed behind the column, necessary for a high detection sensitivity, may be completely eliminated if the chromatographic column with an electrically conductive wall acts as an electrokinetic detector[11–13].

The flow dependence of the background current generated in the column was found to be non-linear at the beginning in normal-phase systems[11]. The contradiction between the experiment and eqn. 1 was explained by the idea of back-discharging of the charge carried by the liquid flowing out of the column[11]. A consequence of this idea was the assumption that the chromatographic column can act as an electrokinetic detector only if mobile phases with conductivities of 10^{-9} $\Omega^{-1}m^{-1}$ or lower are used[12]. However, that assumption has never been confirmed experimentally.

This work was aimed at establishing whether the column with an electrically conductive wall can be used as a detector in reversed-phase systems where the mobile

phase conductivities substantially exceed the limit of 10^{-9} $\Omega^{-1}m^{-1}$. Further, the sensitivity of detection using the column as a detector in reversed-phase systems was tested and the effects of the column wall and the column filling on both background current and solute responses were studied.

EXPERIMENTAL

An HPP 4001 syringe pump (Laboratory Instruments, Prague, Czechoslovakia) served as a pulseless source of the mobile phase flow. Stainless-steel columns with beds of 100 × 2 mm, 150 × 2 mm, 100 × 4 mm and 100 × 6 mm were closed at the outlets with filter-paper and sealed with Teflon (Fig. 1a). The columns were isolated from the injection block with a nylon spacer. Streaming currents were measured with a Vibron Model 33 C electrometer (Electronic Instruments, Richmond, U.K.). A Model 427 current amplifier (Keithley, U.S.A.) was used for model analyses. A reference detector (a refractometer or UV photometer) with an 8-μl cell was connected behind the column. Solutes were injected with a Hamilton (Bonaduz, Switzerland) Model 1801 microsyringe.

The currents generated in the chromatographic column were sensed from the column wall (Fig. 1a) or from the outlet capillary 5 (45 × 0.8 mm I.D.). On sensing from the chromatographic column both the whole chromatograph and the outlet capillary 5 were earthed. On sensing from the isolated capillary 5 the column was earthed.

To sense the streaming current generated in the capillaries, the electrokinetic detector (Fig. 1b) was connected behind the column. A 40 × 0.5 mm I.D. stainless-steel capillary (15), electrically isolated and screened, served as both generation and sensing element. If the generation capillary was filled with a sorbent, its outlet was closed with a cotton-wool wick. The capillary leading out from the column (capillary 5 in Fig. 1a) was earthed. The sensing resistances of the meters (10^5 Ω for acetone and 10^4 Ω for aqueous mobile phases) were chosen so that the conditions for the measurements of current could be achieved[8,18].

Irregular Silasorb 300 silica gel (Lachema, Brno, Czechoslovakia) with a mean particle diameter d_p = 12.4 μm and specific surface area S = 347 m^2/g, and the same material modified with octadecyl groups (Silasorb C_{18}), were used as stationary phases. Prior to use the packed columns were washed with 40 ml of distilled water, 100 ml of 20 mM nitric acid (flow-rate 0.2 ml/min), 25 ml of distilled water and 40 ml of ethanol. Analytical-reagent grade solvents used for the preparation of the mobile phases were not purified. Solutes from different sources were of analytical-reagent grade.

RESULTS AND DISCUSSION

In order that the column may serve as a source of streaming current, the bed outlet must be closed with electrically non-conductive material and the metallic outlet capillary must be isolated from the column wall (Fig. 1a). Except for model analyses, the injected solutes were chosen so that their symmetric zones may be eluted in the dead volume or in its vicinity. The electrokinetic responses of such solutes could be quantified only by the changes in the background current, ΔI_s, in the zone maxima.

The streaming current will reach the maximum if the time of contact between the liquid and the bypassed surface is at least ten times greater than the relaxation time of the liquid[12,19]. The relaxation time of the acetone used was $\tau = 1.9 \cdot 10^{-5}$ s and those of aqueous mobile phases were even shorter[20]. The time the liquid spent in the empty capillary (45 × 0.5 mm I.D.) was 0.1 s at a flow-rate of 5 ml/min. Hence all the capillaries used either as generation or sensing elements guaranteed the maximum charge density in the flowing liquid and its perfect discharge[12,19].

Column as a detector

The possibility of sensing the streaming current generated in a metallic column through which a relatively conductive mobile phase flows was shown by experiments with stainless-steel columns of dimensions 100 × 2 mm, 100 × 4 mm and 100 × 6 mm I.D. filled with Silasorb 300, through which acetone flowed. The streaming current was sensed from the column wall (Fig. 1a). After multiplying streaming currents by a correction factor of $4/d_c^2$, where d_c is the column diameter in millimetres, the flow-rate dependences of the background currents obtained for columns of varying diameter agreed (Fig. 2).

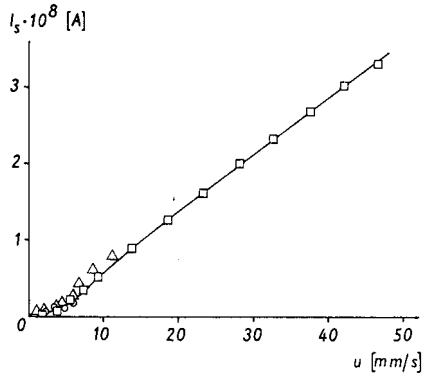

Fig. 2. Dependence of the background current on the linear velocity of the mobile phase in the column standardized to the column of I.D. 2 mm. Stationary phase, Silasorb 300; mobile phase, acetone. Columns: 100 × 6 mm, 100 × 4 mm and 100 × 2 mm I.D.

The streaming current, I_s, is the product of the volumetric flow-rate of the liquid, F and the mean charge density in the streaming liquid, $\bar{q}(u)$:

$$I_s = F\bar{q}(u) \tag{2}$$

The mean charge density at a certain linear velocity of the liquid, u, did not depend on the column diameter and, starting from a linear velocity of 12 mm/s, it did not change at all with the linear velocity. The flow-rate dependence of the background current had the same course as the dependence measured with a hydrocarbon mobile phase[1] whose conductivity was lower by six orders of magnitude than that of the acetone used. This suggests that the initial non-linearity of the background current flow-rate dependence is obviously not associated with the conductivity of the flowing liquid and thus not

even with its relaxation time[12,19]. The reason may rather be the dependence of $\bar{q}(u)$ on the linear velocity of the liquid.

The independence of the streaming current of the time of the liquid transport from the column outlet into the capillary 5 withdrawing the effluent (Fig. 1a) was verified by changing the distance of the capillary from the bed (Table I). The acetone–water (1:1) mobile phase had a specific conductivity of $3.6 \cdot 10^{-5}\ \Omega^{-1}\mathrm{m}^{-1}$. The streaming current did not change even if the outlet capillary 5 was removed from the Teflon sealing and the effluent dripped freely out of the column. These results agree with the observations of Hurd and Hackerman[18].

TABLE I

DEPENDENCE OF BACKGROUND CURRENT, I_s, SENSED FROM THE COLUMN ON THE DISTANCE, d, OF OUTLET CAPILLARY 5 (FIG. 1) FROM THE COLUMN

Column, 100 × 2 mm I.D.; sorbent, Silasorb 300; mobile phase, acetone–water (1:1); flow-rate, 1 ml/min.

d (mm)	$I_s \cdot 10^8$ *(A)*
0.5	−1.1
3	−1.0
5	−1.1

The dependence of the background current, I_s, and solute responses, ΔI_s, on the composition of the separation system is shown in Tables II and III. The differences in Table II can be ascribed unambiguously to modification of the silica gel with octadecyl groups, as Silasorb C_{18} was prepared from Silasorb 300 used in this work. When sensing streaming currents from the outlet capillary, the same phenomenon as during measurements with a hydrocarbon–alcohol[11,13] mobile phase was observed, *i.e.*, the polarities of both the background currents and solute responses reversed, but their absolute values did not change. In electrokinetic and refractometric detection both the retention volumes of the solutes and the peak shapes agreed.

The sensitivity of the detection of retained ionizing solutes in sensing streaming currents from the metallic column was tested for nitrophenols (Fig. 3) and carboxylic acids (Fig. 4). The calculated detection limits (Table IV) generated responses twice as high as the noise. The response was calculated from the measurements in which the

TABLE II

BACKGROUND CURRENTS, I_s, AND SOLUTE RESPONSES, ΔI_s, ON SILASORB 300 AND SILASORB C_{18}

Column, 100 × 4 mm I.D.; mobile phase, acetone; flow-rate, 0.5 ml/min.

Sorbent	$I_s \cdot 10^8$ *(A)*	$\Delta I_s \cdot 10^8$ *(A)*		
		Ethanol	*p-Nitrophenol*	*2,3-Dihydroxynaphthalene*
Silasorb 300	+0.2	+0.2	+0.4	+0.3
Silasorb C_{18}	+0.5	−1.5	−2.0	−2.0

TABLE III

INFLUENCE OF THE MOBILE PHASE COMPOSITION ON BACKGROUND CURRENT, I_s, AND SOLUTE RESPONSES, ΔI_s, GENERATED ON SILASORB C_{18}

For experimental details, see Table II.

Mobile phase	ε_r[a]	κ[b] $(\Omega^{-1}m^{-1})$	$I_s \cdot 10^8$ *(A)*	$\Delta I_s \cdot 10^8$ *(A)*[c]				
				EtOH	*ONA*	*PNA*	*PNP*	*2,3-DHN*
Acetone	23.0	$1.1 \cdot 10^{-5}$	+0.5	−11.5	− 1.8	− 1.85	− 2.0	− 2.0
Acetone–methanol (90:10)	24.9	$3.9 \cdot 10^{-5}$	+1.6	− 1.9	− 1.6	− 1.6	− 1.6	− 1.2
Methanol	34.4	$4.4 \cdot 10^{-5}$	−6.2	+22.3	+10.2	+ 5.6	+ 3.2	+ 2.5
Acetonitrile	39.5	$6.4 \cdot 10^{-5}$	+1.3	−28.0	−25.0	−25.0	−32.0	−22.5
Acetone–water (70:30)	45.0	$1.5 \cdot 10^{-4}$	−0.5	− 0.5	0.0	− 0.1	− 1.3	− 0.7

[a] Relative permittivity.

[b] Electrical conductivity.

[c] EtOH = Ethanol; ONA = *o*-nitroaniline; PNA = *p*-nitroaniline; PNP = *p*-nitrophenol; 2,3-DHN = 2,3-dihydroxynaphthalene.

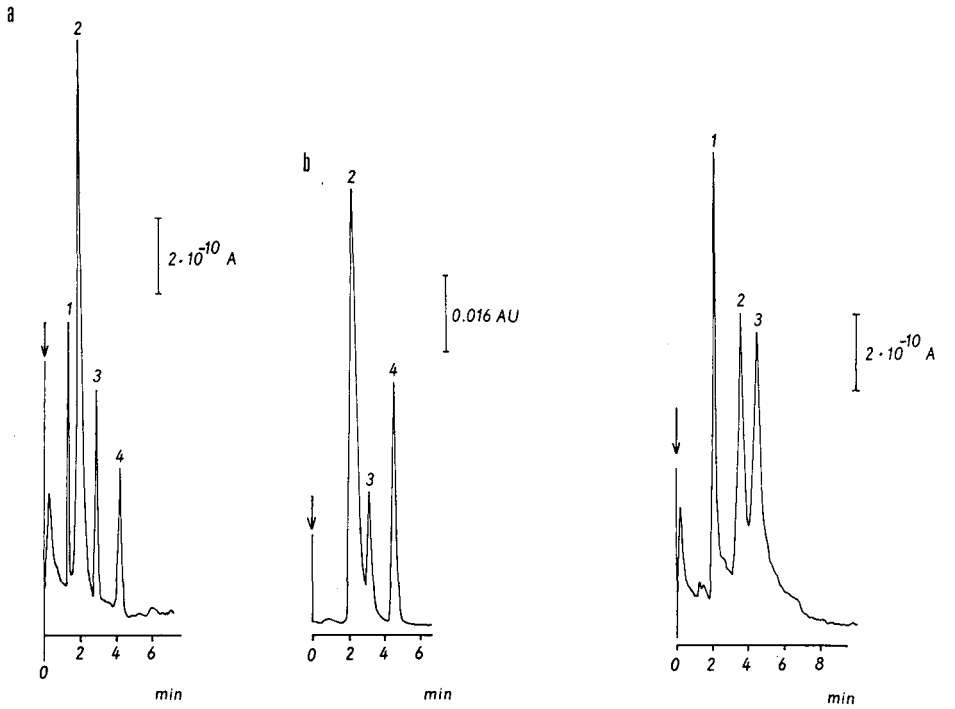

Fig. 3. Chromatogram of a mixture of nitrophenols. Detection: (a) sensing of streaming currents for the column; (b) UV (254 nm). Column, 150 × 2 mm I.D.; stationary phase, Silasorb C_{18}; mobile phase, methanol–water (4:6); flow-rate, 0.2 ml/min; amount of solutes injected, $5 \cdot 10^{-9}$ mol. Noise level (peak to peak): $2.2 \cdot 10^{-11}$ A. Peaks: 1 = methanol; 2 = 2,5-dinitrophenol; 3 = *p*-nitrophenol; 4 = *o*-nitrophenol.

Fig. 4. Chromatogram of a mixture of carboxylic acids. Mobile phase, methanol; amount of solutes injected, $2 \cdot 10^{-9}$ mol; other conditions as in Fig. 3. Noise level (peak to peak): $3.4 \cdot 10^{-11}$ A. Peaks: 1 = caprylic acid; 2 = palmitic acid; 3 = stearic acid.

TABLE IV

CAPACITY FACTORS, k', AND DETECTION LIMITS OF RETAINED IONIZING SOLUTES CALCULATED FROM CHROMATOGRAMS IN FIGS. 3 AND 4

Solute	k'	*Detection limit* ($mol \cdot 10^{10}$)
2,5-Dinitrophenol	0.7	2.7
p-Nitrophenol	3.7	6.7
o-Nitrophenol	7.3	8.8
Caprylic acid	0.8	1.2
Palimitic acid	2.0	1.8
Stearic acid	2.7	1.9

detection sensitivity had not been optimized for individual solutes. In spite of that, the values obtained were comparable to the best results obtained with the electrokinetic detector behind the column[2]. The better resolution of nitrophenols with the electrokinetic than with the photometric detection (Fig. 3) is due to the fact that the eluted zones are detected without extra column broadening. Electrokinetic detection is therefore a promising technique for microcolumns. However, with decreasing column diameter the importance of the wall effect for both background current and solute responses increases.

Wall effect

Let I_1 be the background current influenced by the cylindrical tube wall of radius a and I_2 the streaming current generated by the tube filling. According to eqn. 2, it holds that

$$I_1 = F_1 \bar{q}_1 \tag{3}$$

$$I_2 = F_2 \bar{q}_2 \tag{4}$$

The volumetric flow-rate of the liquid carrying the spatial charge of the double layer on the tube wall, F_1, is

$$F_1 = 2\pi a \kappa^{-1} u \tag{5}$$

where u is the linear liquid velocity; the double-layer thickness, κ^{-1}, depends only on the properties of the flowing liquid[19].

It follows from the Guy–Chapman theory of the electric double layer[1] that the mean charge density in the liquid is directly proportional to the zeta potential. Therefore,

$$\bar{q}_1 = A_0 \zeta_1 \tag{6}$$

where ζ_1 is the zeta potential of the tube wall. The proportionality constant, A_0, depends on the properties of the liquid.

The flow-rate of the liquid carrying the spatial charge of the double layer of the filling not affected by the wall is

$$F_2 = \pi(a - \kappa^{-1})^2 A_2 u \tag{7}$$

where A_2 is the ratio of the cross-section of the liquid in which exists the double layer on the particles of the filling to the total bed cross-section, and depends on the bed geometry and κ^{-1}. It holds for the mean charge density, $\bar{q}_2$, in the liquid fraction, F_2, in analogy with eqn. 7 that

$$\bar{q}_2 = A_0 \zeta_2 \tag{8}$$

where ζ_2 is the zeta potential of the filling particles.

The relative contribution of the current affected by the wall, I_1, to the total current, $I_1 + I_2$, is

$$\beta = I_1/(I_1 + I_2) \tag{9}$$

Substituting into eqn. 9 from eqns. 3–8 and assuming $a \gg \kappa^{-1}$ we can calculate the minimum radius of the filled tube, $a_{\min}$, in which wall effect does not exceed β:

$$a_{\min} = 2\kappa^{-1} \frac{[1 - \beta(1 - A_2\zeta_2/\zeta_1)]}{\beta A_2 |\zeta_2/\zeta_1|} \tag{10}$$

In order to determine $a_{\min}$, let us assume a cylindrical tube filled with spherical particles of $d_p = 12\ \mu$m, with acetone as mobile phase ($\kappa^{-1} = 0.24\ \mu m^{20}$), and assume also that $|\zeta_2/\zeta_1| \approx 1$. For such a system $A_2 = 4 \cdot 10^{-2}$. In this instance the minimum tube diameter having a negligible wall effect ($\beta = 0.01$) is $2a \approx 2.4$ mm.

Analogous considerations concerning the solute responses is not possible, as the generation of solute responses has not yet been sufficiently investigated. The influence of the tube wall and its packing was therefore studied experimentally. The electrokinetic detector behing the column (100 × 4 mm I.D.) with a stainless-steel capillary (45 × 0.5 mm I.D.) acting as a generation element (Fig. 1b), was used. The reference background current and solute responses were sensed from the column used.

In order that identical properties of the silica gel surface in the column and in the capillary may be guaranteed, in contrast to preceding experiments, both the filled column and the capillary were washed only with the mobile phase.

In all the experimental arrangements (Table V) the background current and the responses of methanol and ethanol injected into the empty column were below the sensitivity limit of the meter, $1 \cdot 10^{-9}$ A. Hence the responses of solutes measured from the filled column were generated in the bed of sorbent only. In accordance with refs. 11 and 13, the absolute values of the responses sensed from the column wall or from the outlet capillary 5 (Fig. 1a) were identical.

At a sufficiently high linear velocity of the liquid, with $\bar{q}(u)$ being constant, the streaming current generated by a given volumetric flow-rate, F does not depend on the bed cross-section (eqn. 2, Fig. 2). Therefore, the responses of methanol and ethanol generated on a silica gel bed in the column and the filled capillary of the detector

TABLE V

INFLUENCE OF GENERATING AND SENSING ELEMENTS ON THE MAGNITUDE AND POLARITY OF STREAMING CURRENT RESPONSES, ΔI_s

Mobile phase, acetone; flow-rate, 0.5 ml/min.

Generating element	*Sensing element*	$\Delta I_s \cdot 10^8$ (A)	
		Methanol[a]	*Ethanol*[a]
Column 100 × 4 mm I.D., + Silasorb 300	Column 100 × 4 mm I.D., + Silasorb 300	−2.0	+1.9
Column 100 × 4 mm I.D., + Silasorb 300	Stainless-steel outlet capillary, 40 × 0.8 mm I.D.	−1.9	−1.8
Detector stainless-steel capillary, 40 × 0.5 mm I.D.	Detector stainless-steel capillary, 40 × 0.5 mm I.D.	−0.4	−0.4
As above + Silasorb 300	As above + Silasorb 300	+1.6	+1.4

[a] Volume injected: 10 μl.

behind the column had to be identical. Hence the additivity applies to the solute response affected by the tube wall and its filling in the same way as to background currents. The tube filling evidently increases the detector sensitivity only if the solute responses generated on the tube wall and on the tube filling have the same polarities.

The minimum diameter of the packed tube through which acetone flows and in which the wall effect on the background current is negligible is 2.4 mm. In the filled tube, 0.5 mm in diameter, one sixth of the total charge was generated on the tube wall by the zone passing through the detector with the use of the same mobile phase. With a tube diameter of 4 mm the influence of the wall could not be proved (Table V). It can therefore be judged that with the use of the same mobile phase the minimum tube diameter whose wall does not influence the solute response is comparable to the minimum tube diameter in which the influence of the wall on the background current is negligible. If responses are sensed from the columns behaving as columns of infinite diameter[21], the solute does not come into contact with the tube wall. In such a column the solute responses are not affected at all by the wall.

REFERENCES

1 R. J. Hunter, *Zeta Potential in Colloid Chemistry*, Academic Press, London, 1981.
2 S. Terabe, K. Yamamoto and T. Ando, *Can. J. Chem.*, 59 (1981) 1531.
3 R. Vespalec, *J. Chromatogr.*, 210 (1981) 11.
4 N. Ando, Y. Tanizaki and F. Hasegawa, *U.S. Pat.*, 3 352 643 (1967).
5 S. Terabe, K. Yamamoto and T. Ando, *J. Chromatogr.*, 239 (1982) 515.
6 W. Kemula, B. K. Glod and W. Kutner, *J. Liq. Chromatogr.*, 6 (1983) 1823.
7 W. Kemula, B. K. Glod and W. Kutner, *J. Liq. Chromatogr.*, 6 (1983) 1837.
8 B. K. Glod and W. Kemula, *J. Chromatogr.*, 321 (1985) 433.
9 B. K. Glod and W. Kemula, *J. Chromatogr.*, 366 (1986) 39.
10 R. Vespalec and M. Cigánková, *J. Chromatogr.*, 364 (1986) 233.
11 K. Šlais, *Thesis*, Brno, 1978.
12 K. Šlais and M. Krejčí, *J. Chromatogr.*, 148 (1978) 99.
13 M. Krejčí, K. Šlais and K. Tesařík, *J. Chromatogr.*, 149 (1978) 645.

14 M. Krejčí, D. Kouřilová and R. Vespalec, *J. Chromatogr.*, 219 (1981) 61.
15 H.-S. Jacobasch, G. Bauböck and J. Schurz, *Colloid Polym. Sci.*, 263 (1985) 3.
16 S. M. Neale, *Trans. Faraday Soc.*, 42 (1946) 473.
17 L. Dresner and K. A. Kraus, *J. Phys. Chem.*, 67 (1964) 990.
18 R. M. Hurd and N. Hackerman, *J. Electrochem. Soc.*, 102 (1955) 594.
19 J. Gavis and I. Koszman, *J. Colloid Sci.*, 16 (1961) 375.
20 J. Neča, unpublished results.
21 J. J. De Stefano and H. C. Beachell, *J. Chromatogr. Sci.*, 8 (1970) 434.

Journal of Chromatography, 514 (1990) 171–178
Elsevier Science Publishers B.V., Amsterdam

CHROM. 22 566

Electrochemical detection for high-performance liquid chromatography using a Kel-F wax–graphite electrode

JULIE WANGSA and NEIL D. DANIELSON*
Department of Chemistry, Miami University, Oxford, OH 45056 (U.S.A.)
(First received October 3rd, 1989; revised manuscript received April 24th, 1990)

ABSTRACT

A carbon paste electrode using Kel-F wax as the binder was characterized for electrochemical detection in high-performance liquid chromatography. The resulting electrode was stable in solutions with high organic content and possessed good reproducibility and detection limit. The amperometric response of the Kel-F wax carbon paste electrode by flow injection analysis was about 26% higher than that of Kel-F oil carbon paste electrode in an acetonitrile–water (70:30) solution. This represented a two-fold improvement over the Nujol oil carbon paste electrode. Cyclic voltammetric data indicated the greater response of the Kel-F wax carbon paste electrode in high-acetonitrile-containing solutions was due to a higher surface area caused in part by solvent swelling of the electrode. Three unconjugated estrogens were separated and detected satisfactorily at the pg level using this Kel-F wax carbon paste electrode.

INTRODUCTION

The most common electrodes used for electrochemical detection in high-performance liquid chromatography (HPLC) are based on various types of carbon such as glassy carbon, pyrolytic graphite, and numerous kinds of carbon paste[1–5]. Carbon paste electrodes (CPEs) can be advantageous because they are cheap, easy to prepare and replace, and modifiable to suit the required electrode potential. These CPEs, however, suffer from several drawbacks. The most severe limitation of the CPE is the tendency for the binder (such as Nujol) to dissolve in solutions containing an appreciable content of organic solvent. To overcome this problem, a variety of composite electrodes such as graphite–Kel-F particle[6] and graphite–epoxy electrodes[7] have been developed.

In our previous work[8], we have compared the performance of Nujol and Kel-F oil-based CPEs. The response of identically prepared Kel-F and Nujol oil CPEs to estriol was evaluated by flow injection analysis (FIA) using mobile phases of various acetonitrile content. An enhancement factor of about 1.7 over the response of the Nujol oil CPE was obtained for the Kel-F oil CPE as the acetonitrile content in the

0021-9673/90/$03.50

mobile phase was increased from 0 to 80%. As determined by chronocoulometry, the active surface area of the CPEs increased when immersed in a mixed acetonitrile–water solution.

We report here the use of Kel-F wax as a binder in a CPE for electrochemical detectors in HPLC. Recent preliminary data suggested that Kel-F wax is superior to Kel-F oil in several respects such as solvent stability and lower residual current. Both characterization of the Kel-F wax CPE and applicability of the CPE for HPLC detection of three estrogens will be presented.

EXPERIMENTAL

Chemicals

Kel-F oil (No. 700) and Kel-F wax were obtained from Halocarbon (Hackensack, NJ, U.S.A.) and from Alltech (Arlington Heights, IL, U.S.A.), respectively. The molecular weight of the oil was about 800–1000 while that for the wax was undetermined since it is a mixture of two higher-molecular-weight Kel-F polymers. The graphite particles (Fisher Scientific, Fairlawn, NJ, U.S.A.), determined to be about 10 to 25 μm by light microscopy, were treated successively with hexane, chloroform, acetone, water, 6 *M* nitric acid and finally water until a neutral pH before drying overnight in a vacuum oven at 110°C. The estrogens were purchased from Sigma (St. Louis, MO, U.S.A.) All chemicals were at least reagent grade; the acetonitrile was HPLC grade. Triply distilled water was obtained from a Barnstead Nanopure distillation unit (Sybron/Barnstead, Boston, MA, U.S.A.).

Apparatus

The HPLC arrangement was composed of a Beckman Model 110A pump modified with a SSI pulse dampener (Scientific Systems, State College, Pa, U.S.A.), a Rheodyne Model 7010 injector (Rheodyne, Berkeley, CA, U.S.A.) with a 20-μl sample loop, a 5-μm Lichrospher 100 RP-18 column with dimensions of 20 cm × 4.6 mm I.D. (EM Science, Cherry Hill, NJ, U.S.A.) and a BAS (West Lafayette, IN, U.S.A.) Model LC-3A or a Waters (Milford, MA, U.S.A.) 460 electrochemical detector. The electrochemical cell consisted of a stainless-steel auxiliary cell half, a plastic Kel-F cell half, and an Ag/AgCl reference electrode. Peaks were generated on a Linear Model 1201 (Linear Instruments, Reno, NV, U.S.A.) strip-chart recorder or a Model C-R6A Chromatopac integrator (Shimadzu, Columbia, MD, U.S.A.).

Cyclic voltammetry and chronocoulometry measurements were performed using a BAS-100 electrochemical analyzer. The electrochemical cell was composed of a CPE, a Pt wire counter electrode and a saturated Ag/AgCl reference electrode. Cyclic voltammograms were generated at the scan rate of 100 mV/s. For the chronocoulometry, the potential was stepped from 0 to 600 mV data pulse width of 250 ms. The active surface area of the CPE was calculated from the slope of a plot of charge Q (coulombs) *versus* $t^{\frac{1}{2}}$(ms) based on the Cottrell equation

$$Q = \frac{2nFAC_0D_0^{\frac{1}{2}}}{\pi^{\frac{1}{2}}}(t^{\frac{1}{2}})$$

where n = number of electrons transferred, F = Faraday constant, A = surface area, C_0 = concentration and D_0 = diffusion coefficient.

The diffusion coefficient value of $7.6 \cdot 10^{-6}$ cm^2/s for $K_3Fe(CN)_6$ in 1 *M* KCl solution was used[9]. For the solution containing 70% acetonitrile, the D_0 value of $12 \cdot 10^{-6}$ cm^2/s was appropriate as calculated previously[8].

Procedure

Kel-F oil and wax carbon pastes were prepared in batches by combining graphite powder (pre-dried at 110°C) and the binder in the weight ratios of 1.25. The required amount of Kel-F wax was weighed into a beaker and was heated on a hot plate at low heat until the wax had melted. The graphite powder was added slowly with stirring. The mixture was allowed to cool and then mixed more thoroughly with a mortar and pestle. Small amounts of the paste were then transferred to the flow cell cavity with a spatula and packed by applying pressure with a small brass rod. The electrode surface was smoothed by polishing it on glazed white paper[10]. Electrode repacking was done by replacing approximately one-fifth of the previously used carbon paste. Equilibration of a new CPE was carried out for at least 8 h in 0.025 *M* phosphate buffer containing 30% acetonitrile, pH 3.2. Oxidation of the estrogens was performed at +0.95 V *vs.* Ag/AgCl and the flow-rate was maintained at 1 ml/min. Each data point was generated from at least five injections.

The extent of swelling of the Kel-F wax by an organic solvent was carried out as described in our previous work[8]. Determinations were done in triplicate.

RESULTS AND DISCUSSION

Our primary interest is to develop a stable, easily prepared CPE with a wide range of potential limits. Three estrogens which require high applied potentials for oxidation were chosen to be the test solutes. Using a glassy carbon electrode, a required applied potential of 1.15 V *vs.* Ag/AgCl has been reported for estriol[11]. Hydrodynamic voltammograms of repetitive injections of 60 ng estriol, 76 ng estradiol, and 116 ng estrone are shown in Fig. 1. A potential higher than +1.15 V *vs.* Ag/AgCl must be applied in order to reach the limiting current plateau. A + 0.95 V applied oxidation potential was chosen for the estrogens. At higher applied potentials, oxidation of the mobile phase can occur which results in high background currents. The optimum operating potential for any compound is a compromise between minimizing the background current and maximizing the limiting current.

Fig. 2 illustrates the stability of identically prepared Kel-F oil and wax CPEs used in solution with 70% acetonitrile content. The response to 10 ppm estriol decreases by about 15% and 3% for Kel-F oil and wax, respectively, over a 9-h period. The Kel-F wax CPE is less soluble in this organic solvent and thus, is more suitable for use as a HPLC detector. Also, the response of the Kel-F wax CPE is about 26% higher than that of Kel-F oil CPE (Fig. 3). For the five repetitive measurements, relative standard deviations (R.S.D.) of less than 5% and 3% were calculated for the Kel-F oil and wax CPEs, respectively. The peak width of the Kel-F wax CPE is also about 10% narrower than the Kel-F oil CPE indicating better mass transfer of the solute in and out of the electrode. Better reproducibility and detection limit of the Kel-F wax CPE are expected becauce of the lower noise (Fig. 3). From baseline data (after 8 h of

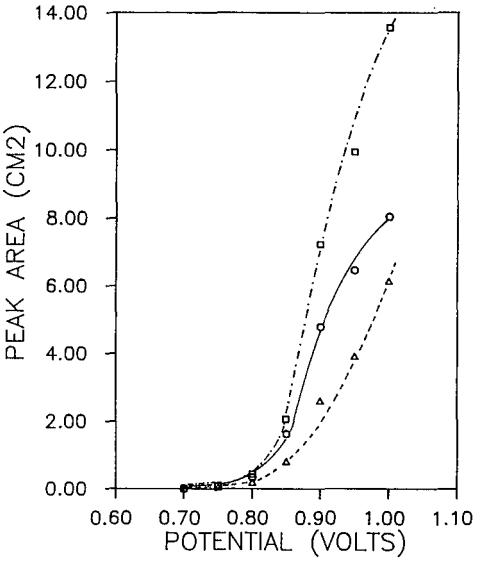

Fig. 1. Hydrodynamic voltammograms for estriol (△), estradiol (○) and estrone (□).

equilibration), values of 0.5 nA and 0.3 nA were observed for Kel-F oil and wax CPEs, in buffer containing 70% acetonitrile, respectively. Compared to the standard Nujol CPE[8], the Kel-F wax CPE has better than a two-fold response.

The Kel-F wax CPE response was found to increase directly with the amount of organic solvent with a moderate solvent polarity parameter (ε^0)[12] such as acetonitrile ($\varepsilon^0 = 0.65$) (Fig. 4). Methanol which possesses a high ε^0 value of 0.95 did not improve the response of the Kel-F wax electrode. Similar results were found for the Kel-F oil CPE[8]. It should be noted, however, that the Kel-F wax CPE is more stable in methanol

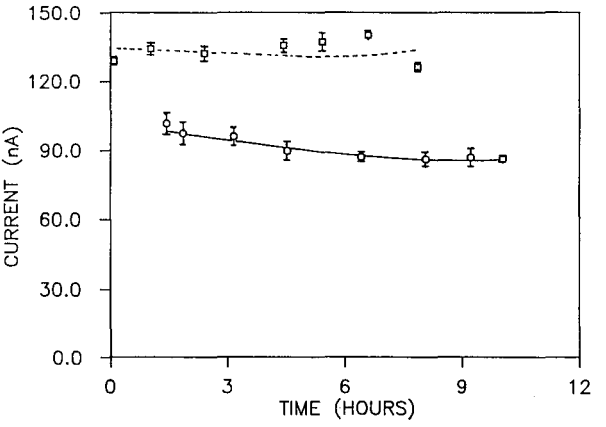

Fig. 2. Lifetimes of Kel-F oil (○) and Kel-F wax (□) CPEs in 0.025 *M* phosphate buffer containing 70% acetonitrile, pH 3.2.

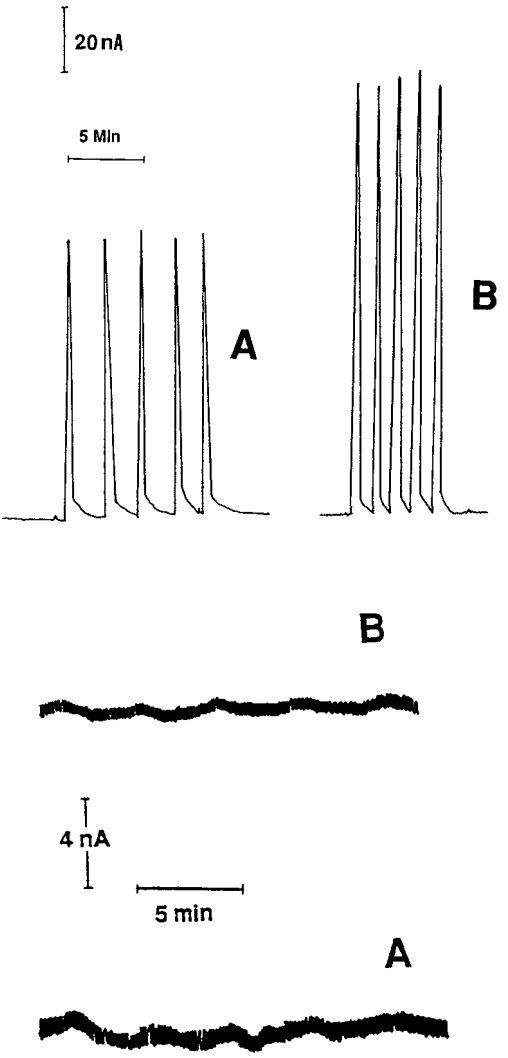

Fig. 3. Five repetitive measurements of 10 ppm estriol with Kel-F oil (A) and Kel-F wax (B) CPEs and baseline noise of CPEs after 8 h of equilibration in 0.025 *M* phosphate buffer containing 70% acetonitrile, pH 3.2.

than the Kel-F oil CPE. The extent of swelling of Kel-F wax measured as percent change in weight in acetonitrile (1.13%) and methanol (0.04%) supports the data in Fig. 4.

For comparison purposes, cyclic voltammetry and chronocoulometry measurements of the Kel-F oil CPE electrode and Kel-F wax CPE in both aqueous and 70% acetonitrile solutions were carried out. These data are tabulated in Table I. The R.S.D. for the active surface area for five different electrodes was about 7.6%. If untreated graphite was used, the precision was about two times worse. The current

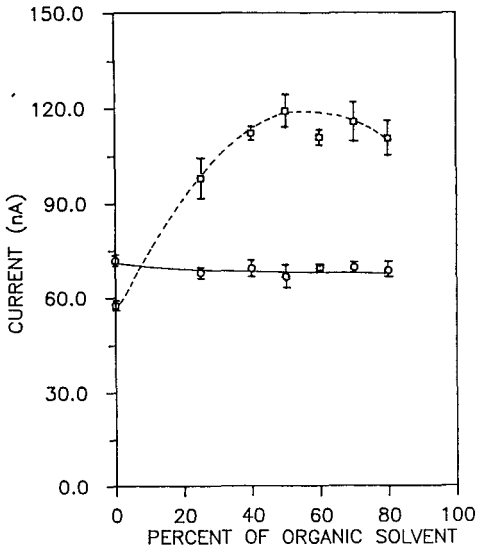

Fig. 4. The effect of organic solvents on the response of the Kel-F wax CPE. □ = Acetonitrile; ○ = methanol.

signals of both electrodes in aqueous solution are comparable but improve in a 70% acetonitrile solution. The peak current ratio (anodic/cathodic) values of close to 1 indicate reversibility although the peak potential separation values of about 100 mV indicate non-Nernstian behavior. The active surface area has increased about four-fold for both electrodes when immersed in a 70% acetonitrile solution after 8 h of equilibration. Without some equilibration time, the current signals and surface areas of both CPEs are comparable to those found in aqueous solution. This increase in

TABLE I

CYCLIC VOLTAMMETRIC AND CHRONOCOULOMETRIC DATA FOR KEL-F OIL AND KEL-F WAX CPEs

All electrodes were equilibrated in its respective solvent for 8 h.

Electrode (n=5)	*Solvents*	*Average cathodic current (μA)*	*Peak current ratio* $(\frac{ipa}{ipc})$	*Average peak potential separation (mV)*	*Average active surface area (cm^2)*
Kel-F oil	0.264 m*M* $K_3Fe(CN)_6$ in acetonitrile–water (70:30) (0.1 *M* KCl) (solvent A)	4.51	1.05	120	0.128
Kel-F oil	0.264 m*M* $K_3Fe(CN)_6$ in 0.1 *M* KCl (solvent B)	5.80	1.00	65.9	0.453
Kel-F wax	A	4.56	1.07	113.2	0.122
Kel-F wax	B	6.83	1.22	86.7	0.501

active surface area is likely due in part to the swelling of both polymers by the organic solvent. The ratio of the acetonitrile active surface area data of the two CPEs relates to the 26% increase in response of the Kel-F wax CPE over the Kel-F oil CPE under hydrodynamic voltammetry conditions. The increase in active surface area is not directly proportional to the increase in current, however.

Three estrogens were separated satisfactorily as shown in Fig. 5A. The order of elution was estriol, estradiol and estrone with retention times of 3.0, 8.6, and 11.8 min, respectively. Comparable detection limits as those obtained by Hayashi *et al.*[13] were observed with our system. Based on a signal-to-noise, ratio of 3, the limit of detections are 60, 76 and 116 pg for estriol, estradiol and estrone, respectively (Fig. 5B). Since α-naphthol is eluted at the same time as estradiol with the specified mobile phase, it is

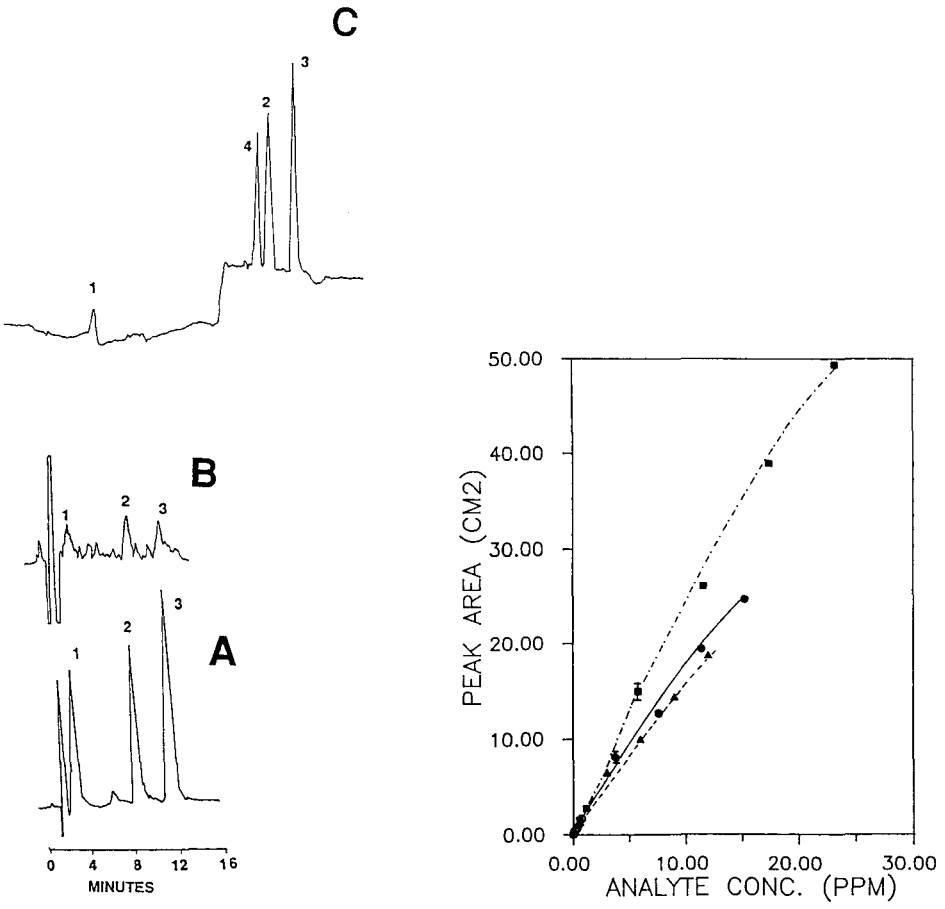

Fig. 5. (A) Separation of estriol (1), estradiol (2) and estrone (3) using 0.025 *M* phosphate buffer with 50% acetonitrile, pH 3.2. (B) Chromatogram showing the detection limits for estriol, estradiol, and estrone. (C) Separation of the three unconjugated estrogens with α-naphthol (4) as an internal standard. The organic content of the mobile phase was stepped from 30 to 50% acetonitrile.

Fig. 6. Calibration curves for estriol (▲), estradiol (●) and estrone (■).

used as an external standard to take into account the slight variation of the electrode response due to the electrode surface area. It is possible to use α-naphthol as an internal standard with the use of step gradient elution, as demonstrated in Fig. 5C.

Calibration curves for the estrogens are depicted in Fig. 6. An external standard, α-naphthol, was injected before each calibration curve. A linear relationship was obtained for the three estrogens up to about 125 ng. The R.S.D. values involved in five repetitive area measurements for the three estrogens are less than 6%. The reproducibility of the Kel-F wax electrode between batches is within 8%. The lifetime of the electrode is satisfactory (at least about five months) when it is stored in a dry environment.

Comparison of response of the Kel-F wax CPE to that of a glassy carbon electrode for the oxidation of NADH to NAD^+ as a function of time has been made. The signal generated by the Kel-F wax CPE was about 1.5 × higher and more stable. Over a 12-h period of repetitive 20-μl injections of 1.5 m*M* NADH, the signal decreased almost 50% for the glassy carbon CPE but only 10% for the Kel-F wax CPE. Electrode fouling due to dimerization of NAD^+ is a well-known problem for glassy carbon but may not be as pronounced for the Kel-F wax CPE.

The results of this study show that the Kel-F wax CPE is suitable for use in HPLC because of its stability in organic solvents enhanced response, and lower background current. Because Kel-F polymers can be chemically modified[14–16], the fabrication of CPEs for specific HPLC applications may be feasible.

REFERENCES

1 C. Bollet, P. Oliva and M. Caude, *J. Chromatogr.*, 149 (1977) 625.
2 R. M. Wightman, E. C. Paik, S. Borman and M. A. Dayton, *Anal. Chem.*, 50 (1978) 1410.
3 R. J. Fenn, S. Siggia and D. J. Curran, *Anal. Chem.*, 50 (1978) 1067.
4 E. Pungor, Z. S. Feher and G. Nagy, *Anal. Chim. Acta*, 52 (1970) 47.
5 K. Stulik, V. Pacakova and B. Starkova, *J. Chromatogr.*, 213 (1981) 41.
6 D. E. Weisshaar and D. E. Tallman, *Anal. Chem.*, 53 (1981) 1809.
7 J. Wang, T. Golden, K. Varughese and I. El-Rayes, *Anal. Chem.*, 61 (1989) 508.
8 N. D. Danielson, J. Wangsa and M. A. Targove, *Anal. Chem.*, 61 (1989) 2585.
9 M. S. Freund and A. Brajter-Toth, *Anal. Chem.*, 61 (1989) 1048.
10 P. T. Kissinger, C. Refshauge, R. Dreiling and R. N. Adams, *Anal. Lett.*, 6 (1973) 465.
11 *LCEC Application Note 35*, Bioanalytical Systems, W. Lafayette, IN.
12 L. R. Snyder and J. J. Kirkland, *Introduction to Modern Liquid Chromatography*, Wiley, New York, 1979, pp. 257–260.
13 N. Hayashi, K. Hayata and K. Sekiba, *Acta Med. Okayama*, 39 (1985) 143.
14 N. D. Danielson, R. T. Taylor, J. A. Huth, R. W. Siergiej, J. G. Galloway and J. B. Paperman, *Ind. Eng. Chem. Prod. Res. Dev.*, 22 (1983) 303.
15 A. J. Dias, T. J. McCarthy, *Macromolecules*, 18 (1985) 1826.
16 L. G. Beaver, *Ph. D. Dissertation*, Miami University, Oxford, OH, 1987.

Journal of Chromatography, 514 (1990) 179–187
Elsevier Science Publishers B.V., Amsterdam

CHROM. 22 503

Identification of products formed during UV irradiation of tamoxifen and their use for fluorescence detection in high-performance liquid chromatography

JAROSLAV ŠALAMOUN*
Institute of Analytical Chemistry, Kounicova 82, 611 42 Brno (Czechoslovakia)
MIROSLAV MACKA and MILOŠ NECHVÁTAL
Research Institute of Pure Chemicals, Lachema, Karásek 28, 621 33 Brno (Czechoslovakia)
MILOŠ MATOUŠEK
Central Testing and Checking Institute of Agriculture, Zemědělská 1a, 658 37 Brno (Czechoslovakia)
and
LUBOMÍR KNESEL
Regional Hygiene Station, Hygiene Laboratories, Cornovova 68, 618 00 Brno (Czechoslovakia)
(First received December 28th, 1989; revised manuscript received March 27th, 1990)

ABSTRACT

During the UV irradiation of tamoxifen, isomerization of the *trans* to the *cis* isomer takes place and consequently corresponding highly fluorescent phenanthrene derivatives are formed. Their formation can be used for the sensitive and selective detection of tamoxifen in high-performance liquid chromatography (HPLC). The structure of photoproducts was identified by ^{1}H NMR spectroscopy, HPLC, gas chromatography–mass spectrometry and liquid chromatography–mass spectrometry. Owing to the variety of products formed and the higher selectivity and fluorescence response, on-line postcolumn photocyclization is preferred to the precolumn mode. A chromatographic system for the separation of isomers and photoproducts is suggested.

INTRODUCTION

Tamoxifen [*trans*-1-(4-β-dimethylaminoethoxyphenyl)-1,2-diphenyl-1-butene] is a non-steroidal antiestrogen used in the treatment of breast cancer[1]. The parent compound is synthesized as a mixture of the *cis* and *trans* isomers, although it is the *trans* isomer that acts as an estrogen antagonist.

Recently, several liquid chromatographic (LC) methods[2–10] have been published for the determination of tamoxifen in human plasma. All the methods involve photochemical conversion of tamoxifen to the fluorescent phenanthrene derivative before or after chromatography. Mendenhall *et al.*[2] identified the main fluorescent

0021-9673/90/$03.50

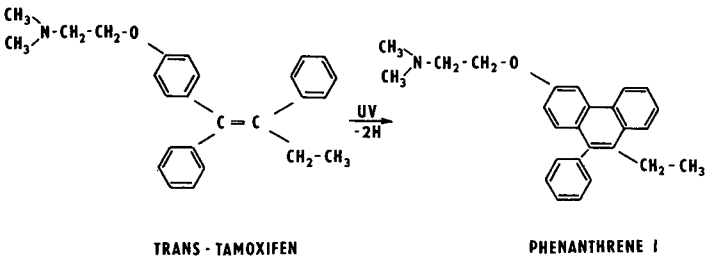

Fig. 1. Photocyclization reaction scheme of *trans*-tamoxifen.

photooxidation product (Fig. 1) by thin-layer chromatography (TLC), NMR spectroscopy and mass spectrometry and (MS). They found, however, that some NMR data are not unequivocal owing to the apparent purity of the isolated products.

The photochemistry of stilbenes, of which tamoxifen is a derivative, has been intensively studied (see ref. 11 and papers cited therein). Most workers accept a reaction mechanism in which stilbene is converted to 4*a*,4*b*-dihydrophenanthrene prior to dehydrogenation. However, dihydrophenanthrene was difficult to isolate, not only because of its oxidation to phenanthrene but also because of the reverse reaction to stilbene.

In none of the papers cited[2–10] was it mentioned whether *cis*- and *trans*-tamoxifen were separated. The only described separations were effected by the use of phenyl[12] or cyclodextrin[13] columns. Both methods have drawbacks, such as poor resolution of isomers on the phenyl column and a poor efficiency of the cyclodextrin column.

In this paper, an improved chromatographic system for the separation of tamoxifen isomers is suggested; the structure of the photooxidation products was identified by ^{1}H NMR spectroscopy, LC with fluorimetric and diode-array photometric detection, gas chromatography (GC)–MS and LC–MS.

EXPERIMENTAL

Chemicals

trans-Tamoxifen [99% purity by high-performance LC (HPLC) and *cis*-tamoxifen (91%), were prepared in the Research Institute of Pure Chemicals (Lachema, Brno, Czechoslovakia). Acetonitrile (LiChrosolv) and tetrahydrofuran (LiChrosolv) were supplied by Merck (Darmstadt, F.R.G.) and 1-octanesulphonic acid by Janssen Chimica (Beese, Belgium). All other chemicals were of analytical-reagent grade.

Equipment and methods

HPLC separations were performed on a Hewlett-Packard (Vienna, Austria) Model HP 1090 liquid chromatograph with a Model HP 1040 diode-array detector, a Model HP 1046 programmable fluorescence detector and a Model HP 310 Chemstation. Fluorescence was measured by using a 280-nm cut-off filter, a 1 × 1 mm slit on the excitation side (12 nm) and a 2 × 2 mm slit on the emission side (25 nm).

Stainless-steel analytical columns (25 × 0.4 cm I.D.) were packed with Silasorb fenyl, d_p = 7.5 μm, and Silasorb SPH C_{18}, d_p = 7.5 μm (Lachema).

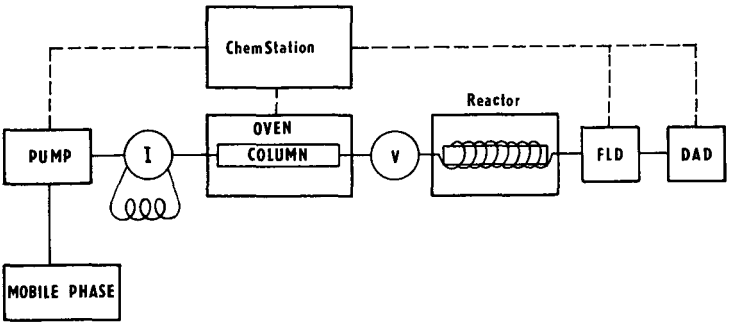

Fig. 2. Schematic diagram of the chromatographic apparatus. Solid lines, liquid connections; dashed lines, electrical connections. I = Injection valve; V = stop-flow valve; FLD = fluorescence detector; DAD = diode-array detector.

Photooxidation was accomplished in a PTFE capillary (400 cm × 0.25 mm I.D. × 1.59 mm O.D.) which was coiled around a tubular 8-W low-pressure mercury lamp (GTE, Sylvania G8T5) inserted in a MINUVIS viewer for TLC (Desaga, Heidelberg, F.R.G.). This light source emits the known mercury spectrum including the most intense line in the UV region at 254 nm. Because of the low power rating of the light source, no active cooling in the photoreactor was necessary. A schematic diagram of the chromatographic apparatus is shown in Fig. 2. A Rheodyne (Cotati, CA, U.S.A.) Model 7125 six-way valve was inserted between the analytical column and the capillary in order to apply the stop-flow technique for the measurement of fluorescence spectra.

The mobile phase for the separation of the two isomers consisted of acetonitrile–water–tetrahydrofuran–glacial acetic acid (68:27:8:0.2, v/v); 0.25 g of sodium octanesulphonate salt was added to 250 ml of this mixture. Acetonitrile–25% ammonia solution (500:0.7, v/v) was used for the separation of the photooxidation products on Silasorb C_{18}.

^{1}H NMR spectra were obtained on a Bruker (Karlsruhe, F.R.G.) WP 80SY spectrometer with a working frequency of 80.13 MHz.

GC–MS measurements were effected with a Hewlett-Packard system consisting of a Model HP 5890 gas chromatograph, an HP 5970 mass-selective detector and an HP 310 workstation.

The LC–MS system consisted of a Model HP 1090 liquid chromatograph, a HP 59888A mass spectrometer with a thermospray interface and a HP 310 workstation.

Photoproducts of *cis*- or *trans*-tamoxifen were extracted from the first of the above mobile phases into benzene after alkalinization in accord with GC–MS requirements. The extraction yield of all the compounds of interest was higher than 95% and was checked by HPLC.

RESULTS AND DISCUSSION

Separation

The separation of *cis*- and *trans*-tamoxifen was carried out on silica gel modified with phenyl groups, in a system similar to that described by Doyle *et al.*[11]

TABLE I

INFLUENCE OF THE ADDITION OF TETRAHYDROFURAN ON THE NUMBER OF THEORETICAL PLATES (N) AND RESOLUTION (R_s) OF ISOMERS

Tetrahydrofuran in mobile phase (%)	N		R_s[a]
	cis-Tamoxifen	*trans-Tamoxifen*	
0	2600	2800	0.5
2	3500	2800	1.25

[a] Peak capacity factor $k = 3$.

Tetrahydrofuran was added to the mobile phase mentioned above to improve the resolution and peak symmetry. The influence of the addition of tetrahydrofuran on the number of theoretical plates (N) and resolution (R_s, calculated by published LC nomenclatures[14]) of isomers is shown in Table I.

The second system with a Silasorb C_{18} packing was used to give a much better resolution of the two main fluorescent photoproducts of tamoxifen. However, all the analytes were poorly eluted from this reversed-phase material. A mobile phase consisting of only pure methanol or acetonitrile completely failed as the solutes were irreversibly adsorbed on the residual silanol groups. Subsequent addition of a small amount of ammonia resulted in the elution of all peaks and an acceptable resolution of all the main compounds present in the reaction mixture. Some workers[10] have previously used precolumn photoderivatization and detected the two main photoproducts as one broad or double peak.

Characteristics of photoproducts

The ^{1}H NMR spectrum (Fig. 3) confirms that the photocatalysed isomerization

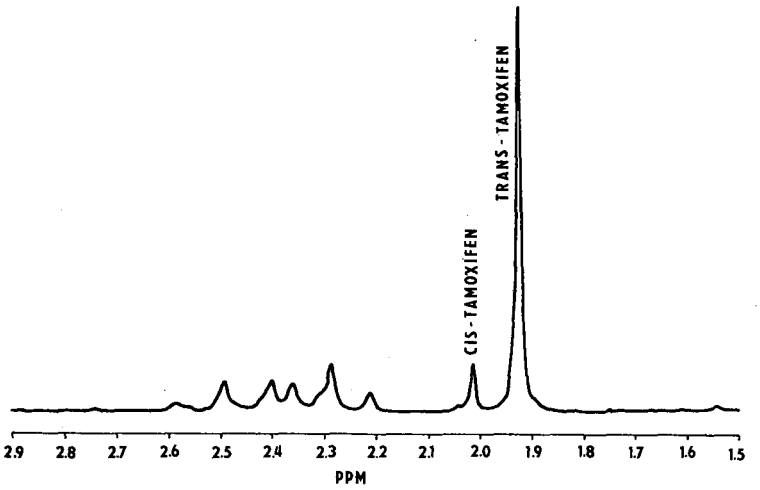

Fig. 3. ^{1}H NMR spectrum of *trans*-tamoxifen solution (0.5 mg/ml) exposed to daylight for 10 h. Solvent, deuterobenzene; spectrum width, 1200 Hz; digital resolution, 0.07 Hz per point; pulse duration, 2.5 μs.

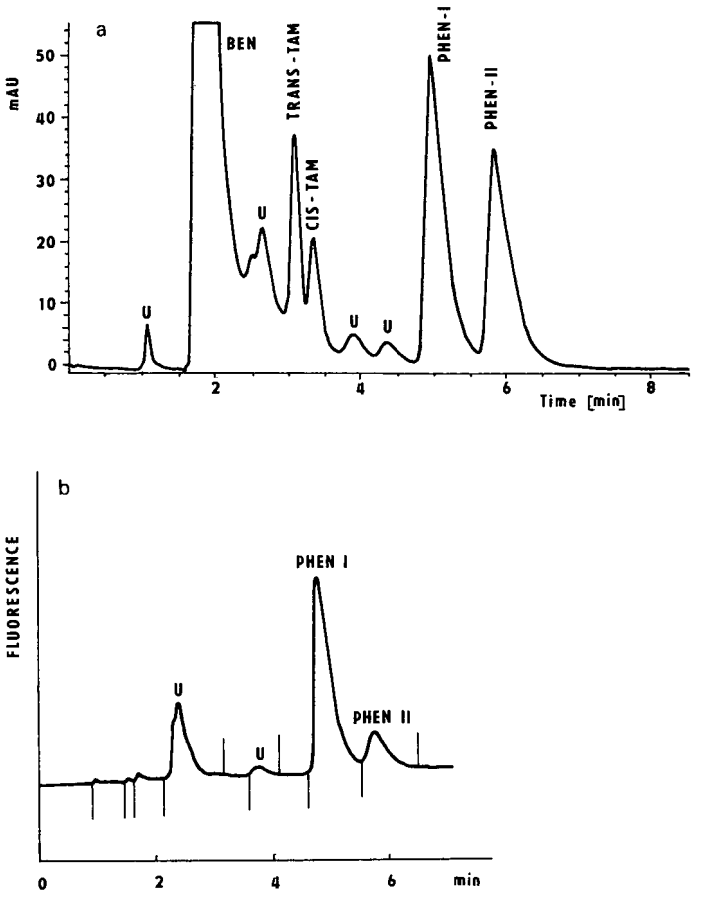

Fig. 4. HPLC of photoproducts of tamoxifen. BEN = benzene; TRANS-TAM = *trans*-tamoxifen; CIS-TAM = *cis*-tamoxifen; PHEN I = phenanthrene I; PHEN II = phenanthrene II; U = unknown. Flow-rate, 1 ml/min; sample, effluent fraction from irradiated PTFE capillary after extraction into benzene; detection, (a) UV (diode-array), 254 nm and (b) fluorescence, λ_{ex} = 245 nm, λ_{em} = 385 nm.

of one isomer to the other occurs with daylight. During irradiation for 10 h in an aqueous solution, 11% of the *trans* isomer was converted to the cis-isomer. This result explains the strict instruction that tamoxifen solution should be stored in the dark[8].

HPLC with diode-array and fluorescence monitoring of the effluent from the PTFE capillary confirmed that this isomerization paralleled the appearance of two other highly fluorescent peaks (Fig. 4). Photochemical cyclization of both isomers appeared to proceed through almost identical reaction sequences and no difference in reaction behaviour was noted when either *cis*- or *trans*-tamoxifen was irradiated. Tamoxifen isomerizes and the corresponding phenanthrenes are produced (Fig. 5). This assumption is supported by the existence of an absorption band at 236 nm in the UV spectra of *trans*-tamoxifen and phenanthrene I (Fig. 6). The UV spectra of both phenanthrene derivatives are similar to that of a photocyclization product published by Mendenhall *et al.*[2] and Nieder and Jaeger[8].

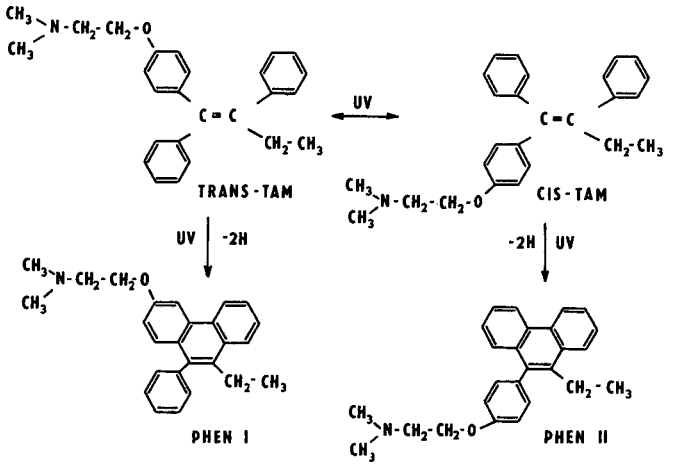

Fig. 5. Reaction scheme derived from identified products and their behaviour.

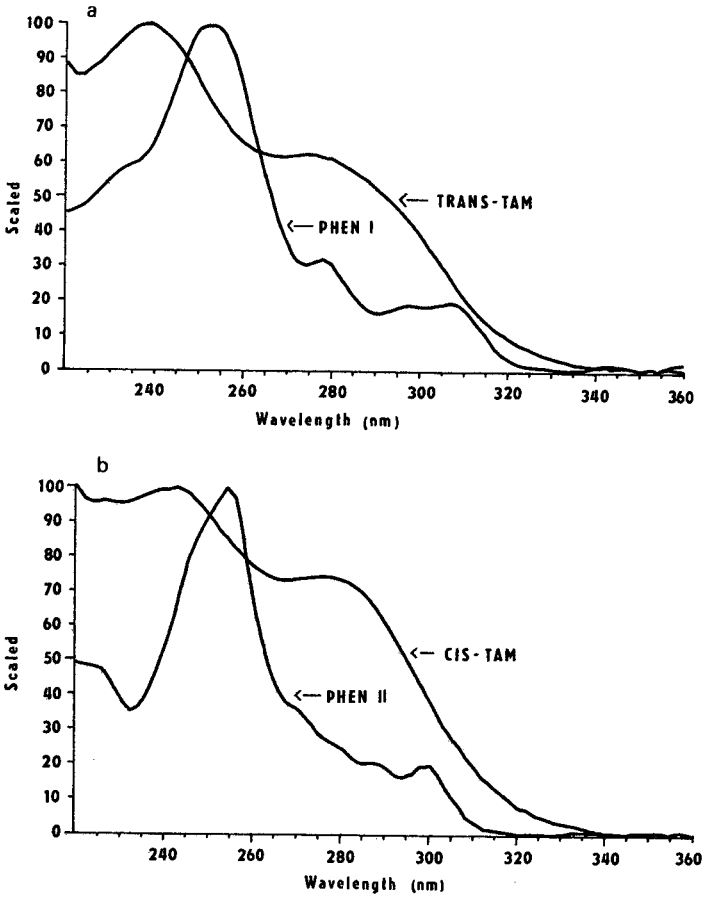

Fig. 6. UV spectra of (a) *trans*-tamoxifen and phenanthrene I and (b) *cis*-tamoxifen and phenanthrene II. For abbreviations, see Fig. 4.

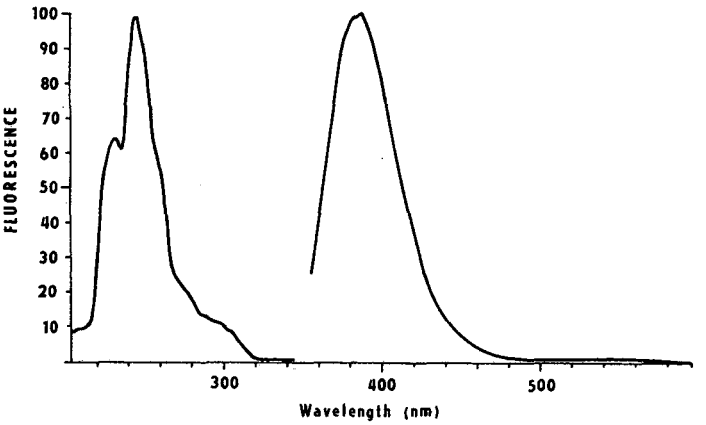

Fig. 7. Fluorescence spectrum of phenanthrene I. λ_{ex} = 245 nm, λ_{em} = 385 nm.

The fluorescence response of phenanthrene I is three times higher than that of phenanthrene II. This difference is probably caused by the presence and the position of the electron-donating group $-OCH_2CH_2N(CH_3)_2$, which tends to enhance the fluorescence by increasing the electron density of the phenanthrene aromatic system. The molecule of phenanthrene I could form a more rigid and planar structure, which is usually favourable for fluorescence.

Both *cis*- and *trans*-tamoxifen exhibit virtually no native fluorescence. The irradiation of effluent containing these compounds results in a rapid increase in the fluorescence response when measured with λ_{ex} = 245 nm and λ_{em} = 385 nm. The

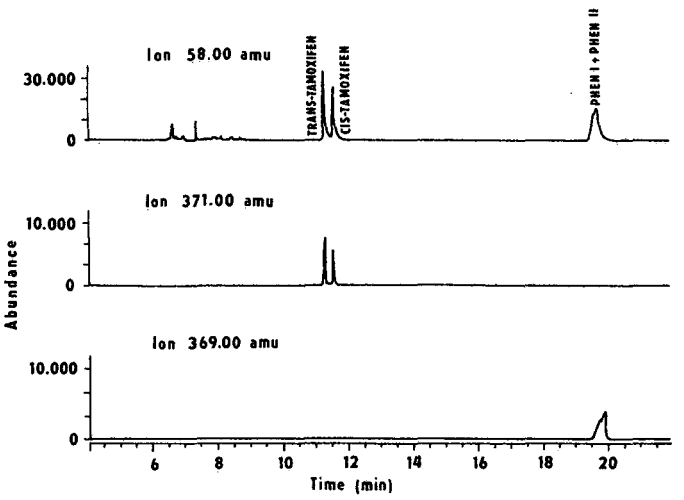

Fig. 8. GC–MS of photoproducts of *trans*-tamoxifen. For abbreviations, see Fig. 4. Chromatographic conditions: column, ULTRA 1 HP (12 m × 0.2 mm I.D.), film thickness 0.33 μm; carrier gas, helium; flow-rate, 0.4 ml/min; temperature programme, 60 to 260°C at 40°C/min; injection port temperature, 280°C. For sample, see Fig. 4.

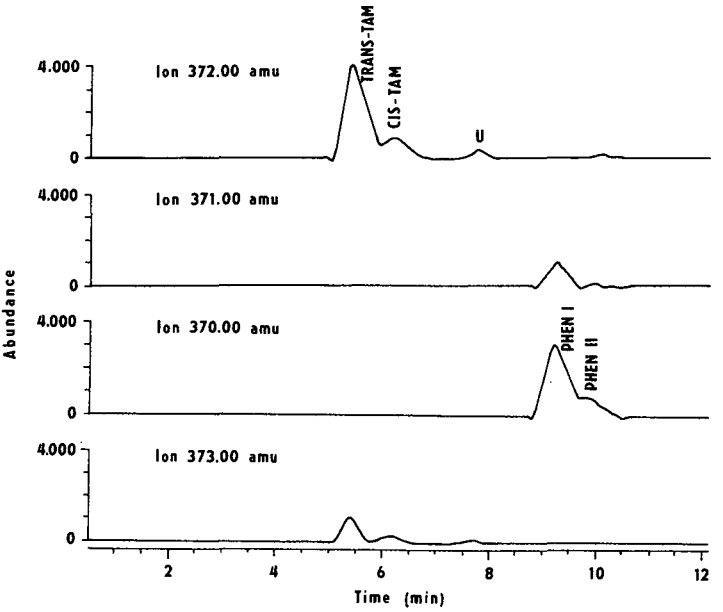

Fig. 9. HPLC–MS of *trans*-tamoxifen photoproducts. Chromatographic conditions: column, packed with Silasorb C_{18}; mobile phase, methanol–water–amonia (1000:50:7, v/v/v) plus 0.2 g/l of ammonium acetate; flow-rate, 1.2 ml/min; stem temperature, 120°C. For sample, see Fig. 4.

published excitation maxima vary from 251 to 266 nm and emission from 320 to 360 nm, depending on the type and the construction of the fluorescence detector[2–10]. The fluorescence spectra (Fig. 7) of the two phenanthrene derivatives are nearly identical when measured with a programmable fluorescence detector in the stop-flow mode. The spectra have maxima at λ_{ex} = 245 nm and λ_{em} = 385 nm. The fluorescence emission spectrum of a cyclization product published by Nieder and Jaeger[8] has two maxima at *ca.* 365 and 390 nm. The difference could be caused by the differences in the slits used for spectral scanning.

The identification of photoproducts was confirmed by GC–MS. All the main photoproducts contain the most intensive dimethylaminoethylene ion at *m/z* 58 produced by cleavage of the side-chain (Fig. 8, top). Although the separation of the two phenanthrene derivatives is not sufficient, it is evident that their mass is 369 u, whereas the separated tamoxifen isomers are detected at mass of 371 u.

Better resolution of all the photoproducts was achieved by LC–MS (Fig. 9). Mass spectra were measured by the use of the thermospray technique and ammonium acetate in the mobile phase so that M + 1 ions were produced. Peaks detected at 372 u are M^{+1} ions of tamoxifen isomers and those at 370 u are M + 1 ions of phenanthrene derivatives. Additionally, other smaller peaks at 371 and 373 u were found to be co-eluting phenanthrene peaks. The origin of these ions is not clear and an explanation would require further research. Unstable dihydrophenanthrene derivatives were not confirmed, although on the chromatogram (Fig. 8), in addition to the two peaks for the tamoxifens, other smaller peaks of mass 372 u were found. However, the disappearance of the yellow colour of irradiated effluents containing higher concen-

trations of tamoxifen could indicate the presence of dihydrophenanthrene derivatives[11].

The time of irradiation strongly influences the fluorescence yield and the formation of reaction products. At shorter times (1–5 s) isomerization mainly takes place and, *e.g.*, from *trans*-tamoxifen more phenanthrene I than II is formed. Prolonged irradiation resulted in a higher fluorescence response with the maximum at 9 s. The longer the irradiation of *trans*-tamoxifen, the more phenanthrene II was found in the reaction mixture and the total fluorescence response decreased.

CONCLUSIONS

This work has clarified that the tamoxifen cyclization used in LC makes it easier to detect trace amounts of tamoxifen, *e.g.*, in biological fluids. The variety of fluorescent products formed by UV irradiation reduces the advantages of precolumn derivatization.

The on-line postcolumn photocyclization of solutes in a PTFE or quartz capillary has the following advantages over precolumn derivatization: a higher fluorescence signal-to-noise ratio, which summarizes the contributions of all fluorescent products formed during photoreactions; and a less selective separation system may be required if the postcolumn reaction is used because a smaller number of peaks are separated.

Generally, this example takes advantage of an on-line and on-the-fly reaction system, permitting a more selective determination of compounds of interest in a biological matrix.

ACKNOWLEDGEMENTS

The authors are indebted to Dr. Hans-Peter Schiefer of Hewlett-Packard for providing the programmable fluorescence detector and Dr. Miloš Krejčí and Dr. Karel Šlais for advice.

REFERENCES

1 S. Iacobelli, M. E. Lippman and G. Robustelli della Cuna (Editors), *The Role of Tamoxifen in Breast Cancer*, Raven Press, New York, 1982.
2 D. W. Mendenhall, H. Kobayashi, F. M. L. Shih, L. A. Sternson, T. Higuchi and C. Fabian, *Clin. Chem.*, 24 (1978) 1518.
3 Y. Golander and L. A. Sternson, *J. Chromatogr.*, 181 (1980) 41.
4 M. Uihlein and E. Schwab, *Chromatographia*, 15 (1982) 140.
5 R. R. Brown, R. Bain and V. C. Jordan, *J. Chromatogr.*, 272 (1983) 351.
6 C. M. Camaggi, E. Strocchi and N. Canova, *J. Chromatogr.*, 275 (1983) 436.
7 B. J. Wilbur, C. C. Benz and M. W. DeGregorio, *Anal. Lett.*, 18 (1985) 1915.
8 M. Nieder and H. Jaeger, *J. Chromatogr.*, 413 (1987) 207.
9 E. A. Lien, P. M. Ueland, E. Solheim and S. Kvinnsland, *Clin. Chem.*, 33 (1987) 1608.
10 D. Stevenson, R. J. Briggs, D. J. Chapman and D. de Vos, *J. Pharm. Biomed. Anal.*, 6 (1988) 1065.
11 T. D. Doyle, N. Filipescu, W. R. Benses and D. Banes, *J. Am. Chem. Soc.*, 92 (1970) 6371.
12 *The United States Pharmacopeia*, 21st Revision, Mack, Easton, PA, 1985, p. 1010.
13 R. D. Armstrong, T. J. Ward, N. Pattabiraman, C. Benz and D. W. Armstrong, *J. Chromatogr.*, 414 (1987) 192.
14 L. S. Ettre, *J. Chromatogr.*, 220 (1981) 29.

Journal of Chromatography, 514 (1990) 189–198
Elsevier Science Publishers B.V., Amsterdam

CHROM. 22 525

Application of micro-scale liquid chromatography with fluorescence detection to the determination of thiols

B. LIN LING[a]

Department of Pharmaceutical Chemistry and Drug Quality Control, Pharmaceutical Institute, State University of Ghent, Harelbekestraat 72, B-9000 Ghent (Belgium)

C. DEWAELE*

Bio-Rad RSL, Begoniastraat 5, B-9731 Nazareth (Belgium)

and

W. R. G. BAEYENS

Department of Pharmaceutical Chemistry and Drug Quality Control, Pharmaceutical Institute, State University of Ghent, Harelbekestraat 72, B-9000 Ghent (Belgium)

(First received February 26th, 1990; revised manuscript received May 1st, 1990)

ABSTRACT

Different thiol compounds of biological and pharmacological interest were separated on a packed reversed-phase fused-silica capillary column and determined with fluorescence detection. Conventional inexpensive liquid chromatographic equipment could be adapted for such purposes, providing a highly efficient analytical system. The different compounds were derivatized with the fluorogenic reagents SBD-F and ABD-F and chromatographed both isocratically and in the gradient mode in order to separate a series of thiols with widely varying polarities. Subsequently the derivatives were measured at $\lambda_{ex.}$ = 380 nm and $\lambda_{em.}$ = 510 nm. Application of the system to biological and pharmacological samples is suggested.

INTRODUCTION

Since the late 1970s, when the groups of Novotny[1] and Ishii[2] introduced capillary columns in liquid chromatography (LC), the development of this technique has shown considerable progress. Numerous laboratories are increasingly interested in its potential, as evidenced by the frequent publication of books[3–8], reviews[9,10] and papers on the developments and/or applications of this technique in different fields. The success of capillary columns is undoubtedly due to their distinct advantages, including the low consumption of mobile phase and stationary phase, better permeability and efficiency, higher mass sensitivity and easy coupling with other

[a] On leave from the Department of Bromatology and Pharmaceutical Analytical Techniques, Faculty of Pharmacy, Complutense University of Madrid, Ciudad Universitaria, 28040 Madrid, Spain.

0021-9673/90/$03.50

separation and detection techniques[11,12]. However, micro-LC instrumentation and technology have still to develop their full potential. Their growth has been slow, the problem most often being the LC detection system[13].

In this work, a conventional LC pumping device and fluorescence detector were adapted to micro-LC analysis. This was possible by employing a split-flow technique for delivering the eluent and by using a laboratory-made square quartz cell for performing the micro-LC fluorescence measurements. As a result, a highly sensitive and efficient separation system was obtained, which was applied to the LC–fluorescence determination of several thiol compounds of biological and pharmacological importance. These compounds were first derivatized with the thiol-specific fluorogenic reagents SBD-F and ABD-F[14], developed by Imai's group[15–17], and for which several applications in high-performance LC[18–28] and in thin-layer chromatography[29–36] have been reported during the last 5 years.

EXPERIMENTAL

Chemicals

The thiol-specific fluorogenic reagents ammonium 7-fluoro-2,1,3-benzoxadiazole (SBD-F) and 4-(aminosulphonyl)-7-fluoro-2,1,3-benzoxadiazole (ABD-F) were obtained from Wako (Neuss, F.R.G.). The thiol compounds were purchased from Janssen Chimica (Beerse Belgium), Merck (Darmstadt, F.R.G.), UCB (Leuven, Belgium) and Aldrich (Beerse, Belgium). Captopril was obtained from Squibb (Brussels, Belgium). All compounds were chemically pure and were used without further purification. Acetonitrile and water for the mobile phase were of HPLC grade (Alltech, Deerfield, IL, U.S.A.).

Disodium EDTA (Merck) was added to all thiol and reagent solutions, at a concentration of 2.0 m*M*, to prevent metal-catalysed thiol oxidation.

All other chemicals and solvents were obtained from Merck and UCB.

Sample preparation: derivatization reaction[15–17]

Equal volumes of SBD-F (1.0 m*M* in 0.1 *M* aqueous sodium borate buffer, pH 9.5, containing 2.0 m*M* disodium EDTA) and of thiol solutions were vortex mixed and heated in a water-bath at 60°C for 60 min, followed by cooling in ice–water. The thiol solutions were freshly prepared in the buffer solution mentioned above. A 60–200-nl aliquot of the derivatized samples was subjected to micro-LC.

A reagent blank solution (no thiol present) was similarly prepared and analysed.

The procedure for derivatization of thiols with ABD-F was performed in the same way as with SBD-F, but with heating at 50°C for 5 min at pH 8.0.

Apparatus and chromatography

The isocratic chromatographic set-up consisted of a Waters Assoc. (Milford, MA, U.S.A.) Model 510 HPLC pump equipped with a split-flow system, a 60–200-nl internal volume injector (CI4W; Valco, Houston, TX, U.S.A.) and a 250 × 0.32 mm I.D. fused-silica capillary filled with 5-μm Nucleosil C_{18} or RoSiL C_{18} (Bio-Rad RSL, Eke, Belgium). The split-flow system was obtained by using a conventional HPLC column (5-μm RoSiL C_{18}, 150 × 4.6 mm I.D.) as a solvent by-pass, placing a T-splitter (Valco) between the pump and the conventional–micro-LC connection system. This

arrangement allowed a constant flow-rate of 1–5 μl min^{-1} to be achieved in the micro-column.

Detection of the derivatized samples was performed with a Shimadzu Model RF-535 fluorescence detector (Pleuger, Wijnegem, Belgium) in which a laboratory-made 312-nl square quartz detection cell (0.25 × 0.25 × 5.0 mm) was included. Excitation was at 380 nm and emission at 510 nm. Recording of the signals was performed with a Model 2020-0000 recorder (Linear, Instruments, Reno, NV, U.S.A.), integrating with a Chromatopac C-R3A (Shimadzu, Kyoto, Japan). Chromatography was carried out isocratically at ambient temperature using 0.15 *M* H_3PO_4–CH_3CN (90:10, v/v) as the mobile phase.

The gradient reversed-phase chromatography set-up was similar to that described above, but using a RoSiL C_{18} column (Bio-Rad RSL) and a Varian Aerograph (Walnut Creek, CA, U.S.A.) Model 5560 gradient pump at a flow-rate of 1.5 ml min^{-1} providing a 2.6 μl min^{-1} flow in the micro-LC column. The T-split system was then connected to a conventional 250 × 4.6 mm I.D. 5-μm RoSiL C_{18} HPLC column.

The flow-rate in the micro-LC column was frequently checked by connecting an empty 10-μl syringe to the column end and timing the advance of the liquid meniscus.

RESULTS AND DISCUSSION

Optimization of the chromatographic system

Chromatography was first applied to the separation of cysteine–, homocysteine–, glutathione– and acetylcysteine–SBD derivatives. Following the method suggested by Toyo'oka and Imai[18], isocratic elution using 0.1 *M* sodium phosphate (pH 6.0)–methanol (95:5, v/v) as the mobile phase was tried out. However, the high concentration of buffer solution caused salt precipitation and the eluent composition was therefore modified. Improved selectivity and efficiency of separation were obtained by replacing methanol with acetonitrile and by using a lower concentration of phosphate buffer solution. Finally, by replacing the salt with the corresponding acid, a considerable gain in resolution was obtained. The optimum mobile phase was 0.15 *M* H_3PO_4–CH_3CN (90:10, v/v).

Fig. 1A shows the analysis of four common thiols labelled with SBD-F, achieving their separation in 15 min and requiring only 60–200 nl of sample. The optimum flow-rate was 5 μl min^{-1}. Sample volumes of up to 1 μl may be injected although there appears some peak tailing. The detection cell used provided improved sensitivity and less background noise than when applying "on-column" detection, a technique in which part of the fused-silica column not containing packing material is used as the detection cell[37]. This is the result of using a square instead of a round cell.

The chromatographic conditions mentioned above could also be applied to the separation of the ABD derivatives of the four thiols although when the same mobile phase is used considerably longer retention times are then obtained, *viz.* 7.2, 12.6, 15.0 and 47.6 min for cysteine, homocysteine, glutathione and acetylcysteine, respectively (Fig. 1B). Blank reagent solutions did not provide any peaks in the chromatogram.

Determination of thiols

SBD-and ABD-labelled cysteine, homocysteine, glutathione and acetylcysteine were analysed on a reversed-phase packed fused-silica column and measured by

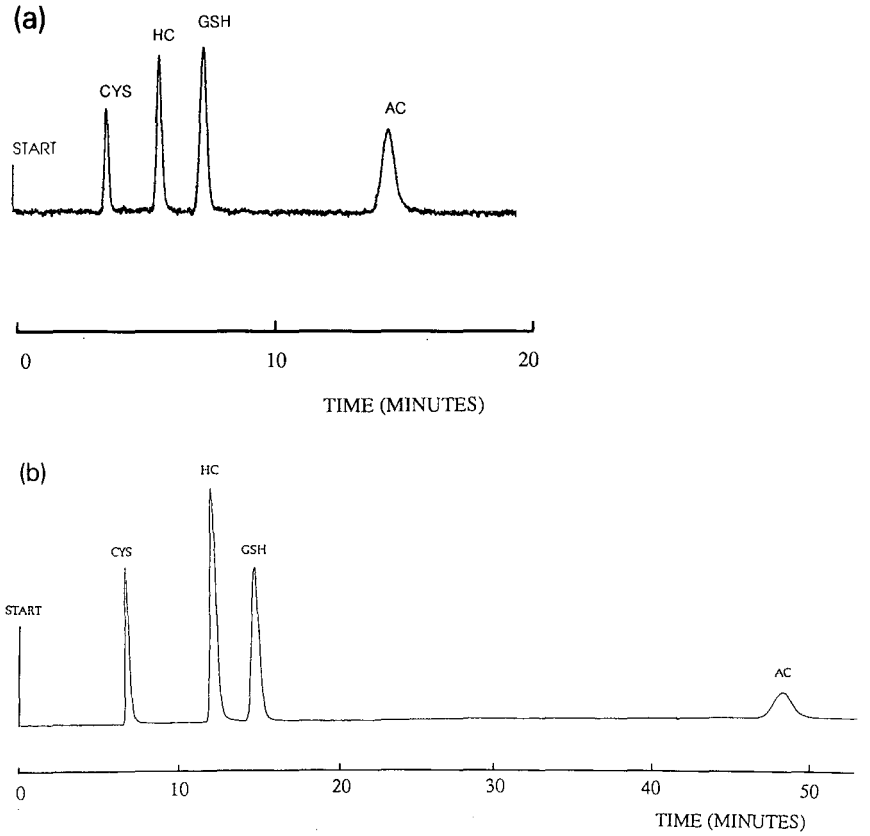

Fig. 1. Micro-LC separation of (A) SBD- and (B) ABD-thiol derivatives. CYS = cysteine; HC = homocysteine; GSH = glutathione; AC = acetylcysteine. Concentrations between 1 and 10 μg ml^{-1}. Column, 250 × 0.32 mm I.D., fused silica, 5-μm Nucleosil C_{18}; mobile phase, 0.15 *M* H_3PO_4–CH_3CN (90:10, v/v); flow-rate, 5 μl min^{-1}; detection, λ_{ex} = 380 nm, λ_{em} = 510 nm.

fluorescence detection. The detection limits for the SBD derivatives were 39, 7.4, 14 and 40 pg per injection (signal-to-noise ratio = 2), respectively, and those for the ABD derivatives were 77, 19, 24 and 29 pg per injection, respectively. The relative standard deviation of the peak areas was 1.86% (n = 10). The SBD derivatives generally yielded higher fluorescence signals than the ABD derivatives under identical conditions. Similar results were obtained from the calibration graphs (fluorescence intensity *versus* thiol concentration) for SBD–cysteine and ABD–cysteine as representative thiol derivatives. Linearity was observed in the range 0–3000 pg per injection (Fig. 2). In comparison with conventional HPLC in combination with concentration-based detectors, the sensitivity is increased in micro-LC as sample dilution is reduced when the same mass of sample is injected into a column of smaller I.D.[11].

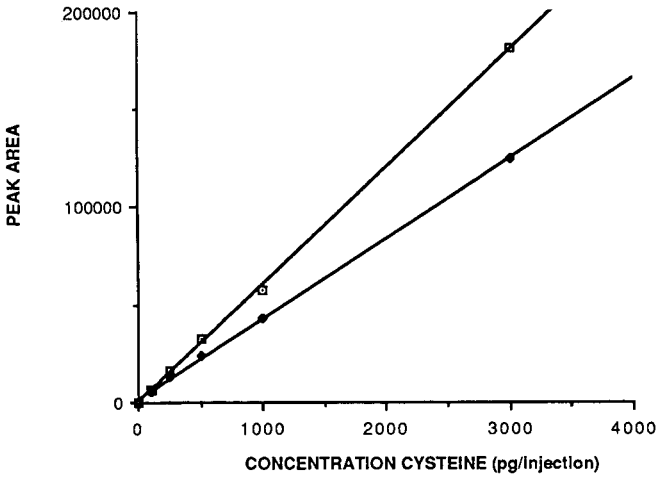

Fig. 2. Calibration graphs (0–3000 pg per 60-nl injection) for SBD- and ABD-cysteine. □ = SBD-cysteine; $y = 483.34 + 59.973x$, $R = 1.00$; ◆ = ABD-cysteine; $y = 2078.3818 + 41.0241x$, $R = 1.00$.

Isocratic and gradient chromatographic behaviour of other thiols

Various other thiol compounds of biological and pharmacological importance were derivatized with SBD-F and ABD-F. However, by using the recommended mobile phase, 0.15 *M* H_3PO_4–CH_3CN (90:10, v/v), most of the thiol derivatives showed inconveniently high retention times (>60 min). With a higher acetonitrile content [0.15 *M* H_3PO_4–CH_3CN (70:30, v/v)], all the derivatives were eluted in less than 10 min, giving the retention times and detection limits shown in Table I.

Gradient elution of these thiol derivatives resulted in a more efficient elution of the latter and also of the originally assayed thiol compounds. Fig. 3 shows the micro-LC gradient separation of several thiol compounds with various polarities, derivatized with both fluorogenic reagents. Blank runs gave stable baselines. It is advisable to follow with an isocratic elution just after the gradient elution to compensate for the volume delay. Eluent sonication and helium flushing for 20–30 min prior to chromatography is likewise advisable. An initial gradient elution trial from 0.15 *M* H_3PO_4–CH_3CN (100:0) to (50:50) over 15 min was initially tried. As expected, gradient elution allowed the elution of all the SBD- and ABD-thiol derivatives. However, certain thiol derivatives gave overlapping peaks for both types of derivatives. Considering the results obtained from the isocratic elution, a gradient elution from 0.15 *M* H_3PO_4–CH_3CN (95:5) to (70:30) was subsequently tried; the chromatogram obtained for the SBD derivatives is shown in Fig. 3A. As observed, the derivatives from a mixture of nine thiol compounds were clearly resolved in less than 30 min.

With the ABD derivatives a small addition of acetonitrile was required to allow a better elution of all the thiol derivatives, as their retention times are slightly higher than those of the corresponding SBD derivatives. Fig. 3B shows the chromatogram of eleven ABD derivatives separated with gradient elution from 0.15 *M* H_3PO_4–CH_3CN (95:5) to (65:35) over 20 min.

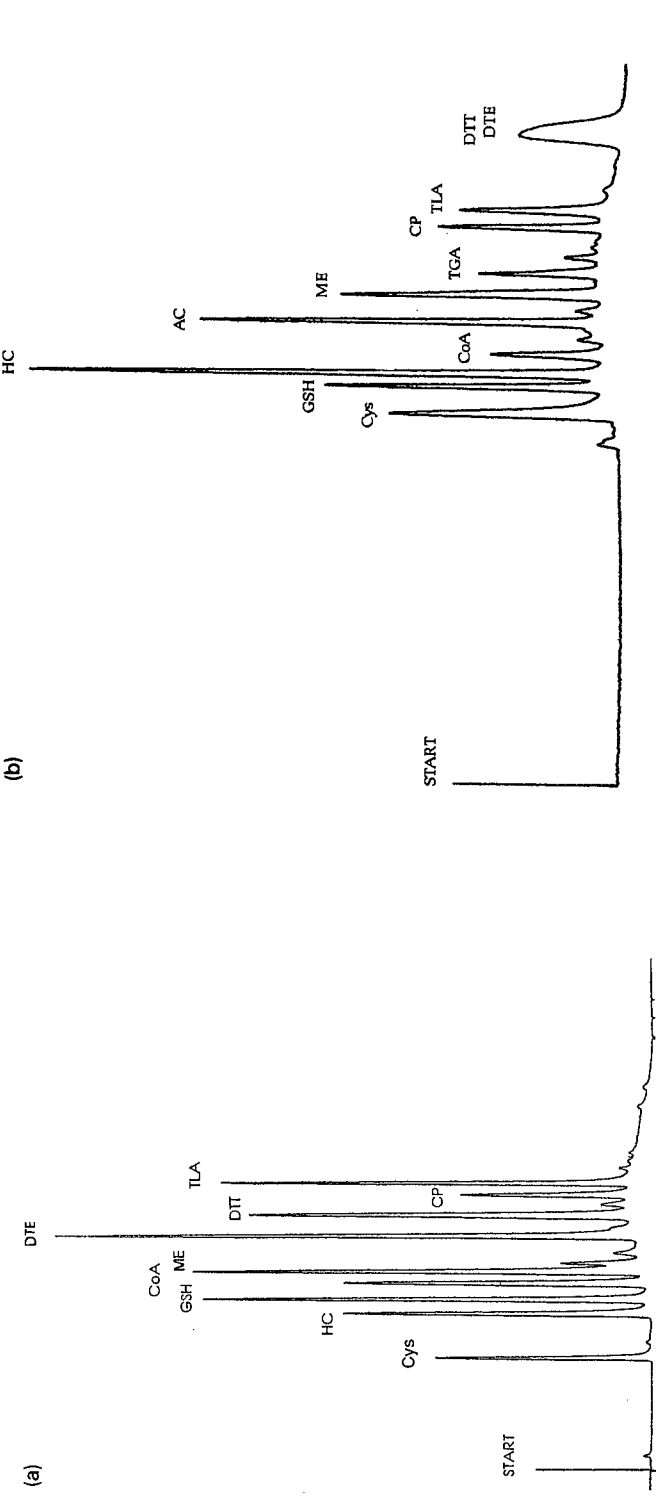

Fig. 3. Micro-LC gradient elution of (A) SBD- and (B) ABD–thiol derivatives. Cys = cysteine; HC = homocysteine; GSH = glutathione; CoA = coenzyme A; DTT = dithiothreithol; DTE = dithioerythritol; ME = mercaptoethanol; CP = captopril; TLA = thiolactic acid; TGA = thioglycolic acid; AC = acetylcysteine. SBD–thiol concentrations are between 1 and 40 μg ml^{-1} and ABD–thiol concentrations are between 10 and 200 μg ml^{-1}. Column, 250 × 0.32 mm I.D., fused silica, 5-μm RoSiL C_{18}; mobile phase, (A) from 0.15 *M* H_3PO_4 (A)–CH_3CN (B) (95:5, v/v) to A–B (70:30) over 15 min followed by isocratic elution with A–B (70:30) for 5 minutes and (B) from A–B (95:5) to A–B (65:35) over 15 min followed by isocratic elution with A–B (65:35) for 5 minutes; flow-rate, 4.0 μl min^{-1}; detection, $\lambda_{ex.}$ = 380 nm, $\lambda_{em.}$ = 510 nm.

TABLE I

RETENTION TIMES AND DETECTION LIMITS OF SBD- AND ABD-THIOL DERIVATIVES

Column, 250 × 0.32 mm I.D., fused silica, 5-μm RoSiL C_{18}; mobile phase, 0.15 *M* H_3PO_4–CH_3CN (70:30, v/v); flow-rate, 5 μl min^{-1}; detection, $\lambda_{ex.}$ = 380 nm, $\lambda_{em.}$ = 510 nm.

Thiol	*Retention time (min)*	*Detection limit (pg per 60-nl injection)*
SBD derivatives		
Acetylcysteine	3.90	39
Captopril	4.45	55
Cysteine	3.75	40
Coenzyme A	3.95	30
Dithioerythritol	4.02	58
Dithiothreitol	4.05	39
Glutathione	3.90	14
Homocysteine	4.80	7
Mercaptoethanol	3.95	8
Thioglycolic acid	4.30	30
Thiolactic acid	4.55	35
ABD derivatives		
Acetylcysteine	5.80	29
Captopril	9.45	102
Cysteine	5.10	77
Coenzyme A	5.80	31
Dithioerythritol	14.25	68
Dithiothreitol	12.95	130
Glutathione	5.30	24
Homocysteine	5.70	19
Mercaptoethanol	6.85	10
Thioglycolic acid	7.55	49
Thiolactic acid	10.45	93

Higher resolution was achieved by using longer columns (Fig. 4). However, direct comparison with the shorter columns is difficult owing to the different gradient profiles. The inconvenience of the long duration of analysis (>2 h) and the obvious dilution effect when using these long columns reduce their practical use.

Application of the described method to the determination of glutathione and cysteine in biological samples (blood, plasma) and to the analysis of pharmaceutical compounds (drug quality control) is currently under investigation. Fig. 5A shows the preliminary isocratic chromatogram obtained from human whole blood treated with trichloroacetic acid and derivatized with SBD-F^{18}. Fig. 5B shows the analysis of a glutathione-spiked human whole blood sample. Disposable 4-mm syringe filters (pore size 0.45 μm; Alltech) were used to inject clear particle-free derivatized sample solutions. Further research on this subject will be reported elsewhere.

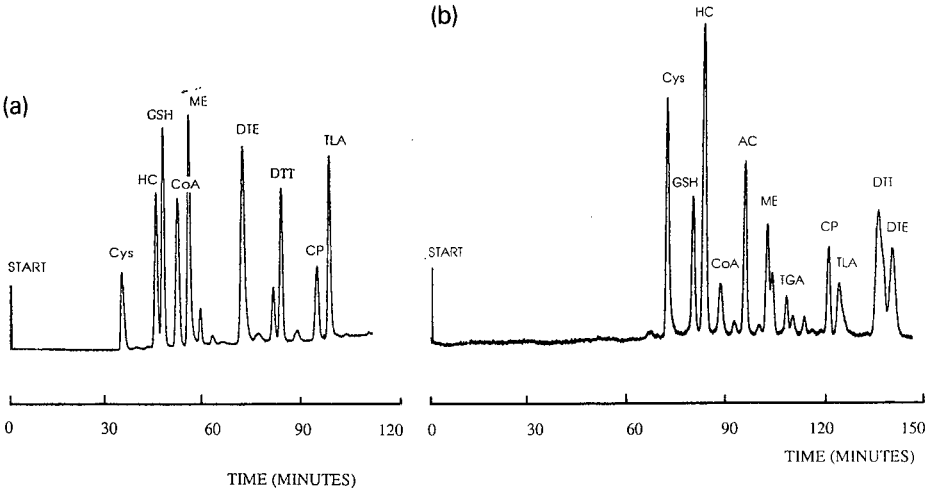

Fig. 4. Micro-LC gradient elution of (A) SBD– and (B) ABD–thiol derivatives on a long fused-silica capillary column (1000 × 0.32 mm I.D.), RoSiL C_{18}, 5 μm. The same compounds as in Fig. 3 were are analysed under similar experimental conditions, except for the flow-rate (2.0 μl min^{-1}) and the mobile phase: (A) from A–B (95:5, v/v) to A–B (70:30) over 90 min followed by isocratic elution with A–B (70:30) for 60 min; (B) from A–B (95:5) to A–B (65:35) over 90 min followed by isocratic elution with A–B (65:35) for 60 min.

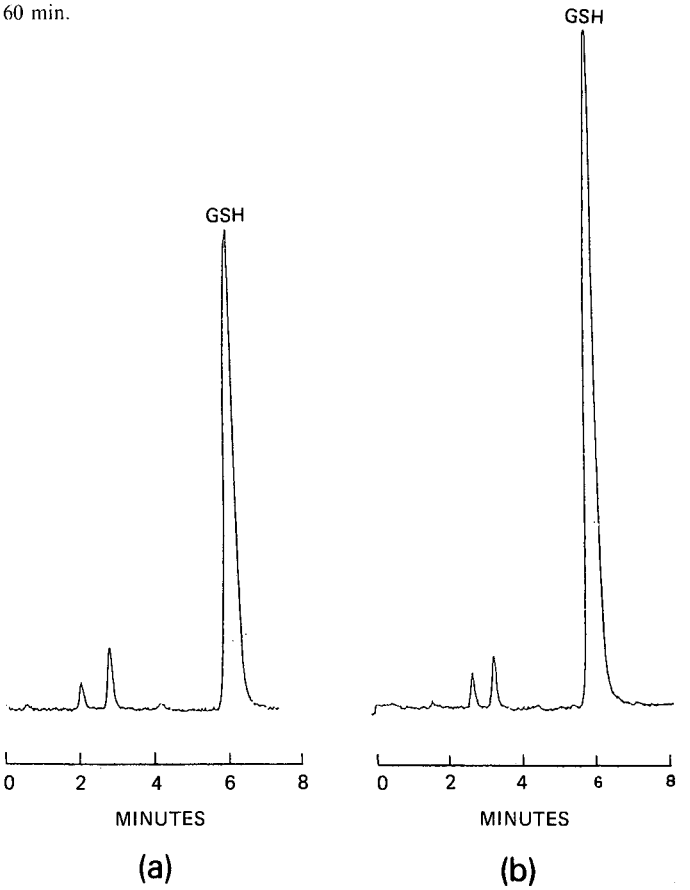

Fig. 5. Chromatogram obtained from human whole blood treated with trichloroacetic acid and derivatized with SBD-F^{17}. (A) Sample as such and (B) sample spiked with 75 μg ml^{-1} of glutathione added to the supernatant. Column, 250 × 0.32 mm I.D., fused silica, 5-μm RoSiL C_{18}; mobile phase, 0.15 *M* H_3PO_4–CH_3CN (90:10, v/v), isocratic; flow-rate, 5 μl min^{-1}; detection, $\lambda_{ex.}$ = 380 nm, $\lambda_{em.}$ = 510 nm.

CONCLUSIONS

The combined use of the micro-LC separation technique with selective and sensitive fluorescence detection allows the specific determination of trace amounts of various thiol compounds of biological and pharmacological interest. Conventional LC equipment may be successfully adapted to capillary columns, providing a suitable analytical method for the determination of thiols in different matrices. Gradient reversed-phase chromatography provided the separation of several fluorescent SBD– and ABD–thiol derivatives covering a wide range of polarities. The application of the system to the identification of glutathione in human whole blood was achieved.

ACKNOWLEDGEMENTS

B.L.L. and W.R.G.B. gratefully acknowledge all the technical facilities (instruments, columns and devices) and stimulating discussions provided by Bio-Rad RSL Laboratories; thanks are especially due to the LC Department. Pleuger (Wijnegem, Belgium) are thanked for the use of the Shimadzu RF-535 fluorescence detector. The authors also express their gratitude to Professor K. Imai (Branch Hospital Pharmacy, Tokyo, Japan) for his continuous and helpful discussions on the fluorobenzoxadiazole labelling topic and for providing some of the reagents and materials. Squibb (Brussels, Belgium) are likewise acknowledged for providing captopril bulk material and relevant scientific information on this compound.

REFERENCES

1 T. Tsuda and M. Novotny, *Anal. Chem.*, 50 (1987) 271.
2 D. Ishii, K. Asai, K. Hibi, T. Jonokuchi and M. Nagaya, *J. Chromatogr.*, 144 (1977) 157.
3 M. Novotny and D. Ishii (Editors), *Microcolumn Separations: Columns, Instrumentation and Ancillary Techniques*, Elsevier, Amsterdam, 1985.
4 F. J. Yang (Editor), *Microbore Column Chromatography. A Unified Approach to Chromatography*, Marcel Dekker, New York, 1988.
5 P. Kucera (Editor), *Microcolumn High-Performance Liquid Chromatography*, Elsevier, Amsterdam, 1984.
6 R. P. W. Scott (Editor), *Small Bore Liquid Chromatography Columns: Their Properties and Uses*, Wiley, New York, 1984.
7 D. Ishii (Editor), *Introduction to Microscale High-Performance Liquid Chromatography*, VCH, New York, 1988.
8 B. G. Belen'kii, E. S. Gankina and V. G. Mal'sfev, *Capillary Liquid Chromatography*, Plenum Press, New York, 1987.
9 M. Novotny, *Anal. Chem.*, 60 (1988) 500A.
10 K. Jinno, *Chromatographia*, 25 (1988) 1004.
11 K. Jinno, *LC · GC*, 7 (1989) 328.
12 M. Verzele, C. Dewaele and M. De Weerdt, *LC · GC*, 6 (1988) 966.
13 G. J. De Jong, in P. Sandra and G. Redaut (Editors), *Proceedings of the 10th International Symposium on Capillary Chromatography, Riva del Garda*, Huethig, Heidelberg, 1989, p. 1476.
14 W. R. G. Baeyens, K. Imai and B. Lin Ling, in L. J. Cline Love and D. Eastwood (Editors), *Progress in Analytical Luminescence*, American Society for Testing and Materials, Philadelphia, PA, 1988, pp. 83–99.
15 K. Imai, T. Toyo'oka and Y. Watanabe, *Anal. Biochem.*, 128 (1983) 471.
16 T. Toyo'oka and K. Imai, *Analyst (London)*, 109 (1984) 1003.
17 T. Toyo'oka and K. Imai, *Anal. Chem.*, 56 (1984) 2461.
18 T. Toyo'oka and K. Imai, *J. Chromatogr.*, 282 (1983) 495.

19 T. Toyo'oka, K. Imai and Y. Kawahara, *J. Pharm. Biomed. Anal.*, 2 (1984) 473.
20 T. Toyo'oka, H. Miyano and K. Imai, *Peptide Chemistry 1985,* Peptide Research Foundation, Osaka, 1986.
21 T. Sueyoshi, T. Miyata, S. Iwanaga, T. Toyo'oka and K. Imai, *J. Biochem.*, 97 (1985) 1811.
22 T. Toyo'oka and K. Imai, *Anal. Chem.*, 57 (1985) 1931.
23 T. Toyo'oka, H. Miyano and K. Imai, *Biomed. Chromatogr.*, 1 (1986) 15.
24 K. Imai and T. Toyo'oka, *Methods Enzymol.*, 143 (1987) 67.
25 T. Toyo'oka, S. Uchiyama, Y. Saito and K. Imai, *Anal. Chim. Acta*, 205 (1988) 29.
26 A. Araki and Y. Sako, *J. Chromatogr.*, 422 (1987) 43.
27 T. Toyo'oka, F. Furukawa, T. Suzuki, Y. Saito, M. Takahashi, Y. Hayashi, S. Uzu and K. Imai, *Biomed. Chromatogr.*, 3 (1989) 166.
28 K. Imai, *J. Pharm. Biomed. Anal.*, in press.
29 B. Lin Ling, W. R. G. Baeyens, B. Del Castillo, K. Imai, P. De Moerloose and K. Stragier, *J. Pharm. Biomed. Anal.*, 7 (1989) 1663.
30 B. Lin Ling, W. R. G. Baeyens, B. Del Castillo, K. Stragier and H. Marysael, *J. Pharm. Biom. Anal.*, 7 (1989) 1671.
31 B. Lin Ling, W. R. G. Baeyens, H. Marysael and K. Stragier, *J. High Resolut. Chromatogr. Chromatogr. Commun.*, 12 (1989) 345.
32 B. Lin Ling, W. R. G. Bayens, H. Marysael, K. Stragier and P. De Moerloose, *J. Liq. Chromatogr.*, in press.
33 B. Lin Ling, W. R. G. Baeyens, A. Raemdonck and H. Marysael, *Anal. Chim. Acta*, 227 (1989) 203.
34 B. Lin Ling, W. R. G. Baeyens and A. Raemdock, *J. Chromatogr.*, 502 (1990) 230.
35 W. R. G. Baeyens, B. Lin Ling and V. Corbisier, *Analyst (London)*, 115 (1990) 359.
36 W. R. G. Baeyens, B. Lin Ling and K. Stragier, *Chromatographia*, in press.
37 M. Verzele, M. De Weerdt, C. Dewaele, G. J. De Jong, N. Lammers and F. Spruit, *LC · GC*, 4 (1986) 1162.

Journal of Chromatography, 514 (1990) 199–207
Elsevier Science Publishers B.V., Amsterdam

CHROM. 22 530

Efficient determination of phytoecdysteroids from *Ajuga* species and *Polypodium vulgare* by high-performance liquid chromatography

FRANCISCO CAMPS*, JOSEP COLL, M. PILAR MARCO and JAIME TOMÁS
Department of Biological Organic Chemistry, CID–CSIC, Jordi Girona 18-26, 08034 Barcelona (Spain)
(First received October 31st, 1989; revised manuscript received March 12th, 1990)

ABSTRACT

Efficient chromatographic conditions were established for the simultaneous determination of eight phytoecdysteroids by high-performance liquid chromatography. Spherisorb ODS-2 columns, ultraviolet detection, isopropanol–water as the mobile phase and temperature control were used. Ecdysteroids were obtained by purification of methanol plant extracts with Sep-Pak C_{18} cartridges. The results compared well with those obtained by other chromatographic methods in terms of resolution, selectivity and efficiency.

INTRODUCTION

Ecdysteroids are a group of steroidal compounds related to the insect moulting hormones. They all have the same rigid 5β-cholestane skeleton with a 7-en-6-one chromophore and a variable number of hydroxyl substituents.

Several methods have been used for the determination of ecdysteroids[1–3]. High-performance liquid chromatography (HPLC) with or without prior derivatization was found to be quicker and easier to use than gas chromatography (GC) although GC with electron-capture detection exhibits a higher selectivity and sensitivity[4]. In addition, HPLC is a non-destructive method and fractions of pure compounds may be collected for identification or bioassay purposes[5].

Baseline resolution of many ecdysteroids can be achieved by HPLC on columns of microparticulate material[6]. Both silica and reversed-phase supports can be efficiently used but the solvent systems have to be optimized. Reversed-phase packings are the most commonly employed and selective effects of different mobile phases have been described[1]. Mixtures of methanol–water and acetonitrile–water with other organic modifiers such as tetrahydrofuran are the most common solvent systems reported. Acid buffers[7,8], cationic detergents[9] and high-performance columns (with a length of 20 or 25 cm) must be used for difficult separations, but these conditions

0021-9673/90/$03.50

usually cause baseline disturbances or lead to long time analysis. Moreover, the inorganic modifiers make work under preparative conditions difficult.

Plants contain ecdysteroids in larger amount than insects. More than 100 ecdysteroids have so far been isolated from plants[10,11], but only some of these compounds have also been detected in insects. During the course of our work on the production of ecdysteroids by plant tissue cultures from different *Ajuga* species and the fern *Polypodium vulgare*, we needed a suitable and efficient chromatographic method to determine these compounds using a peak-area standard. Owing to the number of quantitative analyses required, an important priority in this reasearch was the development of a reliable and effective HPLC separation method for the main ecdysteroids produced by these plants.

In this paper, we report an efficient and rapid chromatographic system for the simultaneous determination of eight different ecdysteroids present in *Polypodium vulgare* and several *Ajuga* species.

EXPERIMENTAL

Chemicals and materials

29-Norsengosterone (NS), 29-norcyasterone (NC). cyasterone (CY) and ajugalactone (AJL) standards were extracted from *Ajuga reptans*, 20-hydroxyecdysone (20-HE), ecdysone (E), 20,26-dihydroxyecdysone (20,26-HE) and polypodine B (PB) were obtained by purification from *Polypodium vulgare* rhizome extracts and makisterone-A (MK) was obtained from *Ajuga chamaepitys*. For the extraction and purification we used procedures already described for the isolation of ecdysteroids from biological samples[12,13], with slight modifications.

High-purity solvents (HPLC grade) were purchased from Merck, Scharlau or Romil. Water for HPLC was purified with a Milli-Q system and, prior to use, filtered through 0.45-μm Millipore filters (Type HA, for aqueous solvents) and degassed in ultrasonic bath under vacuum.

HPLC

Two Waters Assoc. Model 150 pumps were used for solvent delivery, controlled by a Waters Assoc. Model 660 solvent-programming unit. Samples were introduced via a Rheodyne 7105 injector, and compounds were detected with a Waters Assoc. Model 450 variable-wavelength UV spectrophotometer set at 242 nm. Temperature was regulated with a Perkin-Elmer Model 1220 oven. Chromatograms were recorded with a Waters Assoc. Model 740 data module integrator.

The analyses were carried out on a 25 × 0.4 cm I.D. (10 μm particle size) and 10 × 0.4 cm I.D. (5 μm) Spherisorb ODS-2 C_{18} (Tracer Analítica), 12 × 0.4 cm I.D. (3 μm) Spherisorb ODS-2 C_{18} (Scharlau) ad LiChroCART 12.5 × 0.4 cm I.D. (5 μm) LiChrospher 100 RP-18 (Merck) reversed-phase columns under isocratic conditions.

Preparation of samples

Different samples of *Ajuga* species (400–1000 mg) and *Polypodium vulgare* (25–50 mg) were extracted with methanol in an ultrasonic bath or homogenized with methanol and methanol–water mixtures. The methanolic extracts were centrifuged, washed with hexane and, after partial evaporation of the organic solvent, diluted with

water to 10 ml of *ca.* 10% aqueous methanol and retained on a reversed phase Sep-Pak C_{18} cartridge. Isolation of ecdysteroid fractions was carried out by elution of more polar substances than ecdysteroids with 10 ml of 15% aqueous methanol. Ecdysteroids were then eluted with 5.5 ml of 85% aqueous methanol, the first 0.5 ml were discarded and the next 5 ml were used for HPLC analysis. Less polar substances than ajugalactone in the case of *Ajuga* or ecdysone for *Polypodium* were not eluted under these conditions.

The ecdysteroid eluate from the Sep-Pak C_{18} cartridge was injected directly into the HPLC column after mixing with a solution of methyl anthranilate as a peak-area standard for quantitative analysis.

Quantification

Ecdysteroid concentrations were calculated by interpolation on the calibration graph obtained for 20-hydroxyecdysone as a representative of the more polar (first group) phytoecdysteroids and ajugalactone as a representative of the less polar compounds (last group in this present study) with methyl anthranilate (MA) as a peak-area standard. MA elutes between the two groups and does not interfere under

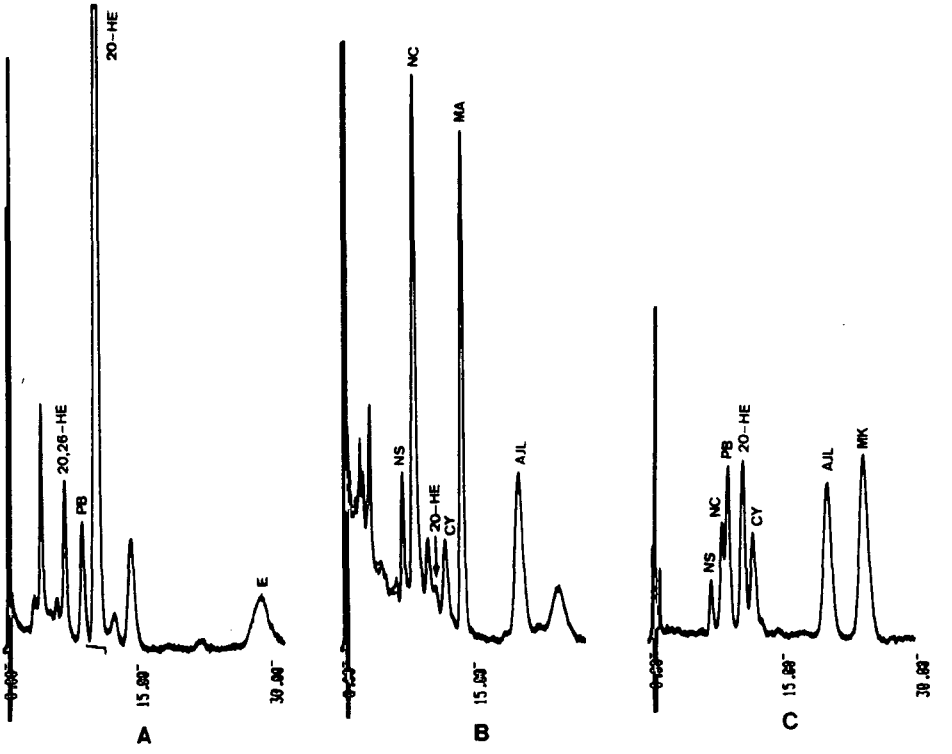

Fig. 1. Chromatographic profiles of plant extracts: (A) *in vitro* growing prothalli of *Polypodium vulgare*; (B) *in vitro* micropropagated plantlets of *Ajuga reptans*; (C) a mixture of standards. Column, LiChrospher 100 RP-18 (5 μm), 12.5 × 0.4 cm I.D., thermostated at 55°C; mobile phase, isopropanol–water (6.5:93.5) at 2 ml/min.

the conditions used. The result obtained was multiplied by a correction factor corresponding to the different absorptivities, the most important element affecting the area of an eluted product in comparison with other factors such as reversible and irreversible absorption on the column.

RESULTS AND DISCUSSION

The separation of polypodine B and 20-hydroxyecdysone, two of the ecdysteroids present in these plants, is regarded as a difficult problem in HPLC analysis[14], even with extended analysis time. However, as will be seen later, we have achieved this separation using isopropanol–water mixtures and a reversed-phase microparticulate support. A comparative study of different eluent systems and temperature conditions allowed us to determine the ecdysteroid content in methanolic extracts of *P. vulgare* and *Ajuga* species. Fig. 1 shows the chromatograms for two methanolic plant extracts.

The aim of all chromatographic analyses is to optimize the resolution in the minimum time. Resolution (R) is a function of the selectivity (α), the number of theoretical plates or efficiency (N) and the capacity factor (k').

The choice of an appropriate solvent system allows the optimization of α and k'. Mixtures of isopropanol and water were tested as eluents and compared with two normal solvent systems used in the chromatography of ecdysteroids, namely methanol–water and acetonitrile–water. A primary consideration was the need to find an isocratic system, if possible, without a buffer in the eluent, in order to be able to apply it for preparative purposes.

The mobile phase was optimized in order to separate 20-hydroecdysone and polpypodine B using the 10-μm column. The three systems were tested with different proportions of organic solvent, but the resolution was always poor when using acetonitrile–water mixtures even with prolonged analysis. The best results were obtained with isopropanol as organic modifier because it showed a higher resolution for a similar capacity factor.

Next, six other ecdysteroids, 29-norsengosterone, 29-norcyasterone, cyasterone, ajugalactone, ecdysone and makisterone-A, were tested, again comparing the three solvent mixtures. In this instance we employed the 5-μm column at room temperature. The best conditions were the use of methanol–water (30:70) or isopropanol–water (7:93), but the latter mixture exhibited a higher resolution. However, in no instance were all peaks completely separated down to the baseline. Ternary mixtures described in the literature, such as methanol–acetonitrile–water[5], were tried but not all the standards were separated under these conditions.

The relative retention times result from the different distribution coefficients of the components of the sample between the eluent and the stationary phase. With some exceptions (*e.g.*, exclusion chromatography) these distribution coefficients are thermodynamic parameters and, in consequence, they depend on the temperature, among other factors. This effect was studied by thermostating the column at various temperatures, employing two different systems and conditions. In the first instance the 5-μm column was used, the mobile phase was isopropanol–water (7:93) at a flow-rate 1 ml/min and the temperature was varied from 35 to 60°C. In the second, a reversed-phase 3-μm column was used, the mobile phase, was isopropanol–water (9:91) at a flow-rate of 0.9 ml/min and the temperature was varied from 23 to 63°C.

TABLE I

EQUATIONS OF ADJUSTED CURVES FOR THE VARIATION OF THE CAPACITY FACTOR WITH TEMPERATURE (T)

Stationary phase, Spherisorb ODS-2, 5 μm; column, 10 × 0.4 cm I.D.; mobile phase, isopropanol–water (7:93) at 1 ml/min. $T_{\frac{1}{2}}$ = exponential decay rate (°C).

Phytoecdysteroid	*Equation of exponential decay*	$T_{\frac{1}{2}}$	r
29-Norsengosterone (NS)	$k' = 21.6e^{-0.045T} + 3.0$	15.20	0.999
29-Norcyasterone (NC)	$k' = 32.0e^{-0.049T} + 3.3$	14.07	0.999
Polypodine B (PB)	$k' = 19.3e^{-0.038T} + 3.7$	17.87	0.998
20-Hydroxyecdysone (20-HE)	$k' = 29.1e^{-0.042T} + 4.1$	16.20	0.999
Cyasterone (CY)	$k' = 39.0e^{-0.046T} + 4.8$	15.06	0.999
Makisterone (MK)	$k' = 75.7e^{-0.044T} + 7.1$	15.60	1
Ajugalactone (AJL)	$k' = 76.8e^{-0.044T} + 8.6$	15.61	1

The same behaviour was observed in both instances. The capacity factor decreased with increase in temperature, following an exponential decay curve. The adjusted curves had similar exponents except for 29-norcyasterone and polypodine B (Table I). The former had a higher exponent and its retention time decayed faster than the others, whereas the exponent for polypodine B was lower and its retention time diminished at slower rate (Fig. 2). Consequently, both curves crossed at *ca.* 40°C, after which the elution of these two compounds was reversed.

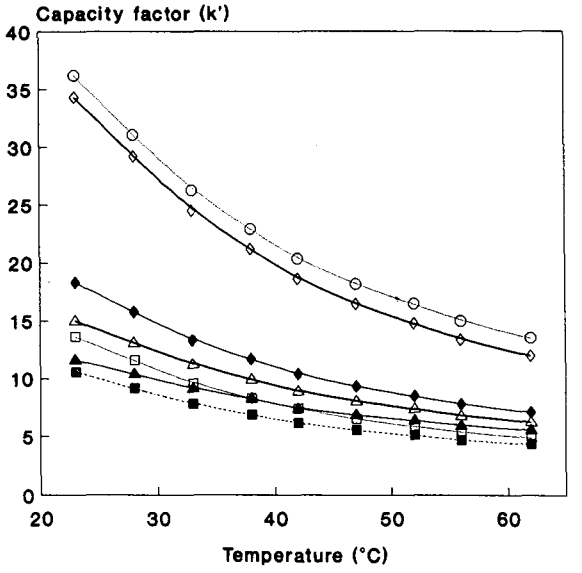

Fig. 2. Effect of temperature on the capacity factor. Column, 12 × 0.4 cm I.D. packed with Spherisorb ODS-2 (3 μm); mobile phase, isopropanol–water (9:91) at 0.9 ml/min. □ = NC; ▲ = PB; ■ = NS; △ = 20-HE; ◆ = CY; ◇ = MK; ○ = AJL.

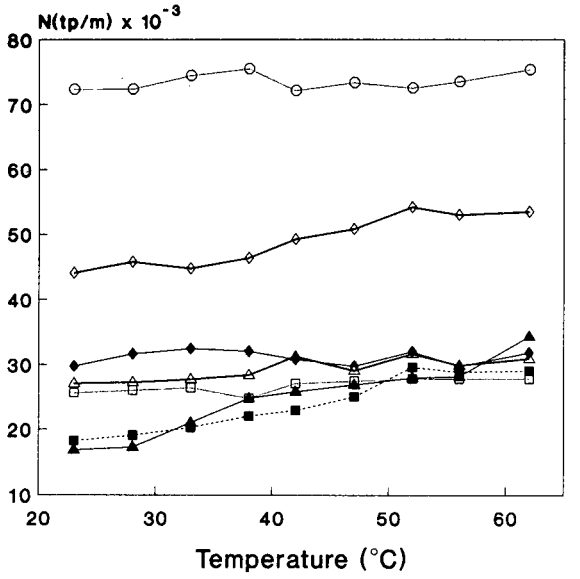

Fig. 3. Effect of temperature on the efficiency. Column, 12 × 0.4 cm I.D. packed with Spherisorb ODS-2 (3 μm); mobile phase, isopropanol–water (9:91) at 0.9 ml/min. N (number of theoretical plates, tp) = 5.54 $(V/W_{\frac{1}{2}})^2$, where V = retention volume of the peak and $W_{\frac{1}{2}}$ = peak width (in volume) at half weight. Symbols as in Fig. 2.

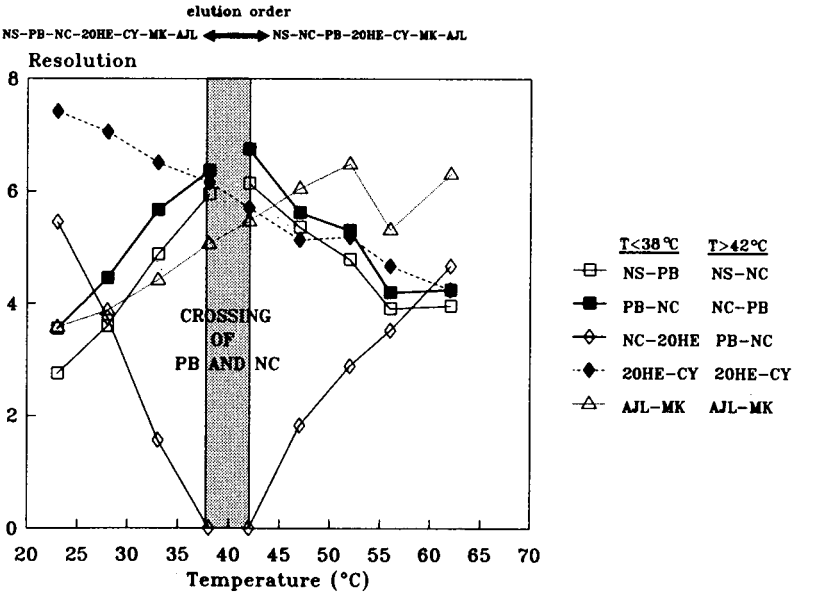

Fig. 4. Variation of the resolution with temperature. The best conditions appear to be in the temperature range 55–60°C. Column, 12 × 0.4 cm I.D. packed with Spherisorb ODS-2 (3 μm); mobile phase, isopropanol–water (9:91) at 0.9 ml/min. $R = (\sqrt{N}/4)[(\alpha-1)/\alpha][k'/(k'-1)]$.

The diminution of the capacity factor has a negative effect on the resolution, but in this instance it is accompanied by a narrowing of the peaks marked enough to produce an increase in the number of theoretical plates. This increment is so important for 29-norsengosterone and polypodine B that the number of plates almost doubled when the temperature was increased from 23 to 60°C. For most of the ecdysteroids, N begins to decrease when the temperature exceeds 50°C (see Fig. 3).

The resolution and selectivity were calculated for pairs of consecutive peaks. As can be seen in Fig. 4, if no peak crossing is involved, the resolution increases with increase in temperature. The discontinuities are due to the crossing of the peaks of 29-norcyasterone and polypodine B, which are not resolved between 35 and 45°C.

The temperature for optimum resolution of all the ecdysteroids was found to be 55°C. At this temperature, under both sets of conditions studied, the value of R was over 3.75 (Fig. 4) and all the peaks were separated near to their bases. With samples that do not contain simultaneously both 29-norcyasterone and polypodine B, optimum resolution was obtained between 40 and 45°C.

The R value for the pair NS–20-HE increased from 7.16 at room temperature to 12.22 at 50°C using the same column (Table II). Moreover, the analysis time was also minimized. The effect of temperature was also studied with the methanol–water mobile phase. An increase in temperature produced a decrease in selectivity and above 30°C 20-hydroxyecdysone was not separated from cyasterone or 29-norcyasterone from polypodine B. In this instance the use of buffers did not result in a better separation (Table II).

After this study, analyses of plants were carried out with isopropanol–water (7:93) at 55°C using he columns described above. Fig. 5 shows the calibration graphs obtained for 20-hydroxyecdysone and ajugalactone. Other ecdysteroids were determined by interpolation on these graphs, taking into account a correction factor corresponding to the different absorptivities. The results found for *P. vulgare* and *Ajuga* species are expressed as percentage of dry weight in Table III.

As no buffer is needed, these conditions might be adapted for preparative or semi-preparative separations. Compounds present in plant extracts together with ecdysteroids show a different behaviour in HPLC with the variation of temperature.

TABLE II

RESOLUTION OBTAINED WITH DIFFERENT TEMPERATURE CONDITIONS

If no buffer is present a clear increase in the resolution is observed from room temperature to 50°C, whereas the use of buffer (formic acid–triethylamine, 0.075 M, pH 3) did not improve it. All analyses were performed using a reversed-phase column, 10 × 0.4 cm I.D.; stationary phase, Spherisorb ODS-2, 5 μm; mobile phase, isopropanol–water (7:93) at 1 ml/min.

Temperature (°C)	*Buffer pH*	*k'*		*α*	*N(BE) (theoretical plates/m)*	*R*
		NS	*20-HE*			
25	–	24.7	36.8	1.49	8000	7.16
25	3	14.5	21.2	1.46	9400	7.29
50	–	15.5	23.6	1.52	22200	12.22
50	3	18.2	12.1	1.47	10300	7.49

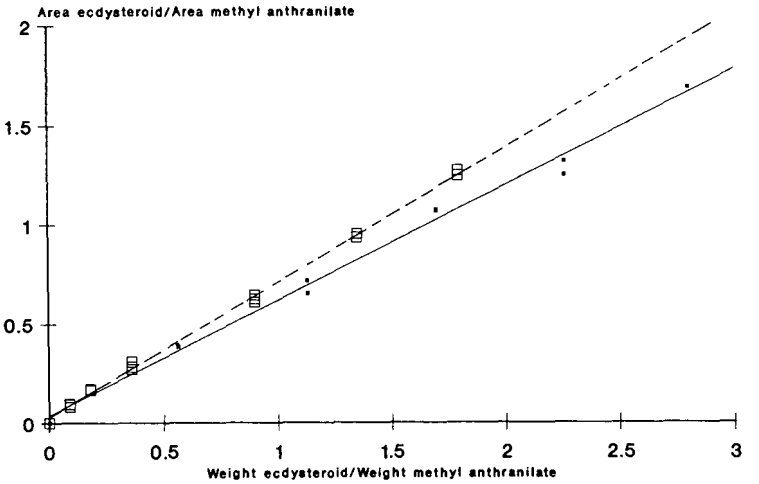

Fig. 5. Linear calibration graphs obtained for 20-hydroxyecdysone (solid line) and ajugalactone (dotted line) with methyl anthranilate as peak-area standard.

Thus, temperature control can be used to optimize the separation conditions around the major peaks to be isolated in each particular problem.

With a semi-preparative column (Tracer Analítica, 15 × 1.0 cm I.D., Spherisorb ODS-2,5 μm) it was possible to obtain 20-hydroxyecdysone or ajugalactone of high purity [300 μg of ecdysteroid (70–85% purity) in 125 μl of methanol in each injection; product recovery 170–200 μg of >99.9% purity by HPLC]. In the same column, up to 8 mg (in 175 μl of methanol) of ecdysteroidal fraction was injected, and the ecdysteroids (>95% pure by HPLC) were recovered in *ca.* 85% of the amount present in the sample.

TABLE III

ECDYSTEROID CONTENTS FOUND IN SOME REAL SAMPLES

Results are ppm dry weight ± S.D. ($n=6$).

Ecdysteroid	*P. vulgare*		*A. reptans*	
	Rhizomes	*Fronds*	*Wild plant*	*Cultivated*
Ecdysone	400 ± 40	300 ± 20		
20-Hydroxyecdysone	4000 ± 200	1200 ± 100	50 ± 20	20 ± 10
Polypodine B	1800 ± 150	100 ± 10		
29-Norsengosterone			210 ± 20	140 ± 20
29-Norcyasterone			450 ± 50	320 ± 30
Cyasterone			110 ± 20	50 ± 10
Ajugalactone			330 ± 20	180 ± 20

CONCLUSIONS

The use of isopropanol–water as eluent in the reversed-phase mode at temperatures above room temperature for the HPLC separation of ecdysteroids proved to be very efficient. The separation of all eight ecdysteroids of this study was accomplished with a short column of only 10 cm. Thermostating of the column allowed a rapid analysis without a decrease in resolution and, in addition, it avoided fluctuations of the retention times of the ecdysteroids. The variation of k' with temperature can be used not only for the optimization of the resolution, but also for identification purposes if the analyses are performed at two different temperatures.

The above conditions allow the quantitative analysis of biological samples that might contain the compounds examined in this work. Further, scale-up to the semi-preparative isolation of pure ecdysteroids has been shown to be readily accomplished. Finally, these conditions can be of great value for the recent liquid chromatograph–mass spectrometer interfaces[15] in order to take maximum advantage of this technique in ecdysteroid analysis.

ACKNOWLEDGEMENTS

Financial support from CICYT (Grant BIO880230) is gratefully acknowledged. Two of us (M.P.M. and J.T.) also thank the Spanish Ministry of Education and Science for predoctoral fellowships.

REFERENCES

1 E. D. Morgan and I. D. Wilson, in J. Koolman (Editor), *Ecdysone, from Chemistry to Mode of Action*, Georg Thieme, Stuttgart, 1989, pp. 114–30.
2 M. Báthori, K. Szendrei and I. Herke, *Chromatographia*, 21 (1986) 234.
3 M. L. De Reggi, M. H. Hirn and M. A. Delaage, *Biochem. Biophys. Res. Commun.*, 66 (1975) 1307.
4 I. D. Wilson, C. R. Bielby, E. D. Morgan and A. E. M. McLean, *J. Chromatogr.*, 194 (1980) 343.
5 I. Kubo, J. A. Klocke, I. Ganjian, N. Ichikawa and T. Matsumoto, *J. Chromatogr.*, 257 (1983) 157.
6 R. Lafont, G. Sommé-Martin and J. C. Chambet, *J. Chromatogr.*, 170 (1979) 185-94.
7 S. Scalia and E. D. Morgan, *J. Chromatogr.*, 346 (1985) 301.
8 M. Báthori, K. Szendrei, H. Kalasz and R. Ohmacht, *J. High Resolut. Chromatogr. Chromatogr. Commun.*, 9 (1986) 539.
9 S. Scalia and E. D. Morgan, *J. Chromatogr.*, 238 (1982) 457.
10 R. Lafont and D. H. S. Horn, in J. Koolman (Editor), *Ecdysone, from Chemistry to Mode of Action*, Georg Thieme, Stuttgart, 1989, pp. 39–64.
11 F. Camps, *Proc. Phytochem. Soc. Eur.*, in press.
12 F. Camps, J. Coll and A. Cortel, *Chem. Lett.*, (1982) 1313.
13 J. Jizba, V. Herout and F. Sorm, *Tetrahedron Lett.*, (1967) 1689.
14 I. D. Wilson, C. R. Bielby and E. D. Morgan, *J. Chromatogr.*, 238 (1982) 97.
15 M. L. Vestal, *Science (Washington, D.C.)*, 221 (1984) 275.

Journal of Chromatography, 514 (1990) 209–218
Elsevier Science Publishers B.V., Amsterdam

CHROM. 22 541

Reversed-phase high-performance liquid chromatographic method for the determination of soil-bound [^{14}C]atrazine and its radiolabeled metabolites in a soil metabolism study

ABU M. RUSTUM*[a], STEVE ASH and ADESH SAXENA
Department of Environmental Fate, Hazleton Laboratories America, Inc., Madison, WI (U.S.A.)
and
K. BALU
Ciba-Geigy Corporation, Greensboro, NC (U.S.A.)
(First received February 6th, 1990; revised manuscript received May 8th, 1990)

ABSTRACT

A rapid and simple reversed-phase high-performance liquid chromatography (RP-HPLC) method has been developed to determine [^{14}C]atrazine and its radiolabeled degradation products using radioisotope detection and liquid scintillation counting quantitation. A 25 cm × 4.6 mm, 5-μm octadecylsilane (C_{18}) column was used with gradient elution of acetonitrile and 0.01 *M* monobasic potassium phosphate (pH 2.0). The mobile phase was delivered at 1.0 ml/min. Fractions of the HPLC eluate were collected and the radioactive peak were quantitated as percent of the total radioactivity injected into the chromatographic system. A histogram of radioactivity (dpm) *versus* fraction number was constructed. Identification of individual radioactive peaks was conducted by comparing the retention time of the peaks in the histogram with the retention time of the peaks of non-radiolabeled standards obtained by ultraviolet detection at 230 nm.

This method was applied to determine the degradation products of [^{14}C]atrazine in a soil metabolism study. Four degradation products in the soil metabolism study were positively identified by co-chromatography technique. The limit of detection of the method for [^{14}C]atrazine and its degradation products was 5 ng/ml for a 100-μl injection volume and when [^{14}C]atrazine had a specific activity of $7.62 \cdot 10^5$ Bq/mg.

INTRODUCTION

Atrazine (2-chloro-4-ethylamino-6-isopropylamino-*s*-1,3,5-triazine) is a triazine herbicide used worldwide for weed control in various agricultural crops. Multiple

[a] Present address: Abbott Laboratories, Division of Pharmaceutical Products Development, Department No. 417, 14th Sheridan Road, North Chicago, IL 60064, U.S.A.

0021-9673/90/$03.50

analytical problems are usually encountered when soil metabolism and other environmental fate studies are conducted using a non-radiolabeled test compound. Most of these analytical problems can be solved by using the test material labeled with ^{14}C, ^{3}H or other appropriate radioactive isotopes.

Paper chromatography has been used to determine several triazine herbicides[1–2]. Gas chromatography (GC) has been used to determine the triazines in different sample matrices[3–6]. Most of the GC methods in the literature to determine the hydroxy-*s*-triazines use a pre-chromatography derivatization step.

Recently, high-performance liquid chromatography (HPLC) has been used extensively to determine atrazine, its residues and its metabolites in soil and other sample matrices[7–16].

Most of the reported procedures for the isolation of atrazine and its degradation products from soil and other sample matrices use complex and multiple-step extraction for sample preparation before HPLC analysis. These HPLC procedures use ultraviolet (UV) detection (typically in the 230- to 220-nm range) to monitor atrazine and its degradation products.

UV detection is usually a non-selective mode of detection. Interference from the sample matrix peak(s) is often a common problem. Hence, long procedures for sample cleanup are usually followed to eliminate the interference peak(s) of the sample matrices.

The use of radioisotopes and liquid scintillation counting quantitation in HPLC eliminates the interference problems involved in UV detection, is usually more sensitive than UV detection, and is an absolute method of quantitation. By knowing the specific activity of the test material, one can directly quantitate the analyte simply by measuring the total disintegrations per minute (dpm) of the chromatographic peak. Therefore, a calibration curve is not required for quantitation of the analyte in an unknown sample. The linear dynamic range of the analytical signal for radioisotope detection is typically six orders of magnitude.

In this report, a simple and sensitive HPLC method has been described to quantitate atrazine and its radiolabeled degradation products in a soil matrix. The use of radioisotopes detection made the method more sensitive than most of the methods reported in the literature. The one-step extraction procedure resulted in a simpler, reproducible, and more accurate method than those reported previously.

EXPERIMENTAL

The HPLC system consisted of a Perkin-Elmer (Norwalk, CT, U.S.A.) Series 410B solvent delivery unit, equipped with a Rheodyne (Cotati, CA, U.S.A.) 7275 sample injector with a 200-μl sample loop. An Applied Biosystem (Ramsey, NJ, U.S.A.) UV–visible detector (Model No. Spectroflow 783) with a flow cell of 8-mm path length was used. The chromatograms were recorded on a Houston Instrument (Austin, TX, U.S.A.) D-5237-2 strip chart recorder. Deionized water was collected from a Milli-Q System (Millipore, Bedford, MA, U.S.A.). A Model 2200 Branson sonicator was used to degas the mobile phase (Branson Cleaning Equipment, Shelton, CT, U.S.A.). The samples were centrifuged using an IEC centrifuge, Model-K (Damon, IEC Division, Needham Heights, MA, U.S.A.). A fraction collector (Model 203, Gilson, Middleton, WI, U.S.A.) was used to collect the fractions from the

chromatographic system. A Model 380I liquid scintillation system was used to determine the radioactivity in the HPLC fraction (Beckman, Fullerton, CA, U.S.A.). A 25 cm × 4.6 mm C_{18} (ODS), 5-μm Econosphere column (Alltech, Deerfield, IL, U.S.A.) was used to test the developed method.

Materials

Acetonitrile and methanol (HPLC grade) were purchased from EM Science (Cherry Hill, NJ, U.S.A.). Atrazine (radiolabeled and non-radiolabeled) and the non-radiolabeled degradation products (GS-17792, GS-28273, GS-17794, G-28279, G-30033 and G-34048) were obtained from Ciba-Geigy (Greensboro, NC, U.S.A.). All standards were used as received without further purification. The standards used in this experiment were at least 98% pure. Potassium phosphate monobasic (KH_2PO_4) and hydrochloric acid were purchased from Fisher Scientific (Fairlawn, NJ, U.S.A.). Liquid scintillation cocktail was purchased from Packard (Downers Grove, IL, U.S.A.).

Chromatographic conditions

The mobile phase consisted of a gradient elution of acetonitrile and 0.01 *M* KH_2PO_4 (pH adjusted to approximately 2.0 with phosphoric acid). The rate of the mobile phase delivery through the analytical column was 1.0 ml/min. The non-radiolabeled standards of atrazine and its degradation products were monitored by a UV–visible absorbance detector at a wavelength of 230 nm and from 0.20 to 0.01 absorbance units full scale (a.u.f.s.). The mobile phase gradient is listed in Table I.

Prechromatography isolation of atrazine and its degradation products from soil

Isolation of atrazine and its degradation products from the soil samples was performed as follows. Approximately 10 g of a soil sample (from a soil metabolism study of atrazine) containing soil-bound atrazine and its degradation products was transferred into a container. This soil was heated at reflux with 1 *M* HCl in methanol (solvent–soil ratio approximately 10:1) and stirred with a magnetic stir bar for 2 h. The refluxed sample was allowed to equilibrate to ambient temperature, and was then vacuum filtered through a 0.45-μm nylon-66 membrane. The solids in the filter were washed with an aliquot of the extraction solvent. The filtered extract was concentrated to 1–2 ml by rotary evaporation at approximately 60°C in vacuum. The concentrated extract was diluted with 0.01 *M* KH_2PO_4 to a total volume of 10.0 ml. A 100- to 200-μl aliquot of this solution was injected directly into the chromatographic system. A flow chart for the extraction of the soil sample for a metabolism study is in Fig. 1.

TABLE I

MOBILE PHASE GRADIENT OF THE HPLC SYSTEM

Step time (min)	*Acetonitrile (%)*	*0.01 M KH_2PO_4 (pH ca. 2.0) (%)*
0 to 10	5	95
10 to 15	20	80
15 to 20	30	70
20 to 35	70	30

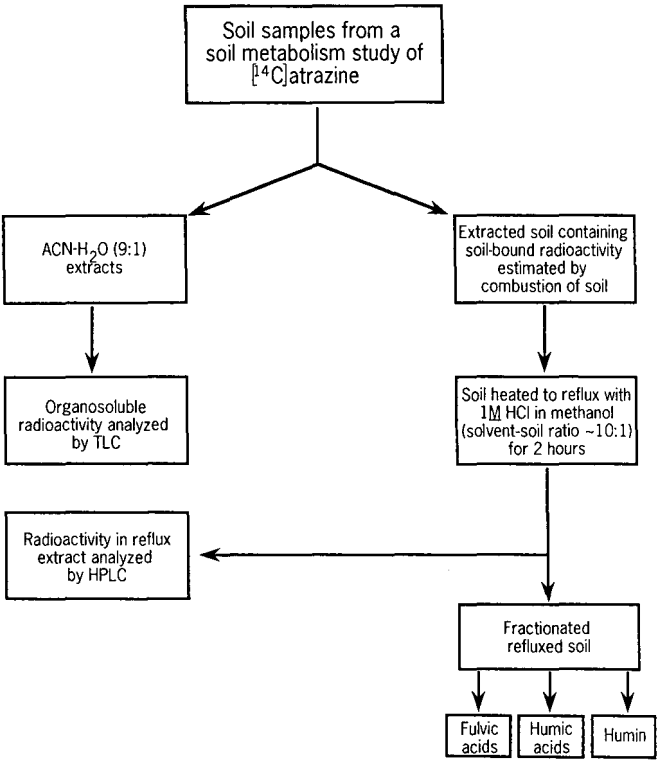

Fig. 1. Flow chart for extraction of [^{14}C]atrazine and its metabolites from soil samples of the soil metabolism study. ACN = Acetonitrile; TLC = thin-layer chromatography.

Fraction collection and histogram of the injected sample radioactivity

For samples containing radioactivity, the eluate from the column was collected in 0.5-ml fractions, which were then analyzed by liquid scintillation counting. A histogram was generated from each HPLC assay by plotting fraction number *versus* radioactivity (dpm).

Preparation of the stock solution

Stock solutions of [^{14}C]atrazine, non-radiolabeled atrazine, and non-radiolabeled degradation products of atrazine were prepared in neat acetonitrile. The chemical structures of the standards used in this experiment are shown in Fig. 2. The retention times of the non-radiolabeled standards (by UV detection) with those of the [^{14}C]atrazine and degradation products (as determined by HPLC–liquid scintillation counting histograms) were compared.

Calculations

The percentage of [^{14}C]atrazine, its individual degradation products in soil, and radioactivity recovered from the HPLC system (after injection) was calculated with respect to total radioactivity injected into the HPLC system.

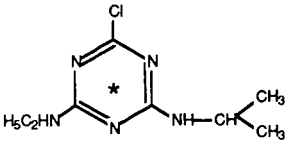

Atrazine
(2-chloro-4-ethylamino-6-isopropylamino-s-triazine)
* Position of radiolabel.

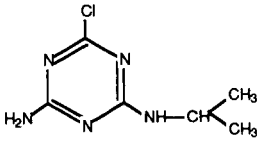

G-30033
(2-amino-4-chloro-6-isopropylamino-s-triazine)

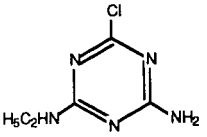

G-28279
(2-amino-4-chloro-6-ethylamino-s-triazine)

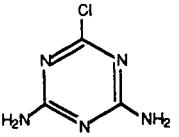

G-28273
(2,4-diamino-6-chloro-s-triazine)

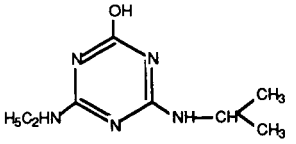

G-34048 (Hyroxy Atrazine)
(2-ethylamino-4-hydroxy-6-isopropylamino-s-triazine)

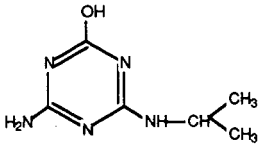

GS-17794
(2-amino-4-hydroxy-6-isopropylamino-s-triazine)

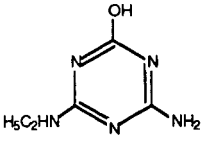

GS-17792
(2-amino-4-ethylamino-6-hydroxy-s-triazine)

Fig. 2. Structure of atrazine and its major degradation products.

$$\% \text{ of } [^{14}\text{C}]\text{atrazine (or degradation product)} = \frac{\text{Radioactivity (dpm) in the fractions of the atrazine peak (or degradation products)}}{\text{Total radioactivity (dpm) injected into the HPLC system}} \times 100$$

$$\% \text{ Radioactivity (dpm) recovered from the HPLC system} = \frac{\text{Sum of the radioactivity (dpm) in all the fractions of the histogram}}{\text{Total radioactivity (dpm) injected into the HPLC system}}$$

The total radioactivity (dpm) injected into the HPLC system was determined directly by liquid scintillation counting using duplicate aliquots of an aliquot (same volume as injected into the HPLC system) of the extract.

Counts per minute (cpm) were converted to disintegrations per minute (dpm) using the external standard method. The background radioactivity of the HPLC fractions was determined by collecting the HPLC eluate (in duplicate) before the

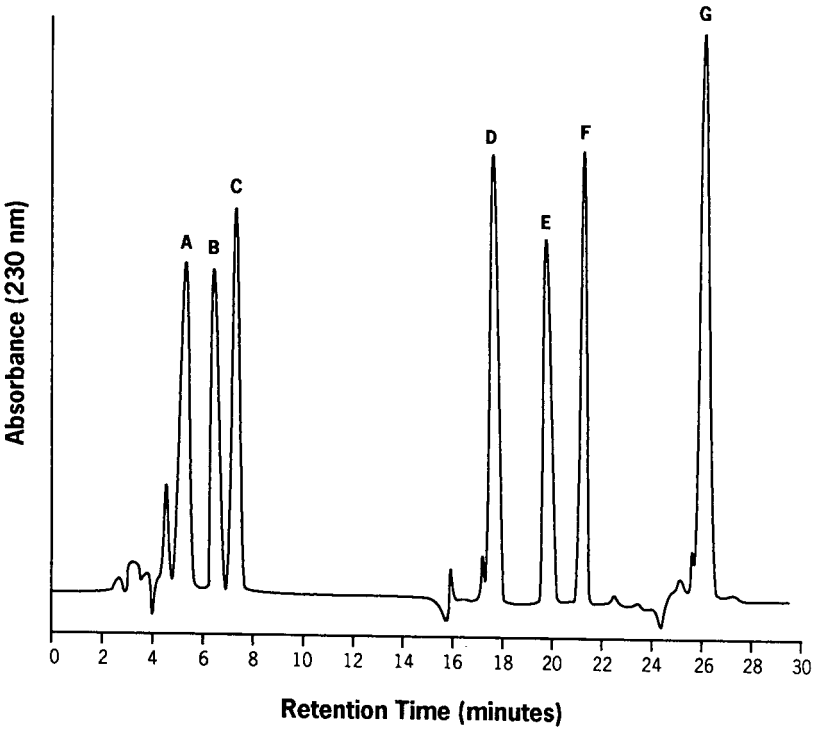

Fig. 3. Representative chromatogram of non-radiolabeled atrazine and its major degradation products. Peaks: A = GS-17792; B = G-28273; C = GS-17794; D = G-28279; E = G-34048; F = G-30033; G = atrazine. The detector was at 230 nm and 0.200 a.u.f.s.

radioactive sample extract was injected. The mean radioactivity of the two blanks was then subtracted from each of the HPLC fractions. Similarly, the background radioactivity for the extract of the soil samples was subtracted to eliminate the matrix effect on chemiluminescence and quenching.

RESULTS AND DISCUSSION

The HPLC method described in this report is capable of separating (baseline) atrazine and its six degradation products in less than 30 min. Fig. 3 shows a chromatogram of the nonradiolabeled standards of the degradation products and atrazine (at 230 nm). The chromatographic conditions used in this experiment were optimum in terms of resolution and sensitivity. The pH of the mobile phase is very critical for the separation of the first three peaks in Fig. 3. When the pH of the mobile phase was greater than 3.0, peaks 2 and 3 coeluted with identical retention times.

Fig. 4 is a representative histogram of a soil reflux extract from a soil metabolism study of atrazine. The atrazine was incubated for 181 days under aerobic conditions. Four degradation products of atrazine were identified in the histogram of the day-181 soil metabolism sample. One unknown degradation product (trace) was also observed in this sample which is not shown in Fig. 4. The peaks in the histogram were identified

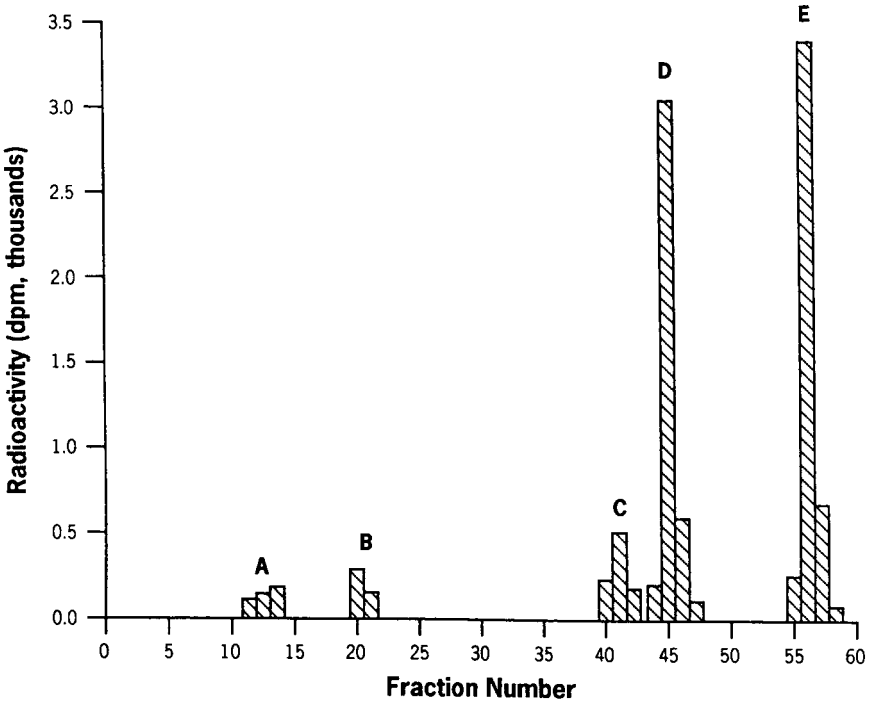

Fig. 4. Representative HPLC histogram of 1 *M* HCl in methanol reflux extract of day-181 sample of soil metabolism of atrazine. Fractions: 12–14 = GS-17792; 20 and 21 = GS-17794; 40–42 = G-28279; 44–47 = G-34048; 55–58 = atrazine.

TABLE II

REPRESENTATIVE HPLC RETENTION TIMES OF NON-RADIOLABELED STANDARDS OF ATRAZINE AND ITS DEGRADATION PRODUCTS

Retention times are representative values. Actual retention times varied slightly in day-to-day analyses with new batches of mobile phase.

Standard identification	*Retention time (min)*
Atrazine	27.0
G-30033	22.0
G-28279	18.5
G-28273	6.5
G-34048	20.5
GS-17792	5.0
GS-17794	8.0

by comparing the retention times of the non-radiolabeled standards (Fig. 3). The retention times of atrazine and its degradation products are listed in Table II.

The extract of a control soil sample was also injected into the HPLC system to determine the retention behavior of the UV-absorbing components extracted from the soil background. It was found that most of these components (at 230 nm) eluted at the void volume of the chromatographic system. Therefore, most of the degradation products of non-radiolabeled atrazine may be quantitated by UV detection in a soil metabolism study.

Recovery of [^{14}C]atrazine from soil by extraction was approximately 93% at day

TABLE III

DISTRIBUTION OF ATRAZINE AND METABOLITES IN BIOLOGICALLY ACTIVE AEROBIC SAMPLES

ND = Not detected.

Incubation time (days)	*Distribution (%)*[a]						
	Atrazine	*G-30033*	*G-28279*	*G-28273*	*G-34048*	*GS-17794*	*GS-17792*
0	90.7	0.8	1.3	0.1	ND	ND	ND
3	85.6	2.1	0.6	0.7	ND	ND	ND
7	80.8	2.2	0.6	0.4	ND	ND	ND
14	77.8	2.6	0.8	0.2	ND	ND	ND
32	67.0	2.1	0.7	0.3	ND	ND	ND
62	59.1	2.7	0.9	ND	0.7	ND	ND
94	56.5	3.0	1.7	ND	0.7	ND	ND
181	33.1	3.5	1.6	ND	0.5	ND	ND
244	26.5	4.3	2.0	0.2	0.6	ND	ND
300	21.2	4.6	1.2	0.1	0.2	ND	ND

[a] The data are mean values (n = 4) based on the percentage of the radioactivity applied to the test system. The R.S.D. for one-step extraction was 10% or less for atrazine and its metabolites.

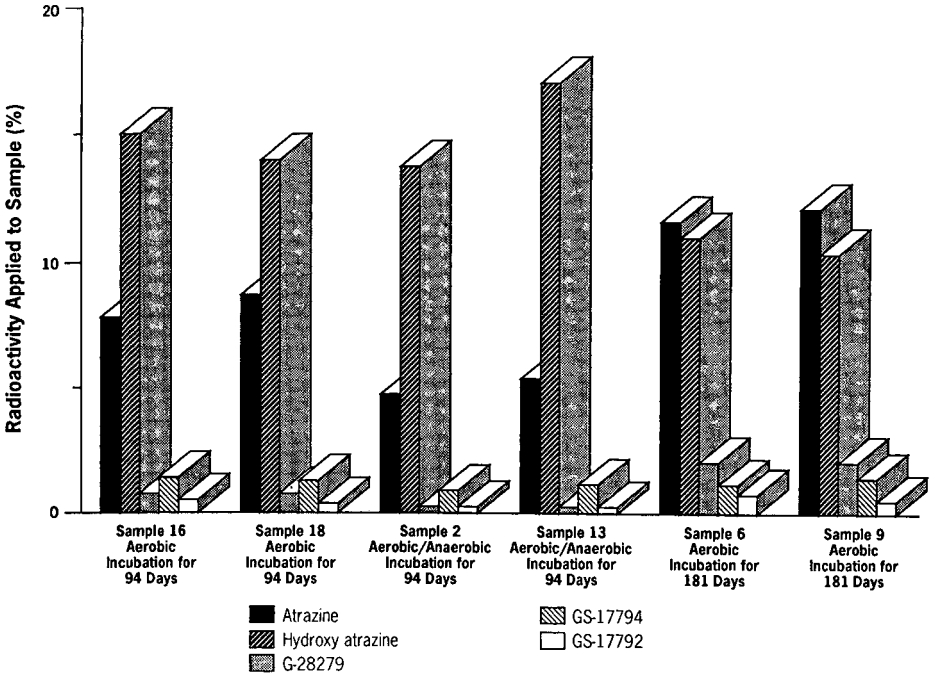

Fig. 5. Recovery of [^{14}C]atrazine and its degradation products under aerobic and anaerobic incubation conditions for days 94 and 181.

0. The total ^{14}C recovery from the soil decreases with time due to binding with soil and soil materials. Approximately 78% of the total ^{14}C material extracted by organic solvent after the [^{14}C]atrazine in soil was incubated for 300 days under aerobic conditions.

The distribution of atrazine and its degradation products during 300 days of incubation is shown in Table III. The relative standard deviation (R.S.D.) for atrazine and its metabolites was 10% or less for four extractions. This indicates that the reproducibility of the single-step extraction procedure used in this experiment is good. No systematic study was conducted to determine the recovery of the hydroxylated atrazine products by the single-step extraction procedure. However, the recovery of the more polar hydroxylated products decreased with the increase of incubation period. The recovery of the parent also decreased with time, but to a lesser extent than the degradation products. The total radioactivity recovered during the study was also calculated. The total radioactivity recovered from day 0 to day 300 was approximately 98.6% $\pm$ 5%. The recovery of atrazine and its metabolites incubated under aerobic and anaerobic conditions for different days is in Fig. 5.

Radiolabeled materials are frequently used in soil metabolism and animal metabolism studies. Most of the reported methods for conducting soil and animal metabolism studies use TLC. TLC methods[17] usually provide poor resolution and are very time consuming compared with HPLC methods. The sample extract for radiolabeled compounds can be injected into a reversed-phase chromatography

system without any preconcentration because large volumes of the extract (up to 500 μl) can be injected into an HPLC system. Therefore, for metabolism studies, an HPLC method is usually more simple, reproducible, and accurate than a TLC method. This method may also be used in animal metabolism studies of [^{14}C]atrazine. The lower limit of quantitation for [^{14}C]atrazine and its metabolites was 20 ng/ml for a 100-μl injection volume and a R.S.D. of less than 10%. Instead of fraction collection and quantitation by liquid scintillation counting, a radioactivity detector for HPLC can be used to conduct on-line quantitation of the analytes.

CONCLUSION

This HPLC method for determining atrazine and its degradation products is rapid, sensitive and more accurate than most of the methods reported in the literature. This method was used to determine atrazine and its metabolites from a soil metabolism study. All of the metabolites of atrazine that were formed in a 300-day soil metabolism study were separated and quantitated by the described HPLC method. No interference peak was observed in any of the sample extracts, obtained at different time points. Because of good selectivity, this method may also be used in animal metabolism studies of atrazine.

REFERENCES

1 L. Fishbein, *Chromatogr. Rev.*, 12 (1970) 167.
2 L. Fishbein, *Chromatography of Environmental Hazards*, Vol. 3, Elsevier, Amsterdam, 1975, Ch. 17.
3 P. G. Stokes and A. W. Schwartz, *J. Chromatogr.*, 168 (1979) 455.
4 D. C. Muir and B. E. Baker, *J. Agric. Food Chem.*, 26 (1978) 420.
5 W. R. Lusby and P. C. Kearney, *J. Agric. Food Chem.*, 26 (1978) 635.
6 L. Stadler and W. Pestemer, *Weed Res.*, 20 (1980) 341.
7 B. A. Demian, V. Borbeby, F. Kerek, B. Bader, M. Cirstea and E. Dragusin, *Rev. Chem.*, 30 (1979) 281.
8 E. Smolkova and V. Pacakova, *Chromatographia*, 11 (1978) 698.
9 J. F. Lawrence and R. Leduc, *Anal. Chem.*, 50 (1978) 1, 161.
10 K. A. Ramsteiner and W. D. Horman, *J. Agric. Food Chem.*, 27 (1979) 934.
11 J. F. Lawrence and D. Turton, *J. Chromatogr.*, 159 (1978) 207.
12 P. H. Plaested and M. L. Thronton, *Contrib. Boyce Thompson Inst.*, 22 (1974) 399.
13 D. C. Muir, *J. Agric. Food Chem.*, 28 (1980) 714.
14 H. M. J. Vermeulen, Z. Apostolides, D. J. J. Potgiester, P. C. Nel and N. S. H. Smit, *J. Chromatogr.*, 240 (1982) 247.
15 M. T. Giardi, M. C. Giardina and E. Brancaleoni, in A. Frigerio (Editor), Chromatography in Biochemistry, Medicine and Environmental Research, 1 (*Analytical Chemistry Symposia Series*, Vol. 13), Elsevier, Amsterdam, 1983, p. 53.
16 M. T. Giardi, M. C. Giardina and G. Filacchioni, *Agric. Biol. Chem.*, 49 (1988) 1551.
17 P. Capriel and A. Haisch, *Z. Pflanzenernaehr. Bodenk.*, 146 (1983) 474.

Journal of Chromatography, 514 (1990) 219–225
Elsevier Science Publishers B.V., Amsterdam

CHROM. 22 476

High-performance liquid affinity chromatography for the purification of immunoglobulin A from human serum using jacalin

SHIU HON CHUI*
Department of Health Sciences, Hong Kong Polytechnic, Kowloon (Hong Kong)
CHRISTOPHER WAI KEI LAM
Department of Chemical Pathology, Prince of Wales Hospital, Chinese University of Hong Kong, Shatin (Hong Kong)
W. H. P. LEWIS
Department of Health Sciences, Hong Kong Polytechnic, Kowloon (Hong Kong)
and
KAR NENG LAI
Department of Medicine, Prince of Wales Hospital, Chinese University of Hong Kong, Shatin (Hong Kong)
(First received April 14th, 1989; revised manuscript received March 29th, 1990)

ABSTRACT

A high-performance liquid affinity chromatographic method for the purification of serum immunoglobulin A (IgA) using a jacalin column is described. The automated procedure takes about 2 with minimal manipulation. The yields of the isolated IgA and of its IgG and IgM contamination were studied by enzyme-linked immunosorbent assay (ELISA) of 30 sera. Purity was assured by immunoelectrophoresis. The ratio of IgA_1 to total IgA was unchanged after purification, as verified by ELISA. The results showed that >90% IgA could be recovered with <0.5% total IgG and >2.0% total IgM remaining in the fractions containing purified IgA.

INTRODUCTION

Immunoglobulin A (IgA) is the second most abundant immunoglobulin in human serum. Circulating IgA is usually monomeric whereas the secretory form is predominently dimeric or polymeric[1], with the presence of a secretory component[2] and the J chain[3]. Studies of IgA are usually carried out with the secretory form because it can be obtained with a reasonable degree of purity. The isolation of immunochemically pure IgA from serum has been difficult, with relatively low yields and heavy contamination with IgG[4]. Moreover, the purification procedure requires several steps, such as ammonium sulphate precipitation, ion-exchange chromatography and gel filtration[5,6]. Mestecky *et al.*[7] reported an immunoprecipitation method for serum IgA

0021-9673/90/$03.50

isolation, using the $F(ab')_2$ fragment of antibody to IgA as immunoadsorbent, followed by gel filtration. Doellgast and Plaut[8] purified human IgA from normal serum and serum from patients with multiple myeloma using salt-mediated hydrophobic chromatography.

Jacalin is an α-D-galactose-binding lectin isolated from jack-fruit seeds[9]. Its unique biospecific binding properties to IgA were first reported by Roque-Barreria and Campos-Neto[10]. They also used immobilized jacalin in the affinity chromatographic purification of IgA from human serum and colostrum, a much improved technique over the methods mentioned above.

Here we report a rapid purification of serum IgA using a jacalin column on a high-performance liquid affinity chromatographic (Fast Protein liquid chromatographic, FPLC) system with the isolated IgA (and its contaminating IgG and IgM) being determined by enzyme-linked immunosorbent assay (ELISA).

EXPERIMENTAL

Chemicals and reagents

Immobilized jacalin attached to cross-linked 6% beaded agarose (No. 20395) was obtained from Pierce (Rockford, IL, U.S.A.).

The binding buffer was 0.02 *M* NaH_2PO_4 (Sigma, St. Louis, MO, U.S.A.) containing 0.15 *M* sodium chloride (Sigma) and 0.02% (w/v) sodium azide (Sigma), with the pH adjusted to 7.4 using 10 *M* sodium hydroxide solution (Sigma). The elution buffer was 0.1 *M* melibiose (Sigma) in binding buffer. Before use, the buffers were filtered with a 0.22-μm Type GS membrane filter (Millipore, Bedford, MA, U.S.A.) and degassed with a Transsonic T460 ultrasonic bath (Elma, Singen/Hohentwiel, F.R.G.).

Equipment

All the chromatographic equipment used was manufactured by Pharmacia (Uppsala, Sweden). The FPLC system consisted of an LCC 500 programmer controlling two P-500 reciprocating pumps and one P-1 peristaltic pump. Each pump delivered one buffer into a dynamic mixing chamber where the buffers passed through a V-7 injection valve for introduction of the sample via a 10-ml superloop onto the jacalin column. An HR 10/10 column (10 cm × 10 mm I.D.) packed with *ca.* 8 ml of immobilized jacalin suspended in binding buffer was used. The eluate was monitored by a single-path UV-1 monitor at 280 nm in a 10-mm path-length high-resolution flow cell and the chromatogram was recorded on an REC-482 two-channel recorder. Fractions (5-min) were collected with a FRAC-100 fraction collector.

Sample preparation

A 1–3-ml volume of serum (*ca.* 1–6 mg of IgA) was diluted 1:1 with binding buffer prior to its application to the column. Immobilized jacalin has a maximum binding of about 3 mg of human IgA per ml of gel. For optimum purification and recovery, it is recommended that a sample size should be chosen such that the expected IgA load on the column is less than 80% of the maximum binding capacity.

ELISA of purified IgA

Fractions of the eluted protein peak were pooled and the concentrations of the isolated IgA and the starting serum were determined by ELISA as described previously[11]. The amount of IgA loaded onto the column and the amount recovered were calculated.

A brief description of the ELISA method is as follows. Purified immunoglobulin fractions of rabbit antisera to human IgA, IgG and IgM (Dako Immunoglobulins, Copenhagen, Denmark) were used at 1:2000 dilution. Microtitre plates were coated by adding 100 μl per well of the appropriate antiserum diluted in 0.015 *M* sodium carbonate–hydrogencarbonate buffer (coating buffer) (pH 9.6). The plates were incubated overnight at 4°C and washed ten times with phosphate-buffered saline (pH 7.4) containing 0.05% (v/v) of Tween 20 (Sigma) (PBS–Tween). Samples and standards appropriately diluted in PBS containing 10% (v/v) fetal bovine serum (FBS) were introduced at 100 μl per well in duplicate. After incubation at 37°C for 3 h, the plates were again washed ten times with PBS–Tween. The same antisera as used for coating, but conjugated with horseradish peroxidose (Dako) and diluted 1:6000 (IgA), 1:6000 (IgG) and 1:2000 (IgM) in PBS–Tween, were then added at 100 μl per well, as appropriate. Incubation at 37°C was continued for 2 h and the washing repeated. A freshly prepared substrate solution containing 20 mg of urea hydrogen peroxide (BDH, Poole, U.K.) and 70 mg of *o*-phenylenediamine dihydrochloride (Sigma) in 100 ml of 0.20 *M* phosphate–citrate buffer (pH 5.0) was added at 100 μl per well and the plates left at room temperature for 15 min. Finally, the reaction was terminated by adding 50 μl per well of 4 *M* sulphuric acid and the absorbances were measured at 450 nm using a Model 2550 EIA reader (Bio-Rad Labs., Richmond, CA, U.S.A.). Immunoglobulin concentrations were determined by reference to the respective calibration graphs.

Immunoelectrophoresis of purified IgA

The purity of the jacalin-isolated IgA was investigated by a standard immunoelectrophoresis technique[12], using Titan IV IEP plates (Helena Labs., Beaumont, TX, U.S.A.), rabbit anti-human serum (Dakopatts) and rabbit anti-IgA (Dakopatts) antisera. Three serum samples [one from NS and two from IgAN patients (where NS is a Normal Subject and IgAN patients are patients with IgA nephropathy)] together with the corresponding purified IgA solution (concentrated) were examined. Volumes of 5 μl of each sample and the albumin marker (Helena Labs.) were applied to appropriate wells in the agarose gel plate. The electrophoresis was carried out with barbitone buffer (pH 8.2) at 150 V for *ca.* 90 min. After electrophoresis, 90 μl of the appropriate antisera were added to the appropriate trough. The plate was allowed to stand overnight at room temperature in the moist chamber. Precipitin arcs were observed. Excessive antisera in the gel were removed by washing the plate with PBS with constant shaking for 48 h. The plate was then stained with Coomassie blue.

ELISA of IgA_1

The IgA_1 concentrations in eight serum samples before and after jacalin purification were determined. The same ELISA protocol as described above was used except that microtitre plates were coated with mouse anti-human IgA_1 monoclonal antibody (Becton-Dickinson Immunocytochemistry Systems, Mountain View, CA,

U.S.A.) at 3 μg per well. The Calbiochem (San Diego, CA, U.S.A.) IgA_1 standard was used for the construction of dose-related curves (from 0 to 200 μg/ml).

RESULTS AND DISCUSSION

Fig. 1 shows the gradient elution chromatogram of human serum IgA. A total of 30 sera were subjected to the same FPLC system and similar chromatograms were obtained for all samples.

The chromatography consisted of three stages lasting 2 h. During the first hour (fractions 1–12) IgA and two other unknown proteins in binding buffer were bound to jacalin, probably via the terminal D-galactose which is absent in other immunoglobulin classes[10]. Thus, the first protein peak should contain most serum proteins not bound to jacalin, except IgA.

Elution of the bound IgA was initiated by switching to the elution buffer at the end of the first hour. Melibiose displaced bound IgA from jacalin, presumably by competing for the binding sites on jacalin. The elution required 30 min and IgA in all samples was eluted as a single peak when monitored at 280 nm. Fractions 13–17 were pooled for ELISA of IgA and also IgG and IgM concentrations. After elution, the column was regenerated with distilled water for 30 min.

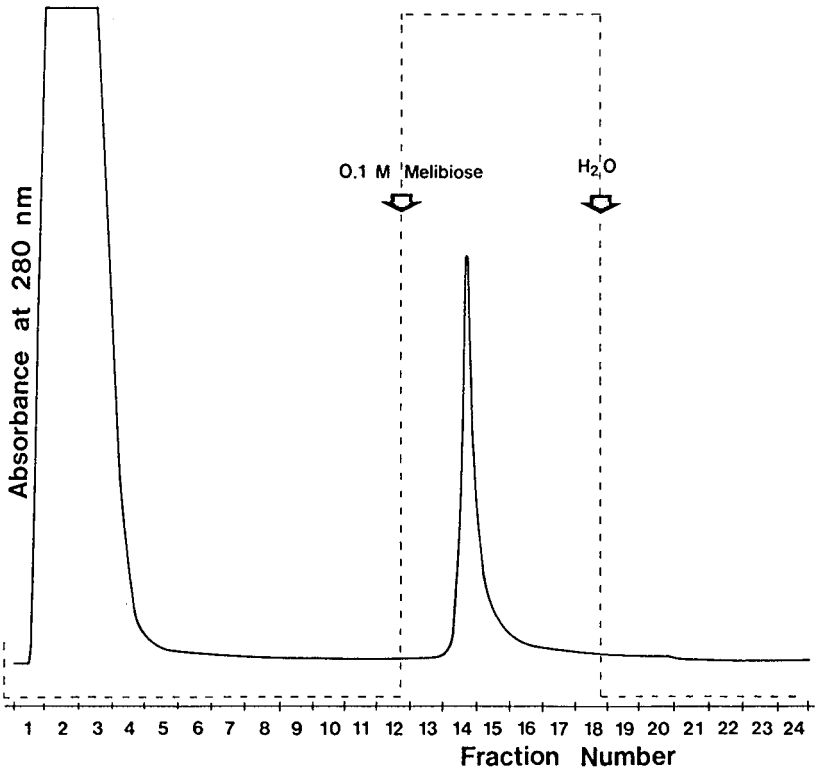

Fig. 1. FPLC purification of human IgA from serum. The dashed line represents the gradient shape.

TABLE I

RECOVERY OF IgA FROM SERUM SAMPLES AND AMOUNTS OF IgG AND IgM IN PURIFIED FRACTIONS

Immunoglobulin	*Amount injected (mg) (n = 30)*	*Amount recovered (mg) (n = 30)*	*Recovery (%) (mean ± S.D.)*
IgA	0.99–5.93	0.90–5.16	93.49 ± 3.91
IgG	5.71–26.81	0.01–0.08	0.22 ± 0.09
IgM	0.71–3.34	0.01–0.05	1.88 ± 0.80

Table I shows the recovery of IgA from 30 serum samples ranging from 1 to 3 ml. All samples showed a yield of IgA of *ca.* 90% or above. These results demonstrate that the FPLC procedure offers an effective purification of IgA.

Fig. 2 shows the results of immunoelectrophoresis of three sera with corresponding purified IgA solutions. Multiple precipitin arcs were observed in areas between serum samples and antiserum raised against human serum. The only prominent precipitin arc was observed in areas between the purified IgA and antiserum

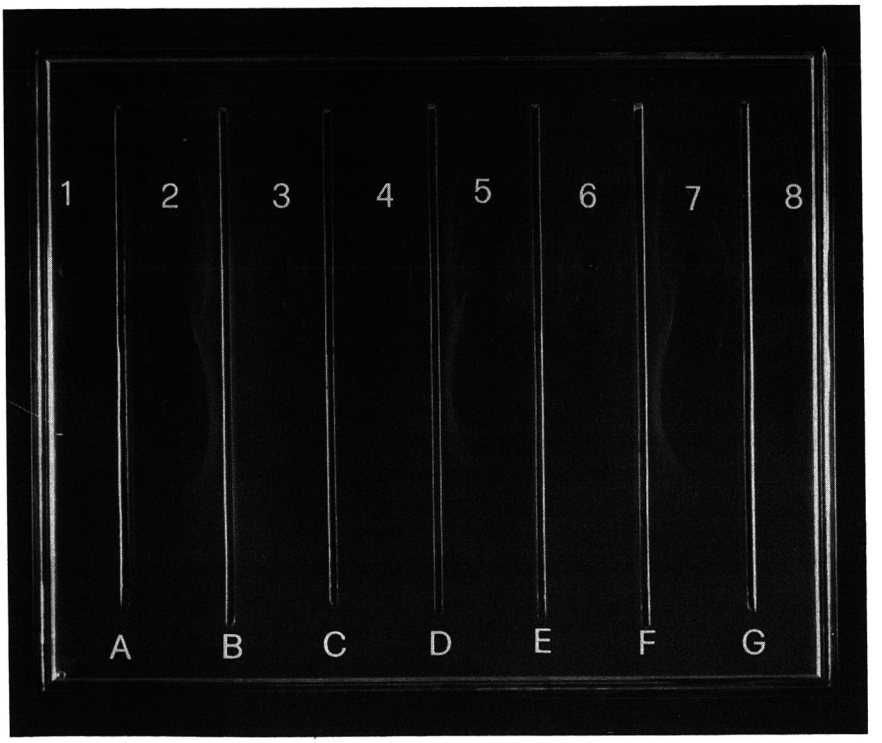

Fig. 2. Immunoelectrophoresis of purified IgA. Antigen wells 2, 5 and 7 contained unpurified serum samples; wells 3, 4 and 6 contained corresponding purified IgA; wells 1 and 8 contained albumin marker. Antiserum troughs A, C, E and G contained antiserum to human IgA. Troughs B, D and F contained antiserum to complete human serum proteins.

TABLE II

PERCENTAGE OF IgA_1 IN TOTAL IgA IN EIGHT SERUM SAMPLES BEFORE AND AFTER JACALIN PURIFICATION

Sample No.	*IgA_1 before purification (%)*	*IgA_1 after purification (%)*
1	89.6	84.0
2	63.9	67.2
3	75.5	79.0
4	81.3	80.4
5	97.2	93.6
6	90.1	93.6
7	73.4	68.4
8	71.4	70.8
Mean ± S.D.	80.3 ± 11.3	79.6 ± 10.5

to human serum, which appeared at the same location as the single arc formed from purified IgA and anti-IgA. These patterns indicated that the purified IgA solutions consisted predominantly (if not exclusively) of IgA.

The purity of the isolated IgA with respect to other immunoglobulin classes was also assessed by measuring IgG and IgM concentrations in both the starting serum and the eluted peak fractions. The results in Table I show that only *ca.* 0.04 μg of IgG and 0.03 μg of IgM were bound and recovered, representing an average of 0.22% IgG and 1.88% IgM in the starting material. Hence the isolated IgA was highly purified with very little contamination of IgG and IgM. This high recovery and purity should permit the study of the physico-chemical properties of IgA more easily.

The subclass of IgA which was purified by this methodology was studied. Table II shows the percentage of IgA_1 in the total IgA of eight serum samples before and after jacalin purification. The mean contents of IgA_1 in the two sample groups, before and after purification, were 80.3 ± 11.3% and 79.7 ± 10.5%, respectively, indicating that the ratio of IgA_1 to total IgA remained unchanged after purification with jacalin.

CONCLUSION

Since its discovery as a potent and selective stimulator of distinctive human T and B cell functions[13], jacalin has been used as an affinity absorbent for the isolation of human serum and colostrum secretory IgA[10,14–16]. The basis of the apparent specificity of jacalin towards IgA due to the presence of D-galactose as the terminal sugar only in IgA has been elucidated[10,17,18]. It has been demonstrated that jacalin apparently binds only three serum proteins, one of them being IgA and the other two not yet having been identified but proved to be non-immunoglobulin proteins[10]. Our results showed that the major component in the isolated protein fraction was IgA. The recovery of IgA was >90% with very little IgG and IgM. Although it has been reported that jacalin binds preferentially to IgA_1[19,20], it was demonstrated by our IgA_1 ELISA results that the ratio of IgA_1 to total IgA remained unchanged after purification.

Previously, jacalin affinity chromatographic procedures for isolating serum IgA were not automated. The availability of an immobilized jacalin attached to cross-linked beaded agarose prompted us to pack our own affinity chromatographic column to be used in the fully automated FPLC system. The whole purification procedure takes only 2 h. Hence prolonged manual operation and the necessity for a cold room can be avoided.

ACKNOWLEDGEMENTS

This work was supported by grants from the Mr. & Mrs. L. C. Liu Research Fund and the Edward Sai Kim Hotung Fund (Hong Kong).

REFERENCES

1 J. Bienenstock and A. D. Befus, *Gastroenterology*, 84 (1983) 178.
2 H. F. Heremans, in M. Sela (Editor), *The Antigens*, Vol. 2, Academic Press, New York, 1974, p. 365.
3 M. S. Halpern and M. E. Koshland, *Nature (London)*, 228 (1970) 1276.
4 J. P. Vaerman, *Studies on IgA Immunoglobulins in Man and Animals*, Sintal, Louvain, 1970, p. 15.
5 R. H. Waldman, J. P. Mach, M. M. Stella and D. S. Rowe, *J. Immunol.*, 105 (1970) 43.
6 H. Khayam-Bashi, R. M. Blanken and C. L. Schwartz, *Prep. Biochem.*, 7 (1977) 225.
7 J. Mestecky, R. Kulhavy and F. W. Kraus, *J. Immunol.*, 107 (1971) 605.
8 G. J. Doellgast and A. G. Plaut, *Immunochemistry*, 13 (1976) 135.
9 G. S. Kumar, P. S. Apukuttan and D. Basu, *J. Biosci.*, 4 (1982) 257.
10 M. C. Roque-Barreira and A. Campos-Neto, *J. Immunol.*, 134 (1985) 1740.
11 K. N. Lai, F. M. Lai, S. H. Chui, Y. M. Chan, G. S. W. Tsao, K. M. Leung and C. W. K. Lam, *Clin. Nephrol.*, 28 (1987) 281.
12 V. S. Mehl and G. M. Penn, in N. R. Rose, F. Herman and J. L. Fahey (Editors), *Manual of Clinical Laboratory Immunology*, 3rd ed., American Society for Microbiology, Washington, DC, 1986, p. 127.
13 M. M. Buno-Moreno and A. Campos-Neto, *J. Immunol.*, 127 (1981) 427.
14 H. Kondoh, K. Kobayashi, K. Hagiwara and T. Kajii, *J. Immunol. Methods*, 88 (1986) 171.
15 H. Kondoh, K. Kobayashi and K. Hagiwara, *Mol. Immunol.*, 24 (1987) 1219.
16 P. Ancouturier, F. Duarte, E. Mihaesco, N. Pineau and J. L. Preud'homme, *J. Immunol. Methods*, 113 (1988) 185.
17 M. E. A. Pereina, M. A. Loures, F. Villalta and A. F. B. Andrade, *J. Exp. Med.*, 152 (1980) 1375.
18 N. Sharon and H. Lis, *Mol. Cell Biochem.*, 42 (1982) 167.
19 D. L. Skea, P. Christopoulos, A. G. Plant and B. J. Underdown, *Mol. Immunol.*, 25 (1988) 1.
20 K. Hogiwara, D. Collet-Cassart, K. Kobayashi and J. P. Vaerman, *Mol. Immunol.*, 25 (1988) 69.

Journal of Chromatography, 514 (1990) 227–239
Elsevier Science Publishers B.V., Amsterdam

CHROM. 22 585

Amino acid analysis by high-performance liquid chromatography with methanesulfonic acid hydrolysis and 9-fluorenylmethylchloroformate derivatization

MARCIA F. MALMER* and LAUREN ALFRED SCHROEDER
Department of Biological Sciences, Youngstown State University, 410 Wick Avenue, Youngstown, OH 44555 (U.S.A.)

(First received December 5th, 1989; revised manuscript received May 16th, 1990)

ABSTRACT

Experiments were undertaken to verify a method for complete amino acid analysis of plant and animal tissues and waste products from a single hydrolysis and high-performance liquid chromatographic run. Using methanesulfonic acid, hydrolysis of cytochrome *c* at 115°C for 22 h yielded recoveries equal to or higher than hydrolysis at 115°C for 70 h or at 150°C for 22 h. Triple evacuation of the hydrolysis tube alternated with nitrogen flush gave recovery improvements over single evacuation. Refrigerated storage of samples under vacuum for up to 4 days between hydrolysis and further analysis was not different from immediate analysis. However, recoveries of several amino acids were reduced by refrigerated storage in air. Recoveries of individual amino acids were determined by hydrolysis of biological samples with and without added cytochrome *c*. Although recoveries from biological samples were lower for several amino acids, precision was sufficient to allow quantitation after correction for incomplete recoveries.

Derivatization with 9-fluorenylmethylchloroformate (FMOC) was chosen because derivatives are formed with both primary and secondary amino acids, derivatives are quite stable, and detection may be either UV absorbance or fluorescence. Derivative yield is sensitive to the pH of the reaction mixture. A pH of 8.0 gave reproducible derivative yield for all physiological amino acids. Solvent extraction of excess FMOC, when compared to addition of amantadine to react with excess FMOC, gave both higher recoveries and greater precision. Following derivatization, samples could be kept at 4°C for at least 24 h before high-performance liquid chromatographic analysis without loss of response. Derivative yield and detector response were constant across a wide range of molar ratio of FMOC to total amino acids.

Gradient elution was required to separate FMOC derivatives on a reversed-phase column. The capability of the pumping system to produce exponential gradients permitted rapid and easy fine-tuning of the gradient.

0021-9673/90/$03.50

INTRODUCTION

Research into methods for amino acid determination has been an active area of investigation during recent years. The Biosis data base lists more than 9000 English papers published on this subject during the 1980s. The focus for much of this research has been on precise determination of amino acid composition from limited quantities of relatively pure proteins. The information obtained is often used in conjunction with sequence analysis to elucidate protein structure. Relatively little attention has been given to the very different problems involved in amino acid analysis on mixed tissue samples for ecological or nutritional purposes[1]. Mixed tissue samples contain, in addition to proteins and free amino acids, varying amounts of carbohydrates and lipids which may interfere with hydrolysis and subsequent analysis. These samples are necessarily heterogeneous in nature, making larger sample sizes an advantage. Some decrease in effciency of recovery and precision of determination is tolerable in exchange for speed and ease in sample preparation.

The present set of experiments was undertaken with the purpose of validating a method whereby complete amino acid composition could be determined for plant and animal tissues and waste products using a single hydrolysis and high-performance liquid chromatographic (HPLC) run. Methanesulfonic acid hydrolysis was chosen because of its ability to preserve tryptophan in the presence of moderate amounts of carbohydrate[2,3] and because derivatization may be carried out on the hydrolysis mixture after only pH adjustment. Since the exclusion of oxygen during hydrolysis is important for the complete recovery of several amino acids, the effect of flushing the sample with nitrogen during evacuation, prior to hydrolysis, was studied. The effects of hydrolysis time and temperature and of sample storage on recoveries were determined by hydrolysis and analysis of cytochrome *c*. Recovery efficiency for each amino acid from cytochrome *c* added to biological samples was determined by hydrolysis of biological samples alone and with added cytochrome *c*.

9-Fluorenylmethylchloroformate (FMOC) was chosen as a pre-column derivatization reagent based on the method of Cunico *et al.*[4]. Other derivatization methods were rejected because of considerations such as long analysis time and necessity for a post-column derivatization system (ninhydrin)[5], inability to detect secondary amino acids (*o*-phthalaldehyde)[6], instability of derivatives (dansyl chlorides)[7,8], or the requirement for evaporation prior to HPLC injection (phenylisothiocyanate)[9]. FMOC reacts with amino acids in dilute, basic solution to form UV absorbing and fluorescent derivatives with 88–98% yield[10]. This derivatization avoids the problems mentioned above and gives a choice of detection by fluorescence in the low pmole range or by UV absorbance at higher concentrations. Also, it is less sensitive to interferences from extraneous sample components than the other methods[4,10].

The effects of conditions during and after derivatization were studied to maximize the yield of amino acid derivatives. Optimum pH and reaction time for derivative formation were determined. Comparison was made between the use of amantadine to scavenge excess FMOC following reaction and the use of pentane to extract the alcoholic by-product. The effect on derivative formation of the molar ratio of FMOC to total amino acids and the stability of FMOC derivatives at both 4°C and at room temperature were determined. The mobile phase gradient was optimized to allow complete separation of all essential amino acids.

MATERIALS AND METHODS

Hydrolysis

Samples of black cherry leaves (*Prunus serotina*), fifth instar cecropia larvae (*Hyalophora cecropia*), and feces produced by the larvae when fed black cherry leaves were lyophilized and ground, using a Wiley Mill, to pass a 40-mesh screen. Samples were weighed on a Cahn Model 49 electrobalance to contain 0.2 to 2 mg of protein and introduced below the neck restriction of a reusable hydrolysis tube with PTFE stopper (Pierce)[11]. Hydrolysis reagent was freshly prepared by diluting methanesulfonic acid (Kodak) to 4 *M* with HPLC-grade water and adding approximately 0.2% 3-(2-aminoethyl)indole (Sigma). A 2-ml volume of reagent was added to each sample and the tube was closed to the first stop. Samples were frozen in dry ice–acetone and evacuated to 50 μTorr. The efficacy of nitrogen flush compared with simple evacuation was tested by flushing the sample tube twice with nitrogen and re-evacuating. Samples were hydrolyzed in an oil bath at 115°C (±2°C) for 22 or 70 h and at 150°C for 22 h.

Except when testing for sample deterioration with storage between hydrolysis and derivatization, samples were either derivatized and analyzed immediately or were kept sealed at 4°C. Cytochrome *c* (1.0 mg) and samples with added cytochrome *c* (about 1 mg total protein) were treated in a similar manner. Equine cytochrome *c* used for standardization has no serine residues[12], therefore serine does not appear in the tables for recovery of amino acids.

Hydrolysis results in conversion of glutamine and asparagine to glutamate and aspartate, respectively. The HPLC conditions used did not resolve glutamine from asparagine. Therefore, these four amino acids are grouped as diamino plus diacid (DAA) in the tables.

Derivatization

Standard amino acids, cytochrome *c* and FMOC were purchased from Sigma. c-Allylglycine (Sigma) was added to each hydrolyzed sample as an internal standard. Samples were transferred quantitatively to 15-ml centrifuge tubes, placed in an ice bath and either neutralized with NaOH and buffered with 0.1 *M* $NaHCO_3$, pH 8.0, or buffered with 0.1 *M* $Na_2B_4O_7$, pH 8.0, and adjusted to pH 8.0 with NaOH. All samples were brought to a final volume of 12 ml. Following centrifugation, 1.0 ml of sample was mixed with 1.0 ml of $6.0 \cdot 10^{-3}$ *M* FMOC in acetone. After completion of the reaction at room temperature, excess FMOC was destroyed by addition of approximately 6 μmol of amantadine or removed by double extraction with 2.0-ml portions of *n*-pentane. The samples were filtered through a 0.45-μm-pore syringe filter. The first few drops were discarded.

Chromatography

The HPLC system (Waters Division of Millipore) consisted of a Model 600 pump with exponential quaternary gradient capability and column heater, a refrigerated WISP autosampler, a 990 photodiode array detector and a NEC APC IV computer with Waters 990+ software. The column was a 150 mm × 4.6 mm I.D. end-capped ODS-80TM Aminotag column supplied by Varian Instruments and was maintained at 30°C.

Solvents used were Baker, HPLC grade. Tetrahydrofuran was distilled under

TABLE I

MOBILE PHASE COMPOSITION

Components were measured separately by volume and mixed without correction to final volume. Buffer composition was $15 \cdot 10^{-3}$ *M* citric acid, $10 \cdot 10^{-3}$ *M* tetramethylammonium chloride, pH adjusted with NaOH.

Mobile phase	*Buffer pH*	*Buffer (%)*	*Aceto-nitrile (%)*	*Tetrahydro-furan (%)*	*Final pH*
A	1.85	73	27	0	3.25
B	4.50	60	35	5	5.30
C	4.50	25	62	13	6.20

nitrogen within 72 h before use. Water was freshly purified by passage through a Continental Modulab, Type 1, HPLC-grade system. All mobile phases were prepared and filtered fresh daily. The mobile phase buffer was $15 \cdot 10^{-3}$ *M* citric acid with $10 \cdot 10^{-3}$ *M* tetramethylammonium chloride, pH adjusted with NaOH. Mobile phase composition and gradient profile are given in Tables I and II, respectively. These are modified from a method developed in the Varian LC Applications Laboratory[13].

Statistical analyses were done using SPSS/PC+ on an IBM/AT computer[14].

RESULTS AND DISCUSSION

Hydrolysis

The Student's *t*-test showed significantly higher mean recoveries from cytochrome *c* hydrolysate for cysteine ($P < 0.01$), methionine ($P < 0.01$) and tyrosine ($P < 0.05$) when the hydrolysis tube was flushed twice with nitrogen during

TABLE II

GRADIENT PROFILE

Composition of buffers A, B and C are given in Table I. Flow-rate, 1.4 ml/min.

Time (min)	*A (%)*	*B (%)*	*C (%)*	*Curve No.*[a]
0	100	0	0	
3	50	50	0	6
17	0	100	0	7
23	0	96	4	7
27	0	85	15	6
31	0	50	50	6
35	0	35	65	6
40	0	0	100	6

[a] Curve No. refers to the exponential gradient designation given in the Waters operating manual for the 600 pump. Curve 6 is a linear gradient, curve 7 is the shallowest of the concave gradients described by the equation: $A = A_s + (A_c - A_s)\,[(t - t_0)/(t - t_1)]^{(n-5)}$, where A = % of A at time t; A_s = % of A at the beginning of the segment; A_c = % of A at the end of the segment; t = elapsed time; t_0 = time at the beginning of the segment; t_1 = time at the end of the segment; n = curve number.

TABLE III

RECOVERY OF AMINO ACIDS FROM HYDROLYZED CYTOCHROME *c* — EFFECT OF NITROGEN FLUSH DURING EVACUATION PRIOR TO HYDROLYSIS

Samples of 1.0 mg cytochrome *c* were hydrolyzed at 115°C for 22 h. Evacuation was to 50 μTorr. For double nitrogen flush, after evacuation, vacuum was turned off, tube was flushed with nitrogen and re-evacuated, then nitrogen flush and evacuation were repeated.

Amino acid	*Evacuation only*		*Double nitrogen flush*	
	Mean recovery (%)	*C.V. (n = 3)*	*Mean recovery (%)*	*C.V. (n = 3)*
Ala	91.8	2.5	91.7	3.1
Arg	90.7	5.8	92.1	4.1
Cys	42.5	5.3	68.4	8.8[b]
DAA[a]	91.2	2.7	92.2	4.5
Gly	96.8	6.1	95.0	5.1
His	89.9	7.5	94.7	5.4
Ile	86.1	2.8	90.2	2.7
Leu	88.0	1.8	90.2	2.7
Lys	88.4	6.8	96.1	3.8
Met	63.1	6.2	92.7	3.1[b]
Phe	88.6	10.3	92.2	4.4
Pro	90.4	4.9	97.8	5.6
Thr	82.6	4.9	85.4	2.4
Trp	78.4	2.6	90.0	6.7
Tyr	73.4	4.3	82.0	6.5[c]
Val	87.6	4.2	89.1	2.5

[a] Sum of Asp, Glu, Asn, Gln.
[b] $P < 0.01$.
[c] $P < 0.05$.

evacuation prior to hydrolysis (Table III). Although individual recoveries of other amino acids were not improved by nitrogen flush, overall recovery was tested for significance of improvement by data transformation. Excluding the three amino acids for which individual recoveries were significantly higher, individual recoveries for nitrogen flush were divided by the corresponding recoveries for evacuation only. The mean of the results was tested against the hypothesis that it was not different from one. It was found to be greater than one by a Student's *t*-test at $P < 0.01$.

Neither longer (115°C for 70 h) nor higher-temperature (150°C for 22 h) hydrolysis yielded any significant improvements for individual or overall recoveries when compared to hydrolysis at 115°C for 22 h (Table IV, one-way ANOVA, Scheffe multiple range test, $P > 0.05$). At 150°C, there was significant loss of cysteine ($P < 0.05$), methionine ($P < 0.05$), threonine ($P < 0.01$) and tyrosine ($P < 0.05$) (one-way ANOVA, Scheffe multiple range test). Since peptide linkages involving branched chain amino acids are particularly difficult to hydrolyze[15], their recovery may be taken as a measure of hydrolysis efficiency. The 115°C, 22 h hydrolysis yielded 86% recovery of isoleucine and 89% recovery of leucine and valine (Table IV).

When replicate hydrolyzed samples ($n = 3$) were derivatized and analyzed immediately, stored at 4°C under vacuum or stored at 4°C after releasing the vacuum

TABLE IV

EFFECT OF HYDROLYSIS CONDITIONS ON RECOVERY OF CYTOCHROME *c*

Samples of 1.0 mg cytochrome *c* were hydrolyzed as indicated.

Amino acid	*22 h, 115°C*		*70 h, 115°C*		*22 h, 150°C*	
	Mean recovery (%)	*C.V. (n = 3)*	*Mean recovery (%)*	*C.V. (n = 3)*	*Mean recovery (%)*	*C.V. (n = 3)*
Ala	96.6	3.0	97.8	7.3	102.3	2.9
Arg	94.2	4.8	100.2	2.9	96.4	3.4
Cys	69.8	3.4	62.2	5.0	53.0	9.4[c]
DAA[a]	94.4	3.0	95.2	4.5	90.3	3.5
Gly	98.3	4.4	99.7	2.6	106.5	8.7
His	92.4	3.1	94.1	5.2	89.2	4.9
Ile	85.5	2.9	86.8	2.9	90.2	3.4
Leu	89.3	2.9	88.6	3.0	91.4	2.8
Lys	93.8	4.3	93.1	4.0	88.1	4.0
Met	90.7	5.6	87.6	10.0	85.7	1.8[c]
Phe	89.7	5.5	88.6	10.4	90.6	5.2
Pro	94.4	3.9	94.5	5.0	95.6	10.5
Thr	84.0	5.5	79.2	5.5	67.5	6.1[b]
Trp	89.5	4.2	85.5	2.3	87.2	3.0
Tyr	84.4	6.1	81.4	5.3	73.2	7.5[c]
Val	88.7	3.1	89.3	3.7	92.6	3.3

[a] Sum of Asp, Glu, Asn, Gln.
[b] $P < 0.01$.
[c] $P < 0.05$.

from the hydrolysis tube, there was found to be no difference between storage under vacuum for up to 4 days and immediate derivatization (Table V). However, there was a significant loss of cysteine, histidine, lysine and tryptophan when samples were stored in air at 4°C for 4 days (Table V, one-way ANOVA, Scheffe multiple range test, $P < 0.05$).

Individual amino acid recoveries from leaves, larvae and feces were tested separately against recoveries from cytochrome *c* using a Student's *t*-test. Most amino acids were recovered from the cytochrome *c* spike in leaves, larvae and feces with efficiencies similar to those from pure protein (Table VI). Exceptions were methionine from all three samples and tryptophan from leaves and feces. However, the coefficient of variation (C.V.) is low enough to allow estimation of total amino acid content to within *ca.* 12% for tryptophan and to less than *ca.* 10% for all others.

Derivatization

An advantage of sulfonic acid hydrolysis over HCl hydrolysis is that sulfonic acid need not be evaporated prior to derivatization. It is sufficient to adjust the pH and buffer the sample prior to addition of the derivatization reagent. No one pH is optimum for derivatization of all amino acids. Many amino acids show maximum derivative formation at a pH of 7.0; however, efficiency falls off quickly at slightly higher or lower pH. At pH 8.0, derivative formation is slightly less than maximum, but

TABLE V

EFFECT OF STORAGE OF HYDROLYZED SAMPLES ON RECOVERY OF AMINO ACIDS FROM CYTOCHROME *c*

Replicate 1.0 mg samples of cytochrome *c* were hydrolyzed at 115°C for 22 h. Three were refrigerated for 4 days without opening the hydrolysis tube. Three were refrigerated for 4 days after opening the hydrolysis tube. Three were derivatized and analyzed immediately.

Amino acid	*Immediate deriv.*		*4°C, Vacuum*		*4°C, Air*	
	Mean recovery (%)	*C.V. (n = 3)*	*Mean recovery (%)*	*C.V. (n = 3)*	*Mean recovery (%)*	*C.V. (n = 3)*
Ala	97.3	2.5	96.2	4.8	96.1	3.6
Arg	92.9	4.5	94.1	4.5	97.7	5.3
Cys	69.8	4.0	70.4	4.0	57.9	4.9[b]
DAA[a]	92.8	2.7	94.3	4.2	93.9	4.8
Gly	95.5	4.9	97.4	3.4	96.5	5.3
His	96.3	3.5	92.4	4.0	78.5	8.8[b]
Ile	85.3	2.6	87.2	3.6	86.8	3.9
Leu	88.7	3.3	88.9	3.9	87.7	3.7
Lys	93.5	5.4	94.3	4.5	78.6	6.2[b]
Met	92.2	5.4	90.9	4.8	92.8	3.3
Phe	89.7	5.7	90.0	6.4	89.3	5.4
Pro	95.2	3.2	94.6	3.8	91.9	5.6
Thr	83.5	2.9	81.4	5.0	82.8	3.5
Trp	89.8	3.3	88.6	6.6	75.0	6.6[b]
Tyr	84.5	6.4	84.5	5.5	85.4	7.9
Val	88.4	4.4	88.8	4.7	89.5	3.0

[a] Sum of Asp, Glu, Asn, Gln.
[b] $P < 0.05$.

is less affected by small variations in pH[16]. A pH of 8.0 gave reproducible results for all amino acids. Mean C.V. was less than 5.0 for all biological samples (Table VII). Sodium borate buffer was easier to use and gave greater precision of recovery than sodium bicarbonate buffer. With sodium bicarbonate it is necessary to approximately neutralize the sample prior to adding the buffer. Otherwise carbon dioxide is evolved reducing the buffering strength of the mixture. With borate buffer, it is possible to add the buffer to the acidic hydrolysis mixture and then adjust pH with a few drops of NaOH. Whichever procedure is used, pH of each individual sample should be verified before proceeding with derivatization because derivative yield is strongly dependent on pH.

Einarsson *et al.*[17] found that the FMOC derivatization reaction is essentially complete in less than 1 min at room temperature. FMOC also reacts with water to produce FMOC-alcohol. The alcohol elutes from the HPLC column at mid-run and has fluorescence and UV absorbance spectra similar to the derivatized amino acids. Large FMOC-alcohol peaks interfere with quantitation of smaller amino acid peaks. Unless derivatization is done on line immediately prior to HPLC injection, excess FMOC must be removed following derivatization. Amantadine, added after amino acid derivatives have formed, reacts with excess FMOC, preventing further formation

TABLE VI

RECOVERY OF AMINO ACIDS FROM HYDROLYZED CYTOCHROME *c* ADDED TO BIOLOGICAL SAMPLES

Three samples each of leaves, larvae and feces containing approximately 1.0 mg of protein were hydrolyzed. Three samples of each containing approximately 0.5 mg of sample protein plus 0.5 mg of cytochrome *c* were hydrolyzed. Amino acids recovered from cytochrome *c* in mixed samples were calculated by subtraction of amino acids from corresponding single component samples.

Amino acid	*Leaves*		*Larvae*		*Feces*	
	Mean recovery (%)	*C.V. (n = 3)*	*Mean recovery (%)*	*C.V. (n = 3)*	*Mean recovery (%)*	*C.V. (n = 3)*
Ala	92.6	3.8	90.5	6.6	90.4	5.5
Arg	96.0	7.1	93.0	6.5	98.0	6.5
Cys	67.3	7.3	72.4	5.5	76.6	6.1
DAA[a]	96.7	1.2	100.7	3.7	92.7	4.4
Gly	95.1	2.4	93.9	1.1	93.6	2.9
His	95.2	4.6	90.1	2.3	92.5	4.5
Ile	86.1	5.6	88.6	4.8	85.7	3.9
Leu	86.2	3.4	90.8	4.5	88.8	2.0
Lys	97.1	4.3	96.4	8.5	91.1	6.4
Met	77.6	3.9[b]	71.4	4.4[b]	75.3	2.2[b]
Phe	89.5	4.2	92.1	5.0	89.3	6.3
Pro	93.8	4.8	101.0	3.5	92.1	6.4
Thr	73.4	4.5	75.4	3.2	71.7	6.1
Trp	64.4	12.1[b]	87.0	1.4	54.0	12.9[b]
Tyr	80.9	4.3	90.5	4.5	82.8	4.9
Val	85.0	3.2	96.6	3.0	90.5	4.4

[a] Sum of Asp, Glu, Asn, Gln.
[b] $P < 0.01$.

of alcohol[6,18]. It does not, however, remove alcohol formed prior to addition. If amantadine is used to scavenge excess FMOC, it must be added at accurately timed intervals within five minutes of reaction time to minimize alcohol formation. Amantadine–FMOC has a reversed-phase retention time longer than any of the physiological amino acids and the HPLC run time must be extended by as much as 10 min to completely remove it from the column. Alternatively, an organic solvent may be used to remove both excess FMOC and previously formed FMOC-alcohol. Since alcohol is extracted along with excess FMOC, it is not necessary to minimize alcohol formation. The derivatization reaction may be carried out for a longer time and exact timing is not so critical. The HPLC run may be terminated shortly after the last amino acid derivative is eluted.

The average specific response (integrated area per pmoles injected) for most amino acids was less with amantadine addition at 5 min than with pentane extraction at 15 min (Tables VIII) (Student's *t*-test). If amantadine addition was delayed to 15 min, the FMOC-alcohol peak completely masked the alanine peak and made quantitation of tyrosine and proline difficult. Although it has been found that pentane extraction may remove some of the more hydrophobic amino acids[18], the data in Table

TABLE VII

MEAN COEFFICIENTS OF VARIATION OF AMINO ACIDS IN BIOLOGICAL MATERIALS

Hydrolysis, derivatization and analysis were performed in duplicate or triplicate for the indicated number of samples. Values given are the mean of the CV's (%) calculated separately for those samples.

Amino acid	*Leaves (n = 15) (%)*	*Larvae (n = 11) (%)*	*Feces (n = 8) (%)*
Ala	2.8	5.0	4.5
Arg	4.7	4.9	5.1
Cys	9.0	8.1	9.3
DAA[a]	3.4	4.5	4.2
Gly	3.8	3.9	4.2
His	3.6	4.4	4.3
Ile	4.7	5.0	4.4
Leu	4.0	3.4	4.0
Lys	4.8	4.6	4.1
Met	4.9	3.7	4.6
Phe	4.7	4.1	4.7
Pro	4.3	4.7	4.1
Thr	2.6	4.7	4.5
Trp	6.2	5.5	9.4
Tyr	7.6	3.9	4.1
Val	3.9	3.5	4.7

[a] Sum of Asn, Gln, Asp and Glu.

VIII indicate that specific response and thereby sensitivity are enhanced by pentane extraction following an extended reaction time.

To study the effect of the molar ratio of FMOC to total amino acids on derivative formation, equimolar standard amino acid mixtures were prepared to contain total amino acids from 30 to 4000 nmol in 1.0 ml. These were derivatized with 6000 nmol of FMOC in 1.0 ml of acetone, giving a molar ratio of FMOC to total amino acids ranging from 200 to 1.5. For each amino acid, a regression equation was calculated for specific response against concentration. Correlation was found to be significant (Student's t-test, $P < 0.05$) only for glycine and the correction was less than 2% over the entire concentration range. Although several researchers have stressed the importance of maintaining the molar ratio of FMOC to amino acids within a certain range[4,15,16], these data do not show any effect due to a 133-fold change in that ratio.

To test for derivative deterioration over time, standard mixtures were derivatized and injected immediately, then reinjected after 1, 2, 6, 12, 18 and 24 h either at 4°C or at room temperature. Regression equations and correlation coefficients were calculated for specific response against time for each amino acid at each temperature. At 4°C, aspartate and glutamate both showed a significant (Student's t-test, $P < 0.05$) positive correlation with storage time following derivatization. In both cases, the correction was less than 2% over a 24-h period. At room temperature only tryptophan was significantly correlated with storage time (Student's t-test, $P < 0.05$). Again the correction was less than 2%. Derivatives were, therefore, sufficiently stable to allow simultaneous preparation of enough samples to load the autosampler for a 24-h run.

TABLE VIII

SPECIFIC RESPONSE USING AMANTADINE OR PENTANE TO REMOVE EXCESS FMOC

Mixtures containing 10 nmoles each of 20 standard amino acids in 1.0 ml buffer were derivatized with 6 μmoles of FMOC in 1.0 ml acetone. Where amantadine was used, 6 μmoles were added after 5 min. If pentane was used, 2.0 ml was added after 15 min. After shaking and centrifugation, pentane was removed and extraction was repeated. Injection size was 20 μl.

Amino acid	*Amantadine*		*Pentane*	
	Response (area/pmol)	*C.V.* (n = 3)	*Response (area/pmol)*	*C.V. (n = 3)*
Ala	16.1	3.2	15.7	2.7
Arg	9.4	2.5	12.1	2.8[b]
Cys	23.8	8.1	22.8	2.8
DAA[a]	15.1	2.8	20.4	3.2[b]
Gly	12.6	6.0	16.8	3.1[b]
His	15.9	2.5	18.5	2.2[b]
Ile	13.6	2.6	18.5	2.1[b]
Leu	15.4	3.2	20.6	1.8[b]
Lys	26.6	2.4	34.3	1.5[b]
Met	12.6	3.4	17.9	1.6[b]
Phe	11.1	3.8	14.6	2.0[b]
Pro	11.6	3.5	13.5	1.8[c]
Thr	10.2	3.0	13.1	2.0[b]
Trp	15.8	8.9	21.4	1.6[b]
Tyr	11.4	2.6	15.2	3.6[b]
Val	13.1	2.4	17.8	2.0[b]

[a] Sum of Asn, Gln, Asp plus Glu.
[b] $P < 0.01$.
[c] $P < 0.05$.

Chromatography

A binary, three-point optimization technique[19] was used in a stepwise manner to effect separation among groups of amino acids which proved difficult to separate. The final gradient (Table II) was a combination of linear and exponential segments. Separation was near baseline for all amino acids with the exception of asparagine and glutamine (Fig. 1). These are non-essential for the larvae studied. Also, hydrolysis converts asparagine and glutamine to aspartate and glutamate, respectively. Therefore separation of this pair was not considered essential to our goals. The injection volune was 20 μl. If this is changed it is necessary to reoptimize the gradient, because the sample buffer disturbs the pH profile of the gradient near the beginning of the run. While much of the separation is insensitive to slight changes in pH or organic content of the elution gradient, the separation among phenylalanine, tryptophan, isoleucine and leucine remained extremely sensitive to such changes as well as to the effects of column ageing. The capability of the pumping system to produce exponential gradients made tuning this section of the chromatogram quite easy using only a change in the curve number.

Histidine and tyrosine form both mon- and di-FMOC derivatives. Quantitation was achieved by summing weighted peak areas. Also, no attempt was made to prevent

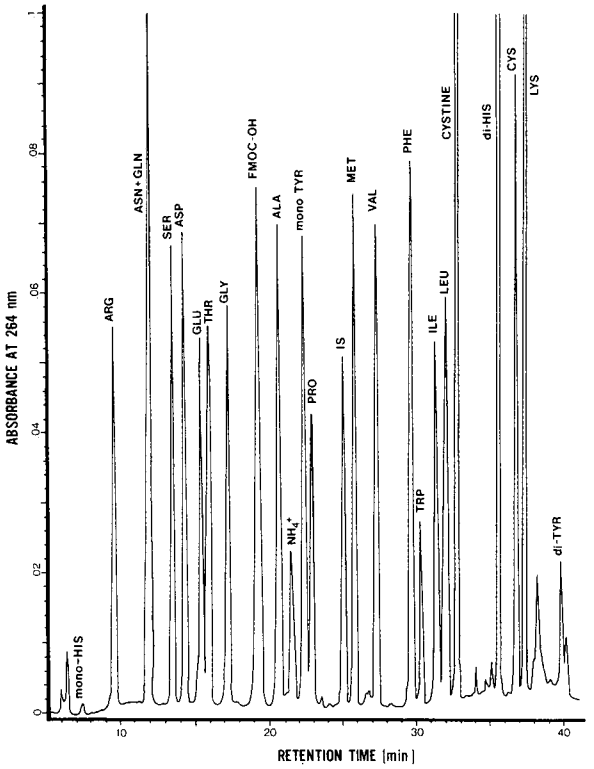

Fig. 1. Separation of FMOC derivatives of standard amino acids. Approximately 1.0 nmole of each amino acid was injected onto a 150 mm × 4.6 mm I.D. ODS-80TM Aminotag column. Internal standard (IS) was c-allylglycine. Gradient elution conditions are given in Tables I and II.

interconversion of cysteine and cystine during hydrolysis. These were quantitated from the weighted-area sum of the two peaks.

Biological samples

Fig. 2 is a typical chromatogram obtained from a sample of larval tissue hydrolyzed, derivatized and chromatographed under the conditions described. All physiological amino acids, with the exceptions noted above, are easily separated and peak areas may be accurately determined.

Biological samples analyzed under the conditions described above generally had C.V. values under 5%. Cysteine and tryptophan were somewhat higher, but under 10%. Our mean C.V. for all amino acids for leaves and larvae was 4.6% and for feces 4.9% (Table VII). These compare favorably with published values of precision for other methods used to analyze mixed biological samples. A recent multi-laboratory study used HCl hydrolysates of fish meal to compare ion-exchange HPLC with gas chromatography (GC) for amino acid analysis[20]. The mean within-laboratory C.V. for all amino acids was 6.4% for ion-exchange HPLC and 5.9% for GC. Adeola *et al.*[21] analyzed soybean meal, corn and triticale using HCl hydrolysis and

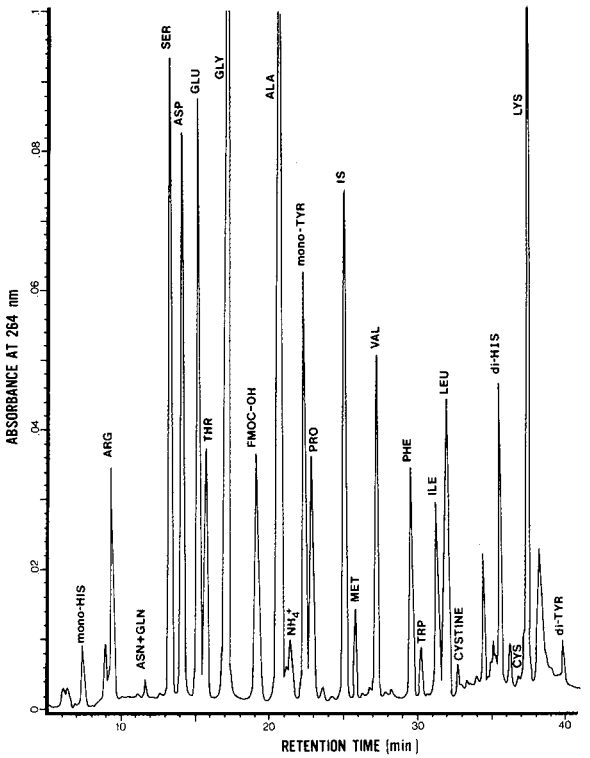

Fig. 2. Separation of FMOC derivatives of amino acids from hydrolyzed cecropia larvae. Approximately 5 mg of sample was hydrolyzed. Final injection represented approximately 4 μg of tissue injected onto a 150 mm × 4.6 mm I.D. ODS-80TM Aminotag column. Internal standard (IS) was c-allylglycine. Gradient elution conditions are given in Tables I and II.

reversed-phase HPLC of phenylthiocarbamyl derivatives or GC of N-heptafluorobutyryl derivatives. Using HPLC, the mean C.V. for soybean meal was 6.7%. Using GC, the mean C.V. for soybean meal was 3.6%, but neither arginine nor histidine, both essential amino acids, were determined. Corresponding mean C.V. values for corn were 6.1% using HPLC and 5.1% using GC and for triticale 5.3% using HPLC and 6.2% using GC.

CONCLUSIONS

Nitrogen flush used in preparation for methanesulfonic acid hydrolysis significantly increased the recovery of cysteine, methionine and tyrosine. Hydrolysis for 22 h at 115°C gave less than complete recoveries of amino acids, but with sufficient precision to allow accurate quantitation after correction for recoveries. Longer (72 h) or higher-temperature (150°C) hydrolysis did not significantly enhance efficiency of recovery and the higher temperature caused partial loss of cysteine, methionine, threonine and tyrosine. Hydrolyzed samples were stored for up to 4 days at 4°C under vacuum without significant loss of amino acids. Storage for 4 days in air resulted in loss of cysteine, histidine, lysine and tryptophan. For some amino acids, recovery efficiency

was lower from biological samples than from pure protein. However, precision was high enough to achieve reliable quantitation of amino acid content when correction was made for recoveries of individual amino acids.

With FMOC derivatization, pH control is important to obtain repeatable derivative yield. Although pH 8.0 did not give maximum yield for all amino acids, yield was less dependent on small changes at pH 8.0 than at lower pH. Borate buffer was judged to be easier to use than bicarbonate. For removal of excess FMOC, pentane extraction, compared with amantadine addition, gave a higher derivative yield for most amino acids. Derivative yield and specific response for UV absorbance was constant for molar ratios of FMOC to total amino acids ranging from 1.5 to 200. Derivatized samples were kept for at least 24 h without significant change in amino acid derivatives.

Complete HPLC separation of FMOC amino acids was achieved during a 40-min run time. Small differences in both pH and organic content of gradients are important for separation among phenylalanine, tryptophan, isoleucine and leucine.

Biological samples were analyzed with a mean C.V. for all amino acids in all samples of under 5%. This could be achieved on a routine basis using an autosampler for 24 or more samples daily.

ACKNOWLEDGEMENTS

We are grateful to Richard Vernell for skillful technical assistance. This work was supported by Youngstown State University, by an Ohio Board of Regents Academic Challenge Grant to Youngstown State University and by a National Science Foundation Grant, BSR-8611882, to L.A.S.

REFERENCES

1 M. L. G. Gardner, in J. M. Rattenbury (Editor), *Amino Acid Analysis*, Wiley, New York, 1981, p. 158.
2 B. Penke, R. Ferenczi and K. Kovacs, *Anal. Biochem.*, 60 (1974) 45.
3 R. J. Simpson, M. R. Neuberger and T.-Y. Liu, *J. Biol. Chem.*, 251 (1976) 1936.
4 R. Cunico, A. G. Mayer, C. T. Wehr and T. L. Sheehan, *BioChromatography*, 1 (1986) 6.
5 S. Moore and W. H. Stein, *J. Biol. Chem.*, 192 (1951) 663.
6 I. Betner and P. Foldi, *Chromatographia*, 22 (1986) 381.
7 E. Bayer, E. Grom, B. Kaltenegger and R. Uhmann, *Anal. Biochem.*, 73 (1976) 52.
8 J.-K. Lin, C.-A. Chen and C.-H. Wang, *Clin. Chem.*, 26 (1980) 579.
9 R. L. Heinrikson and S. C. Meredith, *Anal. Biochem.*, 136 (1984) 65.
10 L. A. Carpino and G. Y. Han, *J. Org. Chem.*, 37 (1972) 3404.
11 C. W. Gehrke, L. L. Wall, Sr., J. S. Absheer, F. E. Kaiser and R. W. Zumwalt, *J. Assoc. Off. Anal. Chem.*, 68 (1985) 811.
12 T. Takano, O. B. Kallai, R. Swanson and R. E. Dickerson, *J. Biol. Chem.*, 248 (1973) 5243.
13 A. G. Mayer, personal communication.
14 M. J. Norusis, *SPSS/PC+ for the IBM PC/XT/AT*, SPSS Inc., Chicago, IL, 1986.
15 S. Hunt, in G. C. Barrett (Editor), *Chemistry and Biochemistry of the Amino Acids*, Chapman & Hall, London, New York, 1985, p. 376.
16 T. Nasholm, G. Sandberg and A. Ericsson, *J. Chromatogr.*, 396 (1987) 225.
17 S. Einarsson, B. Josefsson and S. Lagerkvist, *J. Chromatogr.*, 282 (1983) 609.
18 I. Betner and P. Foldi, *LC·GC*, 6 (1988) 832.
19 S. J. Costanzo, *J. Chromatogr. Sci.*, 24 (1986) 89.
20 E. L. Miller, J. M. Juritz, S. M. Barlow and J. P. H. Wessels, *J. Sci. Food Agric.*, 47 (1989) 293.
21 O. Adeola, J. G. Buchanan-Smith and R. J. Early, *J. Food Biochem.*, 12 (1988) 171.

Journal of Chromatography, 514 (1990) 241–251
Elsevier Science Publishers B.V., Amsterdam

CHROM. 22 489

Comparative analysis of organic acids located on the surface of natural building stones by high-performance liquid, gas and ion chromatography

B. SCHRÖDER, J. MANGELS, K. SELKE, S. WOLPERS and W. DANNECKER*
Institut für Anorganische und Angewandte Chemie, Abt. Angewandte Analytik, Martin-Luther-King-Platz 6, D-2000 Hamburg 13 (F.R.G.)
(First received December 15th, 1989; revised manuscript received April 6th, 1990)

ABSTRACT

Highly polar carboxylic acids located on stone surfaces were analysed with regard to their potential impact on the deterioration of historical sites and monuments. A method for the elution of several organic acids from natural building stones is described. The performance of this method was confirmed by comparative high-performance liquid, gas and ion chromatographic analyses of the extracts obtained from prepared stone samples.

INTRODUCTION

Historical sites and monuments constructed from natural building stones deteriorate by several natural and anthropogenic mechanisms of weathering[1,2]. Buildings constructed from sandstone or marble are especially prone to decay.

Microorganisms such as fungi, bacteria and algae grow on weathered surfaces of buildings made of natural stones; macroorganisms such as moss, lichens and higher plants are also often observed[3]. Several strains of aerobic microorganisms produce mineral acids; in addition, complexing organic acids can be secreted as metabolites of the citric acid cycle, anaerobic glycolysis and other energetic cycles[4]. These metabolites may cause destruction by dissolution of minerals, modification of mineral structures and extension of pore sizes[5,6].

For quantitative determination, carboxylic acids had to be extracted from previously pulverized stones by a suitable method. The samples were ground in a mortar and pestle to avoid decomposition and losses of carboxylic acids, which occur as a consequence of thermal strain if globe mills or mortar mills are used.

The high calcium content of some building stones (up to 30%) was a major problem with regard to the extraction process, because salts formed by the expected carboxylic acids with calcium ions are of very low solubility. Previously described extraction methods[7–10] did not prove suitable for the extraordinary matrix.

0021-9673/90/$03.50

We have shown that mild extraction conditions are necessary to avoid decomposition[22]. The best results were obtained by extraction of acids using cation exchangers. As several commercially available polymeric cation exchangers of analytical-reagent grade display strong chromatographic interferences even if extensively purified, we turned to inorganic ion exchangers. Zeolite A (Na^+ form) had the highest specificity for calcium and other bivalent cations and turned out to be sufficiently purifiable by common laboratory methods.

Methods for determining carboxylic acids by high-performance liquid chromatography (HPLC) have been frequently described. Many workers have tried to enhance the ultraviolet sensitivity by derivatization[11,12]. No satisfactory results were obtained for highly polar carboxylic acids, especially at low concentrations.

Separation of the compounds was first tried by using ion-pairing reagents[13] on reversed phases. High resolution but poor detection limits were characteristics of this method. Direct separation on reversed phases[14,15] is not sufficiently specific for anions in a complex matrix. A combined single-column ion chromatographic–ion exclusion chromatographic method[16] could be adapted to the complex matrix of our samples and thereby solve this special separation problem. Detection limits of 2–570 nmol/g were realized and a highly sufficient group separation was obtained.

Analysis of organic anions by ion-exchange chromatographic (IC) methods is subject to interference by inorganic anions and the strong retention of, *e.g.*, citrate. As an isocratic method can hardly deal with these difficulties, a suitable gradient system was developed. Shintani and Dasgupta[17] described a sodium hydroxide gradient technique which could be adapted to the problem; increased solvent contamination was counteracted by on-line purification of the eluent with an anion-trap column.

Gas chromatographic (GC) analysis of carboxylic acids requires derivatization prior to analysis to increase the volatility of these polar compounds. In our case, the derivatization procedure had to deal with samples containing high concentrations of inorganic salts and at least trace amounts of water. As some of the acids in question are susceptible to decarboxylation, extensive heating had to be avoided.

Promising results were obtained with an esterification procedure employing *n*-butanol and concentrated sulphuric acid as reagents[18]; it is described as being especially suitable for samples containing inorganic salts and small amounts of water. As this method showed poor blanks, especially with regard to oxalic acid, acetyl chloride was used as a reagent instead of sulphuric acid[9,19]. The results obtained after this variation were favourable, and the method established shows good limits of determination and easy handling, is not prone to disturbances and allows large numbers of samples to be processed.

EXPERIMENTAL

Standard solutions

Aqueous standard solutions of nine carboxylic acids were prepared to evaluate the efficiency of the extraction procedure. Oxalic, succinic and formic acid (E. Merck, Darmstadt, F.R.G.) and citric and tartric acid (Riedel-de Haën, Seelze, F.R.G.) were of analytical-reagent grade. Propionic, fumaric and glyoxylic acid (E. Merck) were synthetic grade and malic acid (Riedel-de Haën) was labelled "biosynth". Water doubly distilled in an all-quartz apparatus. Concentrations of the three standard solutions (CA 1–3) are listed in Table I.

TABLE I

CARBOXYLIC ACID CONCENTRATIONS IN STANDARD SOLUTIONS

Acid	*Concentration (mg/l)*		
	CA 1	*CA 2*	*CA 3*
Formic	907	1896	3238
Propionic	1993	3987	9537
Citric	396	985	4138
Succinic	215	1995	3984
Oxalic	231	996	9847
Malic	993	1972	3943
Tartaric	991	1982	3968
Fumaric	26	401	2005
Glyoxylic	391	1140	3184

Stone samples

Three types of building stone often used at historical sites were selected with regard to their different contents of calcium carbonate: the limestone Krenzheimer Muschelkalk (K), the quartzite Worzeldorfer Quarzit (W) and the sandstone Ebenheidener Sandstein (E). The respective contents of the major bivalent cations as measured by inductively coupled plasma atomic emission spectrometry (ICP-AES) are given in Table II. Freshly quarried stones (Pressbau, Oberhausen, F.R.G.) were sawn into 16 ashlars of each type with weights varying from 3.13 to 6.75 g.

Four ashlars of each type were spiked with each of the CA 1–3 solutions. Four samples of each type of stone were chosen to determine blank values and were treated similarly to the spiked samples in the following process.

Extraction procedure

Zeolite A was purified prior to use as follows: 100 g of zeolite A (analytical-reagent grade; Fluka, Buchs, Switzerland) were shaken for 2 h with 500 ml of doubly distilled water and filtered by suction. This process was repeated until no relevant

TABLE II

CONTENTS OF BIVALENT CATIONS IN NATURAL BUILDING STONES DETERMINED BY ICP-AES

Cation	*Concentration (g/kg)*		
	Worzeldorfer Quarzit	*Ebenheidener Sandstein*	*Krenzheimer Muschelkalk*
Ca^{2+}	0.49	0.76	357.00
Mg^{2+}	0.84	2.37	1.75
Fe^{2+}	4.22	8.79	0.85
Ba^{2+}	0.56	0.41	0.08
Sr^{2+}	0.06	0.05	1.24

TABLE III

MAXIMUM CONCENTRATIONS OF CARBOXYLIC ACIDS IN EXTRACTS FROM SPIKED STONE SAMPLES (100% RECOVERY ASSUMED)

Acid	*Concentration (mg/l)*		
	I (spiked with CA 1)	*II (spiked with CA 2)*	*III (spiked with CA 3)*
Formic	4.54	9.48	16.20
Propionic	9.97	19.94	47.70
Citric	1.98	4.93	26.10
Succinic	1.08	9.98	19.92
Oxalic	1.16	4.98	49.25
Malic	4.97	9.86	19.72
Tartaric	4.96	9.91	19.84
Fumaric	0.13	2.01	10.03
Glyoxylic	1.96	5.70	15.95

chromatographic interferents were found in the filtrate. The purified zeolite A was dried overnight at 100°C.

For W and E, 1.0 g of stone powder, 10 ml of doubly distilled water and 2.0 g of zeolite A were placed in a 50-ml screw-capped vial. For K, with regard to its high calcium content, 0.5 g of stone powder, 10 ml of water and 5.0 g of zeolite A were taken. These samples were shaken (7 times per second) for 4 h. After deposition for 16 h they were filtered through a 0.2-μm cellulose membrane (Millipore, Bedford, MA, U.S.A.).

Table III gives the carboxylic acid concentrations in the solutions obtained, corresponding to 100% extraction efficiency.

Instrumental

High-performance liquid chromatography as single-column ion chromatography. The following equipment was used: pump, ConstaMetric III; detector, Spectro-Monitor D; integrator, MP 3000 (all from LDC–Milton Roy, U.S.A.); precolumn, Chromguard anion-exchange column (50 × 3 mm I.D.) (Chrompack, Middelburg, The Netherlands); separation column, ION-300 (ICT, CA, U.S.A.); and a column oven. The separation conditions were 5 m*M* sulphuric acid, flow-rate 0.4 ml/min, 40°C and detection at 210 nm.

Gas chromatography. A sample of 0.1–1.0 ml, depending on concentration, was evaporated *in vacuo* at 30°C on a rotary evaporator. A 1.0-ml volume of 1-butanol (analytical-reagent grade) and 0.5 ml of acetyl chloride (synthetic grade) (both from E. Merck) were added. After 1.5 h at 25°C, 7 ml of water were added and the solution was extracted three times with 0.3 ml of 2,2,4-trimethylpentane (analytical-reagent grade; E. Merck). A 10.0-μl volume of an internal standard solution containing 25.0 μg/ml of *n*-eicosane (Supelco, Bellefonte, PA, U.S.A.) was added to the combined organic extracts. Finally, the sample was evaporated *in vacuo* without heating to a final volume of 0.1 ml.

A Model FV 4160 gas chromatograph equipped with a Model El 490 electrometer, Model 430 temperature programmer, Model G1/M3 split injector and

a flame ionization detector (all from Carlo Erba, Milan, Italy) was used. The integrator was a C-R3A (Shimadzu, Tokyo, Japan). Compressed air and hydrogen (quality 5.0; Linde, Unterschleissheim, F.R.G.) were used as detector gases and the latter also used as carrier gas at a pressure of 40 kPa. The samples were separated on a Superox II column (Alltech Germany, Unterhaching, F.R.G.) (30 m × 0.25 mm I.D.) with a 0.25-μm film thickness. The temperature programme was 80°C start, increased at 30°C/min to 140°C, 3°C/min to 185°C and 15°C/min to 260°C, and a 10-min hold at 260°C.

Ion chromatography. The Model 4000i ion chromatograph (Dionex, Sunnyvale, CA, U.S.A.) includes a gradient programmer, pump and conductivity detector; a C-R3A integrator (Shimadzu) was used. The regenerant was 50 m*M* sulphuric acid (analytical-reagent grade; E. Merck) at a flow-rate of 4 ml/min. Eluent 1 was 0.75 m*M* sodium hydroxide solution (analytical-reagent grade; Baker, Phillipsburg, NJ, U.S.A.) and eluent 2 was 200 m*M* sodium hydroxide solution, with the following gradient: 0 min, 100%; 4 min, 100%; 8 min, 90%; 14 min, 83%; 20 min, 72%; and 30 min, 45% eluent 1; the flow-rate was 1 ml/min. ATC, HPIC-AG5A (5 μm), HPIC-AS5A (5 μm) and AMMS columns (all from Dionex) were used.

RESULTS AND DISCUSSION

This work had two major objectives: first to examine the efficiency of the proposed extraction method and second to investigate the reliability of the three chromatographic methods for this kind of sample. The results for Worzeldorfer Quarzit are presented in Figs. 1 and 2; they were standardized by subtraction of zero

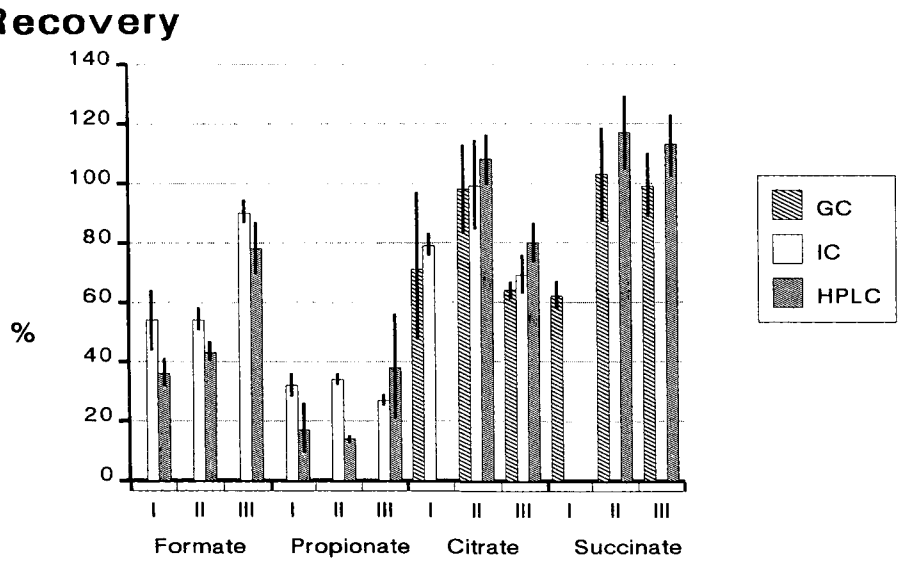

Fig. 1. Recoveries of formate, propionate, citrate and succinate from the quartzite Worzeldorfer Quarzit as determined by GC, IC and HPLC. The error bars represent relative standard deviations. I, II and III: sample concentrations are given in Table III.

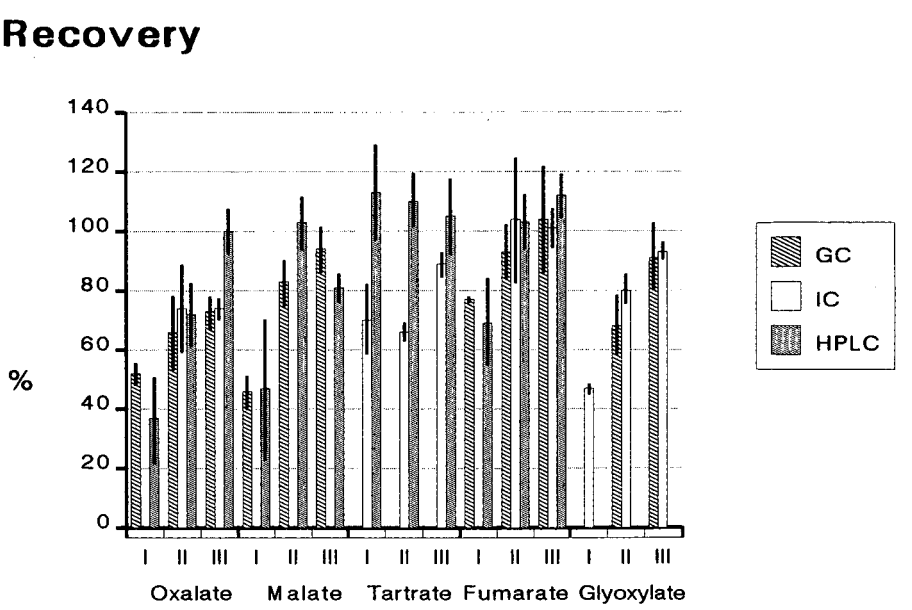

Fig. 2. Recoveries of oxalate, malate, tartrate, fumarate and glyoxylate from the quartzite Worzeldorfer Quarzit as determined by GC, IC and HPLC. The error bars represent relative standard deviations. I, II and III: sample concentrations are given in Table III.

TABLE IV

RECOVERIES (*R*) AND RELATIVE STANDARD DEVIATIONS (R.S.D.) OF HIGHLY POLAR CARBOXYLIC ACIDS EXTRACTED FROM KRENZHEIMER MUSCHELKALK AND EBENHEIDENER SANDSTEIN

R.S.D. values are normalized by the recoveries.

Stone	*Sample*[a]	*Method*	*Formic acid*		*Propionic acid*		*Citric acid*	
			R (%)	*R.S.D.* (%)	*R* (%)	*R.S.D.* (%)	*R* (%)	*R.S.D.* (%)
Krenzheimer Muschelkalk	I	GC	nd[b]		nd		46	3
		IC	nd		nd		82	5
		HPLC	97	15	36	4	97	7
	II	GC	nd		nd		29	2
		IC	nd		84	18	111	14
		HPLC	110	21	79	7	104	24
	III	GC	nd		nd		48	18
		IC	nd		93	11	87	4
		HPLC	102	12	85	19	94	20
Ebenheidener Sandstein	I	GC	nd		nd		51	4
		IC	nd		43	7	73	9
		HPLC	101	7	39	7	nd	
	II	GC	nd		nd		84	12
		IC	97	14	25	4	nd	
		HPLC	63	6	13	4	110	23
	III	GC	nd		nd		67	16
		IC	105	5	24	2	81	5
		HPLC	73	7	23	1	82	8

[a] Sample concentrations are given in Table III.
[b] Not determined.

concentrations. The boxes show percentage recoveries and the error bars represent relative standard deviations (R.S.D.)[20], normalized by the rate of recovery:

$$\text{R.S.D.}\,(\%) = \frac{100}{\bar{x}}\sqrt{\frac{\Sigma(x_i - \bar{x})^2}{n-1}}$$

The results for Krenzheimer Muschelkalk and Ebenheidener Sandstein are given in Table IV. Table V shows which chromatographic methods were applied to determine the different carboxylic acids.

Succinic, fumaric, tartric and citric acid were successfully recovered even from K and from samples with the lowest concentrations of carboxylic acids; the recoveries range from about 70 to 100%. The different chromatographic methods give concordant results. Malic and especially oxalic acid display increasing recoveries from low to high concentration levels. This indicates that a small amount of calcium ions still exists in the extraction solutions containing zeolite A. However, the HPLC and GC data both show that about 75% of oxalic and malic acid were extracted when 50 μg/g oxalic acid or 20 μg/g malic acid were present in the stone sample.

At first glance, the low recoveries obtained for glyoxylic, propionic and formic acid are striking. They are obviously due to the drying process at 60°C, which led to partial vaporization of the volatile carboxylic acids. The degree of vaporization depends on the respective acidities of stones and acids; the alkaline limestone K shows no losses of formic acid and only slight losses of propionic acid. A small amount of

CARBOXYLIC ACIDS EXTRACTED FROM KRENZHEIMER MUSCHELKALK AND EBENHEIDENER

Succinic acid		*Oxalic acid*		*Malic acid*		*Tartaric acid*		*Fumaric acid*		*Glyoxylic acid*	
R (%)	*R.S.D. (%)*	*R (%)*	*R.S.D. (%)*	*R (%)*	*R.S.D. (%)*	*R (%)*	*R.S.D. (%)*	*R (%)*	*R.S.D. (%)*	*R (%)*	*R.S.D. (%)*
73	10	23	3	37	4	nd		77	1	29	7
nd		nd		nd		93	15	nd		109	9
nd		34	2	122	29	94	2	92	22	nd	
78	8	36	6	48	4	nd		91	14	37	8
nd		nd		nd		108	5	nd		nd	
102	3	74	4	60	27	67	8	109	7	nd	
100	16	66	11	98	10	nd		97	9	51	7
nd		nd		nd		115	7	nd		86	17
123	14	84	4	54	22	77	19	111	17	nd	
60	7	29	6	54	4	nd		nd		nd	
nd		nd		nd		87	16	nd		nd	
nd		30	2	60	10	108	35	77	1	nd	
95	7	61	7	86	3	nd		98	10	44	4
nd		74	3	nd		99	7	99	1	45	6
107	8	82	6	95	26	101	25	102	6	58	14
100	7	75	4	100	6	nd		97	14	63	13
nd		37	10	nd		99	11	102	11	59	6
113	9	92	9	27	6	94	18	105	7	nd	

formic acid but more than 50% of propionic acid were lost from the slightly acidic sandstone E. More than 60% of propionic acid and 30–60% of formic acid escaped from the more acidic quartzite W. Owing to the losses, no actual recovery data can be given for E and W. Nevertheless, a good extraction efficiency is indicated by data obtained from K, which is the most difficult matrix because of its very high calcium content; IC and HPLC gave corresponding results.

The thermal evaporation of volatile carboxylic acids indicates that vaporization of these compounds is also to be expected on buildings, especially on walls with a southern alignment where solar irradation can cause great heat on the stone surface.

Glyoxylic acid is probably not vaporized, but decomposes during the drying process. This assumption was confirmed by previous storage experiments with spiked stone powder at −20°C, 6°C and at room temperature. For example, the starting concentration of glyoxylic acid decreased to well below 50% within 3 days at 23°C.

The suitability of the three chromatographic methods employed was judged by the following criteria: (a) interference with other compounds usually present in this matrix, (b) reproducibility of the results and (c) limits of determination. Figs. 3–5 show typical chromatograms of carboxylic acids extracted from stone samples by means of an aqueous suspension of zeolite A.

Using GC, oxalic, glyoxylic and succinic acid are determined without interference and with good reproducibility and determination limits. Fumaric and malic acid usually give reproducible results even at low concentrations, but fumaric acid is badly resolved from maleic acid and small peaks of malic acid may be difficult to distinguish from neighbouring peaks. Citric acid is prone to peak distortion in GC because of its high polarity even after derivatization. Formic, propionic and tartric acid could not be determined with the chosen GC method.

HPLC gives very satisfactory results with most of the carboxylic acids. A very low determination limit for fumaric acid is observed whereas that for glyoxylic acid is surprisingly high. Oxalic acid suffers interference from large amounts of nitrate.

Using gradient IC, formic, propionic and citric acid can be determined with good results. Difficulties with regard to reproducibility were found with oxalic and fumaric acid, and only high concentration levels could be measured. Glyoxylic and tartric acid

TABLE V

METHODS OF CHROMATOGRAPHIC ANALYSIS APPLIED TO THE INVESTIGATED CARBOXYLIC ACIDS

x = Suitable in most instances; (x) = suitable only in some instances; – = usually not suitable.

Acid	*HPLC*	*GC*	*IC*
Formic	×	–	×
Propionic	×	–	×
Citric	×	×	×
Succinic	×	×	–
Oxalic	×	×	(×)
Malic	(×)	×	–
Tartaric	×	–	(×)
Fumaric	×	×	×
Glyoxylic	–	×	(×)

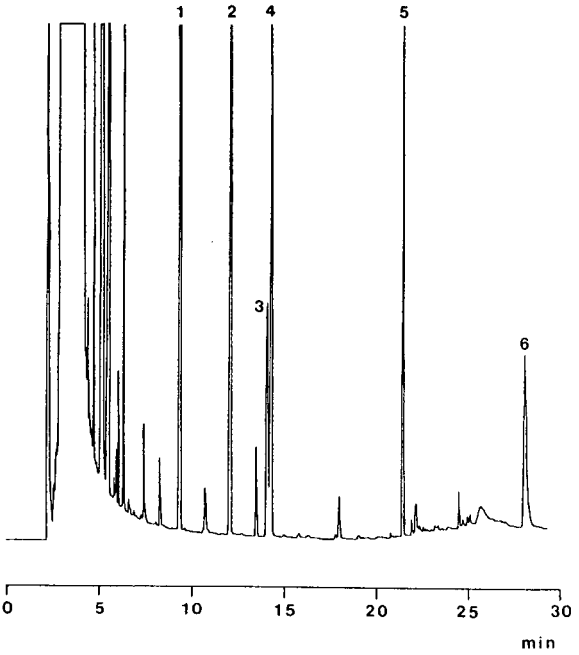

Fig. 3. Typical gas chromatogram of a derivatized extract obtained from a spiked stone sample. 1 = Oxalate; 2 = glyoxylate; 3 = fumarate; 4 = succinate; 5 = malate; 6 = citrate.

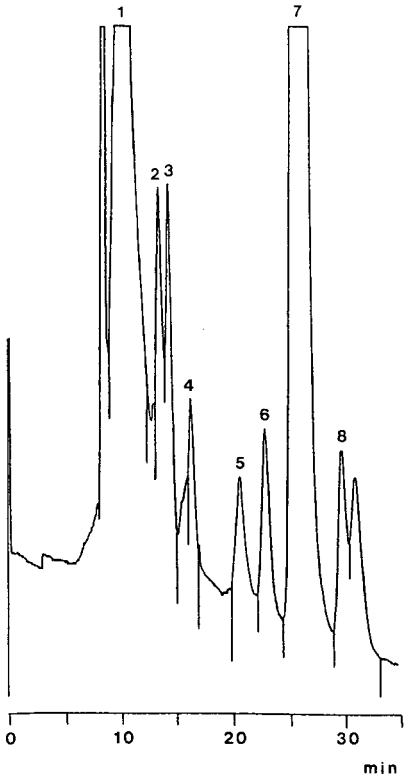

Fig. 4. Typical chromatogram obtained by HPLC from an extract of a spiked stone sample. 1 = Oxalate; 2 = citrate; 3 = tartrate; 4 = malate; 5 = succinate; 6 = formate; 7 = fumarate; 8 = propionate.

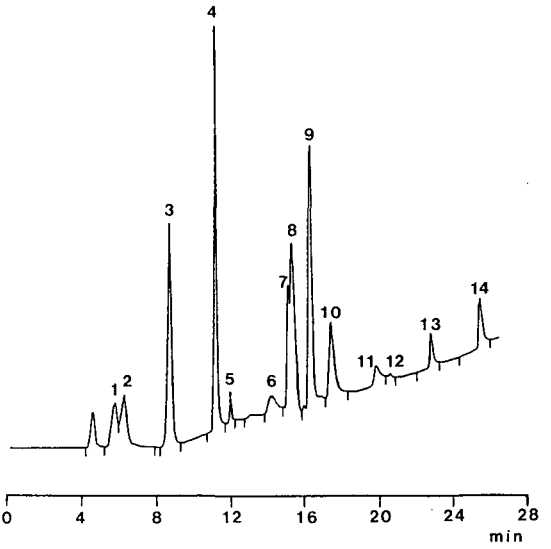

Fig. 5. Typical ion chromatogram of an extract obtained from a spiked stone sample. 1 = Acetate; 2 = propionate; 3 = formate; 4 = glyoxylate + chloride; 5 = nitrite; 6 = carbonate; 7 = malate + nitrate; 8 = succinate; 9 = tartrate + sulphate; 10 = oxalate; 11 = fumarate; 12 = phthalate; 13 = phosphate; 14 = citrate.

are subject to interference from chloride and sulphate, respectively. As succinic and malic acid coelute they cannot be determined with the chosen gradient, which was developed for the simultaneous determination of selected inorganic and organic anions[21]. Improvements in resolution may be achieved by further development.

The results presented show that the three methods employed complement each other and give the possibility of verifying results independently.

CONCLUSION

Zeolite A in an aqueous suspension is a suitable agent for the extraction of highly polar carboxylic acids from calcium-containing stones. It can be easily purified from interfering components. The recoveries and precision of the method are satisfactory down to a concentration of about 10 μg of acid per gram of stone. The described procedure has already been used to examine surface samples from some historical sites; oxalic acid is the most abundant and seems to be almost ubiquitous, but other carboxylic acids have also been found. The results should be compared with microbiological and geological findings.

ACKNOWLEDGEMENT

This research was funded by the German Federal Ministry of Research and Technology (BMFT), which is gratefully acknowledged.

REFERENCES

1 S. Luckat, *Chem. Unserer Zeit*, 16 (1982) 89.
2 K. Kraus, *Doctoral Thesis*, University of Cologne, Cologne, 1985.
3 R. Blaschke, *Bautenschutz Bausanierung*, special edition (1986) 38.
4 H. G. Schlegel, *Allgemeine Mikrobiologie*, Georg Thieme, Stuttgart, 1981.
5 F. E. W. Eckhardt, *Habilitationsschrift*, University of Kiel, Kiel, 1982.
6 M. Wagner and W. Schwartz, *Z. Allg. Mikrobiol.*, 7 (1967) 33.
7 M. K. L. Bicking and C. A. R. Skow, *Chromatographia*, 21 (1986) 157.
8 T. Tsuda, H. Nakanishi, T. Morita and J. Takebayashi, *J. Assoc. Off. Anal. Chem.*, 68 (1985) 902.
9 C. H. McMurray, *J. Chromatogr.*, 378 (1986) 201.
10 J. M. Rosenfeld, M. Mureika-Russel and A. Phatak, *J. Chromatogr.*, 283 (1984) 127.
11 H. D. Durst, M. Milano, E. J. Kiktra, S. A. Connelly and E. Grushka, *Anal. Chem.*, 47 (1975) 1797.
12 R. Badond and G. Pratz, *J. Chromatogr.*, 360 (1986) 119.
13 J. F. Keefer and S. M. Schuster, *J. Chromatogr.*, 383 (1986) 297.
14 W. Distler, *J. Chromatogr.*, 152 (1978) 250.
15 B. Libert, *J. Chromatogr.*, 210 (1981) 540.
16 R. Pecina, G. Bonn, E. Burtscher and O. Bobleter, *J. Chromatogr.*, 287 (1984) 245.
17 H. Shintani and P. K. Dasgupta, *Anal. Chem.*, 59 (1987) 802.
18 I. Molnar-Perl and M. Szakacs-Pinter, *Chromatographia*, 17 (1983) 493.
19 S. L. MacKenzie, *J. Chromatogr.*, 171 (1979) 195.
20 P. Zöfel, *Statistik in der Praxis*, Gustav Fischer, Uni-Taschenbücher, Stuttgart, 1985.
21 K. Selke and W. Dannecker, *Fresenius Z. Anal. Chem.*, 355 (1989) 966.
22 H. Mangels and J. Mangels, unpublished results.

Journal of Chromatography, 514 (1990) 253–257
Elsevier Science Publishers B.V., Amsterdam

CHROM. 22 487

Investigation of parameters in the separation of amino acid enantiomers by supercritical fluid chromatography

XIANWEN LOU, YUFEN SHENG and LIANGMO ZHOU*
Dalian Institute of Chemical Physics, Chinese Academy of Sciences, Dalian 116012 (China)
(First received December 28th, 1989; revised manuscript received April 4th, 1990)

ABSTRACT

The effects of column temperature (T) and pressure on enantioselectivity (α) and capacity factor (k') were investigated by supercritical fluid chromatography (SFC) with carbon dioxide as the mobile phase using a laboratory-made cross-linked chiral capillary column. The column temperature has considerable effects on both α and k' whereas the column pressure (*i.e.*, the density of mobile phase) shows no effect on α. Good linear relationships between $\ln\alpha$ and $1/T$ are obtained. The separation of some amino acid enantiomers is illustrated.

INTRODUCTION

Chromatographic separations of enantiomers have attracted wide attention since the important difference in biological activity of enantiomers became recognized[1]. Generally, gas chromatography (GC) is the method of choice for the separation of thermally stable and volatile molecules, but a high temperature is needed for the separation of amino acid enantiomers and the enantioselectivity decreases with increase in column temperature[2]. We therefore investigated supercritical fluid chromatography (SFC) for the separation of enantiomers under mild conditions and studied the parameters for the separation of amino acid enantiomers. In this paper, the effects of column temperature (T) and pressure (P) (*i.e.*, the density of the mobile phase) on separation factors (α) and capacity factors (k') in SFC are considered.

EXPERIMENTAL

The chiral stationary phase OV-225–L-valine–*tert.*-butylamide was cross-linked within a glass capillary column (20 m × 100 μm I.D.)[3]. GC experiments were carried out with a GC R1A gas chromatograph and SFC with a laboratory made chromatograph with carbon dioxide as the mobile phase. Each chromatographs was equipped with a flame ionization detector. The enantiomers of amino acids were derivertized to N-trifluoroacetyl amino acid isopropyl esters before injection[4].

0021-9673/90/$03.50

RESULTS AND DISCUSSION

The α-values of some amino acid enantiomers were obtained at different pressures by SFC (see Table I) and compared with those given by GC at the same column temperature (see Table II).

The effects of column temperature on α and k' values in SFC and GC are shown in Tables III and Table IV, respectively. The relative deviations of the data for both α and k' are within 2%. Fig. 1 shows the plots of ln α *vs.* $1/T$ and Fig. 2 of ln k' *vs.* $1/T$ for different amino acid enantiomers.

TABLE I

EFFECT OF PRESSURE ON α VALUES IN SFC (60°C)

Amino acid	*Pressure (MPa)*				
	8.0	*9.0*	*10.0*	*10.5*	*11.0*
Leu	1.132	1.129	1.129	1.129	
Met			1.098	1.100	1.098

TABLE II

COMPARISON OF α VALUES IN GC AND SFC

Method	*Ala (70°C)*	*Val (70°C)*	*NVal (80°C)*	*Leu (80°C)*	*NLeu (80°C)*
GC[a]	1.078	1.061	1.075	1.093	1.080
SFC (8.0 Mpa)	1.080	1.060	1.075	1.091	1.080

[a] Carrier gas nitrogen.

TABLE III

EFFECTS OF COLUMN TEMPERATURE ON α AND k' VALUES IN SFC

T(°C)	*Parameter*	*Ala (8.0 MPa)*	*Val (8.0 MPa)*	*NVal (8.0 MPa)*	*Leu (9.0 MPa)*	*NLe (8.0 MPa)*	*Met (10.0 MPa)*
50	α	1.098	1.080	1.107	1.143	1.118	1.115
	k'(L)	0.58	0.67	0.92	0.50	1.13	0.48
60	α	1.090	1.070	1.094	1.129	1.106	1.098
	k'(L)	0.79	0.71	1.13	0.76	1.53	1.27
70	α	1.080	1.060	1.083	1.107	1.091	1.088
	k'(L)	0.69	0.60	1.06	0.80	1.48	2.09
80	α			1.075	1.091	1.080	1.076
	k'(L)			0.91	0.75	1.24	2.22
90	α				1.083		1.066
	k'(L)				0.65		2.15
100	α				1.068		1.058
	k'(L)				0.53		1.95

TABLE IV

EFFECTS OF COLUMN TEMPERATURE ON α AND k' VALUES IN GC

T(°C)	*Parameter*	*Ala*	*Val*	*NVa*	*Leu*	*NLe*	*Met*
70	α	1.078	1.061				
	k'(L)	21.4	28.9				
80	α	1.068	1.054	1.075	1.093	1.080	
	k'(L)	11.7	15.4	27.9	39.2	46.8	
90	α	1.059	1.045	1.067	1.083	1.068	
	k'(L)	6.81	8.70	15.2	21.2	24.9	
100	α	1.051	1.039	1.056	1.068	1.058	
	k'(L)	4.02	5.01	8.49	11.6	13.5	
110	α	1.045	1.034	1.048	1.059	1.048	1.048
	k'(L)	2.61	3.21	5.19	6.70	7.89	59.2
120	α	1.038	1.027	1.040	1.049	1.040	1.040
	k'(L)	1.70	2.01	3.19	4.22	4.89	34.5
130	α						1.034
	k'(L)						19.0
140	α						1.026
	k'(L)						11.5
150	α						1.021
	k'(L)						7.10

As is well known, the enantioselectivity (α) is defined by

$$\alpha = k'_L/k'_D \tag{1}$$

Other than the polarization property, there is no difference between L- and D-antipodes in most of their physical and chemical properties[5]. It is also true that direct separation of enantiomers could only be achieved by chiral–chiral recognition so far. It is reasonable to assume that the effects of an achiral mobile phase (such as carbon

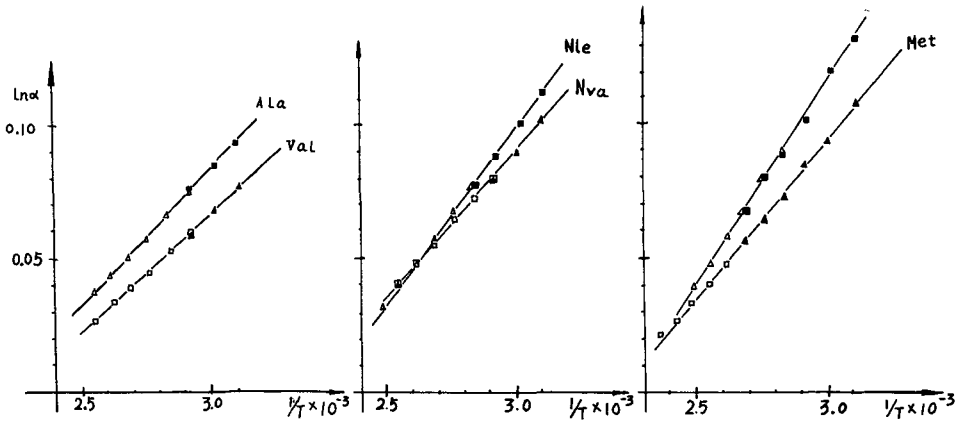

Fig. 1. Plots of ln α *vs.* $1/T$ obtained by (△, □) GC and (▲, ■) SFC.

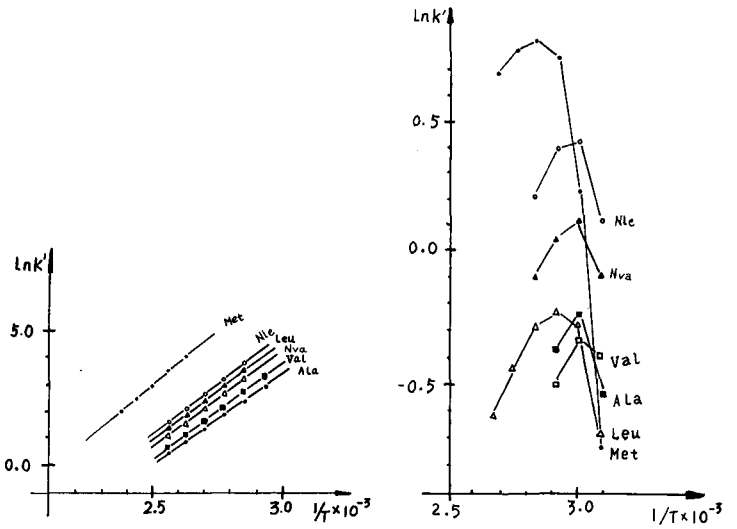

Fig. 2. Plots of ln k' *vs.* $1/T$: (left) GC; (right) SFC.

dioxide) on L- and D-antipodes will be identical, so according to the equations derived by Martire and Boehm[6] the following equations can be easily derived:

$$(\ln \alpha)_{SFC} = (\ln \alpha)_{GC} \tag{2}$$

$$\begin{aligned}(\ln \alpha)_{SFC} &= -(\Delta H_L - \Delta H_D)_{SFC}/RT + (\Delta S_L - \Delta S_D)_{SFC}/R \\ &= -(\Delta H_L - \Delta H_D)_{GC}/RT + (\Delta S_L - \Delta S_D)_{GC}/R\end{aligned} \tag{3}$$

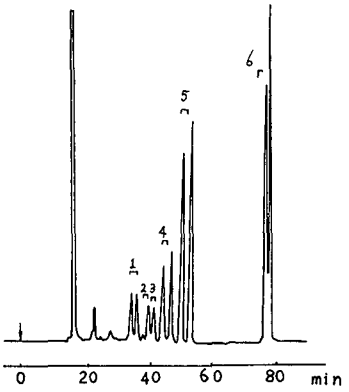

Fig. 3. Chromatogram of amino acid enantiomers obtained by SFC. Column, 20 m × 0.10 mm I.D. cross-linked OV-225–L-Val–tert.-butylamide; mobile phase, CO_2; detector, flame ionization; column temperature, 60°C; pressure, increased from 8 to 16 MPa at 0.1 MPa/min. Peaks: 1 = Val; 2 = allo-Isoleucine; 3 = Ile; 4 = Nva; 5 = Leu; 6 = Met.

(where R is the molar gas constant). Eqns. 2 and 3 indicate that the plots of ln α *versus* $1/T$ are linear in SFC and they are the same as those obtained by GC if the same column is used. The data in Tables II–IV and Fig. 1 confirm and support these points.

The effects of column temperature on capacity factors in SFC are more complicated than those in GC (see Fig. 2), probably because column temperature can affect the solute solubility in the mobile phase and the retention in the stationary phase simultaneously, but the two effects on k' values are in opposite directions. The results shown in Fig. 2 are the consequence of the competition of these effects.

Using SFC, enantiomers could be separated at fairly low column temperatures and have higher α values than in GC. The separation of some amino acid enantiomers with pressure programming by SFC is shown in Fig. 3.

CONCLUSION

The density of the mobile phase has no influence on enantioselectivity under the operating conditions applied. The results further confirm that the linear relationships between ln α and $1/T$ in SFC for the amino acids tested coincide with those obtained in GC. Higher α values are obtained by SFC than GC owing to the lower column temperature used.

ACKNOWLEDGEMENTS

The authors thank Professor Qinghai Wang, Daoqian Zhu and Yafeng Guan for their technical help and valuable discussions. This work was supported by Chinese National Natural Sciences Fund.

REFERENCES

1 G. Blaschke, H. P. Kraft, K. Fickentscher and F. Koehler, *Arzneim.-Forsch.*, 29 (1979) 1640.
2 W. Roeder, F. J. Ruffing and G. Schomburg, *J. High Resolut. Chromatogr. Chromatogr. Commun.*, 10 (1987) 665.
3 L.-W. Zhou, X.-W. Lou and Y.-F. Sheng, *Chin. J. Chromatogr.*, in press.
4 H. Frank, G. J. Nicholson and E. Bayer, *J. Chromatogr.*, 167 (1978) 187.
5 R. W. Souter, *Chromatographic Separation of Stereoisomers*, CRC Press, Boca Raton, FL, 1985, p. 1.
6 D. E. Martire and R. E. Boehm, *J. Phys. Chem.*, 91 (1987) 2433.

Journal of Chromatography, 514 (1990) 259–272
Elsevier Science Publishers B.V., Amsterdam

CHROM. 22 512

Behaviours of siloxane polymers containing phenyl or silarylene as stationary phases for high-temperature gas chromatography

Y. TAKAYAMA*, T. TAKEICHI
Materials Science, Toyohashi University of Technology, Tempaku-cho, Toyohashi 440 (Japan)
S. KAWAI
Gifu College of Pharmacy, Mitahora, Gifu 502 (Japan)
and
M. MORIKAWA
Nippon Chromato Co., 8–15–2 Toshima, Kita-ku, Tokyo 114 (Japan)
(First received December 29th, 1989; revised manuscript received April 24th, 1990)

ABSTRACT

Several kinds of mechanisms have been proposed for the thermal degradation of methylphenylsiloxane and dimethylsiloxane–silarylene copolymer in an inert atmosphere. These polymers have been used as gas chromatographic stationary phases at temperatures as high as 370°C, but there is no report on the thermal stability of the polymers during prolonged use at high temperatures, especially above 400°C. In this work, the thermal stability of these stationary phases at temperatures as high as 420°C was examined using a deactivated metal capillary column, which is much more thermally stable than the fused-silica capillary columns. It was found that these phases degraded at 380–400°C by eliminating arylene-containing moieties, which led to cross-linking, and the peak shapes therefore deteriorated. With a column treated at 420°C, elution of solutes was considerably delayed and the elution order became unusual, which could not be rationalized from the behaviours of these medium-polarity and non-polar columns. It was concluded that the medium-polarity stationary phases in these columns finally became highly cross-linked dimethylsiloxane by losing arylene-containing moieties, thus giving poor peak shapes.

INTRODUCTION

Several mechanisms have been proposed for the thermal degradation of methylphenylpolysiloxane under an inert atmosphere[1,2]. Together with the formation of benzene and cross-linking structures, the formation of methylphenyltricyclosiloxane, which results from the flexibility of the siloxane main chain as in the case of dimethylpolysiloxane, has been reported[1,2]. Arylene-containing dimethylsiloxane–

0021-9673/90/$03.50

silarylene copolymer, whose main chain flexibility is restricted, showed improved thermal stability at 400–450°C in thermogravimetric analysis (TGA)[3–5]. Applications of the copolymer as a stationary phase in capillary gas chromatography (GC) have been proposed[6,7]. Above 350°C, however, scission of the main chain and the formation of branched structures are known to occur owing to the interactions between the main chains[5]. Although these degradations of the copolymer do not result in weight loss and cannot be observed by TGA, the use of the copolymer for high-temperature GC (HTGC) may not be as desirable as expected. Capillary columns of methylphenylsiloxane–silarylene copolymer and methylphenylpolysiloxane have already been characterized[8,9]. The highest temperature examined, however, was only 370°C and further study is required in order to establish the behaviour of the columns at higher temperatures such as those used in HTGC.

We have previously reported on the development of novel deactivated metal capillaries that exhibit superior characteristics for HTGC such as the maintenance of inertness, thermal stability and mechanical strength in comparison with those for fused-silica capillaries[10,11]. In this work, the high-temperature behaviours of methylphenylsiloxane and dimethylsiloxane–silarylene copolymer were investigated, taking advantage of the high-temperature properties of the deactivated metal capillaries.

EXPERIMENTAL

Stationary phase synthesis

Methylphenylsiloxane prepolymer. Siloxanol-type prepolymer containing 50% phenyl groups was prepared from methylphenyldichlorosilane according to the procedure of Madani and Chambaz[12].

Tetramethyldisiloxanediol (TMDSD). To a solution of ammonium carbonate (110 g) in distilled water (410 ml) was added dimethyldichlorosilane (65 ml) over 2.5 h with vigorous stirring at 0°C. The mixture was then kept standing at −5°C for 48 h. The crystals obtained were extracted with light petroleum and dried over magnesium sulphate. Concentration of the filtrate afforded crystalline TMDSD, which was further recrystallized from light petroleum before use.

Dimethylsiloxane–silarylene precopolymer. Prepolymers A and B were prepared from *p*-phenylenebis(dimethylsilanol) (PPBDMS) and TMDSD according to the reported procedure[7] under the conditions shown in Table I. Briefly, PPBDMS and TMDSD were dissolved in 150 g of toluene and tetramethylguanidine di-2-ethylhexanoate (TMG) was added as a catalyst. The mixture was heated to reflux and then filtered. Removal of toluene afforded a viscous product, which was dissolved in diethyl ether, washed with water five times, and dried over magnesium sulphate. Removal of the ether gave the prepolymers.

Column preparation

Methylphenylsiloxane column. Methylphenylsiloxane prepolymer was coated statically on an RAS 25 metal capillary (35 m × 0.25 mm I.D.), prepared by Nippon Chromato, which was heated at 250°C for 15 h under a flow of nitrogen at 1 ml/min and then at 300°C for 24 h under a flow of nitrogen at 0.2 ml/min. Rinsing with 5 ml of methylene chloride gave a 30-m column with a film thickness of 0.25 μm.

Dimethylsiloxane–silarylene columns. Toluene solutions of prepolymers A (5%)

TABLE I

PREPARATION OF DIMETHYLSILOXANE–SILARYLENE PREPOLYMERS

Prepolymer	*Dope*			*Reaction time*[a]
	PPBDMS	*TMDSD*	*Catalyst (TMG)*	
A	4.29 g 19.0 mmol (50.9 mol-%)	2.86 g 18.3 mmol (49.1 mol-%)	0.79 g	9 h
B	5.05 g 22.4 mmol (53.8 mol-%)	3.00 g 19.2 mmol (46.2 mol-%)	0.46 g	5 h

[a] At reflux temperature.

and B (7%) were coated dynamically on an RAS 25 deactivated metal capillary (12.5 m × 0.25 mm I.D.). Column A, coated with prepolymer A, was heated under a flow of hydrogen at 1 ml/min at 250°C for 50 h. Column B, coated with prepolymer B, was heated at 300°C for 20 h under a similar flow of hydrogen. Columns 10 m long were used.

Column evaluation

Methylphenylsiloxane column. The column was evaluated on a Varian 3410 gas chromatograph. Helium was used as the carrier gas and the inlet pressure was adjusted to 12.5 p.s.i. The flow-rate at ambient temperature was 1.0 ml/min and the linear velocity was 24.5 cm/s. Thermal treatment of the column and the subsequent GC measurement to evaluate the column were carried out without removing the column during the experiment, in order to minimize experimental errors. Thermal treatment of the column was carried out successively at 300°C for 15 h, at 350°C for 15 h, at 400°C for 17 h and at 420°C for 5 h, under a flow of helium at 12.5 p.s.i., the same pressure as that in the GC measurement. After each thermal treatment, the column was evaluated with a polarity test mixture (Grob and Grob's test mixture[13]). The GC conditions are given in the figure captions. Separation factors were measured for a mixture of tridecane and 1-decanol.

Dimethylsiloxane–silarylene columns. Thermal treatments of the columns were carried out in an oven under a flow of hydrogen at 1.5 ml/min. After each thermal treatment described below, GC measurement using a simplified polarity test mixture[10] was performed with an Ohkura (Tokyo, Japan) Model 701 instrument to study the changes in peak shapes and elution order. Thermal treatment for column A was at 350°C for 25 h and then at 380°C for 25 h, and for column B at 350°C for 25 h and then at 400°C for 25 h. The baseline shift was also measured for column B.

RESULTS AND DISCUSSION

Variation of methylphenylsiloxane column by thermal treatment

Separation factor (α). Separation factors were measured for a mixture of tridecane and 1-decanol using columns heated at various temperatures. As shown in

TABLE II

VARIATION OF CAPACITY FACTORS (k') AND SEPARATION FACTORS (α) WITH THERMAL TREATMENT OF METHYLPHENYLSILOXANE COLUMN[a]

Thermal treatment[b]	$k'_{(C_{13})}$[c]	$k'_{(C_{10}ol)}$[d]	$\alpha_{(C_{10}ol/C_{13})}$
300°C, 15 h	4.43	7.28	1.64
350°C, 15 h	4.32	7.03	1.63
400°C, 17 h	4.70	7.31	1.56
420°C, 5 h	—[e]	—[e]	—[e]

[a] Measured isothermally, column temperature 110°C, helium flow-rate 24.5 cm/s.
[b] Thermally treated with helium at 12.5 p.s.i., adjusted to 1 ml/min at ambient temperature.
[c] Capacity factor of tridecane.
[d] Capacity factor of 1-decanol.
[e] Peaks did not appear.

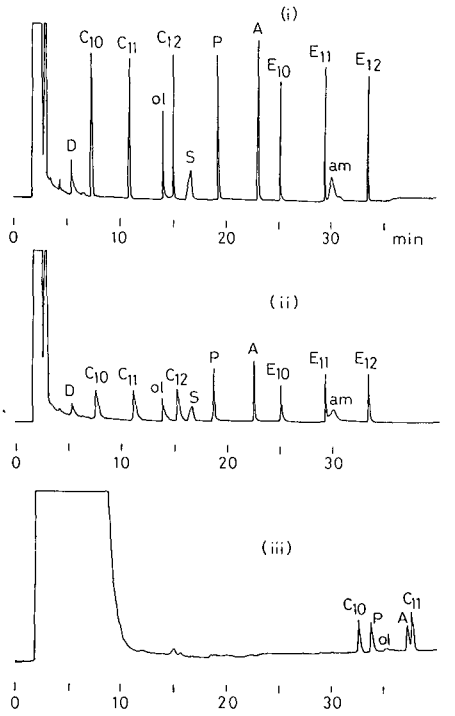

Fig. 1. Gas chromatograms of polarity test mixture on a deactivated metal capillary coated with methylphenylsiloxane prepolymer having terminal OH groups (50% phenyl) (30 m × 0.25 mm I.D.). Thermal treatment: (i) 300°C, 15 h + 350°C, 15 h; (ii) as (i) + 400°C, 17 h; (iii) as (ii) + 420°C, 5 h. Conditions: carrier gas, helium at 12.5 p.s.i. constant pressure; temperature programme, start 60°C, increased at 3°C/min. Peaks: D = 2,3-butanediol; C_{10} = *n*-decane; C_{11} = *n*-undecane; ol = 1-octanol; C_{12} = *n*-dodecane; S = 2-ethylhexanoic acid; P = 2,6-dimethylphenol; A = 2,6-dimethylaniline; E_{10} = methyl decanoate; E_{11} = methyl undecanoate; am = dicyclohexylamine; E_{12} = methyl dodecanoate.

Table II, only slight changes were observed for both the capacity factors (k') and separation factors (α) of the solutes up to 350°C, but with thermal treatment at 400°C an increase in $k'_{(C_{13})}$ and a decrease in α, that is, a decrease of polarity, were observed. The decrease in α is not due to the decrease in the number of terminal OH groups of the stationary phases, as the $k'_{(C_{13})}$ values after treatment at 300 and 350°C are almost the same. The decrease in α is considered to be due to the elimination of arylene-containing moieties. This assumption is supported by the observation that the pak shapes of tridecane and 1-decanol after thermal treatment at 400°C became triangular with a vertical section in front and some tailing. This indicates elimination of arylene-containing moieties and solidification of the remaining phases by cross-linking[8]. An increase in $k'_{(C_{13})}$ after the thermal treatment at 400°C is a sign that the elution time became so long that the solute was not eluted in the normal time after thermal treatment at 420°C.

Variation of peak shapes and elution order of solutes. The chromatograms for the polarity test mixture are shown in Fig. 1. There was little difference up to 350°C. After thermal treatment at 400°C, however, it is clearly seen from the comparison of Fig. 1(i) and (ii) that the peak shape for each hydrocarbon became triangular with a vertical section in front and tailing, and that, although the elution order was same, the elution time became longer, as was observed in Table II.

After thermal treatment at 420°C, the elution time became very long, as shown in Fig. 1(iii), and the elution order changed dramatically. This column was fitted to a Shimadz GC 8A instrument and a gas chromatogram was measured under the same conditions. As shown in Fig. 2, a very long elution time and dramatically changed elution order, similar to those in Fig. 1(iii), were observed. The same phenomenon was confirmed with another methylphenylsiloxane column after treatment at 420°C. With the change in elution order, 2,6-dimethylaniline (A) was eluted earlier than *n*-undecane (C_{11}) in Figs. 1(iii) and 2, which cannot be understood from the behaviours of the original column shown in Fig. 1(i) or the dimethylsiloxane column shown in Fig. 3.

The ratio of the elution times for each solute after and before thermal treatment of the column is shown in Table III as the retardation factor. Table III shows that, with

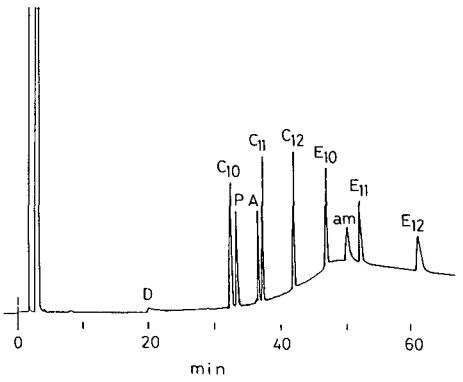

Fig. 2. Gas chromatogram of polarity test mixture on a deactivated metal capillary coated with methylphenylsiloxane prepolymer having terminal OH groups (50% phenyl) (30 m × 0.32 mm I.D.). Thermal treatment: 300°C, 15 h + 350°C, 15 h + 400°C, 17 h + 420°C, 5 h. Conditions: carrier gas, nitrogen at 1.0 ml/min constant flow-rate; other condition and peaks as in Fig. 1.

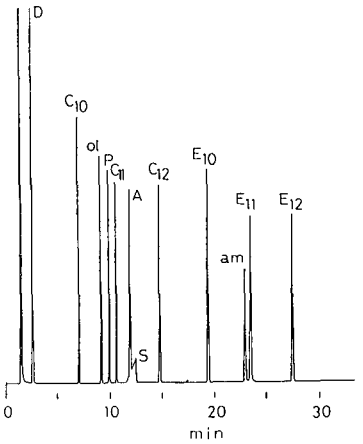

Fig. 3. Gas chromatogram of polarity test mixture on a deactivated metal capillary coated with dimethylsiloxane prepolymer having terminal OH groups and thermally treated (30 m × 0.25 mm I.D.). Conditions and peaks as in Fig. 2.

TABLE III

VARIATIONS OF ELUTION TIME AND ORDER OF SOLUTES ON THERMAL TREATMENT OF METHYLPHENYLSILOXANE

Solute[a]	*Methylphenylsiloxane column*					*Non-polar column*[f]*: elution order*
	Thermal treatment				*Retardation factor*[e]	
	300 → 350°C[b]		*300 → 420°C*[c]			
	Elution order	*Elution time (min)*	*Elution order*	*Elution time (min)*[d]		
D	1	5.5	1	20.0	3.6	1
C_{10}	2	7.3	2	32.9	4.5	2
C_{11}	3	10.8	6	37.7	3.5	5
ol	4	14.0	4	35.0[g]	2.5	3
C_{12}	5	14.9	7	42.5	2.9	8
S	6	16.7	7[h]			7
P	7	19.1	3	33.6	1.8	4
A	8	22.9	5	36.8	1.6	6
E_{10}	9	25.1	9	47.4	1.9	9
E_{11}	10	29.4	11	52.5	1.8	11
am	11	30.0	10	50.6	1.7	10
E_{12}	12	33.4	12	61.5	1.8	12

[a] For abbreviations, see Fig. 1.

[b] 300°C, 15 h + 350°C, 15 h.

[c] 300°C, 15 h + 350°C, 15 h + 400°C, 17 h + 420°C, 5 h.

[d] Calculated value corresponding the elution time in Fig. 1(iii), corrected by multiplying the elution time in Fig. 2 by 1.0086 using the elution time of C_{11} as standard.

[e] Ratio of elution times between the two columns.

[f] See Fig. 3.

[g] Measured value from Fig. 1(iii).

[h] Estimated elution order. Peak did not appear in Fig. 2.

treatment at 420°C, early-eluted solutes are retarded much more than the late-eluted solutes. The retardation factor is relatively small for the solutes which have a cyclic structure in the molecule, such as P, A and am (see Fig. 1 for abbreviations). Basic solutes such as am eluted from the column which was adsorptive-active after treatment at 420°C for 5 h. This indicates that the adsorptive activity is not due to the acidity usually seen with active columns.

Thermal treatment of the column was carried out under helium at a pressure of 12.5 p.s.i., which was the same as that in the GC measurement. Hence it was expected that, on thermal treatment of the column, the front part of the column would lose phenyl groups and become highly cross-linked and non-polar, thus giving triangular peak shapes. The latter part of the column was expected to contain more arylene-containing moieties that have migrated from the front part. Hence the peak shapes with the latter part of the column were expected to be more normal and the elution order should be different from that with the front part of the column.

To confirm the above expectations, the following experiments were carried out. After the measurements in Fig. 2, the column that had been treated at 420°C was divided into four parts to give short columns, (i)–(iv). Every peak that eluted prior to *n*-dodecane (C_{12}) was assigned by measuring each solute by isothermal GC at 100°C. Fig. 4(i) shows a chromatogram using the front 7.5 m of the 30-m column. As expected, the peak shapes were triangular with a vertical section in front. The elution time was short and the elution order was C_{10}, ol, P, C_{11} and A, if ol eluted, the same order as was

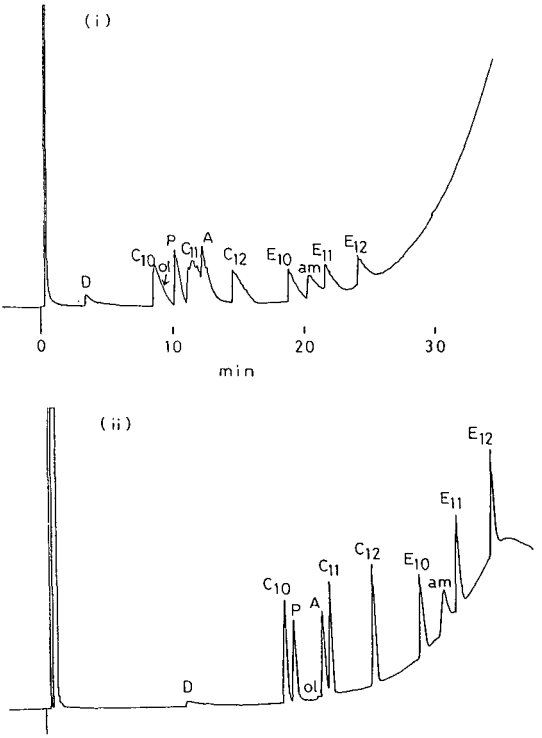

Fig. 4.

(*Continued on p. 266*)

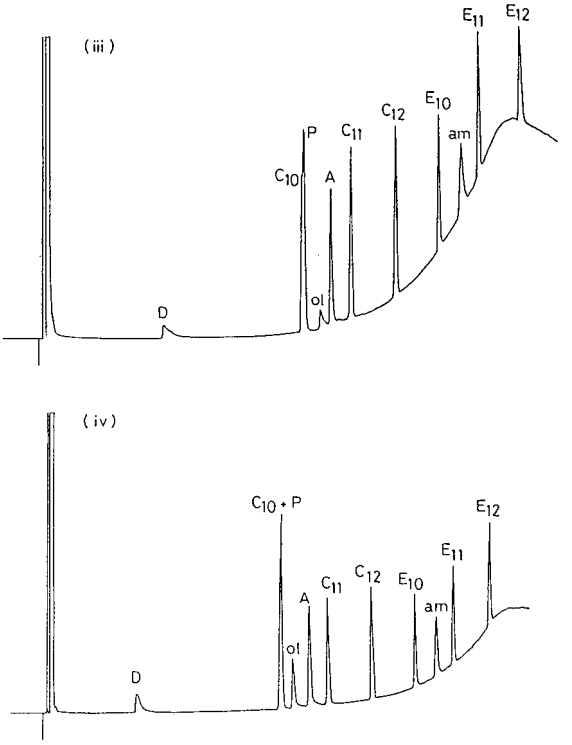

Fig. 4. Gas chromatograms of polarity test mixture on sectioned columns after thermal treatment. Columns coated with methylphenylsiloxane (7.5 m × 0.25 mm I.D.). Thermal treatment: 300°C, 15 h + 350°C, 15 h + 400°C, 17 h + 420°C, 5 h, under a flow of helium at 12.5 p.s.i. Carrier gas nitrogen at 1 ml/min; other test conditions and peaks as in Fig. 1. (i)–(iv): numbered as quartered columns cut from the top of the 30 m column.

seen in Fig. 3 with the non-polar dimethylsiloxane column. As shown in Fig. 4(ii)–(iv), the elution time became large with columns (ii)–(iv) compared with column (i), but P and A were retarded comparably less. P and A shifted forward between C_{10} and C_{11} with the latter column, as shown in Fig. 4(ii)–(iv), the chromatograms of which cannot be understood from the results with the ordinary polymethylphenylsiloxane column [Fig. 1(i)] and polymethylsiloxane column (Fig. 3).

Based on the chromatograms obtained, we interpreted the mechanism of the thermal degradation of the polymethylphenylsiloxan column as follows. At *ca.* 370°C, the column begins to lose polarity by eliminating benzene and forming branched structures[8]. With treatment at 400°C for 17 h, cross-linking proceeds and the stationary phase solidifies[8]. With treatment at 420°C for 5 h, scission of the solidified phase occurs and siloxane oligomers migrate back to the latter part of the column. Hence relatively large holes remain in the solidified phase as a result of the loss of the oligomers. With column (i), the holes are too large to retain solutes, which elute in order to their boiling points without significant retardation. With column (ii), however, the solidified phase with large holes captures siloxane oligomers and swells,

thus making the holes smaller. The smaller holes in column (ii) can retain linear hydrocarbons such as C_{10} and C_{11}, and their retention times become longer. However, aromatic solutes such as P and A are difficult to retain in the smaller holes, and the increases in retention time for the aromatic solutes are smaller than those for the linear solutes, resulting in the order of elution C_{10}, P, A and C_{11}. The peak shapes are greatly improved with column (ii) [Fig. 4(ii)] compared with column (i). Siloxane oligomers may also be acting as tailing reducers. Larger amounts of siloxane oligomers should have migrated into columns (iii) and (iv), making the holes in the solidified phase smaller. P and A are more difficult to retain in the smaller holes of columns (iii) and (iv), thus leading to a shorter elution time for P and A. P eluted at the same time as C_{10} in Fig. 4(iii) and (iv).

The behaviours of ol, S and am, which often cause problems due to adsorption, were examined with the short columns (i)–(iv). As shown in Fig. 4(i)–(iv), the columns show adsorptive activity towards ol and S. The deactivated metal capillary column coated with dimethylsiloxane prepolymer did not show adsorptive activity[10] even after treatment at 450°C, and columns coated with dimethylsiloxane–silarylene precopolymer that had been treated above 420°C did not show adsorptive activity towards ol. There is little possibility of catalytic degradation of the stationary phase by the metal column, as exemplified by the result that no appreciable difference was observed with methylphenylsiloxane between the experiments using the RAS 25 deactivated metal capillary reported here and preliminary experiments using a leached glass capillary column. Hence the adsorptive activity of the columns coated with methylphenylsiloxane prepolymer after high-temperature treatment is due to some kind of

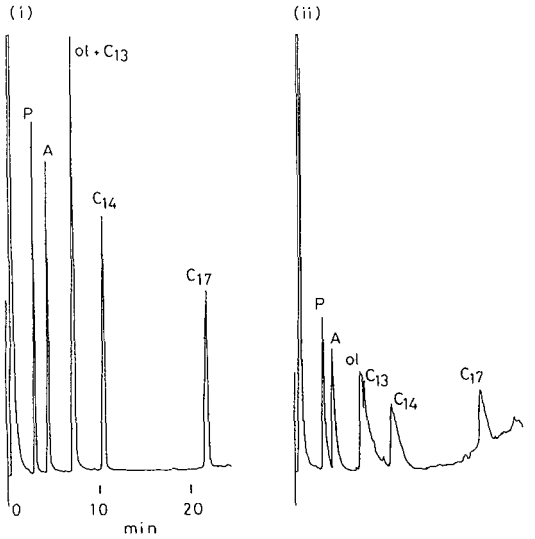

Fig. 5. Gas chromatograms of simplified polarity test mixture on a deactivated metal capillary coated with dimethylsiloxane–silarylene coprepolymer (A) having terminal OH groups (10 m × 0.25 mm I.D.). Thermal treatment under hydrogen at 1.5 ml/min: (i) 350°C, 25 h; (ii) as (i) + 380°C, 25 h. Conditions: carrier gas, nitrogen at 1.5 ml/min constant volume; temperature programme, start 60°C, increased at 3°C/min. Peaks: P = 2,6-dimethylphenol; A = 2,6-dimethylaniline; ol = 1-decanol; C_{13} = *n*-tridecane; C_{14} = *n*-tetradecane; C_{17} = *n*-heptadecane.

degradation of the stationary phase and not to the activation of the deactivated metal capillaries.

Variation of dimethylsiloxane–silarylene column by thermal treatment

Variation in peak shapes and elution order of solutes. Column A, coated with prepolymer A shown in Table I, was heated at 350°C for 25 h and a chromatogram was then obtained with the simplified polarity test mixture. The chromatogram obtained, shown in Fig. 5(i), is similar to that obtained before the thermal treatment. After further heating at 380°C for 25 h, however, the peak shapes, as shown in Fig. 5(ii), became triangular and ol and C_{13} became resolved. This indicates that silarylene-containing moieties began to be eliminated, and at the same time the stationary phase became non-polar accompanied by cross-linking and solidification.

With column B, the chromatograms before and after thermal treatment at 350°C for 25 h were same as that in Fig. 5(i). A baseline shift with column B after thermal treatment at 350°C for 25 h, as shown in Fig. 6, was observed at temperatures from 325°C and degradation of the stationary phase appeared vigorous above 370°C. After an additional thermal treatment at 400°C for 25 h, the peak shapes, as shown in Fig. 7, became triangular, the elution time became long and non-polar solutes were retarded relatively longer, as was described with the methylphenylsiloxane columns.

There appears to be little difference between columns A and B. Fig. 5(ii) with column A can be regarded as the pre-stage of Fig. 7 with column B, and at this stage solutes were retarded only slightly, although the peak shapes were not good. Columns A and B began to eliminate silarylene-containing moieties and cross-link on treatment at 380°C for 25 h, thus becoming less polar. This resulted in a chromatogram as in Fig. 5(ii), in which ol eluted earlier and the peak shapes became triangular. The longer retention time and relatively earlier elution of P and A after treatment at 400°C for 25 h, as shown in Fig. 7, is due to the same reason as suggested for Fig. 4(i). The same chromatogram as shown in Fig. 7 was obtained after rinsing column B that had been thermally treated at 400°C for 25 h, which indicates that considerable cross-linking of the stationary phase occurred.

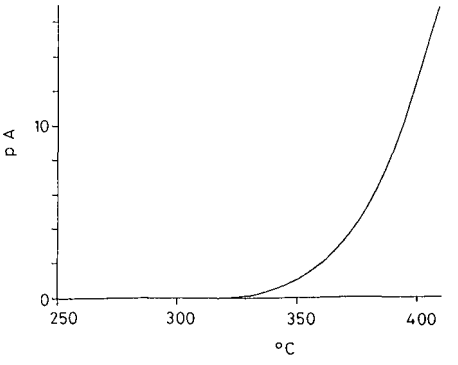

Fig. 6. Baseline shift for dimethylsiloxane–silarylene copolymer (B) after thermal treatment at 350°C, 25 h. Column, 10 m × 0.25 mm I.D.; carrier gas, nitrogen at 1.5 ml/min constant volume; temperature, programmed at 3°C/min.

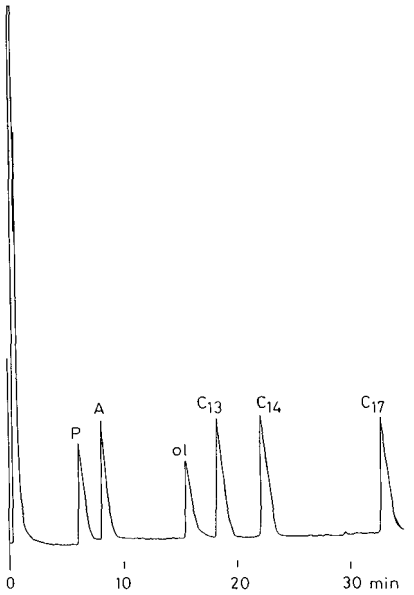

Fig. 7. Gas chromatogram of simplified polarity test mixture on a deactivated metal capillary coated with dimethylsiloxane–silarylene copolymer (B) having terminal OH groups (10 m × 0.25 mm I.D.). Thermal treatment: 350°C, 25 h + 400°C, 25 h. Conditions and peaks as in Fig. 5.

Volatile products obtained by thermal treatment of the precopolymer. Precopolymer was placed in a glass tube and heated gradually from 350 to 420°C under a stream of nitrogen at 2 ml/min and maintained at 420°C for 3 h. Volatile compounds were collected as an oil in a trap cooled with liquid nitrogen. GC–mass spectrometric (GC–MS) measurements were made on the gas phase and methylene chloride solution of the liquid phase from the trap. Using a fused-silica column coated with OV-1, the gas phase was analysed at ambient temperature and the liquid phase with temperature programming from 100 to 300°C at 10°C/min and a hold at 300°C. Benzene was not detected in the gas phase. GC of the liquid phase is shown in Fig. 8. MS measurements were made on the peaks with the underlined scan numbers. As a result, parent peaks or peaks from which hydrogen atoms were abstracted were observed at *m/z* 281 (observed in scan number 27), 341 (scan number 53), 343 (114), 355 (56), 415 (142), 429 (88), 461 (221), 475 (204) and 489 (161).

Among these peaks, that of *m/z* 341 was identified as coming from abstraction of a hydrogen atom from the structure 1 with $n = 2$, which was formed by adding two hydrogen atoms to a corresponding radical. The peaks of *m/z* 415 and 489 were identified as structure 1 with $n = 3$ and 4, respectively. The peak of *m/z* 475 is considered to come from the random copolymer segment 2. A peak observed at *m/z* 281 can be assigned to a hydrogen atom-abstracted product from the cyclic structure of a radical 3, which, however, is hardly possible because of the strain of such a small molecule having a silarylene unit. The peaks of *m/z* 355 and 429, both of which have one more $Si(CH_3)_2$–O unit compared with structure 3, also cannot be assigned either, together with the peaks of *m/z* 343, 461 and 475. This experiment also confirmed that

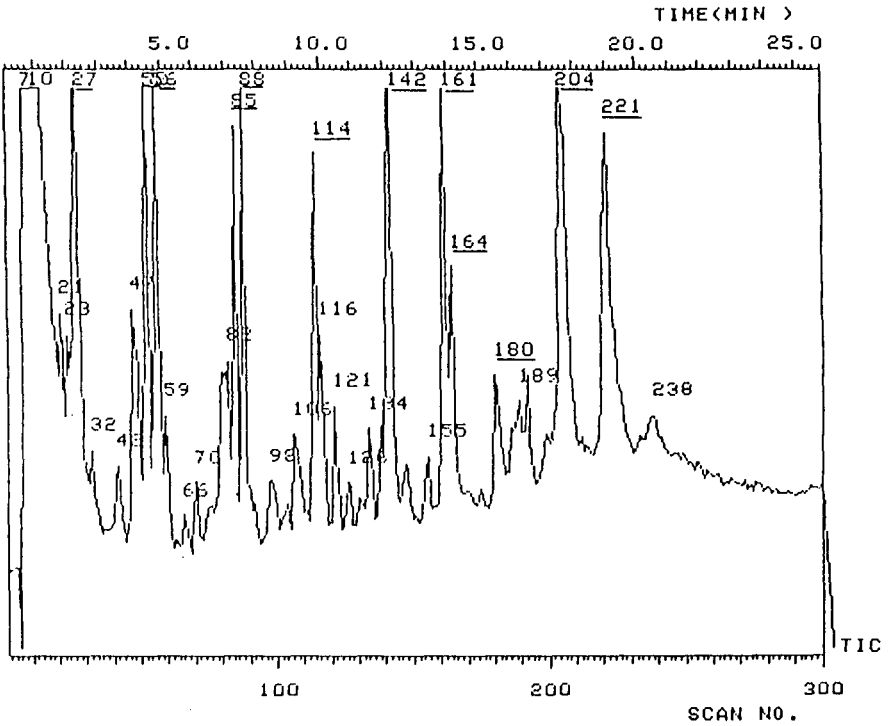

Fig. 8. Gas chromatogram of volatile liquid products obtained by thermally treating dimethylsiloxane–silarylene precopolymer.

columns coated with precopolymer decompose easily by eliminating silarylene-containing moieties.

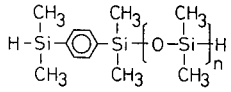

1

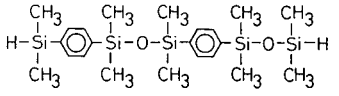

2

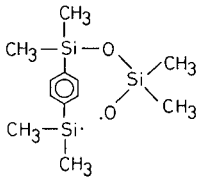

3

CONCLUSIONS

The thermal stabilities of arylene-containing polymers, methylphenylsiloxane polymer and dimethylsiloxane–silarylene precopolymer as stationary phases for HTGC were examined using a deactivated metal capillary column. The thermal stabilities of the stationary phases were evaluated from the variations in peak shapes and elution orders of solutes of a polarity test mixture after prolonged thermal treatment at 300–420°C.

All the phases examined start to lose arylene-containing moieties and to cross-link on prolonged use at 380°C, and the peak shapes became triangular with a vertical section in front.

Although the retention time was expected to become short owing to decomposition and migration of stationary phases after prolonged use at 400–420°C, the retention time became very long for every solute. It was proposed that siloxane oligomers migrated from the solidified stationary phase and holes that were too large to retain solutes remained, thus making the solidified phase porous. Migrating siloxane oligomers were then trapped by the solidified porous stationary phase of the latter part of the column, thus making the phase swell. The smaller holes so obtained can trap solutes, leading to longer retention times. As relatively large cyclic solutes cannot be easily trapped in the smaller holes, the increase in retention time is small compared with that of linear solutes. Consequently, the elution order varied dramatically and became completely different from that of the non-degraded column or non-polar column.

These stationary phases are not suitable for HTGC above 400°C. Their maximum operating temperature is limited to 350–360°C and to 380–400°C for brief periods with temperature programming. Repeated use, however, will result in degradation of the column. The column should not be used further when the peak shapes of hydrocarbon become triangular, otherwise great changes in elution time and elution order will occur.

ACKNOWLEDGEMENT

We are deeply grateful to Dr. Y. Hirata for the GC–MS measurements.

REFERENCES

1 N. Grassie, I. G. Macfarlene and K. F. Francey, *Eur. Polym. J.*, 15 (1979) 415.
2 T. H. Thomas and T. C. Kendrick, *J. Polym. Sci., Part A-2*, 8 (1970) 1823.
3 R. W. Lenz and P. R. Dvornic, *Polym. Prepr. Am. Chem. Soc. Div. Polym. Chem.*, 21, No. 2 (1980) 142.
4 N. Koide and R. W. Lenz, *J. Polym. Sci., Polym. Symp.*, 70 (1983) 91.
5 N. Grassie and S. R. Beattie, *Polym. Degrad. Stabil.*, 7 (1984) 109.
6 I. P. Yudina, K. I. Sakodynskii, V. P. Mipeshkevich, S. B. Dolgoplosk, G. N. Semina and L. I. Ananeba, *Russ. Pat.*, SU 105650 (1983).
7 J. Buijten, L. Blomberg, S. Hoffmann, K. Markides and T. Wännman, *J. Chromatogr.*, 301 (1984) 265.
8 A. Bemgård, L. Blomberg, M. Lymann, S. Claude and R. Tabacchi, *J. High Resolut. Chromatogr. Chromatogr. Commun.*, 11 (1988) 881.
9 A. Bemgård, L. Blomberg, M. Lymann, S. Claude and R. Tabacchi, *J. High Resolut. Chromatogr. Chromatogr. Commun.*, 10 (1987) 302.

10 Y. Takayama, T. Takeichi and S. Kawai, *J. High Resolut. Chromatogr. Chromatogr. Commun.*, 11 (1988) 732.
11 Y. Takayama, *M&E Japan*, Dec. (1988) 138.
12 C. Madani and E. M. Chambaz, *Chromatographia*, 11 (1978) 725.
13 K. Grob and G. Grob, *J. Chromatogr.*, 219 (1981) 13.

Journal of Chromatography, 514 (1990) 273–278
Elsevier Science Publishers B.V., Amsterdam

CHROM. 22 506

Thermal desorption–gas chromatography of some organophosphates and S-mustard after trapping on Tenax

J. STEINHANSES and K. SCHOENE*
Fraunhofer Institut für Umweltchemie und Ökotoxikologie, D-5948 Schmallenberg (F.R.G.)
(First received December 18th, 1989; revised manuscript received April 13th, 1990)

ABSTRACT

Thermal desorption from Tenax coupled with gas chromatographic analysis was performed with bis(2-chloroethyl) sulphide (s-mustard), O,O-diisopropyl phosphorofluoridate (DFP), O-isopropyl methylphosphonofluoridate (sarin), O-(1,2,2-trimethylpropyl) methylphosphonofluoridate (soman) and O,O-dimethyl methylphosphonate (DMMP). Experiments with humidified test atmospheres (48% relative humidity at 20°C) of S-mustard, DFP and soman revealed that the moisture did not impair the sampling of these compounds on Tenax or their thermal desorption from that sorbent. Tenax tubes loaded with the three agents from humidified atmospheres could be stored for up to 2 months without a decrease in recovery.

INTRODUCTION

The objective of this work was to study the applicability of Tenax as the sampling material together with automated thermal desorption–gas chromatography (ATD–GC) in monitoring atmospheres for their content of the toxic compounds bis(2-chloroethyl) sulphide (S-mustard), O,O-diisopropyl phosphorofluoridate (DFP), O-isopropyl methylphosphonofluoridate (sarin), O-(1,2,2-trimethylpropyl) methylphonofluoridate (soman) and, as a simulant, O,O-dimethyl methylphosphonate (DMMP). Additionally, with S-mustard, DFP and soman, the influence of atmospheric moisture on sampling, ATD–GC and storage of loaded sorbent tubes was investigated.

EXPERIMENTAL

Materials and equipment

The chemicals used, with the purity and supplier in parentheses, were Tenax TA, 20–35 mesh (Alltech), 1,1,2-trichlorotrifluoroethane (TCFE; 99%, Aldrich), DMMP (97%, Aldrich), S-mustard (99.7%, Atlanta), DFP (80%, EGA Chemie), sarin (93.5%, Wehrwissenschaftliche Dienststelle der Bundeswehr) and soman (83%, Wehrwissenschaftliche Dienststelle der Bundeswehr). The percentages given for the last three latter compounds were determined by titration according to ref. 1.

0021-9673/90/$03.50

For ATD and GC an ATD 50–GC 8500 system with an LCI 100 integrator from Perkin-Elmer was applied. The ATD sorption tubes, made of stainless-steel (8.9 cm × 0.49 cm I.D.), were filled with 175 mg of Tenax and flushed with nitrogen at 250°C overnight to remove volatile impurities.

The ATD 50 (with a multiple split system) was run with the following operating parameters: helium, 150 kPa; purge, 1.5 ml/min; mode 2; box, 140°C; oven, 250°C; cold trap, −30/300°C; desorb I, 10 min, input split closed, output split 18 ml/min; desorb II, 45 s, input split 12 ml/min, output split closed. With these split settings maximum transfer of sample onto the column was achieved. The cold trap was filled with 15 mg of Tenax. In order to exclude contamination of the cold trap by exudations from the septum of the ATD injector, the septum port was replaced with a stainless-steel screw-cap. With this measure, an appreciable decrease in the noise of blank tube runs and in the detection limits was achieved.

The operating parameters of the GC 8500 were as follows: helium, 150 kPa (4 ml/min at 35°C); column, WCOT (25 m × 0.32 mm I.D.), 1 μm PVMS (Perkin-Elmer); oven, 35°C (4.5 min), increased at 30°C/min to 65°C (2 min) and to 110°C (3 min); flame ionization detector, 250°C, with hydrogen at 85 kPa and air at 155 kPa; flame photometric detector, 300°C, with hydrogen at 135 kPa and air at 145 kPa.

Calibration of the gas chromatograph with flame photometric detection (FPD) and the ATD–GC system with flame ionization detection (FID)

Stock solutions of the test compounds S-mustard, DFP and soman were made up by weight in isooctane. From these, dilutions containing 0.05–1 μg/ml were prepared, so that with 2-μl injections into the GC (FPD) the relevant concentration range could be covered. The calibration functions were linear in each instance.

Another stock solution, also made up by weight, contained a mixture of all five test compounds in TCFE. From this, six different dilutions were prepared covering the concentration range 10–1000 μg/ml. The sorbent beds of ATD tubes were spiked at the upstream side with 1 μl of the six standard mixtures ($n = 6$). The tubes were then subjected to ATD–GC (FID). By means of second ATD runs, it was ensured that a single thermal desorption step was sufficient to remove the sample completely from the sorbent.

As mentioned above, the ATD injector was switched out of operation, so that GC calibrations via the cold trap and the transfer line were not performed.

Test atmospheres

Test atmospheres of DFP and soman (as a mixture) and S-mustard were prepared by means of a dynamic diffusive vapour generator as described previously[2]. The generator was run with dry air, applying a flow-rate of 100 ml/mn (S.T.P.). Based on the operating parameters, the generator should deliver gas concentrations of 0.23 (S-mustard), 0.2 (DFP) and 0.1 ng/ml (soman). The arrangement allowed the admixture of humidified air [*ca.* 100% relative humidity (R.H.) at 20°C] behind the exit of the generator with a flow-rate of 100 ml/min (S.T.P.). Hence, in the experiments with humidified air, a total flow-rate of 200 ml/min was applied, containing half the concentrations as above and a final humidity, as measured by means of an appropriate sensor, of 48% R.H. (at 20°C).

With the humidified atmosphere a series of control experiments were performed

to check the retention of water vapour on the Tenax bed: 100 ml/min of this atmosphere were conducted through a Tenax tube and the downstream humidity, as measured by a sensor, reached the upstream value of 48% R.H. within 30 s or less.

Sampling and analysis of vapours

The technical arrangement and the procedure for sampling the gas mixtures delivered by the vapour generator has been described in detail in a previous paper[2].

For determining the gas concentration, a portion of 80 ml/min was sucked from the main gas stream through two small bubblers, arranged in series in an ice-bath; they were filled by weight with 3 ml of isooctane (density 0.69 g/cm^3). After the sampling period, their actual contents in isooctane (plus analyte) were determined by weight, followed by GC (FPD) analysis and the agent concentration was calculated on this basis. Sampling in isooctane was carried out only from dry atmospheres; sampling times of 80–100 min were applied, so that amounts of 1–3 μg of the agents should be trapped.

The sampling on Tenax was done by sucking 50 ml/min from the main stream through two tubes coupled in series. For analysis, the tubes were subjected to ATD–GC (FID). Samples were taken from both dry (50 ml/min) and humidified (100 ml/min) atmospheres, applying sampling times of 20–40 min, so that 100–450 ng of the agents should be trapped. The loaded ATD tubes were divided into two series: series 1 was subsequently subjected to ATD–GC analysis; the tubes of series 2 were closed with the usual aluminium caps (with integral Viton O-ring seals), stored at ambient temperature and pressure in an empty desiccator and analysed after different storage times.

RESULTS AND DISCUSSION

The ATD–GC (FID) analysis of the spiked Tenax tubes yielded a satisfactory separation of the five components (Fig. 1).

The detection limits were calculated to be three times the respective noise levels of the baseline, which was obtained by ATD–GC (FID) of TCFE-spiked tubes ($n = 6$); there was no noticeable difference between TCFE-spiked and blank tubes. Representative chromatograms are given in Fig. 1. After subtracting the respective noise levels from the individual peak areas, linear calibration functions were obtained in each instance. The respective correlation coefficients resulting from linear regression are given together with the retention times and detection limits in Table I.

The results obtained by sampling the standard atmospheres in isooctane followed by GC analysis, and on Tenax with subsequent ATD–GC, are given in Table II. The contents in the second bubblers were $\leqslant 10\%$ of the total; in the "back-up" tubes none of the analytes could be detected.

The agreement of the results from the two methods substantiates the reliability of calibrating with spiked tubes (at least for the three compounds concerned) and sampling these agents on Tenax. The concentration values found with the humidified atmospheres are, as expected, 50% of those obtained from dry air sampling. With regard to DFP and soman, there is a discrepancy between the precalculated and the measured concentrations. The probable reasons for these deviations from the theoretical values have been discussed elsewhere[2].

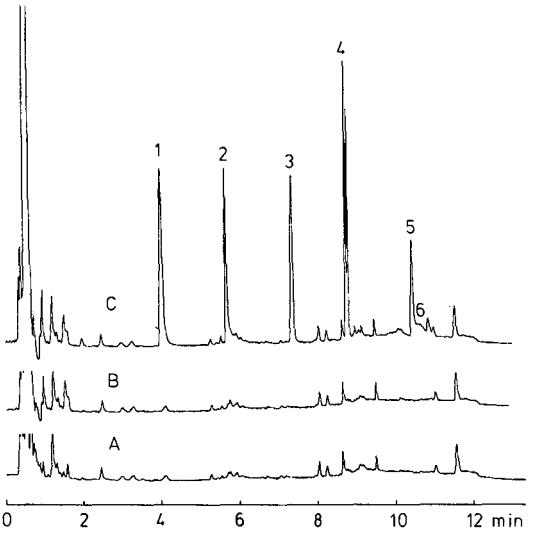

Fig. 1. Chromatograms obtained by ATD–GC with FID (sensitivity, "high"; LCI 100, 10 V, attenuation "2") of Tenax tubes. (A) Blank; (B) spiked with 1 μl of TCFE; (C) spiked with (1) 41.0 ng of sarin, (2) 47.9 ng of DMMP, (3) 35.2 ng of DFP, (4) 34.5 ng of soman (doublet on account of stereoisomers) and (5) 53.7 ng of S-mustard in 1 μl TCFE; an impurity in the DFP batch appeared at 10.8 min (6).

The influence of storage on the loaded Tenax tubes is illustrated by the data in Table III. For calculating the percentage recoveries, the concentration values in Table I and the individual sampling volumes were used to give the 100% value. The original contents of the tubes were in the range 100–300 ng per agent. Tenax tubes loaded with DFP and soman from a dry atmosphere were not stored. The results show that no obvious decrease in recovery occurred on prolonged storage.

Concerning the influence of moisture on the sampling and analysis procedures, the results indicate that, so far as was measured, the humidity did not impair the sampling efficiency, in the thermal desorption step the water content in the tubes (see

TABLE I

ATD–GC (FID) OF THE TEST COMPOUNDS: CORRELATION COEFFICIENTS OF THE CALIBRATION FUNCTIONS, RETENTION TIMES AND DETECTION LIMITS

Compound	*Correlation coefficient (n = 6)*	*Retention time (min)*	*Detection limit (ng per tube)*
Sarin	0.9997	4.0	10
DMMP	0.995	5.8	10
DFP	0.99990	7.2	5
Soman	0.99990	8.8	5
S-Mustard	0.9998	10.4	20[a]

[a] 5 ng per tube as a single compound.

TABLE II

ANALYSIS OF STANDARD ATMOSPHERES

Compound	*Precalculated*[2] *concentration (μg/l)*	*Concentration after sampling (μg/l)*					
		In isooctane (GC)			*On Tenax (ATD–GC)*		
		Concentration	*S.D.*	*n*	*Concentration*	*S.D.*	*n*
S-Mustard:							
Dry	230	221	7	6	229	6	12
Humidified	115				117	5	11
DFP:							
Dry	200	150	11	4	166	8	4
Humidified	100				85	7	4
Soman:							
Dry	100	74	8	4	86	7	4
Humidified	50				42	3	4

TABLE III

ATD–GC RECOVERY OF S-MUSTARD (I), DFP (II) AND SOMAN (III) FROM TENAX AFTER TRAPPING FROM DRY AND HUMIDIFIED ATMOSPHERES AND PROLONGED STORAGE

Storage time (h)[a]	*Recovery (%) after trapping from*			
	Dry atmosphere:	*Humidified atmosphere*		
	I[b]	*I*	*II*	*III*
0.5	94.4	109.7		
	97.4	109.4		
	104.3	94.0		
1.5			75	103
2.3			99	104
23			99	98
26	97.4	99.1		
	105.6	103.4		
96	99.6	99.7		
	95.7	100.9		
221			102	92
308	97.8	103.4		
		105.1		
370			104	98
			97	94
860	106.1	100.0		
1465	80.5	99.1		
Average	97.9	102.1	96	98
S.D.	7.4	4.7	11	5

[a] Excluding analysis time.

[b] With II and III, no samples were stored.

below) did not cause any reduction in the recovery and there was no loss of analyte in the tubes on storage for up to 2 months.

The small influence, if any, of water on the sampling efficiency of Tenax has already been reported by other workers and has been ascribed to the hydrophobic properties of this polymer[3,4]. The lack of effect on the recovery could be due to the purge step in the ATD operation, by which both air and water vapour are removed from the cold tube before the thermal desorption begins.

The stability on storage of samples taken from the humidified atmosphere was unexpected, however. The hydrolytic half-lifes of these agents in aqueous solution at 20°C are[5] 16 min (S-mustard), 61 h (DFP) and 23 h (soman). Without any water adsorption taken into account, the tubes still contained in their free volume the atmospheric moisture of 48% R.H.; with a sorbent weight of 175 mg, its specific density of 1.2 g/cm^3 (ref. 6) and geometric data, this free volume is calculated to be 1.53 cm^3, corresponding to a water content of 12.7 μg per tube, which is, *e.g.*, 40 times more than the content in S-mustard.

Obviously the state of sorption of these compounds prevents the access of (and/or reaction with) water molecules. It seems reasonble to assume that absorption is the reason for this protective effect.

REFERENCES

1 L. K. Beach and S. Sass, *Anal. Chem.*, 32 (1961) 901.
2 K. Schoene and J. Steinhanses, *Fresenius' Z. Anal. Chem.*, 335 (1989) 557.
3 E. Pellizzari, J. E. Bunch, R. F. Berkley and J. McRae, *Anal. Lett.*, 9 (1976) 45.
4 R. H. Brown and C. J. Purnell, *J. Chromatogr.*, 178 (1979) 79.
5 S. Franke, *Militärchemie*, Vol. 2, Deutscher Militärverlag, Berlin, 2nd ed., 1976.
6 K. Schoene, J. Steinhanses and A. König, *J. Chromatogr.*, 455 (1988) 67.

Journal of Chromatography, 514 (1990) 279–286
Elsevier Science Publishers B.V., Amsterdam

CHROM. 22 505

Sorption isotherms of organic vapours on Tenax

K. SCHOENE*, J. STEINHANSES and A. KÖNIG
Fraunhofer-Institut für Umweltchemie und Ökotoxikologie, D-5948 Schmallenberg (F.R.G.)
(First received December 18th, 1989; revised manuscript received April 13th, 1990)

ABSTRACT

Sorption isotherms of *o*-xylene, *n*-octane and tetrachloroethene on Tenax were determined at different temperatures, applying vapour concentrations in the range 10–10 000 ppm. In the range up to 120 ppm the isotherms were derived from the results of breakthrough experiments; for the higher concentrations a headspace gas chromatographic method was applied. At lower gas concentrations, corresponding to bed loads of *ca.* 100 μmol/g Tenax, the sorption follows the Freundlich equation, whereas in the higher ppm range the isotherms become linear. For the Freundlich part of the isotherms, the isosteric heats of sorption were calculated to be in the range 40–> 100 kJ/mol.

INTRODUCTION

The porous polymer Tenax [poly(*p*-2,6-diphenylphenylene oxide)], originally developed for gas chromatographic purposes[1], has proved to be an efficient trapping material for organic vapours. Additionally, it allows most of the substances collected to be desorbed thermally, which facilitates the analytical procedure appreciably[2]. As a consequence, Tenax became one of the most promising sorbents for sampling gaseous pollutants.

On account of its growing practical importance, it seemed of interest to obtain more information about the sorption characteristics of Tenax. In the lower ppm range, the sorption isotherms have been described by both the Freundlich[3] and the Langmuir[4] equations. At higher concentrations, the Tenax isotherms were found to become linear[5].

The investigations described here were undertaken to re-examine these earlier findings and the sorption isotherms of *o*-xylene, *n*-octane and tetrachloroethene on Tenax TA were determined at different temperatures in the concentration range 10–10 000 ppm. The results confirmed the biphasic shape of the Tenax isotherms with a Freundlich-type section at lower and a linear course at higher vapour concentrations.

0021-9673/90/$03.50

EXPERIMENTAL

Tenax TA (20–35 mesh) was purchased from Alltech (Unterhaching, F.R.G.); the characteristic data were (according to the supplier) specific surface area 35 m^2/g, pore volume 2.4 cm^3/g and average pore radius 200 nm. *o*-Xylene ("99+%"), *n*-octane ("99+%") and tetrachloroethene ("99.9%") were purchased from Aldrich (Steinheim/Buch, F.R.G.).

For determining the sorption isotherms in the concentration range 10–120 ppm, a continuous flow of the sample vapour was conducted through a bed of 220 mg of Tenax (bed length 5 cm) in a stainless-steel tube (8.9 cm × 0.49 cm I.D.) housed in a thermostated cabinet (Heraeus-Vötsch, ±0.5°C). At the downstream side, the breakthrough concentrations were measured at time intervals of 3 min by use of a process gas chromatograph. Plotting the measured concentrations against time yielded the breakthrough curve, from which the equilibrium load α, *i.e.*, the capacity of the bed, was calculated. Varying the exposure concentration c led to correspondingly different equilibrium loads α. By plotting α *vs.* c, the sorption isotherm was obtained. Measurements were carried out at 5, 20 and 40.5°C. The procedural details concerning vapour generation, calibrations, controls and evaluation were given in a previous paper[6].

The sorption isotherms at higher vapour concentrations (200–10 000 ppm) were determined by headspace gas chromatography (HSGC). Known amounts of Tenax and the liquid test substance were introduced into an HSGC vial in such a way that the liquid did not touch the sorbent. After closure with a septum, the vessel was stored at the test temperature until the sorption equilibrium (via the gas phase) was established. The equilibrium gas concentration c was then measured by HSGC as usual. The equilibrium load α on the sorbent was calculated as the difference between the amount originally introduced and the amount found in the gas phase. When applying different amounts of test substance (and keeping that of the sorbent constant), correspondingly different results for c and α were obtained. Plotting α against c yielded the sorption isotherm. The details of the experimental and evaluation procedure have been described previously[5]. With the HSGC system used (Perkin-Elmer HS 100), the lowest applicable test temperature is about 40°C. Therefore, sorption measurements were performed at 40.5, 50.1 and 60.5°C.

RESULTS

The complete sorption isotherms obtained at 40.5°C are given in Fig. 1. The curved sections up to 113 ppm represent the results derived from the breakthrough curves and those for the upper range from the HSGC measurements. The shape as shown in Fig. 1 is representative also of the isotherms obtained at the other temperatures; in the range measured, at the higher concentrations no deviation from linearity was observed in any instance.

On account of the biphasic character, in the following the two parts of the isotherm are treated separately and denoted as the "linear section" and the "curved section".

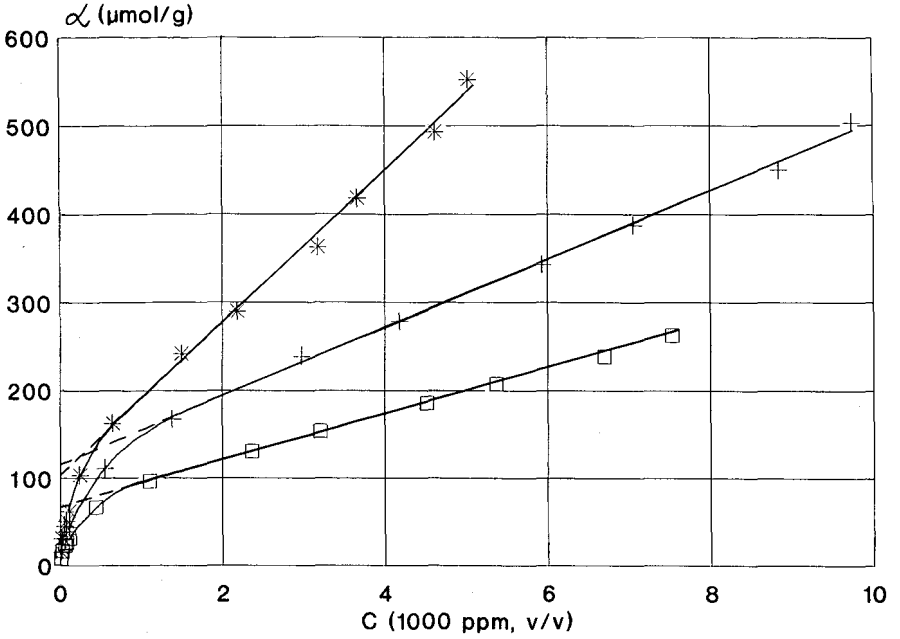

Fig. 1. Sorption isotherms of *o*-xylene (∗), *n*-octane (□) and tetrachloroethene (+) on Tenax at 40.5°C. The straight lines are the result of linear regression according to eqn. 1.

Linear section

Except for the one or two lowest values, the sorption data were subjected to linear regresssion according to

$$\alpha = Sc + \alpha_0 \tag{1}$$

with c in ppm, α in mol/g Tenax and α_0 (mol/g) as the intercept with the ordinate, as shown in Fig. 1. The regression parameters are given in Table I. The temperature functions of S and α_0 follow the equations

$$\log S = A(1/T) + B \tag{2}$$

$$\log \alpha_0 = A'(1/T) + B' \tag{3}$$

The respective data are summarized in Table II. By means of eqns. 2 and 3, the parameters S and α_0 at 20°C, as given in Table I, were calculated.

Curved section

The sorption isotherms obtained with the lower vapour concentrations up to 113 ppm are shown in Fig. 2. The straight lines were drawn on the basis of linear regression according to the Freundlich equation:

$$\log \alpha = p \log c + q \tag{4}$$

TABLE I

LINEAR SECTION: RANGE AND REGRESSION PARAMETERS ACCORDING TO EQN. 1

Compound	*T (K)*	*Range of α (mol/g × 10⁶)*	*S [mol/(g · ppm)]*	*a_0 (mol/g × 10⁶)*	*r*	*n*
o-Xylene	313.65	160–550	8.596	104.5	0.997	7
	323.25	150–480	5.559	87.0	0.9998	7
	333.65	90–320	3.943	62.1	0.9994	6
	293.15[a]		20.98	197		
n-Octane	313.65	100–260	2.550	69.7	0.9997	7
	323.25	80–210	1.880	52.1	0.9997	7
	333.65	50–170	1.826	37.7	0.9992	7
	293.15[a]		3.59	143		
Tetrachloroethene	313.65	170–500	3.872	116.3	0.9990	7
	323.25	140–430	2.875	90.8	0.998	7
	333.65	90–340	1.796	71.9	0.9990	8
	293.15[a]		9.76	203		

[a] Extrapolated using eqn. 2 (S) and eqn. 3 (α_0).

with c in ppm and α in mol/g Tenax. The results are summarized in Table III. Evaluation according to the Langmuir equation led to unsatisfactory results, similar to those reported recently[4].

Heats of sorption

For calculating the heats of sorption (the differential molar enthalpy of sorption[7]), the sorption isotherms in eqn. 4 were converted into the respective sorption isosteres:

$$\log c = (1/p) \log \alpha - q/p \tag{5}$$

For four arbitrarily chosen α values (10, 30, 50 and 70 μmol/g), the corresponding c values were calculated at each of the three test temperatures. From these sets of data, the temperature functions of c were evaluated according to

$$\log c = f(1/T) + g \tag{6}$$

TABLE II

LINEAR SECTION: TEMPERATURE FUNCTIONS OF S AND α_0 ACCORDING TO EQNS. 2 AND 3

Parameter	*o-Xylene*	*n-Octane*	*Tetrachloroethene*
A	1770	757	1747
B	−12.72	−10.03	−12.97
r (n = 3)	0.997	0.90	0.9998
A'	1184	1397	1093
B'	−7.74	−8.61	−7.42
r (n = 3)	0.990	0.9997	0.9998

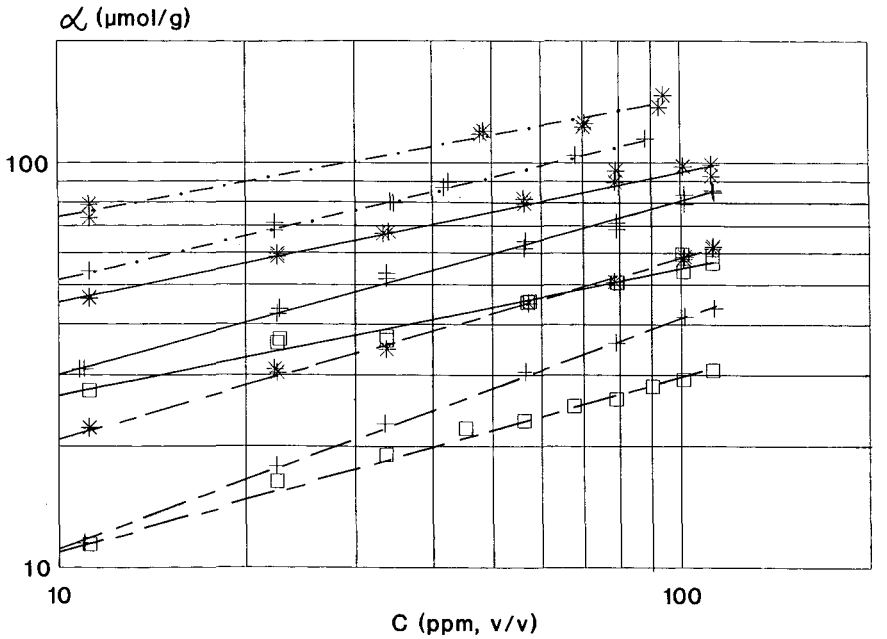

Fig. 2. Sorption isotherms of *o*-xylene (*), *n*-octane (□) and tetrachloroethene (+) on Tenax according to the Freundlich equation (eqn. 4) at 5°C (– · –), 20°C (——) and 40.5°C (– – –).

The correlation coefficients r resulting for *o*-xylene and tetrachloroethene were $\geqslant 0.996$. For technical reasons, the measurements with *n*-octane could be done at two temperatures only, so that the respective values are based tentatively on two point-calculations.

The heats of sorption, Q_s, were calculated from the slopes f by use of the equation

$$Q_s \text{ (kJ/mol)} = 19.147\,[T_1T_2/(T_1 - T_2)] \log (c_1/c_2) \quad (7)$$

TABLE III

CURVED SECTION: REGRESSION PARAMETERS OF THE FREUNDLICH EQUATON (EQN. 4)

Compound	*T (K)*	*p*	*q*	*r*	*n*
o-Xylene	278.15	0.2854	−4.417	0.990	8
	293.15	0.3357	−4.684	0.997	14
	313.65	0.4497	−5.134	0.999	12
n-Octane	293.15	0.3181	−4.895	0.990	14
	313.65	0.4390	−5.404	0.997	11
Tetrachloroethene	278.15	0.3656	−4.652	0.998	9
	293.15	0.4218	−4.940	0.997	14
	313.65	0.5721	−5.526	0.9994	7

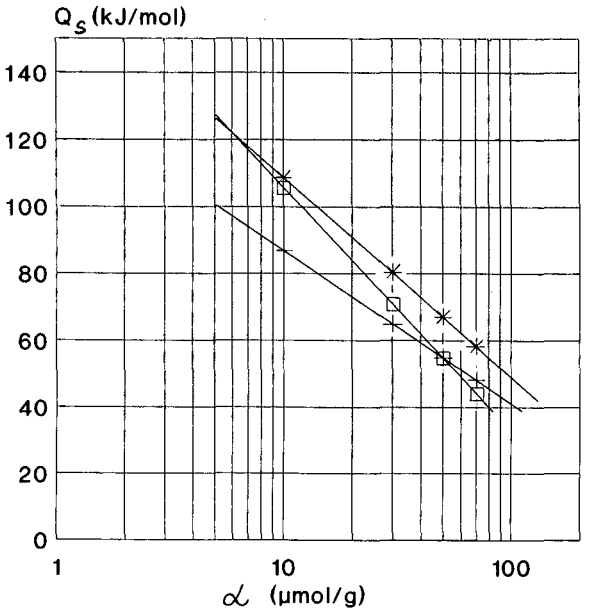

Fig. 3. Heats of sorption, Q_s, on Tenax in the range of the Freundlich isotherm for *o*-xylene (∗), *n*-octane (□) and tetrachloroethene (+) as a function of the bed load α.

The resulting Q_s was found to be related to the bed load α according to

$$Q_s = -F \log \alpha - G \tag{8}$$

as shown in Fig. 3. The regression parameters are given in Table IV.

DISCUSSION

The previously reported biphasic character of the sorption isotherm of tetrachloroethene on Tenax[5] was verified by breakthrough measurements in the lower concentration range. Biphasic isotherms were also found with *o*-xylene and *n*-octane, which suggests that this shape is typical of the sorption behaviour of Tenax.

With regard to the analytical application of Tenax, the relevant part of the isotherm is that following the Freundlich equation (eqn. 4)[6]. The range of validity of

TABLE IV

CURVED SECTION: REGRESSION PARAMETERS OF EQN. 8 (r = 1.00)

Compound	*F*	*G*
o-Xylene	59.5	189
n-Octane	72.7	258
Tetrachloroethene	45.7	142

TABLE V

UPPER LIMITS OF THE FREUNDLICH-TYPE SORPTION AND LINEAR REGRESSION DATA OF THE EQUATION LOG $c_0 = v(1/T) + w$

Compound	*T (K)*	α_0 *(μmol/g)*	c_0 *(ppm)*	v	w	r
o-Xylene	278.15	329[a]	1876	1730	−2.963	0.998
	293.15	197	822			
	313.65	105	367			
n-Octane	293.15	143	2004	2066	−3.744	
	313.65	70	694			
Tetrachloroethene	278.15	323[a]	1500	963	−3.000	0.993
	293.15	203	907			
	313.65	116	605			

[a] Extrapolated by means of eqn. 3.

this equation is smaller than the curved part of the isotherm (this becomes obvious from a log α *vs.* log c plot up to the regression line). Hence, it seems reasonable to conclude that the α_0 values (Table I) indicate the upper end-points of the Freundlich-type sorption. Introducing the α_0 values into eqn. 5 yields the corresponding concentration limits c_0. The results in Table V show that, as for α_0, the c_0 values decrease with increasing temperature; the plots of log c_0 *vs.* $1/T$ appear to be linear.

Interestingly, there is a clear correlation ($r \geqslant 0.998$) between the α_0 values and the respective molar volumes, V_M (cm^3/mol), according to

$$\log \alpha_0 = n \log (1/V_M) + m \tag{9}$$

The V_M values were calculated using the temperature functions of the specific densities[8].

Multiplying α_0 by V_M yields the volume occupied by the quantity α_0 per gram of Tenax. At 20°C these "specific volumes", V_s (cm^3/g), are 0.024 (*o*-xylene), 0.023 (*n*-octane) and 0.021 (tetrachloroethene), *i.e.*, 1% of the total pore volume.

Calculation of the specific surface areas, A_s (m^2/g), according to $A_s = \alpha_0 N(V_M/N)^{2/3}$ (N = Avogadro's number) at 20°C gave 40.5 (*o*-xylene), 35.6 (*n*-octane) and 37.1 (tetrachloroethene), which are in satisfactory agreement with the values of 35 m^2/g given by the supplier. It should be noted, however, that with increasing temperature the A_s values decrease, *e.g.*, down to 9–13 m^2/g at 60.5°C.

The heats of sorption, Q_s, decrease with increasing load, α. The regression lines (according to eqn. 8) in Fig. 3 were extrapolated to the respective heats of condensation, Q_c (kJ/mol)[9] of 41.9 (*o*-xylene), 38.6 (*n*-octane) and 38.7 (tetrachloroethene). Hence, the differential heat evolved in the Freundlich-type sorption exceeds the heat of condensation up to loads of *ca.* 100 μmol/g Tenax.

In the literature, Tenax is generally referred to as an adsorbent. Following this view, and taking into account the structural characteristics and the curve shape, the isotherms should be considered as type IV isotherms in the Brunauer classification[7],

the Freundlich-type part indicating adsorption at the pore walls in the form of monomolecular layers and the linear part representing the formation of multilayers.

There are, however, several findings, which do not satisfactorily fit into this concept. The pronounced temperature dependence of the heats of sorption on the load α is not consistent with that theory[7]. After sampling vapours of hydrolysable compounds on Tenax from a humid atmosphere (50% relative humidity), the sampling tubes could be stored (up to at least 2 months) and subsequently thermally desorbed without loss of analyte, despite the relatively high water content in the tubes[10]. Obviously the state of sorption of the organic compounds prevented the access of (and/or the reaction with) water molecules, which seems hardly to be compatible with the concept of wall adsorption in open pores. Finally, Tenax is reported to be soluble in, for example, lower chlorinated hydrocarbons, tetrahydrofuran, carbon disulphide, dioxane, pyridine and cyclohexanone[1].

Hence it seems reasonable to assume that after the adsorption step, absorption will also occur to a certain extent and, consequently, to interpret the linear section in terms of Henry's law with the magnitude S as the solute–gas equilibrium constant. Clarification of this question, however, needs further investigation.

REFERENCES

1 R. van Wijk, *J. Chromatogr. Sci.*, 8 (1970) 418.
2 R. H. Brown and C. J. Purnell, *J. Chromatogr.*, 178 (1979) 79.
3 N. van den Hoed and M. T. H. Halmans, *Am. Ind. Hyg. Assoc. J.*, 48 (1987) 364.
4 J. Vejrosta, M. Mikesova, A. Ansorgova and J. Drozd, *J. Chromatogr.*, 447 (1988) 170.
5 K. Schoene, J. Steinhanses and A. König, *J. Chromatogr.*, 455 (1988) 67.
6 K. Schoene, J. Steinhanses and A. König, *Fresenius' Z. Anal. Chem.*, 336 (1990) 114.
7 S. J. Gregg and K. S. W. Sing, *Adsorption, Surface Area and Porosity*, Academic Press, London, 2nd ed., 1982.
8 *Beilsteins Handbuch der Organischen Chemie*, Springer, Berlin, Göttingen, Heidelberg, 1958, E III: 1, 457 (*n*-octane), 664 (tetrachloroethene), 5, 808 (*o*-xylene).
9 R. C. Weast (Editor), *CRC Handbook of Chemistry and Physics*, CRC Press, Boca Raton, FL, 67th ed., 1986/1987, p. C-673.
10 J. Steinhanses and K. Schoene, *J. Chromatogr.*, 514 (1990) 273.

Journal of Chromatography, 514 (1990) 287–292
Elsevier Science Publishers B.V., Amsterdam

CHROM. 22 511

Application of pyrolysis–high-resolution gas chromatography–pattern recognition to the identification of the Chinese traditional medicine Mai Dong

XINGCHUN FANG
Department of Pharmaceutical Analysis, China Pharmaceutical University, Nanjing 210009 (China)
BOYANG YU
Department of Pharmacognosy, China Pharmaceutical University, Nanjing 210009 (China)
and
BINGREN XIANG and DENGKUI AN*
Department of Pharmaceutical Analysis, China Pharmaceutical University, Nanjing 210009 (China)
(First received January 23rd, 1990; revised manuscript received April 12th, 1990)

ABSTRACT

Pyrolysis–high-resolution gas chromatography–pattern recognition (Py–HRGC–PaRe) was used to develop a potential technique for identifying the Chinese traditional medicine Mai Dong. About 1 mg of crude drug powder was pyrolysed in a furnace pyrolyser and the products were directly carried into a gas chromatograph with an FSOT capillary column (30 m × 0.265 mm I.D.) coated with DB-1701 (d_f 0.25 μm). The Py–HRGC data were analysed by non-linear mapping PaRe. The results showed that Mai Dong samples could be classified into two categories: *Ophiopogon japonicus* (L.f.) Ker-Gawl (included in the Chinese Pharmacopoeia) and *Liriope spicata*.

INTRODUCTION

Mai Dong is a Chinese traditional drug widely used for the treatment of dipsosis, dry throat, tussiculation bloody sputum, palpitations and anxiety. Mai Dong as specified in the Chinese Pharmacopoeia must be the tuberous root of the plant *Ophiopogon japonicus* (L.f.) Ker-Gawl, but a recent survey of the drug revealed that the general name Mai Dong could involve the tuberous roots of several plants of different origins. They belong mainly to the genuses *Ophiopogon* and *Liriope*. Other varieties of crude drug may also be sold as Mai Dong. These unofficial products make up around 40% of Mai Dong samples purchased from the markets, hence the identification of Mai Dong samples sold in the markets is very important. Usually, the botanical source of a Mai Dong sample can be identified morphologically by a qualified, experienced pharmacognosist, but this process is complicated and time consuming. The accuracy of the morphology may also be affected by environmental factors.

0021-9673/90/$03.50

Analytical pyrolysis–gas chromatography (Py–GC) is a rapid and reliable method for distinguishing biological organisms, polymers, etc.[1–4]. Py–GC is a degradative technique in which the molecular fabric of a plant is thermally fragmented in the absence of oxygen. The resulting pyrolysate components are then subjected to GC. Pyrograms of crude drug powders are very complex and overall patterns of variation are not easily discernible by visual inspection. Therefore, a multivariate pattern recognition (PaRe) method has been utilized to analyse the pyrograms and elucidate the chemical features (pyrogram peaks) that could be used to discriminate plants[5]. The use of Py–high-resolution (HR) GC–PaRe as a powerful technique for the identification of Chinese drugs has also been demonstrated in our laboratory[6,7]. In this work, non-linear mapping[8] was applied to data obtained from Py–HRGC profiles of Mai Dong samples purchased from the market in order to distinguish Mai Dong and its substitutes.

EXPERIMENTAL

Sample preparation

Seventeen Mai Dong samples purchased from the market were ground into a fine powder (40 mesh). The varieties present were identified to be *O. japonicus* and *L. spicata* (see Table I).

Pyrolysis–high-resolution gas chromatography

A quartz tube was heated at 500°C using a Shimadzu Py-2A furnace pyrolyser. About 1 mg of crude drug powder was placed on the platinum boat, then the sample rod with the platinum boat was introduced into the quartz tube connected directly in the inlet of the chromatograph and remained there for 1 min. The resulting pyrolysate products were separated on a J&W Scientific DB-1701 fused-silica capillary column (30 m × 0.265 mm I.D.; d_f 0.25 μm) using a Shimadzu GC-9A gas chromatograph equipped with a flame ionization detector. High-purity nitrogen (99.999%) was used as the carrier gas and peak areas were obtained from a Shimadzu CR-3A Chromatopak integrator. The injector and detector temperature was maintained at 250°C. The gas chromatograph oven was maintained at 50°C for 3 min, then heated

TABLE I

BOTANICAL SOURCES AND LOCATIONS OF MAI DONG SAMPLES STUDIED

Sample No.	*Botanical source*	*Location*[a]
1–10	*O. japonicus*	Zhejiang[b], Yunan, Jiangxi, Sichuan HubeiXianning, Guizhou, Hunan
11–17	*L. spicata*	Hubei[c], Fujian, Henan, Guangxi[d], Shanxi

[a] Location of collection (market).
[b] Four batches of samples.
[c] *L. spicata* (Thunb.) Lour. var. *prolifera* Y. T. Ma, called Hubei Mai Dong.
[d] Three batches of samples.

from 50 to 150°C at 5°C/min and from 150 to 200°C at 3°C/min. A typical pyrolysis gas chromatogram of the sample is shown in Fig. 1.

Numerical method

The resulting pyrograms (retention times *vs.* percentage of peak areas) are represented by data vectors $X_l(x_{l1}, x_{l2}, x_{l3}, \ldots, x_{lj}, \ldots, x_{lm})$, where component x_{lj} is the percentage area of the jth peak in the lth sample. The feature selction is important for pattern recognition because more features give rise to difficulties in the classification between the plants. If we have two classes, class r and class k, the feature selection is as follows[9]:

$$W_j = \frac{|\bar{x}_j^k - \bar{x}_j^r|}{s_j^{rk}} \tag{1}$$

where W_j is weighing factor, $\bar{x}_j^k$ is the average percentage area of the jth peak in the kth class:

$$\bar{x}_j^k = \frac{1}{N_k} \sum_{i=1}^{N_k} x_{ij} \tag{2}$$

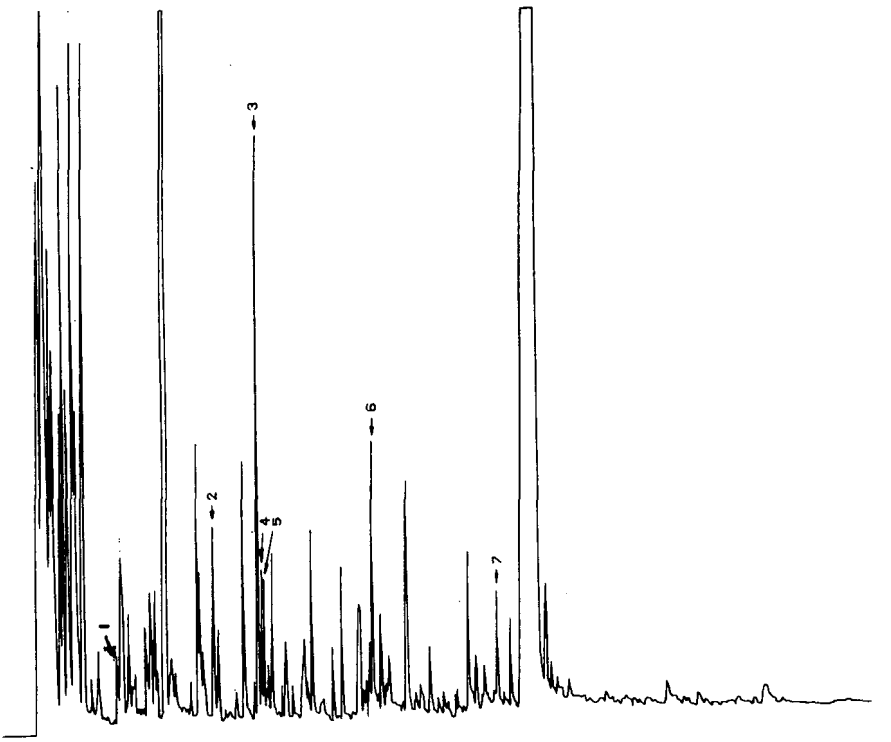

Fig. 1. Typical Py–GC profile of the sample.

N_k is number of sample in class k.

$$s_j^{rk} = \{2(s_j^r)^2 (s_j^k)^2/[(s_j^k)^2 + (s_j^r)^2]\}^{\frac{1}{2}} \tag{3}$$

s_j^r is the standard deviation of percentage area of the jth peak of all samples in class r.

Seventeen samples were divided into classes (see Table I). We selected seven features (peaks) as the original data vector of pattern recognition based on the rule of Max W_j. Each sample data vector was then normalized to sum 100 over the seven peaks.Thus, a 17 × 7 data matrix constituted the empirical material for the non-linear mapping (NLM).

NLM by error minimization according to Sammon[10] is a display method that is commonly used. The method starts by calculating the m variable means $\bar{x}_j (j = 1\text{–}m)$ as

$$\bar{x}_j = \frac{1}{N} \sum_{i=1}^{N} x_{ij} \; (j = 1,2, \ldots, m) \tag{4}$$

where m is the number of variables (peaks) and N is the total number of points (objects). Then the covariance matrix C is generated, each element C_{ij} of which compares variables i and j as

$$C_{ij} = \sum_{l=1}^{N} (x_{li} - \bar{x}_i)(x_{lj} - \bar{x}_j) \tag{5}$$

Next, the eigenvalues λ_j and eigenvectors μ_j for $j = 1\text{–}m$ are calculated by solving

$$C\mu_j = \lambda_j \mu_j \tag{6}$$

The basis vectors μ_1 and μ_2, which correspond to the two largest eigenvalues λ_1 and λ_2, are used as the starting configuration for NLM map. All of the m-space interpoint distances, d_{ij}^*, are calculated as

$$d_{ij}^* = \left[\sum_{k=1}^{m} (x_{ik} - x_{jk})^2 \right]^{\frac{1}{2}} \tag{7}$$

and all of the two-space interpoint distances, d_{ij}, are calculated as

$$d_{ij} = [(y_{i1}^* - y_{j1})^2 + (y_{i2} - y_{j2})^2]^{\frac{1}{2}} \tag{9}$$

where the y values are found by the rotation matrix that diagonalizes C in eqn. 6. The object here is iteratively to change the two coordinates (y_{l1} and y_{l2}) for each point y_l so as to minimize an error function E, defined as

$$E = \frac{1}{\sum_{i<j} d_{ij}^*} \sum_{i<j} \frac{(d_{ij}^* - d_{ij})^2}{d_{ij}^*} \tag{10}$$

The minimization attempts to preserve interpoint distances by finding d_{ij}s that are as close as possible to d_{ij}^*s.

In order to change iteratively the two-space coordinate and minimize E, a gradient method should be used. Sammon[10] suggested the method of steepest descent. As this method is adequately described elsewhere[10], the details will not be given here.

NLM was implemented using an IBM PC/XT microcomputer and the program in True BASIC was written by the authors.

RESULTS AND DISCUSSION

NLM was applied to the 17 × 7 data matrix in Table I. NLM results are given in Fig. 2.

Py–GC can be used to obtain a chemical fingerprint of the herbs. Efforts to use these chromatograms for the classification of different samples in the same family have often been difficult, owing to the characteristic peaks of different varieties in same family. On the other hand, the large apparent variability of repetitive chromatograms was measured on the same type of samples. Of course, part of the variability between repetitive chromatograms measured on the same type of herbs was systematic. This systematic variability could be overcome automatically by means of the normalization of peak areas and pattern recognition. At the same time, pattern recognition techniques can be used to handle the complex chromatograms to give the correct classification of herbs.

In Fig. 2, *O. japonicus* was clearly separated from *L. spicata*. The botanical source of Mai Dong included in the Chinese Pharmacopoeia must be the tuberous root of the plant *O. japonicus* (L.f.) Ker-Gawl. The family of *L. spicata* contains two varieties, *L. spicata* (Thunb.) Lour and *L. spicata* (Thunb.) Lour. var. *prolifera* Y. T. Ma (from Hubei, also called Hubei Mai Dong) which is debated by

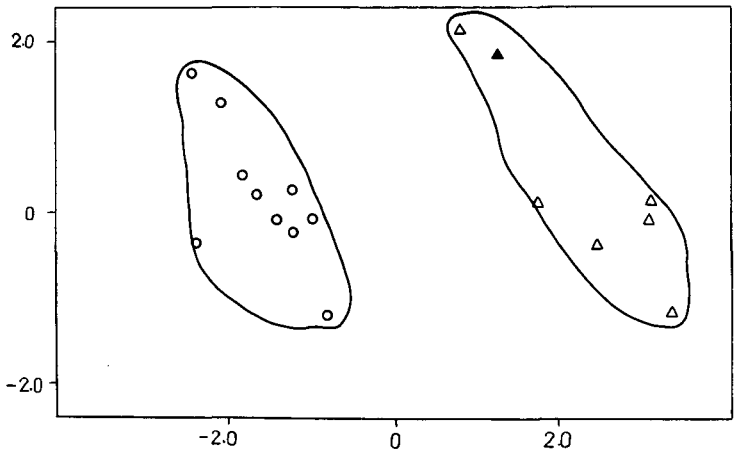

Fig. 2. Classification of Mai Dong samples obtained by NLM. ○ = *O. japonicus* (L.f.) Ker-Gawl; △ = *L. spicata* (Thunb.) Lour.; ▲ = *L. spicata* (Thunb.) Lour. var. *prolifera* Y. T. Ma. Horizontal axis represents y_1, vertical axis represents y_2.

pharmamognosists; some think that Hubei Mai Dong is same as *L. spicata* (Thunb.) Lour. In this paper, we use Py–HRGC–PaRe to attempt a chemical classification of these two type of samples; this method was not able to distinguish between the different varieties in the same family.

The combination of Py–HRGC and NLM (Py–HRGC–PaRe) gave a good classification with the present example of 17 Mai Dong samples chosen to illustrate this potential method. This method also has simplicity, rapidity and reliability. Without any prior chemical treatment, micro-amounts were sufficient to complete the identification, which makes the technique especially valuable for use with expensive or rare herbs. The identification of herbs by pharmacognosists is very important, hence this work must be seen as an illustration of the possibilities of the methodology being developed for the physical and chemical identification of Chinese drugs and not as a final method for a working identification of herbs. However, the application of Py–HRGC–PaRe to the identification of herbs will provide an independent means of classifying these herbs.

REFERENCES

1 W. J. Irwin, *Analytical Pyrolysis: a Comprehensive Guide*, Marcel Dekker, New York, 1982.
2 G. Blomquist, E. Johansson, B. Söderström and S. Wold, *J Chromatogr.*, 173 (1979) 19.
3 E. Kullik, M. Kaljurand and M. Koel, *J. Chromatogr.*, 126 (1976) 249.
4 R. Valcaece and G. G. Smith, *Chemometr. Intell. Lab. Systems*, 6 (1989) 157.
5 B. R. Xiang and D. K. An, *Guowai Yixue Yaoxue Fence*, 10 (1983) 204.
6 X. C. Fang, B. R. Xiang and D. K. An, *Acta Pharm. Sin.*, 25 (1990) in press.
7 X. C. Fang, X. Yin, B. R. Xiang and D. K. An, *J. China Pharm. Univ.*, 21 (1990) 91.
8 D. L. Massart, B. G. M. Vandeginste, S. N. Deming, Y. Michotte and L. Kaufman, *Chemometrics: a Textbook*, Elsevier, Amsterdam, 1988, p. 366.
9 I. Juricskay and G. E. Veress, *Anal. Chim. Acta*, 171 (1985) 61.
10 W. J. Sammon, Jr., *IEEE Trans. Comput.*, C-18 (1969) 401.

Journal of Chromatography, 514 (1990) 293–304
Elsevier Science Publishers B.V., Amsterdam

CHROM. 22 488

Controlled thermal degradation for the identification and quantification of amine N-oxides in urine

BOEL LINDEGÅRD*, LENNART MATHIASSON and JAN ÅKE JÖNSSON
Department of Analytical Chemistry, University of Lund, S-221 00 Lund (Sweden)
and
BENGT ÅKESSON
Department of Occupational and Environmental Medicine, University Hospital, S-221 85 Lund (Sweden)
(First received December 5th, 1989; revised manuscript received April 11th, 1990)

ABSTRACT

Studies of amine N-oxides in urine are important for the evaluation of occupational exposure to amines. These thermolabile compounds are difficult to handle by either gas or liquid chromatography, so a device for controlled thermal degradation has therefore been developed. It consists of a short precolumn with shut-off valves at both ends and an aluminium block for heating, and it was connected to the injection port of a gas chromatograph. After injection of amine N-oxides onto the precolumn and thermal degradation, the degradation products were allowed to enter the analytical column.

Trimethylamine N-oxide (TMAO) and triethylamine N-oxide (TEAO) were investigated. Their thermal degradation patterns could be used for identification and quantification in aqueous solutions and in urine. Linear calibration graphs based on degradation product peaks (trimethylamine and O,N,N-trimethylhydroxylamine from TMAO and diethylamine and triethylamine from TEAO) were obtained for concentrations up to 500 ppm. Detection limits in aqueous solutions were 0.2 ppm (*ca.* 1 ng) for TMAO and 1 ppm for TEAO and the precisions were 6% and 9%, respectively. In urine, similar values were obtained for TEAO. The detection limit for TEAO corresponds to the expected concentration in urine after an 8-h exposure to air containing 0.8 mg/m^3 of triethylamine.

INTRODUCTION

Amine N-oxides are formed in the body as metabolites of tertiary amines from natural sources, such as the enterobacterial metabolism of dietary choline and lecithin[1]. Another source is marine fish which contains N-oxides[2,3].

Occupational exposure to amines is another cause of the formation of amine N-oxides. Amines occur as pollutants in many industrial environments[4], *e.g.*, in polymer production, and various adverse health effects due to this exposure have been

0021-9673/90/$03.50

reported[5,6]. Biological monitoring of industrial pollutants, involving the analysis of urine, blood, etc., is increasingly used to measure individual exposure, in addition to conventional measurements of pollutants in workplace air. For biological monitoring of amine exposure, however, determinations of both the amine N-oxide and the corresponding amine are recommended[7].

The determination of volatile amines both in air and in body fluids can readily be performed using gas chromatography (GC)[8,9]. Amine N-oxides, however, cannot be determined in this way, as they are thermally unstable, non-volatile and very polar. In a recent study[10] the thermal degradation of amine N-oxides in a hot injection port was demonstrated.

Modern liquid chromatography (LC) usually offers good opportunities for the determination of thermolabile compounds in biological samples. However, problems arise when the compounds of interest do not contain functional groups which give a response from the most frequently used LC detectors, *e.g.*, UV, electrochemical and conductimetric detectors. Further, thermolabile substances are not easily identified with LC–mass spectrometric (MS) equipment, as the temperature of the interface is often held relatively high.

With their low UV absorbance, amine N-oxides are difficult to determine with LC at trace levels. For example, a recent LC method with UV detection at 208 and 214 nm gave a detection limit for trimetylamine N-oxide (TMAO) in standard solutions as high as 5 μg[11].

Other direct methods for the determination of amine N-oxides exist, based on IR spectrometry[12], polarography[13] and potentiometry[14]. In all these methods the sensitivity is insufficient for trace analysis and the compound has to be separated from the matrix. Polarograms and cyclic voltammograms obtained at our laboratory for TMAO at pH 1.3, 5.0 and 11.0 showed that high reductive or oxidative voltages (-1.3 and $+1.6$ V *vs.* SCE, respectively) were needed before any reaction occurred. Hence electrochemical LC detectors are expected to give poor selectivity and high background currents.

To avoid the problems mentioned above, amine N-oxides are frequently determined after reduction to the corresponding amines[15–17]. However, in this instance it must be verified that the amines found really emanate from the amine N-oxides.

In this paper we present an alternative method for the identification and quantification of amine N-oxides in urine. It is based on thermal degradation under controlled conditions followed by GC analysis. Additionally, an approach for the simultaneous quantification of volatile tertiary amines and the corresponding amine N-oxides is discussed.

EXPERIMENTAL

Chemicals

Trimethylamine N-oxide (TMAO) dihydrate, trimethylamine (TMA) hydrochloride, ethylamine and dimethylamine (DMA) hydrochloride were obtained from Janssen Chimica (Beerse, Belgium), triethylamine (TEA) from Fluka (Buchs, Switzerland), diethylamine (DEA) from BDH (Poole, U.K.) and triethylamine N-oxide (TEAO) from ICN Pharmaceuticals (Planview, NY, U.S.A.).

Stock solutions (1000 ppm) of amines and amine N-oxides were prepared in 50 m*M* sulphuric acid and 1 m*M* sodium hydroxide solution, respectively. Standard solutions for GC measurements were prepared by dilution with 0.5 *M* sodium hydroxide solution and stored in screw-capped vials sealed with Mininert valves (Alltech, Arlington Heights, IL, U.S.A.).

Equipment

The gas chromatograph (Model 3700; Varian, Walnut Creek, CA, U.S.A.) used for the measurements was equipped with a nitrogen-sensitive detector (TSD; Varian) and connected to a recorder and an integrator (Model 3390A; Hewlett-Packard, Palo Alto, CA, U.S.A.). A thermal decomposition device (see below) was connected to the injection port of the gas chromatograph.

Typical parameter settings were: bias voltage −10 V, bead current 650 scale divisions, detector temperature 200°C, injector temperature 150°C, air flow-rate 170 ml/min and hydrogen flow-rate 3 ml/min. Nitrogen was used as the carrier gas at a flow-rate of 30 ml/min.

A glass column (190 cm × 3 mm I.D.) was used, packed with *ca.* 10 g of 28% Pennwalt 223 with 4% potassium hydroxide on Gas-Chrom R (Alltech)[a]. Further details concerning the chromatographic conditions are given in the figure legends.

A gas chromatograph–mass spectrometer (Model 4021; Finnigan MAT, San José, CA, U.S.A.) was used for the identification of degradation products. The thermal decomposition device was connected to the injection port of the GC–MS system. A glass column of the same type as above was used for the GC stage.

Thermal decomposition device

The thermal decomposition device (Fig. 1) consisted of a precolumn with shut-off valves at both ends. The precolumn was heated by a thermostated aluminium

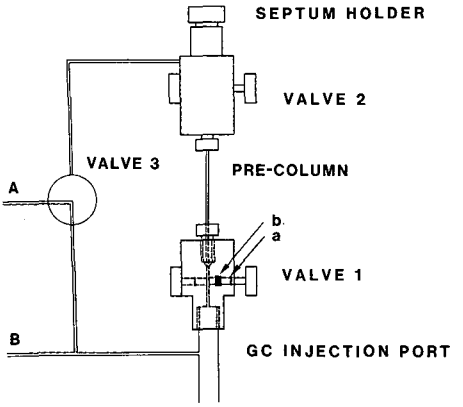

Fig. 1. Thermal degradation apparatus.

[a] Pennwalt 223 is no longer available, but a replacement (Alltech 223) is offered, which is claimed to be identical.

block with a slit, in which the precolumn fitted. The whole device can be easily connected to the injection port of any gas chromatograph with packed columns.

The precolumn was made of steel (7.6 cm × 1 mm I.D.) and packed with *ca.* 24 mg of Chromosorb 103 (Alltech). The rods of the valves were made of PTFE and sealed with O-rings (a) against the surrounding Kel-F blocks. A piece of silicone-rubber tubing (b) ensured complete shut-off in the closed position. In the upper block, a septum holder with a PTFE-lined septum (Microsep F-174; Alltech) was included.

The lower block was directly screwed to the injection port of the gas chromatograph, which was equipped with two independent carrier gas controllers, A and B. One of these (B) was connected to the injector in the normal way. The carrier gas controller A was connected, via a switching valve (3), either to the top of the precolumn or to the injector. In this way, the flow through the precolumn could be adjusted to any value and also switched off while keeping the carrier gas flow-rate through the main column constant. The configuration of the gas streams was the same as described previously[18] in a similar context.

Before packing, the precolumn was rinsed with dilute (15%) ammonia followed by a saturated solution of potassium hydroxide in methanol, which was allowed to dry, leaving a layer of potassium hydroxide on the inner wall of the tubing. The channels in the Kel-F blocks were rinsed with dilute ammonia and water.

Injection procedure for amine N-oxides

Samples (usually 5 μl) were injected through the septum onto the precolumn using a 10-μl Hamilton syringe with a fixed needle. On injection the carrier gas was led through the precolumn with valves 1 and 2 (see Fig. 1) open. After 5 s the lower valve (1) and the upper valve (2) were closed and valve 3 was switched, in that order. The precolumn was then heated by applying the aluminium block for typically 5 min at 175°C for TMAO and 3 min at 150°C for TEAO. The degradation products were transferred to the analytical column by switching the carrier gas valve 3 and opening valves 1 and 2, in that order.

To ensure complete transfer of all degradation products, the heating block was kept surrounding the precolumn for 1 min after the opening of the valves. During the entire chromatographic run the valves were kept open and 20 ml/min of carrier gas were passed through the precolumn and 10 ml/min through the lines leading to the injector in order to prevent backflushing.

Injection procedure for a mixture of amines and amine N-oxides

A simultaneous determination of amines and the corresponding amine N-oxides could be performed by keeping the valves open for 30 s after injection at a precolumn temperature of 80°C, permitting the elution of the amines. At this temperature no degradation of the amine N-oxides investigated here was observed. The precolumn was then closed and the amine N-oxides could be determined after thermal degradation at a higher temperature as described above. If needed to complete the amine chromatogram, the degradation can be started later.

Sample pretreatment

Urine samples were stored in acidic solution (pH ≈ 2.0) before further work-up. After centrifugation, the solutions were, if necessary, filtered through 0.45-μm

Millipore membranes. An equal amount of diisopropyl ether was added, the sample was shaken and the organic layer discarded. The aqueous layer was made alkaline (pH 14) by addition of sodium hydroxide. This solution contains both amines and amine N-oxides and was analysed by direct injection followed by thermal degradation as described.

It is also possible to remove the amines by extracting the alkaline solution with diisopropyl ether or diethyl ether. The aqueous phase containing the amine N-oxides was then injected onto the pre-column and treated as above.

Thin-layer chromatographic (TLC) preparation of TEAO

Urine samples collected during exposure to TEA and normal urine samples, with and without addition of TEA and TEAO, were extracted with portions of diethyl ether, in order to remove TEA. The urine samples were lyophilized, extracted with ethanol to remove inorganic salts, dissolved in 50 ml of 0.1 *M* hydrochloric acid and applied to a column of Dowex 50W-X8 (H^+; 200–400 mesh), as described by Baker and Chaykin[12]. The column was washed with water and 0.1% aqueous ammonia. TEAO was eluted with 20 ml of 1% aqueous ammonia. A 10-μl volume of the eluate was transferred to the precoated TLC plate (silica gel 60 F_{254}; Merck, Darmstadt, F.R.G.) and dried by a hot air stream. The plate was developed and the solvent [butanol–acetic acid–water (60:15:25)] was allowed to reach a level of 1 cm from the upper end of the plate. The plate was air-dried overnight. A second elution was made with methanol–acetic acid–water (80:10:10). The plate was sprayed with 0.2% bromocresol green in ethanol from an air-driven atomizer. After a few seconds, bluish spots were seen on the yellow background with R_F values of 0.55 and 0.63 for TEA and TEAO, respectively.

The different spots containing substance and silica were scraped off, transferred to centrifuge tubes, extracted with 500 μl of 0.5 *M* sodium hydroxide solution , shaken

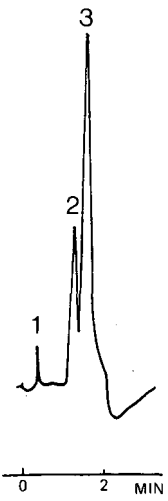

Fig. 2. Chromatogram of 10 ppm of TMAO in 0.5 *M* NaOH, after thermal degradation at 175°C. Attenuation, $8 \cdot 10^{-12}$ a.u.f.s. Temperature programming from 90°C (1 min) at 40°C/min to 155°C. Peaks: 1, sammonia; 2, TMA; 3, Meisenheimer rearrangement product TMHA (see text).

for 40 min and centrifuged. During these steps the test-tubes were capped. Aliquots of the clear solutions were then transferred to capped vials and injected onto the precolumn as above.

RESULTS AND DISCUSSION

Thermal degradation

The thermal degradation of amine N-oxides results in fragmentation patterns typical of a certain compound. The relative concentration of the degradation products varies with the conditions during the procedure.

TMAO. Fig. 2 shows a chromatogram obtained after thermal degradation of TMAO in 0.5 *M* sodium hydroxide solution. Peaks 1 and 2 were identified by their retention times as ammonia and TMA. The identification of peak 2 was confirmed by MS. The formation of the parent amine by deoxygenation has been observed previously[19]. Peak 3 is probably a result of a Meisenheimer[20] rearrangement of the amine N-oxide to O,N,N-trimethylhydroxylamine (TMHA), which, on further heating, may degrade to DMA and formaldehyde according to Hattori[21]. Thus the following reaction scheme can be written:

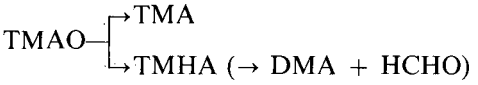

Using MS detection the latter step seems to occur in the hot (*ca.* 250°C) transfer line between the column and the ion source, since peak 3 was identified as DMA, which should have a shorter retention time even than peak 2. This step does not occur to a significant extent in the precolumn as no DMA peak was observed. After peak 3, a negative peak due to the elution of water appears.

Triethylamine N-oxide (TEAO). Fig. 3 shows the fragmentation pattern obtained after thermal degradation of TEAO in 0.5 *M* sodium hydroxide solution. Peaks 1–4 were identified by their retention times as ammonia, ethylamine, DEA and TEA, respectively, and were further confirmed by MS.

The Meisenheimer rearrangement product O,N,N-triethylhydroxylamine (TEHA), formed in a similar way as with TMAO above, seems to decompose to DEA

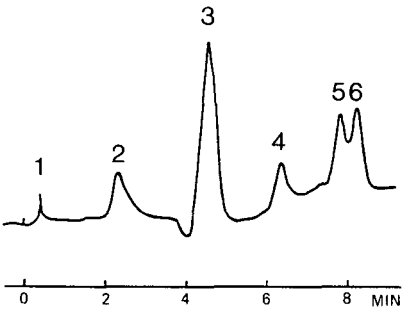

Fig. 3. Chromatogram of 55 ppm of TEAO in 0.5 *M* NaOH after thermal degradation at 150°C. Attenuation, $4 \cdot 10^{-12}$ a.u.f.s. Temperature programming from 75°C (4 min) at 40°C/min to 140°C. Peaks: 1, ammonia; 2, ethylamine; 3, DEA; 4, TEA; 5 and 6, rearrangement products of TEAO.

and acetaldehyde in the precolumn, reflected by a large DEA peak. The acetaldehyde is not present in Fig. 3 as a nitrogen-sensitive detector was used, but at the beginning of the total ion chromatogram obtained by GC–MS a broad peak with $m/z = 44$ is observed.

Peaks 5 and 6 give almost identical mass spectra and obviously result from other rearrangements and degradation reactions in the precolumn. According to the mass spectrum, one of these peaks could be a result of the Cope reaction[22], resulting in the formation of N,N-diethylhydroxylamine (N,N-DEHA) from TEAO after elimination of ethene. The ethene is not observed with the nitrogen-sensitive detector. The other peak could be O,N-diethylhydroxylamine (O,N-DEHA), which should give a very similar mass spectrum and a similar retention time.

Thus, the following reaction scheme is suggested:

$$\text{TEAO} \rightarrow \begin{cases} \text{TEA} \\ \text{TEHA} \rightarrow \text{DEA} + \text{CH}_3\text{CHO} \\ \text{N,N-DEHA} \\ \text{O,N-DEHA} \end{cases}$$

The Cope reaction cannot occur with TMAO owing to the lack of a β-hydrogen.

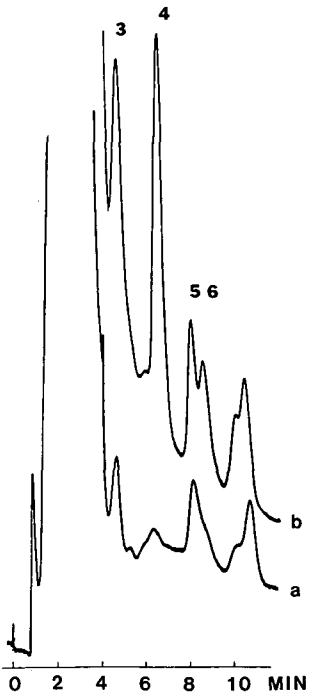

Fig. 4. Chromatograms after thermal degradation at 150°C. Attenuation, $1 \cdot 10^{-11}$ a.u.f.s. (a) Urine; (b) urine spiked with 10 ppm of TEAO. Temperature programme and peak identities as in Fig. 3.

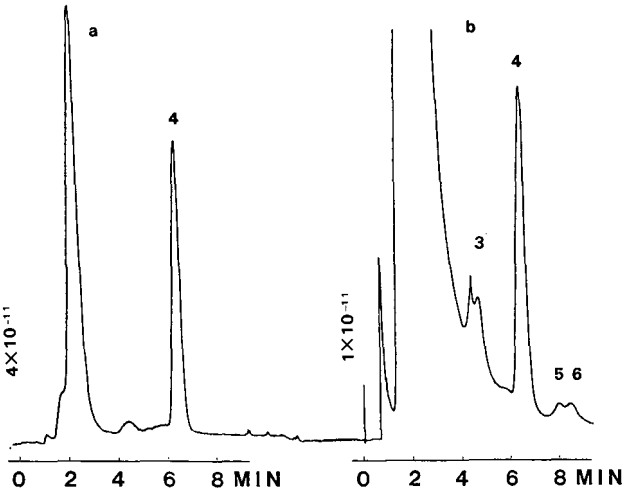

Fig. 5. Chromatograms of urine spiked with 10 ppm of TEAO and 30 ppm of TEA. (a) Direct injection through precolumn at 80°C; attenuation, $4 \cdot 10^{-11}$ a.u.f.s. (b) Chromatogram after heating of precolumn to 150°C; attenuation, $1 \cdot 10^{-11}$ a.u.f.s. Temperature programme and peak identities as in Fig. 3.

Identification of amine N-oxides in urine

These results clearly show that the degradation patterns of TMAO and TEAO can be used as strong evidence for their presence in a sample. It can also be expected that other amine N-oxides can be identified in a similar way.

Urine is an especially interesting matrix in connection with amine N-oxides. The influence of a urine background on the degradation pattern is illustrated in Fig. 4, which shows a direct injection of urine spiked with TEAO, one of the major metabolites after exposure to air containing TEA. It can be seen that the short-chain amines which are abundant in urine do not appreciably influence the degradation pattern. However, in the analysis of urine samples from workers after exposure to TEA in air, the TEA peak will emanate both from TEA and from the degradation of TEAO.

A chromatogram of a mixture of TEAO and TEA in urine is shown in Fig. 5. In this instance the injection procedure for a mixture (described above) was used. The main peak (4) in chromatogram (a) is TEA, which eluted through the precolumn at a temperature of 80°C with the valves open before the thermal degradation was started. Chromatogram (b) shows thermal degradation products of TEAO. The TEA peak is larger here than expected, owing to incomplete elution from the precolumn at 80°C. In spite of this, the first TEA peak is reproducible and could be used for the quantification of TEA.

If only amine N-oxides are of interest, an extraction of an alkalinized sample with *e.g.*, diisopropyl ether minimizes amine interferents. TEA is completely removed from urine samples in this way.

A further clean-up of urine samples by TLC may give a more reliable identification and protects the precolumn. It demands, however, considerably more work and leads to lower quantitative accuracy. Fig. 6 shows a chromatogram obtained after precleaning a urine sample spiked with TEAO. The spot giving the chromato-

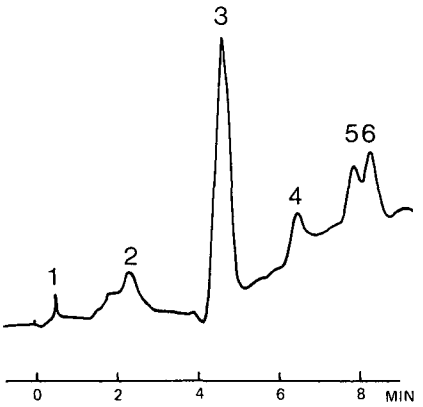

Fig. 6. Chromatogram of urine spiked with 10 ppm of TEAO after precleaning with TLC and thermal degradation. Other conditions and peak identities as in Fig. 3.

gram was identified as TEAO by comparison of the R_F value with that of a standard. The degradation pattern in Fig. 6 is very similar to that in Fig. 3, confirming the identity. Authentic urine samples obtained from exposed workers also gave the same pattern.

For shorter chained amine N-oxides than TEAO, the problem with direct injection of urine increases, as the thermal degradation products will be obscured by the amine background. However, with removal of the amines in an extraction or TLC step and a further optimization of the chromatographic separation, it should be possible to identify even small amounts of the shortest chained amine N-oxide, TMAO, using the peak of TMHA.

Optimization of the system

To perform quantitative determinations of amine N-oxides using the thermal degradation technique, it is necessary to obtain a high and reproducible yield of one or several characteristic degradation products. Several parameters that influence the degradation process were investigated. These include precolumn temperature, heating time and amount of water present in the precolumn. The optimization procedure was performed for both TMAO and TEAO.

TMAO. At a temperature of 125°C significant degradation was observed. However, better conditions from an analytical point of view were obtained using 175°C. At this temperature adsorption of the degradation products in the precolumn was less pronounced, resulting in sharper peaks in the final chromatograms. Furthermore, the degradation was more efficient, giving higher peaks. A temperature of 175°C was chosen, considering the temperature restrictions of the polymeric material (Kel-F) used for the valve blocks.

The thermal degradation procedure was optimized with respect to the amount of water injected and heating time at 175°C. It was found that the most interesting peak, the supposed rearrangement product of TMAO to TMHA (peak 3 in Fig. 2), was largest using a heating time of 5 min and a total injection volume of at least 4 μl.

The injection of large water volumes (up to 17 μl was tested) demands a longer

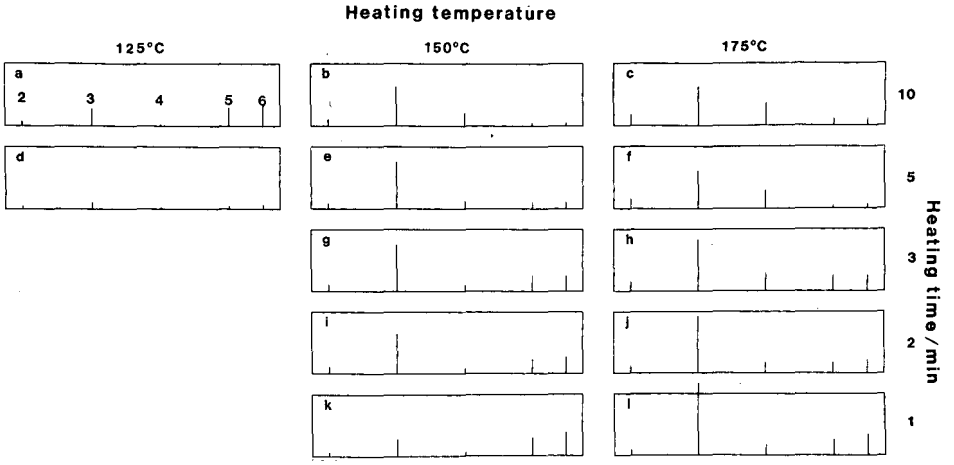

Fig. 7. Schematic chromatograms showing the degradation patterns of TEAO (100 ppm in 0.5 *M* NaOH) after heating in the precolumn for different times and temperatures. Peak identities as in Fig. 3.

heating time. The small inner volume of the precolumn also makes injection of large water volumes difficult. On the other hand, too small water samples are not desirable because of memory effects, *i.e.*, peaks of TMA and TMHA which appear in the following run. This may be due to incomplete degradation of TMAO. As prolongation of the heating time does not decrease the memory effects significantly, access to sufficient amounts of water seems to be necessary for rapid degradation at the chosen temperature.

Taking all these effects into consideration, we chose a sample volume of 5 μl in the subsequent experiments. Under these conditions the memory peaks are of the order of 20% at a concentration of 10 ppm of the TMAO injected and decrease to about 5% in a second blank injection. This must be taken into consideration when quantitative analysis is attempted.

TEAO. With TEAO, more complex influences on the degradation patterns are observed. Fig. 7 shows schematic degradation patterns as a function of temperature and heating time with a 5-μl aqueous sample injection. The conditions for chromatogram (g), heating for 3 min at 150°C, were used in further studies. Chromatogram (h) gives about the same height of the DEA peak, preferably used for quantification of TEAO, but the TEA peak is higher than in chromatogram (g). However, a relative low TEA peak is favourable with respect to possible memory effects in quantitative measurements of TEA in a mixture of TEA and TEAO.

Band broadening

The band broadening process in the precolumn was investigated by direct injection of TMA onto the analytical column. It was found that the peak width was the same, within experimental uncertainty, with and without precolumn. This was also expected as the dead volume in the precolumn (*ca.* 0.05 ml) is small compared with that of the analytical column (*ca.* 9 ml).

Quantification

Alkaline aqueous standard solutions of TMAO and TEAO with concentrations up to 500 ppm gave linear calibration graphs passing close to the origin. For TMA, however, the graph deviated from linearity above 200 ppm. The quantification was based on the peaks from TMA or the supposed rearrangement product THMA in the case of TMAO and on the peaks from either DEA or TEA for TEAO.

The linear correlation coefficients (based on nine points) were 0.996 for TMA, 0.997 for THMA, 0.9997 for DEA and 0.9991 for TEA. In all instances the intercepts on the ordinate did not differ significantly from zero.

The overall precision for TMAO in aqueous solutions was determined using triple injections at a concentration of 10 ppm. Peak heights of TMA and TMHA were measured, giving relative standard deviations of 12% and 6%, respectively. For TEAO at the same concentration, the corresponding figures were 9% based on the peak of DEA and 12% based on the peak of TEA. The detection limits were *ca.* 0.2 ppm (1 ng) for TMAO and *ca.* 1 ppm (5 ng) for TEAO.

The determination of TEAO in a urine matrix is interesting with respect to occupational air exposure. Calibration graphs for TEAO in spiked urine samples were linear in the range 5–100 ppm. The correlation coefficient for DEA was 0.997 and that for TEA was 0.992 and the intercepts on the ordinate did not differ significantly from zero. The precision was 5% for DEA and 8% for TEA (triple injections of urine spiked with 10 ppm of TEAO). The detection limit of TEAO in spiked urine, based on the TEA peak, was *ca.* 1 ppm. Based on the DEA peak it was *ca.* 3 ppm, mostly owing to a higher background.

In urine from workers exposed to TEA, the detection limit for TEAO based on the TEA peak will be higher owing to the contribution from TEA in the urine. Even when TEA is eluted before thermal degradation on the precolumn as in Fig. 5, some memory effects from TEA remain. However, this problem can be eliminated by a preceding basic extraction of TEA from the urine.

With an exposure to 8 mg/m^3 of TEA in air (the Swedish Hygiene Threshold Limit Value from 1990[23]), the concentration in urine of TEAO after 8 h is of the order of 20 ppm[7]. This corresponds to about ten times the detection limit, as the concentration in the sample before the final injection onto the GC column is almost the same as that in the urine.

CONCLUSION

Controlled thermal degradation followed by GC can be used for the identification and quantification of amine N-oxides. As the conditions during the thermal degradation step can easily be varied, *e.g.*, by incorporating different catalysts in the precolumn, it should also be possible to apply this procedure to other thermolabile substances.

ACKNOWLEDGEMENT

This work was supported by a grant from the Swedish Work Environment Fund.

REFERENCES

1 S. H. Zeisel, J. S. Wishnok and J. K. Blusztajn, *J. Pharmacol. Exp. Ther.*, 225 (1983) 320.
2 R. C. Lundstrom and L. D. Racicot, *J. Assoc. Off. Anal. Chem.*, 66 (1983) 1158.
3 M. Al-Waiz, S. C. Mitchell, J. R. Idle and R. L. Smith, *Xenobiotica*, 17 (1987) 551.
4 B. Åkesson, S. Skerfving, B. Ståhlbom and T. Lundh, *Am. J. Ind. Med.*, 16 (1989) 211.
5 B. Åkesson, M. Bengtsson and I. Florén, *Int. Arch. Occup. Environ. Health*, 57 (1986) 297.
6 W. N. Albrecht and R. L. Stephenson, *Scand. J. Work Environ. Health*, 14 (1988) 209.
7 B. Åkesson, *Thesis*, Lund, 1989.
8 G. Audunsson and L. Mathiasson, *J. Chromatogr.*, 315 (1984) 299.
9 G. Audunsson, *Anal. Chem.*, 60 (1988) 1340.
10 F. Devínsky and J. W. Gorrod, *J. Chromatogr.*, 466 (1989) 347.
11 R. B. H. Wills, J. Silalahi and M. Wootton, *J. Liq. Chromatogr.*, 10 (1987) 3183.
12 J. R. Baker and S. Chaykin, *J. Biol. Chem.*, 237 (1962) 1309.
13 H. Hoffmann, *Arch. Pharm.*, 304 (1971) 614.
14 S. Bagnasco, *Anal. Biochem.*, 149 (1985) 572.
15 F. A. Hoppe-Seyler, *Z. Biol.*, 90 (1930) 433.
16 M. Brewester, H. Schedewie and J. A. MacDonald, *Clin. Chem.*, 26 (1980) 1011.
17 B. Åkesson, S. Skerfving and L. Mathiasson, *Br. J. Ind. Med.*, 45 (1988) 262.
18 P. Lövkvist and J. Å. Jönsson, *J. Chromatogr.*, 286 (1984) 279.
19 G. P. Shulman and W. E. Link, *J. Am. Oil Chem. Soc.*, 41 (1964) 329.
20 J. Meisenheimer, *Chem. Ber.*, 52 (1919) 1667.
21 Y. Hattori, *J. Pharm. Soc. Jpn.*, 60 (1940) 24.
22 A. C. Cope, T. T. Foster and P. H. Towle, *J. Am. Chem. Soc.*, 71 (1949) 3929.
23 Swedish National Board of Occupational Safety and Health, *Hygieniska gränsvärden*, Arbetarskyddsstyrelsens författningssamling, Liber, Stockholm, 1990.

Journal of Chromatography, 514 (1990) 305–308
Elsevier Science Publishers B.V.; Amsterdam

CHROM. 22 588

Note

Analytical gas chromatographic separations of diastereomeric *tert.*-butylmethoxyphenylsilyl ethers

CHARLES J. W. BROOKS* and W. JOHN COLE
Chemistry Department, University of Glasgow, Glasgow G12 8QQ (U.K.)
and
ROBERT A. ANDERSON
Department of Forensic Medicine and Science, University of Glasgow, Glasgow G12 8QQ (U.K.)
(Received April 9th, 1990)

Chiral acylating agents are extensively used for converting enantiomeric alcohols into diastereomeric esters suitable for analysis on achiral columns by gas–liquid chromatography (GLC). The analogous use of chiral silylation appears to be unreported, but would be of practical value [especially in GLC combined with mass spectrometry (MS)] if suitable reagents could be developed. Unfortunately, there are two major difficulties: many chiral silyl halides have limited optical stability, and the stereochemical course of nucleophilic displacements of the halide ions is far from uniform[1,2]. Nevertheless, there are reported examples of silyl halides with moderate optical stability and of etherifications that proceed either with complete retention of configuration or with substantial inversion[1–3]. Pending the design of reagents that would afford ethers without loss of stereochemical control, we have examined the extent of separation, by GLC, of diastereomeric *tert.*-butylmethoxyphenylsilyl (TBMPS) ethers of various alcohols. The chiral silane compound *tert.*-butylmethoxyphenylsilyl bromide (TBMPSBr), in racemic form, was introduced by Guindon *et al.*[4] as a versatile protecting reagent for alcohols, yielding derivatives that are stable towards hydrolysis: the TBMPS ethers can, however, be selectively cleaved by tetrabutylammonium fluoride in the presence of other stable silyl ethers such as *tert.*-butyldimethylsilyl ethers. Under appropriate conditions, the formation of TBMPS ethers may be selective for primary hydroxyl groups[2], and this feature has been applied in the reported analysis of the arachidonic acid metabolite, 12,20-diHETE (a 12,20-dihydroxyeicosatetraenoic acid): the derived methyl 12,20-dihydroxyeicosanoate yielded a 12-trimethylsilyl, 20-TBMPS ether suitable for GLC–MS[5].

EXPERIMENTAL

Gas chromatographic separations of four examples of diastereomeric silyl ethers containing chiral silicon have been reported earlier[6].

0021-9673/90/$03.50

TBMPS ethers were prepared from the secondary alcohols (100 μg) by reaction at 80°C, in a sealed vial, for 5 min, with TBMPSBr (Aldrich, Gillingham, Dorset, U.K.) [4 μl: 20–30 molar proportions (mol. prop.)] in a mixture of acetonitrile (20 μl) and dry pyridine (20 μl). The reagents were removed by evaporation under nitrogen, and the residual products extracted with cyclohexane and purified on a column (4 cm × 1 cm I.D.) of silica gel 60 DCC (ICN Biomedicals: Park Scientific, Northampton, U.K.). The TBMPS ether of *trans,trans*-β-decalol was also purified by thin-layer chromatography (TLC) on silica gel 60 F_{254} (Merck; BDH, Poole, U.K.): analytical TLC in the mobile phase chloroform–ethyl acetate (3:1, v/v) gave a single spot at R_F 0.69, and recovery from a preparative TLC plate gave the pure product in good yield as judged by GLC.

GLC was carried out with a Hewlett-Packard 5880 A instrument equipped with CP Sil5 CB and CP Sil19 CB fused-silica capillary columns (25 m × 0.32 mm I.D.; Chrompack, London, U.K.) and dual flame ionisation detectors. Helium carrier-gas and make-up gas flow-rates were 3 and 25 ml/min, respectively. The column temperature programming conditions are presented in Figs. 1 and 2.

GLC–MS was performed with a Hewlett-Packard 5890 gas chromatograph interfaced to a VG 70-250S instrument. The column temperature programming conditions were similar to those presented in Figs. 1 and 2. Mass spectra (40 eV) were acquired using the following conditions: accelerating voltage, 8 kV; filament current, 4 A; trap current, 100 μA; source and interface temperatures, 240 and 290°C, respectively.

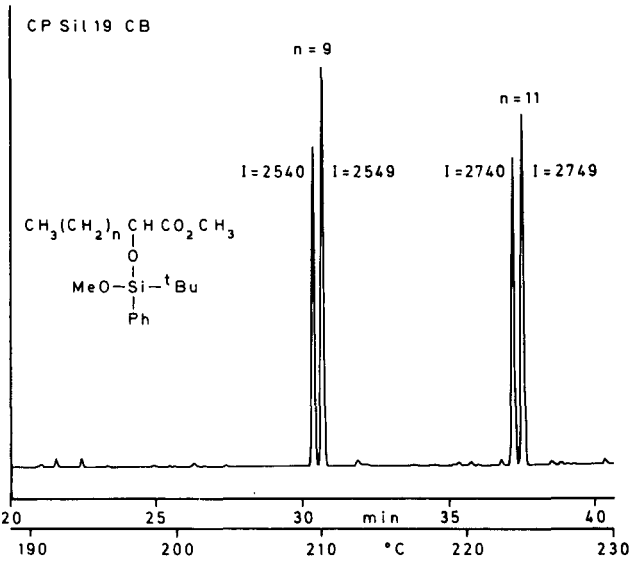

Fig. 1. Gas chromatographic separation of the TBMPS derivatives of (±)-methyl-2-hydroxylaurate (n = 9) and (±)-methyl-2-hydroxymyristate (n = 11). Column, CP Sil19 CB fused-silica capillary (25 m × 0.32 mm I.D.; film thickness, 0.18 μm); column temperature, programmed from 80°C (2 min) to 160°C (1 min) at 30°C/min, and then at 2°C/min to 240°C; helium flow-rate, 3 ml/min. ^{t}Bu = *tert.*-Butyl; Me = methyl; Ph = phenyl.

RESULTS AND DISCUSSION

Fig. 1 shows the pairs of diastereomer peaks observed for TBMPS ethers of methyl 2-hydroxylaurate and methyl 2-hydroxymyristate. The retention index increments (ΔI) resulting from TBMPS ether formation were 788 and 782, respectively, on the CP Sil19 CB phase. In these examples, and in many others studied, the proportions of diastereomers formed were unequal, indicating a not unexpected stereoselectivity in the rates of etherification. As only the racemic forms of the silylation reagent and substrates were employed, no evidence has been obtained as to the stereochemical course of the displacement of bromide ion.

Derivatives of two isomeric racemic bicyclic alcohols, *trans,trans*-α-decalol and *cis,cis*-α-decalol, each afforded diastereomeric TBMPS ethers that were well separated, particularly on the more polar stationary phase CP Sil19 CB as shown in Fig. 2. Separations (as ΔI values) observed for the four decalols studied are cited in Table I.

The mass spectra [40 eV e.i. (electron impact)] of the derivatives cited in this note were dominated by ions of type $(M-57)^+$ (resulting from the loss of a *tert.*-butyl radical from the molecular ion) and by several ions comprising reagent moieties. For example, the decalin TBMPS ethers yielded prominent ions at *m/z* 153, for which high-resolution MS indicated a mass of 153.0383 corresponding to $C_7H_9O_2Si$ as expected for the ion $(C_6H_5(OCH_3)SiOH)^+$. For the hydroxy-ester derivatives (Fig. 1) minor fragmentations involving losses of MeO· were also observed. The presence of other substituents capable of directing favourable cleavages (as exemplified in ref. 5) would afford mass spectra of a more structurally informative nature.

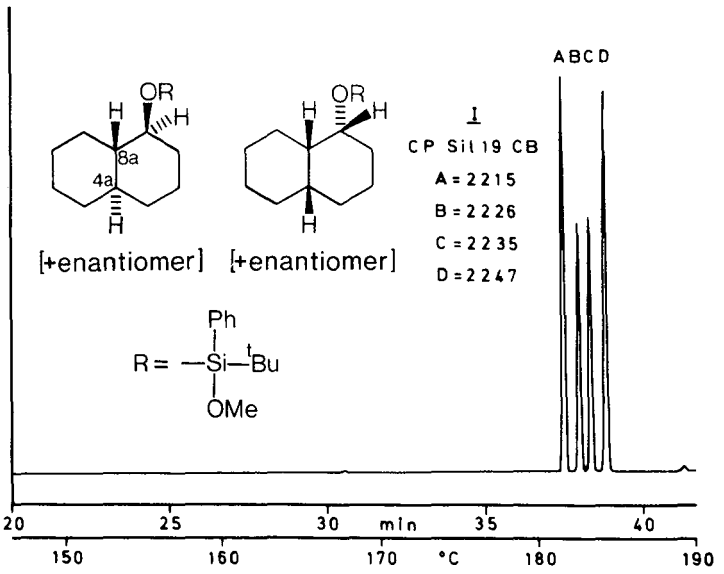

Fig. 2. Gas chromatographic separation of the TBMPS derivatives of (±)-*trans,trans*-α-decalol (A/B) and (±)-*cis,cis*-α-decalol (C/D). Column, CP Sil19 CB fused-silica capillary (25 m × 0.32 mm I.D.; film thickness, 0.18 μm); column temperature, programmed from 80°C (2 min) to 115°C (1 min) at 30°C/min, and then at 2°C/min to 190°C; helium flow-rate, 3 ml/min. ^{t}Bu = *tert.*-Butyl; Me = methyl; Ph = phenyl.

TABLE I

RETENTION INDEX DATA FOR TBMPS ETHERS OF (±)-DECALOLS

Decalols	*CP Sil5 CB*[a]		*CP Sil19 CB*[b]	
	I	*ΔI*	*I*	*ΔI*
cis,cis-α- (1*RS*, 4a*SR*, 8a*SR*)	2122, 2132	10	2235, 2247	12
trans,trans-α- (1*RS*, 4a*SR*, 8a*RS*)	2105, 2115	10	2215, 2226	11
cis,cis-β- (2*RS*, 4a*SR*, 8a*RS*)	2146, 2150	4	2264, 2269	5
trans,cis-β- (2*RS*, 4a*RS*, 8a*RS*)	2136, 2141	5	2244, 2249	5

[a] A dimethylsiloxane polymer.

[b] A siloxane copolymer containing 7% cyanopropyl, 7% phenyl, 85% methyl and 1% vinyl substituents.

The results indicate that the substituents in the TBMPS group are bulky enough to produce significantly different partition coefficients, in GLC, for the derived diastereomeric ethers, and to allow, in many instances, complete resolution of the corresponding peaks. The development of practical applications will require the design of optically stable silylation reagents: on existing evidence[1–3], the incorporation of vinyl, naphthyl and ferrocenyl groups may be advantageous in this respect, while consideration might be given to the use of chiral silyl hydrides which tend to have greater configurational stability than halides. Meanwhile, the reactions of TBMPBr with a variety of hydroxylic substrates are being further explored.

ACKNOWLEDGEMENTS

We thank Dr. A. R. Bader for helpful discussions. The decalols were kindly provided by Dr. A. J. Baker from the sample collection bequeathed by Professor Sir James Cook to the Chemistry Department.

REFERENCES

1 R. J. P. Corriu, C. Guérin and J. J. E. Moreau, *Topics Stereochem.*, 15 (1984) 43.
2 R. J. P. Corriu, C. Guérin and J. J. E. Moreau, in S. Patai and Z. Rappoport (Editors), *The Chemistry of Organic Silicon Compounds*, Wiley, Chichester, 1989, Vol. 1, p. 305.
3 R. J. P. Corriu and G. Royo, *J. Organometal. Chem.*, 14 (1968) 291.
4 Y. Guindon, R. Fortin, C. Yoakim and J. W. Gillard, *Tetrahedron Lett.*, 25 (1984) 4717.
5 A. I. Mallet, R. M. Barr and J. A. Newton, *J. Chromatogr.*, 378 (1986) 194.
6 B. Feibush and L. Spialter, *J. Chem. Soc. B*, (1971) 115.

Journal of Chromatography, 514 (1990) 309–316
Elsevier Science Publishers B.V., Amsterdam

CHROM. 22 499

Note

Comparison of helium head pressure carbon dioxide and pure carbon dioxide as mobile phases in supercritical fluid chromatography

T. GÖRNER, J. DELLACHERIE and M. PERRUT*
Ecole Nationale Supérieure des Industries Chimiques, 1 Rue Grandville, 54000 Nancy (France)
(First received February 9th, 1990; revised manuscript received April 19th, 1990)

In supercritical fluid chromatography (SFC), the solvating power of the mobile phase can be continuously varied and controlled by regulating the density. The density is a function of pressure and temperature and its variations become particularly important as the critical point is approached. The retention decreases sharply when the density of the eluent is decreased.

In these experiments we used two different sources of supercritical carbon dioxide as the mobile phase: helium head pressure carbon dioxide (HHPCD) and pure carbon dioxide. The retention times obtained with HHPCD were much higher than those obtained with pure carbon dioxide at the same temperature, pressure and flow-rate.

The few papers that have reported the use of HHPCD led to some controversy: Porter *et al.*[1] had problems with HHPCD in terms of reproducibility of retention times and peak areas, whereas Schwartz *et al.*[2] and Rosselli *et al.*[3] did not experience severe problems. Porter *et al.*[1] and Rosselli *et al.*[3] reported a slight increase in retention times when HHPCD was used instead of pure carbon dioxide. We observed a considerable increase in retention times with HHPCD.

EXPERIMENTAL

Instrumentation

All experiments were carried out on the device described elsewhere[4].

A Milton Roy Dosapro (Pont St. Pierre, France) minipump was used with a numerical manometer (Touzart & Matignon, Vitry sur Seine, France) of 0–40 MPa, assuming regulation of the pressure. The pump head was cooled to 1°C. To improve the pumping of liquid carbon dioxide, sapphire ball checks and seats were replaced with stainless-steel parts. Carbon dioxide cooled to 1°C in a thermostated bath was pumped without any problems at least up to 32 MPa.

Injections were made with a Rheodyne Model 7413 valve with a 1-μl internal loop (Touzart et Matignon, Vitry sur Seine, France).

0021-9673/90/$03.50

A Perkin-Elmer LC-75 spectrophotometric detector (St. Quentin en Yvelines France) with an 8-μl cell was used. Aromatic compounds were detected at 254 nm and fatty acid esters at 212 nm. A Spectra-Physics SP 4270 (Les Ulis, France) integrator was used.

Pressure was measured at the column inlet and outlet with the numerical manometer; column pressure drops were *ca.* 1 MPa. Pressure reduction was done after the detector in two steps by two mechanical pressure regulators, the first being heated to the column temperature to avoid condensation of carbon dioxide.

Materials

Carbon dioxide of N 45 quality (99.995%) from Air Gaz France (Vigy, France) was delivered in cylinders of 5 MPa, liquefied in our laboratory in a cooling bath at 1°C and pumped up to the working pressure.

Helium head pressure carbon dioxide (HHPCD) (Carbolium[5]) of HP quality from Carboxyque Française (Paris-La Défense, France) was delivered in cylinders of 20 MPa with helium as pressuriser gas. HHPCD was used without a pump at the cylinder pressure, or if necessary was pumped up to desired pressure with the above mentioned pump.

Columns

The columns used were reversed-phase Hypersil C_{18}-bonded silica (5 μm) (135 × 4.6 mm I.D.) and polar Hypersil silica (5 μm) (235 × 4.6 mm I.D.), purchased from Chromatofield (Chateauneuf les Martigues, France).

The above-mentioned phenomenon of a weaker elution strength of HHPCD relative to pure carbon dioxide under the same chromatographic conditions was seen on both types of columns and with various solutes. As can be seen from the following examples, at different temperatures different complementary pressures of HHPCD had to be used to obtain the same retention as with pure carbon dioxide.

On the silica column (41.9°C, flow-rate 1.04 l/min) the methyl esters of fatty acids eluted with pure carbon dioxide at 13.0 MPa have retention times of 17.7 and 21.0 min, respectively, if HHPCD is used, a much higher presure of 19.5 MPa must be applied to give the same retention. As illustrated in Fig. 1, pure carbon dioxide at 19.5 MPa gives very short retention times of 8.6 and 9.8 min respectively. The aromatic compounds benzene, naphthalene and dibenzyl were deluted under milder elution conditions (49.4°C, flow-rate 0.85 l/min) with pure carbon dioxide at 13.5 MPa with retention times of 2.0, 2.9 and 4.0 min, respectively. To obtain the same retention with HHPCD a pressure of 18.5 MPa was necessary. On the C_{18}-bonded silica column (54.5°C, flow-rate 0.85 l/min) at 12.9 MPa with pure carbon dioxide the retention times of the fatty acid methyl esters $C_{20:5}$ and $C_{22:6}$ were 5.2 and 6.6 min, respectively. To obtain the same retention with HHPCD a pressure of 16.4 MPa was necessary.

At first we suspected the presence of traces of water in the carbon dioxide cylinder, acting as a polar modifier. To avoid moisture, a 20 × 2 cm drying column filled with glass-wool and phosphorus pentoxide was introduced between the carbon dioxide cylinder and the pump; no changes in chromatographic behaviour were observed, so the hypothesis of water presence was rejected. A systematic study of a test mixture of aromatic solutes on the silica column at different pressures using HHPCD and pure carbon dioxide was undertaken. The test mixture consisted of benzene, which

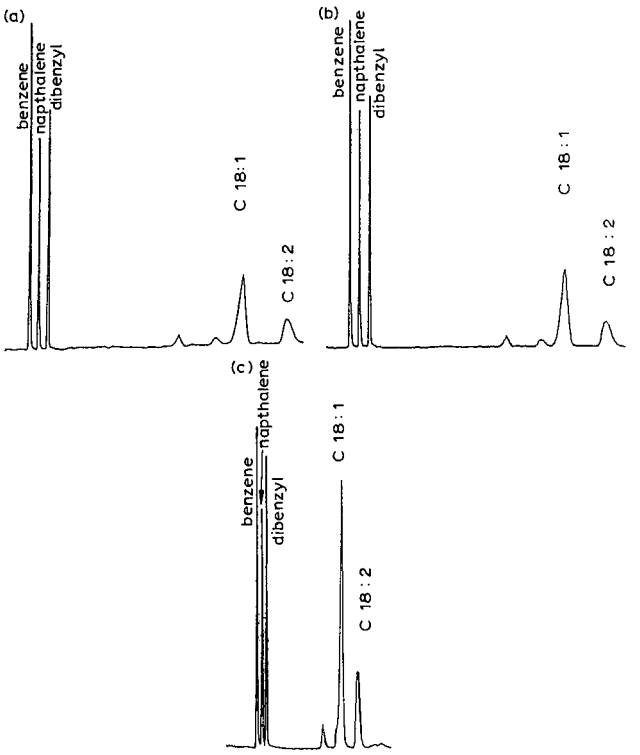

Fig. 1. Methyl esters of fatty acids and aromatic compounds. Silica column, 235 × 4.6 mm I.D., 41.9°C, flow-rate 1.04 l/min. Pressure: (a) 19.5 MPa of HHPCD; (b) 13.0 MPa of pure carbon dioxide; (c) 19.5 MPa of pure carbon dioxide. Retention times: (a) $C_{18:1}$ 17.6 min, $C_{18:2}$ 20.9 min; (b) $C_{18:1}$ 17.7 min, $C_{18:2}$ 21.0 min; (c) $C_{18:1}$ 8.6 min, $C_{18:2}$ 9.8 min.

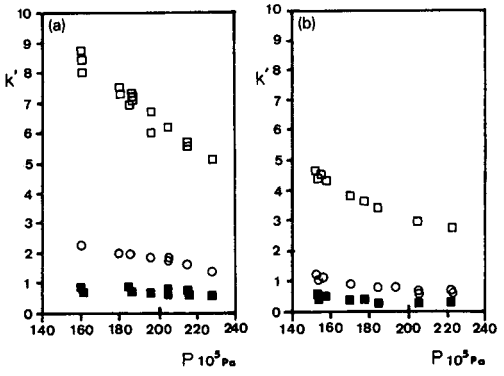

Fig. 2. $k' = f(P)$. Temperature, 39.6°C; flow-rate, 0.85 l/min. Mobile phase: (a) HHPCD; (b) pure carbon dioxide. ■ = Benzene; ○ = dibenzyl; □ = methyl benzoate.

is slightly retained, dibenzyl and methyl benzoate with relatively long retention times of 6–12 min in our conditions (39.6°C; flow-rate 0.85 l/min).

Capacity factors (k') were calculated using the eluent residence time t_0, obtained from the model proposed by Perrut[6] based on Darcy's law.

We expected, and it was confirmed experimentally, that the retention time of benzene (an almost non-retained substance) was hardly influenced by the pressure and nature of the eluent. With dibenzyl and methyl benzoate there are obviously different interactions with the column, resulting in different k' values with the two eluents (Fig. 2).

Determination of density

In the literature we could not find any density values for carbon dioxide mixed with helium under our pressure and temperature conditions, so we estimated the HHPCD and carbon dioxide densities with the same method based on tables of the Lee–Kesler equation of state[7].

Carbon dioxide. The density of pure carbon dioxide, D, was calculated from the equation

$$D = MP/ZRT \tag{1}$$

where M is the molar mass of CO_2, P is pressure, T is temperature, R is the gas constant and Z is the compressibility factor. The compressibility factor Z, correlated with the reduced temperature $T_r = T/T_c$ and reduced pressure $P_r = P/P_c$, were found in the Lee–Kesler tables. The critical temperature T_c and critical pressure P_c are 304.15 K and 7.38 MPa, respectively, and the acentric factor $\omega = 0.239$.

With this method the carbon dioxide densities were found to be higher than those obtained by using the Peng–Robinson equation of state, and closer to the experimentally based values published by IUPAC[13]. The calculated values are plotted in Fig. 3 at different temperatures.

Helium head pressure carbon dioxide. The chromatographic analysis showed that the carbon dioxide leaving the HHPCD cylinder at 20 MPa at 15°C has a helium concentration of 5.8% (v/v), which diminishes linearly to 4.4% as the cylinder pressure decreases to 15 MPa. The real concentration of helium in the HHPCD varies slightly with the cylinder pressure, but we chose a simplified approach, considering a constant concentration (mean value of 5%) over the whole range of 15–20 MPa cylinder pressure in subsequent calculations.

We could not find published liquid–vapour equilibrium data for the He–CO_2 system for our pressure and temperature ranges. However, the data for slightly lower pressures or temperatures[8,9] permitted it to be verified that the above-mentioned concentrations correspond well to the published values, assuming linearity.

To calculate the pseudocritical pressure and temperature of this mixture we followed the recommendations of Solen *et al.*[10]. Subscripts 1 and 2 are used for carbon dioxide and helium, respectively. For quantum gases (helium), slightly temperature-dependent critical constants T_c and P_c must be used.

$$T_{C2} = T_C^0/(1 + C_1/M_2T) \tag{2}$$

$$P_{C2} = P_C^0/(1 + C_2/M_2T) \tag{3}$$

$$V_{C2} = 0.291\ RT_C^0/P_C^0 \tag{4}$$

where T_C^0 = 10.5 K, P_C^0 = 0.676 MPa, C_1 = 21.8 K, C_2 = 44.2 K, V_{C2} = critical volume of helium = 38.2 $cm^3\ mol^{-1}$, V_{C1} = critical volume of carbon dioxide = 93.9 $cm^3\ mol^{-1}$ and M_2 = molar mass of helium.

For a mixture, the interaction constants must be calculated[11]:

$$k_{12} = 1 - \frac{8(V_{C1}V_{C2})^{1/2}}{(V_{C1}^{1/3} + V_{C2}^{1/3})^3} \tag{5}$$

$$V_{C12} = (V_{C1}^{1/3} + V_{C2}^{1/3})^3/8 \tag{6}$$

$$M_{12} = \frac{2}{(1/M_1) + (1/M_2)} \tag{7}$$

where M_1 = molar mass of carbon dioxide.

Whenever either component is a quantum gas, we calculate

$$T_{C12} = \frac{(T_{C1}T_{C2})^{1/2}(1-k_{12})}{1 + (C_1/M_{12}T)} \tag{8}$$

For the utilization of Lee–Kesler tables (as was done with pure carbon dioxide) we applied the laws for mixtures proposed by Plocker *et al.*[12].The following laws permit the pseudocritical constants of HHPCD to be calculated for molar fractions y_1 and y_2 of carbon dioxide and helium, respectively:

$$V_{CM} = y_1^2V_{C1} + 2y_1y_2V_{C1} + y_2^2V_{C2} \tag{9}$$

$$T_{CM} = \frac{1}{V_{CM}^{1/4}}(y_1^2V_{C1}T_{C1} + 2y_1y_2V_{C12}^{1/4}\ T_{C12} + y_2^2V_{C2}^{1/4}T_{C2}) \tag{10}$$

$$\omega_M = y_1\omega_1 + y_2\omega_2 \qquad (\omega_1 = 0.239;\ \omega_2 = 0.0) \tag{11}$$

$$P_{CM} = (0.2905 - 0.085\omega_M)RT_{CM}/V_{CM} \tag{12}$$

The reduced parameters $T_r = T/T_{CM}$ and $P_r = P/P_{CM}$ were calculated for HHPCD and with the compressibility factor Z from Lee–Kesler tables the density of the mixture was obtained from eqn. 1, where M is replaced by the molar mass of HHPCD.

RESULTS AND DISCUSSION

The pure carbon dioxide (CO_2) and HHPCD densities at different temperatures and pressures are given in Fig. 3. As it can be seen, the corresponding CO_2 densities are

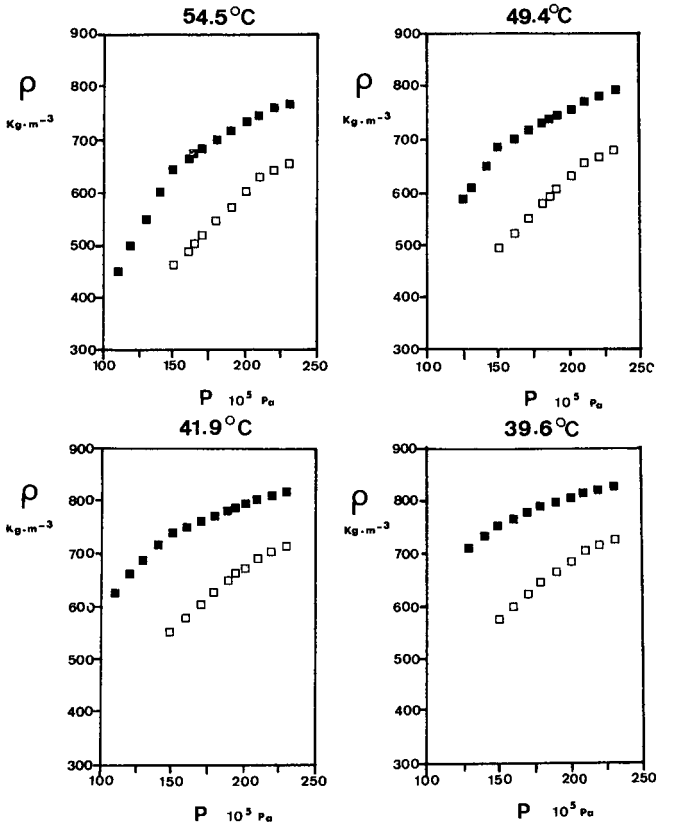

Fig. 3. Densities of (□) HHPCD and (■) pure carbon dioxide at different pressures and temperatures. Concentration of 5% of helium in carbon dioxide.

much higher than those of HHPCD, which explains the higher elution strength of CO_2 under the same conditions.

Table I gives some values referring to our experiments. The pressures and temperatures of the experiments and the calculated densities of HHPCD (D_{HC}) and of CO_2 (D_{CO2}) at a given temperature and pressure are listed in the first four columns. As can be seen the CO_2 values are much higher than those of HHPCD.

TABLE I

COMPARISON OF PRESSURES AND CORRESPONDING DENSITIES OF PURE CARBON DIOXIDE AND HHPCD

Temperature (°C)	*Pressure (MPa)*	D_{HC} *(kg/m³)*	D_{CO_2} *(kg/m³)*	$P_{CO_2 eqv.}$ *exp. (MPa)*	D_{CO_2} *theor. (kg/m³)*	$P_{CO_2 eqv.}$ *(MPa)*	*Δ (%)*
41.9	19.5	660	790	13.0	690	12.0	8
54.5	16.4	501	672	12.9	545	12.0	7
49.4	18.5	591	739	13.5	630	12.5	7

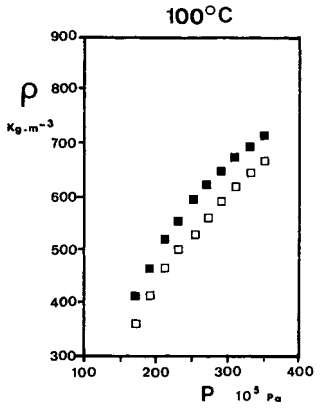

Fig. 4. Densities of (□) HHPCD and (■) pure carbon dioxide at 100°C and at different pressures. Concentration of 3% of helium in carbon dioxide.

We calculated the density of CO_2 at the pressures experimentally observed (fifth column) and giving the same retention as HHPCD. The CO_2 densities obtained (sixth column) are very close to those of HHPCD (third column), which explains why a lower CO_2 pressure was needed to obtain the same retention.

We also calculated the theoretical pressures at which CO_2 would have the same density as HHPCD. As can be seen, the calculated pressures (seventh column) are slightly lower, by 7–8% (last column) than those observed experimentally (fifth column).

We can consider that the simplified hypothesis (taking into consideration only density changes as a function of helium concentration) explains very well the higher retention times obtained with the HHPCD, and the first approximation presented here leads to a satisfactory interpretation of the results.

The fact that Rosselli *et al.*[3] and Porter *et al.*[1] observed only slightly higher retention times in the case of HHPCD is explained as follows. In both instances the HHPCD was used in cylinders of pressure *ca.* 10.75 MPa. According to the equilibrium data, at 20°C there is about 3% of helium dissolved in carbon dioxide. We made density calculations assuming 3% of helium CO_2 under the experimental conditions of Rosselli *et al.*[3] and, as can be seen from Fig. 4, the differences between HHPCD and CO_2 are much smaller than those under our experimental conditions (Fig. 3).

CONCLUSIONS

The lower elution strength of HHPCD compared with CO_2 at the same temperature, pressure and flow-rate is due mainly to its lower density. It is surprising that the presence of a relatively small concentration of helium decreases the elution strength of the HHPCD so much, but the important density variations can explain this phenomenon. This fact must be taken into consideration if different sources of supercritical carbon dioxide are used.

ACKNOWLEDGEMENTS

The authors thank Mr. Rigal for his contribution to the calculations.

REFERENCES

1 N. L. Porter, B. E. Richter, D. J. Bornhop, D. W. Later and F. H. Bayerlein, *J. High Resolut. Chromatogr. Chromatogr. Commun.*, 10 (1987) 477.
2 H. E. Schwartz, P.J. Barthel and S. E. Moring, *J. High Resolut. Chromatogr. Chromatogr. Commun.*, 10 (1987) 668.
3 A. C. Rosselli, D. S. Boyer and R. K. Houck, *J. Chromatogr.*, 465 (1989) 11.
4 T. Gorner and M. Perrut, *LC · GC Int.*, 2, No. 7 (1989) 36.
5 *Carbolium, Technical Note*, Carboxyque Française, Paris-La Défense, 1987.
6 M. Perrut, *J. Chromatogr.*, 396 (1987) 1.
7 B. I. Lee and H. G. Kesler, *AIChE J.*, 5 (1975) 510.
8 R. F. MacKendrick, C. K. Heck and P. L. Barrick, *J. Chem. Eng. Data*, 13 (1968)352.
9 D. W. Burfield, H. P. Richardson and R. A. Guereca, *AIChE J.*, 16 (1970) 97.
10 K. A. Solen, P. L. Chuen and J. M. Prausnitz, *Ind. Eng. Chem., Process Des. Dev.*, 9 (1972) 310.
11 R. R. Tarakad and R. P. Danner, *AIChE J.*, 23 (1977) 685.
12 U. Plocker, H. Knapp and J. M. Prausnitz, *Ind. Eng. Chem., Process Des. Dev.*, 17 (1978) 324.
13 S. Angus et al., *IUPAC International Thermodynamical Tables of the Fluid State —Carbon Dioxide*, Pergamon, Oxford, 1974.

Journal of Chromatography, 514 (1990) 317–324
Elsevier Science Publishers B.V., Amsterdam

CHROM. 22 533

Note

Separation of alkanes in *Citrus* essential oils by on-line coupled high-performance liquid chromatography–high-resolution gas chromatography

GIUSEPPE MICALI, FRANCESCO LANUZZA, PAOLINA CURRÒ and GIUSEPPE CALABRÒ*
Istituto di Merceologia dell'Università degli Studi di Messina, Piazza S. Pugliatti, 98100 Messina (Italy)
(First received January 3rd, 1990; revised manuscript received May 2nd, 1990)

The development of gas chromatography (GC) and especially high-resolution GC (HRGC) has made it possible to study essential oils in depth. The high resolving power of capillary columns has allowed separations of the many components present, but the great complexity of the matrices often requires the use of different stationary phases and the use of mass spectrometry (MS) in order to identify the components accurately. Sometimes not even MS is able to identify all the components because similar components give similar fractionation patterns, *e.g.*, as happens with sesquiterpenes[1].

The recently developed coupling of high-performance liquid chromatography (HPLC) with HRGC has been a great help towards improving our knowledge of the composition of essential oils[2,3], because it is possible to use simultaneously the high separating power of HPLC and HRGC to separate the numerous components which are present. The components are first separated by HPLC into relatively small volume of eluate which can be introduced on-line into the gas chromatograph, thus avoiding too much handling of the sample, which can lead to errors.

The alkanes in *Citrus* essential oils have not been studied much up to now[4–7]. On-line HPLC–HRGC with concurrent solvent evaporation[8–10] has been used in our research to study the alkane fraction of cold-pressed *Citrus* essential oils. The HPLC eluate is injected into the gas chromatograph by using the concurrent solvent evaporation technique. The temperature of the GC column is maintained at a higher value than boiling point of the HPLC eluent, taking into account both the composition of the eluent and the inlet pressure of carrier gas[11,12].

EXPERIMENTAL

Equipment

The liquid chromatograph was a Perkin-Elmer Series 4 with a Rheodyne 7125 S microinjection valve equipped with a 6-μl loop. The column was Hypersil Silica (5 μm) (10 × 0.21 cm I.D.). A Perkin-Elmer LC 55 S spectrophotometric detector was used.

0021-9673/90/$03.50

The gas chromatograph was a Carlo Erba Fractovap 2900 equipped with a flame ionization detector. An OV-1 glass capillary column (22 m × 0.32 m I.D.) with a 0.4-μm film thickness was used, with a fused-silica retention gap (4 m × 0.53 mm I.D.). A Perkin-Elmer LCI 100 computing integrator was used.

Other equipment consisted of Valco six-way and four-way valves ($\frac{1}{16}$ in.), a Valco T-piece ($\frac{1}{16}$ in.) and Carlo Erba needle valves.

Reagents

n-Hexane of HPLC grade was obtained from Omnia Res, methylene chloride of HPLC grade from Koch-Light, eneicosane, docosane, tricosane, tetracosane, pentacosane, hexacosane, heptacosane, octacosane, triacontane, dotriacontane and tri-triacontane from Fluka and nonacosane from Aldrich.

Chromatographic analysis

The liquid and gas chromatographs were coupled using the interface shown in Fig. 1, which consists of a six-way sample valve (A), connected to the HPLC detector exit, equipped with a sample loop, and a four-way valve (B) connected to the flow regulator of the carrier gas. The two valves are connected by a steel capillary with two needle valves (C_1 and C_2) and by a T-piece. Valve A is connected to the T-piece by a 25-cm steel capillary and valve B is connected to the same T-piece by a fused-silica capillary (2 m × 0.32 mm I.D. × 0.45 mm O.D.) which passes through it, entering the precolumn to a distance of 1.5 cm (Fig. 1). The transfer steps are shown in Fig. 2.

During the GC analysis the loop with the eluent must be washed because it was

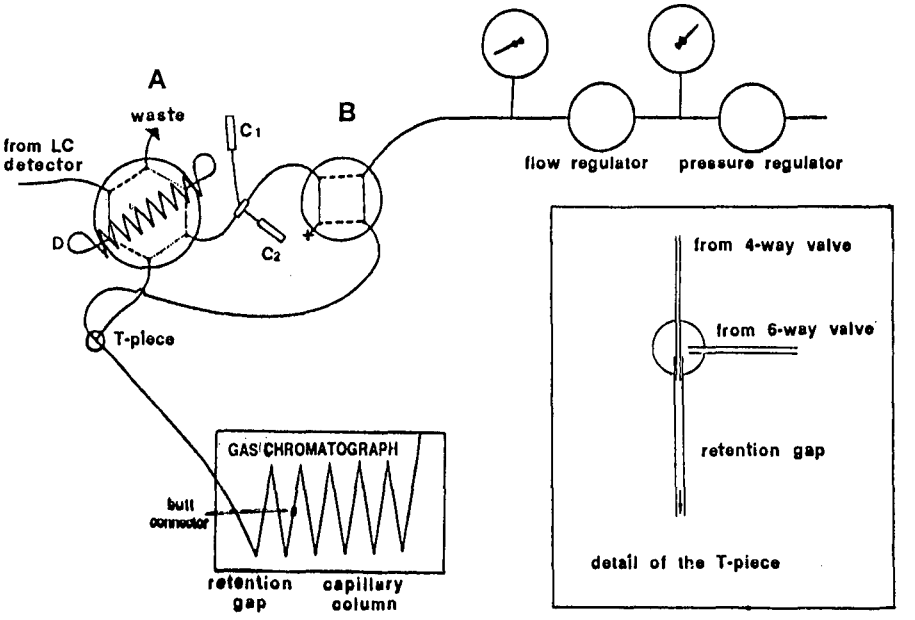

Fig. 1. HPLC–HRGC coupling interface. A = sampling valve; B = carrier gas valve; C_1 and C_2 = needle valves; D = sampling loop.

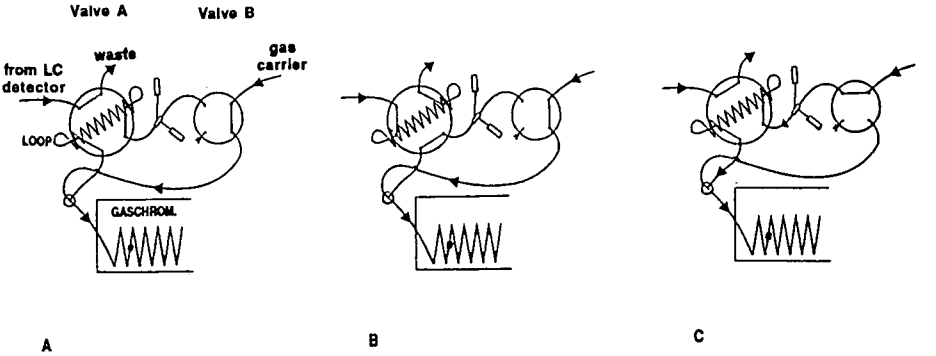

Fig. 2. Configuration of the interface during the transfer steps. (A) Basic working condition; (B) isolation of the fraction of interest in the loop; (C) transfer of the loop content into the capillary column.

observed that, owing to component carryover, washing the loop only with the carrier gas, as proposed by Grob and Stoll[9], proved to be insufficient. For this purpose, valve A is made to rotate so that the mobile phase flows through the loop; the interface appears as shown in Fig. 2B. At the end of the GC analysis, in the cooling phase of the GC oven, valve A is returned to the position in Fig. 2A. The eluent trapped in the loop is removed by opening the needle valve C_1 simultaneously.

The needle valve C_2, regulated at a flow-rate of 2 ml/min, controls any eventual increases in pressure of the system, making the evaporation of the solvent more regular.

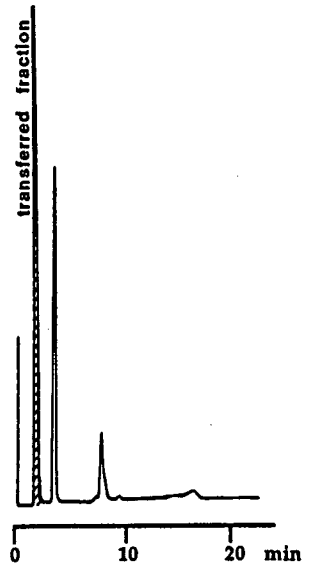

Fig. 3. HPLC of a mandarin essential oil.

The *Citrus* essential oils diluted in hexane (1:5) were injected into the liquid chromatograph through a Rheodyne valve with a 6-μl loop. A 10 × 0.21 cm I.D. Hypersil Silica 5-μm silica gel column was used with hexane at a flow-rate of 0.2 ml/min and UV detection at 220 nm. The UV absorption of terpenes was a marker for the non-absorbing hydrocarbons (Fig. 3). Alkanes were eluted in a single peak together with terpenes and sesquiterpenes. This fraction of 250-μl volume was directly transferred to the gas chromatograph.

For the GC analysis we used an OV-1 glass capillary column, connected by a butt-connector to an untreated fused-silica column (4 m × 0.53 mm I.D.) which comes out of the GC oven and is connected to the T-piece. We used hydrogen as the carrier gas at a column flow-rate of 4.5 ml/min, obtained by regulating the inlet pressure at 3 atm and the flow regulator at 1.15 atm. This regulation was performed at 124°C, which was the temperature of concurrent solvent evaporation. The temperature was programmed from 124°C (isothermal for 12 min) at 4°C/min to 180°C and rat 6°C/min to 285°C. Under these conditions, the alkanes in the sample were separated whereas the terpenes and the sesquiterpenes were eluted with the solvent in a single peak.

During the GC analysis, the LC column was washed for 15 min with methylene chloride in order to elute the oxygenated compounds left in the column; finally, it was reconditionated with hexane.

The chromatographic identification of the alkanes was carried out by using pure

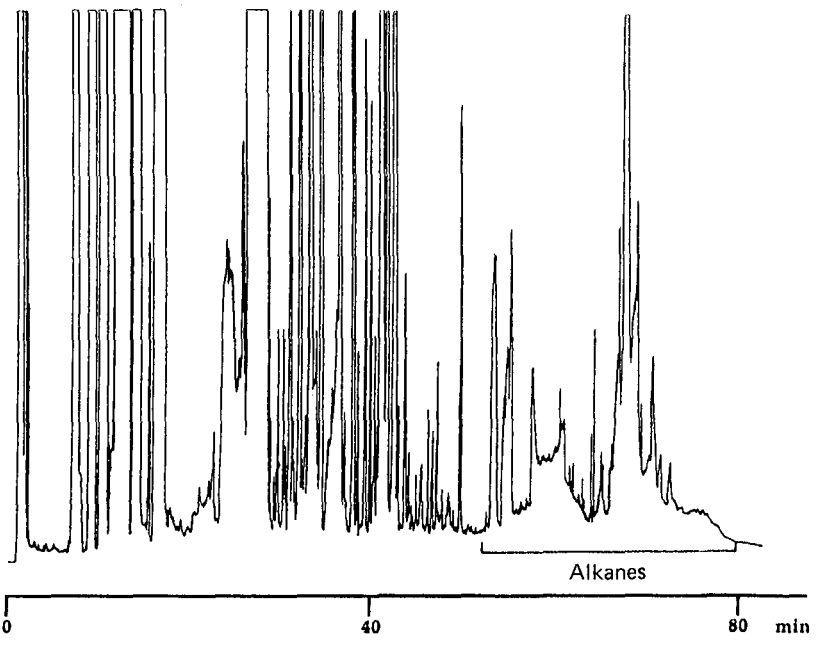

Fig. 4. Gas chromatogram of a bergamot essential oil. Injection "on-column" of 0.5 μl of essential oil solution diluted 1:5 in hexane. Temperature programme: 45°C for 2 min, increased at 2°C/min to 120°C, at 5°C/min to 230°C and at 10°C/min to 300°C. Carrier gas, hydrogen; flow-rate, 3.5 ml/min; detector temperature, 320°C.

standards; the isoalkanes were identified by using the few data available in the literature[4–7].

RESULTS AND DISCUSSION

The "on-column injection" GC analysis generally used to study *Citrus* essential oils does not give sufficient information on the alkanes because there are only small amounts present and also because of interferences from other compounds (Fig. 4). On-line HPLC–HRGC coupling allowed us to overcome this problem. A suitable amount of the sample can be injected for the accurate detection of the alkanes. The chromatograms thus obtained are less complex and the alkanes are separated without interferences, which makes their identification easier and more reliable.

Fig. 5 shows typical chromatograms of alkanes in lemon, bergamot, mandarin, sweet and bitter orange essential oils. For each essential oil ten different genuine samples were analysed.

The examination of the chromatograms obtained showed that, in the essential oils analysed all the alkanes in the range C_{21}–C_{33} and the isoalkanes in the range C_{23}–C_{31} are present. The concentrations of the various *n*-alkane components vary, sometimes greatly, from one essential oil to another. The highest concentration was found in sweet orange essential oil and the lowest in bitter orange. In all the essential oils analysed, the contents of alkanes with odd numbers of carbon atoms are generally higher than those with even numbers. In mandarin essential oil, the *n*-C_{24} concentration is comparable to that of the alkanes with an odd number of carbon atoms.

In lemon, bergamot and sweet orange essential oils, the *n*-alkanes present in the greatest concentrations are generally in sequence *n*-C_{29}, *n*-C_{31}, *n*-C_{27} and *n*-C_{25}.

We found the same composition in bitter orange essential oil. There were, however, small concentrations of other compounds, probably isomers of the various *n*-alkanes. In mandarin essential oil, the *n*-alkanes present in the greatest concentrations are generally *n*-C_{23}, *n*-C_{24}, *n*-C_{25}, *n*-C_{27} and *n*-C_{29}. In all the essential oils analysed we found the isoalkanes between *i*-C_{23} and *i*-C_{31}, which precede the corresponding *n*-alkanes in the chromatograms. As there are no pure standards available, their identification was carried out on the basis of the few data reported in the literature[4–7], according to which data the even-carbon isoalkanes are the 3-methylalkanes and the odd-carbon compounds are the 2-methylalkanes.

In all the essential oils analysed, the isoalkane found in the greatest amount is *i*-C_{25} (2-methyl-$C_{24}H_{49}$). The concentration of the other isoalkanes normally decreases as the number of carbon atoms increases, until they are scarcely detectable in the range *i*-C_{28} (3-methyl-$C_{27}H_{55}$) to *i*-C_{31} (2-methyl-$C_{30}H_{61}$).

In sweet orange and bergamot essential oil the isoalkanes have lower concentrations than the corresponding *n*-alkanes. Bitter orange, mandarin and lemon essential oils often had concentrations of *i*-C_{23}–*i*-C_{26} isoalkanes comparable with those of the *n*-alkanes.

The proposed combined technique is new and easier to perform than the traditional method, which requires isolation on an open alumina column of the various classes of compounds present in essential oils, followed by GC analysis of the fraction of interest after having adequately concentrated the sample[6,7,13]. The preseparation of the alkane fraction and its direct transfer to the gas chromatograph are carried out very

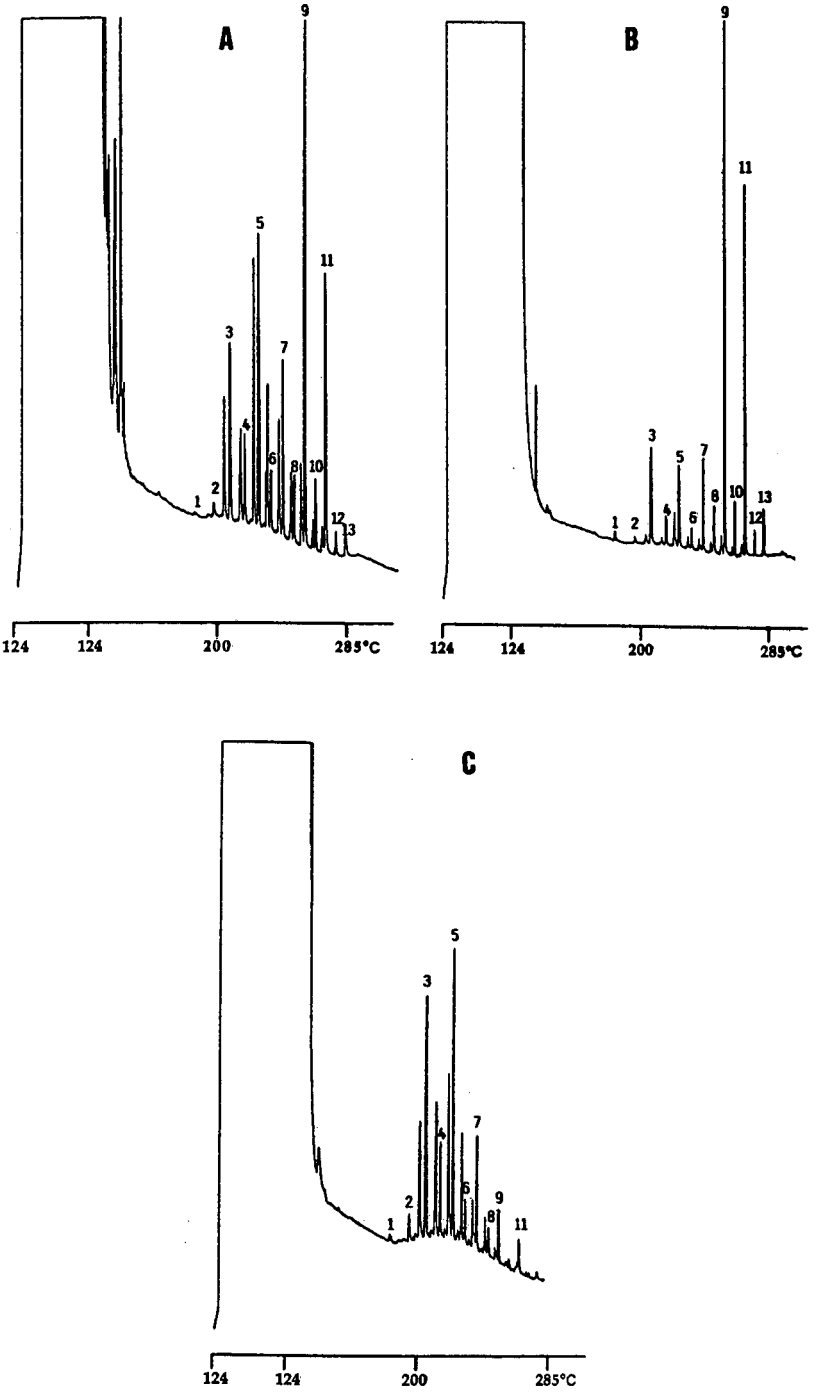

Fig. 5.

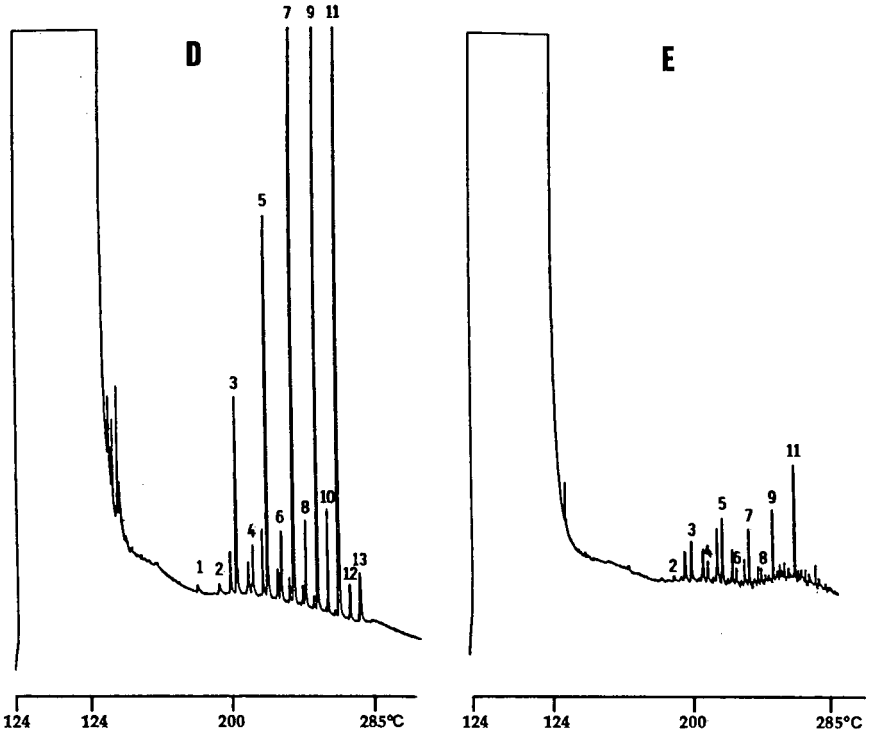

Fig. 5. Chromatograms obtained by HPLC–HRGC with flame ionization detection. (A) Lemon essential oil; (B) bergamot essential oil; (C) mandarin essential oil; (D) sweet orange essential oil; (E) bitter orange essential oil. Peaks: 1 = n-C_{21}; 2 = n-C_{22}; 3 = n-C_{23}, 4 = n-C_{24}; 5 = n-C_{25}; 6 = n-C_{26}; 7 = n-C_{27}; 8 = n-C_{28}; 9 = n-C_{29}; 10 = n-C_{30}; 11 = n-C_{31}; 12 = n-C_{32}; 13 = n-C_{33}. The peaks preceding the n-alkanes are the respective isoalkanes.

rapidly. The amount of sample required is small, and the analytical sample is obtained by simple dilution in an appropriate solvent, thus avoiding possible causes of errors, *e.g.*, due to isomerization on the alumina column. The analysis is carried out in a short time and peak identification is simplified and more certain.

REFERENCES

1 T. Shibamoto, in G. Charalambous (Editor), *Analysis of Food and Beverages: Modern Techniques*, Academic Press, New York, 1984, p. 104.
2 P. Currò, F. Lanuzza, G. Micali and G. Calabrò, *Rass. Chim.*, 41 (1989) 125.
3 F. Munari and G. Dugo, presented at the *10th International Symposium on Capillary Chromatography, Riva del Garda, May 22–25, 1989.*
4 G. Eglinton, A. G. Gonzalez, R. J. Hamilton and R. A. Raphael, *Phytochemistry*, 1 (1962) 89.
5 G. L. K. Hunter and W. B. Brodgen, Jr., *Phytochemistry*, 5 (1966) 807.
6 G. D'Amore, G. Calabrò and P. Currò, *Ann. Fac Econ. Commer. Univ. Stud. Messina*, 6, No. 3 (1968) 3.
7 G. Calabrò and P. Currò, in S. Fossataro (Editor), *Atti del VII Convegno Internazionale della Qualità, Cagliari–Sassari, 17–22 Maggio 1971*, 1971, pp. 587–598.
8 H. J. Cortes, C. D. Pfeiffer and B. E. Richter, *J. High Resolut. Chromatogr. Chromatogr. Commun.*, 8 (1985) 469.

9 K. Grob and J. M. Stoll, *J. High Resolut. Chromatogr. Chromatogr. Commun.*, 9 (1986) 518.
10 K. Grob, C. Walder and B. Schilling, *J. High Resolut. Chromatogr. Chromatogr. Commun.*, 9 (1986) 95.
11 K. Grob, *J. High Resolut. Chromatogr. Chromatogr. Commun.*, 10 (1987) 297.
12 K. Grob and T. Läubli, *J. High Resolut. Chromatogr. Chromatogr. Commun.*, 10 (1987) 435.
13 G. Dugo, G. Lamonica, A. Cotroneo, A. Trozzi, F. Crispo, G. Licandro and D. Gioffrè, *Essenze Deriv. Agrum.*, 57 (1987) 456.

Journal of Chromatography, 514 (1990) 325–329
Elsevier Science Publishers B.V., Amsterdam

CHROM. 22 517

Note

Separation of enantiomeric protected dipeptides by chiral high-performance liquid chromatography

SHIH-HSIUNG WU*, SHU-LING LIN, SU-YUAN LAI and TAI-HUNG CHOU
**Institute of Biological Chemistry, Academia Sinica, P.O. Box 23-106, Taipei 10798 (Taiwan) and Graduate Institute of Biochemical Sciences, National Taiwan University, Taipei (Taiwan)*
(First received March 19th, 1989; revised manuscript received April 23rd, 1990)

Diastereomers of protected peptides can be separated by reversed- and normal-phase high-performance liquid chromatography (HPLC)[1–3] and can also be analysed by ^{1}H NMR spectroscopy[4]. These methods have been applied to the study of racemization in peptide synthesis[5–8]. However, there are no powerful or convenient methods for the determination of enantiomers of protected dipeptides, which may be produced in the asymmetric formation of peptide bonds by chemical or enzymatic methods[9,10].

Enantiomers of free dipeptides have been separated by thin-layer chromatography (TLC), gas chromatography (GC) and HPLC. Günther *et al.*[11] developed a direct method for the resolution of enantiomeric free dipeptides on chiral TLC plates, Lindner *et al.*[12] reported the separation of enantiomeric glycine dipeptides after dansylation by reversed-phase HPLC with chiral metal chelate additives and enantiomeric dipeptides with esterification in the carboxyl-terminal position and perfluoroacylation in the N-terminal position can be separated by GC on a chiral stationary phase[13]. Owing to the inaccuracy of quantification in TLC and the possibility of racemization of protected dipeptides in the deprotecting and derivatization steps for analysis by GC, it is imperative to develop a facile means of analysing for protected dipeptides directly and quantitatively in order to study racemization and asymmetric induction in peptide synthesis. In this work, the separation of eight sets of enantiomeric protected dipeptides, (*Z*)-AA_1-AA_2-OBzl (Bzl is benzyl), where AA_1 and AA_2 are Ala and Phe, respectively, were studied by chiral HPLC.

EXPERIMENTAL

L-Amino acids were purchased from Kyowa Fermentation (Tokyo, Japan) and D-amino acids from Sigma (St. Louis, MO, U.S.A.). All solvents were obtained from Alps Chemical (Taipei, Taiwan). A chiral Pirkle type 1-A column (25 cm × 4.6 mm I.D.) and Pirkle-concept Sumipax OA-1100 and OA-2200 chiral columns (15 cm × 4.6 mm I.D., 5 μm) were obtained from Regis Chemical (Morton Grove, IL, U.S.A.) and a Chiralcel OD column (25 cm × 4.6 mm I.D.) from Daicel Chemical Industries (Tokyo, Japan).

0021-9673/90/$03.50

Protected dipeptides were synthesized by the dicyclohexylcarbodiimide coupling method and their purity was checked by TLC on silica gel type 60 (E. Merck, Darmstadt, F.R.G.) with detection by the chlorine–tolidine method[14]. The HPLC system from Waters Assoc. (Milford, MA, U.S.A.) used for the analytical separations consisted of an M6000A solvent delivery unit and a U6K universal injector, coupled to a Model M450 variable-wavelength UV spectrophotometer and an SIC Chromatocorder 12 integrator (System Instruments, Tokyo, Japan). Enantiomers of protected dipeptides were separated on chiral columns using isopropanol (IPA) in *n*-hexane as the mobile phase at room temperature and detected by UV spectrophotometry at 254 nm.

RESULTS AND DISCUSSION

Free D,L-amino acids and enantiomers of free dipeptides are easily converted into diastereomers, which could be separated using general reversed-phase or ion-exchange columns[15]. In recent years, they have also been separated directly by TLC or HPLC with the chiral ligand-exchange method[11,12,16]. Because of the lack of free amino and carboxyl groups, protected amino acids and peptides cannot form diastereomers of ligand complexes with metal ions in the mobile phase and a chiral stationary phase. Therefore, other types of commercially available chiral columns have been introduced to separate enantiomers of protected dipeptides. Among the chiral columns tested, the Pirkle type 1-A chiral column is the best. According to Table I and Fig. 1, four pairs of D–D/L–L protected dipeptides and the D–L/L–D

TABLE I

SEPARATION OF ENANTIOMERIC PROTECTED PEPTIDES USING PIRKLE-TYPE 1-A, CHIRALCEL OD AND SUMIPAX OA 1100 CHIRAL COLUMNS

k' = Capacity factor; α = separation factor.

Compound	*Enantiomers*	*Pirkle-type 1-A*			*Chiralcel OD*		*Sumipax OA 1100*	
		k'	α	*Isopropanol–n-hexane eluent*	k'	α	k'	α
(*Z*)-Phe-Phe-OBzl	L–L	5.10	1.16	1:6	3.64	1.29	1.26	1.00
	D–D	6.64			4.70		1.26	
	L–D	7.41	1.15	1:6	4.70	1.08	1.59	1.08
	D–L	8.53			5.10		1.47	
(*Z*)-Phe-Ala-OBzl	L–L	7.29	1.18	14:100	2.90	1.03	2.18	1.06
	D–D	8.59			3.00		2.06	
	L–D	7.76	1.17	14:100	3.00	1.20	2.18	1.00
	D–L	9.12			3.60		2.18	
(*Z*)-Ala-Phe-OBzl	L–L	6.72	1.18	1:6	3.60	1.44	1.59	1.35
	D–D	7.94			5.20		1.18	
	L–D	8.53	1.08	1:6	4.00	1.13	1.94	1.22
	D–L	9.18			4.50		1.59	
(*Z*)-Ala-Ala-OBzl	L–L	4.76	1.14	1:6	2.80	1.34	1.71	1.16
	D–D	5.43			3.76		1.47	
	L–D	6.18	1.09	1:6	3.04	1.05	1.94	1.13
	D–L	6.67			3.20		1.71	

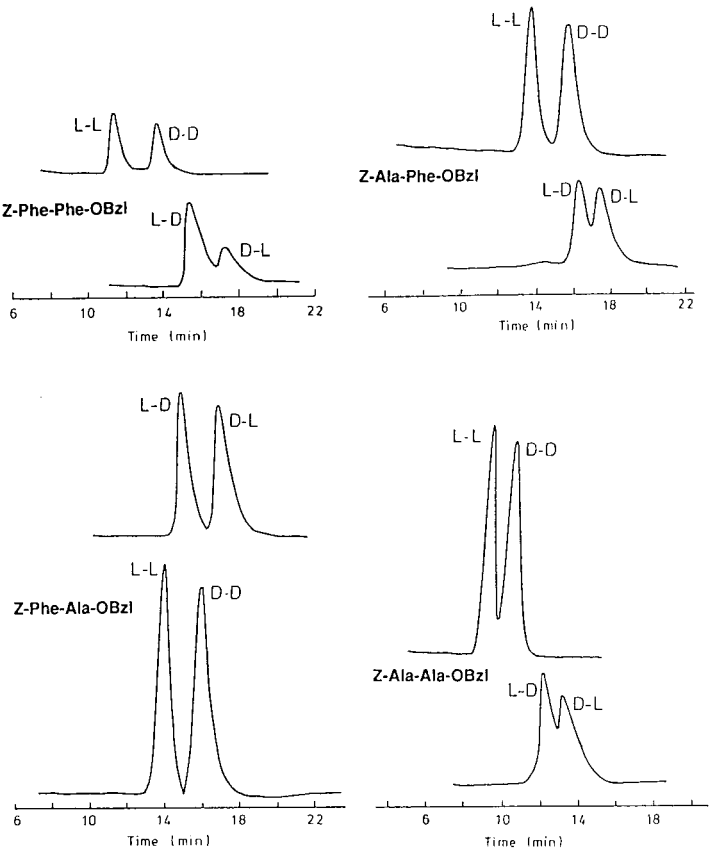

Fig. 1. Separation of stereoisomers of protected dipeptides on a chiral Pirkle type 1-A column. Mobile phase, as in Table I; flow-rate, 1.0 ml/min; detection, 254 nm at room temperature.

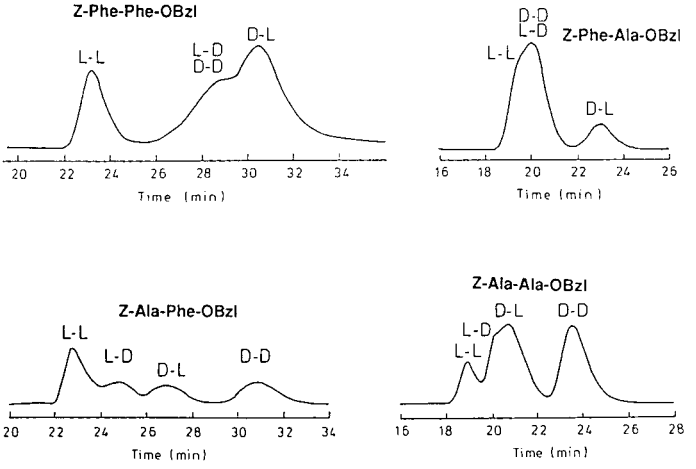

Fig. 2. Separation of stereoisomers of protected dipeptides on a Chiralcel OD column. Mobile phase, *n*-hexane–isopropanol (5:1); flow-rate, 0.45 ml/min; detection, 254 nm at room temperature.

enantiomers of (*Z*)-Phe-Ala-OBzl are separated well by the Pirkle type 1-A chiral column, and three other D–L/L–D pairs are partially separated with tailing peaks. The elution order of the four protected dipeptides for each set is L–L, D–D, L–D and D–L, except the reverse order of L–D and D–D in the case of (*Z*)-Ala-Phe-OBzl.

The L–L/D–D isomers of (*Z*)-Ala-Ala-OBzl, (*Z*)-Ala-Phe-OBzl and (*Z*)-Phe-Phe-OBzl and the D–L/L–D enantiomers of (*Z*)-Phe-Ala-OBzl show good separations on the Chiralcel OD column. However, other enantiomers are only partially separated (Fig. 2). The elution order on the Chiralcel OD column for each set is L–L, L–D, D–L and D–D. Apparently, D-amino acid residues undergo greater interaction with the stationary phase of the Chiralcel OD column, which contains cellulose tris-3,5-dimethylphenyl carbamate coated on silica gel.

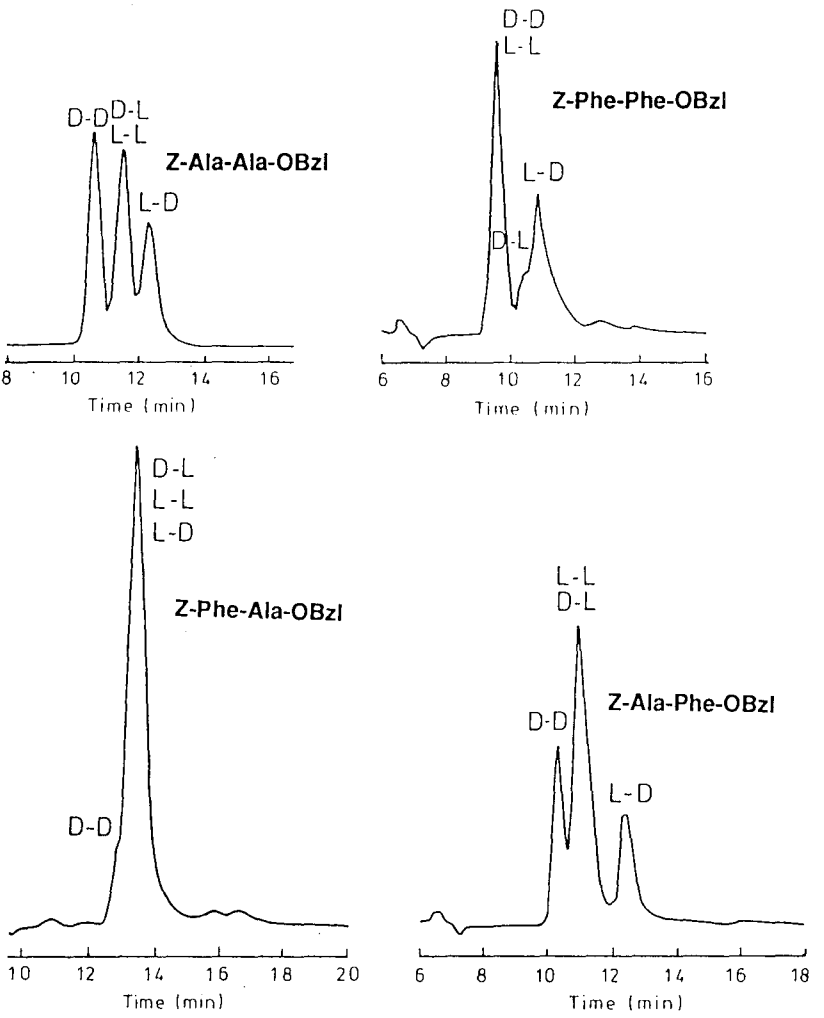

Fig. 3. Separation of stereoisomers of protected dipeptides on a Regis Sumipax OA 1100 column. Mobile phase, *n*-hexane–isopropanol (5:1); flow-rate, 0.4 ml/min; detection, 254 nm at room temperature.

Four sets of enantiomers, D–D/L–L and D–L/L–D of (*Z*)-Ala-Ala-OBzl and D–D/L–L and D–L/L–D of (*Z*)-Ala-Phe-OBzl, can be separated on the Regis Sumipax OA 1100 chiral column (Fig. 3), but none of the sets of enantiomers could be separated on the Regis Sumipax OA 2200 column.

It is believed that Pirkle-concept chiral columns have a similar theoretical basis of separation in which the mechanism of separation of small molecules is explained by three-point interactions involving hydrogen bonding, π–π hydrophobic forces and dipole stacking[17]. The chiral interactions between protected dipeptides and chiral stationary phases are possibly multi-point and more complicated than three-point interactions. The explanation of these interactions by molecular modelling is in progress. Although the four stereoisomers (L–L, L–D, D–L and D–D) are not well separated simultaneously, this enantiomeric separation, combined with diastereomeric separation, will provide an analytical method for studying the asymmetric reactions in peptide synthesis.

REFERENCES

1 L. C. Lo, S. T. Chen, S. H. Wu and K. T. Wang, *J. Chromatogr.*, 472 (1989) 336.
2 R. Seinauer, F. M. F. Chen and N. L. Benoiton, *J. Chromatogr.*, 325 (1985) 111.
3 T. Yamada, Y. Manabe, T. Miyazama and S. Kuwata, in S. Sakakibara (Editor), *Peptide Chemistry 1982*, Protein Research Foundation, Osaka, 1983, pp. 69–80.
4 N. L. Benoiton, K. Kuroda and F. M. F. Chen, *Int. J. Pept. Protein Res.*, 13 (1979) 403.
5 N. L. Benoiton, K. Kuroka, S. T. Cheung and F. M. F. Chen, *Can. J. Biochem.*, 57 (1979) 776.
6 S. T. Cheung and N. L. Benoiton, *Can. J. Chem.*, 55 (1977) 911.
7 T. Yamada, M. Shimamura, T. Miyazawa and S. Kuwata, in E. Munekata (Editor), *Peptide Chemistry 1983*, Protein Research Foundation, Osaka, 1984, pp. 31–36.
8 T. Yamada, M. Nakao and S. Kuwata, in Y. Kiso (Editor), *Peptide Chemistry 1985*, Protein Research Foundation, Osaka, 1986, pp. 333–338.
9 I. B. Stoineva and D. D. Petkov, *FEBS Lett.*, 183 (1985) 103.
10 K. T. Wang, in T. B. Lo, T. Y. Liu and C. H. Li (Editors), *Biochemical and Biophysical Studies of Proteins and Nucleic Acids*, Elsevier, Amsterdam, 1984, pp. 341–348.
11 K. Günther, J. Martens and M. Schickedanz, *Angew. Chem., Int. Ed. Engl.*, 25 (1986) 278.
12 W. Lindner, J. N. Le Page, G. Davies, D. E. Seitz and B. L. Karger, *J. Chromatogr.*, 185 (1979) 323.
13 N. Oi, M. Horiba, H. Kitahara and H. Shimada, *J. Chromatogr.*, 202 (1980) 302.
14 B. F. Rydon and P. W. G. Smith, *Nature (London)*, 169 (1952) 922.
15 T. Nambara, in W. S. Hancock (Editor), *Handbook of HPLC for the Separation of Amino Acids, Peptides and Proteins*, Vol. I, CRC Press, Boca Raton, FL, 1984, pp. 383–389.
16 K. Günther, J. Martens and M. Schickedanz, *Angew. Chem., Int. Ed. Engl.*, 23 (1985) 506.
17 W. H. Pirkle and T. C. Pochapsky, *Chem. Rev.*, 89 (1989) 347.

Journal of Chromatography, 514 (1990) 330–333
Elsevier Science Publishers B.V., Amsterdam

CHROM. 22 501

Note

Separation and identification of impurities in the dye intermediate 8-amino-1-naphthol-3,6-disulphonic acid (H-acid) by high-performance liquid chromatography

CHANDRASHEKHAR D. GAITONDE* and PRITA V. PATHAK

Applications and Methods Development Laboratory, Anamed Instruments (Pvt.) Ltd., Plot D-165, T.T.C. Area, M.I.D.C., New Bombay 400 706 (India)

(First received January 18th, 1990; revised manuscript received March 27th, 1990)

H-acid is the aminonaphthol derivative of naphthalenedisulphonic acid derived from the sulphonation of naphthalene under drastic conditions[1]. It is currently used particularly in the manufacture of other important dyes and dye intermediates, principally azo dyes, textile auxiliaries, food dyes, hair dyes and polymer coatings.

The determination of H-acid as obtained from the industrial process was effected in the past by paper[2] or thin-layer chromatography[3], which are time consuming with poor accuracy and precision. A spectrophotometric titration procedure which required derivatization was developed by Kuznetsov *et al.*[4]. High-performance liquid chromatography (HPLC) for the separation of different naphthalenesulphonic acids and their derivatives using sodium sulphate as the mobile phase additive was introduced by Jandera and co-workers[5–8]. A number of other HPLC methods for the separation of these compounds using efficient anion-exchange methods[9–13] and tetraalkylammonium salts as ion-pairing agents[14–23] have been developed. The application of sodium sulphate-containing mobile phases for the quality control of H-acid has been reported[24].

The present method involves reversed-phase HPLC using sodium sulphate as the mobile phase with UV detection. Its advantage is the separation of impurities without extraction or derivatization. The method is suitable for monitoring H-acid quality in routine production and allows the determination of purity levels of H-acid without interferences from other dye intermediates.

EXPERIMENTAL

Apparatus

The equipment consisted of a ConstaMetric III dual-piston reciprocating pump (LDC/Milton Roy, Riviera Beach, FL, U.S.A.) and a SpectroMonitor III Model 1204D UV–visible detector (LDC/Milton Roy) with a Rheodyne Model 7125 injector with a 20-μl fixed loop. The column (250 mm × 4.6 mm I.D.) contained Spherisorb S5

0021-9673/90/$03.50

ODS (5 μm) (LDC/Milton Roy). All chromatograms were recorded on an LDC/Milton Roy Model CI-10 computing integrator with a Sekonics (Tokyo, Japan) printer–plotter.

Reagents and chemicals

Dry, purified sodium sulphate (analytical-reagent grade) was obtained from E. Merck (Darmstadt, F.R.G.). Standards of H-acid, chromotropic acid (1,8-dihydroxynaphthalene-3,6-disulphonic acid), Koch acid (8-aminonaphthalene-1,3,6-trisulphonic acid) and omega acid (8-amino-3-naphthol-1,6-disulphonic acid) from Zenith Chemicals (Boisar, Tarapur, India) and G-salt (2-naphthol-6,8-disulphonic acid) and Nevile–Winther acid (1-naphthol-4-sulphonic acid) from Sahyadri Dyestuff (Pune, India). Doubly distilled, deionized water was used for preparing mobile phase, standard and sample solutions (500 μg/ml each). The samples of H-acid were supplied by Zenith Chemicals.

The mobile phase was 0.30 *M* sodium sulphate at a flow-rate of 1.0 ml/min. The UV–visible detector was set at 235 nm with a sensitivity of 0.05 a.u.f.s.

RESULTS AND DISCUSSION

In the manufacture of H-acid, isomers of disulphonic acids, namely chromotropic acid and omega acid, and Koch acid, a trisulphonic acid, are also formed in appreciable amounts. Their structures are shown in Fig. 1. Fig. 2 shows a typical chromatogram obtained from a sample of H-acid. Reference standards of Koch acid, omega acid and chromotropic acid were injected separately in order to confirm the identities of the components in the sample of H-acid. Unknown concentrations in the H-acid sample were obtained by using the equation:

$$\text{Unknown concentration } (X_i) = \text{response factor } (\text{RF})_{(X_i)} \times \text{area } (X_i)$$

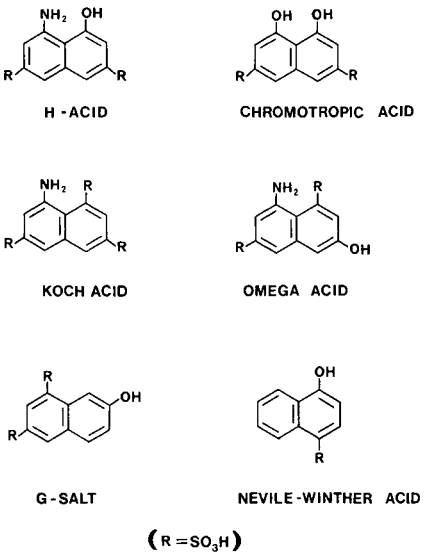

Fig. 1. Structures of dye intermediates.

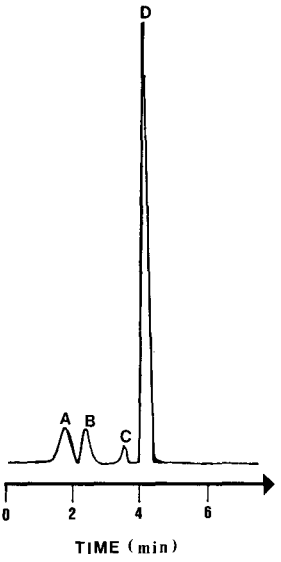

Fig. 2. Chromatogram of H-acid sample (500 μg/ml). Peaks: A = Koch acid; B = omega acid; C = chromotropic acid; D = H-acid.

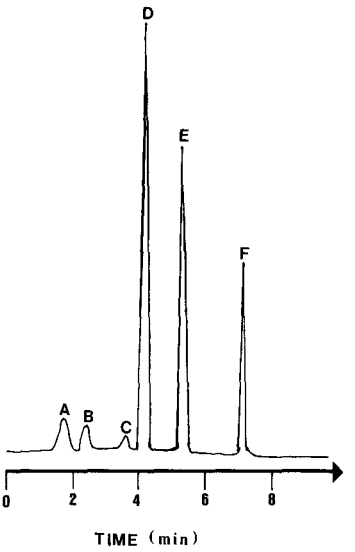

Fig. 3. Chromatogram of a mixture containing 500 μg/ml each of G-salt, Nevile–Winther acid and H-acid. Peaks: A = Koch acid; B = omega acid; C = chromotropic acid; D = H-acid; E = G-salt; F = Nevile–Winther acid.

where X_i is either H-acid or impurities present in H-acid, and $(RF)_{(X_i)}$ the response factor of H-acid or impurities.

TABLE I

SUMMARY OF METHOD VALIDATION DATA FOR THE DETERMINATION OF H-ACID OBTAINED FROM INDUSTRIAL SULPHONATION

Concentration added (μg/ml)	*Concentration found (μg/ml) (mean ± standard deviation, n = 15)*	*Relative standard deviation (%)*
Within-day variation:		
100	99.5 ± 0.11	0.11
150	148.8 ± 0.12	0.08
250	249.9 ± 0.14	0.05
350	350.0 ± 0.16	0.04
400	398.5 ± 0.19	0.04
Day-to-day variation:		
100	98.5 ± 0.10	0.10
150	149.5 ± 0.11	0.07
250	250.0 ± 0.13	0.05
350	348.9 ± 0.16	0.04
400	399.9 ± 0.20	0.05

The method was applied to the separation of other commonly used dye intermediates, G-salt and Nevile–Winther acid, the structures of which are shown in Fig. 1. A chromatogram resulting from a mixture of H-acid, G-salt (peak E) and Nevile–Winther acid (peak F) is shown in Fig. 3. Both the components added were well separated and do not interfere with H-acid or its impurities.

A calibration graph was prepared for H-acid and for impurities such as omega acid, chromotropic acid and Koch acid in the concentration range 100–500 μg/ml. The regression equations (with x = concentration of the component and y = peak area of the component) were $y = 0.0165x + 1.0485$, $y = 0.0819x + 0.8564$, $y = 0.0183x + 2.1325$ and $y = 0.0523x + 0.5529$ for H-acid, omega acid, chromotropic acid and Koch acid, respectively. Each point on the calibration graph was measured at least ten times. The detection limits were found to be 105 μg/ml for H-acid, 120 μg/ml for omega acid, 140 μg/ml for chromotropic acid and 110 μg/ml for Koch acid at 235 nm, 0.05 a.u.f.s.

Results of the method validation study for H-acid samples are shown in Table I. The reproducibility of the analytical procedure was obtained by determining the within-day and day-to-day variations. The relative standard deviations for five different concentrations in both instances varied between 0.04 and 0.11%, demonstrating excellent precision.

REFERENCES

1 N. Donaldson, *The Chemistry and Technology of Naphthalene Compounds*, Edward Arnold, London, 1972, Ch. 22.
2 S. B. Savrin, T. G. Akimova and A. N. Besesnev, *Zh. Anal. Khim.*, 33 (1978) 1813.
3 H. W. Langfeld and D. Ildiko, *Rev. Chim.*, 29 (1978) 873.
4 V. V. Kuznetsov, M. Benamor and O. M. Petrukhin, *Anal. Chim. Acta*, 186 (1986) 223.
5 P. Jandera, J. Churáček and J. Bartosova, *Chromatographia*, 13 (1980) 485.
6 P. Jandera and J. Churáček, *J. Chromatogr.*, 197 (1980) 181.
7 P. Jandera and H. Engelhardt, *Chromatographia*, 13 (1980) 18.
8 P. Jandera, J. Churáček and B. Taraba, *J. Chromatogr.*, 262 (1983) 121.
9 P. Jandera and J. Churáček, *J. Chromatogr.*, 86 (1973) 423.
10 M. Singh, *J. Assoc. Off. Anal. Chem.*, 58 (1975) 48; 60 (1977) 173, 1067, 1105.
11 J. J. Kirkland, *Anal. Chem.*, 43 (1971) 374.
12 E. S. Jacobs and R. J. Passarelli, *J. Chromatogr. Sci.*, 13 (1975) 153.
13 J. A. Schmit and R. A. Henry, *Chromatographia*, 3 (1970) 497.
14 S. Eksborg, P. O. Lagerstrom, R. Modin and G. Schill, *J. Chromatogr.*, 83 (1973) 99.
15 S. Eksborg and G. Schill, *Anal. Chem.*, 45 (1973) 2092.
16 J. H. Knox and G. R. Laird, *J. Chromatogr.*, 122 (1976) 17.
17 D. P. Wittmer, N. O. Nuessle and W. G. Haney, Jr., *Anal. Chem.*, 47 (1975) 1422.
18 E. Tomlinson, T. M. Jefferies and C. M. Riley, *J. Chromatogr.*, 159 (1978) 315.
19 R. Gloor and F. L. Johnson, *J. Chromatogr. Sci.*, 15 (1977) 413.
20 C. Prandi and T. Venturini, *J. Chromatogr. Sci.*, 19 (1981) 308.
21 H. V. Ehmcke, H. Kelker, K. H. König and H. Ullner, *Fresenius' Z. Anal. Chem.*, 294 (1979) 251.
22 K.-S. Lee and T.-L. Yeh, *J. Chromatogr.*, 260 (1983) 97.
23 A. Kraslawski and J. M. Kulawinek, *J. Chromatogr.*, 254 (1983) 322.
24 S. Wang, *Fenxi Huaxue*, 11 (1983) 836.

Journal of Chromatography, 514 (1990) 334–342
Elsevier Science Publishers B.V., Amsterdam

CHROM. 22 532

Note

Separation of peracetylated flavanoid and flavonoid polyphenols by normal-phase high-performance liquid chromatography on a cyano-silica column and their determination

MARCO VINCENZO PIRETTI* and PAOLA DOGHIERI[a]

Dipartimento di Biochimica, Sezione di Biochimica Veterinaria, Università di Bologna, Via Zanolini 3, 40126 Bologna (Italy)

(First received October 25th, 1989; revised manuscript received April 23rd, 1990)

The characteristics of many plant products, *i.e.*, taste, palatability, nutritional value, pharmacological and toxic effects and microbial decomposition, depend substantially on their polyphenol content. For this reason, studies on such widespread natural compounds are not only of scientific interest, but also of considerable practical significance. In the last 10 years, in this journal alone, at least 40 papers relating to high-performance liquid chromatographic (HPLC) separations of flavanoid and flavonoid polyphenols have been published. Usually the separations were carried out by reversed-phase HPLC, and only in about 10 instances was the normal-phase mode used. Recently, however, Cooper and Smith[1,2] published two important papers describing the advantages of a cyanopropyl-bonded phase as a normal phase. This phase, in fact, seems to be a "universal phase"[2], which can exhibit a different character depending on the polarity of the liquid system, which normally consists of a binary mixture of *n*-hexane and another more polar solvent[1,2].

In this work we studied the effectiveness and versatility of this phase for the separation of complex mixtures of paracetylated polyphenols.

EXPERIMENTAL

Materials

In the course of previous investigations on polyphenols from grapes (*Vitis vinifera*), we were able to isolate in the pure state, as their corresponding peracetyl derivatives, (+)-catechin, (−)-epicatechin, kaempferol glucoside (glucose position not known), quercetin 3-glucoside (isoquercitrin) and the four procyanidins B_1–B_4[3–7]. (−)-Epigallocatechin, (−)-epicatechin 3-gallate and (−)-epigallocatechin 3-gallate

[a] Holder of a fellowship from Tecnofarmaci SpA, Pomezia (Rome).

0021-9673/90/$03.50

were recently isolated from green tea and (+)-gallocatechin was obtained from *Trebbiano* grapes[5]. Apigenin and tricin were isolated from *Alfalfa*[8], persicoside was extracted from the bark of *Prunus persica*[9] and naringin was supplied by Fluka (Buchs, Switzerland).

Hesperetin and naringenin, which are the aglycones of persicoside and naringin, respectively, were obtained by acidic hydrolysis of the corresponding glycoside according to Harborne[10]. Quercetin and kaempferol were prepared in the same way.

Polyphenol acetylation

A 100-mg amount of each polyphenolic compound was dissolved in a mixture of 150 μl of anhydrous pyridine and 500 μl of anhydrous acetic anhydride. The solutions were allowed to stand at room temperature. After *ca.* 12 h the solutions were poured into ice–water and the precipitated acetates were recovered by filtration. Incomplete acetylations were never observed.

Thin-layer chromatography (TLC)

Silica gel plates (20 × 20 cm, thickness 250 nm; Stratocrom SI RS, Carlo Erba, Milan, Italy) were employed and were developed with benzene–acetone (8:2) at room temperature. After development, the plates were sprayed with sulphuric acid–40% formaldehyde (9:1, v/v) and heated at 150°C until coloured spots appeared.

HPLC conditions

All measurements were obtained using a Varian LC 5060 ternary liquid chromatograph equipped with a 10-μl loop, combined with a Varian UV-100 variable-wavelength detector. The retention times and the quantitative parameters were determined with a Spectra-Physics Model 4270 integrator. The data system output was fixed at 2.0 absorbance/V and the integrator attenuation was maintained at × 8.

A 5-μm Spherisorb S-5 Nitrile column (250 × 4.6 mm I.D.) (Phase Separations, Queensferry, U.K.) was used, coupled with a precolumn (100 × 4.6 mm I.D.) packed with Partisil-10 PAC (Whatman, Clifton, NJ, U.S.A.).

n-Hexane (A) and ethyl acetate (B) solvents of HPLC grade were supplied by Merck-Bracco (Milan, Italy). Two different elution profiles were chosen for the separations of the mixtures of the above-mentioned compounds: the first was isocratic with A–B (60:40) (Fig. 1), and the second was programmed as follows: 0–15 min, isocratic with A–B (60:40); 15–17 min, linear gradient to A–B (55:45); 17–30 min (end of chromatogram), isocratic with A–B (55:45) (Fig. 2). Separations were usually performed by injecting 10-μl aliquots of each sample in ethyl acetate solution, using a flow-rate of 1 ml/min. Peaks were monitored at 278 nm.

Regeneration of column activity

When the column performance deteriorates, *i.e.* the separations are no longer optimum, the original activity can be regenerated by washing the column with ethyl acetate (flow-rate 1 ml/min) for 1 h.

Calibration graphs

All the quantitative determinations were performed under isocratic conditions

with A–B (60:40). For each pure compound, available in a sufficient amount, ten solutions were prepared with concentrations of 500, 400, 250, 200, 100, 75, 50, 25, 10 and 5 mg/l. The calibration graphs were constructed by plotting the peak-area counts of each chromatographic peak *versus* the corresponding concentration. In our graphical representations, the following units were chosen: 1 mm on the abscissa = 4 mg/l and 1 mm on the ordinate = 2000 peak-area counts. The slopes (m) of the curves $y = mx + q$ are given in Table II, together with the intercepts (q) and with the corresponding correlation coefficients; these parameters were determined according to the least-squares calibration mode. For this purpose, only the experimental data were used, and the points 0,0 were never considered.

Extraction of polyphenolic constituents from the peel of Golden Delicious apples and green tea

From 2 kg of Golden Delicious apples 150 g of peel were obtained, which was cut into small pieces and immediately immersed in 1500 ml of methanol. The mixture was heated at 30°C for 10 min with stirring and left for 24 h at room temperature. After filtration and distillation of the methanol, the residue was dissolved in 500 ml of distilled water and extracted five times with 100-ml portions of ethyl acetate. The remaining aqueous solution was discarded and the organic phase was dried over anhydrous sodium sulphate.

The solvent was then removed under vacuum and the residue was dispersed in 50 ml of chloroform, in which polyphenols are insoluble. After filtration, 360 mg of polyphenols were recovered.

One third of the material extracted was acetylated and analysed by HPLC (Fig. 3a). The remaining part was hydrolysed with ethanol–2 *M* hydrochloric acid according to Harborne[10].

After evaporation of the ethanol, the polyphenol aglycones were extracted from the reaction mixture with ethyl acetate as described above. The corresponding peracetylated material weighed 160 mg; its HPLC profile is shown in Fig. 3b.

In the same way, from 10 g of green tea leaves 1.3 g of polyphenols were extracted. After acetylation of such material 1.5 g of the peracetyl derivative was obtained, the composition of which determined by HPLC is shown in Fig. 3c.

Quantitative determinations

A 100-mg amount of peracetylated material from green tea was dissolved in ethyl acetate and diluted to 50 ml with the same solvent in a volumetric flask. The average values of the peak-area counts, recorded for each component for three successive 10-μl injections, are reported in Table III, together with the corresponding concentrations determined using our calibration graphs. In Table III are also reported the calculated percentage concentration of each component in its free state.

A 25-mg amount of the peracetyl aglycone (quercetin) isolated from the apple-peel extract was diluted to 50 ml with ethyl acetate in a volumetric flask. The average value of the peak-area counts, obtained as described above for the only peak in the chromatogram (Fig. 3b), was 175 371. According to our calibration graph this value corresponds to 30 mg/l of peracetylquercetin in the prepared solution. Hence, one can calculate that the polyphenolic material extracted from apple peel contains 4.3 mg of free quercetin per kg of apples or 5.7 mg per 100 g of peel.

RESULTS

Twenty peracetylated polyphenolic compounds, representative of the various classes (3-flavanols, 4-flavanones, flavones and 3-flavonols) were isolated as their peracetyl derivatives in the course of previous investigations[3–9]. This provided the opportunity to study their separation by normal-phase HPLC using a column packed with a cyanopropyl-bonded phase.

Figs. 1 and 2 show the HPLC profiles obtained under two different separation conditions, with isocratic elution (Fig. 1) and programmed elution (Fig. 2). The separation of peracetylated polyphenolic mixtures extracted from some vegetable matters is reported in Fig. 3.

The data given in Table I show the good agreement between the TLC separation of the above-mentioned polyphenolic compounds on silica gel plates and their corresponding HPLC separation by programmed elution. In Table II the analytical parameters are reported, by means of which it is possible to construct the calibration graphs, useful for performing quantitative determinations of some of the compounds under examination. Using such calibration graphs the quantitative composition of the polyphenols contained in a sample of green tea was calculated. The results obtained employing 10 g of vegetable matter (Table III) are in good agreement with those in the

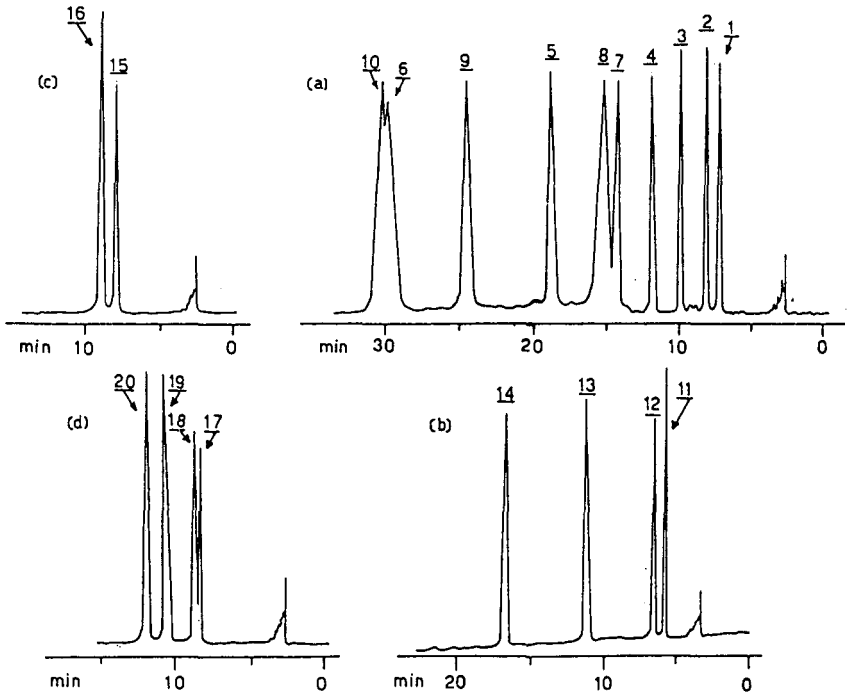

Fig. 1. Separation of selected mixtures of peracetylated polyphenolic compounds by isocratic elution (see Experimental). (a) 3-Flavanols; (b) 4-flavanones; (c) flavones; (d) 3-flavonols. The chromatograms were obtained by injection of 10 μl of a solution containing amounts of each peracetylated polyphenol sufficient to produce chromatographic peaks higher than 50% of full-scale. For peak identification, see Table I.

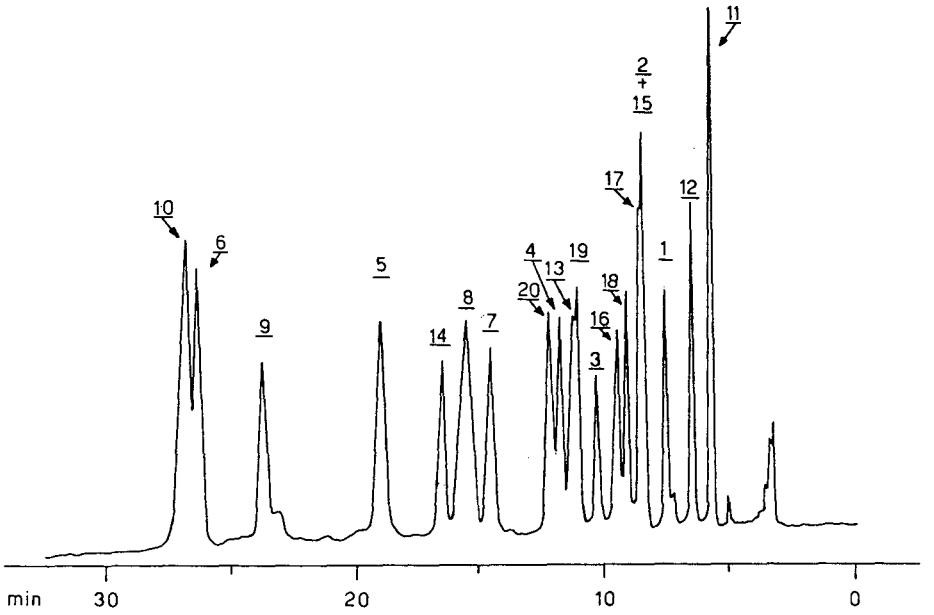

Fig. 2. Separation of a mixture of all the peracetylated polyphenolic compounds by programmed elution (see Experimental). The chromatogram was obtained by injection of 10 μl of a solution containing amounts of each peracetylated polyphenol sufficient to produce chromatographic peaks higher than 50% of full-scale. For peak identification, see Table I.

literature[11]. The amount of quercetin aglycone contained in apple peel was determined in the same way.

DISCUSSION

The results obtained clearly show that the cyano-silica column used to separate the peracetyl derivatives of flavanoid and flavonoid polyphenols by normal-phase HPLC under the conditions described here offers a good performance. Because of the necessity to evaluate simultaneously compounds with UV maxima at different wavelengths[12], 278 nm was chosen as a compromise. This wavelength is intermediate between the absorbance maxima of the acetylated flavones (*ca.* 270 nm) and the acetylated flavanones and flavonols (*ca.* 300 nm) and is sufficiently distant from that of ethyl acetate (256 nm), which is a component of the mobile phase used. The small amounts of substance (25–100 ng) necessary to produce a peak intensity corresponding to 5% of full-scale (Table II) suggest that the wavelength chosen allows satisfactory qualitative and quantitative evaluations.

We shall now discuss the reasons for choosing *n*-hexane–ethyl acetate in order to separate the acetylated polyphenols on a cyano-silica phase. According to the solvent classification proposed by Snyder[13], nitriles and esters belong to the same group VIa, which within the triangular diagram[13] occupies an almost equidistant position from the two oblique sides, shifted towards the base. In accord with their

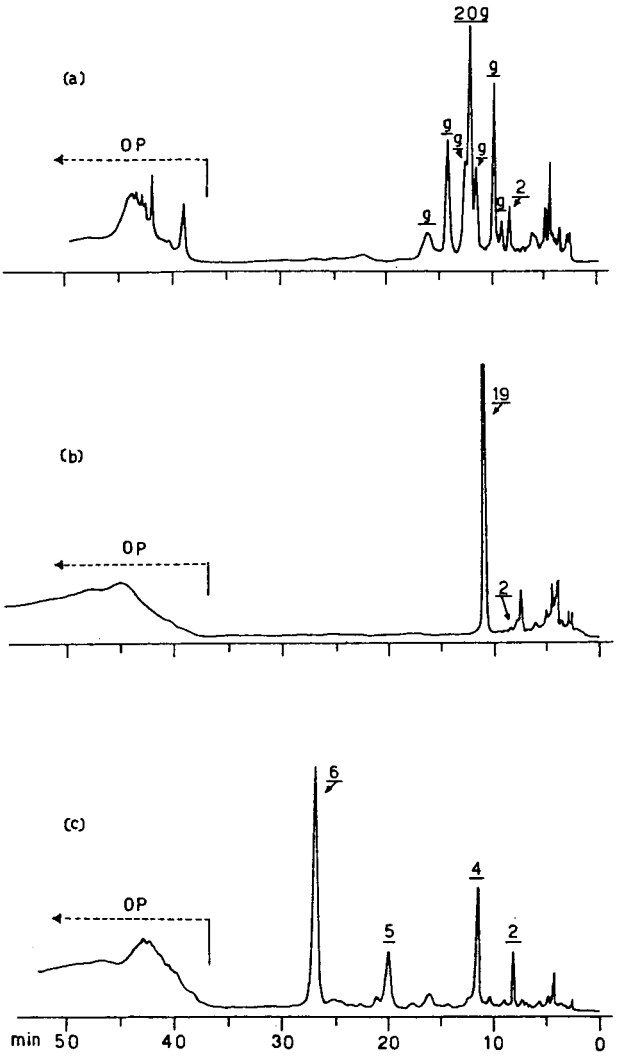

Fig. 3. Separation of peracetylated polyphenolic mixtures extracted from vegetable matter by programmed elution (see Experimental). (a) Quercetin glycosides from Golden Delicious apple peel. Peak 20 g corresponds to quercetin 3-glucoside (isoquercitrin); the others, indicated by g, are unknown glycosides. (b) Aglycones (quercetin only) of the above mixture. (c) Polyphenolic mixture extracted from green tea. The chromatograms were obtained by injection of 10 μl of a solution containing amounts of each peracetylated polyphenol sufficient to produce chromatographic peaks higher than 50% of full-scale. For peak identification in (b) and (c), see Table I.

limited tendency to act as proton donors or proton acceptors, these molecules exhibit low x_e and x_d values (0.33–0.34 and 0.26–0.25, respectively), while their x_n values (0.41 and 0.42, respectively) are markedly higher, as would be expected from their strong tendency to give rise to dipole–dipole interactions owing to their relatively high dipolar moment.

TABLE I

COMPARISON OF THE TLC AND HPLC BEHAVIOUR OF THE PERACETYL DERIVATIVES OF THE POLYPHENOLIC COMPOUNDS UNDER INVESTIGATION

No.	*Peracetyl derivative*	*TLC*[a]: R_F	*HPLC*[b]	
			Retention time (min)	k'[c]
1	(+)-Catechin	0.44	7.4	1.31
2	(−)-Epicatechin	0.40	8.4	1.62
3	(+)-Gallocatechin	0.37	10.2	2.19
4	(−)-Epigallocatechin	0.33	11.7	2.66
5	(−)-Epicatechin 3-gallate	0.26	19.9	5.22
6	(−)-Epigallocatechin 3-gallate	0.18	26.4	7.25
7	Procyanidin B_1	0.31	14.7	3.59
8	Procyanidin B_2	0.28	15.7	3.91
9	Procyanidin B_3	0.24	23.7	6.40
10	Procyanidin B_4	0.20	26.9	7.40
11	Naringenin	0.52	5.5	0.72
12	Hesperetin (persicoside aglycone)	0.50	6.3	0.97
13	Naringin	0.35	11.1	2.47
14	Persicoside (hesperetin glucoside)[d]	0.33	16.5	4.16
15	Apigenin	0.40	8.4	1.62
16	Tricin	0.39	9.4	1.94
17	Kaempferol	0.47	8.5	1.66
18	Kaempferol glucoside[d]	0.37	9.0	1.81
19	Quercetin	0.39	10.9	2.40
20	Isoquercitrin	0.32	12.2	2.81

[a] The conditions used for the TLC separation are described under Experimental.
[b] The data reported refer to programmed elution (see Experimental).
[c] Capacity factor.
[d] Glucose position not known.

In spite of their different polarities ($P' = 6.2$ for nitriles and 4.3 for esters)[13], these two classes of compounds exhibit almost identical selectivities. If the interaction between the solute and uncoated silanol groups can be disregarded, the interaction between the cyano-silica stationary phase and the solute molecules (acetylated polyphenols, *i.e.*, polyesters) must be attributed mainly to dipole–dipole interactions among molecules with different polarities but almost identical selectivities. This is why we considered that the most suitable eluent for separating the test compounds was a binary mixture of *n*-hexane (solvent of the group 0 according to Snyder) and ethyl acetate which, as an ester, according to Snyder belongs to the same group VIa as the solute and the stationary phase. The above mixture indeed possesses the same selectivity as the stationary phase and the solute with a more or less marked polarity depending on the concentration of ethyl acetate.

As shown by the results, our choice fully met the expectations. In order to eliminate possible overlappings which could originate during the separation of complex mixtures, it is necessary only to modify slightly the elution mixture considered to be the optimum, *i.e.*, *n*-hexane–ethyl acetate (60:40) (Fig. 2); in this way, only the polarity of the elution mixture and not its selectivity is changed.

TABLE II

HPLC DETERMINATION OF SOME PERACETYLATED POLYPHENOLS BY ISOCRATIC ELUTION

Slope, intercept and correlation coefficient (r) of the calibration graphs $y = mx + q$.

Compound[a]	*Isocratic retention time (min)*[b]	*m*	*q*	*r*	*5% amount*[c] *($g \times 10^{-9}$)*
1	7.4	1.73	− 2.80	0.9993	100
2	8.4	1.28	− 0.17	0.9988	100
4	11.7	1.19	+ 0.13	0.9990	100
5	19.9	1.25	− 1.84	0.9993	100
6	29.8	1.17	+ 0.35	0.9998	100
7[d]	14.8	1.46	− 0.03	0.9988	100
8[d]	15.8	1.17	− 2.06	0.9965	100
9[d]	24.7	1.60	− 5.31	0.9993	100
10[d]	30.4	1.14	+ 4.98	0.9983	100
11	5.5	1.57	− 0.86	0.9998	50
13	11.1	2.97	+ 1.60	0.9986	50
14	16.8	3.55	+ 3.49	0.9995	50
15	8.4	18.96	+20.67	0.9996	25
16	9.4	11.32	− 7.08	0.9978	25
18	9.0	4.21	− 0.08	0.9981	50
19	10.9	11.60	+ 1.04	0.9996	25
20	12.2	5.63	+ 0.63	0.9980	50

[a] Compound numbers as in Table I.

[b] The retention times of compounds 6, 8, 9, 10 and 14 differ from those given by programmed elution (*cf.*, Table I). With isocratic elution these compounds show capacity factors of 8.31, 3.94, 6.72, 8.50 and 4.25, respectively.

[c] Amount sufficient to produce a peak intensity corresponding to 5% of full-scale.

[d] For the calibration graphs for these compounds the three most dilute solutions were disregarded (see Experimental).

TABLE III

QUANTITATIVE COMPOSITION OF THE POLYPHENOLIC CONSTITUENTS OF GREEN TEA

Compound[a]	*Peak-area counts*[b]	*Concentration as peracetyl derivative (mg/l)*	*Concentration as free compound (mg/l)*	*Content (%)*
1	5260	12	7	1
2	60 082	94	55	6
4	178 174	299	164	18
5	153 302	251	150	17
6	535 737	915	528	58

[a] Compound numbers as in Table I.

[b] Determined using a Spectra-Physics 4270 data system as integrator.

With complex mixtures (Fig. 1) where separation under isocratic conditions is not feasible, we believe that modification of the elution mixture at very short intervals (1–2 min) is more suitable than the use of a linear gradient for long periods, thus obtaining a step-like elution profile through a succession of isocratic states.

The observation that the performance of the column remains almost unchanged during use lends support to our choice of the eluent system for the separation of these mixtures. When a reduction in the retention times or a poor resolution of a pair of substances which were previously completely resolved was observed, the original activity could be regenerated simply by washing the column with ethyl acetate.

The column used for the separations described in this paper has been used every day in our laboratory for more than 4 years, and under the above conditions has retained its full starting efficiency.

ACKNOWLEDGEMENT

The authors are grateful to Dr. Ezio Bombardelli (Indena S.p.A., Milan, Italy) for the assistance in preparing the manuscript.

REFERENCES

1 W. T. Cooper and P. L. Smith, *J. Chromatogr.*, 355 (1986) 57.
2 P. L. Smith and W. T. Cooper, *J. Chromatogr.*, 410 (1987) 249.
3 K. Weinges and M. V. Piretti, *Justus Liebigs Ann. Chem.*, 748 (1971) 218.
4 K. Weinges and M. V. Piretti, *Ann. Chim. (Rome)*, 62 (1972) 29.
5 M. V. Piretti, M. Ghedini and G. Serrazanetti, *Ann. Chim. (Rome)*, 66 (1976) 429.
6 M. V. Piretti, M. Ghedini and G. Spezialetti, *Ann. Chim. (Rome)*, 66 (1976) 761.
7 M. V. Piretti, G. Serrazanetti and R. Pistore, *Ann. Chim. (Rome)*, 70 (1980) 615.
8 M. V. Piretti, F. Zeli and R. Pistore, *Gazz. Chim. Ital.*, 112 (1982) 47.
9 M. V. Piretti, M. Arias and S. Sansavini, *Frutticoltura*, 51 (1989) 53.
10 J. B. Harborne, *Phytochemistry*, 4 (1965) 107.
11 K. Weinges, W. Bähr, W. Ebert, K. Göritz and H. D. Marx, L. Zechmeister (Editor), *Progress of the Chemistry of Organic Natural Products*, Springer, Vienna and New York, 1969, pp. 158–260.
12 R. Galensa and K. Herrmann, *J. Chromatogr.*, 189 (1980) 217.
13 L. R. Snyder, *J. Chromatogr.*, 92 (1974) 223.

Journal of Chromatography, 514 (1990) 343–347
Elsevier Science Publishers B.V., Amsterdam

CHROM. 22 595

Note

High-performance liquid chromatographic analysis of octopinic acid, lysopine and nopalinic acid as sensitive indicators of *Agrobacterium*-induced crown gall tumours

J. L. FIRMIN
John Innes Institute and AFRC Institute of Plant Science Research, Colney Lane, Norwich NR4 7UH (U.K.)
(First received January 12th, 1990; revised manuscript received May 15th, 1990)

Octopinic acid, lysopine and nopalinic acid are members of a group of iminocarboxylic acids collectively termed opines (Fig. 1) which are characteristically found in crown gall tumours —plant tumours induced by the soil-living bacterium *Agrobacterium tumefaciens*[1]. Depending on the strain of *A. tumefaciens* which initiated the tumour, the tissue will contain either the octopine family (I–IV) or the nopaline family (V and VI). Octopine also occurs in some marine invertebrates[2].

The presence of opines in plant tissue is generally taken to indicate that the tissue has been genetically transformed by *A. tumefaciens*. Thus opines are useful markers of transformation. Opines occur in *Agrobacterium*-transformed plant tissue at levels from *ca.* 20 μg/g dry weight (d.w.) (octopine) to *ca.* 20 mg/g d.w. (nopaline)[3]. The validity of using opines as markers of transformation has been questioned by several workers[4–6]. Thus it has been reported that untransformed soybean callus can synthesise nopaline when cultured on a medium supplemented with arginine[6]. In addition lysopine has been reported to occur in untransformed tomato and tobacco tissue[4]. However, there are no reports of untransformed plant tissue containing, or able to synthesize, either octopinic acid or nopalinic acid.

Detection of opines in transformed plant tissue has generally relied on detection of the guanidino group of octopine or nopaline using either the Sakaguchi reagent[7] or the more sensitive fluorescence reagent phenanthrenequinone[8], after paper chromatography or paper electrophoresis of the tissue extract.

The non-guanidino opines octopinic acid, lysopine and nopalinic acid can be detected on paper chromatograms using ninhydrin[9–11] and ninhydrin has also been used in conjunction with ion-exchange column chromatography to detect octopinic acid and lysopine[12]. The detection limits for these opines are not reported.

Gas chromatography of the heptafluorobutyric-*n*-propyl derivatives of the non-guanidino opines has been used[3]; however, this method requires a time-consuming derivatization step and does not have the sensitivity of the fluorescence method.

This paper reports the detection of octopinic acid, lysopine and nopalinic acid in

0021-9673/90/$03.50

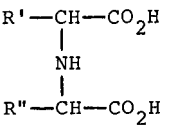

	OPINE	R'	R"
I	Octopine	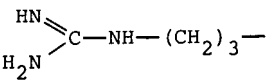	CH_3—
II	Octopinic acid	H_2N—$(CH_2)_3$—	CH_3—
III	Lysopine	H_2N—$(CH_2)_4$—	CH_3—
IV	Histopine	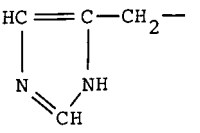	CH_3—
V	Nopaline	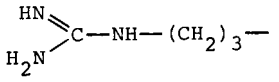	HO_2C—$(CH_2)_2$—
VI	Nopalinic acid	H_2N—$(CH_2)_3$—	HO_2C—$(CH_2)_2$—

Fig. 1. Structures of the iminocarboxylic opines found in crown gall tumours. Depending on the strain of *A. tumefaciens* which initiated the tumour, the tissue will contain either the octopine family (I–IV) or the nopaline family (V and VI).

transformed plant tissue, using reversed-phase separation of the *o*-phthaldialdehyde (OPA) derivatives of these opines.

MATERIALS AND METHODS

Octopine and octopinic acid were obtained from Sigma. Lysopine was synthesized by hydrolysis of homooctopine with barium hydroxide[13]. Nopaline was synthesized as described by Cooper and Firmin[14]. Nopalinic acid was synthesized by hydrazinolysis of nopaline[10]. Paper chromatography and detection of the non-guanidino opines with ninhydrin was carried out as described in ref. 10.

Tissue extraction and derivatization

Samples [*ca.* 10 mg fresh weight (f.w.)] of plant tissue were extracted by grinding with acid-washed sand and aqueous ethanol (70%, v/v, 20 μl/mg f.w. of tissue). After

centrifugation (10 000 *g*, 5 min) the supernatant was stored at −20°C until required. OPA derivatives were prepared immediately prior to injection onto the column by mixing 10 μl of the tissue extract with 90 μl of OPA reagent [OPA reagent is 10 ml, 0.5 *M*, pH 10.4 potassium borate + 100 μl OPA solution (80 mg/ml methanol) + 20 μl 2-mercaptoethanol]; 10–100 μl of the derivative was injected onto the column. For further details about preparation and stability of the OPA reagent see ref. 15.

High-performance liquid chromatography (HPLC)

Separation of the OPA derivatives was carried out on a reversed-phase C_8 column (Brownlee RP300, 7 μm), 25 cm × 4.6 mm I.D., fitted with a 3 cm × 4.6 mm I.D. guard column. The column was eluted with a pH 6.8 citrate (0.1 *M*, pH adjusted with KOH) methanol gradient (see Fig. 2 for details) at 1 ml/min. OPA derivatives in the eluate were detected by fluorescence (excitation 340 nm, emission 455 nm, bandwidth 10 nm).

RESULTS AND DISCUSSION

The fluorescence traces obtained from extracts of normal and *Agrobacterium*-transformed plant tissue after derivatization with OPA are shown in Fig. 2. Gradient elution was required to separate the opines from other amino acids present in the extract. The OPA derivatives of the opines show a similar instability to that found with the OPA derivatives of ornithine and lysine; thus the derivatized sample should be injected onto the column immediately after it is prepared.

The short half life of the OPA derivatives of octopinic acid, lysopine and nopalinic acid can be useful in the event of ambiguity in peak identification since delaying injection of the derivatized sample by 15 min results in a three-fold decrease in the size of the opine peak relative to peaks given by most other amino compounds *e.g.* glutamate and aspartate. Replacing 2-mercaptoethanol with ethanedithiol, an alternative reducing agent which is reported to increase the stability of several OPA-amino acids, including OPA-ornithine and lysine[16], did increase the stability of OPA-octopinic acid, -lysopine and -nopalinic acid, presumably for the same reasons that OPA-ornithine and -lysine are stabilized. However, the resulting increased retention times together with some loss of resolution would require modification of the elution conditions. N-Acetyl-L-cysteine, another alternative reducing agent[17], also increased the stability of the OPA-opine derivatives but resulted in loss of resolution of the OPA-opines from other amino acids present in the extract.

The guanidino opines octopine and nopaline do not react with OPA under the conditions described here to yield UV-absorbing or fluorescent derivatives.

Reducing the pH of the citrate buffer below 6.8 resulted in loss of resolution of the opines from other amino acids. Octopinic acid, lysopine and nopalinic acid had a response factor (normalized to glutamic acid) of *ca.* 0.5. The limit of detection for these opines was *ca.* 0.5 pmol. By contrast, the limit of detection for these opines with ninhydrin on paper was *ca.* 20 nmol.

The method described in this paper provides a rapid and sensitive assay for the non-guanidino opines octopinic acid, lysopine and nopalinic acid, and has been used successfully with several other plant species *e.g.* sunflower, pea, flax and tobacco.

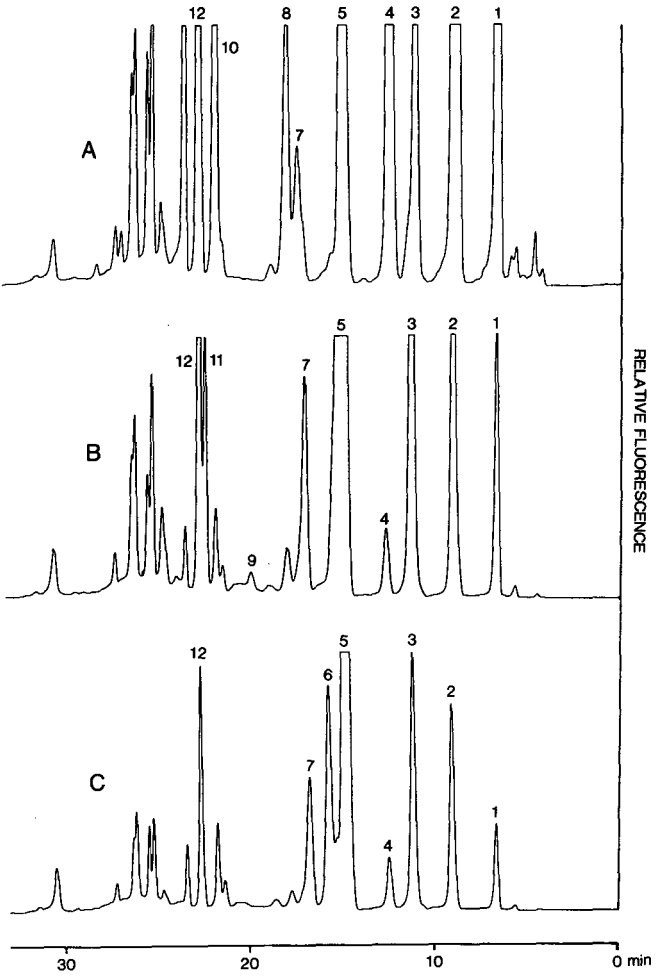

Fig. 2. HPLC of OPA derivatives from (A) untransformed mint (*Mentha citrata*), (B) mint transformed with an octopine strain of *A. tumefaciens* (strain A384) and (C) mint transformed with a nopaline strain of *A. tumefaciens* (C58). The traces shown are equivalent to 50 μg f.w. of tissue with the exception of sample B, which was injected at a higher level (100 μg f.w.) because of the lower relative concentration of octopinic acid. The column was eluted with a pH 6.8 (0.1 *M*) citrate–methanol (B) gradient: 0 min: 20% B, 13.2 min: 35% B, 19.8 min: 75% B, 26.4 min: 75% B, 33 min: 20% B. A further 10 min were allowed for re-equilibration. All increments are linear. Peaks: 1 = aspartate; 2 = glutamate; 3 = asparagine, 4 = serine; 5 = glutamine; 6 = nopalinic acid; 7 = arginine; 8 = threonine; 9 = octopinic acid; 10 = alanine; 11 = lysopine; 12 = γ-aminobutyric acid.

ACKNOWLEDGEMENTS

I am grateful to Andrew Spenser, AFRC Institute of Food Research, Norwich, U.K., for supplying crown gall tumours and untransformed plant tissue, and to Dr. J. Tempé, Institut des Sciences Végétales, Centre National de la Recherche Scientifique, France, for supplying a sample of homooctopine.

REFERENCES

1 A. Petit, D. Chatal, G. A. Dahl, J. G. Ellis, P. Guyon, F. Casse-Delbart and J. Tempé, *Mol. Gen. Genet.*, 190 (1983) 204.
2 E. Moore and D. W. Wilson, *J. Biol. Chem.*, 119 (1937) 573.
3 I. M. Scott, J. L. Firmin, D. N. Butcher, L. M. Searle, A. K. Sogeke, J. Eagles, J. F. March, R. Self and G. R. Fenwick, *Mol. Gen. Genet.*, 176 (1979) 57.
4 E. W. Seitz and R. M. Hochster, *Can. J. Bot.*, 42 (1964) 999.
5 M. F. Wendt-Gallitelli and I. Dobrigkeit, *Z. Naturforsch., C*, 28C (1973) 768.
6 P. Christou, S. G. Platt and M. C. Ackermann, *Pl. Physiol.*, 82 (1986) 218.
7 R. Acher and C. Crocker, *Biochim. Biophys. Acta*, 9 (1952) 704.
8 S. Yamada and H. A. Itano, *Biochim. Biophys. Acta*, 130 (1966) 538.
9 A. Ménagé and G. Morel, *C.R. Acad. Sci. Paris*, t 261 (1965) 2001.
10 J. L. Firmin and G. R. Fenwick, *Phytochemistry*, 16 (1977) 761.
11 K. Biemann, C. Lioret, J. Asselineau, E. Lederer and J. Polonsky, *Bull. Soc. Chim. Biol.*, 42 1960) 979.
12 C. Lioret, *Physiol. Veg.*, 4 (1966) 89.
13 J. Tempé and G. Morel, *Ann. Physiol. Veg.*, 8 (1966) 75.
14 D. Cooper and J. L. Firmin, *Org. Prep. Proced. Int.*, 9 (1977) 99.
15 P. Lindroth and K. Mopper, *Anal. Chem.*, 51 (1979) 1667.
16 S. S. Simons, Jr. and D. F. Johnson, *Anal. Biochem.*, 82 (1977) 250.
17 N. Nimura and T. Kinoshita, *J. Chromatogr.*, 352 (1986) 169.

Journal of Chromatography, 514 (1990) 348–354
Elsevier Science Publishers B.V., Amsterdam

CHROM. 22 596

Note

High-performance liquid chromatographic determination of several quinolone antibacterials in medicated fish feed

JOHN F. BAUER*, SPENCER HOWARD and ANDREW SCHMIDT
PPD Analytical Research Department, Abbott Laboratories, North Chicago, IL 60064-4000 (U.S.A.)
(First received March 6th, 1990; revised manuscript received May 17th, 1990)

Aquaculture is growing as a commercial source of consumable fish products. During the growth stages of aquaculture, antibacterial agents are used to prevent the development of gram-negative bacterial infections in the fish.

Quinolone analogues of nalidixic acid[1] (I), 1-ethyl-1,4-dihydro-4-oxo-7-methyl-1,8-naphthyridine-3-carboxylic acid, are wide-spectrum antibacterial agents. Some of these are being developed for use in aquaculture. A validated analytical procedure was developed to measure various concentrations of the quinolones in feed. Feed–drug admixtures were studied to determine effectiveness and dosage levels for various fish species.

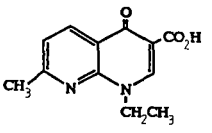

I

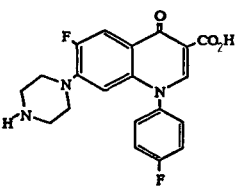

II

Although methodology for various quinolones have been reported in several matrices including fish tissue[2–6], none has been reported for feed. Animal feeds, in general, are an admixture of several grains and soy products containing numerous polar and non-polar compounds. This can often lead to the co-extraction of interfering components along with the drug of interest. In order to minimize this problem, it is preferable to extract the drug from the feed using a solvent of moderate polarity such as acetonitrile. Additionally the natural products present in the feed provide favorable binding sites for many drugs which often makes quantitative extraction difficult.

Sarafloxacin (II) is a quinolone which is a potent wide-spectrum antibacterial. Sarafloxacin is presently being used successfully in aquaculture trials.

Sarafloxacin is quite insoluble in water (0.3 mg/ml) and in most organic solvents (< 1 mg/ml) and therefore presents a formidable analytical problem when mixed with

0021-9673/90/$03.50

feed. Sarafloxacin will be commercially available as a pre-mix with soy flour which is then mixed with the appropriate fish feed (trout, salmon and catfish) before feeding. It was therefore necessary to develop analytical methodology for quantitating sarafloxacin in both the pre-mix and in the various fish feeds.

Due to the low solubility of sarafloxacin in organic solvents, it is impossible to use moderate-polarity solvents such as acetonitrile to extract the drug from the feed. As a result of an unusual synergistic effect, however, sarafloxacin is significantly more soluble in an equal mixture of acetonitrile and water (>4 mg/ml) than in either of the individual solvents. This equal mixture of acetonitrile and water was chosen as the extraction solvent, even though it resulted in the extraction of numerous other components from the feeds. The extraction was further complicated by the fact that sarafloxacin is amphoteric and has a tendency to bind to the feed.

This paper presents validated methods developed for both the soy flour pre-mix of sarafloxacin and the various fish feed admixtures.

MATERIALS AND METHODS

Instrumentation and reagents

A Polytron Model PT 35/4 homogenizer (Brinkmann Instruments, Westbury, NY, U.S.A.) was used for sample extraction. The column liquid chromatography (LC) system used throughout this work consisted of a Model SIL-6A autosampler (Shimadzu, Kyoto, Japan) and a Spectroflow 783 variable-wavelength UV detector (Kratos Analytical Instruments). Chromatograms were processed using a Chromatopac Model C-R4A integrator (Shimadzu). A C_{18} chromatographic column (10 μm, 25 cm × 4.6 mm I.D.) was used (Alltech, Deerfield, IL, U.SA.). Chemicals and solvents were reagent grade and high-performance liquid chromatography (HPLC) grade, respectively. Bulk sarafloxacin and difloxacin were prepared at Abbott Laboratories, North Chicago, IL, U.S.A. Bulk ciprofloxacin and norfloxacin were purchased from Miles Pharmaceutical Division, New Haven, CT, U.S.A. and Merck, Sharpe and Dohme, West Point, PA, U.S.A., respectively. The catfish, salmon and trout feed mixtures were prepared at Clear Springs Trout Co., Buhl, ID, U.S.A. and Mississippi State University, Oxord, MS, U.S.A., respectively. *p*-Nitroacetophenone and *p*-bromoacetophenone used as internal standards were purchased from Aldrich, Milwaukee, WI, U.S.A.

Chromatographic conditions

Pre-mix analysis. The LC eluent was an aqueous buffer containing 0.02 *M* sodium citrate and 0.02 *M* citric acid (pH adjusted to 2.4 with perchloric acid) mixed with acetonitrile at a ratio 65:35. After filtering through a 0.45-μm nylon membrane (Cuno, Meriden, CT, U.S.A.) the eluent was pumped at 1.5 ml/min. The UV detector was set at a detection wavelength of 280 nm. The internal standard was *p*-nitroacetophenone.

Feed admixtures. The LC eluent was an aqueous buffer containing 0.1 *M* sodium dodecyl sulfate (pH adjusted to 4.0 with phosphoric acid) mixed with acetonitrile and tetrahydrofuran at a ratio 66.5:28.5:5.0. After filtering through a 0.45-μm nylon membrane, the eluent was pumped at 1.5 ml/min. The UV detector was set at a detection wavelength of 280 nm. The internal standard was *p*-bromoacetophenone.

Assay procedure

Pre-mix. An internal-standard solution was prepared by dissolving approximately 250 mg of *p*-nitroacetophenone accurately weighed in 1 l of acetonitrile–water (1:1). A standard was prepared by weighing accurately approximately 23 mg of sarafloxacin reference standard and dissolving in 100.0 ml of internal standard solution. This solution was then diluted 5:50 with eluent. Samples were analyzed by weighing accurately approximately 400 mg of pre-mix into a tall-form beaker and pipeting 100 ml of internal standard into the beaker. The sample was then blended at approximately 5500 rpm for 2 min. The mixture was allowed to settle for 10 min and a portion of the supernatant was centrifuged. A portion of the clear supernatant was then diluted 5:50 with eluent. Peak area ratios were determined and the sarafloxacin content was calculated *versus* the standard.

Feed admixtures. An internal standard solution was prepared by accurately weighing 18 mg of *p*-bromoacetophenone into 1.0 l of acetonitrile–water (1:1). A standard curve was prepared by weighing four individual 3-g samples of blank feed into separate tall-form beakers and spiking into the respective samples 0, 50, 100 and 150% of the anticipated amount of drug in the unknown feed samples. These samples were spiked by adding an appropriate volume of a methanol solution of sarafloxacin and evaporating to dryness. An appropriate volume of internal standard (50 ml for feeds containing < 500 ppm drug and 100 ml for feeds containing $\geqslant 500$ ppm drug) was pipeted into the sample. The mixture was blended in a high-speed homogenizer for 2 min at approximately 5500 rpm. The mixture was allowed to settle for 5–10 min, then a portion of the supernatant was centrifuged. Samples of 50 μl of each standard preparation were injected into the chromatograph and ratios of peak heights of the drug to internal standard were plotted *versus* the drug concentration (mg/g of feed) to produce a standard curve.

Samples of feed containing sarafloxacin were assayed by weighing 3 g into a tall-form beaker and extracting as described for the standard curve. Peak height ratios were determined for the samples and the sarafloxacin content was calculated from the standard curve.

RESULTS AND DISCUSSION

In this work, our purpose was to develop procedures for determining sarafloxacin in both soy flour pre-mix and in actual fish feed admixtures. Because of the large number of binding sites available in the natural products used and the amphoteric nature of sarafloxacin, neither prolonged, vigorous shaking nor sonification were sufficient to quantitatively extract the drug from either the soy flour or the feed. High-speed blending with a homogenizer at 5500 rpm was found to give recoveries ranging from 99 to 101% for spiked soy flour samples. In order to avoid errors due to solvent evaporation during the blending, an internal standard of *p*-nitroacetophenone was added in the extraction solvent.

Typical chromatograms for a sarafloxacin standard and pre-mix sample preparation are show in Fig. 1. The precision of the analysis was determined by performing the analysis several times on the same lot over a two day period. The measurements were made by two analysts and the results are shown in Table I. As shown, the relative standard deviation (R.S.D.) was $\pm$ 0.69%. The linearity of the

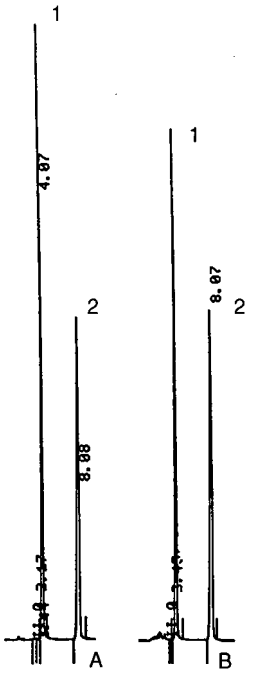

Fig. 1. Chromatograms of sarafloxacin. (A) Standard preparation; (B) pre-mix assay preparation. Peaks: 1 = *p*-nitroacetophenone; 2 = sarafloxacin. Retention times in min.

detector response was demonstrated by chromatographing solutions of sarafloxacin in internal standard solution containing concentrations from 2.4 to 24 μg/ml. A plot of peak area ratios *versus* concentration was linear. The regression line showed a *y*-intercept of 0.004 (not statistically different from the origin, $P \leqslant 0.05$) and a correlation coefficient of 0.9999.

A similar extraction was attempted on fish feed containing sarafloxacin but complete recovery was not obtained. When blank feed was added to a clear

TABLE I

PRECISION DATA FOR ANALYSIS OF SARAFLOXACIN IN PRE-MIX

	Analyst I (mg/g)	*Analyst II* (mg/g)
	45.0	45.8
	45.5	45.6
	45.3	45.8
	45.2	45.9
	45.4	45.9
Average	45.5	
S.D.	0.31	
R.S.D.	0.69%.	

TABLE II

PRECISION DATA FOR THE ANALYSIS OF SARAFLOXACIN IN FISH FEED

	Sample I (ca. 300 μg/g)		*Sample II (ca. 700 μg/g)*	
	Analyst I (μg/g)	*Analyst II (μg/g)*	*Analyst I (μg/g)*	*Analyst II (μg/g)*
	344.7	324.3	831.6	753.2
	338.7	327.6	836.5	812.7
	347.4	326.7	834.4	816.2
	338.7	335.4	837.9	831.6
	344.7	324.9	833.7	826.7
Average	335.3		821.5	
S.D.	8.87		25.4	
R.S.D.	2.6%		3.1%	

homogeneous solution of sarafloxacin, only 85% of the sarafloxacin remained in solution indicating that a partitioning of drug was occurring between the fish feed and the extraction solvent. Direct extraction of sarafloxacin from feed, using the HPLC eluent, which contained the surfactant sodium dodecyl sulfate, did not result in improved recoveries. Analysis of spiked blank feed with levels of sarafloxacin ranging from 100 to 765 μg/g were performed. Plotting the peak height ratios *versus* concentration of drug in feed gave linear relationships with correlation coefficients

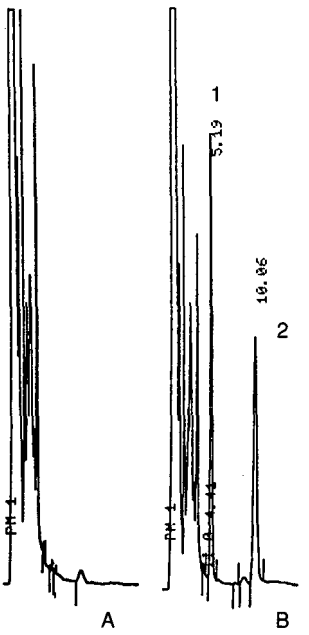

Fig. 2. (A) Chromatogram of blank fish feed. (B) Typical chromatogram of sarafloxacin assay preparation from fish feed. Peaks: 1 = *p*-bromoacetophenone; 2 = sarafloxacin.

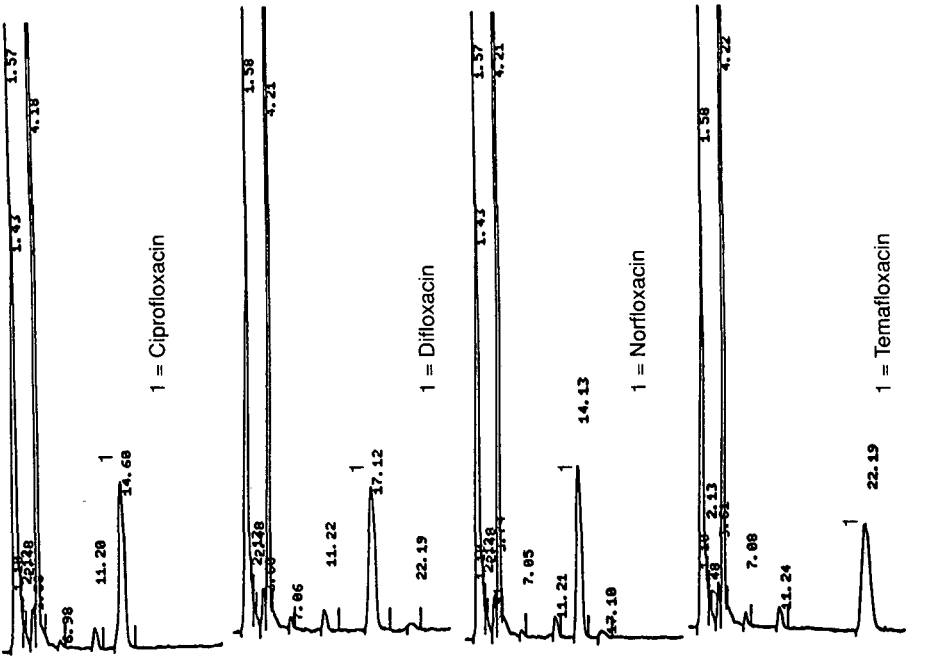

Fig. 3. Application of procedure to other quinolones in fish feed.

typically $\geqslant 0.999$. For this reason, a calibration curve was prepared as part of the analysis to determine the recovery and demonstrate its reproducibility. Samples were then analyzed *versus* the standard curve. Standard addition/recovery experiments using the procedure demonstrated good accuracy (100–105% of spike amount). Due to the co-extraction and co-elution of several other components from the feed, a change in eluent was made to increase the retention of sarafloxacin on the column and allow the other components to elute quickly.

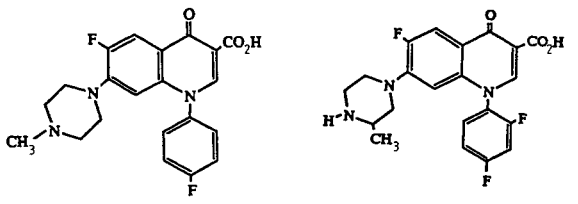

III

IV

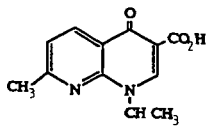

V

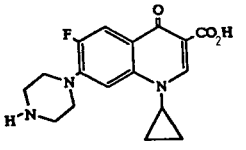

VI

The internal standard was changed to *p*-bromoacetophenone to avoid interference from the feed. The precision of the analysis was determined by performing the analysis several times on a single lot. Two analysts performed the analysis over a two-day period. The results are shown in Table II. Fig. 2 shows typical chromatograms for sarafloxacin in fish feed.

The present investigation focused on the determination of sarafloxacin in pre-mix and fish feed; however, the described technique is applicable to several other quinolones: difloxacin (III), temafloxacin (IV), norfloxacin (V) and ciprofloxacin (VI). Fig. 3 shows chromatograms for these compound. The correlation coefficients for standard curves of these quinolones in feed were all greater than 0.9999.

REFERENCES

1 G. Bourguignon, M. Levitt and R. Sternglanz, *Antimicrob. Agents Chemother.*, 4 (1973) 479.
2 P. Fernandes and D. Chu, *Ann. Rep. Med. Chem.*, 22 (1987) 117–126.
3 M. Horii, K. Saito, Y. Hoshino, N. Nose, E. Mochizuki and E. Nakazawa, *J. Chromatogr.*, 402 (1987) 301–308.
4 G. R. Granneman and L. T. Sennello, *J. Chromatogr.*, 413 (1987) 199–206.
5 S. Horii, C. Yasuoka and M. Motsumoto, *J. Chromatogr.*, 388 (1987) 459–461.
6 A. Weber, D. Chaffin, A. Smith and K. E. Ophum, *Antimicrob. Agents Chemother.*, 27 (1985) 531–534.

Journal of Chromatography, 514 (1990) 355–361
Elsevier Science Publishers B.V., Amsterdam

CHROM. 22 502

Note

Ion chromatography of nitrite, bromide and nitrate ions in brine samples using a chloride-form anion-exchange resin column

SOUJI ROKUSHIKA*, KAZUKO KIHARA, PRECILLA F. SUBOSA[a] and WEN-XUE LENG[b]
Department of Chemistry, Faculty of Science, Kyoto University, Sakyo-ku, Kyoto 606 (Japan)
(First received January 22nd, 1990; revised manuscript received April 20th, 1990)

In aquaculture research, maintenance of water quality is of great importance[1–4]. Recent improvements in fishpond management and fish culture systems, such as intensive feeding and fertilization, have created complex problems. Deterioration of water quality is primarily the resulting effect of these improvements. For example, high-protein feeds and nitrogen fertilizers applied in fishponds produce considerable amounts of nitrite in the water. Moreover, their synergistic effects cannot be ignored. Hence the routine determination of nitrite in fishpond water is required.

Since its introduction by Small *et al.*[5], ion chromatography has been widely used for the determination of ions in water. However, the presence of very high concentrations of chloride is the main obstacle in the analysis of seawater samples, affecting the separation and detection not only of nitrite but also of other anions.

Itoh and Shinbori[6] applied ion chromatography to the analysis of seawater using a 125-cm long column and a conductimetric detector. This technique provided a simple and sensitive analytial method for brine samples. However, nitrite could not be determined owing to the presence of a large chloride peak.

Attempts to determine nitrite in seawater also led to innovations in the methodology. Lee and Field[7] employed a post-column cerium fluorescence detection system to determine nitrite and nitrate in drinking water and seawater. The use of a pretreatment column in the silver form for removal of chloride has been reported[5].

Various detectors have been applied in ion chromatography in addition to the conductimetric detector. The UV detector has been shown to be useful detector for several kinds of inorganic anions[8]. Selective detection of specified inorganic ions can be achieved by tuning the wavelength of the UV detector in ion chromatography[9,10] and also in ion-exclusion chromatography[11]. The elimination of the chloride matrix

[a] Present address: Aquaculture Department, Southeast Asian Fisheries Development Centre, P.O. Box 256, Iloilo City, Philippines.
[b] Present address: Department of Chemical Industry, Jin-Xi Chemical Industry Institute, Jin-Xi, Liao-Ning, China.

0021-9673/90/$03.50

interference in the sub-ppm determination of nitrite in seawater was achieved by a heart-cutting and recycling method using a dual detection system consisting of conductimetric and a UV detectors[12]. This method, however, requires valve switching during analysis and needs a long analysis time.

This paper describes a simple and rapid method for UV-absorbing anions, such as nitrite, nitrate and bromide, in brine samples using a chloride-form anion-exchange resin column combined with a UV detector.

EXPERIMENTAL

Apparatus

The chromatographic system consisted of a Model IC 100 ion chromatographic analyser, a Type 3300 strip-chart recorder (Yokogawa Electric, Tokyo, Japan), a Model 638 variable-wavelength UV monitor (Hitachi, Tokyo, Japan) operated at 210 nm and a Chromatopak C-R1A integrator (Shimadzu, Kyoto, Japan). The sample loop size of the Rheodyne Model 7125 loop injector was 50 μl.

A Yokogawa PAM 3-035 guard column (30 mm × 4.6 mm I.D.) and a SAM 3-125 separation column (125 mm × 4.9 mm I.D.) were used. The gel for the separation column was composed of a hydroxyalkylated polyacrylate matrix and covalently introduced quaternary ammonium residues, of particle diameter 10 μm and ion-exchange capacity 50 μequiv./ml. The column temperature was maintained at 40 $\pm$ 1°C. The suppresser system was removed.

Stainless-steel column, tubing and filter components were used, hence daily washing of the system by pumping pure water was required in order to prevent corrosion problems due to the chloride ions in the eluents.

Reagents

The eluent was prepared by dissolving the appropriate amount of potassium chloride (E. Merck, Darmstadt, F.R.G. in deionized water, and was filtered through a 0.45-μm membrane filter (Toyo Roshi, Tokyo, Japan) and degassed before use. The flow-rate of the eluent was 1.5 ml/min throughout. Sample solutions containing various concentrations of sodium chloride as matrix ions were prepared from Suprapur-grade reagent (E. Merck). Other reagents were of analytical-reagent grade from Nacalai Tesque (Kyoto, Japan) and Wako (Osaka, Japan).

Deionized water was prepared with a Nanopure water purification system (Barnstead, Newton, MA, U.S.A.).

Seawater samples were obtained from fish aquaria in the Seto Marine Biological Laboratory (Kyoto University, Wakayama, Japan). The sample from the Pacific Ocean was provided by Dr. Nakayama (Kyoto University).

RESULTS AND DISCUSSION

Principle of matrix ion evicted chromatography

The problems encountered in the determination of minor ions coexisting in a major matrix ion are the peak overlapping on the matrix ion peak and the peak broadening due to the overwhelming amount of the matrix ion.

In ion chromatography with conventional eluents, *e.g.*, carbonate solutions, the

fixed ions on the ion-exchange sites are replaced by the matrix ions as the ions are passed along the column. It requires a long time to recover the ion-exchange equilibrium after the matrix ion has eluted from the column. The chaotic state in the column makes the retention volumes fluctuate, and moreover the analyte peak shapes are badly distorted.

To prevent this disordered state in the column, we selected the counter ion in the eluent to be the same as the anion included in the matrix. By using neutral chloride salt solutions, such as potassium or sodium salts, the eluent contains only the matrix anion species, and therefore all the ion-exchange sites on the resin are occupied by the single ion species. Under these conditions, the matrix ion apparently is retained on the column and subsequently eluted at the void volume in a narrow peak, whereas analyte ions are retained and eluted in order of their ion-exchange selectivity. Using this system, sharp and symmetrical peaks of analyte ions were obtained.

Relationship between eluent concentration and capacity factors

Prior to the analysis, the column was thoroughly washed with potassium chloride solution for equilibration.

The logarithmic retention volume of the nitrite, bromide and nitrate peaks decreased linearly with increasing logarithmic chloride concentration in the eluent.

For the analysis of brine samples, the concentration of the potassium chloride eluent was set at 50 m*M*, considering the resolution and the analysis time.

Effects of the chloride matrix ion concentration on the chromatographic data

Chromatograms were obtained by the injection of synthetic brine samples with various chloride matrix ion concentrations and containing 1.0 μg/ml of nitrite, 5.0 μg/ml of bromide and 1.0 μg/ml of nitrate ions.

Chloride matrix ion eluted at the column void volume in a narrow peak. The retention volumes of the analyte peaks were independent of the matrix ion

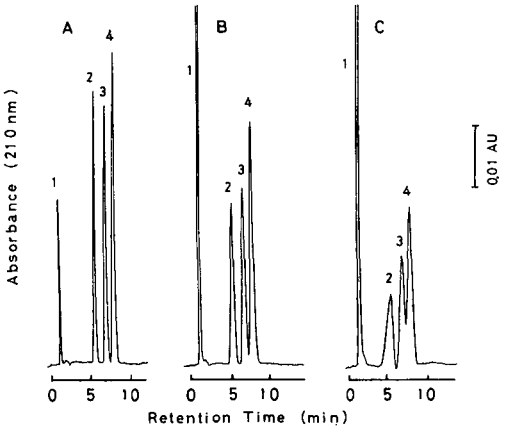

Fig. 1. Effect of chloride ion concentration in the sample solution on the peak shape of anions. Chloride ion concentrations: (A) 5; (B) 20; (C) 50 μg/ml. Peaks: 1 = Cl^-; 2 = NO_2^- (1 μg/ml); 3 = Br^- (5 μg/ml); 4 = NO_3^- (1 μg/ml). Eluent, 50 m*M* potassium chloride solution; flow-rate, 1.5 ml/min; column temperature, 40 ± 1°C; sample volume, 50 μl; detection, UV absorption at 210 nm.

concentrations up to 50 mg/ml. The peak shape of the analytes and the column efficiency varied with the matrix ion concentration. Fig. 1 shows the effect of the chloride matrix ion concentration on the peak shape and the resolution.

Below a matrix ion concentration of 5 mg/ml (141 m*M*), the peak shapes of three anions are symmetrical and well separated from each other. Above this level, the peak width of the analyte ions increased owing to leading of the peak and the peak height decreased with increasing matrix ion concentration. At 20 mg/ml ppm (563 m*M*) of chloride matrix, the peak became skewed, but acceptable resolution between neighbouring peaks were attained. This matrix concentration is equivalent to that in the ocean sample. The analyte anion peak area was not affected by the matrix ion, which implies that the system is applicable to the direct injection of the seawater samples for quantitative analysis.

At 50 mg/ml (1.4 *M*) of chloride matrix ion, the anion peaks become skewed and the front part of the nitrate peak overlaps the tail of the bromide peak. Leading of the analyte peak caused the theoretical plate number, N, to decrease. The value of N for each peak was determined and the ratio N/N_0 is plotted in Fig. 2 as a function of the matrix ion concentration (N_0 is the N value obtained with a matrix-free sample). At higher matrix concentrations, N/N_0 decreased with increasing matrix concentration. The effect of the matrix on the column efficiency was greater for ions with shorter retention times. Peak broadening of the nitrite ion was particularly apparent among the three analyte peaks, but it was still separated from the bromide ion peak with up to 50 mg/ml of matrix coexisting, as shown in Fig. 1.

Determination of anions in seawater samples and contaminants in chemical reagents

Chromatograms obtained by the injection of 50 μl of seawater sample are demonstrated in Fig. 3. The seawater samples contained chloride ion at levels from 18 to 20 mg/ml. Trace A is for a sample taken from the Pacific Ocean, with a concentration of bromide ion of 65 μg/ml. Trace B is for a sample taken from an aquarium and included a considerable amount of nitrate ion produced by biological

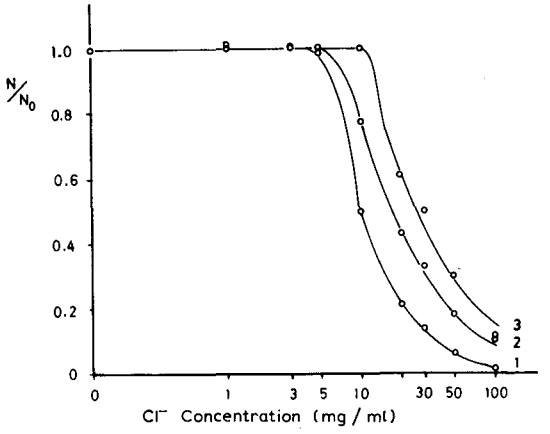

Fig. 2. Effect of chloride ion concentration in the sample solution on the column efficiency. 1 = NO_2^-;)2 = Br^-; 3 = NO_3^-. Conditions as in Fig. 1.

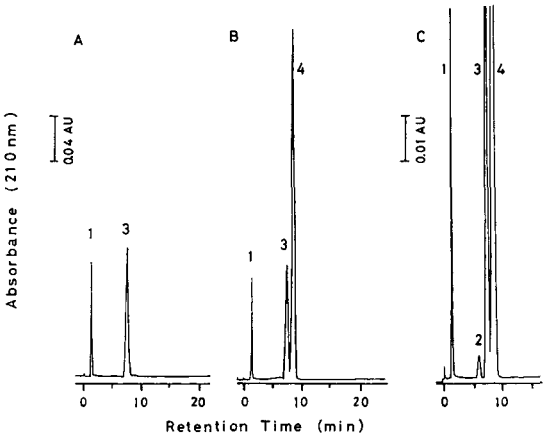

Fig. 3. Chromatograms of seawater samples. (A) Pacific Ocean; (B) aquarium; (C) sample B spiked with 0.5 μg/ml of nitrite. Peaks: 1 = Cl^-; 2 = NO_2^-; 3 = Br^-; 4 = NO_3^-. Conditions as in Fig. 1.

activities of fish, but nitrite was not detected. The result for an aquarium sample spiked with 0.5 μg/ml of nitrite is shown in the trace C.

The relationship between the peak area and the nitrite concentration was obtained at levels up to 20 μg/ml by injecting samples from the Pacific Ocean spiked with various concentrations of nitrite ion. The detection limit was 8 ng/ml (2.4 ng/ml as NO_2-N) for a signal-to-noise ratio of 2.

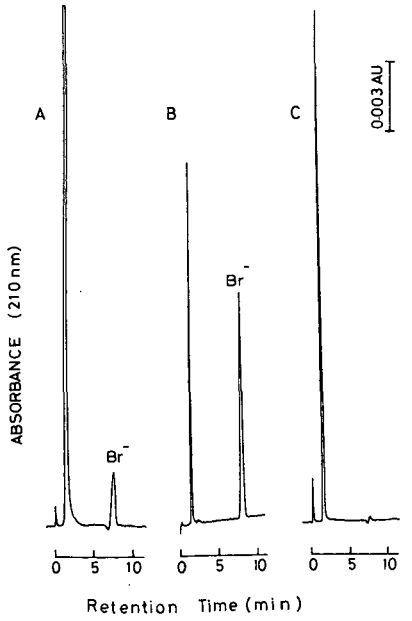

Fig. 4. Chromatograms of chemical reagents. (A) 1.0 *M* NaCl (brand A); (B) 0.2 *M* KCl (brand A); (C) 0.3 *M* KCl (brand B). Conditions as in Fig. 1.

Contaminants in commercially available sodium chloride and potassium chloride reagents were determined by this method. Fig. 4 shows the peak of the bromide ion present as a contaminant in the analytical-reagent grade reagents.

When the detector attenuation was set at high sensitivity, a small negative peak was observed just before the bromide peak. Fig. 4A shows this negative peak when 50 μl of 1.0 *M* sodium chloride solution (35.5 mg/ml as Cl^-) was injected. The negative peak is not observed in Fig. 4B, where a lower concentration of a 0.2 *M* potassium chloride (7.1 mg/ml Cl^-) was applied. The size of the negative peak increased with increasing concentration of chloride ion in the sample solutions. The origin of this negative peak is unknown, but the tail of the nitrite peak and the front of the bromide peak overlapped with it. This peak yields the error in the quantitative determination of nitrite and bromide ions at low concentration levels. The problem with the determination of nitrite was solved by the addition of 5–10% of methanol to the eluent, but the negative peak still overlapped the bromide peak.

Effect of the pH of the sample solution

The effect of the pH of the sample solution on the retention behaviour of analytes was studied. The pH of the sample solution was adjusted by adding dropwise a 0.05 *M* sulphuric acid or a 0.1 *M* sodium hydroxide solution. The retention volume and peak area of the three anions did not vary when the pH of the sample solutions ranged from 2.0 to 11.8, except for the peak area of the nitrite ion, which below pH 2.8 decreased with decrease in the sample pH. This may caused by the decomposition of nitrite ion in an acidic solution; however, no significant increase in the nitrate peak was observed in the sample pH range examined.

Separation of monocarboxylic acids from inorganic acids

Small monocarboxylic acids such as formic or acetic acid are often found as contaminants in practical samples. As carboxylic acids can be detected with a UV detector[13], such compounds sometimes interfere in the analysis of inorganic anions.

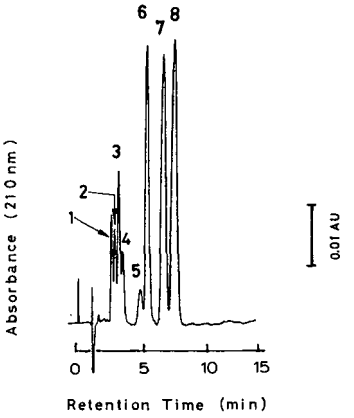

Fig. 5. Chromatogram of a mixture of monocarboxylic acids and inorganic anions. Peaks: 1 = unknown; 2 = acetic acid (20 μg/ml); 3 = formic acid (20 μg/ml) + *n*-propionic acid (20 μg/ml); 4 = *n*-butyric acid (20 μg/ml); 5 = *n*-valeric acid (20 μg/ml); 6 = NO_2^- (1 μg/ml); 7 = Br^- (5 μg/ml); 8 = NO_3^- (1 μg/ml). Conditions as in Fig. 1.

Fig. 5 shows the chromatogram of a mixture of five monocarboxylic acids and three inorganic anions using 50 m*M* potassium chloride solution as eluent. The five acids were eluted before the nitrite peak and did not interfere in the analysis of the inorganic anions. Acetic acid eluted first, followed by formic and *n*-propionic acid. Baseline resolution between *n*-valeric acid and nitrite was obtained when 30 m*M* potassium chloride solution was employed as the eluent.

The present method is also applicable to the analysis of monocarboxylic acids in a solution with a chloride ion matrix.

REFERENCES

1 J. E. M. Almendras, *Aquaculture*, 61 (1987) 33.
2 C. E. Smith and W. G. Williams, *Trans. Am. Fish. Soc.*, 103 (1974) 389.
3 R. E. Crawford and G. H. Allen, *Trans. Am. Fish. Soc.*, 106 (1977) 105.
4 G. A. Wedemeyer and W. T. Yasutake, *J. Fish. Res. Board Can.*, 35 (1978) 822.
5 H. Small, T. S. Stevens and W. C. Bauman, *Anal. Chem.*, 47 (1975) 1801.
6 H. Itoh and Y. Shinbori, *Bunseki Kagaku*, 29 (1980) 239.
7 S. H. Lee and L. R. Field, *Anal. Chem.*, 46 (1974) 1971.
8 R. N. Reeve, *J. Chromatogr.*, 177 (1979) 393.
9 S. Rokushika, Z.-Y. Qiu, Z.-L. Sun and H. Hatano, *J. Chromatogr.*, 280 (1983) 69.
10 T. Okada and T. Kuwamoto, *J. Chromatogr.*, 325 (1985) 327.
11 T. Takaka, *Bunseki Kagaku*, 30 (1981) 661.
12 P. F. Subosa, K. Kihara, S. Rokushika, H. Hatano, T. Murayama, T. Kubota and Y. Hanaoka, *J. Chromatogr. Sci.*, 27 (1989) 680.
13 S. Rokushika, Z.-L. Sun and H. Hatano, *J. Chromatogr.*, 253 (1982) 87.

Journal of Chromatography, 514 (1990) 362–370
Elsevier Science Publishers B.V., Amsterdam

CHROM. 22 524

Note

Analysis of atmospheric precipitation by reversed-phase ion-pair chromatography

Q. XIANREN* and W. BAEYENS
Department of Analytical Chemistry, Vrije Universiteit Brussel, Pleinlaan 2, 1050 Brussels (Belgium)
(First received April 11th, 1989; revised manuscript received April 5th, 1990)

In recent years much effort has been applied to the use of high-performance liquid chromatography (HPLC) for the separation and determination of inorganic anions. The use of a low-capacity anion-exchange column combined with an eluent consisting of a dilute aromatic acid anion solution (*e.g.*, Vydac IC and Hamilton PRP-X100 columns) or with an eluent containing a dilute carbonate–hydrogencarbonate buffer (*e.g.*, the chemically suppressed Dionex ion chromatography system) for the determination of anions is the most common approach[1–3]. The use of other chromatographic methods, especially in the reversed-phase mode, has also been studied in order to extend the applicability and to permit the use of universal HPLC instrumentation. For the separation of some common inorganic anions, ion-pair chromatography (IPC) or ion-interaction chromatography (IIC) using octadecyl-bonded silica as a non-polar stationary phase has been reported[4,5]. The theoretical dependence of the capacity factor on the mobile phase variables and the optimization of the mobile phase composition has been studied by various workers[6–10] and previously in our laboratory[11,12].

In this work, a reversed-phase Partisil 10 ODS-3 column was evaluated for the rapid determination of several anions (chloride, nitrite, bromide, nitrate and sulphate) in environmental samples. It was found that a combination of 8 m*M* tetrabutylammonium iodide (TBAI) and 1 m*M* potassium hydrogenphthalate (KHP) at pH 6 as the eluent was very suitable for the separation of those anions with this column. The method was applied to rainwater and aerosol samples and the results were compared with those obtained with a PRP-X100 (Hamilton) ion-exchange column. The reproducibility of triplicate measurements ranged between 0.5 and 0.9% for Cl^-, NO_2^-, Br^-, NO_3^- and SO_4^{2-}. The detection limit was 0.1–0.2 ppm with a 100-μl injection sample volume. The results of the field measurements are presented.

EXPERIMENTAL

Sampling

Single rain event samples and monthly averaged rainwater samples were collected at the roof of the highest university building at the VUB–Oefenplein campus

0021-9673/90/$03.50

(an urban site) and simultaneously at the university rooftop and a more rural site (Massart garden) 4 km from the university in a southeast direction. The Massart garden is located at the border of the Zonienwoud (a forest surrounding the southern part of Brussels) and distant from major pollutant sources. Rainwater samples were stored at 4°C until further chemical analysis.

Single rain event samples. A wet-only collector was used for the sampling of single rain events. The collection system consisted of a 31-cm diameter polyethylene funnel which was mounted 1 m above the roof of the building of the Science Faculty (Building G), 35 m above the ground level, at the Free University of Brussels. The funnel was attached via a short PTFE tube directly to a fraction collector covered with a Plexiglas box. The funnel was covered between rain events to avoid dry fall-out. The funnel and tubing were rinsed and cleaned with Milli-Q water before a collection sequence was started. The rainwater was collected in glass tubes that had been washed with phosphoric acid and thoroughly rinsed with Milli-Q water. After collecting a volume of 20 ml of subsample, the fraction collector advanced to the next tube. The pH of each of the subsamples was measured shortly after collection.

Monthly averaged rainwater samples. During a period of 1 year (April 1986 to March 1987), a total of twelve parallel samplings (at the University rooftop and the Massart garden) of precipitation were carried out. Samples were collected using a rainwater collector. A funnel coupled to a 2-l polyethylene bottle was placed at a height of 1 m.

Sampling of aerosols. Total suspended particulates (TSP) were collected on Millipore 0.45-μm HA filters using a high-volume air sampler (CA G004, Contigea Schlumberger SA, Belgium). They also were taken at the top of Building G (VUB–Oefenplein campus). The total sampling time of each sample was 24 h. The sampling rate was 1.05 m^3/h. Seventeen samples were collected from January 29th to February 24th, 1987. During this sampling period, three snow samples were collected in parallel with the atmospheric aerosol samples. After the total amount of aerosols had been determined, the water-soluble components of the aerosol samples were extracted with 10 ml of Milli-Q water. The sample was shaken overnight in a mechanical shaker and then placed in an ultrasonic bath. The liquid extract was filtered using a low-volume Millipore filtration system (a 15-ml capacity glass funnel; a glass microanalysis frit support, 25 mm; a glass vacuum filtering flask, 125 ml; a Millipore HVLP 02500 filter of 0.45 μm porosity; and a Millipore vacuum pump), and also using an Acrodisc syringe filter (Gelman Sciences; 0.45-μm pore size and 3-mm diameter), and stored in a refrigerator at 4°C until analysis.

Chemicals and apparatus

The chromatographic technique (equipment, reagents and preparation of eluent) has been described in detail previously[11,12]. In addition, a 1 m*M* KHP (analytical-reagent grade, R.C.B., Belgium) eluent at pH 5.5 and a 4 m*M* *p*-hydroxybenzoic acid (analytical-reagent grade, Aldrich-Chemie, F.R.G.) eluent at pH 8.6 were used for the anion-exchange column.

The columns used were a slurry-packed 250 × 4.6 mm I.D. Partisil 10 ODS-3 RP column (Whatman) protected with a 60 × 2.1 mm I.D. guard column with the same packing and a 150 × 3.9 mm I.D. PRP-X100 ion-exchange prepacked column protected with a PRP-X100 Cartridge Guard column (Hamilton). The particle size of the column packings was 10 μm.

RESULTS AND DISCUSSION

Evaluation of the retention behaviour of anions on the reversed-phase Partisil 10 ODS-3 column

Factors that affect the retention of inorganic anions. Ion-interaction or ion-pair reversed-phase chromatography carried out with an aqueous eluent containing a quaternary ammonium salt and a phthalate buffer was found to be an efficient system for the separation of various inorganic anions.

The capacity factors (k') of the anions increase with increasing TBAI concentration, reach a maximum and then decrease with further increase in TBAI concentration. A linear relationship was found between $1/k'$ and the ionic strength of buffer and also the mobile phase pH. An increase in the buffer concentration and/or pH thus results in a decrease in the capacity factor. The relevant figures for the dependence of k' (or $1/k'$) on the TBAI concentration (or the buffer concentration or the pH of the mobile phase) have been given in a previous paper[11]. The results can be converted into a mathematical model, using the equations

$$1/k'_x = a\{1/[Q^+]_m\} + b[C^-]_m + c[B^-]_m + d[X^-]_m \quad (1)$$

$$1/k'_x = a'\{[(QCA)_S + A_S]/[Q^+]_m\} + b'[B^-]_m + c'[X^-]_m \quad (2)$$

where $[Q^+]_m$ and $[C^-]_m$ are the concentrations of the quaternary ammonium ion and the co-anion in the mobile phase, respectively, $[B^-]_m$ and $[X^-]_m$ are the concentrations of the buffer anion and sample anion, respectively; $(QCA)_S$ is the amount of TBAI adsorbed on the stationary phase, A_S is the number of free sites on the stationary phase and a, a', b, b', c, c' and d are constants. Details of the experimental results and discussion have been presented elsewhere[11].

Factors controlling the resolution of anion peaks and the peak height. Experimental evidence demonstrates that the concentration of the ion-interaction reagent (IIR), the buffer concentration and the pH of the eluent are the major factors that affect the retention of anions in the chromatographic process. These factors should therefore also affect the resolution of anion peaks and detection sensitivity of analytes according to the well known resolution and peak-height equations:

$$R_S = \tfrac{1}{4}\sqrt{N}[k'/(k' + 1)](\alpha - 1) \quad (3)$$

and

$$h = (4Sm\sqrt{N})/[p\,\varepsilon_c\,(k' + 1)\,L\,d_c^2\sqrt{2p}] \quad (4)$$

where R_S is the resolution, N is the column plate number, k' is the mean solute capacity factor of two adjacent peaks in eqn. 3 or the solute capacity factor in eqn. 4, α is the selectivity factor (k'_2/k'_1), S is the response factor of the detector, m is the amount of sample injected, ε_c is the adsorbent porosity, d_c is the column diameter and L is the column length.

As can be understood from eqn. 3, the resolution of an adjacent pair of peaks can be affected and controlled by three parameters, N, k' and α. The resolution R_S is

a function of $\sqrt{N}$, so that any increase in the plate number results in an increase proportional to the square root of N. As for a given column the changes in plate number are relatively small with changes in mobile phase conditions[11], this factor has only a small influence on R_S. The effect of the term $k'/(k' + 1)$ on the resolution is also generally minor; if the nominator increases (decreases) by an amount $\Delta k'$, the denominator also increases (decreases) by the same amount. The lower the k' value and the larger the change $\Delta k'$, the more important the term $k'/(k' + 1)$ will be. This term varies by a factor 2 between eluent buffer concentrations of 1 and 4 mM for Cl^-–NO_2^-, Br^-–NO_3^- and NO_3^-–SO_4^{2-}. The selectivity factor, and hence the capacity factors of the two adjacent peaks, has a major influence on the separation. Previously obtained results showed the dependence of R_S on the on TBAI concentration and mobile phase pH. The large variation of $R_S(NO_3^-$–$SO_4^{2-})$ with respect to $R_S(NO_2^-$–$Br^-)$, $R_S(Cl^-$–$NO_2^-)$ and $R_S(Br^-$–$NO_3^-)$[12] is primarily due to the change in selectivity ($\alpha = k'_2/k'_1$) as a function of the TBAI concentration or pH.

The peak height or detection sensitivity of analytes is also a function of these factors, as in eqn. 4, k', S and N are present. These parameters are affected by the eluent composition (other parameters being constant). The dependence of the peak height on [TBAI] has also been presented previously[12]. The peak height of nitrate and sulphate is considerably increased and that of chloride only slightly with increasing TBAI concentration. This increase should be mainly due to an increasing amount of adsorbed TBA on the stationary phase when the mobile phase concentration of TBA is increased; at higher TBA concentrations, k' decreases, thus increasing the peak height, but in the low TBA concentration range the plate number or the response factor of the detector must be the peak-height controlling factor.

Optimum mobile phase composition and column performance. Based on the above discussion, it is clear that the most important parameter affecting the values of the resolution factor and peak height is the capacity factor. This factor depends on mobile phase variables such as ionic strength, pH and quaternary ammonium salt concentration. Optimization of these mobile phase variables should therefore lead to a well resolved chromatogram and a rapid and sensitive analytical method. A three-factor central composite design with a computer-aided multifactor statistical optimization approach was carried out for the optimization of the mobile phase composition. Unique optimum mobile phase conditions which meet all the requirements (rapid analysis of five anions with adequate resolution and high sensitivity) were to be [TBAI] = 8–8.5 mM, [KHP] = 0.5–1 mM and pH = 6–6.5. These values agree very well with the best results we observed experimentally. Details of the optimization approach have been presented elsewhere[12].

Laboratory slurry-packed ODS-3 columns and a low-capacity anion-exchange pre-packed PRP-X100 column were used for the performance study. The ODS-3 column gives the highest theoretical plate number when an eluent containing 0.5 mM TBAI and 1 mM KHP was used. Under these conditions, the resolution of the peak pair NO_2^-–Br^- and the peak heights of chloride, nitrate and sulphate, however, were low. If the optimum mobile phase composition of a more concentrated TBAI eluent (8 mM) is used at a higher pH (6), the column gives a lower theoretical plate number, but an adequate resolution for the NO_2^-–Br^- peak pair. In addition, we obtained the highest conductance responses (peak heights) for chloride, nitrate and sulphate, and the shortest overall retention time. The plate numbers and resolutions (see Table II in

ref. 11) show that the efficiency of the ODS-3 column when used with TBAI–KHP eluent is as good as that of the commercially pre-packed PRP-X100 column. If we compare the performances obtained with the ODS-3 column for eluent conditions 8 m*M* TBAI, 1 m*M* KHP and pH 6.0 and the Hamilton PRP-X100 column for eluent conditions 1 m*M* KHP and pH 5.5 in detail, we observe that the numbers of theoretical plates per metre are almost identical, the resolutions of the peak pair NO_2^-–Br^- are identical, the elution times of the last peak (SO_4^{2-}) are very close, the analysis times for five anions are both 8–9 min and the peak height of the anions is much better with the ODS column, especially for nitrate and sulphate.

Two negative system peaks occur at 10 and 20 min with the ODS-3 column for the above-mentioned eluent conditions. If one performs a new injection at the moment of the appearance of the first negative peak (every tenth minute), the sytem peaks will not interfere with the peaks of the analytes and the total analysis time will not increase. The number of analyses that can be performed on the ODS column without reconditioning the packing amounts to 500 and sometimes up to 1500 injections, depending on the nature of the sample and also on the frequency of analysis. In addition, a column regeneration technique (column repacking) can be used to prolong the lifetime of the column[11,13].

Application to the determination of anions in precipitation samples

Reproducibility of retention time and concentration of anions in a rainwater sample. Variaton of the retention time of the separated anions in a rainwater sample using the reversed-phase column was tested. Table I shows the reproducibility of the retention times of each anion, which is very good. Moreover, the higher the retention time, the better is the relative standard deviation (R.S.D.): chloride has a mean retention time of 233 s and an R.S.D. of 2.85%, whereas sulphate has a retention time of 556 s and an R.S.D. of 1.70%. In addition, concentrations of three major anions (Cl^-, NO_3^- and SO_4^{2-}) in a given rainwater sample were repeatedly determined after separation (Table II). The S.D.s for the three anions were between 0.37 and 0.41 and the R.S.D.s between 4 and 13%; these are satisfactory results for rainwater analyses on a routine basis.

Determination of anion concentrations in rainwater and aerosol samples. Table III compares the results for Cl^-, NO_3^- and SO_4^{2-} concentrations (ppm) in some aerosol samples. The results were determined by using ion exchange (PRP-X100 column) and reversed-phase (ODS-3 column) chromatographic methods and the agreement of the

TABLE I

REPRODUCIBILITY TEST ON THE RETENTION TIMES OF THE SEPARATED ANIONS IN A RAINWATER SAMPLE WITH THE RP ODS-3 COLUMN

Chromatographic conditions: TBAI, 8 m*M*; KHP, 1 m*M*; pH, 5.4; flow-rate, 2 ml/min; sample injection volume, 25 μl. $n = 10$.

Parameter	Cl^-	NO_2^-	Br^-	NO_3^-	SO_4^{2-}
Mean value (s)	233	303	337	461	556
S.D. (s)	6.65	7.39	7.79	8.46	9.45
R.S.D. (%)	2.85	2.44	2.31	1.84	1.70

TABLE II

REPRODUCIBILITY TEST ON THE ANION CONCENTRATIONS IN A RAINWATER SAMPLE WITH THE RP ODS-3 COLUMN

Chromatographic conditions: as in Table I. $n = 9$.

Parameter	Cl^-	NO_3^-	SO_4^{2-}
Mean value (ppm)	4.61	3.22	8.51
S.D. (ppm)	0.37	0.41	0.34
R.S.D. (%)	8	13	4

results between the two method is satisfactory. Figs. 1 and 2 show an example of a reversed-phase ion-pair chromatogram of some anions in aerosol and rainwater, respectively. Fig. 3 shows the calibration graphs for the determination of Cl^-, NO_3^- and SO_4^{2-}. Fig. 4 shows the variation in the concentration of anions determined in sequentially collected rainwater samples. These results clearly indicate that the anion concentrations in rain decrease in a hyperbolic way with the amount of precipitation. Similar profiles were observed for trace metals in rainwater above the North Sea[14]. The hyperbolic relationship reflects the fact that in the last stages (sequences) of the rainwater samples, the anion concentration tends to a constant value which corresponds to the initial or cloud vapour concentration. This concentration is a measure of the background concentration of the dissolved anions in raindrops. Also, in the initial stages (sequences) of the rainwater samples, the anion concentration is much higher owing to an additional amount of salts which will be incorporated and solubilized in the raindrops during their fall. This additional amount is thus a measure of the scavenging efficiency of anions from aerosols by the raindrops.

TABLE III

COMPARISON OF ANALYTICAL RESULTS FOR AEROSOL SAMPLES OBTAINED USING A REVERSED-PHASE COLUMN (ODS-3) AND AN ION-EXCHANGE COLUMN (PRP-X100)

All data represent the average of duplicate runs for each sample. Chromatographic conditions: TBAI, 8 m*M*; KHP, 1 m*M*; pH 6 for the ODS-3 column; 4 m*M* *p*-hydroxybenzoic acid at pH 8.5 for the PRP-X100 column; flow-rate, 2 ml/min; sample injection volume, 50 μl.

Sample No.	Cl^- *(ppm)*		NO_3^- *(ppm)*		SO_4^{2-} *(ppm)*	
	ODS-3	*PRP-X100*	*ODS-3*	*PRP-X100*	*ODS-3*	*PRP-X100*
1	0.5	0.4	0.9	1.0	4.3	4.5
2	37.8	40.6	8.3	10.0	21.7	20.0
3	59.2	60.8	25.2	27.8	18.4	18.8
4	6.2	5.3	4.4	5.5	17.8	17.3
5	1.2	1.2	5.6	5.5	14.9	15.3
6	0.9	0.9	0.5	–	20.5	21.8
7	9.5	8.7	11.2	12.1	7.6	7.9
8	22.4	22.4	20.6	21.6	5.4	–
9	6.6	5.7	5.6	6.3	5.4	–

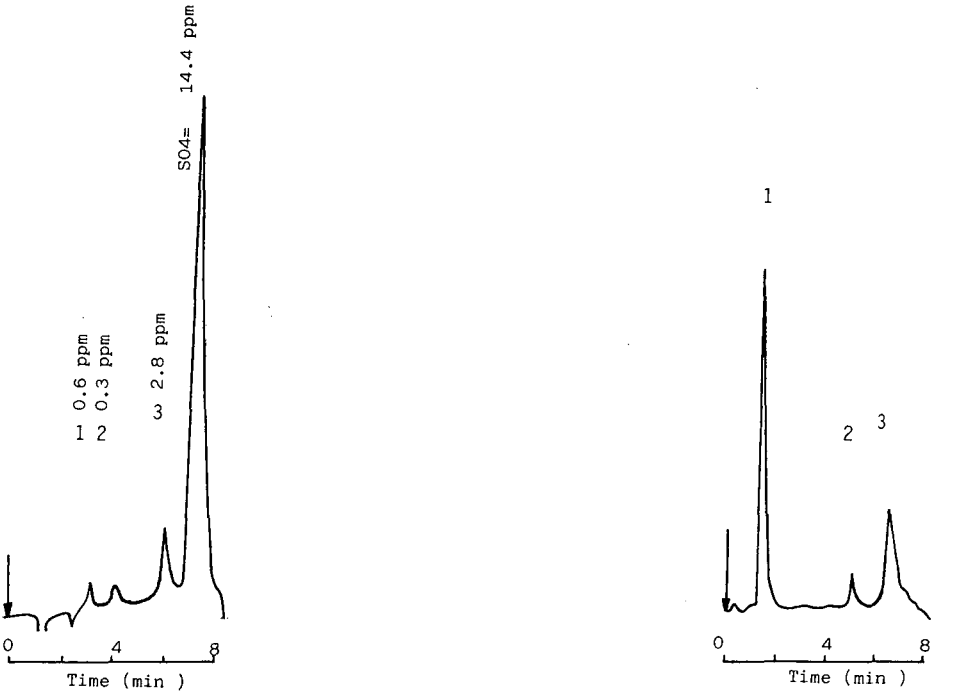

Fig. 1. Example of a reversed-phase ion chromatogram for an aerosol sample. Chromatographic conditions: TBAI, 8 m*M*; KHP, 1 m*M*; pH, 6; flow-rate, 2.5 ml/min; sample injection volume, 50 μl. Peaks: 1 = Cl^-; 2 = NO_2^-; 3 = NO_3^-.

Fig. 2. Example of a reversed-phase ion chromatogram for rainwater. Chromatographic conditions: pH, 5.4; sample injection volume, 25 μl; other conditions as in Fig. 1. Peaks: 1 = Cl^-; 2 = NO_3^-; 3 = SO_4^{2-}.

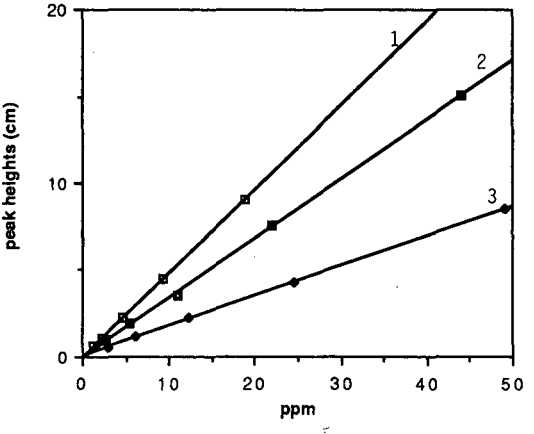

Fig. 3. Calibration graphs for (1) Cl^-, (2) SO_4^{2-} and (3) NO_3^- for the determination of sample anions in atmospheric precipitation. Chromatographic conditions: TBAI, 8 m*M*; KHP, 1 m*M*; pH, 5.4; flow-rate, 2.0 ml/min; injection of standard, 25 μl.

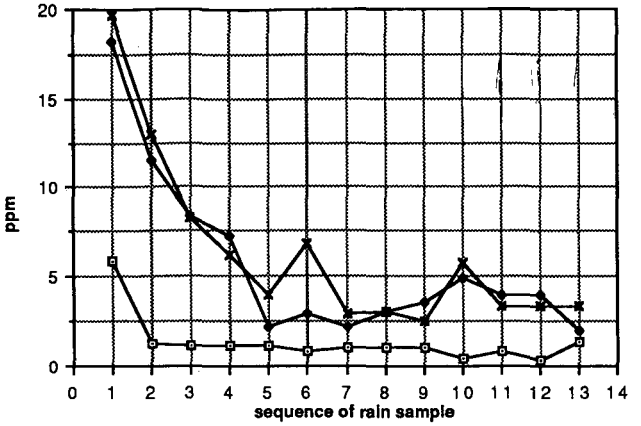

Fig. 4. Diagram showing the variation of anion concentrations in rainwater, determined in sequentially collected rainwater samples (determined on each 20 ml from the start of raining; sampled on June 1st, 1986 at Building G, VUB–Oefenplein, Brussels). Chromatographic conditions: TBAI, 8 m*M*; KHP, 1 m*M*; pH, 6; flow-rate, 2.0 ml/min. □ = Cl^-; ● = NO_3^-; × = SO_4^{2-}.

Environmental atmospheric samples such as wet precipitation (rainwater or snow) and aerosols were also regularly collected. Fig. 5 shows an example of the variation of the sulphate concentration with monthly collected rainwater. In January 1987 high sulphate concentrations were observed. That month the temperature was very low, leading to an increased consumption of fuel and an increased output of sulphate. The SO_4^{2-} concentrations in the samples that were collected at the urban site were generally slightly higher than those collected at the rural site.

Typical inorganic anion compositions of some aerosol samples are shown in Table IV. Using an injection volume of 100 μl a limit of detection of about 0.1 mg/l and a linear calibration range up to 60 mg/l for the anions are obtained.

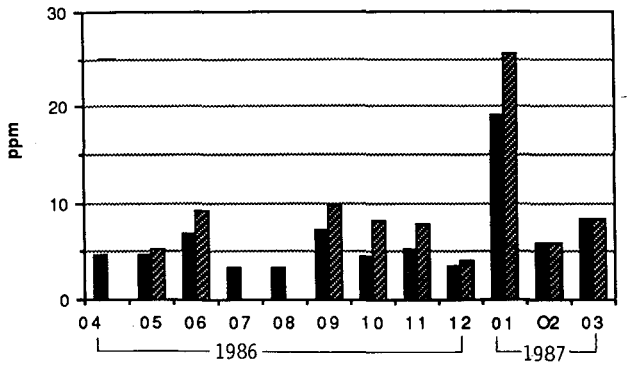

Fig. 5. Example of the variation of the sulphate concentration collected rainwater samples and comparison between two sampling sites: black boxes = more rural; hatched boxes = urban.

TABLE IV

TYPICAL INORGANIC ANION COMPOSITION OF AEROSOL SAMPLES

Sampling date (Feb. 1987)	*Air volume (m^3)*	*Concentration (nequiv./m^3)*				
		Cl^-	NO_2^-	Br^-	NO_3^-	SO_4^{2-}
2–3	24.10	155.8	1.81	0.52	293.4	311.8
6–7	25.03	147.3	0.52	1.50	82.3	347.3
11–12	24.65	135.7	1.41	1.02	116.6	233.4
19–20	25.71	62.5	1.18	0.24	152.0	227.1
22–23	25.00	181.6	0.61	1.50	124.1	283.5
23–24	25.41	172.4	1.54	2.46	117.3	184.9

REFERENCES

1 H. Small, T. S. Stevens and W. C. Banman, *Anal. Chem.*, 47 (1975) 1801.
2 P. R. Haddad, P. E. Jackson and A. L. Hechenberg, *J. Chromatogr.*, 346 (1985) 139.
3 D. T. Gjerde and J. S. Fritz, *Ion Chromatography*, Hüthig, Heidelberg, 2nd ed., 1987.
4 I. Molnar, H. Knauer and C. Wilk, *J. Chromatogr.*, 201 (1980) 225.
5 M. Dreux, M. Lafosse, P. Agbo-Hazoume, B. Chaabane-Doumandji, M. Gibert and Y. Levi, *J. Chromatogr.*, 354 (1986) 119.
6 W. E. Barber and P. W. Carr, *J. Chromatogr.*, 316 (1984) 211.
7 R. L. Smith, Z. Iskandarani and D. J. Pietrzyk, *J. Liq. Chromatogr.*, 7 (1984) 1935.
8 A. Bartha and Vigh, *J. Chromatogr.*, 265 (1983) 171.
9 A. Bartha and Vigh, *J. Chromatogr.*, 395 (1987) 1503.
10 Y. Baba, N. Yoza and S. Ohashi, *J. Chromatogr.*, 348 (1985) 27.
11 Q. Xianren and W. Baeyens, *J. Chromatogr.*, 456 (1988) 267.
12 Q. Xianren, W. Baeyens and Y. Michotte, *J. Chromatogr.*, 467 (1989) 15.
13 N. C. Avery and N. Light *J. Chromatogr.*, 328 (1985) 341.
14 W. Baeyens, H. Dedeurwaerder and F. Dehairs, *Atmos. Environ.*, in press.

Journal of Chromatography, 514 (1990) 371–376
Elsevier Science Publishers B.V., Amsterdam

CHROM. 22 509

Note

Simultaneous determination of extractable sulphate and malate in plant extracts using ion chromatography

E. SMOLDERS, M. VAN DAEL and R. MERCKX*

Laboratory of Soil Fertility and Soil Biology, Faculty of Agricultural Sciences, K.U. Leuven, K. Mercierlaan 92, 3030 Leuven (Belgium)

(First received December 8th, 1989; revised manuscript received March 30th, 1990)

Since its introduction in the mid-1970s, ion chromatography (IC) has become widely used for the determination of all types of anions or cations. Its importance in soil science and plant analysis has increased considerably in recent years[1–6].

Of all plant macroconstituents, SO_4^{2-} has been the most resistent to quantitative determinations[7]. Turbidimetric, gravimetric, titrimetric and spectrophotometric methods[8] are time consuming, difficult to perform or require expensive equipment[9]. With an ion chromatographic technique, however, SO_4^{2-} can be rapidly quantified at an acceptable level of accuracy with a rather simple procedure. An additional advantage of this method in plant and soil research is that many other anionic compounds, such as Cl^-, NO_3^-, $H_2PO_4^-$ and some organic acids can also be determined in the same run.

The determination of SO_4^{2-} in plant materials has been described previously[2], but the resolution of the SO_4^{2-} and organic acid (malate) peaks is poor, probably owing to their nearly equal ionic radii. Nevertheless, methods have been developed to overcome this problem making use of a programmed run with a specific column. In this work we explored the possibility of a simple isocratic system with tandem detectors (a conductivity cell and UV absorbance detector). Double monitoring has been used before by others to widen the range of applications of ion chromatography[10]. In this instance nitrite could be quantified in a large background of chloride by combined monitoring.

EXPERIMENTAL

Ion chromatography

The system used was a Dionex (Sunnyvale, CA, U.S.A.) Model QIC analyser. Details of the operating parameters are given in Table I. The instrument consists of a high-performance liquid chromatograph with an analytical column and precolumn, both containing an anion-exchange resin in the HCO_3^- form. Other components are a single-piston pump with pulse damper and an injection valve with a 50-μl sample loop. The first detector was a Dionex conductivity detector preceded by a cation-

0021-9673/90/$03.50

TABLE I

OPERATING PARAMETERS FOR THE QIC ANALYSER AND THE UV ABSORBANCE DETECTOR

Instrument	*Parameter*	*Value*
QIC analyser	Sample loop volume	50 μl
	Guard column	HPIC-AG4A (50 × 3 mm I.D.)
	Separator column	HPIC-AS4A (250 × 3 mm I.D.)
	Eluent	1.8 m*M* Na_2CO_3 + 1.7 m*M* $NaHCO_3$
	Eluent flow-rate	2.0 ml/min
	Pump pressure	*ca.* 70 bar (1000 p.s.i.)
	Suppressor	Anion fibre suppressor 1-2 P/N
	Regenerant for suppressor	12.5 m*M* H_2SO_4
	Regenerant flow-rate	3.0 ml/min
	Background conductivity	21 μS
	Conductivity full-scale	100 μS
UV absorbance detector	Wavelength	190 nm
	Filter	0.5 s
	Minimum absorbance	0.001

exchange membrane in the H^+ form to suppress the background conductivity of the eluent. The second detector was a variable-wavelength UV monitor (Waters Assoc. Model 484) connected through 30 cm × 0.3 mm I.D. tubing in series with the conductivity cell. The reference cell in the UV monitor was left empty. Absorbance was measured at the highest sensitivity at 190 nm. Sufficient back-pressure was achieved by connecting a 160 cm × 0.3 m I.D. tubing after the outlet of the UV monitor. Data acquisition and peak-area calculation were performed using Shimadzu C-R6A and C-R3A integrators connected to the first and second detectors, respectively.

Extraction of plants and preparation of standards

A commercially available spinach (*Spinacia oleracea* L.) sample was dried for 3 days at 70°C and ground to pass through a 0.4-mm screen (Tecator Cyclotec 1092 sample mill). A 150-mg amount of the ground sample was extracted with 1.8 m*M* Na_2CO_3–1.7 m*M* $NaHCO_3$ solution. The mixture was heated for 30 min in a water-bath at 70°C and the extract was centrifuged for 15 min at 20 000 *g* before injecting the supernatant into the ion chromatographic system. Standards (between 0.02 and 0.1 m*M* for SO_4^{2-} and between 0.05 and 0.25 m*M* for malate) were prepared by dissolving appropriate weights of analytical-reagent grade potassium sulphate (UCB) and DL-malate (Riedel-de Haën) in deionized water that had been filtered and purified through a Millipore Milli-Q purification system. Aliquots (*ca.* 2 ml) of the extract and standards were used to flush and fill the sample loop using a plastic syringe equipped with a Swinnex filter holder with Schleiger & Schüll membrane filters (0.45 μm, diameter 13 mm). Colloidal particles which are retained on the membrane filter act as an ion exchanger and reduce the recovery of the anions. Alkaline instead of aqueous extraction has been found[11] to reduce this effect.

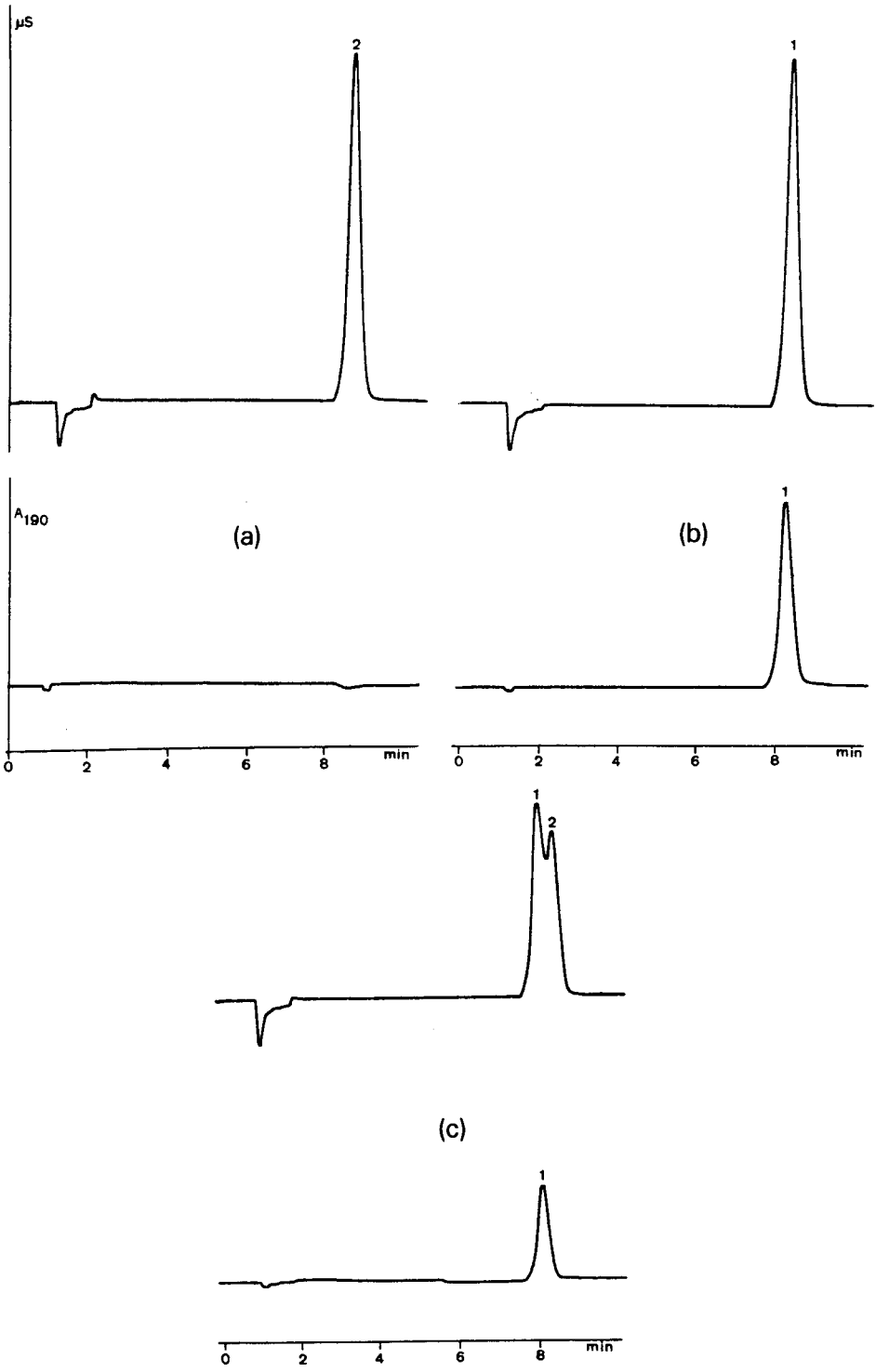

Fig. 1. Typical chromatograms of aqueous standard solutions of (a) 0.1 m*M* SO_4^{2-}, (b) 0.25 m*M* malate and (c) 0.05 m*M* SO_4^{2-} + 0.125 m*M* malate monitored with the conductivity cell (upper chromatograms) or the UV absorbance detector (lower chromatograms). Operating conditions are given in Table I. Peaks: 1 = malate; 2 = SO_4^{2-}.

TABLE II

DETERMINATION OF SO_4^{2-} AND MALATE CONCENTRATIONS IN PURE AQUEOUS MIXTURES BY ION CHROMATOGRAPHY WITH DOUBLE MONITORING

Results are expressed as means (m*M*) ± standard deviation (S.D.) of duplicate injections.

Sample composition	*[SO_4^{2-}] (mM) (x ± S.D.)*	*[malic acid] (mM) (x ± S.D.)*
0.05 m*M* SO_4^{2-} + 0.1 m*M* malate	0.048 ± 0.001	0.104 ± 0.003
0.1 m*M* SO_4^{2-} + 0.25 m*M* malate	0.102 ± 0.001	0.250 ± 0.001

RESULTS AND DISCUSSION

Some typical chromatograms obtained after injecting solutions of SO_4^{2-} or malate and of their mixtures are shown in Fig. 1. When introduced as a single compound the absorbance at 190 nm of SO_4^{2-} does not exceed the noise of the baseline. Therefore, the double peak on the conductivity detector of SO_4^{2-} and malate in Fig. 1c is reduced to a single peak of malate in the UV absorbance detection mode. In all runs a small peak (not shown) was registered by the second detector at a retention time of 23 min. Whether this was an impurity in the malate or a component of malate formed during separation was not investigated further.

When both constituents were present the SO_4^{2-} concentration could be calculated as follows: the concentration of malate was obtained from the area of the single detected peak in the UV absorbance mode; the corresponding area on the conductivity detector was calculated using a calibration graph for pure malate standards and was subtracted from the total area of the unresolved peaks from this detector. The remaining area was used to calculate the SO_4^{2-} concentration.

TABLE III

DETERMINATION OF SO_4^{2-} AND MALATE CONCENTRATIONS IN AQUEOUS EXTRACTS OF SPINACH USING STANDARD ADDITIONS BY ION CHROMATOGRAPHY WITH DOUBLE MONITORING

Results are expressed as means (m*M*) ± standard deviation (S.D.) of duplicate injections. The expected values of the total concentrations are given in parentheses and were calculated with the mean SO_4^{2-} and malate concentrations as the correct value.

Sample composition	*[SO_4^{2-}] (mM) (x ± S.D.)*	*[Malic acid] (mM) (x ± S.D.)*
Spinach extract	0.094 ± 0.005	0.164 ± 0.015
Spinach extract, diluted 1:2	0.045 ± 0.004 (0.047)	0.079 ± 0.001 (0.082)
Spinach extract + SO_4^{2-} and malate solution	0.081 ± 0.001 (0.078)	0.210 ± 0.001 (0.22)
Spinach extract, diluted 1:2 + SO_4^{2-} and malate solution	0.057 ± 0.001 (0.056)	0.128 ± 0.002 (0.132)

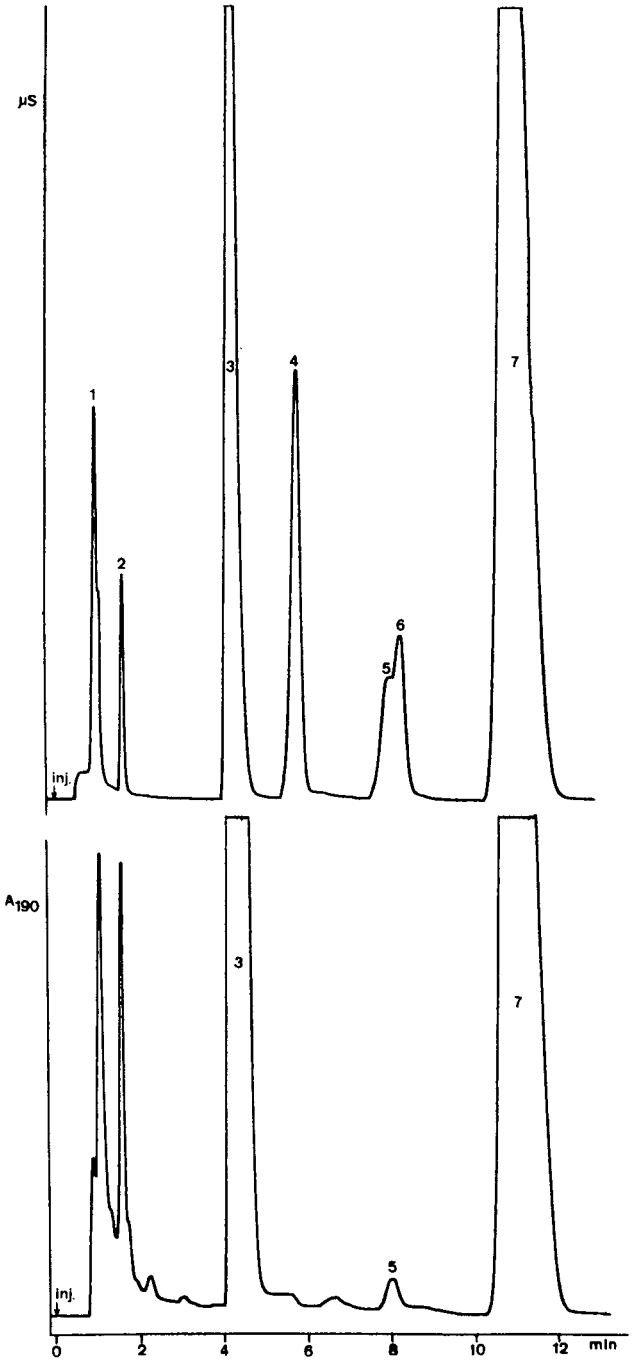

Fig. 2. Typical ion chromatogram of an aqueous spinach extract monitored with the conductivity cell (upper chromatogram) or the UV absorbance detector (lower chromatogram). Operating conditions are given in Table I. Peaks: 1 = unknown; 2 = Cl^-; 3 = NO_3^-; 4 = $H_2PO_4^-$; 5 = malate; 6 = SO_4^{2-}; 7 = oxalate.

To test the assumption that the conductivity peak caused by a mixture of SO_4^{2-} and malate can be obtained by a linear summation of the separate contributions, well standardized mixtures of both components were analysed. On the above basis the concentrations were calculated with the results given in Table II, and are considered to be satisfactory.

To test the appropriateness of the method for plant extracts dilution and standard addition procedures were applied to a spinach extract and the results are given in Table III. Typical chromatograms of the pure extract obtained with both detectors are shown in Fig. 2. The identification of the first peak remains unclear. The results in Table III indicate that SO_4^{2-} can be quantified by the described system with double monitoring within an accepted level of accuracy ($\leqslant 5\%$) except for the diluted sample (The second sample in Table III). This indicates that the detection limit is within this range. However, this limit seems to depend on the malate concentration, as indicated by the smaller relative standard deviation for the last sample ($<2\%$).

CONCLUSIONS

In the isocratic ion chromatographic system described, SO_4^{2-} and malate peaks show poor resolution. However, using the double monitoring system (conductivity cell and UV absorbance at 190 nm), both can be quantified at an accepted level of accuracy with a simple procedure. In spinach extracts (150 mg in 100 ml of 1.8 m*M* Na_2CO_3–1.7 m*M* $NaHCO_3$) SO_4^{2-} and malate were determined with relative standard deviations of 5 and 9%, respectively, for sequential injections. As could be inferred from standard addition procedures, the recoveries of both constituents were satisfactory.

ACKNOWLEDGEMENTS

Financial support of the Onderzoeksraad K.U. Leuven (project OT/87/22) is gratefully acknowledged. E. S. gratefully thanks the Nationaal Fonds voor Wetenschappelijk Onderzoek for a research position as Research Assistant.

REFERENCES

1 L. M. Busman, R. P. Dick and M. A. Tabatabai, *Soil. Sci. Soc. Am. J.*, 52 (1983) 1167.
2 M. Kalbasi and M. A. Tabatabai, *Commun. Soil Sci. Plant Anal.*, 16 (1985) 787.
3 J. A. Grunau and J. M. Swiader, *Commun. Soil Sci. Plant Anal.*, 17 (1986) 321.
4 J. A. Grunau and J. M. Swiader, *Commun. Soil Sci. Plant Anal.*, 20 (1989) 383.
5 C. C. Dupreez, D. J. Laubscher and P. J. Dutoit, *Commun. Soil Sci. Plant Anal.*, 20 (1989) 113.
6 C. A. Hordijk, J. J. M. Van Engelen, F. A. Jonker and T. E. Cappenberg, *Water Res.*, 23 (1989) 853.
7 V. J. G. Houba and J. Uittenbogaard, *International Plant Analytical Exchange, Report 1988*, Department of Soil Science and Plant Nutrition, Wageningen Agricultural University, Wageningen, 1988, p. 51.
8 J. D. Beaton, G. R. Burns and J. Platou, *Sulphur Inst. Tech. Bull.*, No. 14, 1968.
9 I. Novozamsky, R. van Eck, J. J. van der Lee, V. J. G. Houba and E. Temminghof, *Commun. Soil Sci. Plant Anal.*, 17 (1986) 1147.
10 P. Pastore, I. Lavagnini, A. Boaretto and F. Magno, *J. Chromatogr.*, 475 (1989) 331.
11 W. Op de Beeck, *Thesis Landbouwkundig Ingenieur*, Katholieke Universiteit, Leuven, 1989.

Journal of Chromatography, 514 (1990) 377–382
Elsevier Science Publishers B.V., Amsterdam

CHROM. 22 568

Note

Indirect thin-layer chromatography–fast atom bombardment and chemical ionization mass spectrometry determination of carbohydrates utilizing simple and rapid microtransfer techniques

GARY W. CALDWELL*, JOHN A. MASUCCI and WILLIAM J. JONES
Department of Chemical Research, Janssen Research Foundation at McNeil Pharmaceutical, Spring House, PA 19477 (U.S.A.)
(First received January 22nd, 1990; revised manuscript received May 15th, 1990)

Thin-layer chromatography (TLC) and mass spectrometry (MS) can be combined in both direct and indirect modes[1]. The TLC plate can be sampled directly by MS. In this case, two approaches can be taken: a sample can be analyzed directly from a TLC plate mounted inside the ion source, using for example secondary ion mass spectrometry (SIMS)[2–5], or laser mass spectrometry[6,7] for the ionization process, or the sample can be desorbed from the TLC plate and transferred to the ion source through a heated line[8]. In some cases, small segments of the TLC plate are cut out and attached to an MS insertion probe[9,10]. While direct-mode techniques offer many advantages over indirect methods, they do have some disadvantages such as differential compound sensitivity, selection of suitable matrix, prevention of diffusion of spots on the TLC plate, and the unavailability of direct TLC–MS accessories and/or dedicated TLC–MS instrumentation. The indirect mode requires that the TLC spot (analyte plus adsorbent) be removed from the plate and inserted into the MS ion source or that the sample be eluted from the TLC adsorbent with suitable organic solvents, evaporated and the resulting extract analyzed by standard MS techniques[11]. Thus, the usefulness of indirect TLC–MS techniques [fast atom bombardment (FAB), chemical ionization (CI) or electron ionization (EI)] depend heavily on efficient microtransfer techniques.

We wish to communicate simple and rapid microtransfer techniques for indirect TLC–FAB-MS and TLC–CI- (or EI-)MS. Various techniques have been described in the literature for performing these operations on the microscale. For example, studies using TLC–FAB-MS established detection limits of approximately 20 μg for lasalocid, septamycin and monensin when analyte was still deposited on the TLC adsorbent[12]. Their microtransfer technique involved covering the tip of the FAB probe tip with double-faced masking tape. The above compounds were sampled by pressing the probe tip against the TLC spot of interest and acquiring FAB mass spectra in the usual manner. Microtransfer elution approaches have included more elaborate systems[13].

0021-9673/90/$03.50

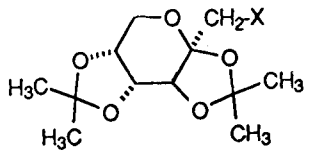

	X	Molecular Mass (amu)
1	OH	260
2	OSO_2NH_2	339
3	$OC(O)NH_2$	303

Fig. 1. Structure and molecular mass of 2,3:4,5-bis-O-(1-methylethylidene)-β-D-fructopyranose (**1**), sulfamate (**2**) and carbamate (**3**).

For example, these devices consist of a filtration section, a collector section and a suction pump. We have developed microtransfer techniques which require no special equipment and are much simpler than any previously reported method.

EXPERIMENTAL

Materials

The carbohydrates 2,3:4,5-bis-O-(1-methylethylidene)-β-D-fructopyranose (**1**), sulfamate (**2**) and carbamate (**3**) derivatives were synthesized according to the literature[14]. The structures and molecular masses are given in Fig. 1. All solvents used were HPLC grade, other materials were of laboratory grade and used as purchased. Common capillary tubes (90 × 1.5–1.8 mm I.D.) and borosilicate glass disposable pasteur pipettes (14 cm) were used.

Preparation of TLC plates

The TLC chromatographic analysis was performed on glass plates coated with silica gel (Whatman MK6F 60A 7.6 × 2.5 cm; Whatman, Clifton, NJ, U.S.A.). A standard mixture (5 mg/ml) of compounds **1–3** was spotted in two separate rows and developed. The mobile phase was cyclohexane–isopropanol (5:1) with R_F values for compounds **1** (0.60), **2** (0.48) and **3** (0.40). After development, one side of the TLC plate was covered while the other side was charred with sulphuric acid for visualization. The covered TLC spots were used for TLC–MS analysis.

Equipment

A VG 7070E mass spectrometer (VG Analytical, Manchester, U.K.) was utilized for obtaining FAB-MS data with 3-mercapto-1,2-propanediol (thioglycerol) as the matrix and argon as the gas for the FAB gun. The acceleration voltage was 5 kV with a mass range of 50–1000 daltons. A Finnigan 3300 or the VG 7070E mass spectrometer was utilized in the CI mode (ammonia) over a mass range of 50–700 daltons.

Microtransfer method for TLC–FAB-MS

A microtransfer method was developed by which the above compounds could be sampled by indirect TLC–FAB-MS. In general, a small amount of thioglycerol was placed on the end of a capillary tube. By touching the capillary tube to the TLC spot of interest, the silica gel was softened and removed (sample plus adsorbent). The silica adsorbent containing analyte was deposited directly on the FAB probe tip and analyzed. Additional thioglycerol was added (1 μl) prior to inserting the FAB probe into the MS.

Microtransfer method for TLC–CI- or EI-MS

The TLC–CI- (or EI-)MS microtransfer method involved a simple one-step

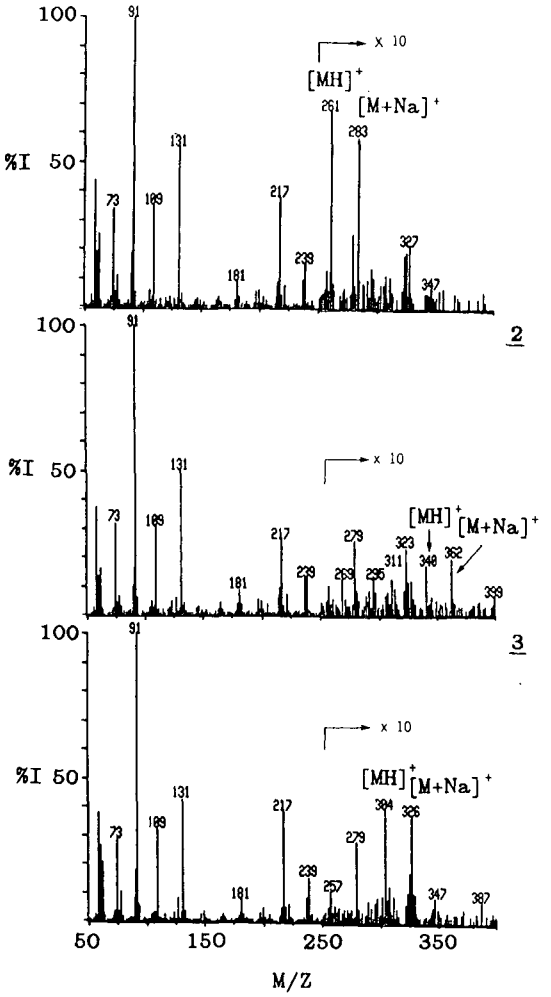

Fig. 2. The TLC–FAB-MS (thioglycerol) spectra of compounds **1–3** are shown. Spectra were obtained from a developed TLC plate (silica gel) where **1–3** were spotted at 5 μg each. The compound plus adsorbent were removed from the TLC plate and inserted directly into the mass spectrometer. I = Relative intensity.

extraction prior to MS analysis. This method involved utilizing a disposable pipette to scrape the TLC spot of interest. After scraping, the sample and adsorbent were located in the tip of the pipette and were transferred to a vial. By holding the vial at approximately a 45° angle and adding approximately 25–50 μl of a chloroform–methanol (50:50) mixture, the vial was slowly rotated in such a manner that the adsorbent remained at the top of the vial and the solution containing the compound of interest was at the bottom of the vial. The pipette was again used to remove the solution by capillary action. This solution, which contained the sample plus a small amount of adsorbent, was placed on an MS insertion probe, evaporated and analyzed.

RESULTS AND DISCUSSION

A glass-backed silica gel TLC plate was used to chromatographically separate a mixture of carbohydrates **1–3**. The TLC–FAB-MS results indicated that spectra of the above compounds could be obtained with reasonable sensitivity at 5 μg per spot (Fig. 2). The $[M + H]^+$ and $[M + Na]^+$ ions were clearly observed in all spectra and could be used for molecular-mass verification. The remaining ions in Fig. 2 are due primarily to the thioglycerol matrix as evident by comparing these ions to background ions in Fig. 3 (top). Background ions from the TLC adsorbent were not observed. The

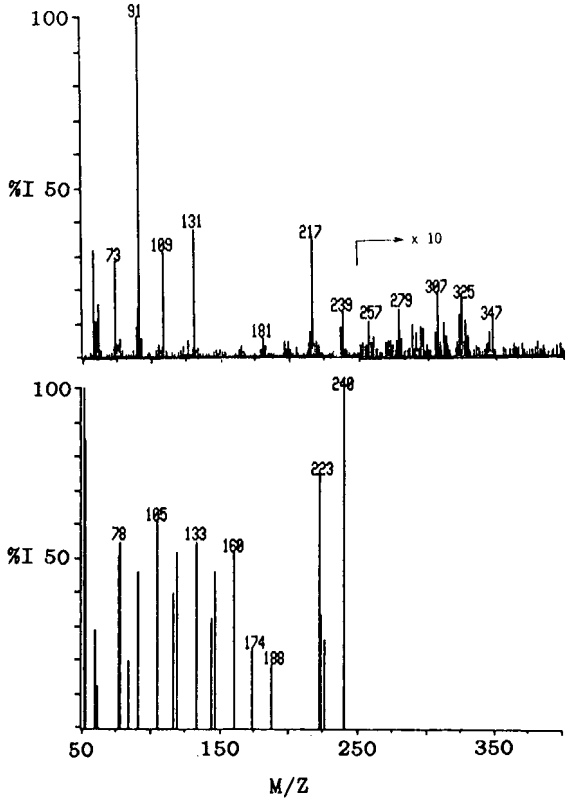

Fig. 3. The background ions are shown for TLC–FAB-MS (top, thioglycerol) and TLC–CI-MS (bottom, ammonia).

TLC–CI-MS (ammonia) results indicated that the $[M + NH_4]^+$ ion could be clearly observed at 5 μg per spot for compounds **1–3** (Fig. 4) along with fragment ions. The base peak was m/z 278. The m/z ion is probably produced for compounds **2** and **3** by ammonia substitution reactions or thermal decomposition, *i.e.*, **2** to **1** and **3** to **1**. Background ions from the TLC adsorbent were not observed (Fig. 3, bottom).

It is significant to note that the TLC plates utilized are those commonly used by organic chemists for monitoring reactions. Thus no special information is required by the chemist to submit samples for MS analysis. It is also important to note that the small amount of silica which is deposited on the probe tip for TLC–FAB-MS or TLC–CI-MS remains primarily on the tip and is removed after MS analysis. Therefore no additional MS source cleaning is required for μg-type analysis.

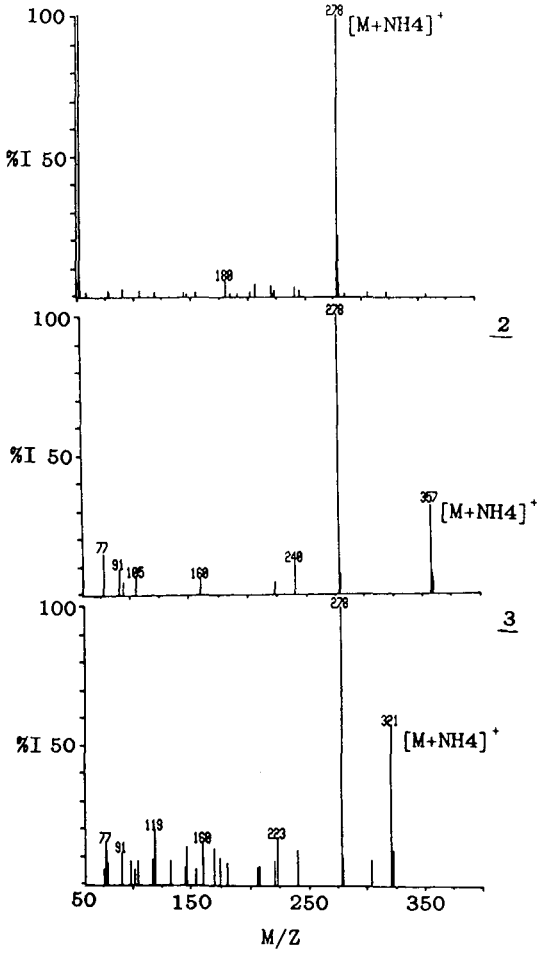

Fig. 4. The TLC–CI-MS (ammonia) spectra of compounds **1–3** are shown. Spectra were obtained from a developed TLC plate (silica gel) where **1–3** were spotted at 5 μg each. The compounds were eluted from the adsorbent prior to CI analysis.

CONCLUSION

We have developed very simple microtransfer techniques for TLC–MS which allow for rapid turn-around-times (2 min per spot) and efficient throughput of samples. In fact, we analyze approximately 400 TLC plates per year with these methods. Useful MS data can be obtained with a high degree of confidence for a wide range of samples and problems when both TLC–FAB-MS and TLC–CI-MS are used in combination. We have found that these microtransfer methods can be applied to most compounds that are separated on TLC plates.

REFERENCES

1 C. F. Poole and S. K. Poole, *J. Chromatogr.*, 492 (1989) 539–584.
2 K. Masuda, K. Harada, M. Suzuki, H. Oka, N. Kawamura and M. Yamada, *Org. Mass Spectrom.*, 24 (1989) 74–75.
3 K. L. Busch, *J. Planar Chromatogr.*, 2 (1989) 355.
4 K. L. Busch, *Trends Anal. Chem.*, 6 (1987) 95–100.
5 G. C. DiDonato and K. L. Busch, *Anal. Chem.*, 58 (1986) 3231–3232.
6 A. J. Kubis, K. V. Somayajula, A. G. Sharkey and D. M. Hercules, *Anal. Chem.*, 61 (1989) 2516–2523.
7 F. P. Novak and D. M. Hercules, *Anal. Lett.*, 18 (1985) 503–518.
8 L. Ramaley, M.-A. Vaughan and W. D. Jamieson, *Anal. Chem.*, 57 (1985) 353–358.
9 H. Iwabuchi, A. Nakagawa and K.-I. Nakamura, *J. Chromatogr.*, 414 (1987) 139–148.
10 Y. Kushi and S. Handa, *J. Biochem.*, 98 (1985) 265–268.
11 C. J. Clemett, *Anal. Chem.*, 43 (1971) 490.
12 T. T. Chang, J. O. Lay and R. J. Francel, *Anal. Chem.*, 56 (1984) 109–111.
13 D. Dekker, *J. Chromatogr.*, 168 (1979) 508–511.
14 B. E. Maryanoff, S. O. Nortey, J. F. Gardocki, R. P. Shank and P. Dodgson, *J. Med. Chem.*, 30 (1987) 880–890.

Journal of Chromatography, 514 (1990) 383–388
Elsevier Science Publishers B.V., Amsterdam

CHROM. 22 531

Note

Determination of arbutin in uvae-ursi folium (bearberry leaves) by capillary zone electrophoresis

E. KENNDLER* and Ch. SCHWER
Institute for Analytical Chemistry, University of Vienna, Währingerstrasse 38, A 1090 Vienna (Austria)
and
B. FRITSCHE and M. PÖHM
Institute of Pharmacognosy, University of Vienna, Währingerstrasse 25, A 1090 Vienna (Austria)
(First received March 16th, 1990; revised manuscript received May 2nd, 1990)

Uvae-ursi folium are the dried leaves of *Arctostaphylos uva-ursi* (L.) Sprengel (bearberry). The crude drug consists mainly of three groups of pharmaceutically relevant compounds: phenols, tanning agents and flavonoids[1,2]. The main phenolic constituent is arbutin (hydroquinone β-D-monoglucopyranoside), with a content of 6–15% (w/w) relative to the dry plant material. Other phenolic compounds found are methylarbutin (up to 2.5%) and hydroquinone (in low concentration). Tanning agents are present in uvae-ursi folium at concentrations of 15–20%, mainly as gallotannins but also as catechotannins, as derivatives of ellagic acid and as galloyl arbutin esters. Free gallic acid is also found in the leaves, and is used with other compounds as an indicator substance to prove the identity of the crude drug[1,2]. The main flavonoid found is quercetin-3-O-galactoside (hyperoside).

The aqueous extract of the crude drug acts as a urinary disinfectant[1,3]. The pharmacologically active compound is hydroquinone, originating from arbutin by *in vivo* glucoside cleavage. Free hydroquinone formed in this way is then conjugated, leading to (non-active) glucuronides and sulphates, which are cleaved in alkaline urine to free hydroquinone, a process supported by simultaneous application of sodium carbonate.

The determination of arbutin and the proof of the identity of the crude drug, as specified in DAB 9[1], are carried out not by a single but by at least two different methods. The identity of the drug is controlled either by microsublimation and determination of hydroquinone, formed by the procedure described, or by the qualitative analysis of arbutin, hydroquinone and gallic acid by thin-layer chromatographic separation followed by derivatization.

The determination of arbutin according to DAB 9 is carried out photometrically, based on the derivative formed by the so-called Emerson reaction[4] after treatment with 4-aminoantipyrine, ammonia and potassium hexacyanoferrate(III). By this procedure an overall parameter for phenolic compounds in general is determined, although the result is related to arbutin.

0021-9673/90/$03.50

In addition to the procedures specified by DAB 9, arbutin has been determined in crude drugs by high-performance liquid chromatography (HPLC) in the presence of other hydroquinone derivatives[5,6]. The identity of the drug, however, was not proved by this method in accordance with DAB 9, because gallic acid, specified as an indicator substance besides arbutin and hydroquinone, was not determined.

In this paper, a simple procedure based on capillary zone electrophoresis is introduced, which simultaneously provides proof of the identity of the drug and the determination of arbutin.

EXPERIMENTAL

All chemicals and solvents used for the preparation of the buffering electrolytes were of analytical-reagent grade (E. Merck, Darmstadt, F.R.G.). Water was distilled twice from a quartz apparatus before use. Resorcinol, used as the internal standard, hydroquinone and gallic acid were also of analytical-reagent grade (E. Merck). Arbutin was isolated on a semipreparative scale from uvae-ursi folium[7].

The aqueous extracts of the crude drugs were prepared as follows: 4 g of sliced dried bearberry leaves were suspended in 100 ml of water, the solution was boiled for 30 min and filtered twice and the resulting filtrate was centrifuged at 15000 rpm, representing a maximum of 15850 *g* at the bottom of the centrifugation tubes, for 5 min (Microfuge E; Beckman, Palo Alto, CA, U.S.A.). A 5-ml volume of the supernatant solution was diluted to an appropriate volume, the internal standard was added and an aliquot of a few nanolitres was injected directly.

Zone electrophoresis was performed on a P/ACE System 2000 instrument (Beckman) equipped with a separation capillary made from fused silica (75 μm I.D., 50 cm lenght to the detector). The field strength was about 350 V/cm at an electric current of about 70 μA. Hydrodynamic injection was carried out pneumatically for 1 s. Between separations, two washing steps were carried out automatically: rinsing with sodium hydroxide solution (0.1 mol/l) for 2 min was followed by washing the capillary with working buffer (sodium borate of different pH values, borate concentration 0.1 mol/l) for 2 min.

Detection by UV absorbance was carried out at 214 nm. Recording and processing of the data were performed with a computerized system (System Gold, Beckman).

RESULTS AND DISCUSSION

Qualitative analysis

Important characteristics of an analytical procedure are sufficiently high precision and accuracy and also the time of analysis. Therefore, often it is not relevant in method developement to maximize the resolution of the sample components without fulfilling the demands on analysis time.

Arbutin and hydroquinone (one of the components used to prove the identity of uvae-ursi folium) are weakly acidic phenols with pK_a values of about 10. A high pH of the buffering electrolyte is therefore required in order to separate these analytes via the different effective mobilities of the anions formed. It can be seen from Fig. 1 that at pH 9, both analytes exhibit about equal migration times, which are very close to that of an

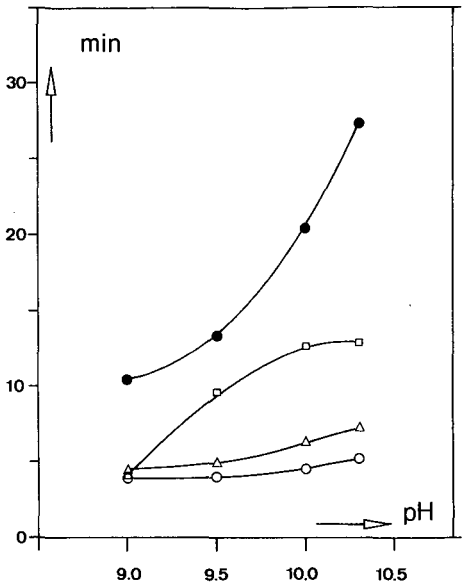

Fig. 1. Dependence of the migration times of arbutin, hydroquinone and gallic acid on the pH of the buffering electrolyte. The migration time of neutral compounds, transported by electroosmosis, was measured from the occurrence of a negative signal on the UV detector due to water injected as the solvent of the standards. ○, Neutral compounds; △, arbutin; □, hydroquinone; ●, gallic acid. Buffers: sodium borate of different pH (0.1 mol/l).

uncharged species. Migration is caused mainly by the electroosmotic flow of the bulk solvent, directed towards the cathode, which originates from the electric double layer between the surface of the fused-silica material and the buffering electrolyte. Increasing the pH of the buffer leads to an increase in the degree of dissociation of these phenols, and the times of migration are enhanced in this way. In fact, it can be seen from Fig. 1 that the difference in the migration times is drastically affected by changing the pH from 9.0 to 9.5. This difference is not influenced significantly by a further increase in pH. On the other hand, the time of migration of gallic acid, which is also an important marker substance for proving the identity of the crude drug under consideration, increases steeply from about 10.5 min at pH 9 to more than 27 min at pH 10.3.

Based on the dependence of the migration times on pH (Fig. 1), it can be concluded that the most favourable electrolyte system is that with pH 9.5. Therefore, this system was applied for the determination of arbutin, and also for monitoring hydroquinone and gallic acid in the extracts of the leaves. At pH 9.5 it was found that arbutin is sufficiently separated from non-ionic compounds, which migrate due to electroosmosis and are detected at about 4 min, arbutin is well separated from hydroquinone and the time of analysis, given by the migration time of the last-eluting component of interest (gallic acid), is only about 13 min, which can be considered to be acceptable.

A typical electropherogram obtained from an aqueous extract of uvae-ursi folium with a buffering electrolyte of pH 9.5 is shown in Fig. 2. Arbutin, hydroquinone

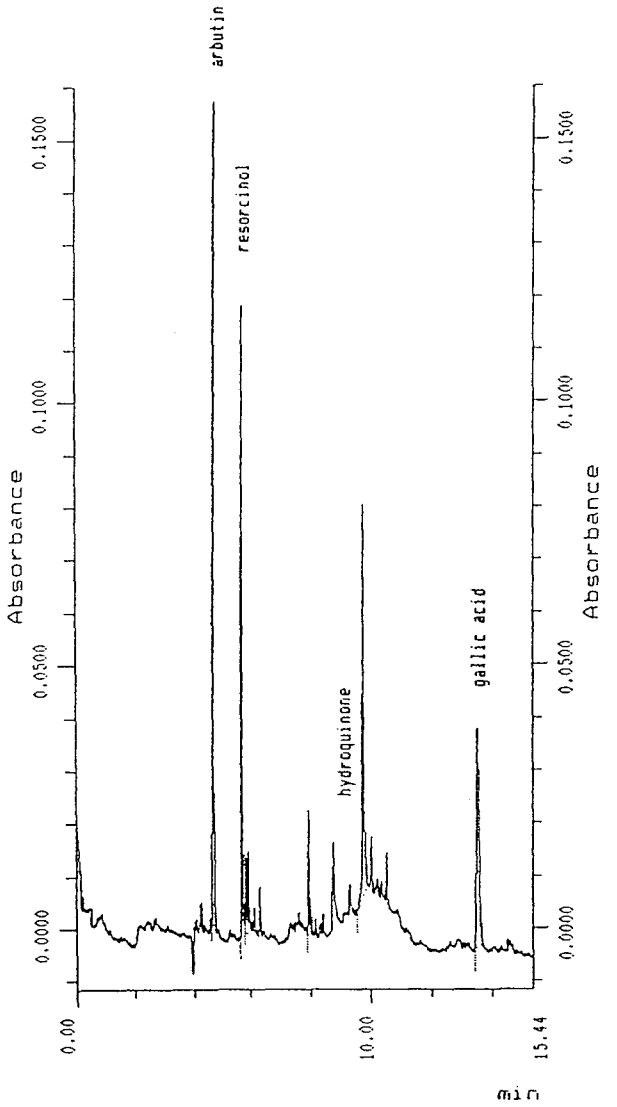

Fig. 2. Typical electropherogram of an aqueous extract of uvae-ursi folium. The electropherogram was obtained from sample 1 in Table I. Conditions: separation capillary, fused silica, 75 μm I.D., 50 cm length to detector; 350 V/cm; 70 μA; buffer, pH 9.5 (sodium borate, 0.1 mol/l); detection, UV, 214 nm.

and gallic acid are clearly distinguished; therefore, the identity of the drug is easily proved. Further, arbutin is well separated from other components under the given conditons permitting an appropriate determination of this compound. The main fraction of anionic components (probably flavonoids), which are detected between 7 and 9 min, do not interfere with this determination.

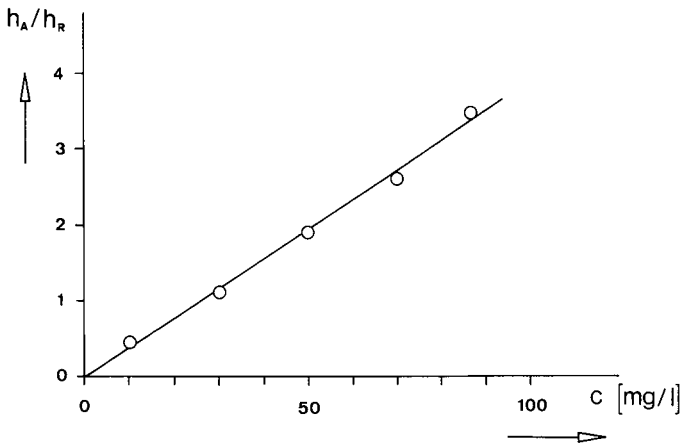

Fig. 3. Calibration graph for the determination of arbutin in crude drugs. h_A/h_R = ratio of the peak heights of arbutin and resorcinol (internal standard); c = concentration of arbutin (mg/l) in the solution injected.

Determination of arbutin

In addition to the proof of identity of the plant drug, arbutin was determined in the extracts of crude drugs using an internal standard. Resorcinol was selected for this purpose, because it does not occur naturally in uvae-ursi folium and it has similar chemical properties to the phenolic analyte. Peak heights of the analyte and the internal standard were used because they are not as strongly affected by variations in the electroosmotic flow as peak areas. The calibration graph is shown in Fig. 3. The linearity was good (linear correlation coefficient 0.998).

The detection limit for arbutin, defined for a signal-to-noise ratio of 3, is about 10 fmol. It is of minor importance for the samples of interest.

The results of the determination of arbutin in four different commercially available crude drugs, obtained from different sources, are given in Table I. The values were calculated from duplicate measurements. In all instances the content of arbutin is within the range specified by DAB 9 (6–15%).

The precision, expressed as the standard deviation, determined, *e.g.*, from eight measurements on extract 4, (Table I), was 0.135%, related to a concentration of 6.4% of arbutin. The corresponding relative confidence interval (for $P=95\%$) is 1.8%.

TABLE I

RESULTS OF THE DETERMINATION OF ARBUTIN IN UVAE-URSI FOLIUM

Sample No.	*Arbutin content (%, w/w)*[a]
1	7.0
2	7.2
3	7.6
4	6.4

[a] The content is relative to the dry leaves.

Hence it can be concluded that the precision of the measurement meets the demands for this type of analysis.

ACKNOWLEDGEMENTS

The authors acknowledge financial support from E. Merck, and appreciate the help of Beckman Instruments in providing the capillary zone electrophoresis instrument.

REFERENCES

1 *Deutsches Arzneibuch 9 (DAB 9)*, Ausgabe 1986, Deutscher Apothekerverlag, Stuttgart, 1986.
2 H. Wagner,in *Pharmazeutische Biologie*, Vol. 2, Gustav Fischer, Stuttgart, New York, 4th ed., 1988, p. 238.
3 D. Frohne, *Z. Phytother.*, 7 (1986) 45.
4 K. H. Müller and E. Hackenberg, *Arzneim. Forsch.*, 9 (1959) 529.
5 O. Sticher, F. Soldati and D. Lehmann, *Planta Med.*, 35 (1979) 253.
6 E. Stahl and L. Kraus, *J. Chromatogr.*, 170 (1979) 269.
7 E. Stahl and W. Schild, in *Pharmazeutische Biologie*, Vol. 4, Gustav Fischer, Stuttgart, New York, 1981, p. 90.

Journal of Chromatography, 514 (1990) 389–393
Elsevier Science Publishers B.V., Amsterdam

CHROM. 22 527

Note

Capillary zone electrophoretic separation of chlorophenols in industrial waste water with on-column electrochemical detection

CHANDRASHEKHAR D. GAITONDE* and PRITA V. PATHAK
Applications and Methods Development Laboratory, Anamed Instruments (Pvt.) Ltd., D-165, T.T.C. Area, M.I.D.C., New Bombay 400706 (India)
(First received January 25th, 1990; revised manuscript received April 18th, 1990)

Phenolic compounds, in particular chlorinated phenols as pollutants in drinking water, cause concern because of their high toxicity and wide distribution. The release of these chlorophenols through waste water has led to the need for methods for monitoring these compounds in industrial effluents and natural waters.

A variety of methods such as liquid–liquid extraction[1–3] ion-exchange techniques[4,5], gas chromatography (GC) with different derivatization procedures[6–8], spectrophotometry[9,10], colorimetry[11] and high-performance thin-layer chromatography[12] have been used for the determination chlorophenols in waters. However, these were either tedious and time consuming or often tiresome. Reversed-phase high-performance liquid chromatography (HPLC) as applied to isomeric chlorophenols in waste waters with UV[13–16], fluorescence[17] and electrochemical[18–20] detection has already been reported. Electrokinetic chromatography with micellar solutions for the separation of chlorophenols as reported by Terabe *et al.*[21] and Otsuka *et al.*[22] employed UV detection, providing detection levels in the nanogram range.

The objective of this work was to study the suitability of capillary zone electrophoresis (CZE) for the separation of chlorinated phenols in industrial waste waters. A fused-silica capillary was employed with an applied potential of 20 kV. Detection was performed with an on-column electrochemical detector modified with carbon fibres. Detection levels in the picomole range were achieved with separation efficiencies of the order of 320 000 theoretical plates.

EXPERIMENTAL

Reagents and chemicals

The standards of chlorinated phenols (2-chloro-, 4-chloro-, 2,4-dichloro-, 2,6-dichloro-, 2,4,6-trichloro-, 2,3,4,6-tetrachloro- and pentachlorophenol) were obtained from Sigma (St. Louis, MO, U.S.A.) and phenol, *o*-phenylphenol, catechol

0021-9673/90/$03.50

and 4,5,6-trichloroguiacol from S. D. Fine Chemicals (Boisar, Tarapur, India). They were dissolved in methanol–water (1:1) to give a concentration of 5 ng/l of each of the components. Sodium dihydrogenphosphate and sodium borate were obtained from E. Merck (India) (Worli, Bombay, India). Other reagents were of analytical-reagent grade from S. D. Fine Chemicals and were used as received.

Industrial waste water samples containing isomeric chlorophenols and neutral phenols were the gifts from Dharamsi Morarji Chemicals (Ambernath, India). Millipore Milli-Q water was used wherever necessary and to prepare sodium dihydrogenphosphate (0.045 *M*) and sodium borate (0.015 *M*) buffers for mixing in an appropriate ratio to give pH 8.0.

Extraction and CZE apparatus

Waste water samples (5 ml) were shaken with 5 ml of chloroform–diethyl ether (1:1) in a separating flask. An aliquot (1 ml) of the organic layer was diluted with sodium dihydrogen orthophosphate (0.045 *M*)–sodium borate (0.015 *M*) (1:1) and the pH was adjusted to 8.0. This was used directly for CZE.

All CZE experiments were performed using a 650 mm × 25 μm I.D. fused-silica capillary (Scientific Glass Engineering). On-column measurements were carried out 300 mm from the negative end of the capillary using an electrochemical detector modified using carbon fibres (10-μm diameter) as described by Knecht *et al.*[23]. The connections of the capillary to the electrochemical detector were the same as employed by Ewing *et al.*[24], except for the porous-glass joint assembly connector. Detection was performed in the amperometric mode with an oxidation potential of + 1.4 V *vs.* SCE. The temperature in the separation capillary unit was maintained at 20–25°C during the separation using a thermostated oven. A capillary was immersed in a mixture of buffer

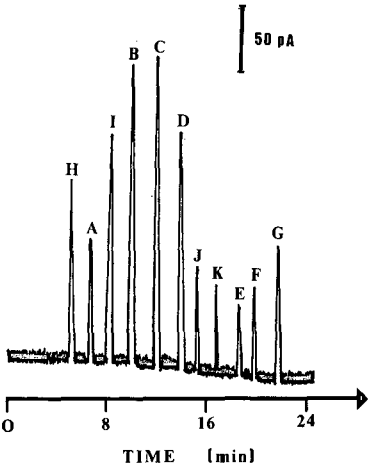

Fig. 1. Electropherogram of a standard mixture of isomeric chlorophenols, 4,5,6-trichloroguiacol and neutral phenols (5–8 ng/l of each). Electrochemical detection at an applied voltage of 20 kV, carbon fibres, + 1.4 V *vs.* SCE. Peaks: A = 2-chlorophenol; B = 2,4-dichlorophenol; C = 2,6-dichlorophenol; D = *o*-phenylphenol; E = 2,3,4,6-tetrachlorophenol; F = 4,5,6-trichloroguiacol; G = pentachlorophenol; H = phenol; I = 4-chlorophenol; J = catechol; K = 2,4,6-trichlorophenol.

solution from the two buffer reservoirs which were kept at the same levels. Sample introduction was accomplished as described by Rose and Jorgenson[25], at a constant voltage (20 kV, high-voltage d.c. power supply, Siemens, Amberg, F.R.G.) at the anodic end for exactly 30 s. The detector signal was recorded on an Omniscribe Model 5000 strip-chart recorder (Digital Electronics, Andheri, Bombay, India).

RESULTS AND DISCUSSION

An electropherogram of a standard mixture of seven chlorophenols together with phenol, *o*-phenylphenol catechol and 4,5,6-trichloroguiacol is shown in Fig. 1. The amount of each component in the mixture injected was estimated to be 5–8 ng/l. The applied voltage between the two ends of the 650-mm capillary was 20 kV. Detection was performed on-column using an oxidation potential of +1.4 V *vs.* SCE. All the compounds were completely resolved within 24 min, the minimum detectable amount being 0.001 ng/ml. The use of a small-diameter capillary (25 μm) enhances the detection with a signal-to-noise ratio of 4.5. Attempts were made to optimize the separation conditions by using different capillary lengths of 400, 500, 600, 650, 800 and 1000 mm and an applied voltage of 20 kV. The theoretical plate number (N) was calculated using the equation[24]

$$N = \frac{(\mu_e + \mu_{eo})V}{2D}$$

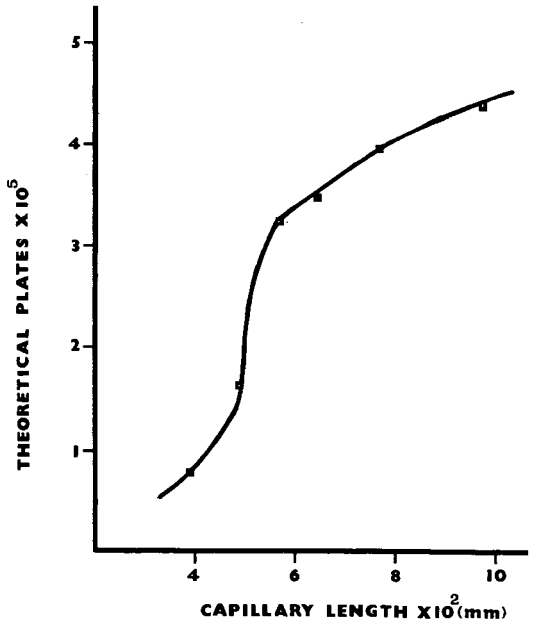

Fig. 2. Theoretical plate number as a function of capillary length (25 μm I.D.) with a buffer mixture of sodium dihydrogenphosphate (0.045 *M*)–sodium borate (0.015 *M*) adjusted to pH 8.0. Detection conditions as in Fig. 1. Sample, 2-chlorophenol.

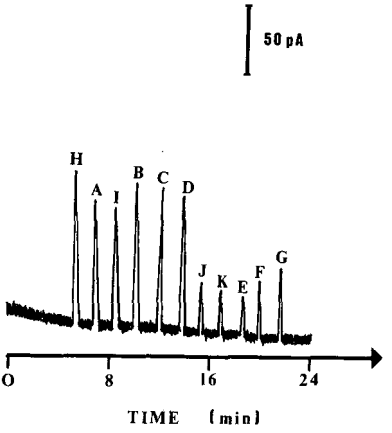

Fig. 3. Electropherogram of an industrial waste water sample with a 2-chlorophenol concentration of 50 ng/ml. Conditions and peaks as in Fig. 1.

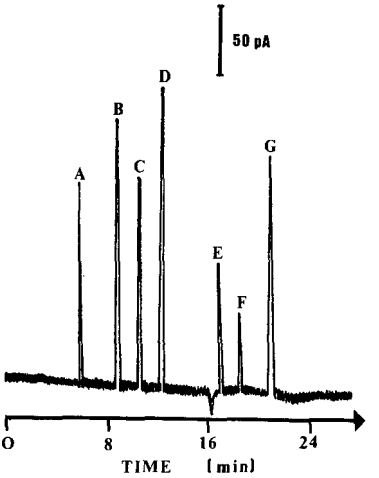

Fig. 4. Electropherogram of an industrial waste water sample with a 2-chlorophenol concentration of 100 ng/ml. Conditions and peaks as in Fig. 1.

where, μ_e and μ_{eo} are the electrophoretic and electroosmotic mobilities, respectively, at *the applied voltage V* and *D* is the diffusion coefficient.

The values of *N* were then plotted against capillary length for 2-chlorophenol as shown in Fig. 2. The results of this experiment clearly indicate that, as the length of the capillary increases beyond 650 mm, the theoretical plate number increases, thereby prolonging the separation of 2-chlorophenol (>60 min) from other components and causing peak broadening. This was also observed for other chlorophenols (results not shown). Important contributors to the peak broadening effect were found to be longitudinal diffusion resulting in a flat flow profile and interactions between the capillary walls and analytes, as noted by others[26].

TABLE I

RETENTION TIME DATA FOR THE COMPOUNDS ANALYSED BY CZE

Results obtained on a 650 mm × 25 μm I.D. capillary, 20 kV, +1.4 V *vs.* SCE.

Compound[a]	*Retention time (min)*	*Compound*[a]	*Retention time (min)*
Phenol (H)	5.8	Catechol (J)	15.6
2-Chlorophenol (A)	7.1	2,4,6-Trichlorophenol (K)	17.0
4-Chlorophenol (I)	8.1	2,3,4,6-Tetrachlorophenol (E)	19.1
2,4-Dichlorophenol (B)	10.1	4,5,6-Trichloroguiacol (F)	20.0
2,6-Dichlorophenol (C)	12.0	Pentachlorophenol (G)	22.0
o-Phenyl phenol (D)	13.8		

[a] Letters in parentheses indicate peaks in Figs. 1, 3 and 4.

Two samples of industrial waste water containing chlorophenol isomers and neutral phenols were subjected to CZE. The chlorophenols were well separated, as shown in Figs. 3 and 4. The limits of detection of each of these components in waste water were found to be 0.005 ng/ml and the analysable concentration range was the same as for model compounds. Table I gives retention time data for these compounds, demonstrating the effective resolution achieved with this system. No interferences from the impurities present in industrial waste water samples were observed.

CONCLUSION

The proposed method of CZE as applied to the separation of chlorophenols and other phenols in industrial waste water samples is more promising than techniques such as HPLC and GC. The use of an on-line electrochemical detector provides excellent sensitivity and selectivity without derivatization or tedious extraction of the sample.

REFERENCES

1 L. Rudling, *Water Res.*, 4 (1970) 533.
2 A. S. Y. Chau and J. A. Coburn, *J. Assoc. Off. Anal. Chem.*, 57 (1974) 289.
3 L. F. Faas and J. C. Moore, *J. Agric. Food Chem.*, 27 (1979) 554.
4 L. Renberg, *Anal. Chem.*, 46 (1979) 459.
5 J. J. Richard and J. S. Fritz, *J. Chromatogr.*, 18 (1980) 35.
6 L. L. Lamparski and T. J. Nestrick, *J. Chromatogr.*, 156 (1978) 143.
7 L. Renberg and K. Lindstrom, *J. Chromatogr.*, 214 (1981) 327.
8 K. Abrahamsson and T. M. Xie, *J. Chromatogr.*, 279 (1983) 199.
9 F. Bosch, G. Font and G. J. Manes, *Analyst (London)*, 112 (1987) 1335.
10 S. Amalathe, S. Upadhyay and V. K. Gupta, *Analyst (London)*, 112 (1987) 1463.
11 S. M. Hassan, F. B. Salem and N. Abd El-Salem, *Anal. Lett.*, 20 (1987) 677.
12 L. Lepri, P. G. Desideri and D. Heimler, *J. Chromatogr.*, 248 (1982) 308.
13 P. Alaroon, A. Bustos, B. Canas, M. D. Andres and L. M. Polo, *Chromatographia*, 24 (1987) 613.
14 F. P. Bigley and R. L. Grob, *J. Chromatogr.*, 350 (1985) 407.
15 G. Blo, F. Dondi, A. Betti and C. Bighi, *J. Chromatogr.*, 257 (1983) 69.
16 D. N. Armentrout, J. C. McLean and M. W. Long, *Anal. Chem.*, 51 (1979) 1039.
17 C. S. Giam, D. A. Trujillo, S. Kira and Y. Hrung, *Bull. Environ. Contam. Toxicol.*, 25 (1980) 824.
18 C. De Ruiter, J. F. Bhole, G. J. De Jong, U. A. Th. Brinkman and R. W. Frei, *Anal. Chem.*, 60 (1988) 666.
19 C. W. Whang, *J. Chin. Chem. Soc. (Taipei)*, 34 (1987) 81.
20 P. Trippel, W. Maasfeld and A. Kettrup, *Int. J. Environ. Anal. Chem.*, 23 (1985) 97.
21 S. Terabe, K. Otsuka, K. Ichikawa, A. Tsuchiya and T. Ando, *Anal. Chem.*, 56 (1984) 111.
22 K. Otsuka, S. Terabe and T. Ando, *J. Chromatogr.*, 348 (1985) 39.
23 L. A. Knecht, E. J. Guthrie and J. W. Jorgenson, *Anal. Chem.*, 56 (1984) 479.
24 A. G. Ewing, R. A. Wallingford and T. M. Olefirowicz, *Anal. Chem.*, 61 (1989) 292A.
25 D. J. Rose and J. W. Jorgenson, *Anal. Chem.*, 60 (1988) 642.
26 X. Huang, W. F. Coleman and R. N. Zare, *J. Chromatogr.*, 480 (1989) 95.

Author Index

Errata

J. Chromatogr., 506 (1990) 371–377

Page 371, the footnote to O. Chiantore is incorrect and should be deleted.

J. Chromatogr., 507 (1990) 389–398

Page 392, Table I: the k' value for IUPAC 138 should be 0.94. IUPAC 138 is then completely separated from IUPAC 163, $k' = 1.10$.

Page 396, Fig. 5: the peak denoted "?" should be labelled 138/163 in Fig. 5A, 138 in Fig. 5B and 163 in Fig. 5C. The text in the second paragraph on page should be interpreted in the same way

Vol. 514, No. 2

journal of
chromatography news section

SYMPOSIUM PROGRAMME

3rd INTERNATIONAL ION CHROMATOGRAPHY SYMPOSIUM, SAN DIEGO, CA, U.S.A., SEPTEMBER 30–OCTOBER 3, 1990

The third in a continuing series of symposia on Ion Chromatography will be held in the San Diego area, September 30th - October 3rd 1990.

Designed to provide a forum for recent developments in this field, the Symposium will offer plenary and keynote sessions of interest to the entire audience, several concurrent sessions devoted to specific interest areas, and a poster session.

The preliminary program includes over sixty-five podium and poster presentations featuring original research reports, reviews of special interest areas, and authoritative summaries of methodologies or experiences within ion chromatography (IC). The Symposium will cover the theory and applications of analytical and preparative separation methods for ionic analytes.

Plenary Lecture

"Twenty" Years of Ion Chromatography

Hamish Small
Leland, MI

An historical look at some of the developments in detection and separation that have made IC what it is today.

Review Lectures

Developments in Ion-exclusion Chromatography
James S. Fritz, Iowa State University, Ames, IA

Development of Moderate Capacity Pellicular Ion Exchange Packing Materials for Ion Chromatography
Christopher A. Pohl, Dionex Corporation, Sunnyvale, CA

Indirect Detection in Ion Chromatography
Donald J. Pietrzyk, University of Iowa, Iowa City, IA

Post-column Reaction Detection in IC
Richard M. Cassidy, University of Saskatchewan, Saskatoon, Saskatchewan, Canada

Optimization of Detection Sensitivity in the Capillary Electrophoresis of Inorganic Ions
Petr Jandik and William Jones, Waters Chromatography Division of Millipore, Milford, MA

Developments in Stationary Phases for Non-suppressed IC
Guenther K. Bonn, Innsbruck University, Innsbruck, Austria

Application of Macrocyclic Ligands to Ion Chromatography
John D. Lamb, Brigham Young Univ., Provo, UT

Evaluation of Eluents for Gradient Elution and SPR - Conductivity Detection of Anions
Douglas T. Gjerde, Sarasep, Inc., Santa Clara, CA

IC in the 90's: A Powerful Tool for the Analysis of Ionic and Polar Componds
Joachim Weiss, Dionex Corporation, FRG

Sample Handling Procedures for Ion Chromatography
Paul R. Haddad, University of New South Wales, Kensington, Australia

Contributed Presentations

Separation Methods and Stationary Phases

A Sensitive, Linear, Practical Method for the Analysis of Monovalent and Divalent Cations by Ion Chromatography
Peter G. Alden, Petr Jandik, and Jim Krol, Waters Chromatography Division of Millipore, Milford,MA

A Cation Exchange Chromatography Column for the Isocratic Elution of Alkali Metals and Alkaline Earth Cations
John R. Stillian, Christopher A. Pohl, and Dan Campbell, Dionex Corporation, Sunnyvale, CA

Controlled Changes of Selectivity in the Separation of Ions by Capillary Electrophoresis
William R. Jones and Petr Jandik, Waters Chromatography Division of Millipore, Milford, MA

Universal Stationary Phase for the Separation of Anions on Suppressor-based and Single-Column IC Systems
Raaidah Saari-Nordhaus, Inga K. Henderson and James M. Anderson, Jr., Alltech Associates, Deerfield, IL

The Separation of Inorganic and Organic Analyte Ions on Dye-Coated Stationary Phases
Thomas A. Walker, Marion Merrell Dow, Inc., Kansas City, MO

Ion Chromatographic Methods for the Detection of Starch Hydrolysis Products in Ruminal Digesta
Karen Barsuhn and Susan F. Kotarski, The Upjohn Company, Kalamazoo, MI

Separation of Transition Metals, Lanthanides and Actinides using Dynamic Ion-Exchange Chromatography with Mandelic Acid
Steve Elchuk and Charles A. Lucy, Atomic Energy of Canada Ltd., Chalk River, Ontario, Canada

Versatility of Multi-Phase Cation Exchange HPLC Columns
Maria A. Rey and Rosanne W. Slingsby, Dionex Corporation, Sunnyvale, CA

Electrochemical Eluent Generation and Suppression in Ion Chromatography: Is Electric Eclectic?
Purnendu K. Dasgupta, Texas Tech University, Lubbock, TX

Analysis of Transition Metals using Dynamically Coated Reverse Phase Columns and Post-Column Derivatization
Jim Krol, Peter E. Jackson, and Allan Heckenberg, Waters Chromatography Division of Millipore, Milford, MA

Monitoring of Free Cyanide in Mine Process Liquors using a Coupled Ion Chromatographic System
Peter Fagan and Paul R. Haddad, University of New South Wales, Kensington, Australia

Analysis of Chelates by HPLC
Marilou E. Lonsdale, W.R. Grace & Co., Nashua, NH

Separation of Inorganic Anions and Aliphatic Organic Acids Using a Solvent Compatible Anion Exchange Column
R.E. Kiser, C.E. DeVasa, and C.A. Pohl, Dionex Corporation, Sunnyvale, CA

Temperature Programming in Macrocycle-Based Ion Chromatography
Robert G. Smith, Phillip A. Drake, and John D. Lamb, Brigham Young University, Provo, UT

Ruthenium (II) 1, 10-Phenanthroline Salts as Mobile Phase Additives for the Separation and Indirect Detection of Free Amino Acids
Donald J. Pietrzyk and Dongxing Yuan, The University of Iowa, Iowa City, IA

Ion Exchange-Adsorption on Low Capacity Polymeric Ion Exchangers
Donald J. Pietrzyk and Shon Meek, The University of Iowa, Iowa City, IA

Detection

Determination of Saccharides in Biological Materials by Anion-Exchange Chromatography with Pulsed Amperometric Detection
Dean A. Martens and W.T. Frankenberger, Jr., University of California, Riverside, CA

Practical Application of SPR-Conductivity Detection in Ion Chromatography
Peter E. Jackson and Jeanne Li, Waters Chromatography Division of Millipore, Milford, MA

An Overview of Detection in Ion Chromatography
Roy D. Rocklin, Dionex Corp., Sunnyvale, CA

Separation and Detection of Non - Chromophoric, Anionic Surfactants
Jeanne B. Li and Petr Jandik, Waters Chromatography Division of Millipore, Milford, MA

Ion Chromatography of UV-Absorbing Ions in High Chloride Matrices
Andrew R. McTaggert, Marheni and Paul R. Haddad, University of New South Wales, Kensington, Australia

Separation and Detection of Group I and II Cations by Ion Chromatography
Daniel L. Campbell, John Stillian, Steve Carson, Robert Joyce, and Shawn Heberling, Dionex Corporation, Sunnyvale, CA

Applications

The Determination of Soluble Hexavalent Chromium in Industrial Wastewater Effluents using Ion Chromatography and Post-Column Derivatization with Diphenylcarbazide
Elizabeth J. Arar, Technology Applications, Cincinnati, OH and John D. Pfaff, Environmental Protection Agency, Cincinnati, OH

Developments and Updates in EPA Method 300 - The Determination of Inorganic Anions in Waters by Ion Chromatography
John D. Pfaff, Environmental Protection Agency, Cincinnati, OH and Elizabeth J. Arar, Technology Applications, Cincinnati, OH

High Performance Ion-Exchange Chromatography as an Approach for Trace Element Analysis. I. Beryllium
Maria Betti, University of Pisa, Pisa, Italy and S. Cavelli, Dionex Corporation, Rome, Italy

Novel Ion Chromatographic Applications in Industrial Problem-Solving
Virgil T. Turkelson, Dow Chemical Company, Midland, MI

Determination of Lanthanide Metals in Geological Samples using Chelation Ion Chromatography
M. Harrold and John Riviello, Dionex Corporation, Sunnyvale, CA and A. Siriraks and H.M. Kingston, NIST, Gaithersburg, MD

Individual Spread of Concentration of Alkali and Alkaline Earth Elements in Seawater by Suppressed Ion Chromatography
P. Papoff, M. Betti, and G. Giovannoni, University of Pisa, Pisa, Italy

Specification of ppb Levels of Metal Cyanide Complexes in Environmental Water Samples
Chatvalee Kalambaheti and Paul R. Haddad, University of New South Wales, Kensington, Australia

Application of Ion Chromatography to Statistical Process Control of Chemical Milling
Melinda R. Fisher, Aerochem, Adelanto, CA and Shawn Heberling, Dionex Corp., Sunnyvale, CA

Applications of IC to Environmental Analysis in China
Mou Shifen, Academia Sinica, Beijing, China

Determination of Tartaric, Malic and Citric Acids in Grape Juice and Wine using Gradient Chromatography
S.A. Kupina, Heublein Wines, Madera, CA and C.A. Pohl and J.L. Gannotti, Dionex Corporation, Sunnyvale, CA

Azide Determination in Protein Samples by Ion Chromatography
Paul L. Annable and Laurie Sly, Marion Merrell Dow, Inc., Kansas City, MO

Automated Determination of Free and Total Cyanide Using Photodissociation and Gas Dialysis Followed by Ion Chromatographic Determination
S. Shawn Heberling, Robert J. Joyce, and Yan Liu, Dionex Corporation, Sunnyvale, CA

Ion Chromatography for the Analysis of Household Consumer Products
David Murawski, Church & Dwight Co., Princeton, NJ

Ion Chromatography in the Manufacture of Multilayer Circuit Boards
Robert E. Smith, Allied-Signal Inc., Kansas City, MO and Shawn Heberling, Dionex Corporation Sunnyvale, CA

Vitamins as Growth Factors in the Soil Rhizosphere
Dean A. Martens and W.T. Frankenberger, University of California, Riverside, CA

Determination of Total Nitrogen in Animal Feeds and Other Foods using Kjeldahl Digestion and Ion Chromatography
Peter E. Jackson, Jim Krol and Allen Heckenberg, Waters Chromatography Division of Millipore, Milford, MA

Determination of Contaminants in Amine Scrubber Solutions Using Gradient Ion Chromatography
James C. Thompsen, Conoco, Ponca City, OK

Ion Chromatography of Alkyl and Alkanol Amines
Jim Krol, Allan Heckenberg and Peter E. Jackson, Waters Chromatography Division of Millipore, Milford, MA

Applications of Chelating Resins for the Determination of Transition Metals by Ion Chromatography
John Riviello, Dionex Corporation, Sunnyvale, CA and A. Siriraks and H.M. Kingston, NIST, Gaithersburg, MD

Optimization of Inorganic Capillary Electrophoresis for the Analysis of Real Samples
Joe Romano, Petr Jandik, William Jones and Peter E. Jackson, Waters Chromatography Division of Millipore, Milford, MA

Application of Ion Chromatography to Failure Analysis of Advanced Electronics Packaging
Marina Plat and Judy DeLeo, IBM Corporation, Hopewell Junction, NY

Improved Separation and Detection of Alkanolamines Using Liquid Chromatography and Electrochemical Detection
Dan Campbell, Steve Carson, and Shawn Heberling, Dionex Corporation, Sunnyvale, CA

Progress in Optimization of Transition Metal Cation Chromatography and Its Application to Analysis of Silicon Wafer Contamination
Kenneth A. Ruth and Roger W. Shaw, MEMC Electronic Materials Co., St. Peters, MO

Industrial Applications of Ion Exclusion Chromatography and Pulsed Amperometry
Sunil K. Chaudhary, Dow Chemical Canada, Fort Saskatchewan, Alberta, Canada

Determination of Inorganic Anions and Organic Acids in Fruit Juice Products using the Omni-pac PAX-100 Column and Conductivity Detection
Patrick E. Williams, Dionex Corporation, Sunnyvale, CA

Cation Analysis of Fermentation Broth by HPLC/IC
Robert G. Bell, A.L. Laboratories, Chicago Heights, IL

Approaches to the Determination of Fluoride and Chloride in Ore Concentrates
Paul R. Haddad, Marheni, and Colin Stace, University of New South Wales, Kensington, Australia

Suppressed and Non-Suppressed IC Applications in Pharmaceutical Analysis
Jay B. Nair and Paul T. Kurtulik, Bristol-Myers Squibb Pharmaceutical Research Institute, New Brunswick, NJ

Online Analyses of Anions and Cations at Low Part-Per-Trillion Levels in BWR High Purity Waters
Norman S. Davis, Grand Gulf Nuclear Station, Port Gibson, MS

The Separation of Explosive Residues by Multiphase Resin
Gregory Conklin, Dionex Corp., Sunnyvale, CA

The Determination of the Effects of Preservation on Nitrite and Nitrate in Three Types of Water Samples Utilizing TRAACS 800 AutoAnalyzer and Single Column Ion Chromatography
Miriam Roman, Bob Dovi, Rhonda Yoder, Frank Dias, and Bruce Warden, Waste Management/ EML, Geneva, IL

General Topics

A New Sample Treatment Technique for Ion-Exclusion Chromatography
David W. Togami, Interaction Chemicals, Mountain View, CA

Development of an Automated Sample Pretreatment System for Simultaneous ICAP/AES Analysis
J.M. Riviello, Dionex Corporation, Sunnyvale, CA; R.M. Manabe, Thermo Jarrell Ash, Menlo Park, CA; and A. Siriraks, NIST, Gaithersburg, MD

Sample Preparation for Ion Chromatography Using Solid-Phase Extraction
Inga K. Henderson, Raaidah Saari-Nordhaus and Jim M. Anderson, Alltech Associates, Deerfield, IL

Peak Interaction under Concave Isotherm Conditions in Preparative Ion Chromatography
Charles A. Lucy and Steve Elchuk, Atomic Energy of Canada Ltd., Chalk River, Ontario, Canada

A Systematic Evaluation of Retention Methods for Non-Suppressed Ion Chromatography of Anions
Andrew Sosimenko and Paul R. Haddad, University of New South Wales, Kensington, Australia

A Generic Approach to Matrix Elimination in Ion Chromatography
Steven R. Villaseñor, Mallinckrodt Speciality Chemical Company, St. Louis, MO

Comparisons and Contrasts of Ion Chromatography Techniques: How Can I Choose the Best for My Analysis?
Michael J. Doyle, Dionex Corporation, Sunnyvale, CA

Comparison of Gradient Elution Techniques for Analysis of Organic Acids and Anions
Sam Harvey, Houston Lighting and Power Company, Wadsworth, TX

Symposium Management
Century International, Inc.
P.O. Box 493, Medfield, MA 02052
508/359-8777 • 508/359-8778 (FAX)

AWARD

MARCEL GOLAY AWARD TO DR. GERHARD SCHOMBURG

On the occasion of the 11th International Symposium on Capillary Chromatography held in Monterey, CA, U.S.A., May 14–17, 1990, the M.J.E. Golay Award was presented to Dr. Gerhard Schomburg by Dr. David Nelson, vice-president of the Perkin Elmer Corporation and Prof. Dr. Pat Sandra, chairman of the symposium (see Fig. 1).

This award consisting of a medal (Fig. 2), a scroll and an endorsement is sponsored by the Perkin Elmer Corporation. The award is presented at the yearly International Symposia on Capillary Chromatography to scientists who made significant contributions to the evolution of capillary chromatography.

Dr. Gerhard Schomburg — born in Bochum, F.R.G., on August 22, 1929 — studied chemistry at the University of Bonn. His doctoral thesis, prepared under nobel laureate K. Ziegler, dealt with infrared spectroscopy. Since 1956 Dr. Schomburg is head of the chromatography department of the Max Planck Institut für Kohlenforschung and leads since 1965 also the chromatography laboratories of the Max Planck Institut für Strahlenchemie, both in Mülheim a/d Ruhr, F.R.G.

Schomburg is Vice-chairman of the board of the Chromatography Group of the Gesellschaft Deutscher Chemiker, one of the editors of *Chromatographia* and member of the editorial board of the *Journal of Chromatography*. He is author or coauthor of more than 200 scientific publications and wrote a textbook on gas chromatography.

The following events mark his career in chromatography:

1978 Tswett Medal for contributions to the development of chromatography by the Board for Chromatography of the U.S.S.R., Tallinn, U.S.S.R.

1983 Tswett Medal of the U.S.A., received at the International Symposium on Advances in Chromatography in Amsterdam, The Netherlands.

Fig. 1.

1984 A.J.P. Martin Award by the Chromatography Society of Great Britain at the 15th International Symposium on Chromatography in Nürnberg, F.R.G.

1986 Stephen Dal Nogare Award through the Chromatography Forum of Delaware Valley at the Pittsburgh Conference in Atlantic City, U.S.A.

1987 Honorary doctoral degree from the University of Duisburg, F.R.G.

1990 Appointed professor at the Faculty of Chemistry of the University of Wuppertal, F.R.G.

Fig. 2.

The award was presented to Dr. Schomburg for his creative and innovative contributions to capillary chromatography and electrophoresis. To mention a few highlights:

In colum technology for GC, LC and electrophoresis:

- dynamic coating of capillary columns, especially from glass or fused silica using the mercury plug technique;
- etching of glass surfaces in capillaries by HCl and HF for deactivation and the improvement of the adhesion of the stationary phase polymers;
- deactivation of glass and fused silica surfaces by the PSD-technique (polysiloxane degradation);
- immobilization of alkylpolysiloxanes by either γ-radiation or the common radical starters;
- polymeric coatings in LC;
- coating of separation capillaries for electrophoresis by immobilized polymers for the control of the electroosmotic flow in micellar electrokinetic capillary electrophoresis, development of a simple method of production of polyacrylamide gel filled fused-silica capillaries for the separation of charged large oligomeric biomolecules, such as oligonucleotides, using γ-radiation.

In instrumentation for capillary methods of separation:

- sample manipulation and introduction: on column, PTV (programmed temperature vaporization) and CNS (cooled needle) sampling techniques;
- design of automated, valve-free multidimensional systems of coupled capillary colums and coupled packed-capillary columns; design of double oven instruments and special coupling pieces for capillary colums, band focusing by intermediate trapping between the coupled colums, by-passing of detectors by eluate flow switching;
- design and systematical investigations of valve based sampling techniques for SFC;
- design of miniaturized equipment for capillary electrophoresis with special sample introduction and detection techniques (in-column detection).

PUBLICATION SCHEDULE FOR 1990

Journal of Chromatography and Journal of Chromatography, Biomedical Applications

MONTH	J	F	M	A	M	J	J	A	S	O	N	D[a]
Journal of Chromatography	498/1 498/2 499	500 502/1	502/2 503/1 503/2 504/1	504/2 505/1	505/2 506 507 508/1	508/2 509/1 509/2 510	511 512 513	514/1 514/2 515	516/1 516/2 517 518/1	518/2 519/1	519/2 520 521/1 521/2	
Cumulative Indexes, Vols. 451–500		501										
Bibliography Section		524/1		524/2		524/3		524/4		524/5		
Biomedical Applications	525/1	525/2	526/1	526/2 527/1	527/2	528/1 528/2	529/1	529/2 530/1	530/2	531 532/1	532/2 533	

[a] The publication schedule for further issues will be published later.

INFORMATION FOR AUTHORS

(Detailed *Instructions to Authors* were published in Vol. 513, pp. 413–416. A free reprint can be obtained by application to the publisher, Elsevier Science Publishers B.V., P.O. Box 330, 1000 AH Amsterdam, The Netherlands.)

Types of Contributions. The following types of papers are published in the *Journal of Chromatography* and the section on *Biomedical Applications*: Regular research papers (Full-length papers), Notes, Review articles and Letters to the Editor. Notes are usually descriptions of short investigations and reflect the same quality of research as Full-length papers, but should preferably not exceed six printed pages. Letters to the Editor can comment on (parts of) previously published articles, or they can report minor technical improvements of previously published procedures; they should preferably not exceed two printed pages. For review articles, see inside front cover under Submission of Papers.

Submission. Every paper must be accompanied by a letter from the senior author, stating that he is submitting the paper for publication in the *Journal of Chromatography*. Please do not send a letter signed by the director of the institute or the professor unless he is one of the authors.

Manuscripts. Manuscripts should be typed in double spacing on consecutively numbered pages of uniform size. The manuscript should be preceded by a sheet of manuscript paper carrying the title of the paper and the name and full postal address of the person to whom the proofs are to be sent. As a rule, papers should be divided into sections, headed by a caption (*e.g.*, Abstract, Introduction, Experimental, Results, Discussion, etc.). All illustrations, photographs, tables, etc., should be on separate sheets.

Introduction. Every paper must have a concise introduction mentioning what has been done before on the topic described, and stating clearly what is new in the paper now submitted.

Abstract. Full-length papers and Review articles should have an abstract of 50–100 words which clearly and briefly indicates what is new, different and significant. (Notes and Letters to the Editor are published without an abstract.)

Illustrations. The figures should be submitted in a form suitable for reproduction, drawn in Indian ink on drawing or tracing paper. Each illustration should have a legend, all the *legends* being typed (with double spacing) together on a *separate sheet*. If structures are given in the text, the original drawings should be supplied. Coloured illustrations are reproduced at the author's expense, the cost being determined by the number of pages and by the number of colours needed. The written permission of the author and publisher must be obtained for the use of any figure already published. Its source must be indicated in the legend.

References. References should be numbered in the order in which they are cited in the text, and listed in numerical sequence on a separate sheet at the end of the article. Please check a recent issue for the layout of the reference list. Abbreviations for the titles of journals should follow the system used by *Chemical Abstracts*. Articles not yet published should be given as "in press" (journal should be specified), "submitted for publication" (journal should be specified), "in preparation" or "personal communication".

Dispatch. Before sending the manuscript to the Editor please check that the envelope contains four copies of the paper complete with references, legends and figures. One of the sets of figures must be the originals suitable for direct reproduction. Please also ensure that permission to publish has been obtained from your institute.

Proofs. One set of proofs will be sent to the author to be carefully checked for printer's errors. Corrections must be restricted to instances in which the proof is at variance with the manuscript. "Extra corrections" will be inserted at the author's expense.

Reprints. Fifty reprints of Full-length papers, Notes and Letters to the Editor will be supplied free of charge. Additional reprints can be ordered by the authors. An order form containing price quotations will be sent to the authors together with the proofs of their article.

Advertisements. Advertisement rates are available from the publisher on request. The Editors of the journal accept no responsibility for the contents of the advertisements.

Journal of Chromatography Library, Volume 45

Chromatography and Modification of Nucleosides

edited by **C.W. Gehrke** and **K.C.T. Kuo**, *Department of Biochemistry, University of Missouri-Columbia, and Cancer Research Center, P.O. Box 1268, Columbia, MO, U.S.A.*

Part A

Analytical Methods for Major and Modified Nucleosides - HPLC, GC, MS, NMR, UV and FT-IR

Chromatography and Modification of Nucleosides is a four-volume work which provides state-of-the-art chromatography and analytical methods for use in a wide spectrum of nucleic acid modification research.

The focus of Part A, is the presentation of advanced methods for modification research on tRNAs, mRNAs, mtRNAs, rRNAs and DNAs. HPLC-UV, GC-MS, NMR, FT-IR and affinity chromatography approaches to nucleic acid modification studies are presented, as are nucleoside, oligonucleotide and nucleic acid isolation techniques.

1990 liii + 400 pages, ISBN 0-444-88540-4
Price: US$ 141.00 / Dfl. 275.00

Part B

Biological Roles and Function of Modification

Part B, the second of the four-volume work *Chromatography and Modification of Nucleosides*, has as its central theme the modified nucleosides of tRNA and the current analytical means for studying rRNA modifications. Modified nucleoside synthesis, function, structural conformation, biological regulation, and occurrence of modification in a wide range of tRNAs are presented, as is a chapter on DNA modification and a chapter on solid phase immunoassay for determining a particular modification.

The chapters are written by leading scientists in their respective fields and present an up-to-date review on the roles of modified nucleosides in nucleic acids which will be extremely useful for workers in chromatography, molecular biology, genetics, biochemistry, biotechnology and the pharmaceutical industry.

1990 xliv + 370 pages, ISBN 0-444-88505-6
Price: US$ 153.75 / Dfl. 300.00

Elsevier Science Publishers
P.O. Box 211, 1000 AE Amsterdam,
The Netherlands

Elsevier Science Publishing Co. Inc
P.O. Box 882, Madison Square Station
New York, NY 10159, U.S.A